

UNIVERSIDAD COMPLUTENSE DE MADRID
FACULTAD DE CIENCIAS FÍSICAS



TESIS DOCTORAL

**Cosmological and astrophysical signatures of alternative dark
sector models**

**Señales cosmológicas y astrofísicas de sectores oscuros
alternativos**

MEMORIA PARA OPTAR AL GRADO DE DOCTOR

PRESENTADA POR

Héctor Villarrubia Rojo

Directores

José Alberto Ruiz Cembranos
Antonio López Maroto

Madrid

© Héctor Villarrubia Rojo, 2020

UNIVERSIDAD COMPLUTENSE DE MADRID
FACULTAD DE CIENCIAS FÍSICAS



TESIS DOCTORAL

**Cosmological and astrophysical
signatures of alternative dark
sector models**

**Señales cosmológicas y astrofísicas
de sectores oscuros alternativos**

MEMORIA PARA OPTAR AL GRADO DE DOCTOR

PRESENTADA POR

HÉCTOR VILLARRUBIA ROJO

DIRECTOR

JOSÉ ALBERTO RUIZ CEMBRANOS
ANTONIO LÓPEZ MAROTO



UNIVERSIDAD
COMPLUTENSE
MADRID

**Cosmological and astrophysical
signatures of alternative dark
sector models**

**Señales cosmológicas y astrofísicas
de sectores oscuros alternativos**

por

HÉCTOR VILLARRUBIA ROJO

bajo la supervisión de

JOSÉ ALBERTO RUIZ CEMBRANOS

ANTONIO LÓPEZ MAROTO

*Tesis presentada en la
Universidad Complutense de Madrid
para el grado de Doctor en Física*

*Departamento de Física Teórica
Facultad de Ciencias Físicas
Junio 2020*

Publications

- J. A. R. Cembranos, A. L. Maroto and H. Villarrubia-Rojo. “Constraints on hidden gravitons from fifth-force experiments and stellar energy loss”. *JHEP* 09 (2017). DOI: [10.1007/JHEP09\(2017\)104](https://doi.org/10.1007/JHEP09(2017)104). arXiv: [1706.07818](https://arxiv.org/abs/1706.07818).
- J. A. R. Cembranos, A. L. Maroto, S. J. Núñez Jareño and H. Villarrubia-Rojo. “Constraints on anharmonic corrections of Fuzzy Dark Matter”. *JHEP* 08 (2018). DOI: [10.1007/JHEP08\(2018\)073](https://doi.org/10.1007/JHEP08(2018)073). arXiv: [1805.08112](https://arxiv.org/abs/1805.08112).
- J. A. R. Cembranos, A. L. Maroto and H. Villarrubia-Rojo. “Non-comoving Cosmology”. *JCAP* 1906 (2019). DOI: [10.1088/1475-7516/2019/06/041](https://doi.org/10.1088/1475-7516/2019/06/041). arXiv: [1903.11009](https://arxiv.org/abs/1903.11009).
- J. A. R. Cembranos, A. L. Maroto and H. Villarrubia-Rojo. “Magnetic fields from cosmological bulk flows”. arXiv: [1911.04988](https://arxiv.org/abs/1911.04988).

Contents

Publications	v
Introduction	xiii
I STANDARD COSMOLOGY OVERVIEW	1
1 Observational basis	3
1.1 CMB temperature anisotropies	3
1.1.1 Past, present and future of CMB surveys	3
1.1.2 <i>Planck's</i> sky	5
1.1.3 Λ CDM model	7
1.2 Large-scale structure	10
1.2.1 LSS surveys	11
1.2.2 Angular correlations	13
1.3 Galactic structure	14
1.4 Stellar evolution	15
1.4.1 Sun	17
1.4.2 Red giants	18
1.4.3 Supernova SN1987A	19
1.5 Fifth-force tests	20
2 Components of the Universe	23
2.1 Fluid description	23
2.1.1 Energy-momentum tensor	23
2.1.2 Perfect fluids	24
2.2 Field description	25
2.2.1 Energy-momentum tensor	26
2.2.2 Scalar field	27
2.2.3 Vector field	27
2.2.4 Tensor field	29
2.3 Kinetic description	31
2.3.1 Phase space	32
2.3.2 Volume element	33
2.3.3 Distribution function	34
2.3.4 Collisions and the Boltzmann equation	36
2.3.5 Boltzmann equation in flat space-time	38
2.3.6 Energy-momentum tensor	39

3	ΛCDM Cosmology	41
3.1	Background dynamics	41
3.2	Kinetic approach	43
3.2.1	Background	44
3.2.2	Perturbations	45
3.3	Boltzmann equation	47
3.3.1	Liouville operator	47
3.3.2	Collision term	50
3.3.3	Boltzmann equation for different components	54
3.4	Harmonic analysis	56
3.4.1	Scalar-vector-tensor decomposition	56
3.4.2	Boltzmann hierarchy	58
3.4.3	Truncation	59
3.5	Einstein equations and gauge transformations	60
3.5.1	Einstein equations	60
3.5.2	Gauge transformations	61
3.5.3	Newtonian and synchronous gauge	62
3.6	Approximation schemes	63
3.6.1	Tight coupling	64
3.6.2	Radiation streaming	65
3.7	Initial conditions	66
3.7.1	Super-Hubble expansion	66
3.7.2	Adiabatic mode	69
3.8	Line-of-sight integration	70
3.8.1	Neutrinos	71
3.8.2	Photons	72
3.9	Observables	73
3.9.1	Power spectra	74
3.9.2	CMB temperature anisotropy	74
II	BEYOND THE STANDARD PICTURE	77
4	Hidden Gravitons	79
4.1	Massive gravitons	79
4.2	Interaction with matter	83
4.2.1	Fifth-force constraints	83
4.2.2	Coupling to QED	85
4.3	Boltzmann equation and energy loss	86
4.3.1	$2 \rightarrow 2$ process	86
4.3.2	External field process	89
4.3.3	Two-particle annihilation	89
4.4	Plasma processes	90
4.4.1	Photon-photon annihilation	90
4.4.2	Gravi-Compton process	90
4.4.3	Electron-positron annihilation	92

4.4.4	Gravi-bremsstrahlung	93
4.4.5	Nucleon bremsstrahlung	94
4.5	Astrophysical constraints	95
5	Repulsive Fuzzy Dark Matter	99
5.1	FDM and coherent cosmological fields	99
5.1.1	Astrophysical behaviour	99
5.1.2	Cosmological behaviour	100
5.1.3	Axion-like particles	101
5.2	Repulsive FDM	102
5.2.1	Exact description	103
5.2.2	Averaged description	105
5.2.3	Heuristic analysis	108
5.3	Cosmological evolution and constraints	110
5.3.1	Numerical implementation	110
5.3.2	Physical effects	111
5.3.3	Observational constraints	114
6	Non-comoving Cosmology	119
6.1	Cosmology with large-scale motions	119
6.2	Perfect fluids with bulk velocity	121
6.2.1	Physical setting	121
6.2.2	Evolution	123
6.3	Kinetic approach	124
6.3.1	Background	125
6.3.2	Perturbations	127
6.4	Boltzmann equation	129
6.4.1	Liouville operator	129
6.4.2	Collision term	132
6.4.3	Boltzmann equation for different components	133
6.5	Harmonic analysis	135
6.5.1	Helicity basis	136
6.5.2	Boltzmann hierarchy	140
6.5.3	Truncation	142
6.6	Einstein equations and gauge transformations	143
6.6.1	Einstein equations	143
6.6.2	Gauge transformations	144
6.7	Reduced system: fluid approximation	145
6.7.1	Bulk velocities	146
6.7.2	Scalar modes	147
6.7.3	Vector modes	152
6.8	Initial conditions	154
6.8.1	Scalar modes	155
6.8.2	Vector modes	158
6.9	Numerical implementation and first results	159
6.9.1	Implementation details	159

6.9.2	Time evolution and transfer functions	161
6.10	Observables	162
6.10.1	Power spectra	162
6.10.2	CMB temperature anisotropy	166
7	Non-comoving Cosmology: CMB	173
7.1	Generic two-point function	173
7.1.1	Temperature perturbation and transfer function	173
7.1.2	Alternative power spectrum	176
7.1.3	Solar System motion	177
7.2	Modified line-of-sight integral	177
7.2.1	Modified source	177
7.2.2	Modified two-point function	180
8	Non-comoving Cosmology: Magnetic fields	183
8.1	Magnetic fields in the Universe	183
8.2	Electron-proton-photon plasma	184
8.2.1	Full system	184
8.2.2	Electron-proton plasma	185
8.2.3	Maxwell equations	187
8.2.4	Time scales	187
8.2.5	Evolution of subsystems	188
8.3	Magnetic field production	192
III	CONCLUSIONS AND APPENDICES	197
	Concluding remarks	199
A	Conventions	203
A.1	Semantic conventions	203
A.2	Acronyms	203
A.3	Miscellanea	204
B	Useful numbers	207
C	Special functions	211
C.1	Spherical Bessel functions	211
C.2	Legendre polynomials	212
C.3	Associated Legendre functions	213
C.4	Spherical harmonics	213
C.5	Proof of some results	214
D	Metric Formulae	219
D.1	Definitions	219
D.2	Perturbations on a FLRW space-time	220
D.2.1	Background	220
D.2.2	General perturbations	221

D.2.3	Scalar perturbations	223
D.2.4	Vector perturbations	225
D.2.5	Tensor perturbations	227
D.3	Geodesics	228
D.4	Energy-momentum tensor conservation	230
E	Collision term with bulk flows	233
F	Electrodynamics in a perturbed FLRW universe	235
F.1	Lorentz force in General Relativity	235
F.2	Electric current	236
F.3	Maxwell equations	236
F.3.1	Full Maxwell equations	236
F.3.2	Simplified Maxwell equations	237
F.4	Physical fields and gauge transformations	238
F.5	Liouville operator with electromagnetic fields	239
	Abstract	241
	Resumen	243
	References	245

Introduction

Theoretical cosmology has grown to be a mature discipline, owing to the collaborative effort of observationalists and theorists over the last century. We could place its birth after the formulation of General Relativity (GR) and the discovery of the first cosmological solutions of the Einstein equations

$$G_{\mu\nu} = 8\pi G T_{\mu\nu} . \quad (1)$$

These solutions allowed the first mathematical description of the Universe as a whole. Quite generically, the cosmological solutions represented non-stationary universes, either expanding or contracting. Some years after, equally impressive advances in observational cosmology led to the first Hubble diagrams. These observations supported the basic picture of a dynamical (expanding) Universe.

The community quickly realized that the expanding cosmological models, when extrapolated back in time, predicted that the early Universe must have been extremely hot and dense. This gave rise to the “Hot Universe” (or Big Bang) paradigm. This idea proved extraordinarily successful at explaining the relative abundance of light elements, through the so-called Big Bang nucleosynthesis (BBN) process, and also *predicted* a remanent background of microwave radiation.

In the 60s, the cosmic microwave background (CMB) radiation was measured, putting the “Hot Universe” paradigm on a solid footing. On the theory side, the basic framework needed to describe the state of the Universe, from the first few seconds to the present time, was also developed during this decade. Taking GR and standard atomic physics as its backbone, it allowed to understand how the ionized plasma became neutral as the Universe expanded. By the mid 80s, cosmological perturbation theory was a mature and solid framework able to make definite predictions about the evolution of the primordial density fluctuations in the plasma, from the moment they were generated to (almost) the present time. There were competing cosmological models at the time aiming to explain the formation of structures but the observations were not precise enough to discriminate between them.

During the last 25 years the situation has changed and cosmology has become an observationally driven discipline. The wealth of data has allowed to rule out many cosmological models and has also revealed puzzling features of our Universe. Provided that we keep our most cherished assumptions, like the homogeneity and isotropy at large scales or the validity of the Einstein equations at all scales, it seems unavoidable to add a *dark sector* in order to explain current observations. The dark sector can be regarded as an exotic fluid that constitutes most of the energy content of the Universe, i.e. the right-hand side of (1), and whose interaction with the visible sector, i.e. the Standard Model (SM) of particle physics, is so feeble that we can only detect it through its gravitational effects.

In this context, the so-called Λ CDM model has been firmly established as the standard cosmological model. It has withstood many tests and provides a consistent

explanation of a large number of independent observations over a wide range of scales. One of its central features is its minimal dark sector. Within Λ CDM, the dark sector is a two-component fluid composed of a cosmological constant (Λ) and cold dark matter (CDM). Notwithstanding its success, it is important to stress that the dark sector in Λ CDM, as it stands, is purely phenomenological. It provides a good fit to the observations with a small number of parameters and additional assumptions, but it lacks a solid theoretical foundation.

The dark sector plays a paramount role in modern cosmology and yet it is poorly understood. If we want to unveil the nature of the dark sector, it is essential to propose and test alternatives to the simplest Λ +CDM model, exploring their phenomenology and searching for new observable signatures. There are essentially three ways to move beyond a Λ +CDM dark sector:

- I) *Add new species.* The Λ +CDM dark sector is already a two-component fluid so it seems natural to enlarge it, adding components that may change its overall behaviour. Dark radiation is a good example of this procedure. Even a small amount of a radiation-like fluid can modify the early time evolution of the dark sector while recovering the standard Λ +CDM behaviour at late times. Even if they do not modify the cosmological evolution, these new species may also lead to other observational signatures that are worth exploring.
- II) *Change the simplest paradigm.* Both the cosmological constant and the cold dark matter can be substituted by more complex models. For instance, it has become very popular to drop the assumption that Λ is constant and consider instead dynamical *dark energy* models. In the dark matter context, many alternatives have been proposed: warm DM, self-interacting DM, milicharged DM...
- III) *Modify a fundamental assumption.* This is generally, by far, the hardest way to go. Sometimes one can modify only a mild assumption that is easy to handle, e.g. including interactions within the dark sector, but typically a careful theoretical analysis is needed to build a consistent model.

This thesis explores the three routes, providing a representative example in each category. For each alternative model, we first build the theoretical framework, extracting then its phenomenology and finally addressing its observability. Given the wide variety of topics, it has been difficult to provide an adequate background for all of them. Nonetheless, a huge effort has been invested in providing a thorough general introduction, that comprises Part I of this thesis. The selection of topics and the presentation have been made with Part II in mind. Its main objective is to present a clear splitting between what belongs to standard cosmology and what is new in the models that we will present later. Even though the reader familiar with modern cosmology can skip most of Part I, it may be worth skimming through it. The structure of this part goes as follows.

- If we want to discriminate between alternative dark sector models we must find new signatures and compare with observations. Chapter 1 provides the necessary observational background, focusing on the observations used in this work.

- When trying to modify the dark sector one should first learn how to describe it. Chapter 2 tackles this question, presenting three different ways to describe a cosmological component.
- Since we are interested in modifying Λ CDM we must first learn how it works and what are its standard assumptions. In Chapter 3 we develop, in detail, the Λ CDM cosmology.

Part II of this work explores the implications of three alternatives to the standard Λ +CDM dark sector.

- In Chapter 4 we add a new particle to the Λ +CDM dark sector: hidden gravitons. The hidden gravitons are generic massive spin-2 particles, that could be the effective description of a more fundamental theory. The model that we consider only contains two free parameters: the mass and the coupling to matter. Both parameters can be constrained using fifth-force tests and astrophysical data. In particular, we compute the energy lost in stars through the emission of hidden gravitons.
- Chapter 5 contains a full cosmological analysis of a new dark matter model: repulsive fuzzy dark matter. Building upon previous work on the fuzzy dark matter paradigm, where dark matter is an ultralight particle, we add a repulsive self-interaction and analyze its phenomenology. This model contains two more free parameters with respect to CDM: the mass and self-coupling of the dark matter particles. We constrain both parameters using CMB and large-scale structure (LSS) observations.
- Chapter 6 relaxes one of the fundamental assumptions of Λ CDM: we investigate the impact of a primordial bulk motion between the dark and the visible sector. As we will show, a sizeable bulk flow can be introduced without spoiling the isotropy of the background. While the background behaviour is preserved, a very rich phenomenology arises at the perturbation level. The model contains a single free parameter: the amplitude of the primordial bulk motion. While there is no leading order effect on the usual LSS and CMB observables, in this chapter we identify new LSS observable features. In Chapter 7 we move on to the CMB analysis, identifying new features beyond the temperature power spectrum. Finally, Chapter 8 studies the production of magnetic fields in the presence of cosmological bulk flows. While the amplitude of the observed magnetic fields in the Universe is difficult to explain within Λ CDM, we find that, in this scenario, the fields produced are large enough to be the origin of the galactic magnetic fields.

The main text is supplemented by a number of appendices. Appendix A gathers the conventions and acronyms used in the thesis. Appendix B contains some important numerical factors and some of the most important cosmological parameters. In Appendix C we have collected several properties of special functions that are used in the text and some mathematical derivations. Useful formulae for cosmological perturbations of the metric tensors, and related results, can be found in Appendix

D. Appendix E derives the Thomson collision term in the presence of cosmological bulk flows. Appendix F studies the Maxwell equations in an expanding universe with perturbations and bulk flows.

I

STANDARD COSMOLOGY OVERVIEW

1

Observational basis

This chapter summarizes some key observations in cosmology and astrophysics, ranging from cosmological to laboratory scales. Arguably, the most powerful source of cosmological information is the distribution of anisotropies in the CMB, that we cover in Section 1.1. The distribution of matter at large scales, that we discuss in Section 1.2, is an independent, increasingly important, probe of the late-time Universe. Section 1.3 is devoted to studies of galactic structure, that play a central role in discriminating dark matter models. Section 1.4 covers the basics of stellar evolution. We will learn how the detailed knowledge that we possess about the evolution of different stars may allow us to rule out the existence of new particles. We conclude in Section 1.5 with a summary of the ongoing effort to detect deviations from the Newtonian law of gravity, from Solar-System to laboratory scales.

1.1 CMB temperature anisotropies

1.1.1 Past, present and future of CMB surveys

A history of the CMB *anisotropies* could start with the launch of the COBE satellite in 1989. It was equipped with three different instruments: 1) DIRBE, aimed at measuring the cosmic infrared background, 2) FIRAS, to observe the spectrum of the cosmic microwave background, 3) DMR, designed to find temperature fluctuations in the CMB. After only one year of operation, COBE found the first (cosmological) anisotropies [Smo+92]. The basic picture of the CMB after COBE is summarized in Figure 1.1. The main findings, as reported in [Fix+96; Ben+96], were:

- I) The background is extremely isotropic with a mean temperature¹ $T_0 = 2.728 \pm 0.004$ K.
- II) There is a dipolar anisotropy with an amplitude $\Delta T = 3.353 \pm 0.024$ mK pointing toward galactic coordinates $(l, b) = (264^\circ 26' \pm 0^\circ 33', 48^\circ 22' \pm 0^\circ 13')$. It is com-

¹This is the FIRAS value [Fix+96], that we comment below. Actually, despite of being a *differential* measurement instrument, DMR also gave an estimate $T_0 = 2.725 \pm 0.020$ K. In addition to the motion of the Solar System with respect to the CMB rest frame, that gives rise to the kinematic dipole

$$T(\theta) = T_0(1 + \beta_{\text{CMB}}^\circ \cos\theta + \mathcal{O}(\beta^2)),$$

there are additional Doppler boosting effects due to the orbital motions. These motions within the Solar System are known with such precision that T_0 can be inferred from the time-varying regular signal, after fitting to a blackbody distribution using the six frequency channels of DMR. The method is described in detail in [Kog+93].

patible with a kinematical origin: it is a Doppler-shifting effect caused by the motion of the Solar System with respect to the CMB rest frame.

- III) The quadrupole and higher order anisotropies are at the level of $\Delta T \sim 10^{-5}$ K. Their origin is cosmological.

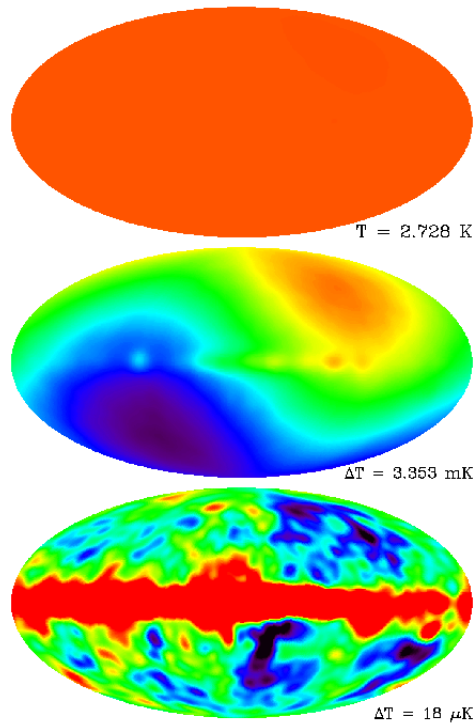


Figure 1.1: COBE observations of the monopole, dipole and higher order cosmological anisotropies. Credit: Legacy Archive for Microwave Background Data (lambda.gsfc.nasa.gov).

Before moving on to modern CMB surveys, it is worth mentioning the relevance of the FIRAS instrument. FIRAS measured with exquisite precision the CMB *spectrum*, i.e. the intensity at many different frequencies. Its main results for the monopole and dipole are represented in Figure 1.2. We can see that the blackbody description of the CMB is staggeringly accurate. It can be inferred that the early Universe was extremely close to thermal equilibrium. As has been phrased in different ways in the literature, “the CMB spectrum is the best-measured black body in nature” [Akr+18a]. The relevance of FIRAS for modern cosmology goes beyond the historical remark: it remains the best determination of the CMB spectrum. This measurement still provides the best bounds on the so-called spectral distortions, that could be produced by exotic energy injections in the early Universe (e.g. due to the decay of dark matter particles). For more details on spectral distortions, see [HS93b; HS93a; CS12].

The study of CMB anisotropies took a leap forward after the launch of the

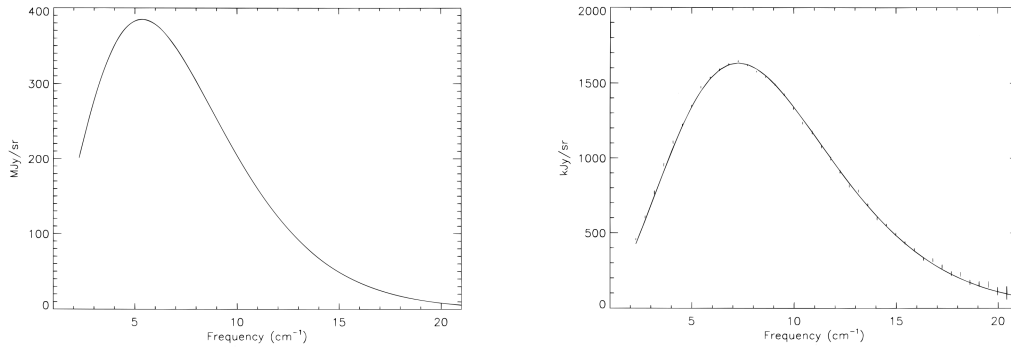


Figure 1.2: Monopole (left) and dipole (right) spectra of the CMB as measured by COBE. Note that the error bars (68% limit) on the monopole spectrum are smaller than the thickness of the curve. Credit: [Fix+96].

WMAP satellite in 2001. COBE had an angular resolution² of about 7° , while WMAP reached an angular resolution of 0.2° . After the arrival of WMAP the amount and quality of data increased so much that it became common, in the cosmological community, to talk about the advent of “the era of precision cosmology”. WMAP laid down the basic ingredients of the Universe as we know it today [Kom+11]. Shortly after, the *Planck* satellite was launched in 2009. It confirmed the basic picture of WMAP, reaching even higher resolution in temperature and polarization measurements. In the next section we will review what we have learnt about the Universe after *Planck*. Looking towards the future, the scientific target of the next-generation surveys is the CMB polarization. The main experiments that have been already approved are the LiteBIRD satellite [Haz+19] and the ground-based Simons Observatory [Ade+19] and CMB-S4 [Aba+16].

1.1.2 *Planck*’s sky

The *Planck* satellite measured the CMB in nine frequency bands (from 30 to 857 GHz) with unprecedented angular resolution. The Figure 1.3 shows the temperature map at 100 GHz before the masking and foreground subtraction (but after subtracting the dipole). The contamination of the galactic plane is clearly visible in the central regions, but in the poles the cosmological anisotropies dominate the map. The different sources of noise need to be modelled and subtracted from these maps. Since different foregrounds have different spectral behaviour, it is crucial to measure the CMB at different frequencies for a correct modelling of these uncertainties. After taking into account these effects and its associated systematic errors, the temperature measurement of *Planck* are extremely precise. Within the angular scales it is aimed at, *Planck* has exhausted all the information in the CMB temperature, i.e. its measurements have reached the ‘cosmic variance limit’, that we will comment below.

The effect of the (kinematic) dipole needs to be corrected in these maps. *Planck* has also provided an extremely precise measurement of the solar dipole

$$\Delta T_{\text{dip}} = 3362.08 \pm 0.99 \mu\text{K}, \quad (1.1)$$

²A useful reference to keep in mind is that a full moon subtends $\sim 0.5^\circ$.

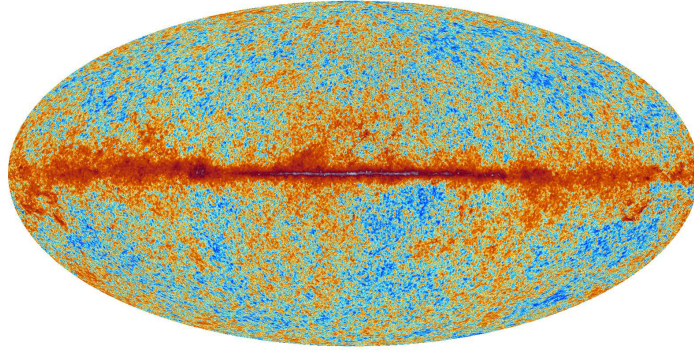


Figure 1.3: *Planck* temperature map at 100 GHz. The dipole has been subtracted. Credit: [Akr+18a].

where $T_0 = 2.7255$ K [Fix09] is needed to convert to temperature units. This corresponds to a relative CMB-Solar System motion

$$\beta_{\text{CMB}}^{\circ} = (1.23357 \pm 0.00036) \times 10^{-3}, \quad (1.2a)$$

$$(l, b) = (264^{\circ}.021 \pm 0^{\circ}.011, 48^{\circ}.253 \pm 0^{\circ}.005), \quad (1.2b)$$

or $v = (369.82 \pm 0.11)$ km s⁻¹. This measurement is based on the observation of the regular Doppler-shifting effects produced by the orbital motions of the satellite, that are exceedingly well known. Observing this orbital modulation effect (at the μ K level) the amplitude of the dipole $\Delta T_{\text{dip}}/T_0$ can be measured.

Once the dipole has been subtracted, it is common to decompose the temperature over the sphere into a set of multipoles

$$\Theta(\hat{n}) \equiv \frac{T(\hat{n}) - T_0}{T_0} = \sum_{\ell=2}^{\infty} \sum_{m=-\ell}^{\ell} a_{\ell m} Y_{\ell}^m(\hat{n}), \quad (1.3)$$

where $Y_{\ell}^m(\hat{n})$ are spherical harmonics. From the theoretical point of view, no cosmological description can aim at explaining the values of every $a_{\ell m}$. It is assumed that the observed anisotropy pattern is the result of stochastic processes, from which we observe one realization. We can build statistical observables and predict, under some assumptions, averages, $\langle \dots \rangle$, over many possible realizations. The main observable is the two-point function

$$C(\hat{n}, \hat{n}') \equiv \langle \Theta(\hat{n}) \Theta(\hat{n}') \rangle, \quad (1.4)$$

that essentially measures the variance of the temperature difference³ in directions \hat{n} and \hat{n}' , i.e. $\langle (T(\hat{n}) - T(\hat{n}'))^2 \rangle / T_0^2$. Moreover, if the Universe has no privileged direction, we have *statistical isotropy*

$$C(\hat{n}, \hat{n}') = C(\hat{n} \cdot \hat{n}'), \quad (1.5)$$

and all the information in the temperature map can be encoded into the power spectrum C_{ℓ}

$$\langle a_{\ell m}^* a_{\ell' m'} \rangle = \delta_{\ell \ell'} \delta_{m m'} C_{\ell}. \quad (1.6)$$

³This is a common definition but notice that it differs from the C_{ℓ} reported in the *Planck*'s papers by a factor T_0^2 .

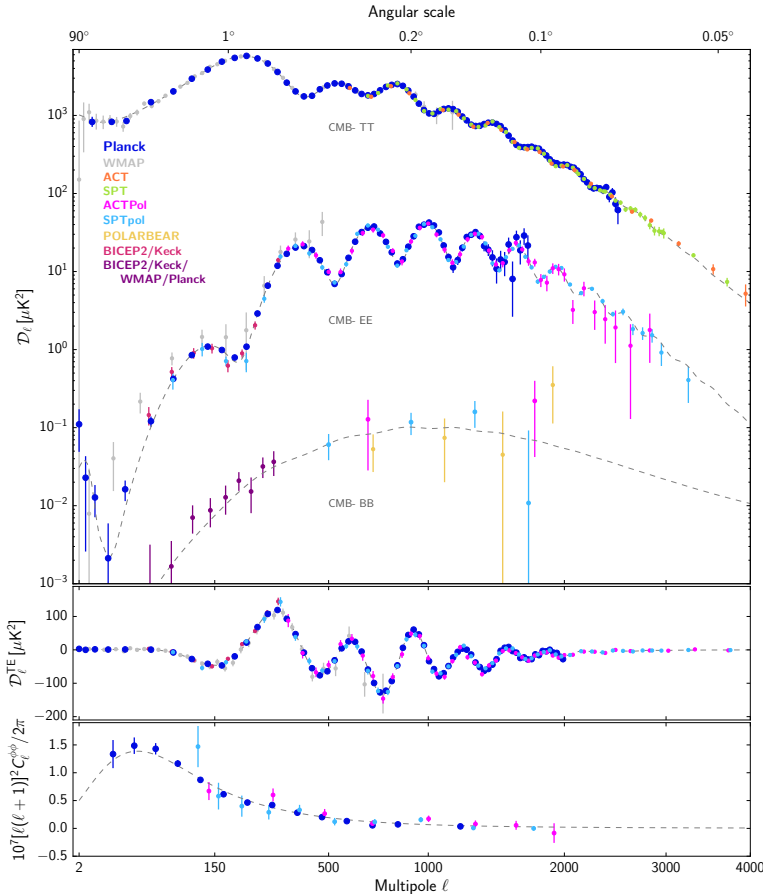


Figure 1.4: Compilation of different observations of the CMB temperature, polarization and lensing spectra. The dotted line is the best Λ CDM fit. Credit: [Akr+18a].

Instead of the average over realizations, the observationally accessible quantity is the average over m

$$C_\ell^{\text{obs}} = \frac{1}{2\ell+1} \sum_m |a_{\ell m}|^2. \quad (1.7)$$

The theoretical computation of the temperature spectrum will be the subject of the next chapter. We will discuss the fundamental limit that arises when performing statistics with a *single realization*, known as cosmic variance. This effect is more pronounced at large scales, i.e. low ℓ , and it is the dominant source of uncertainty in the *Planck* temperature measurements shown in Figure 1.4.

1.1.3 Λ CDM model

Planck has cemented the role of Λ CDM as the leading cosmological model. This model is remarkably simple and has proved successful at explaining many different observations. Among other hypotheses, see [Akr+18a], Λ CDM assumes that the Universe is extremely homogeneous and isotropic, with tiny deviations at early times that can be handled in a perturbative way.

We will now briefly summarize the evolution of the Λ CDM model after Big Bang nucleosynthesis (BBN), i.e. after the formation of light elements at $z \simeq 10^{10}$. The detailed mathematical description can be found in Chapter 3.

- I) The Universe is composed of baryons, photons, neutrinos, cold dark matter (CDM) and a cosmological constant (Λ). The initial conditions for all the fluids can be related to a primordial curvature perturbation \mathcal{R}_k , i.e. only the so-called adiabatic mode is present. The primordial curvature perturbation \mathcal{R}_k is a stochastic Gaussian variable with zero mean, so its statistics can be completely characterized through its standard deviation or power spectrum (two-point function).
- II) Baryons and photons are the only interacting species. In the early Universe, they form a tightly coupled fluid that undergoes acoustic oscillations, i.e. density waves, in the gravitational wells created by⁴ CDM. As the Universe expands and lower its temperature, most of the protons and electrons combine into hydrogen atoms (*recombination* at $z \simeq 1300$). Shortly after, photons decouple from the baryon fluid (*decoupling* at $z \simeq 1090$) and free-stream. The formation of the first structures reionize the Universe at $z \simeq 10$ and some CMB photons rescatter before reaching us at $z = 0$. The main component of the photon anisotropy observed today is an imprint of the acoustic oscillations that took place at decoupling.
- III) CDM only interacts gravitationally and its density perturbations grow throughout the history of the Universe. Once the baryons decouple from photons, they fall in the potential wells created by CDM and the density contrast of both components grows (gravitational instability). At some point, the density perturbations on the smallest scales are so large that linear perturbation theory breaks down. Finally, the non-linear structures observed today, e.g. galaxies or filaments, form.
- IV) Λ becomes dominant at very late times and drives the current accelerated expansion of the Universe.

All this phenomenology is captured in the so-called base Λ CDM, or just Λ CDM, with six free parameters: $\{\Omega_b h^2, \Omega_c h^2, \log(10^{10} A_s), n_s, 100\theta_*, \kappa_{\text{reio}}\}$. These parameters can be classified into different categories.

Energy budget. $\Omega_b h^2$ and $\Omega_c h^2$ are the (reduced) densities⁵ of baryons and CDM, respectively. The amount of photons is set by the CMB temperature, $T_0 = 2.7255$ K [Fix09], which for a blackbody translates into a density $\Omega_\gamma h^2 = 2.47 \times 10^{-5}$. The energy density of neutrinos can be related at early times with that of the photons [Les+13]. For massive neutrinos, the energy density today is⁶

$$\Omega_\nu h^2 = \frac{\sum m_\nu}{93.14 \text{ eV}}. \quad (1.8)$$

⁴CDM is the dominant contribution, but of course all the species source the gravitational potentials.

⁵Sometimes are denoted as ω_b and ω_c . Remember that h is the reduced Hubble parameter, defined as $H_0 \equiv 100 h \text{ kms}^{-1} \text{ Mpc}^{-1}$.

⁶If we neglect the neutrino masses, the energy density today is $\Omega_\nu h^2 \simeq 1.7 \times 10^{-5}$. The difference arises because for massive neutrinos the equation of state changes with time while, if they are massless, the photon-neutrino ratio remains constant and equal to its primordial value, as given in Appendix B.

The base Λ CDM model features two massless neutrinos and one massive, with $\Sigma m_\nu = 0.06$ eV. This model also assumes that the Universe is flat, so

$$\Omega_{\text{tot}} = \Omega_\Lambda + \Omega_c + \Omega_b + \Omega_\nu + \Omega_\gamma = 1. \quad (1.9)$$

This expression fixes the value of Ω_Λ .

Initial conditions. A_s and n_s are the amplitude and spectral index of the primordial power spectrum for scalar perturbations. Λ CDM assumes that the initial conditions are adiabatic, Gaussian and given by the power-law spectrum

$$\mathcal{P}_{\mathcal{R}}(k) = A_s \left(\frac{k}{k_*} \right)^{n_s - 1}, \quad (1.10)$$

where the pivot scale is $k_* = 0.05 \text{ Mpc}^{-1}$. We will come back to this point in Section 3.7.

Distance calibration. θ_* is the angular scale of the sound horizon at the last-scattering surface⁷. This parameter represents the angle subtended by a transverse physical scale at a given redshift, in this case the sound horizon at $z = 1090$. For a precise definition see [Ade+14a]. It is the best measured cosmological parameter, since it is related to the position of the acoustic peaks. The base Λ CDM model can also be parameterized using the reduced Hubble parameter h instead of θ_* as a distance indicator.

Thermal history. CMB physics is very sensitive to the evolution of the ionization fraction, i.e. the number of free electrons. The thermal history at early times, the details of recombination in particular, can be computed with extraordinary precision since it only relies on ordinary atomic physics. However, at late times, the formation of the first stars and quasars led to the emission of ultraviolet photons that produced a sharp reionization of the Universe. CMB photons, freely streaming since decoupling, have a non-negligible probability of rescattering in the late Universe. To take into account this effect, a new parameter needs to be introduced: the optical depth⁸ to reionization $\kappa_{\text{reio}} = \kappa(z_{\text{reio}})$.

Extensions. Λ CDM extensions have been widely considered in the literature. Here, we will only cover one-parameter extensions to the base, i.e. six-parameter, model that are still traditionally associated with Λ CDM. One of the most important is the curvature parameter $\Omega_K = 1 - \Omega_{\text{tot}}$. While the six-parameter model can be tightly constrained using CMB data alone, it is very well-known that, if we relax the flatness assumption, CMB data shows a slight preference for a closed universe [Agh+18]. This is because the angular scale θ_* is highly degenerated with

⁷*Planck's* papers actually use the closely related parameter θ_{MC} . See [Ade+14a] for details.

⁸Notice that, in *Planck's* papers, the same quantity is denoted as τ . Reionization is taken to be sharp, usually modelled as a hyperbolic tangent with midpoint at a redshift z_{reio} and width $\Delta z = 0.5$ [Ade+14a]. This assumption has also been put to test by *Planck* [Agh+18].

the spatial curvature. Including external data⁹ is crucial to break this degeneracy and obtain a strong constraint on the curvature. Another parameter that is commonly fitted is the sum of neutrino masses $\sum m_\nu$. While from oscillation experiments we have a lower bound on this quantity, from the CMB (and in combination with other probes) we can get an extremely competitive upper bound¹⁰. Finally, on top of scalar perturbations, most models of inflation predict the presence of tensor perturbations. These primordial tensor modes are important for the evolution of the polarization and are usually included with a power-law spectrum with an amplitude A_t (or through the parameter $r = A_t/A_s$) and a spectral index n_t . Current observations can only place an upper bound on r , but it is the main target of future CMB surveys.

Nuisance parameters. It is important to mention that the full *Planck* analysis includes several *nuisance parameters*. These parameters model foregrounds and instrumental uncertainties. Even though there are reasonable priors on these parameters, they are non-trivially correlated with the cosmological ones. When comparing a model with CMB observations, the nuisance parameters must also be fitted and marginalized over to obtain the cosmological information.

The best constraints on Λ CDM, and some selected one-parameter extensions, using only CMB data can be found in Table 1.1. The best constraints, using multiple probes, can be found in Appendix B.

1.2 Large-scale structure

The distribution of matter at large scales provides cosmological information that complements the CMB anisotropies. The CMB can be thought as a snapshot of the state of the Universe at early times. After decoupling, CMB photons travelled almost¹¹ freely until reaching the Solar System today. Hence, the CMB is very weakly sensitive to the late-time evolution of the Universe, a gap that can be filled with the aid of large-scale structure (LSS) surveys. The clustering of matter is mainly affected by the late-time expansion history and it is also a sensitive probe of the gravitational behaviour of dark matter at late times. Relying on LSS observations we have access to objects with different redshift, belonging to different evolutionary epochs. Then, it is in principle possible to recover all the ‘3D information’, encoded in LSS snapshots and its evolution in time. However, there are two main disadvantages with respect to CMB data. In the first place, since we are dealing with fully formed astrophysical objects, the measurements are unavoidable plagued with as-

⁹In particular the baryon acoustic oscillation (BAO) measurements that we will cover in the next section.

¹⁰See [Les+13] and Chapter 25 of [Tan+18] for the bounds arising from different combinations of observations.

¹¹The two main effects that modify the free-streaming are reionization, that introduces a non-negligible probability of rescattering and modifies the low- ℓ temperature spectrum through the ISW effect, and the weak lensing produced by the metric potentials along the line of sight, whose overall effect is a smoothing of the acoustic peaks.

Parameter	TT+lowE	TT,TE,EE+lowE+lensing
$\Omega_b h^2$	0.02212 ± 0.00022	0.02237 ± 0.00015
$\Omega_c h^2$	0.1206 ± 0.0021	0.1200 ± 0.0012
$100\theta_*$	1.04097 ± 0.00046	1.04110 ± 0.00031
κ_{reio}	0.0522 ± 0.0080	0.0544 ± 0.0073
$\log(10^{10} A_s)$	3.040 ± 0.016	3.044 ± 0.014
n_s	0.9626 ± 0.0057	0.9649 ± 0.0042
Ω_K	$-0.056^{+0.044}_{-0.050}$	$-0.011^{+0.013}_{-0.012}$
$\sum m_\nu$ [eV]	< 0.537	< 0.241
$r_{0.002}$	< 0.102	< 0.101

Table 1.1: Constraints on the base- Λ CDM model (68% limits) using only CMB data, as reported in [Agh+18]. The second column considers only the temperature (TT) and polarization at low- ℓ (lowE), the latter being very important to constrain reionization. The third column includes the full E-mode polarization spectrum (EE), the cross-correlation with temperature (TE) and the information on the lensing potentials inferred from the CMB lensing (lensing). On the lower part some one-parameter extensions are included with 95% limits. The tensor-to-scalar ratio r is evaluated at a pivot scale 0.002 Mpc^{-1} .

trophysical uncertainties, caused by complex physical processes that must be correctly modelled. In the second place, if we want to access the smallest scales not only do we have to deal with baryonic effects but also with non-linearities. While these scales could, at decoupling time, be analyzed using cosmological perturbation theory, in the present we must deal with the additional complexity of non-linear evolution. In spite of these caveats, there is a wealth of information lurking in LSS, while the information in the temperature anisotropies of the CMB has been mostly exhausted.

1.2.1 LSS surveys

The distribution of (mainly dark) matter can be probed observing the so-called tracers: sources of light (galaxies, quasars or clouds of gas) that populate the underlying dark matter structures. The main observable characteristics of a tracer are its position in the sky, brightness, spectrum and shape. Most surveys operate in the optic or near infrared, and fall into two broad categories.

Photometric. Photometric (or imaging) surveys take extremely detailed pictures of the sky, in a few bands of frequency. This kind of experiments offer a poor redshift resolution, thus losing some of the 3D information, but trade it for measuring a large number of galaxies. A very important goal of photometric observations is to characterize the ellipticity of galaxies, that is affected by the weak lensing effects (cosmic shear) produced by the intervening matter along the line of sight. Performing statistics over the ellipticity field one can learn about the (integrated) metric potentials that produce the lensing, and thus about the matter distribution.

Another target of these experiments is the identification of clusters, since the abundance of clusters of a given mass¹² depends on the cosmological model. Besides measuring the clustering of matter, imaging surveys that monitorize a large region of the sky can be used as supernova hunters. Once a supernova has been identified, dedicated experiments can follow up its evolution. Among photometric surveys, we should highlight the currently operating DES [Abb+18] and two surveys that will start running during the next decade and will take LSS surveys to the next level: LSST [Abe+09] and *Euclid* [Ame+18].

Spectroscopic. The aim of a spectroscopic survey is to identify as many tracers as possible and characterize their individual spectra. This type of surveys can make up for a small number of tracers, compared to photometric surveys, with an accurate redshift determination. This allows for a tomographic analysis, where the large-scale structure can be ‘sliced’ and analyzed at different redshifts. Redshift information also entails velocity information. The peculiar¹³ velocity field of matter contains cosmological information on its own but, in general, the peculiar velocity of the tracers can be used to infer the matter density field, e.g. matter falls into overdense regions. Finally, one of the targets of these experiments is the measurement of the baryonic features in the matter distribution, the so-called baryon acoustic oscillations (BAO) that we will comment below. These features provide us with a length scale, a *standard ruler*, whose evolution in time can be used to infer the expansion history of the Universe. This observation complements the methods based on *standard candles* (supernovae Ia) and the recently available *standard sirens* (gravitational wave events). Many spectroscopic surveys have produced high-quality data over the years, with some recent examples being BOSS [Ala+17], WiggleZ [Par+12] and 6dF [Beu+11]. The next generation of spectroscopic surveys has just started with DESI [Agh+16] and it will continue with *Euclid*.

It is important to mention that not all surveys fall into these two categories. The J-PAS survey [Ben+14], that has just started operating, can be thought of as a mixed model. It is photometric in nature, but with a number of filters large enough to allow for a very precise determination of redshift, which has been traditionally the main advantage of spectroscopic surveys. On the other hand, there are also alternatives to the traditional optic and near-infrared surveys. The SKA project [Maa+15] is a next-generation radio survey that will use the 21 cm emission of neutral hydrogen as a tracer.

¹²Once a cluster has been identified, it is possible to infer its mass either through the lensing effects that it produces or through a knowledge of its temperature. The temperature in its turn can be measured from its X-ray emission or from the SZ distortions produced in the CMB. See e.g. [Dod03] for details.

¹³‘Peculiar’ in this context means that the cosmological redshift produced by the expansion of the Universe has been subtracted. Interpreted as a velocity, the cosmological contribution is sometimes dubbed ‘Hubble flow’.

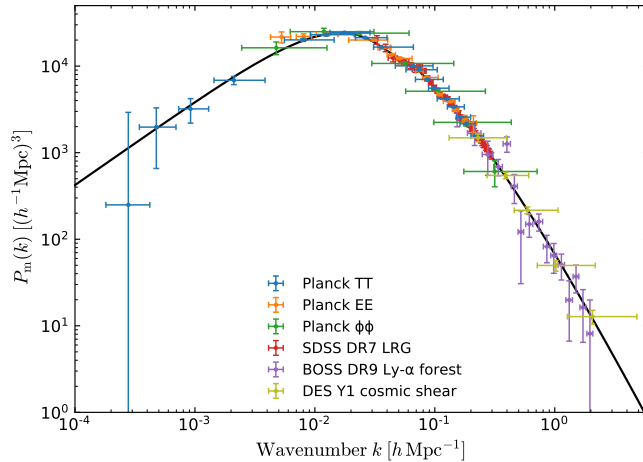


Figure 1.5: Compilation of different measurements of the matter power spectrum at $z = 0$. The BAO signal appears as wiggles around $k \sim 0.1 h \text{ Mpc}^{-1}$, but here it is hidden below the error bars. Credit: [Akr+18a].

1.2.2 Angular correlations

In a similar way to the definition of the temperature perturbation (1.3), one can define the matter overdensity as the fractional deviation from the homogeneous background density $\bar{\rho}_m$

$$\delta_m(t, \mathbf{x}) \equiv \frac{\rho_m(t, \mathbf{x}) - \bar{\rho}_m(t)}{\bar{\rho}_m(t)}, \quad (1.11)$$

It can be estimated from the observed *number* density of tracers [BD11]. Working in Fourier space, and omitting the time dependence, the *matter power spectrum* can be defined as

$$\langle \delta_m(\mathbf{k}) \delta_m^*(\mathbf{k}') \rangle \equiv (2\pi)^3 \delta(\mathbf{k} - \mathbf{k}') P_m(k). \quad (1.12)$$

The paramount objective of most LSS surveys is to measure $P_m(k)$. The most readily observable quantity is the closely related *correlation function* in real space

$$\xi(\mathbf{r}) \equiv \langle \delta(\mathbf{x}) \delta(\mathbf{x} + \mathbf{r}) \rangle = \int \frac{d^3k}{(2\pi)^3} e^{i\mathbf{k} \cdot \mathbf{r}} P_m(k). \quad (1.13)$$

As we mentioned before, these quantities also evolve in time (or redshift). Owing to their clean redshift determination, spectroscopic surveys can follow the evolution of the matter power spectrum back in time. Several measurements of the matter power spectrum (today) are collected in Figure 1.5. There is one feature in this curve that is worth noting: the baryon acoustic oscillations. These baryonic features appear as wiggles in $P_m(k)$ and correspond to the same acoustic oscillations imprinted in the CMB, but this time imprinted in the baryonic component, that represents a non-negligible fraction of the total matter content. This baryonic effect also appears, quite spectacularly, as a bump in the correlation function. The physical interpretation goes as follows. The initial density perturbations in the photon-baryon plasma propagated with a finite sound speed, that dropped to zero when baryons decoupled from photons. This means that, starting from an initial inhomogeneity, the density wave-fronts travelled a finite distance, also known as

sound horizon. This produced an enhanced probability of finding large overdensities separated by this characteristic distance. The sound horizon can be computed from first principles in a given cosmological model. It provides an absolute length scale (standard ruler) that can be used to probe the expansion of the Universe. See for instance [Akr+18a] for a collection of these measurements.

1.3 Galactic structure

Nowadays, the existence of a dark matter component, detected only gravitationally, belongs to the mainstream of cosmology. In the preceding sections we showed how the assumption that most of the matter exists in the form of a non-baryonic, cold dark matter component can explain all cosmological observations, ranging from clustering to CMB. Even though it has worked exceedingly well in cosmology, historically the dark matter hypothesis was proposed to explain the observed galactic structure. For the reader interested in the historical development of the paradigm, we recommend [Wei08] or the excellent review [BH18].

The rotation curves of galaxies are one of the observations that asks for a dark matter explanation. Using simple Newtonian dynamics it is possible to relate the circular velocity of an orbiting object with the mass enclosed in a spherical shell. If galaxies were only composed of baryonic matter, i.e. stars and gas that we observe, it would be impossible to explain the observed rotation curves. These curves tell us that there must be much more matter in a galaxy than what we can see (with electromagnetic signals). According to present knowledge, the galaxy disk lies at the center of a larger, extended structure: the dark matter halo.

The study of astrophysical structures is more involved than the cosmological observations in at least two aspects. First, it is more difficult to obtain clean observables. We usually need to deal with limited information on the astrophysical parameters and the observations are plagued with baryonic, i.e. gas, effects that need to be properly modelled. In the second place, while usually on cosmology we can rely on perturbation theory, the collapsed structures are in the fully non-linear regime. Numerical simulations are unavoidable in this field.

In the 90s, the first N -body simulations for CDM became available. These results allowed for the first quantitative studies on the expected halo properties. Based on several simulations, Navarro, Frenk and White (NFW) proposed the universal halo profile that bears their names [NFW97]

$$\rho_{\text{NFW}}(r) = \frac{\rho_0}{\frac{r}{R_s} \left(1 + \frac{r}{R_s}\right)^2}, \quad (1.14)$$

where the parameters ρ_0 and R_s vary from one halo to another. Even though there are other popular profiles, NFW is the leading phenomenological model to fit the results of N -body simulations with CDM.

Workers in the field quickly realized that there was a mismatch in the rotation curves inferred from simulated halos and the observed ones. The simulated halos invariably present dense and cuspy central regions ($\rho \propto r^{-\gamma}$ with $\gamma \simeq 0.8 - 1.4$) while core-like structures are preferred by observations ($\gamma \simeq 0 - 0.5$) [BB17]. This came to

be known as the *core-cusp problem* [FP94; Moo94; BB17]. It is one of the longest-standing discrepancies faced by the Λ CDM paradigm. This is not the only challenge for Λ CDM on galactic scales, see [BB17] for a comprehensive review of the small-scale problems.

There is an important caveat in the previous discussion: we are comparing CDM-only simulations with real galaxies that also contain *baryons*. Simulations with baryons are extremely expensive compared with CDM-only. It has been traditionally very difficult to achieve large volumes and high resolution, though recent progress has been made, e.g. the NIHAO [Wan+15; Tol+16] and FIRE [Hop+18] simulations. It seems feasible to obtain cores once we introduce baryonic effects, see [BB17], but the results depend on the model and parameters used to take into account the baryonic feedback, e.g. the effect of supernovae.

The next alternative that comes to mind is that maybe we have chosen the wrong dark matter model for the simulations. We know that we need something that resemble CDM on cosmological scales. This still leaves plenty of room for modifications that change the small-scale behaviour. There is a plethora of models that behave as CDM on a cosmological setting and yet yield unambiguously different predictions for small-scale observables [OS03]. Three broad classes of dark-matter models, that may solve in particular the core-cusp problem, have been proposed:

- *Warm dark matter*. Any thermal dark matter component is endowed with a characteristic free-streaming length, below which thermal motions prevent clustering and formation of structures. The free-streaming length depends on the mass and for CDM, i.e. very massive particles, it is effectively assumed to be zero. Warm dark matter consists of particles with masses in the range of the keV, so the effect of a finite mass is irrelevant for cosmology but affects structure formation at astrophysical scales. The original proposal is [BOT01] and some recent constraints can be found in [Irs+17].
- *Self-interacting dark matter*. Self-interaction between dark matter particles can produce an additional source of pressure and diminish clustering at small scales, whenever the densities are high and the additional pressure becomes important. See [CMH92; SS00] for some early works and [TY18] for a recent review.
- *Fuzzy dark matter*. If the dark matter is extremely light (and non-thermal), it may display a wavelike behaviour at small scales. This candidate will be analyzed in detail in Chapter 5.

These alternative models have the same cosmological behaviour but differ on smaller scales. If dark matter only interacts gravitationally, galactic-structure observations may be our best hope for discriminating between different models.

1.4 Stellar evolution

Stars have become one of the best laboratories to study light and weakly interacting particles. For instance, by using the observational evidence accumulated over

decades and the theoretical insight on the inner workings of different stellar objects, it has been possible to constrain many neutrino properties [Raf96]. The most spectacular among these results is probably the observation of neutrino oscillations, that started as a mismatch between the predicted solar flux and the one measured on Earth and ended up being an evidence of the neutrino masses. In addition to constraining properties of known particles, many astrophysical objects are sensitive to the presence of any new particle interacting with the plasma.

One of the main advantages of stars as laboratories is their size. Even a feebly interacting (light¹⁴) particle can be copiously produced and either modify the stellar evolution or lead to a flux that could be detected on Earth. Another advantage is that extreme conditions of temperature, density and magnetic fields, extremely challenging to reproduce in a laboratory, are naturally present in different types of stars.

In this work we will focus on low-mass particles, that can be thermally produced and perturb the star's life in a significant way. We leave aside for instance heavy-particle capture by stars, that could also modify its evolution (e.g. WIMP capture [JKG96]), and light-particle emission that, while leaving the Sun unperturbed, leads to a measurable flux on Earth (e.g. axion helioscopes [Red08]). According to its coupling strength, any new particle that is light enough to be thermally produced can have two effects on a star:

- *Energy loss.* If the particle interacts weakly enough, so that once produced it can freely escape, it acts as an energy sink and modifies different evolutionary time scales. It typically leads to a higher burning rate or to a faster cooling. In either case, the star shines for a shorter time. In some cases it can also increase some scales. For instance, as we will see, a delay of the helium ignition increases the time a low-mass star spends as a red giant.
- *Energy transfer.* If the particle gets trapped, it contributes to the energy transfer. Particles with large mean free paths (but smaller than the star's size) can transfer energy more efficiently than photons¹⁵, modifying the stellar structure.

We will only be concerned with the energy-loss argument in this work. It has been successfully applied for instance to hidden photons [DFK12; APP13], sterile neutrinos [Raf90a; ABK19] and especially to axions [KMW84; Raf86; PK86; Raf90b]. Before explaining the observational basis of the energy-loss argument for different objects, we will briefly review some basic concepts of stellar evolution.

Stars are self-gravitating systems. There are three sources of pressure that can support the star against gravitational collapse: thermal, radiation and degeneracy pressure. *Radiation pressure* ($P \propto T^4$) is only relevant for supermassive stars. Compact stars, like white dwarfs or neutron stars, are supported by the *degeneracy pressure* ($P \propto \text{const.}$). Once the density is high enough, the electron (or neutron) gas becomes degenerated, providing a temperature-independent pressure¹⁶. Any energy loss cools down the object, decreasing its temperature and its luminosity.

¹⁴Light enough to be thermally produced.

¹⁵Note that the mean free path of a photon in the Sun is about 2 cm.

¹⁶Once it reaches the zero-temperature limit, $k_B T \ll E_F$, where E_F is the Fermi energy of the gas.

Standard, i.e. nuclear-burning, stars are supported by the *thermal pressure* ($P \propto T$) of the gas. The simplest version of the virial theorem, for a monoatomic gas in hydrostatic equilibrium [Sch65], states that the thermal (E_T) and the gravitational (E_G) energy of a star are related

$$E_T = -\frac{1}{2}E_G . \quad (1.15)$$

This simple relation can help us to understand the stellar evolution. If these are the only energy sources, the total energy is

$$E_{\text{total}} = E_T + E_G = \frac{1}{2}E_G = -E_T . \quad (1.16)$$

This means that a star that is radiating (losing energy) must contract ($E_G \propto R^{-1}$) and increase its temperature ($E_T \propto T$). In general, energy loss in thermally supported stars leads to an increase of their temperature. This treatment is valid for a contracting gas cloud but, once the temperature is high enough, the nuclear fuel is ignited, acting as a new source of internal energy. The equilibrium configuration is reached when the energy losses are perfectly balanced by the energy produced. If the energy produced is less than the energy emitted, as we have seen, the star contracts. The contraction increases the temperature and hence the energy produced in nuclear reactions also increases. The same logic applies in the opposite situation. This regulation mechanism accounts for the stability of stars.

Once the nuclear fuel is used up, the star contracts again until either it reaches the degeneracy point of the gas or it is hot enough to burn heavier elements. For a full account of a star's life see [Raf96; Sch65; CG68].

At each point of the star, energy conservation requires

$$\frac{dL_r}{dr} = 4\pi r^2 \rho \epsilon , \quad \epsilon = \epsilon_{\text{nuc}} + \epsilon_{\text{grav}} - \epsilon_{\nu} - \epsilon_x , \quad (1.17)$$

where L_r is the luminosity and ϵ is the emissivity. The impact of a new particle is accounted for in ϵ_x , the energy loss rate per unit of mass. This quantity can be computed from first principles once we know how the hypothetical particle interacts with the plasma. From the observational point of view, we will describe now how this new term modifies relevant evolutionary time scales in three very different objects: Sun, red giants and the supernova SN1987A.

1.4.1 Sun

The effect of a novel channel of energy loss in degenerate stars (white dwarfs or neutron stars) is straightforward: it increases the cooling rate. However, in a main sequence star, the nuclear production (ϵ_{nuc}) is readjusted to compensate additional energy losses. While the Sun is very well understood and seems the most promising candidate to apply the energy-loss argument, it is not obvious what observational effects can be expected. Frieman, Dimopoulos and Turner [FDT87] were able to

This does not mean that the star is “cold”, according to the common use of the word, e.g. the central temperature of a neutron star is $\sim 10^9$ K.

tackle this problem in a semianalytic fashion assuming that the new equilibrium configuration (with ϵ_x) is obtained as a homologous contraction¹⁷.

The main conclusion is that an increased energy-loss rate produces modifications in the luminosity and the radius of the star, thus changing its lifetime. If the Sun were emitting more light particles, it would burn its nuclear fuel faster and shine brighter. However, it is important to notice that these quantities are not directly observed. Solar models are actually fitted to achieve the observed luminosity, e.g. changing the amount of helium. We can obtain bounds on the efficiency of particle production either by imposing that the solar age is not significantly modified or that the initial helium fraction has at least the primordial value. Both criteria agree to yield a bound [Raf96]

$$L_x < L_\odot \quad \rightarrow \quad \epsilon_x < \epsilon_\odot, \quad (1.18)$$

where $\epsilon_\odot = 1 \text{ erg g}^{-1} \text{ s}^{-1}$ is the standard emissivity in the Sun and ϵ_x is the emissivity due to the new type of particle. The theoretical luminosities must be evaluated under the conditions of the solar core

$$\begin{aligned} \rho &= 156 \text{ g cm}^{-3}, & n_e &= 6.3 \times 10^{25} \text{ cm}^{-3}, \\ T &= 1.3 \text{ keV}, & X &= 0.35, \end{aligned} \quad (1.19)$$

where ρ is the density in the solar core, n_e the number density of electrons, T the temperature and X the mass fraction of hydrogen. The numerical values in this section come either from [Raf96] or [Raf90a].

1.4.2 Red giants

After depleting the hydrogen in the center, low-mass stars ($M \lesssim 2M_\odot$) develop a degenerate, inert, helium core and ascend along the red giant branch (RGB). The evolutionary track of these stars is represented in Figure 1.6. For a complete, pedagogical account of this fascinating process see [Raf96]. In these red giants, the region surrounding the helium core is still burning hydrogen and then depositing more helium into the core. The core keeps accreting material and contracts, increasing its temperature. At some point it reaches a temperature high enough to ignite helium, the so-called helium flash, and the star moves to the horizontal branch (HB).

Additional energy losses would lead to a cooling of the degenerate core. In this case, the ignition of helium is delayed, and could be prevented in an extreme case.

¹⁷For a detailed discussion see the chapter 22 of [CG68]. In simple terms, two stars are said to be homologous if they are related only by a scale transformation of its parameters. The simplest example is the following: If the configuration at the point r of one star can be computed from the configuration of a different star at the point r_0 as

$$r = \frac{R}{R_0} r_0,$$

where R and R_0 are the radii of the two stars, these two stars are said to be homologous. In general, more parameters may need to be scaled.

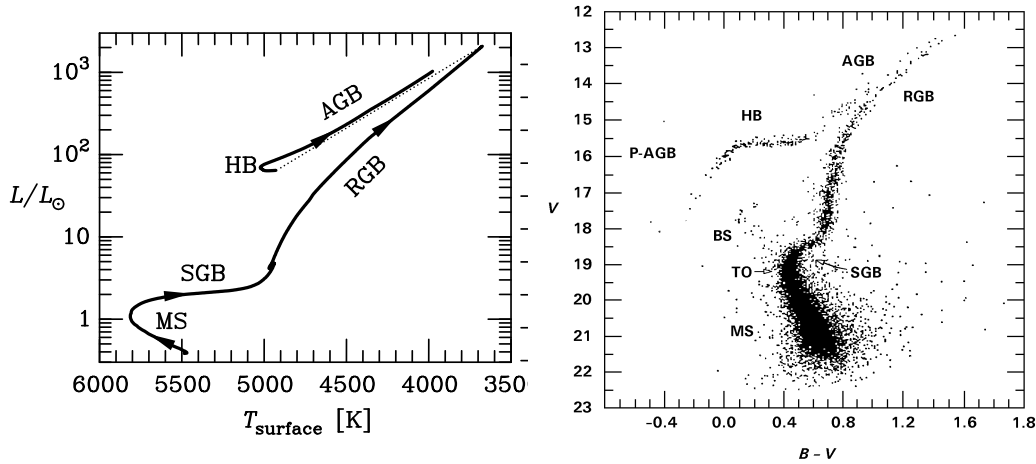


Figure 1.6: (Left) Evolutionary track of a low-mass star ($M \lesssim 2M_{\odot}$) in the temperature-luminosity diagram. The star starts its evolution in the main sequence (MS), where it spends most of its life. Then, as it exhausts the hydrogen in the core, it ascends along the subgiant branch (SGB) and the red giant branch (RGB). After the helium flash, it moves to the horizontal branch (HB) and finally it ascends again along the asymptotic giant branch (AGB). (Right) Hertzsprung-Russell diagram of the globular cluster M3. Credit: (Left) [Raf96], (Right) [Raf99].

Different observables can be found studying the Hertzsprung-Russell diagrams¹⁸ of globular clusters, like Figure 1.6, and performing statistics with the stellar population, e.g. the brightness of the RGB tip or the ratio of HB/RGB stars. More details can be found in [Raf90a; Raf96]. A simple analytical bound for new energy losses is

$$\epsilon_x < 10 \text{ erg g}^{-1} \text{ s}^{-1}, \quad (1.20)$$

to be evaluated at average conditions for the core of a red giant near the helium flash

$$\begin{aligned} \rho &= 2 \times 10^5 \text{ g cm}^{-3}, & n_e &= 6 \times 10^{28} \text{ cm}^{-3}, \\ T &= 8.6 \text{ keV}, & Y_e &= 0.5, \end{aligned} \quad (1.21)$$

where Y_e is the inverse of the mean molecular weight for the electrons, such that $n_e = Y_e \rho / m_u$ where m_u is the atomic mass unit.

1.4.3 Supernova SN1987A

The energy-loss argument for the supernova (SN) case is a bit different. When a neutron star is born, during the core collapse in a type II supernova, a huge amount of energy is emitted in the form of neutrinos. In fact, the neutrino emission ($\sim 10^{53}$ erg) dominates over the radiation and kinetic energy ($\sim 10^{51}$ erg). Most of the neutrino signal is emitted as a pulse during the first second, see Figure 1.7. Afterwards, see the tail in Figure 1.7, neutrinos are the main cooling mechanism of the nascent neutron star.

¹⁸Each dot in the Hertzsprung-Russell diagram represents a star, classified according to its luminosity and temperature.

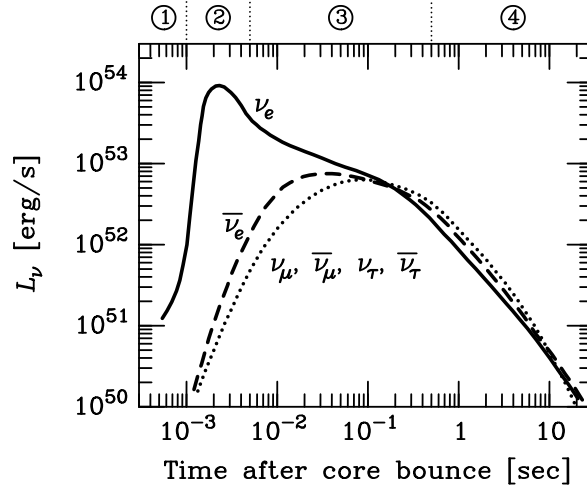


Figure 1.7: Neutrino emission from a type II supernova. The region 4 represents the cooling of the nascent neutron star. Credit: [Raf96].

The basic theoretical picture was confirmed in 1987 when the neutrino signal of the SN1987A event was measured in different observatories. Not only was the initial pulse measured, but also the tail of the emission, with neutrinos received several seconds after the pulse. If any additional cooling mechanism was at work, at least it could not be much more efficient than neutrinos. Raffelt [Raf90a; Raf96], based on numerical simulations of supernova evolution, proposes the following criterion

$$\epsilon_x < 10^{19} \text{ erg g}^{-1} \text{ s}^{-1}, \quad (1.22)$$

where it is assumed that the particles escape freely and the energy-loss rate is to be evaluated under conditions

$$\rho = 8 \times 10^{14} \text{ g cm}^{-3}, \quad T \sim (40 - 60) \text{ MeV}. \quad (1.23)$$

1.5 Fifth-force tests

The inverse-square law (ISL) for gravity has been, since its inception in the XVII century, extremely successful at describing gravitational phenomena over a wide range of scales. The Newtonian force between two bodies can be derived from the interaction potential

$$V(r) = -\frac{Gm_1m_2}{r}. \quad (1.24)$$

A remarkable property of this interaction is that it gives rise to *closed* orbits (ellipses, in particular). Of course, the planets in the Solar System do not undergo perfectly elliptical motions around the Sun. The interactions between different planets, given again by (1.24), perturb the orbits introducing, in general, precession effects: the orbits fail to close. This is a generic feature of any small perturbation of (1.24). The observation of anomalous effects on the orbit of Uranus, along with the firm belief that (1.24) was correct, led to the prediction of the existence of the planet Neptune. The persisting anomalous precession of Mercury, on the other hand, was

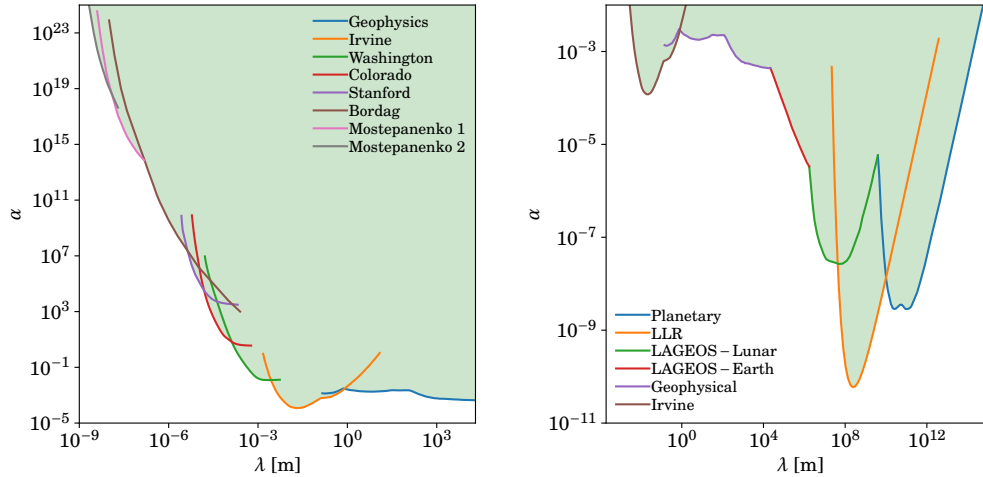


Figure 1.8: Constraints on deviations from the inverse-square law, from laboratory (Left) and Solar System (Right) tests. The curves have been adapted from the following references: planetary, LLR, LAGEOS-Lunar, LAGEOS-Earth, geophysics [AHN03], Irvine [Hos+85], Washington, Colorado [Lon+03], Stanford [Chi+03], Bordag [BMM01], Mostepanenko 1 and 2 [MN01].

the first observational hint of deviations from (1.24), which could be eventually explained within General Relativity.

From the particle-physics perspective, the interaction (1.24) could arise from the exchange of a massless, even spin (0 or 2) boson. The carrier of the force in Einstein gravity is the graviton, a massless spin-2 particle. A similar potential can be obtained for a massive boson mediator

$$V(r) = \frac{\kappa}{r} e^{-mr}, \quad (1.25)$$

where κ is a generic coupling and m is the mass of the carrier. The potential (1.25) is known as Yukawa potential. More exotic possibilities, like the force arising from the exchange of two neutrinos, are reviewed in [FT99]. Clearly, if the carrier is heavy enough its effects on the force are negligible but light mediators can lead to observable deviations from the ISL.

Over the last decades there has been an ongoing effort to measure possible deviations from the inverse-square law, without success so far. As a result of this effort, there exists a wealth of experimental data, ranging from microscopic to Solar System scales, that can be used to put stringent bounds on the parameter space of any light mediator. The interaction potential for ISL tests is traditionally parameterized as

$$V(r) = -\frac{Gm_1m_2}{r} \left(1 + \alpha e^{-r/\lambda}\right). \quad (1.26)$$

The relevant bounds for laboratory and Solar System constraints are shown in Figure 1.8. We will now briefly summarize the content of the experiments quoted and refer the reader to the original references and topical reviews [AHN03; Ade+09] for further details.

- I) *Planetary* ($10^9 - 10^{13}$ m). One of the effects produced by a modification of the ISL over Solar System scales is an anomalous precession of planetary orbits.

This fact was used in [Tal+88] to set bounds on possible modifications of Newtonian gravity, analyzing the orbits of Mercury and Mars.

- II) *Earth-LAGEOS-Moon* ($10^5 - 10^{10}$ m). The first curve (LLR) corresponds to a measure of the anomalous precession of the Moon, which is the same effect as in the previous point. The other two correspond to measurements of the spatial variation of G , based on the orbits of the Moon and the LAGEOS satellite (in an orbit of about 1.2×10^7 m). More details can be found in [De 86].
- III) *Geophysical* ($1 - 10^4$ m). There are several experiments halfway between Solar-System and laboratory scales, which aim to measure spatial variations of G within the Earth. These include measurements in towers, seas, mines and are reviewed in [Sta+87].
- IV) *Cavendish* ($10 \mu\text{m} - 1 \text{cm}$). In this range lie the laboratory probes of the force of gravity with torsion balances. For a review, see [AHN03].
- V) *Casimir* ($1 \text{nm} - 10 \mu\text{m}$). Although experimentally challenging, it is possible to measure the Casimir force between two bodies, e.g. using atomic-force microscopes. As reviewed in [MN01], these measurements can be used to constrain the existence of a new force.

Recent observations of the orbit of the S0-2 star in the Galactic Center have allowed to test the Newtonian law at even larger scales [Hee+17], but the constraints are not competitive yet with the ones already displayed. On the opposite end, neutron scattering experiments are starting to probe ISL deviations at shorter distances than Casimir experiments [BFP18; Saf+18; Had+18].

2

Components of the Universe

The mathematical description of a cosmological model requires defining a matter content, i.e. an energy-momentum tensor, and then solving the Einstein equations (1) for this matter content. Usually, this energy-momentum tensor arises as the combination of different species. In this chapter we cover three different ways to describe the components of the Universe: as fluids (Section 2.1), as fields (Section 2.2) or using kinetic theory (Section 2.3).

2.1 Fluid description

The word fluid is widely used in cosmology to denote any component that sources the right-hand side of the Einstein equations. Even though we may also indulge in this practice, in this section we will try to clarify what we regard as a proper *fluid description*. A fluid is commonly understood as a coarse-grained picture of a collection of particles. The state of the fluid is characterized by a set of macroscopic variables, e.g. density and velocity, that vary smoothly over space-time. Using simple physical arguments, e.g. see [Wei72], it is possible to define an energy-momentum tensor that codifies the energy and momentum fluxes of the fluid. More details on the construction and its physical motivation can be found in the classic references [LL59] and [Wei72].

In practice, a fluid description takes the energy-momentum tensor as the starting point¹. The density and the velocity are the main dynamical variables in this approach. The next section will introduce the fluid variables for a generic energy-momentum tensor. Section 2.1.2 particularize the results to perfect fluids, that are the simplest description for a cosmological component.

2.1.1 Energy-momentum tensor

The total energy-momentum tensor on the right-hand side of the Einstein equations (1) can be endowed with a hydrodynamic interpretation. Following the 1+3 covariant treatment of [EE99], we choose a normalized timelike vector u^μ ($u^\mu u_\mu = -1$) and define the associated projector² on the subspace transverse to u^μ

$$\mathcal{P}^\mu{}_\nu \equiv \delta^\mu{}_\nu + u^\mu u_\nu . \quad (2.1)$$

Any symmetric tensor field can be decomposed relative to u^μ

$$T_{\mu\nu} \equiv \rho u_\mu u_\nu + 2q_{(\mu} u_{\nu)} + P \mathcal{P}_{\mu\nu} + \Pi_{\mu\nu} , \quad (2.2)$$

¹It may be supplemented with other four-vectors, like the entropy or number fluxes.

²It satisfies $\mathcal{P}^\mu{}_\nu u^\nu = 0$ and $\mathcal{P}^\mu{}_\sigma \mathcal{P}^\sigma{}_\nu = \mathcal{P}^\mu{}_\nu$.

where q_μ is transverse ($q^\mu u_\mu = 0$) and $\Pi_{\mu\nu}$ is transverse ($\Pi_{\mu\nu} u^\mu = 0$) and traceless ($\Pi^\mu{}_\mu = 0$). These variables can be defined in terms of the energy-momentum tensor and physically interpreted

$$\rho = u^\mu u^\nu T_{\mu\nu} , \quad (\text{Energy density}) \quad (2.3a)$$

$$P = \frac{1}{3} T_{\mu\nu} \mathcal{P}^{\mu\nu} , \quad (\text{Pressure}) \quad (2.3b)$$

$$q^\mu = -T_{\nu\rho} \mathcal{P}^{\mu\nu} u^\rho , \quad (\text{Momentum density}) \quad (2.3c)$$

$$\Pi_{\mu\nu} = \left(\mathcal{P}^\rho{}_\mu \mathcal{P}^\sigma{}_\nu - \frac{1}{3} \mathcal{P}_{\mu\nu} \mathcal{P}^{\rho\sigma} \right) T_{\rho\sigma} , \quad (\text{Anisotropic stress}) \quad (2.3d)$$

The vector u^μ can be for instance the four-velocity of an observer at rest ($u^i = 0$). In this case we get $q^i \propto T^i{}_0$ and it is possible to define the velocity of the (imperfect) fluid as the velocity of the frame in which $q^i = 0$, i.e. as the velocity of energy transport.

The total energy-momentum tensor satisfies the conservation equation³

$$\nabla_\mu T^\mu{}_\nu = 0 . \quad (2.4)$$

In general, for a multicomponent system, the individual fluids do not satisfy (2.4)

$$T^\mu{}_\nu = T_{(1)}^\mu{}_\nu + T_{(2)}^\mu{}_\nu \quad \rightarrow \quad \nabla_\mu T_{(1)}^\mu{}_\nu = -\nabla_\mu T_{(2)}^\mu{}_\nu . \quad (2.5)$$

The transfer of energy and momentum between two subsystems is characterized by a four-vector

$$\nabla_\mu T_{(1)}^\mu{}_\nu = S_\nu , \quad (2.6a)$$

$$\nabla_\mu T_{(2)}^\mu{}_\nu = -S_\nu . \quad (2.6b)$$

It is very common to have additional conserved quantities, like the number of particles or the electric charge. These quantities can be represented by a four-vector current satisfying a conservation law⁴

$$\nabla_\mu N^\mu = 0 . \quad (2.7)$$

In the presence of conserved charges it is possible to define the velocity of the fluid as the velocity of the frame in which $N^i = 0$. Except in some limiting cases, this velocity *does not* coincide with the velocity of energy transport.

2.1.2 Perfect fluids

Perfect fluids are defined by the further physical requirement

$$q^\mu = 0 , \quad \Pi_{\mu\nu} = 0 . \quad (2.8)$$

³Using the Gauss law, this equation implies the conservation of a four-vector (the four-momentum in this case).

⁴Again, this kind of equation implies the conservation of a scalar, e.g. baryonic number or electric charge.

The energy-momentum tensor for a perfect fluid is

$$T_{\mu\nu} = (\rho + P)u_\mu u_\nu + P g_{\mu\nu} . \quad (2.9)$$

Since $q^\mu = 0$, the u^μ that defines this splitting can be regarded as the velocity of the fluid. The description of the fluid must be supplemented with a prescription to compute P . This prescription is parameterized in terms of the *equation of state*

$$w \equiv \frac{P}{\rho} . \quad (2.10)$$

In cosmology, it is common to choose phenomenological equations of state that provide an effective description for the problem at hand. The evolution of a collisionless perfect fluid is described by (2.4), that can be splitted into

$$u^\mu \nabla_\mu \rho + (\rho + P) \nabla^\mu u_\mu = 0 , \quad (2.11a)$$

$$(\rho + P) u^\mu \nabla_\mu u^\nu + (g^{\mu\nu} + u^\mu u^\nu) \nabla_\mu P = 0 . \quad (2.11b)$$

In the appropriate limits, these expressions reproduce the continuity and Euler equations of Newtonian fluid mechanics.

The perfect fluid approach is a good starting point for a more detailed description. The next level of complexity is to consider nearly-perfect fluids, introducing small perturbations δq^μ and $\delta \Pi_{\mu\nu}$. The density, pressure and the metric are perturbed accordingly. The perturbed energy-momentum tensor is

$$\delta T_{\mu\nu} = (\delta \rho + \delta P) u_\mu u_\nu + \delta P g_{\mu\nu} + P \delta g_{\mu\nu} + 2\delta q_{(\mu} u_{\nu)} + \delta \Pi_{\mu\nu} . \quad (2.12)$$

It must be used now to source the perturbed version of the Einstein tensor. It is customary to trade the momentum perturbation for a velocity perturbation

$$\delta q^\mu = (\rho + P) \delta u^\mu . \quad (2.13)$$

When dealing with perturbed perfect fluids, the analog of the equation of state is the *sound speed*

$$c_s^2 \equiv \frac{\delta P}{\delta \rho} . \quad (2.14)$$

Closely related is the *adiabatic sound speed*

$$c_{\text{ad}}^2 \equiv \frac{\dot{P}}{\dot{\rho}} . \quad (2.15)$$

2.2 Field description

A classical field can be regarded as a smooth function over the space-time. It can be characterized through its behaviour under different types of transformations, e.g. parity or Lorentz transformations. The metric tensor $g_{\mu\nu}$ in the Einstein equations is an example of a classical field.

2.2.1 Energy-momentum tensor

The field description takes the *action* functional as the starting point. It is defined in terms of the Lagrangian. In flat space-time it can be schematically written as

$$S_M^{\text{flat}}[\psi] = \int d^4x \mathcal{L}(\psi(x), \partial\psi(x); \eta_{\mu\nu}), \quad (2.16)$$

where ψ is a generic field and $\eta_{\mu\nu}$ is the Minkowski metric. There is a well-known *minimal coupling* procedure to promote an action from flat to curved space-time, see [Wal10]. The action in curved space-time is⁵

$$S_M[\psi] = \int d^4x \sqrt{-g} \mathcal{L}(\psi(x), \nabla\psi(x); g_{\mu\nu}(x)), \quad (2.17)$$

where g is the determinant of the metric $g_{\mu\nu}$ and ∇ is the covariant derivative. The equations of motion of the field are obtained through the functional derivative

$$\frac{\delta S_M}{\delta \psi} = 0. \quad (2.18)$$

If the field is interacting, the functional derivative must be taken with the total action. The interaction of this matter field with gravity is described by the action

$$S[\psi, g^{\mu\nu}] = S_G[g^{\mu\nu}] + S_M[\psi, g^{\mu\nu}]. \quad (2.19)$$

The gravitational part is described by the Einstein-Hilbert action

$$S_G[g^{\mu\nu}] = \frac{1}{16\pi G} \int d^4x \sqrt{-g} R, \quad (2.20)$$

with functional derivative

$$\frac{\delta S_G}{\delta g^{\mu\nu}} = \frac{\sqrt{-g}}{16\pi G} \left(R_{\mu\nu} - \frac{1}{2} g_{\mu\nu} R \right). \quad (2.21)$$

Varying the total action we obtain the Einstein equations (1)

$$\frac{\delta S}{\delta g^{\mu\nu}} = 0 \quad \rightarrow \quad R_{\mu\nu} - \frac{1}{2} g_{\mu\nu} R = -\frac{16\pi G}{\sqrt{-g}} \frac{\delta S_M}{\delta g^{\mu\nu}} = 8\pi G T_{\mu\nu}. \quad (2.22)$$

In this way we can define the energy-momentum tensor of the field

$$T_{\mu\nu} \equiv -\frac{2}{\sqrt{-g}} \frac{\delta S_M}{\delta g^{\mu\nu}}. \quad (2.23)$$

Using the results of the previous Section 2.2, it is possible to establish a fluid analogy and define the density, momentum, pressure and anisotropic stress of a field.

⁵This assignment may be ambiguous though. One can always add terms proportional to R that vanish in flat space-time, see [Wal10].

2.2.2 Scalar field

The Lagrangian for a free scalar field in flat space-time is

$$\mathcal{L}_\phi^{\text{flat}} = -\frac{1}{2}\eta^{\mu\nu}\partial_\mu\phi\partial_\nu\phi - \frac{1}{2}m^2\phi^2. \quad (2.24)$$

We can promote it to curved space-time

$$\mathcal{L}_\phi = -\frac{1}{2}g^{\mu\nu}\nabla_\mu\phi\nabla_\nu\phi - \frac{1}{2}m^2\phi^2. \quad (2.25)$$

Remember that for scalar fields $\nabla_\mu\phi = \partial_\mu\phi$. The action is

$$S_\phi = -\frac{1}{2}\int d^4x\sqrt{-g}(\nabla^\mu\phi\nabla_\mu\phi + m^2\phi^2). \quad (2.26)$$

Performing a general variation⁶

$$\begin{aligned} \delta S_\phi = -\frac{1}{2}\int d^4x\sqrt{-g}\left\{\left(\nabla_\mu\phi\nabla_\nu\phi - \frac{1}{2}g_{\mu\nu}(\nabla^\sigma\phi\nabla_\sigma\phi + m^2\phi^2)\right)\delta g^{\mu\nu}\right. \\ \left.+ 2(-\nabla^\mu\nabla_\mu\phi + m^2\phi)\delta\phi\right\}. \end{aligned} \quad (2.27)$$

If the scalar field is not directly coupled to any other particle, the equations of motion are

$$\frac{\delta S_\phi}{\delta\phi} = 0 \quad \rightarrow \quad -\nabla^\mu\nabla_\mu\phi + m^2\phi = 0. \quad (2.28)$$

Sometimes it is useful to rewrite the equations of motion as

$$-\frac{1}{\sqrt{-g}}\partial_\mu(\sqrt{-g}\partial^\mu\phi) + m^2\phi = 0. \quad (2.29)$$

The energy-momentum tensor, defined in (2.23), is

$$T_{\mu\nu} = \nabla_\mu\phi\nabla_\nu\phi - \frac{1}{2}g_{\mu\nu}(\nabla^\sigma\phi\nabla_\sigma\phi + m^2\phi^2). \quad (2.30)$$

2.2.3 Vector field

The Lagrangian for the scalar field is so simple that we wrote it right away. When the fields possess more structure we must motivate our choice. In general, we will look for the most general⁷ Lagrangian quadratic in the field and its first derivatives and that is free from instabilities. Our main concern will be the presence of ghost instabilities that may arise when considering general kinetic terms, see [Sbi15; Woo15]. We illustrate this procedure in this section applying it to a vector field, following the exposition of [Rha14].

⁶We have integrated by parts too, assuming that the boundary terms vanish. We also need the result

$$\frac{\delta\sqrt{-g}}{\delta g^{\mu\nu}} = -\frac{1}{2}\sqrt{-g}g_{\mu\nu}.$$

⁷Most general respecting Lorentz invariance, or any other symmetry that we want to enforce.

Let us start with the most general kinetic term for a vector field A^μ

$$\mathcal{L}_{\text{kin}}^{\text{flat}} = a_1 \partial_\mu A^\nu \partial^\mu A_\nu + a_2 \partial_\mu A^\mu \partial_\nu A^\nu + a_3 \partial_\mu A^\nu \partial_\nu A^\mu . \quad (2.31)$$

The last two terms are equivalent upon integration by parts, so without loss of generality one can write

$$\mathcal{L}_{\text{kin}}^{\text{flat}} = a_1 \partial_\mu A^\nu \partial^\mu A_\nu + a_2 \partial_\mu A^\mu \partial_\nu A^\nu . \quad (2.32)$$

Note that from now on the equality between Lagrangians is meant to be equality modulo integration by parts. The field can be splitted into a transverse and a longitudinal part

$$A_\mu \equiv A_\mu^T + \partial_\mu \chi , \quad \partial_\mu A^{T\mu} = 0 . \quad (2.33)$$

Plugging this splitting in the Lagrangian

$$\begin{aligned} \mathcal{L}_{\text{kin}}^{\text{flat}} &= a_1 \partial_\mu A^{T\nu} \partial^\mu A_\nu^T + a_1 \partial_\mu \partial^\nu \chi \partial^\mu \partial_\nu \chi + a_2 \partial^\mu \partial_\mu \chi \partial^\nu \partial_\nu \chi \\ &= a_1 \partial_\mu A^{T\nu} \partial^\mu A_\nu^T + (a_1 + a_2) \square \chi \square \chi , \end{aligned} \quad (2.34)$$

where the d'Alembertian is $\square \equiv \eta^{\mu\nu} \partial_\nu \partial_\mu$. Unless $a_1 = -a_2$, higher-order time derivatives appear in the action, leading to an Ostrogradsky instability [Sbi15; Woo15]. There are different ways to see, e.g. [Rha14], that one of the two degrees of freedom⁸ hidden in χ is always a ghost, i.e. it carries a wrong sign in the kinetic term.

The normalization $a_1 = -1/2$ leads to the Maxwell Lagrangian

$$\mathcal{L}_{\text{kin}}^{\text{flat}} = -\frac{1}{2} (\partial_\mu A_\nu \partial^\mu A^\nu - \partial_\mu A^\nu \partial_\nu A^\mu) = -\frac{1}{4} F_{\mu\nu} F^{\mu\nu} , \quad (2.35)$$

with the conventional definition $F_{\mu\nu} \equiv \partial_\mu A_\nu - \partial_\nu A_\mu$. There is only one possibility for the mass term. Adding it, we arrive at the Proca Lagrangian

$$\mathcal{L}_A^{\text{flat}} = -\frac{1}{4} F_{\mu\nu} F^{\mu\nu} - \frac{1}{2} m^2 A^\mu A_\mu , \quad (2.36)$$

that describes the behaviour of a massive spin-1 particle. We can promote this Lagrangian to curved space-time

$$\mathcal{L}_A = -\frac{1}{4} F_{\mu\nu} F^{\mu\nu} - \frac{1}{2} m^2 A^\mu A_\mu . \quad (2.37)$$

The equations of motion are

$$\nabla_\nu F^{\nu\mu} - m^2 A^\mu = 0 . \quad (2.38)$$

The first term can be rewritten as

$$\nabla_\nu F^{\nu\mu} = \frac{1}{\sqrt{-g}} \partial_\nu (\sqrt{-g} F^{\nu\mu}) . \quad (2.39)$$

⁸It seems uncanny that a scalar possesses two degrees of freedom. The reason is very simple and stems from ordinary classical mechanics. The presence of accelerations in the action functional leads to a modification of the Euler-Lagrange equations. The equations of motion turn out to be *fourth* order, so we need four initial conditions to specify a solution, i.e. two degrees of freedom.

Two important properties of the strength tensor are

$$F_{\mu\nu} = 2\nabla_{[\mu}A_{\nu]} = 2\partial_{[\mu}A_{\nu]} , \quad (2.40)$$

$$\nabla_{[\mu}F_{\nu\sigma]} = \partial_{[\mu}F_{\nu\sigma]} = 0 . \quad (2.41)$$

Finally, the energy-momentum tensor is

$$T_{\mu\nu} = F_{\mu\sigma}F_{\nu}{}^{\sigma} - \frac{1}{4}g_{\mu\nu}F^{\rho\sigma}F_{\rho\sigma} + m^2A_{\mu}A_{\nu} . \quad (2.42)$$

The strength tensor $F_{\mu\nu}$ is the first antisymmetric tensor field we come across. A 1+3 decomposition similar to (2.2) can be defined for antisymmetric tensors. Choosing a timelike vector u^{μ} , we can split the strength tensor into an electric and magnetic parts [BMT07; EE99]

$$F_{\mu\nu} \equiv 2u_{[\mu}E_{\nu]} + \eta_{\mu\nu\sigma}B^{\sigma} , \quad (2.43)$$

where $\eta_{\mu\nu\sigma} \equiv \sqrt{-g}\varepsilon_{\mu\nu\sigma\rho}u^{\rho}$ and $\varepsilon_{\mu\nu\sigma\rho}$ is the Levi-Civita symbol. As usual, the electric and magnetic vectors are transverse ($E_{\mu}u^{\mu} = B_{\mu}u^{\mu} = 0$) and can be written in terms of the strength tensor

$$E_{\mu} = F_{\mu\nu}u^{\nu} , \quad (2.44a)$$

$$B_{\mu} = \frac{1}{2}\eta_{\mu\nu\sigma}F^{\nu\sigma} . \quad (2.44b)$$

In the massless case, i.e. Maxwell electromagnetism, the energy-momentum tensor can be rewritten in terms of these fields [BMT07]

$$T_{\mu\nu}^{(m=0)} = \frac{1}{2}(E^2 + B^2)u_{\mu}u_{\nu} + \frac{1}{6}(E^2 + B^2)\mathcal{P}_{\mu\nu} + 2S_{(\mu}u_{\nu)} + \Pi_{\mu\nu} , \quad (2.45)$$

where the Poynting vector and the stress tensor are

$$S_{\mu} \equiv \eta_{\mu\nu\sigma}E^{\nu}B^{\sigma} , \quad (2.46)$$

$$\Pi_{\mu\nu} \equiv \frac{1}{3}(E^2 + B^2)\mathcal{P}_{\mu\nu} - E_{\mu}E_{\nu} - B_{\mu}B_{\nu} . \quad (2.47)$$

Notice in particular that, in the fluid analogy, the equation of state of the fluid is

$$w = \frac{P}{\rho} = \frac{1}{3} , \quad (2.48)$$

and that we have $g^{\mu\nu}T_{\mu\nu}^{(m=0)} = 0$.

2.2.4 Tensor field

The programme that led us to the Proca Lagrangian for vector fields can be applied to tensor fields. We will restrict ourselves to symmetric tensor fields⁹. The most general kinetic term¹⁰ has four pieces

$$\mathcal{L}^{\text{flat}} = \frac{1}{2}\partial^{\alpha}h^{\mu\nu}(b_1\partial_{\alpha}h_{\mu\nu} + b_2\partial_{(\mu}h_{\nu)\alpha} + b_3\eta_{\mu\nu}\partial_{\alpha}h + 2b_4\eta_{\alpha(\mu}\partial_{\nu)}h) , \quad (2.49)$$

⁹The case for antisymmetric tensor fields is analyzed in [Van73]. The ghost-free Lagrangian that one would obtain is the square of the strength tensor for a two-form field.

¹⁰Up to total derivatives, that we neglect.

where $h \equiv \eta^{\mu\nu} h_{\mu\nu}$. The field can be splitted into a transverse tensor ($\partial^\mu h_{\mu\nu}^T = 0$) and a vector contribution

$$h_{\mu\nu} = h_{\mu\nu}^T + 2\partial_{(\mu}\chi_{\nu)}. \quad (2.50)$$

With this substitution, the kinetic term gives

$$\begin{aligned} \mathcal{L}_{\text{kin}}^{\text{flat}}(h_{\mu\nu}) &= \mathcal{L}_{\text{kin}}^{\text{flat}}(h_{\mu\nu}^T) + 2(b_3 + b_4)h^T \square \partial_\mu \chi^\mu + (b_1 + b_2)\chi^\mu \square^2 \chi_\mu \\ &\quad + (b_1 + 3b_2 + 2b_3 + 4b_4)\chi^\mu \square \partial_\mu \partial_\nu \chi^\nu. \end{aligned} \quad (2.51)$$

The absence of higher derivative terms imposes

$$b_4 = -b_3 = -b_2 = b_1. \quad (2.52)$$

Setting the normalization $b_1 = -1$, we finally obtain

$$\mathcal{L}^{\text{flat}} = -\frac{1}{2}\partial^\alpha h^{\mu\nu} (\partial_\alpha h_{\mu\nu} - 2\partial_{(\mu} h_{\nu)\alpha} - \eta_{\mu\nu} \partial_\alpha h + 2\eta_{\alpha(\mu} \partial_{\nu)} h). \quad (2.53)$$

This Lagrangian describes the evolution of a massless spin-2 particle. It is the same Lagrangian that would be obtained linearizing the Einstein-Hilbert Lagrangian (2.20) over Minkowski space-time. As a result of our choice for the parameters b_i , the Lagrangian is invariant under gauge transformations $h_{\mu\nu} \rightarrow h_{\mu\nu} + \partial_{(\mu} \xi_{\nu)}$. This is the linearized version of the diffeomorphism invariance in GR. Integrating by parts, the Lagrangian can be recast into

$$\mathcal{L}_{\text{kin}}^{\text{flat}} = \frac{1}{2}h^{\mu\nu} \mathcal{E}^{\alpha\beta}_{\mu\nu} h_{\alpha\beta}. \quad (2.54)$$

We have introduced the operator

$$\mathcal{E}^{\alpha\beta}_{\mu\nu} \equiv \left(\delta^\alpha_{(\mu} \delta^\beta_{\nu)} - \eta^{\alpha\beta} \eta_{\mu\nu} \right) \square - 2\delta^{(\alpha}_{(\mu} \partial_{\nu)} \partial^\beta) + \eta^{\alpha\beta} \partial_\mu \partial_\nu + \eta_{\mu\nu} \partial^\alpha \partial^\beta, \quad (2.55)$$

with the following properties.

- *Symmetries.*

$$\mathcal{E}_{\alpha\beta|\mu\nu} = \mathcal{E}_{\beta\alpha|\mu\nu} = \mathcal{E}_{\alpha\beta|\nu\mu} = \mathcal{E}_{\mu\nu|\alpha\beta}. \quad (2.56)$$

- *Action on a symmetric tensor.*

$$\mathcal{E}^{\alpha\beta}_{\mu\nu} h_{\alpha\beta} = \square h_{\mu\nu} - 2\partial^\alpha \partial_{(\mu} h_{\nu)\alpha} + \partial_\mu \partial_\nu h - \eta_{\mu\nu} \left(\square h - \partial_\alpha \partial_\beta h^{\alpha\beta} \right). \quad (2.57)$$

- *Contractions.*

$$\eta_{\alpha\beta} \mathcal{E}^{\alpha\beta}_{\mu\nu} = 2(\partial_\mu \partial_\nu - \eta_{\mu\nu} \square), \quad (2.58a)$$

$$\eta_{\alpha\beta} \eta^{\mu\nu} \mathcal{E}^{\alpha\beta}_{\mu\nu} = -6\square. \quad (2.58b)$$

Our next task is to find a suitable mass term. There are two possible contributions

$$\mathcal{L}_{\text{mass}}^{\text{flat}} = -\frac{1}{2}m^2 (h_{\mu\nu} h^{\mu\nu} - c h^2). \quad (2.59)$$

Splitting the degrees of freedom as in (2.50) we get

$$\mathcal{L}_{\text{mass}}^{\text{flat}} = -\frac{1}{2}m^2 \left(h_{\mu\nu}^T h^{T\mu\nu} - c h^{T2} \right) - m^2 \left(\partial^\mu \chi^\nu \partial_\mu \chi_\nu + (1-2c) \partial_\mu \chi^\mu \partial_\nu \chi^\nu \right). \quad (2.60)$$

From the discussion in the previous section we learnt that the avoidance of instabilities in the vector field Lagrangian requires $c = 1$. Joining the kinetic and the mass term we arrive at the Fierz-Pauli Lagrangian

$$\mathcal{L}_h^{\text{flat}} = -\frac{1}{2} \partial^\alpha h^{\mu\nu} \left(\partial_\alpha h_{\mu\nu} - 2 \partial_{(\mu} h_{\nu)\alpha} - \eta_{\mu\nu} \partial_\alpha h + 2 \eta_{\alpha(\mu} \partial_{\nu)} h \right) - \frac{1}{2} m^2 \left(h_{\mu\nu} h^{\mu\nu} - h^2 \right), \quad (2.61)$$

that describes a massive spin-2 particle. It can be succinctly rewritten as

$$\mathcal{L}_h^{\text{flat}} = \frac{1}{2} h^{\mu\nu} \mathcal{O}^{\alpha\beta}_{\mu\nu} h_{\alpha\beta}, \quad (2.62)$$

where

$$\mathcal{O}^{\alpha\beta}_{\mu\nu} \equiv \left(\delta^\alpha_{(\mu} \delta^\beta_{\nu)} - \eta^{\alpha\beta} \eta_{\mu\nu} \right) (\square - m^2) - 2 \delta^\alpha_{(\mu} \partial_{\nu)} \partial^\beta + \eta^{\alpha\beta} \partial_\mu \partial_\nu + \eta_{\mu\nu} \partial^\alpha \partial^\beta. \quad (2.63)$$

It shares the properties of \mathcal{E} , with the trivial substitution $\square \rightarrow \square - m^2$. The study of a massive spin-2 particle in curved space-time is more complex than for lower spins, especially when we couple it to matter [Hin12; Rha14; SS16; Hei19]. In this work we will not be concerned with these subtle issues and we will restrict ourselves to flat space-time. The equations of motion that can be derived from (2.62) are

$$\mathcal{O}^{\mu\nu}_{\alpha\beta} h^{\alpha\beta} = 0, \quad (2.64)$$

which after a few manipulations can be cast in the form

$$(\square - m^2) h_{\mu\nu} = 0, \quad (2.65a)$$

$$\partial^\mu h_{\mu\nu} = 0, \quad (2.65b)$$

$$h = 0. \quad (2.65c)$$

This is the usual Klein-Gordon equation for a symmetric (10 degrees of freedom), transverse (-4), traceless (-1) tensor field, describing a total of 5 propagating degrees of freedom. This naive count is supported by a full Hamiltonian analysis [Hin12].

2.3 Kinetic description

Kinetic theory generalizes the fluid description to situations where the particles that constitute the fluid have very large mean free paths. It also allows to make a connection between the microphysics of the collisions in the fluid and its macroscopic behaviour. The starting point in Newtonian kinetic theory is the *distribution function*, that expresses the probability that a cell in phase space is occupied by a particle. Using this distribution function one can define the usual energy-momentum density of the fluid. In a general relativistic context, we must first define carefully both the phase space and the volume element. We address this questions in Sections 2.3.1 and 2.3.2. In Section 2.3.3 we move on to the definition of the

distribution function in GR. Section 2.3.4 discusses the underlying assumptions in the Boltzmann equation, that describes the evolution of the distribution function, and in Section 2.3.5 we make the connection with the usual Boltzmann equation in special relativity. Finally, in Section 2.3.6 we write the energy-momentum tensor in terms of the distribution function. The presentation in this section follows mainly [Ehl73] and [Ste71]. For a cosmology-oriented introduction to kinetic theory in curved space-time see [Ber88] and [Dur08].

2.3.1 Phase space

Let us start with a curved space-time $(\mathcal{M}, g_{\mu\nu})$. The free motion of a test particle can be described, in terms of an affine parameter σ , by the Lagrangian

$$\mathcal{L}\left(x^\mu, \frac{dx^\mu}{d\sigma}\right) = \frac{1}{2} g_{\mu\nu}(x) \frac{dx^\mu}{d\sigma} \frac{dx^\nu}{d\sigma}. \quad (2.66)$$

The conjugate momenta are

$$P_\mu = \frac{\partial \mathcal{L}}{\partial \left(\frac{dx^\mu}{d\sigma}\right)} = g_{\mu\nu}(x) \frac{dx^\nu}{d\sigma}, \quad (2.67)$$

and the Hamiltonian is defined as

$$H(x^\mu, P_\nu) = \frac{1}{2} g^{\mu\nu}(x) P_\mu P_\nu. \quad (2.68)$$

All the possible states of a particle comprise the one-particle phase-space. Mathematically, the momentum P_μ belongs to the cotangent space $T_x^*(\mathcal{M})$ and all the pairs (x^μ, P_ν) form the cotangent bundle $T^*(\mathcal{M})$ ¹¹. The one-particle phase-space \mathcal{P} (abbreviated as phase-space) is a subset of the cotangent bundle

$$\mathcal{P} \equiv \left\{ (x, P) \in T^*(\mathcal{M}) \mid P_\mu P^\mu \leq 0, P_0 < 0 \right\}. \quad (2.69)$$

i.e. states of particles that follow time-like or light-like future-directed trajectories. As usual in analytical mechanics [JS+98], we can define the vector field associated with the phase flow

$$\begin{aligned} L &\equiv \frac{dx^\mu}{d\sigma} \frac{\partial}{\partial x^\mu} + \frac{dP_\mu}{d\sigma} \frac{\partial}{\partial P_\mu} \\ &= \frac{\partial H}{\partial P_\mu} \frac{\partial}{\partial x^\mu} - \frac{\partial H}{\partial x^\mu} \frac{\partial}{\partial P_\mu}. \end{aligned} \quad (2.70)$$

We will refer to L as the Liouville operator. The Lie derivative \mathcal{L}_L can then be used to compute the rate of change of any tensor field in \mathcal{P} along the integral curves of L , i.e. the physical trajectories of particles. In particular, for the Hamiltonian we have

$$\mathcal{L}_L H = L(H) = 0. \quad (2.71)$$

¹¹Note that the metric structure allows us to establish a correspondence between $P_\mu \in T_x^*(\mathcal{M})$ and elements of the tangent space $P^\mu \equiv g^{\mu\nu} P_\nu = \frac{dx^\mu}{d\sigma} \in T_x(\mathcal{M})$. In this sense, the definitions of the space of physical states as a subset of the cotangent or tangent bundles are equivalent. Some authors like Ehlers [Ehl73] start with the cotangent bundle while others like Lindquist [Lin66] and Stewart [Ste71] choose the tangent bundle.

The Hamiltonian is conserved along the trajectories and it is simply related to the mass of the particles. We can define the 7-dimensional phase spaces for states associated with a given mass

$$\mathcal{P}_m \equiv \left\{ (x, P) \in T^*(\mathcal{M}) \mid P_\mu P^\mu = -m^2 \leq 0, P_0 < 0 \right\}. \quad (2.72)$$

In a similar way, we can define the restriction of L to these subspaces

$$L_m = \frac{\partial H}{\partial P_\mu} \frac{\partial}{\partial x^\mu} - \frac{\partial H}{\partial x^i} \frac{\partial}{\partial P_i}, \quad (2.73)$$

where P_0 is obtained from the mass-shell condition.

2.3.2 Volume element

Our final objective is to find a sensible definition of the distribution function in the general relativistic domain. We need to adapt the Newtonian definition: ‘number of particles per unit of phase-space volume’. This section is devoted to the definition of volume elements.

- In the space-time \mathcal{M} we have the volumen element¹²

$$\eta \equiv \sqrt{-g} d^4x = \frac{1}{4!} \epsilon_{\mu\nu\sigma\rho} dx^{\mu\nu\sigma\rho}, \quad (2.74)$$

and there is defined a covariant hypersurface element

$$\sigma_\mu = \frac{1}{3!} \epsilon_{\mu\nu\sigma\rho} dx^{\nu\sigma\rho}. \quad (2.75)$$

Using a four-velocity vector u^μ ($u^\mu u_\mu = -1$, $u^0 > 0$) to define a time slicing, we can introduce the spatial volume element

$$dV = \frac{1}{3!} \epsilon_{\mu\nu\sigma\rho} u^\mu dx^{\nu\sigma\rho}, \quad (2.76)$$

or alternatively

$$\sigma_\mu = -u_\mu dV. \quad (2.77)$$

- In the phase-space \mathcal{P} we can define the canonical volume element from analytical mechanics¹³

$$\Omega \equiv -d^4x d^4P. \quad (2.78)$$

¹² We define $\epsilon_{\mu\nu\sigma\rho} = \sqrt{-g} \varepsilon_{\mu\nu\sigma\rho}$ where $\varepsilon_{\mu\nu\sigma\rho}$ is the Levi-Civita symbol ($\varepsilon_{0123} = 1$). We also have

$$dx^{\mu\nu\sigma\rho} \equiv dx^\mu \wedge dx^\nu \wedge dx^\sigma \wedge dx^\rho.$$

¹³Note that

$$d^4x = dx^0 dx^1 dx^2 dx^3,$$

while

$$d^4P = dP_0 dP_1 dP_2 dP_3,$$

- In a similar way it is possible to define a volume element on the tangent or cotangent spaces

$$\pi \equiv -\frac{1}{4!} \epsilon_{\mu\nu\sigma\rho} dP^{\mu\nu\sigma\rho} = \frac{1}{\sqrt{-g}} d^4 P . \quad (2.79)$$

This volume element can be restricted to particles of a given mass. This restriction can be introduced as

$$\pi_m \equiv \mathcal{N} H(P) \delta(m^2 + P^\mu P_\mu) \pi , \quad (2.80)$$

where $H(P) = 1$ if $P^0 > 0$ and 0 otherwise. The normalization constant \mathcal{N} will be fixed later, using physical arguments. The integration over P_0 being understood, it is usually rewritten as

$$\pi_m = \frac{\mathcal{N}}{2\sqrt{-g}P^0} d^3 P . \quad (2.81)$$

These volume elements are related as

$$\Omega = -\eta \wedge \pi . \quad (2.82)$$

Starting with a spatial surface on \mathcal{M} and a volume element π , we can define a surface element on \mathcal{P}

$$\Sigma_\mu = \sigma_\mu \wedge \pi . \quad (2.83)$$

It can be proven, see [Ehl73], that the 7-form

$$\omega = P^\mu \Sigma_\mu = P^\mu \sigma_\mu \wedge \pi , \quad (2.84)$$

as well as the volume element are preserved under the phase flow

$$\mathcal{L}_L \omega = 0 , \quad (2.85)$$

$$\mathcal{L}_L \Omega = 0 . \quad (2.86)$$

This is known as the *Liouville theorem*. Moreover, the integral $\int_\Sigma \omega$ can be regarded as the flux of the vector field L across the spatial surface Σ and thus have the physical interpretation of the number of trajectories intersecting Σ (inward and outward trajectories contribute with opposite signs). The same results can be found using the phase space \mathcal{P}_m .

2.3.3 Distribution function

The previous two sections have been devoted to setting up the mathematical framework. We have constructed the phase space as the space of physical states. Given a Hamiltonian, the physical evolution of test particles is represented by trajectories in the phase space. Finally we have defined a volume element (Ω) and a hypersurface element (ω) that are conserved along these trajectories, i.e. along the phase flow. In particular, ω represents the number of trajectories that intersect a given surface element.

The classical picture of a gas represents it as a collection of a large number of (small) particles. The representation of a gas in phase space is depicted in Figure

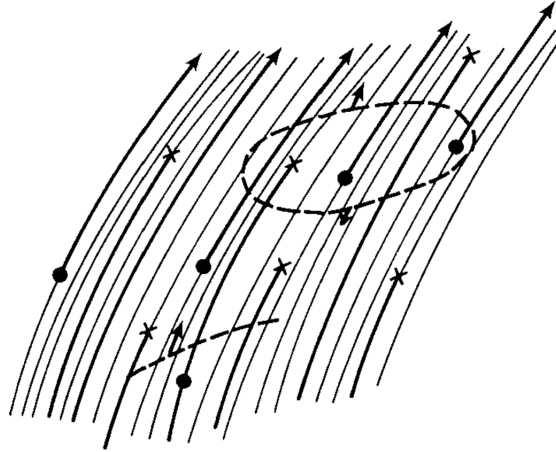


Figure 2.1: Phase-space picture of a gas. Thick lines represent trajectories occupied by a particle. Dots and crosses are creations and annihilations of states, respectively, either due to collisions or to actual creation and annihilation of particles (that we will also denote as collisions). Dotted lines represent open and closed hypersurfaces in phase space. Credit: Fig. 22b from [Eh173].

2.1. The trajectories in phase space can be empty or occupied by a particle of the gas. Clearly, this occupancy may have a beginning and an end, if the particle experience a localized collision that changes abruptly its momentum or if there is creation and annihilation of particles¹⁴.

Such fine-grained description is not needed in practice. Kinetic theory deals with a *large number* of particles and it seeks to obtain information about macroscopic (average) properties of the gas. The key element in this case is the distribution function¹⁵ $f(x,P)$. The distribution function represents the average occupation number of a given phase-space volume. Then, the average number of particles could be tentatively defined as

$$dN = f \omega , \quad (2.87)$$

i.e. the number of trajectories times its average occupation. The rate of change of dN along the phase flow is

$$\mathcal{L}_L dN = L(f)\omega , \quad (2.88)$$

since ω is invariant. We see that the Liouville operator acting on f gives us the change in the number of particles along the phase flow. Putting it in a different way: it gives us the number of collisions, that kick particles in and out the volume. In the absence of such collisions, the number of particles is conserved and the evolution of f is described by the *Liouville equation* (or collisionless Boltzmann equation)

$$L(f) = 0 . \quad (2.89)$$

Before discussing collisions and the Boltzmann equation we should make the results a bit more concrete. The treatment of kinetic theory in General Relativity

¹⁴Collisions will be the subject of the next section.

¹⁵As we will see later, this is properly the one-particle distribution function, defined over the one-particle phase space.

provides a solid, covariant foundation. However, we must reduce the level of abstraction to find expressions that fit our purposes. Besides, we need to reelaborate (2.87) to include a couple of non-classical aspects.

First of all, we will drop the continuous-mass phase space \mathcal{P} as we will be only interested in gases with particles of a given (maybe zero) mass. The preceding results carry through to this case, see [Ehl73], and in the next sections we will drop the ‘ m ’ subscript. Different particles¹⁶ live in different phase spaces and their corresponding distribution functions will be distinguished with a subscript. In the second place, we will be interested only in the kind of “special surfaces” mentioned in [Ste71]. We build these hypersurfaces Σ in \mathcal{P}_m out of a spatial hypersurface in \mathcal{M} and a volume in momentum space. More details can be found in [Ste71; Ehl73].

$$\omega_m = P^\mu \sigma_\mu \wedge \pi_m = (-P^\mu u_\mu) dV \wedge \pi_m \quad (\text{in } \Sigma). \quad (2.90)$$

For an observer locally at rest with the volume ($u^i = 0$) we obtain the classic result

$$\omega_m = \frac{\mathcal{N}}{2} d^3x d^3P. \quad (2.91)$$

The constant \mathcal{N} can be fixed comparing this case with the non-relativistic result. From ordinary kinetic theory, or statistical physics, we know that the average number of particles per unit of phase-space volume is

$$dN_m = g_* f_m \frac{d^3x d^3P}{(2\pi)^3}, \quad (2.92)$$

where $(2\pi)^3$ is the volume of the elementary phase-space cell, i.e. $(2\pi\hbar)^3$ with $\hbar = 1$, and g_* is the number of internal degrees of freedom. The f_m so described reduces to the Fermi-Dirac or Bose-Einstein distributions in equilibrium situations. Comparing with our result

$$dN_m = \frac{\mathcal{N}}{2} f_m d^3x d^3P, \quad (2.93)$$

we get $\mathcal{N} = 2g_*/(2\pi)^3$ and the momentum volume element (2.80) is

$$\pi_m = \frac{g_*}{(2\pi)^3} \frac{d^3P}{\sqrt{-g} P^0}. \quad (2.94)$$

2.3.4 Collisions and the Boltzmann equation

The full Boltzmann equation describes the evolution of the distribution function in realistic multicomponent systems with collisions. The main physical assumptions are the following.

- I) The interactions can be classified into long-range and short-range.

¹⁶This ‘differentiation’ includes particles with different charge or masses. Other properties, like spin, may be included as an internal degree of freedom or not, depending whether it is relevant for the scattering process at hand.

- The particles interact through long-range gravitational and electromagnetic forces. It is assumed that each particle moves in a mean field created by all its neighbours. These fields, like $g_{\mu\nu}$ or A_μ , are in turn sourced by the macroscopic (average) properties of the gas. The effects of long-range interactions, including any external field, is incorporated in the Liouville operator, that describes the trajectories of test particles in phase space.
- The particles also interact in localized, close-by, encounters that are denoted as collisions, even though they may include creation and annihilation of particles. Formally, anything that produces creations and destructions in phase space, like in Figure 2.1, and that induces deviations from the Liouville equation (2.89), will be defined as a collision. Another underlying assumption is that the long-range fields are weak enough so that their effects can be neglected during the collision. As we will see, this fact, along with the hypothesis of point-like collisions, will make possible to compute the collision term in a special relativistic setting.

II) The medium is diluted. This is tantamount to saying that the mean free path is large compared with the range of the short-range interactions. This assumption also supports our phase-space description in terms of the one-particle distribution function. In Newtonian kinetic theory, one may start instead with the N -particle distribution function $f_{(N)}(x_1, P_1, \dots, x_N, P_N)$ that expresses the probability of having N particles in the positions (x_1, P_1) to (x_N, P_N) . This function $f_{(N)}$ satisfies the Liouville equation. It is possible then to marginalize over the momenta to obtain $f_{(1)}(x, P)$, $f_{(2)}(x_1, P_1, x_2, P_2)$ etc. The evolution of $f_{(1)}$ depends on $f_{(2)}$ and, in general, $f_{(k)}$ depends on $f_{(k+1)}$. Thus one arrives at the so-called BBGKY (Bogoliubov-Born-Green-Kirkwood-Yvon) hierarchy, see e.g. [Cha+90].

In our treatment we assume that all the relevant information is encoded in $f_{(1)}$, so in particular we are neglecting the correlations

$$f_{(2)}(x_1, P_1, x_2, P_2) \simeq f_{(1)}(x_1, P_1) f_{(1)}(x_2, P_2) . \quad (2.95)$$

Even though the correlations will be negligible for us, they play an important role in plasma physics [Cha78]. For an elementary derivation of the correlation function in a Newtonian setting see [TB17].

In what follows, we will present the Boltzmann equation for a multicomponent gas with binary collisions. The generalization to other scenarios is straightforward. Consider a gas composed of particles (a, b, c, d) interacting through processes of the form

$$a + b \leftrightarrow c + d . \quad (2.96)$$

A collision is a process taking place at a point x that destroys particles (a, b) with momenta (p_a, p_b) and creates particles (c, d) with momenta (p_c, p_d) (or viceversa). Clearly, the Liouville equation is not satisfied and there must be a term on the right-hand side of (2.89) taking into account the number of collisions

$$L(f_s) = \text{Coll}_s^+ - \text{Coll}_s^- , \quad s = a, b, c, d \quad (2.97)$$

where the sign $+$, $-$ denotes that the collisions may increase or decrease the number of particles in the volume. Of course, this expression is only schematic and we must give a proper formulation of the collision term. Instead of delving into the subtleties of this construction in curved space-time, we take a more pragmatic approach.

In the next section we will present the Boltzmann equation in flat space-time, where the structure of the collision term is well established. The two assumptions above will then allow us to immediately promote this collision term to curved space-time.

2.3.5 Boltzmann equation in flat space-time

The Liouville operator (2.70) is usually substituted in Newtonian kinetic theory by the closely related *material derivative*

$$\frac{Df}{dt} = \frac{\partial f}{\partial t} + \frac{dx^i}{dt} \frac{\partial f}{\partial x^i} + \frac{dp_i}{dt} \frac{\partial f}{\partial p_i}. \quad (2.98)$$

We will call it indistinctively material derivative or Liouville operator. The collision term is *defined* as the right-hand side of the Boltzmann equation

$$\frac{Df}{dt} = C[f]. \quad (2.99)$$

The same definition of the Boltzmann equation (2.99) also applies in special relativity, where t is the time coordinate of an inertial observer. The particular form of the collision term for a binary process $a + b \leftrightarrow c + d$ is (for the species a) [LL00]

$$\begin{aligned} C[f_a] = & \frac{S}{2E_a} \int \mathcal{D}p_b \mathcal{D}p_c \mathcal{D}p_d (2\pi)^4 \delta(p_a + p_b - p_c - p_d) |\mathcal{M}|^2 \\ & \times \left[\underbrace{f_c f_d (1 \pm f_a)(1 \pm f_b)}_{cd \rightarrow ab} - \underbrace{f_a f_b (1 \pm f_c)(1 \pm f_d)}_{ab \rightarrow cd} \right] \begin{cases} + \text{ bosons} \\ - \text{ fermions} \end{cases} \end{aligned} \quad (2.100)$$

The meaning of the different pieces is:

- There are two terms, for the direct $cd \rightarrow ab$ and the inverse process $ab \rightarrow cd$. The first one is proportional to the probability of having c - and d -particles with momenta p_c and p_d , i.e. $f_c f_d$, and expresses the gain of a -particles in a phase-space volume centered at p_a . The second term expresses the lost of a -particles in phase space.
- The matrix element $|\mathcal{M}|^2$ is the probability of the transition $a(p_a) + b(p_b) \leftrightarrow c(p_c) + d(p_d)$. It is the same for the direct and the inverse process, under very general assumptions [Wei95]. It can be computed from first principles and it is the link to the microphysics of the problem.
- The collision is only allowed if it conserves energy and momentum, hence the Dirac δ .
- In order to consider all the possible processes that modify the number of particles in the phase-space volume of the a -particles, we must integrate over the

momentum of all the remaining particles (and possibly sum over every internal degree of freedom). The integration measures are the Lorentz-invariant phase-space volumes

$$\mathcal{D}p_s \equiv \frac{d^3 p_s}{(2\pi)^3 2E_s}, \quad s = a, b, c, d. \quad (2.101)$$

- The factor S is a symmetry factor, e.g. $S = 1/2$ for identical particles in the initial or final state.
- The factor $1/E_a$ ensures that the Boltzmann equation is the same for all boost-related inertial observers.
- The factors $(1 \pm f)$ are quantum statistical factors that modify the final phase-space volume available. They are responsible for the Bose enhancement (stimulated emission) and Pauli blocking (exclusion principle) effects.

How do we promote this result to curved space-time? In the first place, remember that, on the tangent space at a given space-time point, we can always define an orthonormal basis e_a (tetrad) given by

$$e_a = e^\mu{}_a \frac{\partial}{\partial x^\mu}, \quad e^\mu{}_a e^\nu{}_b g_{\mu\nu} = \eta_{ab}. \quad (2.102)$$

This basis defines a locally Minkowskian observer in curved space-time. In the second place, notice that the collision term only accounts for local information. We can compute it in the locally Minkowskian frame and use the flat space-time form (2.100) as long as we interpret the momenta as those measured in this frame

$$p_a = e^\mu{}_a P_\mu. \quad (2.103)$$

Finally, the Boltzmann equation (2.99) applies to the physical time of a locally inertial observer defined by

$$dt = e_\mu{}^0 dx^\mu, \quad (2.104)$$

where we have used the inverse tetrad. We will see an example of this procedure in Section 3.3.

2.3.6 Energy-momentum tensor

The energy-momentum tensor in the kinetic approach is defined as [Ehl73; MB95; Dod03]

$$T_{\mu\nu} \equiv \int P_\mu P_\nu f \pi = \frac{g_*}{(2\pi)^3} \int \frac{d^3 P}{\sqrt{-g}} \frac{P_\mu P_\nu}{P^0} f. \quad (2.105)$$

If we compute the components for a locally inertial frame (2.103), we have in the first place

$$\frac{d^3 P}{\sqrt{-g} P^0} = \frac{d^3 p}{E}, \quad (2.106)$$

with $E \equiv p^0$, and then

$$T^a{}_b = g_* \int \frac{d^3 p}{(2\pi)^3 E} p^a p_b f. \quad (2.107)$$

This expression provides the basis for the physical interpretation of the fluid variables

$$\rho = g_* \int \frac{d^3 p}{(2\pi)^3} E f = -T^0_0, \quad (\text{Energy density}) \quad (2.108a)$$

$$Q_i = g_* \int \frac{d^3 p}{(2\pi)^3} p_i f = T^0_i, \quad (\text{Momentum density}) \quad (2.108b)$$

$$P\delta^i_j + \Pi^i_j = g_* \int \frac{d^3 p}{(2\pi)^3} \frac{p^i p_j}{E} f = T^i_j. \quad (\text{Pressure and stress tensor}) \quad (2.108c)$$

This formalism can be applied to define the current of particles

$$N_\mu \equiv \int P_\mu f \pi = \frac{g_*}{(2\pi)^3} \int \frac{d^3 P}{\sqrt{-g}} \frac{P_\mu}{P^0} f. \quad (2.109)$$

Again, for a locally inertial observer we obtain

$$N^a = g_* \int \frac{d^3 p}{(2\pi)^3} \frac{p^a}{E} f, \quad (2.110)$$

and the familiar definitions from flat space hold

$$n = g_* \int \frac{d^3 p}{(2\pi)^3} f, \quad (\text{Number density}) \quad (2.111a)$$

$$V^i = g_* \int \frac{d^3 p}{(2\pi)^3} \frac{p^i}{E} f. \quad (\text{Particle flux}) \quad (2.111b)$$

Another interesting result concerns the possibility of translating the conservation laws from the fluid approach, (2.4) and (2.7), to the kinetic language. It can be proven, see [Ehl73], that

$$N^\mu{}_{;\mu} = \int L(f) \pi, \quad (2.112)$$

$$T^{\mu\nu}{}_{;\nu} = \int P^\mu L(f) \pi. \quad (2.113)$$

Recalling the form of the Liouville operator (2.70), if we choose a particular time parameterization $dx^0 = d\sigma \equiv d\tau$, it can be rewritten in terms of the material derivative (2.98)

$$L(f) = \frac{\partial f}{\partial \tau} + \frac{dx^i}{d\tau} \frac{\partial f}{\partial x^i} + \frac{dP_i}{d\tau} \frac{\partial f}{\partial P_i} = \frac{Df}{d\tau}. \quad (2.114)$$

Using this time parameterization, the previous results can be recast as

$$N^\mu{}_{;\mu} = \frac{g_*}{(2\pi)^3} \int \frac{d^3 P}{\sqrt{-g} P^0} \frac{Df}{d\tau}, \quad (2.115)$$

$$T^{\mu\nu}{}_{;\nu} = \frac{g_*}{(2\pi)^3} \int \frac{d^3 P}{\sqrt{-g}} \frac{P^\mu Df}{P^0 d\tau}. \quad (2.116)$$

3

Λ CDM Cosmology

This chapter reviews, in detail, the building blocks of the Λ CDM cosmology. The background evolution, based on perfect fluids, is analyzed in Section 3.1. The kinetic description, at the background and perturbation levels, is the subject of Section 3.2. In Section 3.3 we introduce the Boltzmann equation, deriving the equations that govern the evolution of all the species. Section 3.4 introduces the usual scalar-vector-tensor decomposition and develops the Boltzmann hierarchy. The Einstein equations and the gauge-transformation rules are presented in Section 3.5. The usual approximation schemes to follow the evolution of the perturbations (tight coupling and radiation streaming) are covered in Section 3.6. The initial-condition analysis is carried out in Section 3.7, where we identify the usual adiabatic and isocurvature modes. The line-of-sight approach, crucial to describe ultrarelativistic species, is developed in Section 3.8. Finally, in Section 3.9 we define the main observables of the theory: the temperature and matter power spectra.

3.1 Background dynamics

The background metric in Λ CDM is a flat Robertson-Walker (RW) metric

$$ds^2 = a^2(\tau)(-d\tau^2 + d\mathbf{x}^2) , \quad (3.1)$$

where τ is the conformal time and a is the scale factor¹. The Hubble parameter, H , and the conformal Hubble parameter, \mathcal{H} , are defined as

$$\mathcal{H} \equiv \frac{\dot{a}}{a} , \quad H \equiv \frac{1}{a} \mathcal{H} , \quad (3.2)$$

where $\dot{} \equiv d/d\tau$. This metric can be sourced with a perfect fluid (2.9)

$$T^\mu_{\nu} = (\rho + P)u^\mu u_\nu + P\delta^\mu_{\nu} . \quad (3.3)$$

This cosmic fluid is made out of three components with constant equations of state.

- Radiation: $w = 1/3$. The radiation includes photons and neutrinos².
- Matter: $w = 0$. Takes into account baryons³ and cold dark matter.
- Cosmological constant (Λ): $w = -1$. It is usually included as a fluid, instead of as a term in the Einstein equations.

¹Remember that the scale factor is related to the redshift as $a = (1+z)^{-1}$.

²For simplicity, we restrict ourselves to massless neutrinos.

³Following usual practice in cosmology, we denote protons, electrons and bound atoms collectively as baryons.

The Einstein equations (1) allow us to compute the evolution of the scale factor

$$\mathcal{H}^2 = \frac{8\pi G a^2}{3} \rho(\tau) = \frac{8\pi G a^2}{3} (\rho_r(\tau) + \rho_m(\tau) + \rho_\Lambda(\tau)) , \quad (3.4)$$

$$\dot{\mathcal{H}} + \frac{1}{2} \mathcal{H}^2 = -4\pi G a^2 P(\tau) = -4\pi G a^2 \left(\frac{1}{3} \rho_r(\tau) - \rho_\Lambda(\tau) \right) . \quad (3.5)$$

These are the celebrated Friedmann equations that describe the expansion history of the Universe. This kind of background, or universe, is named after Friedmann, Lemaître, Robertson and Walker (FLRW). Since the different components do not interact, at this level, each of them satisfies the conservation equation

$$T_{(s)}^{\mu}{}_{\nu;\mu} = 0 , \quad s = r, m, \Lambda \quad (3.6)$$

separately. For an observer comoving with the fluid, the conservation equation can be written as

$$\dot{\rho} = -3\mathcal{H}(1+w)\rho . \quad (3.7)$$

It can be solved for a constant equation of state⁴

$$\rho = \rho_0 a^{-3(1+w)} , \quad (3.8)$$

where ρ_0 is the density today. The first Friedmann equation (3.4) can be rewritten as

$$\mathcal{H}^2 = a^2 H_0^2 (\Omega_r a^{-4} + \Omega_m a^{-3} + \Omega_\Lambda) , \quad (3.9)$$

where H_0 is the Hubble parameter today and the reduced densities Ω_s are the densities evaluated today and normalized by the critical density

$$\Omega_s = \frac{\rho_s 0}{\rho_{\text{crit}}} , \quad \rho_{\text{crit}} = \frac{3H_0^2}{8\pi G} . \quad (3.10)$$

Another consequence of (3.9) is that

$$\Omega_\Lambda = 1 - \Omega_r - \Omega_m . \quad (3.11)$$

Once the expansion history $\mathcal{H}(a)$ is known, it is possible to compute the conformal time

$$\tau = \int \frac{da}{a\mathcal{H}} . \quad (3.12)$$

If there is only one component in the universe, with a constant equation of state w , we find

$$\mathcal{H} = H_0 a^{-(1+3w)/2} , \quad \tau = \frac{2}{(1+3w)H_0} a^{(1+3w)/2} , \quad (3.13)$$

$$\mathcal{H} = \frac{2}{(1+3w)} \tau^{-1} , \quad a = \left(\frac{(1+3w)H_0}{2} \tau \right)^{2/(1+3w)} . \quad (3.14)$$

The only relevant quantities in the early Universe ($a \ll 1$) are matter and radiation. From (3.9)

$$\mathcal{H}^2 \simeq a^2 H_0^2 (\Omega_r a^{-4} + \Omega_m a^{-3}) . \quad (3.15)$$

⁴It is customary to normalize the scale factor such that today $a(\tau_0) = a_0 = 1$.

For this two-component fluid, it is possible to obtain analytic expressions for $\mathcal{H}(\tau)$ and $a(\tau)$ that will prove handy later

$$\mathcal{H} = \frac{1 + 2\tau/\tau_m}{\tau(1 + \tau/\tau_m)}, \quad \tau_m^{-1} \equiv \frac{H_0\Omega_m}{4\sqrt{\Omega_r}}, \quad (3.16)$$

$$a = H_0\sqrt{\Omega_r}\tau(1 + \tau/\tau_m). \quad (3.17)$$

3.2 Kinetic approach

The perfect fluid description of the previous section is appropriate to describe the homogeneous and isotropic FLRW background. However, a realistic description of our Universe must accommodate the presence of small inhomogeneities, that will be introduced as small perturbations over the RW background metric.

The perfect fluid approach can be adapted to this scenario by including small perturbations in the density, pressure and velocity of the fluid. The photon-baryon plasma in the early Universe and non-relativistic species, like baryons and CDM, can be approximated as perfect fluids and described within this formalism. Unfortunately, important events in cosmology do not admit a fluid description, particularly the details of the photon-baryon decoupling and the free streaming of neutrinos. The introduction of a kinetic approach is unavoidable to describe accurately these processes.

Kinetic theory in curved space-time has been amply discussed in Section 2.3. We briefly summarize here the main ingredients. The presentation and notation follow, inasmuch as possible, that of [MB95]. The phase space of a given component is described by:

- Three positions x^i .
- Three conjugate momenta P_i . These conjugate momenta are defined as the spatial components of the four-momentum

$$P^\mu \equiv m \frac{dx^\mu}{d\lambda}, \quad P_\mu P_\nu g^{\mu\nu} = -m^2, \quad (3.18)$$

where $d\lambda \equiv \sqrt{-ds^2}$ is the proper time and the spatial index i has been lowered with the full metric $g_{\mu\nu}$.

The number of particles per unit of phase-space volume is

$$dN = g_* f(\tau, x^i, P_j) \frac{d^3x d^3P}{(2\pi)^3}, \quad (3.19)$$

where g_* is the number of internal degrees of freedom, e.g. the number of helicity states, and f is the phase-space distribution. The energy-momentum tensor can be defined as (2.105)

$$T_{\mu\nu} = \frac{g_*}{(2\pi)^3} \int \frac{d^3P}{\sqrt{-g}} \frac{P_\mu P_\nu}{P^0} f(\tau, x^i, P_j). \quad (3.20)$$

The next two sections introduce the kinetic description of a fluid in a cosmological setting, rederiving first the background results and then extending the discussion to a perturbed FLRW universe.

3.2.1 Background

Starting with the RW metric (3.1) and denoting the components of the four-momentum as

$$\epsilon \equiv -P_0, \quad q_i \equiv P_i, \quad (3.21)$$

such that $q^i \equiv q_i$. From the mass-shell condition (3.18) we get

$$\epsilon^2 = m^2 a^2 + q^2. \quad (3.22)$$

We will call ϵ and q the comoving energy and momentum of the particles. It is common to define the physical energy and momentum

$$E \equiv \epsilon/a, \quad p_i \equiv q_i/a. \quad (3.23)$$

If we write f_0 for the background distribution function, we can define the fluid variables

$$\begin{aligned} \rho &\equiv a^{-4} g_* \int \frac{d^3 q}{(2\pi)^3} \epsilon f_0, & P &\equiv a^{-4} g_* \int \frac{d^3 q}{(2\pi)^3} \frac{q^2}{3\epsilon} f_0, \\ Q^i &\equiv a^{-4} g_* \int \frac{d^3 q}{(2\pi)^3} q^i f_0, & n &\equiv a^{-3} g_* \int \frac{d^3 q}{(2\pi)^3} f_0, \\ \Pi^{ij} &\equiv a^{-4} g_* \int \frac{d^3 q}{(2\pi)^3} \left(\frac{q^i q^j}{\epsilon} - \frac{q^2}{3\epsilon} \delta^{ij} \right) f_0, & V^i &\equiv a^{-3} g_* \int \frac{d^3 q}{(2\pi)^3} \frac{q^i}{\epsilon} f_0, \end{aligned} \quad (3.24)$$

that represent the usual energy, momentum, shear tensor, pressure, number and velocity densities of the fluid. The components of the energy-momentum tensor (3.20) in terms of these variables are

$$T^0_0 = -\rho, \quad (3.25a)$$

$$T^0_i = Q_i, \quad (3.25b)$$

$$T^i_j = P \delta^i_j + \Pi^i_j \quad (3.25c)$$

In order to source a homogeneous and isotropic RW metric with a single component we need to impose that the distribution function is homogeneous and isotropic

$$f_0 = f_0(\tau, q). \quad (3.26)$$

It is straightforward to prove that this choice leads us to the perfect fluids discussed in Section 3.1, with $Q_i = 0$ and $\Pi^{ij} = 0$. This connection also provides a microscopic basis for the equations of state proposed for radiation and matter, at the beginning of Section 3.1. It is customary to refer collectively to massless, or nearly massless, particles as radiation. For these light particles

$$\epsilon = q + \mathcal{O}\left(\frac{m^2 a^2}{q^2}\right), \quad (3.27)$$

and the density and pressure are

$$\rho = a^{-4} g_* \int \frac{d^3 q}{(2\pi)^3} q f_0 + \mathcal{O}\left(\frac{m^2 a^2}{q^2}\right), \quad (3.28)$$

$$P = a^{-4} g_* \int \frac{d^3 q}{(2\pi)^3} \frac{q}{3} f_0 + \mathcal{O}\left(\frac{m^2 a^2}{q^2}\right) \simeq \frac{1}{3} \rho, \quad (3.29)$$

so $w = 1/3$ for massless particles. On the other hand, for heavy particles the non-relativistic (NR) limit is appropriate

$$\epsilon = ma + \mathcal{O}\left(\frac{q^2}{m^2 a^2}\right). \quad (3.30)$$

In this limit

$$\rho = a^{-3} g_* \int \frac{d^3 q}{(2\pi)^3} m f_0 + \mathcal{O}\left(\frac{q^2}{m^2 a^2}\right) \simeq mn, \quad (3.31)$$

$$P = 0 + \mathcal{O}\left(\frac{q^2}{m^2 a^2}\right), \quad (3.32)$$

so $w \simeq 0$. This limit is implicitly assumed when some component is denoted as ‘matter’. If there is risk of confusion, the appellation ‘cold’ may be added. For instance, in Λ CDM, the name ‘cold dark matter’ points to a heavy dark matter candidate with $w = 0$. Alternative models of ‘warm dark matter’ are constructed with lighter candidates whose equation of state, while being small, differs from zero⁵.

3.2.2 Perturbations

Our starting point is a perturbed flat RW metric

$$ds^2 = a^2(\tau) \left(-(1 - A)d\tau^2 + 2B_i d\tau dx^i + (\delta_{ij} + H_{ij})dx^i dx^j \right). \quad (3.33)$$

Reparameterizing the momentum as

$$P_0 \equiv -aE + \delta P_0, \quad (3.34)$$

$$P_i \equiv a \left(\delta_i^j + \frac{1}{2} H_i^j \right) p_j, \quad (3.35)$$

from the mass-shell condition (3.18) we obtain

$$E^2 = m^2 + p^2, \quad (3.36)$$

$$\delta P_0 = \frac{1}{2} A a E + a p_i B^i. \quad (3.37)$$

The change from P_i to p_i can be regarded just as a redefinition but it has a very simple interpretation in terms of the tetrad (2.102). Our choice of momentum, $P_\mu = e_\mu^a p_a$, corresponds to a choice of tetrad with components

$$\begin{aligned} e_0^0 &= a \left(1 - \frac{1}{2} A \right), & e_i^0 &= 0, \\ e_i^j &= a \left(\delta_j^i + \frac{1}{2} H_j^i \right), & e_0^i &= a B^i. \end{aligned} \quad (3.38)$$

⁵The discussion above obviates the fact that when we talk about light or heavy particles we are comparing their mass with another scale, built in the distribution function. If the dark matter candidate was in thermal equilibrium, as for example WIMPs, this energy scale is simply the temperature of the plasma. However, in Chapter 5, we will discuss what is usually called an ultralight dark matter candidate. These candidates still behave as CDM, but they have a different origin and were never in thermal equilibrium with the plasma.

With these definitions, p_i are the physical momenta measured by a locally inertial observer at a fixed spatial position. It is convenient to work with a closely related set of variables, ϵ and q^i defined as in (3.23), and it will also be useful to split the momentum into direction and magnitude

$$q^i \equiv q n^i, \quad n_i \delta^{ij} n_j = 1. \quad (3.39)$$

As we will see, written in terms of q_i instead of p_i , the Boltzmann equation does not contain a zero order term. The phase-space distribution is also perturbed

$$f(\tau, \mathbf{x}, \mathbf{q}) = f_0(\tau, q) + \delta f(\tau, \mathbf{x}, \mathbf{q}). \quad (3.40)$$

We define the corresponding perturbed fluid variables

$$\begin{aligned} \delta\rho &\equiv a^{-4} g_* \int \frac{d^3 q}{(2\pi)^3} \epsilon \delta f, & \delta P &\equiv a^{-4} g_* \int \frac{d^3 q}{(2\pi)^3} \frac{q^2}{3\epsilon} \delta f, \\ \delta Q^i &\equiv a^{-4} g_* \int \frac{d^3 q}{(2\pi)^3} q^i \delta f, & \delta n &\equiv a^{-3} g_* \int \frac{d^3 q}{(2\pi)^3} \delta f, \\ \delta\Pi^{ij} &\equiv a^{-4} g_* \int \frac{d^3 q}{(2\pi)^3} \left(\frac{q^i q^j}{\epsilon} - \frac{q^2}{3\epsilon} \delta^{ij} \right) \delta f, & \delta V^i &\equiv a^{-3} g_* \int \frac{d^3 q}{(2\pi)^3} \frac{q^i}{\epsilon} \delta f. \end{aligned} \quad (3.41)$$

The components of the perturbed energy-momentum tensor in terms of these variables are

$$\delta T^0_0 = -\delta\rho, \quad (3.42a)$$

$$\delta T^0_i = \delta Q_i, \quad (3.42b)$$

$$\delta T^i_j = \delta P \delta^i_j + \delta\Pi^i_j. \quad (3.42c)$$

Defining the sound speed as⁶

$$c_s^2 \equiv \frac{\delta P}{\delta\rho}, \quad (3.43)$$

for massless particles we find $c_s^2 = 1/3$. On the other hand, in the non-relativistic limit

$$c_s^2 = 0 + \mathcal{O}\left(\frac{q^2}{m^2 a^2}\right), \quad (3.44)$$

$$\delta\Pi^i_j = 0 + \mathcal{O}\left(\frac{q^2}{m^2 a^2}\right), \quad (3.45)$$

$$\delta\rho = m\delta n + \mathcal{O}\left(\frac{q^2}{m^2 a^2}\right), \quad (3.46)$$

$$\delta Q^i = m\delta V^i + \mathcal{O}\left(\frac{q^2}{m^2 a^2}\right). \quad (3.47)$$

All the relevant information for NR particles is encoded in their density and velocity perturbations, so they can be appropriately described as perfect fluids. The kinetic approach has allowed us to justify this assertion and it is essential to follow the evolution of ultrarelativistic species⁷.

⁶Remember that in Section 2.1.2 we also defined the adiabatic sound speed $c_{\text{ad}}^2 = \dot{P}/\dot{\rho}$. They are generally different.

⁷Sometimes it is possible to approximate ultrarelativistic species as *imperfect* fluids [Hu98].

3.3 Boltzmann equation

The information about the time evolution of the distribution function is encoded in the Boltzmann equation. In the locally Minkowskian frame it takes the form (2.99)

$$\frac{Df}{dt} = C[f], \quad (3.48)$$

where $dt \equiv e_{\mu}^0 dx^{\mu}$ is the time measured by the locally Minkowskian observer, which, for the tetrad choice (3.38), reads $dt = \alpha(1 - A/2)d\tau$. We shall find convenient to express the distribution function as a function of the space-time coordinates that appear in (3.33) and the momenta q^i defined in (3.23). Rewritten in conformal time, the Boltzmann equation is

$$\frac{Df}{d\tau} = \alpha \left(1 - \frac{1}{2}A \right) C[f]. \quad (3.49)$$

The left-hand side, the so-called material derivative or Liouville operator, describes the free streaming of particles in phase space. It is defined as (2.98)

$$\frac{Df}{d\tau} \equiv \frac{\partial f}{\partial \tau} + \frac{dx^i}{d\tau} \frac{\partial f}{\partial x^i} + \frac{dq^i}{d\tau} \frac{\partial f}{\partial q^i}. \quad (3.50)$$

This operator contains the information about the space-time geometry, through its effects on the geodesics of the particles. The functional on the right-hand side of (3.48) is the so-called collision term, that we discussed in Sections 2.3.4 and 2.3.5. It takes into account how the number of particles per unit of phase-space volume change due to collisions, i.e. local interactions. The collision term takes the same form as in flat space-time when written in terms of the momenta measured by a locally inertial observer, p_a , defined in (3.34) and (3.35).

The next section is devoted to the left-hand side of the Boltzmann equation, i.e. the Liouville operator, particularizing to massless and non-relativistic particles. This analysis exhausts all the information needed to follow the evolution of non-interacting particles, like CDM and neutrinos. However, to describe the photon-baryon plasma, we must move on to the full Boltzmann equation. We will derive the collision term for the interaction between photons and electrons and we will finally gather the Boltzmann equations for all the relevant components.

3.3.1 Liouville operator

In order to compute the time derivatives appearing in (3.50), we need the geodesics in the metric (3.33). A detailed computation of the geodesics can be found in Appendix D. Using the definition of the four-momentum (3.18) and the parameterization (3.34), (3.35) and (3.23), the final results are⁸

$$\frac{dx^i}{d\tau} = \frac{q^i}{\epsilon} \left(1 - \frac{1}{2}A \right) - B^i - \frac{1}{2\epsilon} H^i_k q^k, \quad (3.51)$$

$$\frac{dq_i}{d\tau} = \frac{1}{2}\epsilon \partial_i A + q^j C_{ij} + \frac{q^j q^k}{\epsilon} D_{ijk}, \quad (3.52)$$

⁸Notice that, with this choice, the geodesic equation (3.52) is already first order in perturbations.

where the following combinations of metric variables have been defined

$$C_{ij} \equiv \partial_i B_j - \frac{1}{2} \dot{H}_{ij}, \quad (3.53)$$

$$D_{ijk} \equiv \frac{1}{2} (\partial_i H_{jk} - \partial_k H_{ij}). \quad (3.54)$$

Splitting the distribution function into a background part plus a perturbation, as in (3.40), the Liouville operator (3.50) up to first order in perturbation theory is

$$\frac{Df}{d\tau} = \frac{\partial f_0}{\partial \tau} + \frac{\partial \delta f}{\partial \tau} + \frac{dx^i}{d\tau} \frac{\partial \delta f}{\partial x^i} + \frac{dq^i}{d\tau} \frac{\partial f_0}{\partial q^i}. \quad (3.55)$$

We will restrict our attention to massless and non-relativistic particles.

Massless particles

Since there are no collisions at the background level⁹, to leading order the Boltzmann equation is

$$\frac{\partial f_0}{\partial \tau} = 0. \quad (3.56)$$

For massless particles, this entails that the unperturbed distribution f_0 only depends¹⁰ on q

$$f_0(\tau, q) = f_0(q). \quad (3.57)$$

It is convenient to work with the reduced phase-space density, integrating out the dependence on the momentum magnitude, defined as

$$\mathcal{F}(\tau, \mathbf{x}, \hat{n}) \equiv \frac{1}{\mathcal{N}} \int q^3 dq \delta f(\tau, \mathbf{x}, \mathbf{q}), \quad (3.58)$$

where the constant \mathcal{N} is related to the comoving energy density

$$\mathcal{N} \equiv \int q^3 dq f_0(q) = \frac{2\pi^2}{g_*} a^4 \rho = \text{const.} \quad (3.59)$$

Plugging the geodesic equations (3.51) and (3.52) into the right-hand side of (3.50) and integrating out the momentum magnitude, we obtain

$$\int q^3 dq \frac{Df}{d\tau} = \mathcal{N} \left[\dot{\mathcal{F}} + n^i \partial_i \mathcal{F} - 2n^i \partial_i A - 4n^i n^j C_{ij} \right]. \quad (3.60)$$

⁹We assume that thermodynamic equilibrium is maintained at the background level and that departures from it appear as small perturbations. Hence, the collision term at the background level (in equilibrium) is zero.

¹⁰We are tacitly assuming that we have a blackbody spectrum

$$f_0(q) = \frac{1}{e^{q/T_0} - 1}.$$

where T_0 is the temperature today. In particular, we assume that there is no chemical potential. Check [KT94; Pad93; Pad00] for more details.

The first moments of the angular distribution can be found performing the appropriate integrals over \hat{n}

$$\int \frac{d\Omega}{4\pi} \int q^3 dq \frac{Df}{d\tau} = \mathcal{N} \left[\dot{\delta} + \frac{4}{3} \partial_i \delta v^i - \frac{4}{3} \delta^{ij} C_{ij} \right], \quad (3.61)$$

$$\int \frac{d\Omega}{4\pi} n^i \int q^3 dq \frac{Df}{d\tau} = \frac{4}{3} \mathcal{N} \left[\delta \dot{v}^i + \frac{3}{4} \partial_j \pi^{ij} + \frac{1}{4} \partial^i \delta - \frac{1}{2} \partial^i A \right], \quad (3.62)$$

where we have defined

$$\delta \equiv \int \frac{d\Omega}{4\pi} \mathcal{F} = \frac{\delta \rho}{\rho}, \quad (3.63)$$

$$\delta \mathbf{v} \equiv \frac{3}{4} \int \frac{d\Omega}{4\pi} \hat{n} \mathcal{F} = \frac{\delta \mathbf{Q}}{\rho + P}, \quad (3.64)$$

$$\pi^{ij} \equiv \int \frac{d\Omega}{4\pi} \left(n^i n^j - \frac{1}{3} \delta^{ij} \right) \mathcal{F} = \frac{\delta \Pi^{ij}}{\rho}. \quad (3.65)$$

Massive particles

The results for massive particles are much more involved. However, since we will focus on non-relativistic particles, it will be enough to restrict the analysis to the lowest moments of the Boltzmann equation: the number density, energy and velocity perturbations.

- *Number density.*

$$a^{-3} g_* \int \frac{d^3 q}{(2\pi)^3} \frac{Df}{d\tau} = a^{-3} \frac{\partial}{\partial \tau} (a^3 n) + a^{-3} \frac{\partial}{\partial \tau} (a^3 \delta n) + \partial_i \delta V^i - n \delta^{ij} C_{ij}. \quad (3.66)$$

- *Energy.*

$$a^{-4} g_* \int \frac{d^3 q}{(2\pi)^3} \epsilon \frac{Df}{d\tau} = \dot{\rho} + 3\mathcal{H}(\rho + P) + \rho (\dot{\delta} + 3\mathcal{H} \delta (c_s^2 - w)) + \partial_i \delta Q^i + \delta (\dot{\rho} + 3\mathcal{H}(\rho + P)) - (\rho + P) \delta^{ij} C_{ij}. \quad (3.67)$$

- *Momentum.*

$$a^{-4} g_* \int \frac{d^3 q}{(2\pi)^3} q^i \frac{Df}{d\tau} = a^{-4} \frac{\partial}{\partial \tau} (a^4 \delta Q^i) + \partial_j (\delta^{ij} \delta P + \delta \Pi^{ij}) - \frac{1}{2} (\rho + P) \partial^i A. \quad (3.68)$$

These results are general, for particles of any mass, and in the appropriate limits reproduce (3.61) and (3.62). Equations (3.66) and (3.67) at the background level, and without collisions, express the conservation of the comoving number of particles and the continuity equation (3.7). Assuming that the zero-order Boltzmann equation, without collisions, is satisfied, the results to first NR order are:

- *Number density.*

$$a^{-3} g_* \int \frac{d^3 q}{(2\pi)^3} \frac{Df}{d\tau} \simeq n \left[\dot{\delta}_n + \partial_i \delta v^i - \delta^{ij} C_{ij} \right]. \quad (3.69)$$

- *Energy.*

$$a^{-4} g_* \int \frac{d^3 q}{(2\pi)^3} \epsilon \frac{Df}{d\tau} \simeq \rho \left[\dot{\delta} + \partial_i \delta v^i - \delta^{ij} C_{ij} \right]. \quad (3.70)$$

- *Momentum.*

$$a^{-4} g_* \int \frac{d^3 q}{(2\pi)^3} q^i \frac{Df}{d\tau} \simeq \rho \left[\delta \dot{v}^i + \mathcal{H} \delta v^i - \frac{1}{2} \partial^i A \right]. \quad (3.71)$$

We have defined

$$\delta_n \equiv \frac{\delta n}{n}, \quad \delta v^i \equiv \frac{\delta V^i}{n}. \quad (3.72)$$

3.3.2 Collision term

This section is devoted to the calculation of the collision term for Compton scattering between electrons and photons. The notation in this section is slightly different. As we mentioned before, the collision term must be written in terms of the momenta p_i measured by a locally inertial observer at a fixed spatial position. These are related to the momenta q_i we have been using as defined in (3.23), i.e. $q_i = p_i/a$. Some standard physical assumptions underlying the derivation of the collision term are the following.

- When written in terms of the momenta p_i , the collision term is the same as in flat space, since it takes into account local information where the curvature effects are not important. In the same way, the matrix element \mathcal{M} is computed using quantum field theory (QFT) in flat space-time.
- The temperature of the plasma is low enough so that the electrons are non-relativistic. We keep only the first order correction in the NR expansion. This means that we keep the electron velocity but neglect its pressure and sound speed. We consider the NR limit of Compton scattering, i.e. Thomson scattering.
- Electrons and protons are much more tightly coupled between them than to photons. The velocities of free electrons, protons and the full baryonic velocity are the same throughout the evolution.
- The angular dependence of Thomson scattering is neglected. This angular dependence has proven important for 1% accuracy and especially for polarization, but we will not take it into account in this work. We use the angle-averaged matrix element instead.
- The number of internal degrees of freedom is *not* included in the definition of f , i.e. the equilibrium distributions correspond to the usual Bose-Einstein and Fermi-Dirac distributions.
- The medium is diluted enough so that we can neglect the quantum statistical factors ($1 \pm f$) responsible for the Bose enhancement and Pauli blocking effects. We do not take into account any plasma effect from finite temperature QFT.

Thomson scattering

Our starting point is the definition (2.100) for the collision term with binary collisions. With the qualifications above, the process $e(p_e) + \gamma(p) \leftrightarrow e(p'_e) + \gamma(p')$ can be modelled by

$$\begin{aligned} \mathcal{C}[f(\mathbf{p})] = & \frac{1}{4p} \int \mathcal{D}p_e \mathcal{D}p' \mathcal{D}p'_e (2\pi)^4 \delta(p^\mu + p_e^\mu - p'^\mu - p_e'^\mu) \\ & \times \left[f(\mathbf{p}') f_e(\mathbf{p}'_e) - f(\mathbf{p}) f_e(\mathbf{p}_e) \right] \sum_{\text{spins}} |\mathcal{M}|^2, \end{aligned} \quad (3.73)$$

where $\mathcal{D}p \equiv \frac{d^3\mathbf{p}}{(2\pi)^3 2E}$ is the Lorentz-invariant phase-space volume, f and f_e are the distribution functions for photons and electrons and their dependence on space-time coordinates has been omitted, since it does not play any role. Note that it has been necessary to add a factor 1/2 to average over the initial helicity of $\gamma(p)$. For Thomson scattering, the matrix element is¹¹

$$\sum_{\text{spins}} |\mathcal{M}|^2 = 48\pi\sigma_T m_e^2 (1 + \cos^2\theta), \quad (3.74)$$

where θ is the angle between the incident and scattered photons in the electron rest frame and σ_T is the Thomson cross section. We use instead the angle-averaged version, with the substitution

$$\sum_{\text{spins}} |\mathcal{M}|^2 \rightarrow \left\langle \sum_{\text{spins}} |\mathcal{M}|^2 \right\rangle_\theta = \frac{1}{2} \int_{-1}^1 d(\cos\theta) \sum_{\text{spins}} |\mathcal{M}|^2 = 64\pi\sigma_T m_e^2 \quad (3.75)$$

Performing the integral over the three-momentum \mathbf{p}'_e in (3.73)

$$\begin{aligned} \mathcal{C}[f(\mathbf{p})] = & \frac{16\pi^2\sigma_T m_e^2}{p} \int \mathcal{D}p_e \mathcal{D}p' \frac{1}{E(\mathbf{p}'_e)} \delta(p - p' + E(\mathbf{p}_e) - E(\mathbf{p}'_e)) \\ & \times \left[f(\mathbf{p}') f_e(\mathbf{p}'_e) - f(\mathbf{p}) f_e(\mathbf{p}_e) \right]. \end{aligned} \quad (3.76)$$

We introduce the definitions

$$\begin{aligned} \Delta\mathbf{p} = \mathbf{p} - \mathbf{p}', \quad \Delta E = E(\mathbf{p}_e) - E(\mathbf{p}'_e) = E(\mathbf{p}_e) - E(\mathbf{p}_e + \Delta\mathbf{p}), \\ \mathbf{p}'_e = \mathbf{p}_e + \Delta\mathbf{p}, \quad \Delta E' = E(\mathbf{p}_e - \Delta\mathbf{p}) - E(\mathbf{p}_e). \end{aligned} \quad (3.77)$$

All we need to do is to compute two integrals

$$\mathcal{C}[f(\mathbf{p})] = \frac{16\pi^2\sigma_T m_e^2}{p} (I_+ - I_-), \quad (3.78)$$

where

$$\begin{aligned} I_+ & \equiv \int \mathcal{D}p_e \mathcal{D}p' \delta(p - p' + \Delta E) \frac{1}{E(\mathbf{p}'_e)} f_e(\mathbf{p}'_e) f(\mathbf{p}') \\ & = \int \mathcal{D}p_e \mathcal{D}p' \delta(p - p' + \Delta E') \frac{1}{E(\mathbf{p}_e - \Delta\mathbf{p})} f_e(\mathbf{p}_e) f(\mathbf{p}'), \end{aligned} \quad (3.79)$$

$$I_- \equiv \int \mathcal{D}p_e \mathcal{D}p' \delta(p - p' + \Delta E) \frac{1}{E(\mathbf{p}'_e)} f_e(\mathbf{p}_e) f(\mathbf{p}). \quad (3.80)$$

¹¹See [PS95].

Assuming that the energy transfer ΔE is small and expanding to first order we have

$$I_+ = \int \mathcal{D}p_e \mathcal{D}p' f_e(\mathbf{p}_e) f(\mathbf{p}') \frac{1}{E(\mathbf{p}_e)} \left\{ \left(1 - \frac{\Delta E'}{E(\mathbf{p}_e)} \right) \delta(p - p') + \Delta E' \frac{\partial \delta(p - p')}{\partial p} + \mathcal{O}((\Delta E')^2) \right\}, \quad (3.81)$$

$$I_- = \int \mathcal{D}p_e \mathcal{D}p' f_e(\mathbf{p}_e) f(\mathbf{p}') \frac{1}{E(\mathbf{p}_e)} \left\{ \left(1 + \frac{\Delta E}{E(\mathbf{p}_e)} \right) \delta(p - p') + \Delta E \frac{\partial \delta(p - p')}{\partial p} + \mathcal{O}((\Delta E)^2) \right\}. \quad (3.82)$$

Combining them

$$\begin{aligned} I_+ - I_- &= \int \frac{\mathcal{D}p_e \mathcal{D}p'}{E(\mathbf{p}_e)} f_e(\mathbf{p}_e) \left\{ \left(1 - \frac{\Delta E' - \Delta E}{2E(\mathbf{p}_e)} \right) \delta(p - p') \right. \\ &\quad \left. + \frac{\Delta E' + \Delta E}{2} \frac{\partial \delta(p - p')}{\partial p} \right\} \left(f(\mathbf{p}') - f(\mathbf{p}) \right) \\ &\quad + \int \frac{\mathcal{D}p_e \mathcal{D}p'}{E(\mathbf{p}_e)} f_e(\mathbf{p}_e) \left\{ \left(-\frac{\Delta E' + \Delta E}{2E(\mathbf{p}_e)} \right) \delta(p - p') \right. \\ &\quad \left. + \frac{\Delta E' - \Delta E}{2} \frac{\partial \delta(p - p')}{\partial p} \right\} \left(f(\mathbf{p}') + f(\mathbf{p}) \right). \end{aligned} \quad (3.83)$$

Additionally, in the usual NR limit for electrons we have

$$E(\mathbf{p}_e) = m_e + \frac{\mathbf{p}_e^2}{2m_e} + \mathcal{O}(4), \quad (3.84)$$

$$\Delta E' - \Delta E = \frac{\Delta \mathbf{p}^2}{m_e} + \mathcal{O}(4), \quad (3.85)$$

$$\Delta E' + \Delta E = -\frac{2\mathbf{p}_e \cdot \Delta \mathbf{p}}{m_e} + \mathcal{O}(4). \quad (3.86)$$

The only terms from (3.83) that give a contribution to first NR order are

$$I_+ - I_- \simeq \int \frac{\mathcal{D}p_e \mathcal{D}p'}{E(\mathbf{p}_e)} f_e(\mathbf{p}_e) \left\{ \delta(p - p') + \frac{\Delta E' + \Delta E}{2} \frac{\partial \delta(p - p')}{\partial p} \right\} \left(f(\mathbf{p}') - f(\mathbf{p}) \right). \quad (3.87)$$

Substituting in the collision term we have

$$\begin{aligned} \mathcal{C}[f(\mathbf{p})] &= \frac{4\pi^2 \sigma_T}{p} \int \frac{d^3 p_e}{(2\pi)^3} \frac{d^3 p'}{(2\pi)^3} f_e(\mathbf{p}_e) \left\{ \delta(p - p') - \frac{\mathbf{p}_e \cdot \Delta \mathbf{p}}{m_e} \frac{\partial \delta(p - p')}{\partial p} \right\} \\ &\quad \times \left(f(\mathbf{p}') - f(\mathbf{p}) \right). \end{aligned} \quad (3.88)$$

If we define the electron number density and velocity with the *full* distribution

$$n_e^{\text{full}} \equiv 2 \int \frac{d^3 p_e}{(2\pi)^3} f_e(\mathbf{p}_e), \quad n_e \mathbf{u}_e^{\text{full}} \equiv 2 \int \frac{d^3 p_e}{(2\pi)^3} \frac{\mathbf{p}_e}{m_e} f_e(\mathbf{p}_e), \quad (3.89)$$

after some simplifications, we finally obtain

$$\begin{aligned} \mathcal{C}[f(\mathbf{p})] &= \frac{\sigma_T}{4\pi p} \int p' d p' d\Omega \left\{ n_e^{\text{full}} \delta(p - p') \right. \\ &\quad \left. + n_e \mathbf{u}_e^{\text{full}} \cdot (\mathbf{p} - \mathbf{p}') \frac{\partial \delta(p - p')}{\partial p'} \right\} \left(f(\mathbf{p}') - f(\mathbf{p}) \right). \end{aligned} \quad (3.90)$$

Notice that f corresponds to the full photon distribution, i.e. we have not yet expanded in cosmological perturbations. Expanding now to first order in cosmological perturbations, we get

$$\begin{aligned} \mathcal{C}[f(\mathbf{p})] = \frac{n_e \sigma_T}{4\pi p} \int p' d\mathbf{p}' d\Omega' \left\{ \delta(p-p') \left(\delta f(\mathbf{p}') - \delta f(\mathbf{p}) \right) \right. \\ \left. + \delta \mathbf{v}_e \cdot (\mathbf{p} - \mathbf{p}') \frac{\partial \delta(p-p')}{\partial p'} \left(f_0(p') - f_0(p) \right) \right\}. \end{aligned} \quad (3.91)$$

As we anticipated, there is no zero-order (background) contribution. After some simple manipulations, it can be recast as

$$\mathcal{C}[f(\mathbf{p})] = n_e \sigma_T \left\{ \int \frac{d\Omega'}{4\pi} \delta f(p, \hat{n}') - \delta f(p, \hat{n}) + \hat{n} \cdot \delta \mathbf{v}_e f_0(p) \right\}. \quad (3.92)$$

Reintroducing the comoving momenta q_i and integrating out its modulus, we obtain the relevant equation for the evolution of the reduced distribution function (3.58)

$$\frac{1}{\mathcal{N}} \int q^3 dq \mathcal{C}[f(\mathbf{p})] = n_e \sigma_T \left\{ \int \frac{d\Omega'}{4\pi} \mathcal{F}_\gamma(\hat{n}') - \mathcal{F}_\gamma(\hat{n}) + \hat{n} \cdot \delta \mathbf{v}_e \right\}. \quad (3.93)$$

The first two moments of this equation, to match with (3.61) and (3.62), are

$$\frac{1}{\mathcal{N}} \int \frac{d\Omega}{4\pi} \int q^3 dq \mathcal{C}[f(\mathbf{p})] = 0, \quad (3.94)$$

$$\frac{1}{\mathcal{N}} \int \frac{d\Omega}{4\pi} n^i \int q^3 dq \mathcal{C}[f(\mathbf{p})] = -\frac{4}{3} n_e \sigma_T (\delta v_\gamma^i - \delta v_e^i). \quad (3.95)$$

Conserved quantities

We have just computed the collision term *for photons*. However, the whole plasma is described by the coupled system

$$\frac{Df}{dt} = \mathcal{C}[f, f_e], \quad (3.96)$$

$$\frac{Df_e}{dt} = \mathcal{C}_e[f, f_e]. \quad (3.97)$$

We ought to compute the collision term for electrons \mathcal{C}_e as well. Not surprisingly, both terms are not independent. In fact, we can make use of some conservation laws derived from the full Boltzmann equation to save us most of the work. Following [Dod03], we write both collision terms with the compact notation

$$\begin{aligned} c_{e\gamma} = \frac{1}{2} \frac{1}{2E_{p_e}} \frac{1}{2p} \frac{1}{2E_{p'_e}} \frac{1}{2p'} (2\pi)^4 \delta(p^\mu + p_e^\mu - p'^\mu - p_e'^\mu) \\ \times \left[f(\mathbf{p}') f_e(\mathbf{p}'_e) - f(\mathbf{p}) f_e(\mathbf{p}_e) \right] \sum_{\text{spins}} |\mathcal{M}|^2, \end{aligned} \quad (3.98)$$

$$\mathcal{C}_e[f_e(\mathbf{p}_e)] \equiv \int \frac{d^3 p}{(2\pi)^3} \frac{d^3 p'}{(2\pi)^3} \frac{d^3 p'_e}{(2\pi)^3} c_{e\gamma} \equiv \langle c_{e\gamma} \rangle_{pp'p'_e}, \quad (3.99)$$

$$\mathcal{C}[f(\mathbf{p})] \equiv \langle c_{e\gamma} \rangle_{p'p'_ep_e}. \quad (3.100)$$

Integrating over all the momenta, it is easy to see that we have

$$\langle c_{e\gamma} \rangle_{p_e p p'_e p'} = 0, \quad (3.101)$$

$$\langle (\mathbf{p} + \mathbf{E}(\mathbf{p}_e)) c_{e\gamma} \rangle_{p_e p p'_e p'} = 0, \quad (3.102)$$

$$\langle (\mathbf{p} + \mathbf{p}_e) c_{e\gamma} \rangle_{p_e p p'_e p'} = 0, \quad (3.103)$$

corresponding to the conservation of the number of particles, energy and momentum. Using these results, the following equalities hold

$$\int \frac{d^3 p_e}{(2\pi)^3} \mathbf{E}(\mathbf{p}_e) C_e[f_e(\mathbf{p}_e)] = - \int \frac{d^3 p}{(2\pi)^3} p C[f(\mathbf{p})], \quad (3.104)$$

$$\int \frac{d^3 p_e}{(2\pi)^3} \mathbf{p}_e C_e[f_e(\mathbf{p}_e)] = - \int \frac{d^3 p}{(2\pi)^3} \mathbf{p} C[f(\mathbf{p})]. \quad (3.105)$$

This means that we can compute the first two moments of the Boltzmann equation for electrons, the only ones that we need since they are non-relativistic, from the first two moments of the photons, already computed in (3.94) and (3.95).

3.3.3 Boltzmann equation for different components

Photons

The reduced Boltzmann equation for photons is obtained combining the Liouville operator (3.60) and the collision term (3.93). The evolution of the reduced phase-space density is governed by

$$\dot{\mathcal{F}}_\gamma + n^i \partial_i \mathcal{F}_\gamma - 2n^i \partial_i A - 4n^i n^j C_{ij} = an_e \sigma_T [\delta_\gamma - \mathcal{F}_\gamma + 4\hat{n} \cdot \delta \mathbf{v}_b]. \quad (3.106)$$

Since protons and electrons form a single tightly-coupled baryonic fluid, we have substituted $\delta \mathbf{v}_e$ with $\delta \mathbf{v}_b$, the velocity of baryons. The evolution of the fluid variables can be found performing the appropriate angular integrals. The equations for the density, combining (3.61) and (3.94), and the velocity, combining (3.62) and (3.95), are

$$\dot{\delta}_\gamma + \frac{4}{3} \partial_i \delta v_\gamma^i - \frac{4}{3} \delta^{ij} C_{ij} = 0, \quad (3.107)$$

$$\delta \dot{v}_\gamma^i + \frac{1}{4} \partial^i \delta_\gamma + \frac{3}{4} \partial_j \pi_\gamma^{ij} - \frac{1}{2} \partial^i A = -an_e \sigma_T [\delta v_\gamma^i - \delta v_b^i]. \quad (3.108)$$

Baryons

As stated above, since electrons and protons are much more tightly coupled between them than to the photons, they behave as a single baryonic fluid. The evolution of the baryon density can be found using the left-hand side (3.70) and energy conservation (3.104). For the velocity, we must use the left-hand side (3.71) and momentum conservation (3.105). The relevant equations are

$$\dot{\delta}_b + \partial_i \delta v_b^i - \delta^{ij} C_{ij} = 0, \quad (3.109)$$

$$\delta \dot{v}_b^i + \mathcal{H} \delta v_b^i - \frac{1}{2} \partial^i A = \frac{4\rho_\gamma}{3\rho_b} an_e \sigma_T [\delta v_\gamma^i - \delta v_b^i]. \quad (3.110)$$

Neutrinos

Neutrinos are decoupled from the plasma during the period we will be interested in¹². Moreover, since we are neglecting their masses, the equation describing their free-streaming is the same as photons (3.106) without collision term

$$\dot{\mathcal{F}}_\nu + n^i \partial_i \mathcal{F}_\nu - 2n^i \partial_i A - 4n^i n^j C_{ij} = 0. \quad (3.111)$$

The phase-space description of light, massive neutrinos is very complicated [MB95; Les+13]. The effects of neutrino masses cannot be neglected when performing precise (1%) comparisons with observational data. In fact, the measurement of the neutrino masses through their effects on the large-scale structure formation is one of the main scientific goals of different LSS surveys, discussed in Chapter 1. Such a detailed description is beyond the scope of this work and we will stick to massless neutrinos.

Cold dark matter

Cold dark matter behaves as collisionless non-relativistic matter, i.e. it just follows the same equations as baryons without interactions,

$$\dot{\delta}_c + \partial_i \delta v_c^i - \delta^{ij} C_{ij} = 0, \quad (3.112)$$

$$\delta \dot{v}_c^i + \mathcal{H} \delta v_c^i - \frac{1}{2} \partial^i A = 0. \quad (3.113)$$

Total fluid

The total energy-momentum tensor, adding all the components, satisfies a conservation equation

$$T^\mu{}_{\nu;\mu} = 0, \quad (3.114)$$

which is a direct consequence of the Einstein equations. The information encoded in this equation is redundant, i.e. once we evolve all the components it is identically satisfied. However it is advisable to keep in mind that it can be used, in some circumstances, to substitute the evolution equations of one of the components. This conservation law yields the usual continuity and Euler equations, see Section D.4,

$$\dot{\delta} + 3\mathcal{H}(c_s^2 - w)\delta + (1+w)\partial_i (\delta v^i - B^i) + \frac{1}{2}(1+w)\dot{H}^i{}_i = 0, \quad (3.115)$$

$$\delta \dot{v}_i + \mathcal{H}(1-3w)\delta v_i + \frac{\dot{w}}{1+w}\delta v_i + \frac{1}{1+w}\partial_i (c_s^2 \delta) + \frac{1}{1+w}\partial_j \pi^j{}_i - \frac{1}{2}\partial_i A = 0, \quad (3.116)$$

where the different variables are defined in the same way as for the individual components, but using the total energy-momentum tensor, e.g.

$$\delta \equiv \frac{1}{\rho} \sum_s \rho_s \delta_s, \quad (3.117)$$

$$c_s^2 \delta \equiv \frac{1}{\rho} \delta P \equiv \frac{1}{\rho} \sum_s \delta P_s. \quad (3.118)$$

¹²Essentially after BBN, $z < 10^{10}$.

3.4 Harmonic analysis

The system of cosmological perturbations that we have developed so far is linear and, since the background is homogeneous, the only inhomogeneities come from the perturbations. These facts make it natural to turn from real space to Fourier space

$$g(\tau, \mathbf{x}) \rightarrow g(\tau, \mathbf{k}). \quad (3.119)$$

The conventions for the Fourier transform are collected in Appendix A. Unless there is risk of confusion, we will use the same symbol for the Fourier-transformed variables. The spatial derivatives follow a similar rule

$$\partial_i g(\tau, \mathbf{x}) \rightarrow ik_i g(\tau, \mathbf{k}). \quad (3.120)$$

The *homogeneity* of the background allows for a great simplification. The system of cosmological perturbations is transformed from a set of partial differential equations to a system of ordinary ones.

The next sections are mainly devoted to another simplification that arises because of the *isotropy* of the background. This simplification is known as decomposition theorem [KS84; Dod03; Hu04]. It is possible to classify the perturbations according to their behaviour under spatial rotations. In particular, as scalar, vector or tensor perturbations. The decomposition theorem states that if there is no privileged direction, each of these perturbations evolve separately. In Section 3.4.1 we will describe the usual scalar-vector-tensor (SVT) decomposition for the fluid variables and the metric. Sections 3.4.2 and 3.4.3 will cover only the evolution of the scalar mode.

3.4.1 Scalar-vector-tensor decomposition

Any spatial vector, in particular the velocity, can be decomposed into a gradient and a divergenceless part

$$\delta v_i = \partial_i v^S + \chi_i, \quad \partial_i \chi^i = 0, \quad (3.121)$$

where v^S is the scalar part of the velocity and χ is the vector part, i.e. the vorticity. In Fourier space, it can be written as

$$\delta v_i = -\frac{i\hat{k}_i}{k}\theta + \chi_i, \quad \theta \equiv -k^2 v^S. \quad (3.122)$$

A spatial traceless tensor, e.g. the shear tensor, can be decomposed in a similar way

$$\pi_{ij} = \left(\partial_i \partial_j - \frac{1}{3} \delta_{ij} \partial^k \partial_k \right) \pi^S + 2\partial_{(i} \pi_{j)}^V + \pi_{ij}^T, \quad (3.123)$$

where again the vector part π^V is divergenceless and π_{ij}^T is the tensor part, satisfying

$$\partial^i \pi_{ij}^T = 0, \quad \delta^{ij} \pi_{ij}^T = 0. \quad (3.124)$$

Alternatively, we can write it in Fourier space¹³

$$\pi_{ij} = -2 \left(\hat{k}_i \hat{k}_j - \frac{1}{3} \delta_{ij} \right) \sigma + ik \left(\hat{k}_i \pi_j^V + \hat{k}_j \pi_i^V \right) + \pi_{ij}^T, \quad \sigma \equiv \frac{k^2}{2} \pi^S, \quad (3.125)$$

The metric perturbations A , B_i and H_{ij} can be decomposed in a similar way. Adapting the notation of [MFB92] for a generic gauge, the perturbed metric (3.33) can be rewritten as

$$ds^2 = a^2(\tau) \left\{ -(1 + 2\Psi) d\tau^2 + 2(\partial_i B - S_i) dx^i d\tau + \left(\delta_{ij} - 2\Phi \delta_{ij} + 2\partial_i \partial_j E + (\partial_i F_j + \partial_j F_i) + h_{ij} \right) dx^i dx^j \right\}, \quad (3.126)$$

where Ψ , Φ , E and B are scalar perturbations, S and F are vector perturbations, i.e. divergenceless vectors, and h_{ij} is a tensor perturbation, i.e. a divergenceless and traceless tensor. The variables previously defined for a general metric perturbation now take the form

$$A = -2\Psi, \quad (3.127a)$$

$$B_i = \partial_i B - S_i, \quad (3.127b)$$

$$H_{ij} = -2\Phi \delta_{ij} + 2\partial_i \partial_j E + \partial_i F_j + \partial_j F_i + h_{ij}. \quad (3.127c)$$

The scalar perturbations are the origin of the large-scale structure in the Universe and constitute the leading contribution to the temperature anisotropies in the CMB. Before analyzing scalar perturbations in detail we will briefly comment upon the relevance of vector and tensor perturbations in Λ CDM.

There are at least two well grounded reasons to ignore the vector modes in Λ CDM. The first one is that its primordial origin is harder to justify. Inflation is currently the preferred mechanism to explain the origin of primordial perturbations. Quite generically, scalar and tensor perturbations are produced during inflation but most (popular) models do not produce primordial vector perturbations. The second reason to neglect vector perturbations is that, even if initially present, they get diluted with the expansion of the Universe. An easy way to see this is to focus on the equation (3.116) describing the velocity of the total fluid. If we neglect the (small) anisotropic stress and project the velocity into the plane perpendicular to \hat{k} we get the evolution of the vorticity

$$\dot{\chi}_i + \mathcal{H}(1 - 3w)\chi_i + \frac{\dot{w}}{1+w}\chi_i = 0 \quad (3.128)$$

During the matter-dominated era, $w \simeq 0$, we get $\chi_i \propto a^{-1}$. This argument can be generalized to the vorticities of the individual components, but the same conclusion holds: vector modes are suppressed. The key point is that the equations for the vector

¹³Our definition for σ differs slightly from [MB95] as

$$\sigma = \frac{3}{4}(1+w)\sigma_{\text{Ma-Bertschinger}}.$$

It agrees for ultrarelativistic species, like photons and neutrinos.

modes do not contain any metric perturbation so the Einstein equations do not feed back into the fluid equations.

The tensor modes on the other hand are singularly important in modern cosmology. Primordial tensor modes are believed to be produced during inflation with a different spectrum from scalar perturbations. For a given scalar spectrum, currently observable, different inflationary models predict different tensor spectra. One of the objectives of contemporary cosmology is the measurement of this spectrum, since it would allow to discriminate between inflationary models. The amplitude of these primordial modes is currently constrained to be very small [Akr+18b] and its impact is negligible in all the observables that we will consider. Their effects are only important in the polarization of the CMB, that we neglected from the onset in our analysis.

3.4.2 Boltzmann hierarchy

At this point we introduce two new quantities

$$R \equiv \frac{3\rho_b}{4\rho_\gamma}, \quad \tau_c^{-1} \equiv an_e\sigma_T, \quad (3.129)$$

that represent the baryon to photon density ratio and the time scale of Thomson scattering. Considering only scalar perturbations, the evolution of the photon-baryon plasma is described by the following coupled system

$$\begin{aligned} \dot{\mathcal{F}}_\gamma + i(\hat{n} \cdot \mathbf{k})\mathcal{F}_\gamma + 4i(\hat{n} \cdot \mathbf{k})\Psi + 4(\hat{n} \cdot \mathbf{k})^2(B - \dot{E}) - 4\dot{\Phi} \\ = \frac{1}{\tau_c} \left[\delta_\gamma - \mathcal{F}_\gamma - \frac{4i}{k^2}(\hat{n} \cdot \mathbf{k})\theta_b \right], \end{aligned} \quad (3.130)$$

$$\dot{\delta}_b + \theta_b - 3\dot{\Phi} + k^2(B - \dot{E}) = 0, \quad (3.131)$$

$$\dot{\theta}_b + \mathcal{H}\theta_b - k^2\Psi = \frac{1}{R\tau_c} [\theta_\gamma - \theta_b], \quad (3.132)$$

where we have plugged the scalar-vector-tensor decomposition in (3.106), (3.109) and (3.110). Neutrinos and CDM obey the same system of equations but without collisions, i.e. $\sigma_T = 0$. The main obstacle to solve these equations arises from the fact that the reduced photon distribution depends explicitly on the photon direction \hat{n} . One way to overcome this difficulty is to integrate out this dependency, as we did in Section 3.3.3, obtaining equations for the density and velocity

$$\dot{\delta}_\gamma + \frac{4}{3}\theta_\gamma - 4\dot{\Phi} + \frac{4k^2}{3}(B - \dot{E}) = 0, \quad (3.133)$$

$$\dot{\theta}_\gamma - \frac{1}{4}k^2(\delta_\gamma - \sigma_\gamma) - k^2\Psi = -\frac{1}{\tau_c} [\theta_\gamma - \theta_b]. \quad (3.134)$$

There is still one unknown variable σ_γ , i.e. the anisotropic stress of photons, that needs to be fixed to close the system¹⁴. At this point, we can either give it a physically plausible value or compute it dynamically using the Boltzmann equation. We already took the first route with baryons, where we set σ_b to zero based on their NR

¹⁴The metric potentials will be taken care of in the next section.

nature. When the interaction rate is high, the anisotropies are washed out and we can approximately set $\sigma_\gamma \simeq 0$. However, in many important applications, it is necessary to follow all the information encoded in the distribution function. In these cases, we must follow the second route and compute σ_γ dynamically. A further angular integral of the Boltzmann equation, with the structure given by (3.65), is needed. Were we to do this, we would end up with another unknown variable. This is a generic feature of this procedure. This method of solution, based on following the evolution of the moments of the angular distribution, can be systematized as follows.

First, note that all the explicit angular dependencies in (3.130) arise in the combination $\mu \equiv \hat{n} \cdot \mathbf{k}$, since these are the only directions in the problem. Then, the distribution \mathcal{F}_γ only depends on \hat{n} through a parameter μ that varies between -1 and 1 . Under these circumstances, we can expand this angular dependency into a series of Legendre polynomials¹⁵

$$\mathcal{F}_\gamma(\tau, \mathbf{k}, \hat{n}) = \sum_{\ell=0}^{\infty} (-i)^\ell (2\ell + 1) \mathcal{F}_\ell(\tau, \mathbf{k}) P_\ell(\hat{n} \cdot \hat{k}), \quad (3.135)$$

where the prefactors of the expansion are introduced following the convention of [MB95]. Now we can multiply the Boltzmann equation by P_ℓ and integrate over μ , using the orthogonality of the Legendre polynomials to obtain differential equations for the coefficients \mathcal{F}_ℓ . This way we end up with an infinite set of coupled differential equations, the so-called *Boltzmann hierarchy*,

$$\dot{\delta}_\gamma + \frac{4}{3}\theta_\gamma - 4\dot{\Phi} + \frac{4}{3}k^2(B - \dot{E}) = 0, \quad (3.136a)$$

$$\dot{\theta}_\gamma - \frac{1}{4}k^2(\delta_\gamma - 4\sigma_\gamma) - k^2\Psi = -\frac{1}{\tau_c}[\theta_\gamma - \theta_b], \quad (3.136b)$$

$$\dot{\sigma}_\gamma - \frac{4}{15}\theta_\gamma + \frac{3k}{10}\mathcal{F}_3 - \frac{4}{15}k^2(B - \dot{E}) = -\frac{1}{\tau_c}\sigma_\gamma, \quad (3.136c)$$

$$\dot{\mathcal{F}}_\ell - \frac{k}{2\ell + 1}(\ell \mathcal{F}_{\ell-1} - (\ell + 1)\mathcal{F}_{\ell+1}) = -\frac{1}{\tau_c}\mathcal{F}_\ell, \quad (\ell \geq 3). \quad (3.136d)$$

The first three terms are the fluid variables that were defined in (3.63), (3.64) and (3.65) and correspond to the lowest moments

$$\mathcal{F}_0 = \delta, \quad \mathcal{F}_1 = \frac{4\theta}{3k}, \quad \mathcal{F}_2 = 2\sigma. \quad (3.137)$$

The same kind of Boltzmann hierarchy is satisfied by neutrinos.

3.4.3 Truncation

In practice, the infinite Boltzmann hierarchy must be truncated at some ℓ_{\max} . An accurate computation may require $\ell_{\max} = \mathcal{O}(10^3)$. The main effect of the hierarchy structure is to dissipate power at low ℓ , transferring it to the higher moments. The crudest truncation scheme one may think of

$$\mathcal{F}_{\ell_{\max}+1} \simeq 0, \quad (3.138)$$

¹⁵See Appendix C for details.

does not produce this dissipative effect. This leads to spurious growth at high ℓ that is reflected back and affects the results at low ℓ . A better truncation scheme, that introduces dissipation and minimizes the reflection of power from high to low ℓ , was proposed in [MB95]

$$\mathcal{F}_{\ell_{\max}+1} \simeq \frac{2\ell_{\max}+1}{k\tau} \mathcal{F}_{\ell_{\max}} - \mathcal{F}_{\ell_{\max}-1}. \quad (3.139)$$

It is based on the observation that for high ℓ

$$\mathcal{F}_{\ell} \sim j_{\ell}(k\tau), \quad (3.140)$$

where j_{ℓ} is a spherical Bessel function. This can be justified by observing that the differential equation that describes the free streaming for large ℓ , i.e. the left-hand side of (3.136d), is the same as satisfied by j_{ℓ} , see (C.4b). Then, the result (3.139) stems from the properties of the spherical Bessel functions (C.4a).

3.5 Einstein equations and gauge transformations

3.5.1 Einstein equations

The last piece of information needed to close the system can be found in the Einstein equations (1), that describe the evolution of the metric perturbations. The intermediate expressions for the perturbed Einstein tensor are collected in Appendix D. The final results for scalar perturbations are

- (0,0)

$$2k^2\Phi + 6\mathcal{H}(\dot{\Phi} + \mathcal{H}\Psi) - 2k^2\mathcal{H}(B - \dot{E}) = -8\pi G a^2 \delta\rho, \quad (3.141)$$

- (0,i)

$$\dot{\Phi} + \mathcal{H}\Psi = \frac{4\pi G a^2}{k^2} (\rho + P)\theta, \quad (3.142)$$

- (i,j)

$$k^2(\Phi - \Psi) - k^2(\partial_{\tau} + 2\mathcal{H})(B - \dot{E}) = 16\pi G a^2 \rho\sigma, \quad (3.143)$$

$$(\partial_{\tau} + 2\mathcal{H})(\dot{\Phi} + \mathcal{H}\Psi) + \Psi(\dot{\mathcal{H}} - \mathcal{H}^2) = 4\pi G a^2 \left(\delta P - \frac{4}{3}\rho\sigma \right). \quad (3.144)$$

Since the conservation of the total energy-momentum tensor is already built in the equations for the individual components, only two of these four equations are independent. The source terms can be written in terms of the individual components as

$$\delta\rho = \delta\rho_{\gamma} + \delta\rho_b + \delta\rho_{\nu} + \delta\rho_c, \quad (3.145)$$

$$\delta P = \frac{1}{3}(\delta\rho_{\gamma} + \delta\rho_{\nu}), \quad (3.146)$$

$$(\rho + P)\theta = \frac{4}{3}\rho_{\gamma}\theta_{\gamma} + \rho_b\theta_b + \frac{4}{3}\rho_{\nu}\theta_{\nu} + \rho_c\theta_c, \quad (3.147)$$

$$\rho\sigma = \rho_{\gamma}\sigma_{\gamma} + \rho_{\nu}\sigma_{\nu}. \quad (3.148)$$

3.5.2 Gauge transformations

The homogeneity and isotropy of the background define a class of privileged observers: those that observe a RW metric (3.1). Once we consider a perturbed FLRW universe, we split the metric into a RW background and a general perturbation (3.33). However, this splitting is not unique. If we take a new coordinate system

$$\tilde{x}^\mu = x^\mu + \epsilon^\mu, \quad \epsilon \ll 1, \quad (3.149)$$

the background in these coordinates is the same (RW), but now the splitting into background and perturbations is different

$$ds^2 = a^2(\tilde{\tau}) \left(-(1 - \tilde{A}) d\tilde{\tau}^2 + 2\tilde{B}_i d\tilde{\tau} d\tilde{x}^i + (\delta_{ij} + \tilde{H}_{ij}) d\tilde{x}^i d\tilde{x}^j \right). \quad (3.150)$$

These infinitesimal coordinate transformations are known in cosmology as *gauge transformations*. This raises another problem: how do we distinguish between a genuine metric perturbation and a mere coordinate transformation? One possibility is to construct combinations of variables that are gauge-invariant and then free from this ambiguity, see [Bar80; KS84; MFB92; BDE92]. Another possibility is to fix the gauge and perform all the computations in a given coordinate system. In either case, we first need to know how to relate the perturbations in two different gauges.

After an infinitesimal gauge transformation

$$\Delta x^\mu = \epsilon^\mu, \quad \epsilon^\mu \equiv \left(T(\tau, \mathbf{x}), L(\tau, \mathbf{x}) \right), \quad (3.151)$$

a generic tensor $T_{\mu\nu}$ changes as¹⁶

$$\Delta T_{\mu\nu} = \epsilon^\rho \partial_\rho T_{\mu\nu} + T_{\rho\nu} \partial_\mu \epsilon^\rho + T_{\mu\rho} \partial_\nu \epsilon^\rho. \quad (3.152)$$

Notice that, since ϵ^μ is infinitesimal, only the background part of $T_{\mu\nu}$ contributes to the right-hand side of (3.152). Applying this rule to the metric tensor $g_{\mu\nu}$, we get

$$\Delta A = -2(\dot{T} + \mathcal{H}T), \quad (3.153a)$$

$$\Delta B_i = \dot{L}_i - \partial_i T, \quad (3.153b)$$

$$\Delta H_{ij} = 2\mathcal{H}T\delta_{ij} + \partial_i L_j + \partial_j L_i. \quad (3.153c)$$

The components of the full energy-momentum tensor with lower indices are

$$a^2 T_{00} = \rho + \delta\rho - A\rho, \quad (3.154a)$$

$$a^2 T_{0i} = -\delta Q_i - B_i P, \quad (3.154b)$$

$$a^2 T_{ij} = P\delta_{ij} + \delta P\delta_{ij} + \delta\Pi_{ij} + H_{ij}P. \quad (3.154c)$$

The equation (3.152) then yields

$$\Delta\delta\rho = T\dot{\rho}, \quad (3.155a)$$

$$\Delta\delta Q_i = -(\rho + P)\partial_i T, \quad (3.155b)$$

$$\Delta\delta P = T\dot{P}, \quad (3.155c)$$

$$\Delta\delta\Pi_{ij} = 0. \quad (3.155d)$$

¹⁶Note that this is just the Lie derivative $\mathcal{L}_\epsilon T_{\mu\nu}$. More details can be found in [DN13].

It can be checked that the vector and tensor perturbations to the fluid variables are gauge-invariant. The transformation rule for a four vector is

$$\Delta N^\mu = \epsilon^\rho \partial_\rho N^\mu - N^\rho \partial_\rho \epsilon^\mu . \quad (3.156)$$

Taking for instance the particle flux (2.109)

$$N^0 = n + \delta n + \frac{1}{2} n A , \quad (3.157a)$$

$$N^i = \delta V^i - n B^i , \quad (3.157b)$$

we get

$$\Delta \delta n = T \dot{n} + n \mathcal{H} T , \quad (3.158a)$$

$$\Delta \delta V^i = -n \delta^i T . \quad (3.158b)$$

3.5.3 Newtonian and synchronous gauge

The gauge-transformation properties of the metric perturbation (3.153) can be rewritten in terms of the scalar-vector-tensor decomposition (3.126) as

$$\begin{aligned} \Delta \Psi &= \dot{T} + \mathcal{H} T , & \Delta S_i &= -(\delta_{ij} - \hat{k}_i \hat{k}_j) \dot{L}^j , \\ \Delta B &= -\frac{i}{k} \hat{k} \cdot \dot{\mathbf{L}} - T , & \Delta F_i &= (\delta_{ij} - \hat{k}_i \hat{k}_j) L^j , \\ \Delta \Phi &= -\mathcal{H} T , & \Delta h_{ij} &= 0 , \\ \Delta E &= -\frac{i}{k} \hat{k} \cdot \mathbf{L} . \end{aligned} \quad (3.159)$$

Tensor perturbations are gauge-invariant. Even though vector perturbations are not gauge invariant, the combination that appears in the Einstein equations, $(S_i - \dot{F}_i)$, is gauge-invariant. The gauge dependency of scalar perturbations is a problem that must be dealt with. One way to proceed is to fix the gauge, i.e. to give a prescription for T and \mathbf{L} . The most widely used gauges in cosmology are the Newtonian (or longitudinal) and the synchronous gauge.

- *Newtonian gauge.* It is defined by

$$B = E = 0 . \quad (3.160)$$

The two remaining variables Φ and Ψ play the role of the Newtonian potential.

- *Synchronous gauge.* It is defined by

$$\Psi = B = 0 . \quad (3.161)$$

It is customary to take as independent metric variables h and η , defined as

$$\Phi = \eta , \quad (3.162a)$$

$$E = -\frac{1}{2k^2} (h + 6\eta) . \quad (3.162b)$$

It is very easy to obtain the Einstein equations in the Newtonian gauge. Since we will use the synchronous gauge later on, it is useful to rewrite the Einstein equations in this gauge

$$\dot{h} - \frac{2k^2\eta}{\mathcal{H}} = 3\mathcal{H}\delta, \quad (3.163a)$$

$$\dot{\eta} = \frac{3\mathcal{H}^2}{2k^2}(1+w)\theta, \quad (3.163b)$$

$$\ddot{h} + 6\dot{\eta} + 2\mathcal{H}(\dot{h} + 6\dot{\eta}) - 2k^2\eta = -12\mathcal{H}^2\sigma, \quad (3.163c)$$

$$\ddot{h} + \mathcal{H}\dot{h} = -3(1+3c_s^2)\mathcal{H}^2\delta, \quad (3.163d)$$

where $c_s^2\delta$ is defined in (3.118) and we have used the Friedmann equation (3.4). The Newtonian gauge is convenient to obtain analytical expressions and easier to interpret but the synchronous gauge is better suited for numerical integration. It is convenient to be able to change between both gauges. From the gauge-transformation properties of the metric variables, we have

$$\Psi = \dot{T} + \mathcal{H}T, \quad (3.164a)$$

$$0 = -\frac{i}{k}\hat{k}\cdot\dot{\mathbf{L}} - T, \quad (3.164b)$$

$$\Phi - \eta = -\mathcal{H}T, \quad (3.164c)$$

$$\frac{1}{2k^2}(h + 6\eta) = -\frac{i}{k}\hat{k}\cdot\mathbf{L}. \quad (3.164d)$$

That can be solved to yield

$$T = \frac{1}{2k^2}(\dot{h} + 6\dot{\eta}), \quad (3.165a)$$

$$\Psi = \dot{T} + \mathcal{H}T, \quad (3.165b)$$

$$\Phi = \eta - \mathcal{H}T. \quad (3.165c)$$

This T can be used to reconstruct the Newtonian potentials and to transform the fluid variables from the synchronous to the Newtonian gauge, according to

$$\delta(\text{Newt}) - \delta(\text{Syn}) = T\frac{\dot{\rho}}{\rho}, \quad (3.166a)$$

$$\theta(\text{Newt}) - \theta(\text{Syn}) = k^2T, \quad (3.166b)$$

$$\delta P(\text{Newt}) - \delta P(\text{Syn}) = T\dot{P}, \quad (3.166c)$$

$$\sigma(\text{Newt}) - \sigma(\text{Syn}) = 0. \quad (3.166d)$$

3.6 Approximation schemes

There are regimes in the history of the cosmological perturbations where it is possible to introduce an approximate description. The purpose of these approximations is two-fold. On the one hand, under the right physical conditions a simplified, while accurate, description allows us to grasp better the underlying physics of the problem. On the other hand, approximation schemes are unavoidable once we try to

find numerical solutions. Cosmological Boltzmann codes [LCL00; Dor05; BLT11] must rely on a number of approximations to achieve accurate and *fast* computations. Here we will discuss the tight-coupling approximation (TCA), which is important at early times, and the radiation-streaming approximation (RSA), which is important at late times.

3.6.1 Tight coupling

At early times, the time scale of Thomson scattering, $\tau_c \equiv (an_e\sigma_T)^{-1}$, is much shorter than the time scales of evolution of the background, \mathcal{H}^{-1} , or the perturbations, k^{-1} . In this regime, the photon-baryon system becomes computationally hard to solve, since it involves widely different scales. However, we can find approximate expressions to follow the evolution by expanding perturbatively in the small parameter τ_c . This is known as the tight-coupling approximation. We will derive only the lowest order in this expansion. Higher order terms, and the procedure to obtain them systematically, can be found in [BLT11].

The main objective is to compute the velocity difference between baryons and photons when $\tau_c \ll 1$. We need to find an expression correct up to first order and then plug it in (3.136b) to obtain an equation valid to zero order in τ_c . We introduce the definitions

$$\Delta\theta \equiv \theta_\gamma - \theta_b, \quad \mathcal{A} \equiv \frac{R}{1+R}. \quad (3.167)$$

The first step is to get an expression for σ_γ . Its evolution equation (3.136c) can be rewritten as

$$\begin{aligned} \sigma_\gamma &= \frac{4}{15}\tau_c \left(\theta_\gamma - \frac{9k}{8}\mathcal{F}_3 + k^2(B - \dot{E}) \right) - \tau_c \dot{\sigma}_\gamma \\ &= \frac{4}{15}\tau_c \left(\theta_\gamma - \frac{9k}{8}\mathcal{F}_3 + k^2(B - \dot{E}) \right) - \frac{4}{15}\tau_c^2 \left(\dot{\theta}_\gamma - \frac{9k}{8}\dot{\mathcal{F}}_3 \right) + \mathcal{O}(\tau_c^2) \\ &= \frac{4}{15}\tau_c \left(\theta_\gamma - \frac{9k}{8}\mathcal{F}_3 + k^2(B - \dot{E}) \right) + \frac{4}{15}\tau_c \left(\Delta\theta + \frac{9k}{8}\mathcal{F}_3 \right) + \mathcal{O}(\tau_c^2). \end{aligned} \quad (3.168)$$

All we need to know for our purposes is that $\sigma_\gamma = \mathcal{O}(\tau_c)$, but using the same argument it is possible to prove that \mathcal{F}_ℓ for $\ell > 2$ are suppressed by even higher powers of τ_c . Next, if we subtract the equations for the velocity of baryons (3.132) and photons (3.136b), we end up with a differential equation for $\Delta\theta$

$$\Delta\dot{\theta} - \mathcal{H}\theta_b - \frac{1}{4}k^2(\delta_\gamma - 4\sigma_\gamma) = -\frac{1}{\mathcal{A}\tau_c}\Delta\theta. \quad (3.169)$$

Following the previous derivation, it can be recast as

$$\begin{aligned} \Delta\theta &= \mathcal{A}\tau_c \left(\mathcal{H}\theta_b + \frac{1}{4}k^2(\delta_\gamma - 4\sigma_\gamma) \right) - \mathcal{A}\tau_c \Delta\dot{\theta} \\ &= \mathcal{A}\tau_c \left(\mathcal{H}\theta_b + \frac{1}{4}k^2(\delta_\gamma - 4\sigma_\gamma) \right) - (\mathcal{A}\tau_c)^2 (\mathcal{H}\dot{\theta}_b - k^2\dot{\sigma}_\gamma) + \mathcal{O}(\tau_c^2) \\ &= \mathcal{A}\tau_c \left(\mathcal{H}\theta_b + \frac{1}{4}k^2(\delta_\gamma - 4\sigma_\gamma) \right) - \mathcal{A}^2\tau_c \left(\frac{1}{R}\mathcal{H}\Delta\theta + k^2\sigma_\gamma \right) + \mathcal{O}(\tau_c^2). \end{aligned} \quad (3.170)$$

Our final result to first order in τ_c is

$$\Delta\theta = \mathcal{A}\tau_c \left(\mathcal{H}\theta_\gamma + \frac{1}{4}k^2\delta_\gamma \right) + \mathcal{O}(\tau_c^2) . \quad (3.171)$$

We can plug this result back into the photon-baryon system. To zero order in the tight-coupling expansion, the photon-baryon plasma can be described by

$$\dot{\delta}_\gamma + \frac{4}{3}\theta_\gamma - 4\dot{\Phi} + \frac{4}{3}k^2(B - \dot{E}) = 0 , \quad (3.172)$$

$$\dot{\delta}_b + \theta_\gamma - 3\dot{\Phi} + k^2(B - \dot{E}) = 0 , \quad (3.173)$$

$$\dot{\theta}_\gamma + \mathcal{A}\mathcal{H}\theta_\gamma + \frac{k^2}{4}(\mathcal{A} - 1)\delta_\gamma - k^2\Psi = 0 , \quad (3.174)$$

where σ_γ and all higher moments of the photon distribution are set to zero.

3.6.2 Radiation streaming

At late times, photons and neutrinos are decoupled and start oscillating fast. In this case, it is time consuming to follow accurately every oscillation but it is not needed in most applications. Since the ultrarelativistic species at late times make a negligible contribution to the metric potentials, we only need to capture the broadest features of their evolution.

In general, the evolution equations for collisionless ultrarelativistic species, like neutrinos, can be combined into a second-order differential equation

$$\ddot{\delta}_\nu + \frac{k^2}{3}(\delta_\nu - 4\sigma_\nu) + \frac{4}{3}k^2\Psi + \frac{4}{3}k^2(\dot{B} - \ddot{E}) - 4\ddot{\Phi} = 0 . \quad (3.175)$$

As can be seen, when the perturbations are sub-Hubble ($k \gg \mathcal{H}$) the density is highly oscillating. During matter domination, it is possible to ignore the contribution of ultrarelativistic species to the total density but their contribution to the total velocity is still important. The radiation-streaming approximation consists on following only the non-oscillatory particular solution of the system [Dor05; BLT11]. In most realistic scenarios $|\sigma_\nu| \ll |\delta_\nu|$, so we can set $\sigma_\nu \simeq 0$. Then, the particular solution of (3.175) is

$$\delta_\nu \simeq -4\Psi - 4(\dot{B} - \ddot{E}) + \frac{4}{3k^2}\ddot{\Phi} . \quad (3.176)$$

Plugging this result in the first-order differential equation for the density, we get

$$\begin{aligned} \theta_\nu &= -k^2(B - \dot{E}) + 3\dot{\Phi} - \frac{3}{4}\dot{\delta}_\nu \\ &\simeq -k^2(B - \dot{E}) + 3(\dot{\Phi} + \dot{\Psi}) + 3(\ddot{B} - \ddot{E}) - \frac{1}{k^2}\ddot{\Phi} \\ &\simeq -k^2(B - \dot{E}) + 3(\dot{\Phi} + \dot{\Psi}) . \end{aligned} \quad (3.177)$$

These expressions reproduce the ones found in [Dor05] and [BLT11] in the Newtonian and synchronous gauge, respectively. In these references, RSA is justified in detail, making reference to specific results for each gauge.

3.7 Initial conditions

The last ingredients needed to evolve the system of cosmological perturbations are the initial conditions. These must be chosen carefully. As we will see, the initial value of each variable cannot be set arbitrarily. Upon imposing the Einstein and fluid equations, only some initial conditions are free. These free initial values are the so-called *modes* of the system. The modes of this system have been extensively studied and identified over the years. There are five growing modes: the so-called adiabatic mode plus four isocurvature solutions.

The programme for the derivation of the initial conditions is:

- We assume that the perturbations are in the tightly coupled regime so we can use (3.172), (3.173) and (3.174) for the photon-baryon plasma. For simplicity, we also neglect $\mathcal{F}_{\nu 3} \simeq 0$ and every other higher moment of the neutrino distribution. This introduces a small difference in the initial condition for σ_ν with respect to other analysis like [BMT00], that is not important for our purposes.
- We are in an approximately radiation-dominated era so we can use (3.16) and (3.17) for the Hubble parameter and the scale factor and expand them in powers of τ/τ_m .
- We are looking for regular solutions while the perturbations are super-Hubble, so we expand every variable as a power series in τ . Namely, for the photon density,

$$\delta_\gamma = C_{\delta_\gamma}^{(0)} + C_{\delta_\gamma}^{(1)}\tau + C_{\delta_\gamma}^{(2)}\tau^2 + \dots \quad (3.178)$$

- We plug these expansions into the Einstein and fluid equations, solving order by order in τ the system of algebraic equations for the constants $C^{(n)}$.
- For the purposes of this work, we substitute the equations for the evolution of CDM, (3.112) and (3.113), with those of the total fluid, (3.115) and (3.116).
- We work in the synchronous gauge.

3.7.1 Super-Hubble expansion

To start with, we introduce some short-hand definitions

$$S_{\gamma\nu} \equiv \Omega_\gamma + \Omega_\nu, \quad (3.179)$$

$$\mathcal{R}_s \equiv \Omega_s/S_{\gamma\nu}, \quad s = \gamma, \nu, b, c, \quad (3.180)$$

$$\mathcal{R}_{bc} \equiv \mathcal{R}_b + \mathcal{R}_c. \quad (3.181)$$

The Hubble parameter (3.16) can be expanded during radiation domination

$$\mathcal{H} = \frac{1}{\tau} + \frac{H_0 \mathcal{R}_{bc} \sqrt{S_{\gamma\nu}}}{4} - \frac{H_0^2 \mathcal{R}_{bc}^2 S_{\gamma\nu} \tau}{16} + \mathcal{O}(H_0^2 \mathcal{R}_{bc}^2 S_{\gamma\nu} \tau^2), \quad (3.182)$$

$$\mathcal{H}^2 = \frac{1}{\tau^2} + \frac{H_0 \mathcal{R}_{bc} \sqrt{S_{\gamma\nu}}}{2\tau} - \frac{H_0^2 \mathcal{R}_{bc}^2 S_{\gamma\nu}}{16} + \mathcal{O}(H_0^2 \mathcal{R}_{bc}^2 S_{\gamma\nu} \tau^2), \quad (3.183)$$

$$\dot{\mathcal{H}} = -\frac{1}{\tau^2} - \frac{H_0^2 \mathcal{R}_{bc}^2 S_{\gamma\nu}}{16} + \frac{H_0^3 \mathcal{R}_{bc}^3 S_{\gamma\nu}^{\frac{3}{2}} \tau}{32} + \mathcal{O}(H_0^2 \mathcal{R}_{bc}^2 S_{\gamma\nu} \tau^2). \quad (3.184)$$

For the sake of clarity, we present here the full system of equations describing the perturbations during TC in the synchronous gauge. The densities evolve according to

$$\dot{\delta}_\gamma + \frac{4}{3}\theta_\gamma + \frac{2}{3}\dot{h} = 0, \quad (3.185)$$

$$\dot{\delta}_\nu + \frac{4}{3}\theta_\nu + \frac{2}{3}\dot{h} = 0, \quad (3.186)$$

$$\dot{\delta}_b + \theta_\gamma + \frac{1}{2}\dot{h} = 0, \quad (3.187)$$

$$\dot{\delta} + 3\mathcal{H}(c_s^2 - w)\delta + (1+w)\theta + \frac{1}{2}(1+w)\dot{h} = 0. \quad (3.188)$$

The baryon velocity follows the photon velocity, to zero order in TCA, so there are only three equations for the velocities

$$\dot{\theta}_\gamma + \frac{k^2}{4}(\mathcal{A} - 1)\delta_\gamma + \mathcal{A}\mathcal{H}\theta_\gamma = 0, \quad (3.189)$$

$$\dot{\theta}_\nu - \frac{k^2}{4}(\delta_\nu - 4\sigma_\nu) = 0, \quad (3.190)$$

$$\dot{\theta} + (1 - 3w)\mathcal{H}\theta + \frac{\dot{w}}{1+w}\theta - \frac{k^2}{1+w}c_s^2\delta + \frac{4k^2}{3(1+w)}\sigma = 0. \quad (3.191)$$

The neutrinos are the only significant source of anisotropic stress

$$\dot{\sigma}_\nu - \frac{4}{15}\theta_\nu - \frac{2}{15}(\dot{h} + 6\dot{\eta}) = 0. \quad (3.192)$$

The metric variables are described by the Einstein equations (3.163a–3.163d) whose sources are the variables of the total fluid: (3.188), (3.191) and

$$c_s^2\delta = \frac{\mathcal{R}_\gamma\delta_\gamma + \mathcal{R}_\nu\delta_\nu}{3(1 + a\mathcal{R}_{bc})}, \quad (3.193)$$

$$\sigma = \frac{\mathcal{R}_\nu\sigma_\nu}{1 + a\mathcal{R}_{bc}}. \quad (3.194)$$

Finally, plugging the expansions (3.178) into the previous equations and the Einstein equations we find the constants $C^{(n)}$ order by order.

$$C_{\delta\gamma}^{(0)} = C_{\delta\gamma}^{(0)}, \quad C_{\delta\gamma}^{(1)} = -\frac{2C_h^{(1)}}{3} - \frac{4C_{\theta\gamma}^{(0)}}{3}, \quad (3.195)$$

$$C_{\delta\nu}^{(0)} = \frac{C_{\delta\gamma}^{(0)}(\mathcal{R}_\nu - 1)}{\mathcal{R}_\nu}, \quad C_{\delta\nu}^{(1)} = -\frac{2C_h^{(1)}}{3} - \frac{4C_{\theta\gamma}^{(0)}(\mathcal{R}_\nu - 1)}{3\mathcal{R}_\nu}, \quad (3.196)$$

$$C_{\delta b}^{(0)} = C_{\delta b}^{(0)}, \quad C_{\delta b}^{(1)} = -\frac{C_h^{(1)}}{2} - C_{\theta\gamma}^{(0)}, \quad (3.197)$$

$$C_\delta^{(0)} = 0, \quad C_\delta^{(1)} = \frac{C_h^{(1)}}{3}. \quad (3.198)$$

$$C_{\delta\gamma}^{(2)} = \frac{C_h^{(1)}H_0\sqrt{S_{\gamma\nu}}\mathcal{R}_{bc}}{4} + \frac{C_{\theta\gamma}^{(0)}H_0\sqrt{S_{\gamma\nu}}\mathcal{R}_b(\mathcal{R}_\nu - 3)}{4(\mathcal{R}_\nu - 1)} - \frac{k^2(C_{\delta\gamma}^{(0)} + 2C_\eta^{(0)})}{6}, \quad (3.199)$$

$$C_{\delta\nu}^{(2)} = -\frac{C_{\delta\gamma}^{(0)}k^2(\mathcal{R}_\nu - 1)}{6\mathcal{R}_\nu} - \frac{C_\eta^{(0)}k^2}{3} + \frac{C_h^{(1)}H_0\sqrt{S_{\gamma\nu}}\mathcal{R}_{bc}}{4} + \frac{C_{\theta\gamma}^{(0)}H_0\sqrt{S_{\gamma\nu}}\mathcal{R}_b}{4}, \quad (3.200)$$

$$C_{\delta b}^{(2)} = \frac{3C_h^{(1)}H_0\sqrt{S_{\gamma\nu}}\mathcal{R}_{bc}}{16} + \frac{3C_{\theta\gamma}^{(0)}H_0\sqrt{S_{\gamma\nu}}\mathcal{R}_b(\mathcal{R}_\nu - 3)}{16(\mathcal{R}_\nu - 1)} - \frac{k^2(C_{\delta\gamma}^{(0)} + 2C_\eta^{(0)})}{8}, \quad (3.201)$$

$$C_\delta^{(2)} = -\frac{C_\eta^{(0)}k^2}{3} - \frac{H_0\sqrt{S_{\gamma\nu}}(4C_h^{(1)}\mathcal{R}_{bc} + 3C_{\theta\gamma}^{(0)}\mathcal{R}_b)}{12}. \quad (3.202)$$

$$C_{\theta\gamma}^{(0)} = C_{\theta\gamma}^{(0)}, \quad C_{\theta\gamma}^{(1)} = \frac{C_{\delta\gamma}^{(0)}k^2}{4} + \frac{3C_{\theta\gamma}^{(0)}H_0\sqrt{S_{\gamma\nu}}\mathcal{R}_b}{4(\mathcal{R}_\nu - 1)}, \quad (3.203)$$

$$C_{\theta\nu}^{(0)} = \frac{C_{\theta\gamma}^{(0)}(\mathcal{R}_\nu - 1)}{\mathcal{R}_\nu}, \quad C_{\theta\nu}^{(1)} = \frac{C_{\delta\gamma}^{(0)}k^2(\mathcal{R}_\nu - 1)}{4\mathcal{R}_\nu}, \quad (3.204)$$

$$C_\theta^{(0)} = 0, \quad C_\theta^{(1)} = 0. \quad (3.205)$$

$$C_{\theta\gamma}^{(2)} = \frac{C_{\theta\gamma}^{(0)}(9H_0^2S_{\gamma\nu}\mathcal{R}_b(3\mathcal{R}_b + \mathcal{R}_{bc}(\mathcal{R}_\nu - 1)) - 8k^2(\mathcal{R}_\nu - 1)^2)}{48(\mathcal{R}_\nu - 1)^2} + \frac{k^2(9C_{\delta\gamma}^{(0)}H_0\sqrt{S_{\gamma\nu}}\mathcal{R}_b - 4C_h^{(1)}(\mathcal{R}_\nu - 1))}{48(\mathcal{R}_\nu - 1)}, \quad (3.206)$$

$$C_{\theta\nu}^{(2)} = -\frac{k^2(C_h^{(1)}\mathcal{R}_\nu(4\mathcal{R}_\nu + 5) + 2C_{\theta\gamma}^{(0)}(\mathcal{R}_\nu - 1)(4\mathcal{R}_\nu + 9))}{12\mathcal{R}_\nu(4\mathcal{R}_\nu + 5)}, \quad (3.207)$$

$$C_\theta^{(2)} = -\frac{k^2(C_h^{(1)}(4\mathcal{R}_\nu + 5) + 8C_{\theta\gamma}^{(0)}(\mathcal{R}_\nu - 1))}{12(4\mathcal{R}_\nu + 5)}. \quad (3.208)$$

$$C_{\sigma\nu}^{(0)} = 0, \quad (3.209)$$

$$C_{\sigma\nu}^{(1)} = \frac{4C_{\theta\gamma}^{(0)}(\mathcal{R}_\nu - 1)}{3\mathcal{R}_\nu(4\mathcal{R}_\nu + 5)}, \quad (3.210)$$

$$C_{\sigma\nu}^{(2)} = \frac{4C_{\theta\gamma}^{(0)}H_0\sqrt{S_{\gamma\nu}}(\mathcal{R}_\nu - 1)(\mathcal{R}_b + \mathcal{R}_c)}{(4\mathcal{R}_\nu + 5)(4\mathcal{R}_\nu + 15)} + \frac{k^2(3C_{\delta\gamma}^{(0)}(\mathcal{R}_\nu - 1) + 4C_\eta^{(0)}\mathcal{R}_\nu)}{6\mathcal{R}_\nu(4\mathcal{R}_\nu + 15)}. \quad (3.211)$$

$$C_\eta^{(0)} = C_\eta^{(0)}, \quad C_\eta^{(1)} = -\frac{C_h^{(1)}}{6} - \frac{4C_{\theta\gamma}^{(0)}(\mathcal{R}_\nu - 1)}{3(4\mathcal{R}_\nu + 5)}, \quad (3.212)$$

$$C_h^{(0)} = C_h^{(0)}, \quad C_h^{(1)} = C_h^{(1)}. \quad (3.213)$$

$$C_\eta^{(2)} = -\frac{C_{\delta\gamma}^{(0)}k^2(\mathcal{R}_\nu - 1)}{6(4\mathcal{R}_\nu + 15)} - \frac{C_\eta^{(0)}k^2(4\mathcal{R}_\nu + 5)}{12(4\mathcal{R}_\nu + 15)} + \frac{C_h^{(1)}H_0\sqrt{S_{\gamma\nu}}\mathcal{R}_{bc}}{16} + \frac{C_{\theta\gamma}^{(0)}H_0\sqrt{S_{\gamma\nu}}(\mathcal{R}_b(4\mathcal{R}_\nu + 5)(4\mathcal{R}_\nu + 15) + 80\mathcal{R}_{bc}(\mathcal{R}_\nu - 1))}{16(4\mathcal{R}_\nu + 5)(4\mathcal{R}_\nu + 15)}, \quad (3.214)$$

$$C_h^{(2)} = \frac{C_\eta^{(0)}k^2}{2} - \frac{3H_0\sqrt{S_{\gamma\nu}}(C_h^{(1)}\mathcal{R}_{bc} + C_{\theta\gamma}^{(0)}\mathcal{R}_b)}{8}. \quad (3.215)$$

There are five free constants that represent the five independent modes: adiabatic ($C_\eta^{(0)}$), baryon isocurvature ($C_{\delta_b}^{(0)}$), CDM isocurvature (a combination of $C_h^{(1)}$ and $C_{\delta_b}^{(0)}$), neutrino density isocurvature ($C_{\delta_\gamma}^{(0)}$) and neutrino velocity isocurvature ($C_{\theta_\gamma}^{(0)}$). The fact that we have used ($C_h^{(1)}, C_{\delta_\gamma}^{(0)}, C_{\theta_\gamma}^{(0)}$) instead of the traditional ($C_{\delta_c}^{(0)}, C_{\delta_v}^{(0)}, C_{\theta_v}^{(0)}$) is a matter of convention.

3.7.2 Adiabatic mode

Λ CDM only takes into account the adiabatic mode. It is conventional to write it in terms of a *primordial curvature perturbation*¹⁷ $\mathcal{R}_\mathbf{k}$,

$$C_\eta^{(0)} = \frac{4\mathcal{R}_v + 15}{4\mathcal{R}_v + 10} \mathcal{R}_\mathbf{k}. \quad (3.216)$$

The description of the Universe we are aiming at does not include the prediction of the positions of every single galaxy. Our final objective is to predict average quantities, e.g. the statistical distribution of galaxies. It is assumed that the initial conditions $\mathcal{R}_\mathbf{k}$ are stochastic in nature and that the Universe we live in is just one realization of many possible, corresponding to particular choices of $\mathcal{R}_\mathbf{k}$. The ensemble average¹⁸ over such possible realizations is denoted as $\langle \dots \rangle$. These variables are taken to be Gaussian¹⁹ so different \mathbf{k} modes are uncorrelated. The primordial curvature spectrum is defined as

$$\langle \mathcal{R}_\mathbf{k} \mathcal{R}_{\mathbf{k}'}^* \rangle \equiv (2\pi)^3 \delta(\mathbf{k} - \mathbf{k}') P_{\mathcal{R}}(k) \quad (3.217)$$

$$\equiv (2\pi)^3 \delta(\mathbf{k} - \mathbf{k}') \frac{2\pi^2}{k^3} \mathcal{P}_{\mathcal{R}}(k), \quad (3.218)$$

where $\mathcal{P}_{\mathcal{R}}$ is the nearly scale-invariant primordial spectrum parameterized as

$$\mathcal{P}_{\mathcal{R}}(k) = A_s \left(\frac{k}{k_*} \right)^{n_s - 1}. \quad (3.219)$$

The amplitude A_s and tilt n_s of this spectrum are two of the six fundamental parameters of Λ CDM and encode all the information about the initial conditions in this model. The latest *Planck* values are collected in Table 1.1, with the pivot scale $k_* = 0.05 \text{ Mpc}^{-1}$.

The system of cosmological perturbations is a system of linear differential equations. A generic cosmological perturbation $g(\tau, \mathbf{k})$ can be written as a product of

¹⁷The curvature perturbation is usually defined as the gauge-invariant combination $\mathcal{R} = \Phi + \mathcal{H}/k^2 \theta$. Another common definition is $\zeta = \Phi - \delta/3(1+w)$. Both agree on super-Hubble scales.

¹⁸This discussion begs the question: how can we possibly measure an ensemble average with *one* realization? A complete answer to this question is beyond the scope of the present work. We refer the reader to [LL00] and to the thorough discussion in [Wei08] for more details. Essentially one can rely in the ergodic theorem to substitute ensemble averages by spatial averages, over different regions in the sky. Another interesting point, briefly touched upon in [Wei08], is how the expectation values of primordial vacuum fluctuations are finally related with ensemble averages of classical variables $\mathcal{R}_\mathbf{k}$. See also [PS96].

¹⁹This is not only one of the simplest choices, but supported by the preferred mechanism of generation of primordial perturbations: as vacuum expectation values of nearly free fields.

a primordial perturbation, encoding the initial condition, and a transfer function, encoding the subsequent evolution,

$$g(\tau, \mathbf{k}) = T_g(\tau, k) \mathcal{R}_{\mathbf{k}} . \quad (3.220)$$

Since the system is linear, it can be recast into a system for the evolution of the transfer functions with the substitution $g \rightarrow T_g$. It is common practice to abuse slightly of the notation, denoting T_g as g , the perturbation itself, and solving the system as if it had initial conditions $\mathcal{R}_{\mathbf{k}} = 1$. The information about the initial conditions is recovered later, in the computation of the physical spectra, by convolving the transfer function with the primordial spectrum (3.219).

3.8 Line-of-sight integration

At this stage, we have developed a formalism that allows us to follow the evolution of the perturbations from the moment they were generated to the present day. Formally, we have all the ingredients needed for the computation of observables. However, in this section we will linger a bit more on the theoretical side, introducing a technique that was a milestone in the history of CMB computations: the line-of-sight integration.

The main drawback of the formalism presented so far is that it demands the solution of a large number of coupled differential equations. This number can be reduced introducing approximations, motivated by the kind of information we are after and the targeted accuracy. Regardless of the approximation techniques used, for an accurate computation of the CMB it is critical to capture the details of the photon-baryon decoupling. During this period, when photons and baryons are becoming loosely coupled, it is unavoidable to follow the high ℓ moments of the photon distribution.

Theoretical descriptions that could reach the 1% accuracy were a pressing necessity in the 90s, given the projected increase in the amount and precision of CMB data. Early CMB computations, e.g. [MB95], solved the Boltzmann hierarchy in the way we have presented it: truncating at a very large ℓ_{\max} to minimize the errors and compute accurately the high- ℓ moments. This involves solving thousands of coupled differential equations, which made this computations slow. A revolution set in with the development of the line-of-sight approach in [SZ96]. The key insight was the realization that the high- ℓ multipoles can be computed as convolutions of spherical Bessel functions with a source function, instead of solving their differential equations. The source functions only involve the first moments of the distribution. Then, to compute accurately these source functions, it is enough to truncate the Boltzmann hierarchy at low ℓ , e.g. $\ell_{\max} = \mathcal{O}(10)$. Every modern Boltzmann code, starting with CMBFAST in [SZ96], implements this approach. Nowadays it is possible to compute the CMB spectrum in a laptop in $\mathcal{O}(10^{-1}, 1)$ seconds²⁰.

²⁰When we want to find the best-fit parameters for a given model it is usually necessary to compute $\mathcal{O}(10^5)$ CMB spectra (to construct Monte-Carlo Markov chains). Efficiency in the individual steps is of the utmost importance for parameter estimation.

In this section we will develop the traditional line-of-sight integration both for neutrinos and photons. In addition to its numerical advantages, it is very well suited to find (approximate) analytical solutions.

3.8.1 Neutrinos

Massless neutrinos are described by the Boltzmann equation (3.111), which can be written as

$$\dot{\mathcal{F}}_v + ik\mu \mathcal{F}_v = S_v(\tau, k, \mu), \quad (3.221)$$

where $\mu \equiv (\hat{n} \cdot \hat{k})$ and S_v is the source function. It can be expressed in two alternative ways

$$\begin{aligned} S_v(\tau, k, \mu) &\equiv 4\dot{\Phi} - 4ik\mu\Psi - 4k^2\mu^2(B - \dot{E}) \\ &\equiv S_0(\tau, k) + ik\mu S_1(\tau, k) - k^2\mu^2 S_2(\tau, k). \end{aligned} \quad (3.222)$$

To obtain the solution of (3.221) we rewrite it as

$$e^{-ik\mu\tau} \frac{d}{d\tau} \left(\mathcal{F}_v e^{ik\mu\tau} \right) = S_v, \quad (3.223)$$

and then, upon integration,

$$\mathcal{F}_v(\tau, k, \mu) e^{ik\mu\tau} = \mathcal{F}_v(\tau_{\text{ini}}, k, \mu) e^{ik\mu\tau_{\text{ini}}} + \int_{\tau_{\text{ini}}}^{\tau} d\tau' S_v(\tau', k, \mu) e^{ik\mu\tau'}. \quad (3.224)$$

Formally, the integration always starts at a finite time τ_{ini} . In practice, the integration starts when the perturbation is still super-Hubble, $k\tau_{\text{ini}} \ll 1$, so we can safely set $\tau_{\text{ini}} = 0$. Following the discussion of the previous Section 3.7, only the first two moments of the neutrino distribution may have non-zero values. Then, the first term on the right-hand side of (3.224) is

$$\begin{aligned} \mathcal{F}_v(0, k, \mu) &= \mathcal{F}_{v0}(0, k) P_0(\mu) - 3i \mathcal{F}_{v1}(0, k) P_1(\mu) \\ &= \delta_v(0, k) - \frac{4}{k^2} ik\mu \theta_v(0, k). \end{aligned} \quad (3.225)$$

The second term in (3.224) can be written in different ways, depending whether we integrate by parts or not,

$$\begin{aligned} \int_0^{\tau} d\tau' S_v(\tau', k, \mu) e^{ik\mu\tau'} &= \int_0^{\tau} d\tau' S_0 e^{ik\mu\tau'} + \int_0^{\tau} d\tau' S_1 \frac{d}{d\tau'} e^{ik\mu\tau'} \\ &\quad + \int_0^{\tau} d\tau' S_2 \frac{d^2}{d\tau'^2} e^{ik\mu\tau'} \\ &= \int_0^{\tau} d\tau' e^{ik\mu\tau'} (S_0 + \dot{S}_1 + \ddot{S}_2) \\ &\quad + e^{ik\mu\tau} [S_1(\tau, k) - \dot{S}_2(\tau, k) + ik\mu S_2(\tau, k)] \\ &\quad + S_1(0, k) + \dot{S}_2(0, k) - ik\mu S_2(0, k). \end{aligned} \quad (3.226)$$

Finally, the integrated Boltzmann equation (3.224) is transformed into

$$\begin{aligned} \mathcal{F}_v(\tau, k, \mu) &= \delta_v(0, k) e^{-ik\mu\tau} + \frac{4}{k^2} \theta_v(0, k) \frac{d}{d\tau} e^{-ik\mu\tau} + \int_0^{\tau} d\tau' S_0 e^{ik\mu(\tau'-\tau)} \\ &\quad + \int_0^{\tau} d\tau' S_1 \frac{d}{d\tau'} e^{ik\mu(\tau'-\tau)} + \int_0^{\tau} d\tau' S_2 \frac{d^2}{d\tau'^2} e^{ik\mu(\tau'-\tau)}. \end{aligned} \quad (3.227)$$

All the angular dependencies have been absorbed in the exponentials. Using the expansion of the exponential in terms of Legendre polynomials

$$\exp\left(ik\mu(\tau' - \tau)\right) = \sum_{\ell=0}^{\infty} (-i)^{\ell} (2\ell + 1) j_{\ell}\left(k(\tau - \tau')\right) P_{\ell}(\mu), \quad (3.228)$$

it is straightforward to express (3.227) in terms of the multipoles, as defined in (3.135),

$$\begin{aligned} \mathcal{F}_{\nu\ell}(\tau, k) = & \delta_{\nu}(0, k) j_{\ell}(k\tau) + \frac{4}{k} \theta_{\nu}(0, k) j'_{\ell}(k\tau) + 4 \int_0^{\tau} d\tau' \dot{\Phi} j_{\ell}\left(k(\tau - \tau')\right) \\ & + 4k \int_0^{\tau} d\tau' \Psi j'_{\ell}\left(k(\tau - \tau')\right) + 4k^2 \int_0^{\tau} d\tau' (B - \dot{E}) j''_{\ell}\left(k(\tau - \tau')\right). \end{aligned} \quad (3.229)$$

where $j'_{\ell}(x) \equiv dj_{\ell}(x)/dx$. In the absence of metric perturbations, the free streaming of neutrinos is described by spherical Bessel functions. This justifies the assertion at the end of Section 3.4, where the truncation scheme (3.139) was based on $\mathcal{F}_{\ell} \sim j_{\ell}(k\tau)$.

3.8.2 Photons

The presence of a collision term in the Boltzmann equation for photons, see (3.130), modifies the procedure outlined in the previous section. First we need to introduce two variables

$$\kappa \equiv \int_{\tau}^{\tau_0} a n_e \sigma_T d\tau' = \int_{\tau}^{\tau_0} \frac{d\tau'}{\tau_c}, \quad (3.230)$$

$$g \equiv -\dot{\kappa} e^{-\kappa}, \quad (3.231)$$

where τ_0 is the conformal time today. These quantities are usually known as the optical depth, κ , and the visibility function, g . The optical depth grows very large in the early Universe, when the scattering of photons is very efficient. The visibility function is normalized, $\int_0^{\tau_0} g(\tau) d\tau = 1$, so we can regard it as a probability function. It is the probability that a photon last scattered at τ , see [Dod03]. The visibility function is strongly peaked at decoupling, around $z_{\text{dec}} \simeq 1090$ for a standard cosmology. The Boltzmann equation for photons (3.130) can be rewritten as

$$\dot{\mathcal{F}}_{\gamma} + ik\mu \mathcal{F}_{\gamma} - \dot{\kappa} \mathcal{F}_{\gamma} = S_{\gamma}(\tau, k, \mu), \quad (3.232)$$

where the source function S_{γ} is slightly different this time

$$S_{\gamma}(\tau, k, \mu) \equiv 4\dot{\Phi} - \dot{\kappa} \delta_{\gamma} - 4ik\mu \left(\Psi - \frac{\dot{\kappa}}{k^2} \theta_b \right) - 4k^2 \mu^2 (B - \dot{E}). \quad (3.233)$$

The solution is

$$\begin{aligned} e^{ik\mu\tau - \kappa(\tau)} \mathcal{F}_{\gamma}(\tau, k, \mu) = & e^{ik\mu\tau_{\text{ini}} - \kappa(\tau_{\text{ini}})} \mathcal{F}_{\gamma}(\tau_{\text{ini}}, k, \mu) \\ & + \int_{\tau_{\text{ini}}}^{\tau} d\tau' e^{ik\mu\tau'} e^{-\kappa(\tau')} S_{\gamma}(\tau', k, \mu). \end{aligned} \quad (3.234)$$

Since the optical depth is very large at τ_{ini} , the first term on the right-hand side is strongly suppressed and can be neglected. Applying this argument and performing different integrations by parts, the source term is conventionally cast in the form

$$\begin{aligned} \int_0^\tau d\tau' e^{ik\mu\tau'} e^{-\kappa(\tau')} S_\gamma = \int_0^\tau d\tau' e^{ik\mu\tau'} \left\{ g(\delta_\gamma + 4\Psi + 4(\dot{B} - \dot{E})) \right. \\ + 4e^{-\kappa} (\dot{\Phi} + \dot{\Psi} + (\ddot{B} - \ddot{E})) \\ + \frac{4}{k^2} \frac{d}{d\tau'} [g(\theta_b + k^2(B - \dot{E}))] \left. \right\} \\ - 4e^{ik\mu\tau} \left\{ e^{-\kappa(\tau)} [\Psi + (\dot{B} - \dot{E}) - ik\mu(B - \dot{E})] \right. \\ + \frac{g}{k^2} (\theta_b + k^2(B - \dot{E})) \left. \right\}. \quad (3.235) \end{aligned}$$

This approach for photons is usually applied to compute the CMB, so we evaluate it *today*, i.e. at τ_0 . Disregarding a monopole and dipole terms²¹, we have

$$\begin{aligned} \mathcal{F}_{\gamma\ell}(\tau_0, k) = \int_0^{\tau_0} d\tau j_\ell(k(\tau_0 - \tau)) \left\{ g(\delta_\gamma + 4\Psi + 4(\dot{B} - \dot{E})) \right. \\ + 4e^{-\kappa} (\dot{\Phi} + \dot{\Psi} + (\ddot{B} - \ddot{E})) \\ + \frac{4}{k^2} \frac{d}{d\tau} [g(\theta_b + k^2(B - \dot{E}))] \left. \right\}, \quad (\ell > 1). \quad (3.236) \end{aligned}$$

The three terms on the right can be given a physical interpretation²². The first one is the Sachs-Wolfe effect. It contains the intrinsic temperature perturbation and the gravitational redshift produced by the metric potentials in the last-scattering surface. The second term is the integrated Sachs-Wolfe effect. It represents the gravitational redshift caused by potentials that vary in time as the photons propagate from the last-scattering surface to us. The last one is the Doppler term. It is the standard Doppler shift produced by motions in the plasma at the last-scattering surface.

3.9 Observables

After developing the formalism of cosmological perturbation theory, we must learn how to connect our results with the observations. As discussed in Chapter 1, two of the main sources of cosmological information are the statistical properties of the clustering of matter and the distribution of CMB anisotropies. In the next two sections we will describe how to compute the matter and temperature power spectra.

²¹The monopole term is absorbed in the definition of the mean CMB temperature. The dipole is also (directly) unobservable, due to the much larger kinematic dipole produced by the motion of the Solar System with respect to the CMB rest frame.

²²Note that each of the terms appears in gauge-invariant combinations (as it should, since we know that \mathcal{F}_ℓ is gauge-invariant for $\ell > 1$). This is a convenient way to check the consistency of lengthy calculations.

3.9.1 Power spectra

The correlation spectra are one of the most readily observable quantities that we can define. Given a cosmological variable $g(\tau, \mathbf{k})$, we define its power spectrum as

$$\begin{aligned} \langle g(\tau, \mathbf{k})g^*(\tau, \mathbf{k}') \rangle &\equiv (2\pi)^3 \delta(\mathbf{k} - \mathbf{k}') P_{gg}(\tau, k) \\ &= |g(\tau, k)|^2 \langle \mathcal{R}_{\mathbf{k}} \mathcal{R}_{\mathbf{k}'} \rangle \\ &= (2\pi)^3 \delta(\mathbf{k} - \mathbf{k}') |g(\tau, k)|^2 \frac{2\pi^2}{k^3} \mathcal{P}_{\mathcal{R}}(k), \end{aligned} \quad (3.237)$$

where $\mathcal{P}_{\mathcal{R}}(k)$ is the primordial spectrum defined in (3.219). Notice that $g(\tau, k)$ in the second and third lines is the transfer function of the quantity g . Correlation functions are usually computed in real space, instead of Fourier space. The relation between both is straightforward

$$\langle g(\tau, \mathbf{x}), g(\tau, \mathbf{x}') \rangle = \int \frac{d^3k}{(2\pi)^3} P_{gg}(\tau, k) e^{i\mathbf{k} \cdot (\mathbf{x} - \mathbf{x}')} = P_{gg}(\tau, |\mathbf{x} - \mathbf{x}'|). \quad (3.238)$$

In a similar way, we can define the cross-correlation spectrum of two different variables g_1 and g_2 . Since the transfer functions are real, we can just write

$$\begin{aligned} \langle g_1(\tau, \mathbf{k})g_2^*(\tau, \mathbf{k}') \rangle &\equiv (2\pi)^3 \delta(\mathbf{k} - \mathbf{k}') P_{g_1g_2}(\tau, k) \\ &= (2\pi)^3 \delta(\mathbf{k} - \mathbf{k}') g_1(\tau, k) g_2(\tau, k) \frac{2\pi^2}{k^3} \mathcal{P}_{\mathcal{R}}(k). \end{aligned} \quad (3.239)$$

Up to this point we have been working with conformal time τ . While the numerical integration is performed in terms of τ , it is very common to present the final results in terms of the redshift z . While, the redshift of an object is readily observable, if we want to associate a conformal time to a given redshift an expansion history, i.e. a background model, must be chosen. That is why we will usually prefer z over τ when presenting observables.

Arguably, the most important spectrum of this type is the matter power spectrum. We define the matter density perturbation as

$$\delta_m \equiv \frac{\Omega_b \delta_b + \Omega_c \delta_c}{\Omega_b + \Omega_c}, \quad (3.240)$$

and the matter power spectrum is

$$\begin{aligned} \langle \delta_m(z, \mathbf{k})\delta_m^*(z, \mathbf{k}') \rangle &\equiv (2\pi)^3 \delta(\mathbf{k} - \mathbf{k}') P_m(z, k) \\ &= (2\pi)^3 \delta(\mathbf{k} - \mathbf{k}') |\delta_m(z, k)|^2 \frac{2\pi^2}{k^3} \mathcal{P}_{\mathcal{R}}(k). \end{aligned} \quad (3.241)$$

3.9.2 CMB temperature anisotropy

We have already discussed in Section 1.1 the leading role that CMB observations have played in modern cosmology. Here, we will relate our theoretical analysis of cosmological perturbations with these observations.

Temperature perturbation

The first objective is to relate the reduced distribution function \mathcal{F}_γ with a temperature perturbation. The spectrum of the CMB is extraordinarily close to a blackbody. Therefore, the zero order distribution function is

$$f_0 = \frac{1}{e^{p/T} - 1}. \quad (3.242)$$

Deviations from this background distribution can be parameterized as temperature perturbations

$$f(\tau, \mathbf{x}, p, \hat{n}) = \left\{ \exp\left(\frac{p}{T[1 + \Theta(\tau, \mathbf{x}, \hat{n})]}\right) - 1 \right\}^{-1}. \quad (3.243)$$

The temperature perturbation can then be written in terms of the reduced distribution function as

$$(1 + \Theta)^4 - 1 = \frac{\int p^3 dp (f - f_0)}{\int p^3 dp f_0} = \mathcal{F}_\gamma. \quad (3.244)$$

To first order in perturbations, the final result is

$$\Theta = \frac{1}{4} \mathcal{F}_\gamma. \quad (3.245)$$

This way we can relate perturbations in the photon distribution function, that we know how to compute, with temperature perturbations, that are observed in the CMB maps.

Two point function

The temperature function in the previous section was defined in real space. It is related to its Fourier counterpart as

$$\Theta(\tau, \mathbf{x}, \hat{n}) = \frac{1}{4} \int \frac{d^3 k}{(2\pi)^3} \mathcal{F}_\gamma(\tau, \mathbf{k}, \hat{n}) e^{-i\mathbf{k} \cdot \mathbf{x}} = \frac{1}{4} \int \frac{d^3 k}{(2\pi)^3} \mathcal{F}_\gamma(\tau, k, \hat{n} \cdot \hat{k}) e^{-i\mathbf{k} \cdot \mathbf{x}} \mathcal{R}_{\mathbf{k}}. \quad (3.246)$$

On the second equality we are writing separately the transfer function and the primordial perturbation. For the computation of the CMB spectrum we are interested in the temperature anisotropy evaluated today ($\tau = \tau_0$) in the Solar System ($\mathbf{x} = 0$)

$$\Theta(\hat{n}) \equiv \Theta(\tau_0, 0, \hat{n}) = \frac{1}{4} \int \frac{d^3 k}{(2\pi)^3} \mathcal{F}_\gamma(\tau_0, k, \hat{n} \cdot \hat{k}) \mathcal{R}_{\mathbf{k}}. \quad (3.247)$$

The observable that is statistically relevant is the *two-point function*, i.e. the correlation function of temperatures in two different directions, defined as

$$C(\hat{n}, \hat{n}') \equiv \langle \Theta(\hat{n}) \Theta(\hat{n}') \rangle = \frac{1}{16} \int \frac{d^3 k}{(2\pi)^3} \mathcal{F}_\gamma(\tau_0, k, \hat{n} \cdot \hat{k}) \mathcal{F}_\gamma^*(\tau_0, k, \hat{n}' \cdot \hat{k}) P_{\mathcal{R}}(k). \quad (3.248)$$

Using the multipole expansion of the transfer function (3.135)

$$\begin{aligned} C(\hat{n}, \hat{n}') &= \frac{1}{16} \int \frac{k^2 dk}{2\pi^2} P_{\mathcal{R}}(k) \sum_{\ell, \ell'} (-i)^\ell i^{\ell'} (2\ell + 1)(2\ell' + 1) \mathcal{F}_{\gamma\ell}(\tau_0, k) \mathcal{F}_{\gamma\ell'}^*(\tau_0, k) \\ &\quad \times \int \frac{d^2 \hat{k}}{4\pi} P_\ell(\hat{n} \cdot \hat{k}) P_{\ell'}(\hat{n}' \cdot \hat{k}). \end{aligned} \quad (3.249)$$

It can be proven, see (C.35), that

$$\int \frac{d^2 \hat{k}}{4\pi} P_\ell(\hat{n} \cdot \hat{k}) P_{\ell'}(\hat{n}' \cdot \hat{k}) = \frac{\delta_{\ell\ell'}}{2\ell+1} P_\ell(\hat{n} \cdot \hat{n}'). \quad (3.250)$$

Then, the two-point function can be expressed as a multipole expansion

$$C(\hat{n}, \hat{n}') = \sum_{\ell=0}^{\infty} \frac{2\ell+1}{4\pi} \bar{C}_\ell P_\ell(\hat{n} \cdot \hat{n}'), \quad (3.251)$$

with coefficients

$$\bar{C}_\ell \equiv \frac{\pi}{4} \int \frac{dk}{k} \mathcal{P}_{\mathcal{R}}(k) |\mathcal{F}_{\gamma\ell}(\tau_0, k)|^2. \quad (3.252)$$

On the other hand, CMB experiments measure the harmonic decomposition of the temperature field in real space

$$a_{\ell m} = \int d^2 \hat{n} Y_\ell^{m*}(\hat{n}) \Theta(\hat{n}). \quad (3.253)$$

With these coefficients, the temperature power spectrum can also be defined as

$$C_\ell \equiv \frac{1}{2\ell+1} \sum_{m=-\ell}^{\ell} \langle |a_{\ell m}|^2 \rangle. \quad (3.254)$$

Using (3.253) and the addition property of the spherical harmonics (C.33), one can prove

$$\begin{aligned} C_\ell &= \frac{1}{2\ell+1} \sum_{m=-\ell}^{\ell} \int d^2 \hat{n} d^2 \hat{n}' Y_\ell^m(\hat{n}) Y_\ell^{m*}(\hat{n}') \langle \Theta(\hat{n}) \Theta(\hat{n}') \rangle \\ &= \int \frac{d^2 \hat{n} d^2 \hat{n}'}{4\pi} P_\ell(\hat{n} \cdot \hat{n}') C(\hat{n}, \hat{n}'). \end{aligned} \quad (3.255)$$

Finally, we have

$$C_\ell = \bar{C}_\ell. \quad (3.256)$$

In Λ CDM all the CMB temperature information is encoded in the temperature power spectrum.

The most prominent anisotropy in the CMB is the dipole term ($\ell = 1$). As discussed in Section 1.1, it is two orders of magnitude larger than any other anisotropy and can be interpreted as the Doppler shift caused by our motion with respect to the CMB rest frame. This relative motion has subtler effects too. In this section we took as our starting point the isotropic blackbody spectrum (3.242). However, a moving observer would measure instead a *boosted* blackbody spectrum. This will have important consequences in Chapters 6 and 7.

II

BEYOND THE STANDARD
PICTURE

4

Hidden Gravitons

The first way to move beyond a Λ +CDM dark sector is to add a new component. In this chapter we follow this approach, considering the observational impact of a new massive spin-2 particle: a *hidden graviton*. To start with, in Section 4.1, after reviewing different scenarios where massive spin-2 particles appear, we introduce our model. In Section 4.2 we analyze the phenomenology that arises when the hidden gravitons are coupled to ordinary matter. Sections 4.3 and 4.4 focus on how this new particle would be emitted in stars, modifying their evolution. Using the results of the preceding section, in Section 4.5 we use observational bounds on the maximum energy loss in stars to constrain the mass and coupling of the hidden gravitons.

4.1 Massive gravitons

Gravity and electromagnetism are, as far as we know today, the only macroscopic forces in Nature. Their long-range character can be explained according to the masslessness of gravitons and photons. This property, in its turn, is usually justified as a result of the local symmetries of both theories, diffeomorphism and $U(1)$ gauge invariance. Nonetheless, it is natural to ask whether they are exactly massless or they just have small masses, and, as a matter of fact, there have been a lot of efforts over the years to test this assumption. On the experimental side, several bounds have been established for non-zero masses [GN10] while on the theoretical side great efforts have been invested in constructing consistent models of massive gravity and massive electrodynamics. The starting point of massive electrodynamics is the Proca Lagrangian. It consists on the usual Maxwell Lagrangian plus a simple mass term, that explicitly violates the gauge invariance of the theory. This effective approach can be completed at high energies through the Stueckelberg or the Higgs mechanisms. On the phenomenological side, one important application of massive electrodynamics has been the proposal of a new hypothetical field: a hidden photon. This hidden photon has associated a large amount of potential experimental signatures. In particular, it constitutes a viable candidate for dark matter, whose effects have been explored extensively in the literature [NS11; Ari+12; Goo+09; BCW10; Abe+08; CMN17; Cem+12].

On the other hand, massive gravity is usually introduced by using the Fierz-Pauli action [FP39]. It consists on the linearized action from General Relativity plus a suitably chosen mass term. This Lagrangian has been thoroughly studied and its properties are well known and understood. For example, although the free action is consistent, a paradoxical behaviour appears when we turn on the interaction with matter. It was discovered independently [Iwa70; DV70; Zak70] that this theory is not continuous in the massless limit: the $m = 0$ and $m \rightarrow 0$ theories are not

physically equivalent. This is the so-called vDVZ discontinuity.

The problem of the mass discontinuity can be traced back to the number of degrees of freedom that both theories propagate. While a massless spin-2 particle has only two degrees of freedom (two tensor modes), a massive spin-2 particle has five (two tensor modes, two vectors and one scalar). It can be shown [Rha14; Hin12] that when we take the $m \rightarrow 0$ limit, the scalar mode becomes strongly coupled, invalidating the linear theory. In fact, when non-linear effects are taken into account, the zero-mass discontinuity is cured through the so-called Vainshtein mechanism [Vai72]. When the problem of the vDVZ discontinuity seemed solved, Boulware and Deser [BD72] showed that for a broad range of extensions of the theory, these non-linear effects also introduce a sixth degree of freedom, that turns out to be a ghost (BD ghost).

Constructing a fully non-linear, consistent, theory of massive gravity is a big challenge and only very recently it has been possible to evade the BD ghost. In 2010 de Rham, Gabadadze and Tolley (dRGT) constructed a ghost-free non-linear completion of the Fierz-Pauli action, known as ghost-free or dRGT massive gravity [RGT11]. The dRGT action contains parameters fixing the self-interactions and a reference metric. Shortly after, Hassan and Rosen [HR11] reformulated the theory and made this reference metric dynamical. This new formulation is a bimetric theory of gravity, describing at the linear level the evolution of a standard massless graviton plus a massive one, with a Fierz-Pauli mass term. This massive graviton has been proved to be a viable CDM candidate in recent works [Bab+16a; Bab+16b; AM16]. The linearized version of bimetric gravity coincides with the model we will analyze in this work, i.e. massless gravity plus a single massive graviton. For a specialized review on bimetric theory see [SS16].

Massive gravitons also appear naturally in extra-dimensional theories of gravity, like the ADD model [ADD98; Ant+98]. In this model, the Standard Model fields are confined to a 4-brane, while gravitons (described by the usual Einstein-Hilbert action) can explore a number n of extra large dimensions. When duly compactified, the existence of these new dimensions leads to a tower of Kaluza-Klein (KK) excitations of the graviton. The weak interaction of this KK modes can be compensated by their huge multiplicity and lead to significant deviations from standard gravity. A number of ways to test the model were suggested in the original proposal [ADD99] and the experimental constraints were derived in detail in many references [Bar+99; CP99; Han+01; HT99; HR01; HR02; HR03].

We shall not assume any particular framework for our study. In our model, we will add a single massive spin-2 particle to the known particles (that we will denote *hidden graviton*), explore its phenomenological consequences and use the observational evidence to constrain its mass and coupling to other fields. In fact, we will employ two methods that have become standard to test the impact of new light, weakly interacting particles: fifth-force tests and astrophysical energy-loss arguments. They have been applied not only to KK gravitons, but also to hidden photons [DFK12; APP13], sterile neutrinos [Raf90a; ABK19] and especially to axions [KMW84; Raf86; PK86; Raf90b].

Our starting point to describe this new particle, in flat space-time, is the Fierz-

Pauli Lagrangian (2.62)

$$\mathcal{L} = -\frac{1}{2}\partial^\alpha h^{\mu\nu}(\partial_\alpha h_{\mu\nu} - 2\partial_{(\mu}h_{\nu)\alpha} - \partial_\alpha h\eta_{\mu\nu} + 2\partial_{(\mu}h\eta_{\nu)\alpha}) - \frac{1}{2}m^2(h_{\mu\nu}^2 - h^2), \quad (4.1)$$

It consists of the kinetic term that could be obtained linearizing GR over a Minkowski geometry plus a suitably chosen mass term. As discussed in Section 2.2, both terms can be fixed without previous knowledge of GR, just requiring the absence of ghost instabilities. The equations of motion for the free field can be expressed as (2.65)

$$(\square - m^2)h_{\mu\nu} = 0, \quad (4.2a)$$

$$\partial^\mu h_{\mu\nu} = 0, \quad (4.2b)$$

$$h \equiv h^\mu{}_\mu = 0. \quad (4.2c)$$

Their solution can be written as

$$h^{\mu\nu}(x) = \int \frac{d^3p}{(2\pi)^3 2E_p} \sum_\lambda \left[a_{\mathbf{p},\lambda} \epsilon^{\mu\nu}(\mathbf{p},\lambda) e^{ipx} + a_{\mathbf{p},\lambda}^\dagger \epsilon^{\mu\nu*}(\mathbf{p},\lambda) e^{-ipx} \right], \quad (4.3)$$

where λ are the polarization states and the polarization tensor satisfies

$$p_\mu \epsilon^{\mu\nu}(\mathbf{p},\lambda) = 0, \quad (4.4a)$$

$$\eta_{\mu\nu} \epsilon^{\mu\nu}(\mathbf{p},\lambda) = 0, \quad (4.4b)$$

$$\epsilon^{\mu\nu}(\mathbf{p},\lambda) \epsilon_{\mu\nu}^*(\mathbf{p},\lambda') = \delta_{\lambda\lambda'}, \quad (4.4c)$$

$$\sum_\lambda \epsilon^{\mu\nu}(\mathbf{p},\lambda) \epsilon^{\alpha\beta*}(\mathbf{p},\lambda) = \frac{1}{2}(P^{\mu\alpha}P^{\nu\beta} + P^{\mu\beta}P^{\nu\alpha}) - \frac{1}{3}P^{\mu\nu}P^{\alpha\beta}, \quad (4.4d)$$

with $P^{\mu\nu} = \eta^{\mu\nu} + p^\mu p^\nu/m^2$. For a thorough analysis see [Hin12]. Next, to find the propagator we need to solve

$$\mathcal{O}^{\alpha\beta\sigma\lambda}(p)D_{\sigma\lambda\mu\nu}(p) = i\delta_{(\mu}^{\alpha} \delta_{\nu)}^{\beta}, \quad (4.5)$$

where the operator $\mathcal{O}^{\alpha\beta}{}_{\mu\nu}$ has been defined in (2.63). The solution, as can be checked by direct substitution, is

$$D_{\alpha\beta\mu\nu} = \frac{-i}{p^2 + m^2} \left[P_{\alpha(\mu} P_{\nu)\beta} - \frac{1}{3}P_{\alpha\beta}P_{\mu\nu} \right]. \quad (4.6)$$

Now, we need to turn on the interaction. To lowest order, the free Lagrangian (4.1) can be supplemented with a linear interaction with a source $T_{\mu\nu}$

$$\mathcal{L} = \frac{1}{2}h^{\mu\nu} \mathcal{O}^{\alpha\beta}{}_{\mu\nu} h_{\alpha\beta} + \kappa h_{\mu\nu} T^{\mu\nu}, \quad (4.7)$$

where κ is a coupling constant, that we will sometimes rewrite as $\kappa = 1/M_h = \sqrt{8\pi G_h}$. The equations of motion for the new Lagrangian are

$$\mathcal{O}^{\mu\nu}{}_{\alpha\beta} h^{\alpha\beta} = -\kappa T^{\mu\nu}. \quad (4.8)$$

The formalism presented so far is general for a massive spin-2 particle. In order to describe our hidden gravitons we choose the energy-momentum tensor as the

source and take the mass m and coupling κ as free parameters. We only keep terms up to quadratic order in the Lagrangian (4.7) so we neglect the self-couplings that would arise from the contribution of $h_{\mu\nu}$ to the energy-momentum tensor. Seen in this light, the hidden gravitons can be regarded as the linearized version of bi-metric gravity, that is the fully non-linear theory comprising GR plus an additional massive graviton.

Finally, since we will only couple the hidden gravitons to conserved energy-momentum tensors, $\partial^\mu T_{\mu\nu} = 0$, the scattering amplitudes will have the property¹ $p^\mu \mathcal{A}_{\mu\dots} = 0$ on shell. In this case, we can make the identification $P_{\mu\nu} \rightarrow \eta_{\mu\nu}$ in (4.4d) and work with the sum over polarizations given by

$$S^{\mu\nu\alpha\beta} = \eta^{\alpha(\mu}\eta^{\nu)\beta} - \frac{1}{3}\eta^{\mu\nu}\eta^{\alpha\beta}. \quad (4.9)$$

Before moving on to the observational constraints, let us briefly discuss the limitations and relevance of the model. It is important to stress that the constraints that we will derive will be valid insofar as its assumptions, flat space-time and negligible self-interactions, remain valid. If we consider more elaborate theories, it is important to analyze in what region of the parameter-space is (4.7) a good phenomenological description and hence to what extent the constraints can be applied.

Let us take bigravity as a particular example, which is a ghost-free non-linear theory that describes a massless and a massive spin-2 particle [SS16]. The free action, without interactions with matter, is very involved but its linearized version reproduces the Fierz-Pauli Lagrangian (4.1) plus its massless equivalent describing linearized gravity. There are at least two caveats when including matter couplings. In the first place, we have the Vainshtein mechanism. As commented before, it is well-known that in massive gravity non-linear effects become important when $m \rightarrow 0$. These non-linear effects allow the model to evade most Solar-System and terrestrial gravity tests for low masses.

In the second place, we must also be cautious when introducing the matter couplings, since a naive choice could reintroduce the BD ghost. It has been shown [RHR15; RHR14; Hei15] that a healthy procedure is to couple the matter fields to an effective metric, that arises as a combination of the ‘massless’ and ‘massive’ metrics, $g_{\mu\nu}$ and $f_{\mu\nu}$,

$$g_{\mu\nu}^{\text{eff}} = \alpha^2 g_{\mu\nu} + 2\alpha\beta g_{\mu\rho} \left(\sqrt{g^{-1}f} \right)_\nu^\rho + \beta^2 f_{\mu\nu}, \quad (4.10)$$

where α and β are arbitrary parameters². If we restrict ourselves to its linearized version, with $g_{\mu\nu} = \eta_{\mu\nu} + \gamma_{\mu\nu} + \mathcal{O}(\gamma^2)$ and $f_{\mu\nu} = \eta_{\mu\nu} + h_{\mu\nu} + \mathcal{O}(h^2)$, we have

$$g_{\mu\nu}^{\text{eff}} = \eta_{\mu\nu} + (1 - \beta)\gamma_{\mu\nu} + \beta h_{\mu\nu} + \dots \quad (4.11)$$

where we have normalized $\alpha + \beta = 1$. This choice reproduces our model (4.7), where the free parameter β is related to the coupling G_h , that we will later constrain, as

$$\frac{G_h}{G} = \frac{\beta}{1 - \beta}. \quad (4.12)$$

¹We use this property, together with the usual Ward identities from QED, to check our results in subsequent sections.

²More general effective metrics have been studied in [Hei15].

To conclude, let us mention that bigravity is not the only theory that motivates a hidden graviton model as a phenomenological description. The ADD model, that we already mentioned, produces a continuum of Kaluza-Klein states, each of them described by (4.7). Another extra-dimensional theory of gravity, the Randall-Sundrum model [RS99a; RS99b; DHR00; GT00], is even closer to our model since it produces a tower of discrete, widely separated, KK excitations. The Randall-Sundrum model can be effectively described, taking into account only the first resonance, by (4.7).

4.2 Interaction with matter

4.2.1 Fifth-force constraints

The first observational signature we can extract from the model above is the existence of a new force. In order to see the effect of this new force between two matter particles, e.g. two electrons, one could first compute the one graviton exchange amplitude, then take the non-relativistic limit and identify the interaction potential via the Born approximation. A textbook example can be found in [PS95]. This is the standard procedure when particles with non-trivial parity, like pseudoscalars, are present and mediate spin-dependent forces. See [MW84] for an analysis of the axion case and [FT99] for a discussion of spin-dependent forces. However, in our case, to reproduce the results at lowest order it is easier to compute the classical interaction potential.

In the next section we will discuss how this hidden graviton couples to other fields. For now, to compute the macroscopic force that it may produce, we will consider the force mediated between two classical, non-relativistic sources with energy-momentum tensor

$$T_{(i)}^{\mu\nu} = M_i \delta_0^\mu \delta_0^\nu \delta(\mathbf{x} - \mathbf{x}_i), \quad i = 1, 2 \quad (4.13)$$

i.e. two lumps of matter sitting at \mathbf{x}_1 and \mathbf{x}_2 . The interaction potential is

$$\begin{aligned} V &= -\kappa \int d^3x h_{\mu\nu}(x) T_{(2)}^{\mu\nu}(x) = -i\kappa^2 \int d^3x \int d^4y T_{(1)}^{\alpha\beta}(y) D_{\alpha\beta\mu\nu}(x-y) T_{(2)}^{\mu\nu}(x) \\ &= -i\kappa^2 M_1 M_2 \int dy^0 \int \frac{d^4p}{(2\pi)^4} D_{0000}(p) e^{ip_0(x^0-y^0)} e^{-i\mathbf{p}\cdot(\mathbf{x}_1-\mathbf{x}_2)} \\ &= -i\kappa^2 M_1 M_2 \int \frac{d^3p}{(2\pi)^3} D_{0000}(p^0=0, \mathbf{p}) e^{-i\mathbf{p}\cdot(\mathbf{x}_1-\mathbf{x}_2)}. \end{aligned} \quad (4.14)$$

Now, it is worth recalling the form (4.6) of the propagator. For massless gravity one can also derive the propagator, after properly fixing the gauge, and the result is the same as in the massive case, save for a factor 1/2 instead of 1/3 [Hin12]. For the moment, we write the generic form

$$iD_{0000}(p^0=0, \mathbf{p}) = \frac{1-\alpha}{\mathbf{p}^2 + m^2}, \quad (4.15)$$

where $\alpha = 1/2, 1/3$ for massless/massive gravitons. After performing the integral, we obtain what is to be expected from a massive, even spin, boson: a universally attractive Yukawa force

$$V = -\kappa^2 M_1 M_2 \frac{e^{-mr}}{4\pi r} (1-\alpha), \quad r = |\mathbf{x}_1 - \mathbf{x}_2|. \quad (4.16)$$

The standard Newtonian potential is recovered in the massless case ($m = 0$, $\alpha = 1/2$, $\kappa = 1/M_{\text{Pl}} = \sqrt{8\pi G}$)

$$V_{\text{Newt}}(r) = -\frac{GM_1M_2}{r}, \quad (4.17)$$

while in the massive case we have ($\alpha = 1/3$, $\kappa = 1/M_h = \sqrt{8\pi G_h}$)

$$V(r) = -\frac{4}{3}G_hM_1M_2\frac{e^{-mr}}{r}. \quad (4.18)$$

The appearance of the factor $4/3$ may seem surprising. In fact, it could be reabsorbed in the definition of G_h , so that the $m = 0$ and $m \rightarrow 0$ cases would give the same physical results with the identification $G = \frac{4}{3}G_h$. However, this kind of factors reappear when calculating the deflection of light [Rha14]. In that case, the factors cannot be reabsorbed, yielding unambiguously different results. As commented in the first section, this is the vDVZ discontinuity in the massless limit.

So we will stick to this definition of the coupling constant, without reabsorbing the factor $4/3$. The total potential produced by standard gravity and this hypothetical new mediator is

$$V(r) = -\frac{GM_1M_2}{r}\left(1 + \frac{4}{3}\frac{G_h}{G}e^{-mr}\right). \quad (4.19)$$

With this result, we are ready to constrain the possible values of G_h and m using the available data.

As commented in Chapter 1, there is a wealth of observational and experimental data constraining deviations from the inverse square law (ISL) implied by the Newtonian potential (4.17). Our interaction potential (4.19) has already been cast in the traditional form for ISL tests (1.26)

$$V(r) = -\frac{GM_1M_2}{r}\left(1 + \alpha e^{-r/\lambda}\right), \quad (4.20)$$

so we can easily adapt the existing constraints to our case

$$\alpha = \frac{4}{3}\frac{G_h}{G}, \quad (4.21a)$$

$$\lambda = m^{-1}. \quad (4.21b)$$

The relevant bounds are shown in Figure 4.1, for Solar-System and laboratory constraints, respectively. The tightest constraints on the interaction strength come from experiments testing large distances and put, in its turn, strong constraints on the existence of very low mass particles. The situation is reversed for higher masses. In view of the huge experimental challenges, the Casimir experiments, that probe the shortest distances, set significantly looser bounds than its Cavendish counterparts.

The shortest range experiments in the laboratory can only put bounds on masses of about few eVs, and there are no prospects that they can go much further. It is in this range of masses where we need the information provided by astrophysical objects.

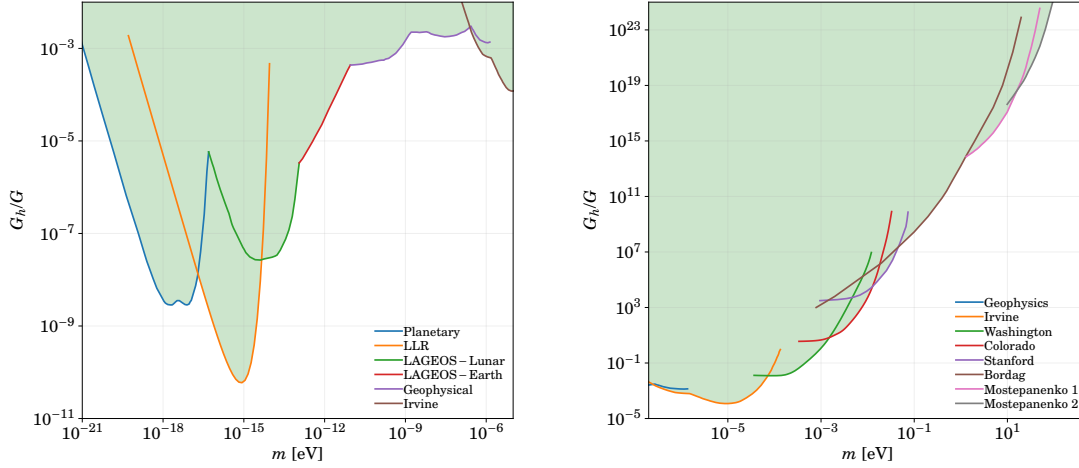


Figure 4.1: Constraints on the hidden-graviton mass and coupling G_h , relative to the standard-graviton coupling. The shadowed region is excluded by fifth-force tests. The limits are adopted from Figure 1.8.

4.2.2 Coupling to QED

The coupling of the hidden graviton is taken to have the same form as the standard graviton, but suppressed by a different energy scale, $\kappa = 1/M_h = \sqrt{8\pi G_h}$. It will couple to matter through the energy-momentum tensor obtained with the usual prescription in GR, as the functional derivative with respect to the metric of a minimally coupled matter action, see (2.23). The most relevant coupling in this work is to quantum electrodynamics (QED) [BD84]

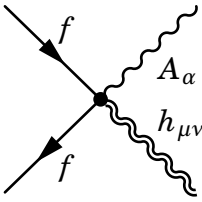
$$\mathcal{L}_{\text{QED}} = -\frac{1}{4}F_{\mu\nu}F^{\mu\nu} + \bar{\psi}(iD - m)\psi, \quad D_\mu \equiv \partial_\mu + iQA_\mu, \quad (4.22)$$

$$T_{\mu\nu}^{\text{QED}} = F_{\mu\alpha}F_\nu{}^\alpha + \frac{i}{2}[\bar{\psi}\gamma_{(\mu}D_{\nu)}\psi - (D_{(\mu}\bar{\psi})\gamma_{\nu)}\psi] + \eta_{\mu\nu}\mathcal{L}_{\text{QED}}, \quad (4.23)$$

where for hidden gravitons on-shell the last term is irrelevant, see (4.4a). From this we can read three kind of vertices. The Feynman rules for these interactions were calculated in [GRW99; HLZ99]. The relevant vertices are

$$h_{\mu\nu} = -2i\kappa V_{(\mu\nu)\alpha\beta}(k_1, k_2), \quad (4.24)$$

$$h_{\mu\nu} = -\frac{i\kappa}{2}W_{(\mu\nu)}(k_1, k_2), \quad (4.25)$$



$$= i\kappa Q \left(\gamma_{(\mu} \eta_{\nu)\alpha} - \eta_{\mu\nu} \gamma_{\alpha} \right), \quad (4.26)$$

and $Q = -e$ for an electron. We have defined the functions

$$V_{\mu\nu\alpha\beta}(p, q) = -\frac{1}{2} \eta_{\mu\nu} (p_{\beta} q_{\alpha} - \eta_{\alpha\beta} p q) - \eta_{\alpha\beta} p_{\mu} q_{\nu} - \eta_{\mu\alpha} (\eta_{\nu\beta} p q - p_{\beta} q_{\nu}) + \eta_{\mu\beta} p_{\nu} q_{\alpha}, \quad (4.27)$$

$$W_{\mu\nu}(p, q) = (p + q)_{\mu} \gamma_{\nu} - \eta_{\mu\nu} (\not{p} + \not{q} + 2m_e). \quad (4.28)$$

Additionally, we must take into account the usual Feynman rules for QED, e.g. see [Sre07].

4.3 Boltzmann equation and energy loss

The Feynman rules derived above can be used in particular to analyze the interaction of hidden gravitons with stellar plasmas. As discussed in Section 1.4 any new light particle interacting with stellar plasmas can lead to modifications of the stellar structure and to deviations from the standard evolutionary track. We will focus on the regime where the hidden gravitons can be thermally produced in stars and act as a new source of energy loss.

It is important to note that these interactions take place in a hot plasma, where the finite temperature and density effects may become important. In this case, the standard vertices and propagators of quantum field theory are modified, new degrees of freedom appear (like the plasmon, a longitudinal mode of the photon) and some collective behaviours may be important (remember the assumptions entering in the Boltzmann equation in Section 2.3.4). These effects, and their importance for some particles like axions, are summarized in [Raf90a; Raf96] and references therein. As a first approximation, we will neglect most of these plasma effects, pointing out some cases where they can decisively suppress a process. To sum up, we will use the Boltzmann equation as derived in Section 2.3.5, computing thermally-averaged cross sections with zero temperature QFT.

The next sections are devoted to the reformulation of the Boltzmann equation in a form suitable for computing the energy loss in three different types of processes.

4.3.1 $2 \rightarrow 2$ process

The evolution of the distribution function for a particle a is described by the Boltzmann equation (2.99)

$$\frac{Df_a}{dt} = \mathcal{C}[f_a]. \quad (4.29)$$

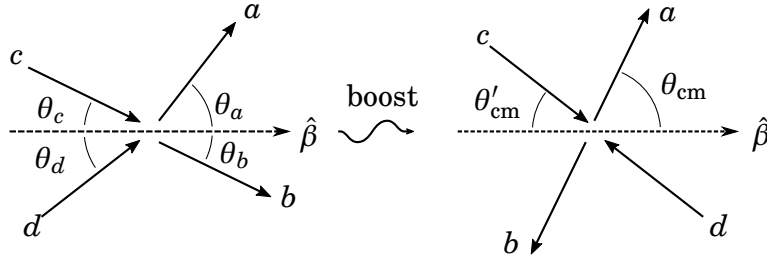


Figure 4.2: Collision in CM and arbitrary frame.

The collision term for a binary process $a + b \leftrightarrow c + d$ is (2.100)

$$\begin{aligned} \mathcal{C}[f_a] = & \frac{S}{2E_a} \int \mathcal{D}p_b \mathcal{D}p_c \mathcal{D}p_d (2\pi)^4 \delta(p_a + p_b - p_c - p_d) |\mathcal{M}|^2 \\ & \times \left[\underbrace{f_c f_d (1 \pm f_a)(1 \pm f_b)}_{cd \rightarrow ab} - \underbrace{f_a f_b (1 \pm f_c)(1 \pm f_d)}_{ab \rightarrow cd} \right] \begin{cases} + \text{bosons} \\ - \text{fermions} \end{cases} \quad (4.30) \end{aligned}$$

If the a -particles are readily emitted, we can neglect the backreaction $a + b \rightarrow c + d$ and the enhancement/blocking factor, i.e. $(1 \pm f_a) \simeq 1$. We also assume that this production do not perturb the local thermal equilibrium, so the distribution functions for the remaining particles are the equilibrium Bose-Einstein/Fermi-Dirac distributions. In order to compute the energy emitted in the form of a -particles, we must integrate over the phase-space of the particle a , weighted with its energy,

$$Q_a \equiv S \int E_a \mathcal{D}p_a \int \mathcal{D}p_b \mathcal{D}p_c \mathcal{D}p_d (2\pi)^4 \delta(p_a + p_b - p_c - p_d) f_c f_d (1 \pm f_b) \sum_{\text{spins}} |\mathcal{M}|^2. \quad (4.31)$$

Many of the following results will prove simpler when written in terms of the Mandelstam variables, that can be expressed in different ways

$$\begin{aligned} s &= -(p_a + p_b)^2 = m_a^2 + m_b^2 + 2(p_a p_b) \\ &= -(p_c + p_d)^2 = m_c^2 + m_d^2 + 2(p_c p_d), \end{aligned} \quad (4.32a)$$

$$\begin{aligned} t &= -(p_a - p_c)^2 = m_a^2 + m_c^2 - 2(p_a p_c) \\ &= -(p_d - p_b)^2 = m_d^2 + m_b^2 - 2(p_d p_b), \end{aligned} \quad (4.32b)$$

$$\begin{aligned} u &= -(p_a - p_d)^2 = m_a^2 + m_d^2 - 2(p_a p_d) \\ &= -(p_c - p_b)^2 = m_c^2 + m_b^2 - 2(p_c p_b), \end{aligned} \quad (4.32c)$$

$$s + t + u = m_a^2 + m_b^2 + m_c^2 + m_d^2, \quad (4.32d)$$

where $(p_a p_b) \equiv \eta_{\mu\nu} p_a^\mu p_b^\nu$ is a scalar product of four-vectors. We can perform first the integrals over a and b

$$\begin{aligned} Q_a &= S \int f_c \mathcal{D}p_c \int f_d \mathcal{D}p_d \mathcal{I} \\ &= \frac{S}{2(2\pi)^4} \int_{m_c}^{\infty} f_c(E_c) p_c dE_c \int_{m_d}^{\infty} f_d(E_d) p_d dE_d \int_{-1}^1 dz_{cd} \mathcal{I}. \end{aligned} \quad (4.33)$$

where now p_c and p_d stand for the magnitude of the three-momentum and $z_{cd} \equiv \cos(\theta_c + \theta_d)$. The easiest way to compute \mathcal{I} is to change to the center of mass (CM)

frame, see Figure 4.2. Boosting to the CM we get³

$$\begin{aligned}
\mathcal{I} &\equiv \int E_a \mathcal{D}p_a \int \mathcal{D}p_b (1 \pm f_b(E_b)) (2\pi)^4 \delta(p_a + p_b - p_c - p_d) \sum_{\text{spins}} |\mathcal{M}|^2 \\
&= \int \frac{E_a}{2E_a^{\text{cm}}} \frac{d^3 p_a^{\text{cm}}}{(2\pi)^2} \int \frac{d^3 p_b^{\text{cm}}}{2E_b^{\text{cm}}} (1 \pm f_b(E_b)) \delta(\mathbf{p}_a^{\text{cm}} + \mathbf{p}_b^{\text{cm}}) \delta(E_a^{\text{cm}} + E_b^{\text{cm}} - \sqrt{s}) \sum_{\text{spins}} |\mathcal{M}|^2 \\
&= \frac{1}{8\pi} \int_{-1}^1 dz_{\text{cm}} (1 \pm f_b(E_b)) \frac{p_{\text{cm}} E_a}{\sqrt{s}} \theta(\sqrt{s} - m_a - m_b) \sum_{\text{spins}} |\mathcal{M}|^2, \tag{4.34}
\end{aligned}$$

where

$$p_{\text{cm}} \equiv p_a^{\text{cm}} = p_b^{\text{cm}} = \frac{1}{2\sqrt{s}} \sqrt{s^2 - 2(m_a^2 + m_b^2)s + (m_a^2 - m_b^2)^2}, \tag{4.35a}$$

$$p'_{\text{cm}} \equiv p_c^{\text{cm}} = p_d^{\text{cm}} = \frac{1}{2\sqrt{s}} \sqrt{s^2 - 2(m_c^2 + m_d^2)s + (m_c^2 - m_d^2)^2}, \tag{4.35b}$$

$$E_b^{\text{cm}} = \frac{1}{2\sqrt{s}} (s + m_b^2 - m_a^2), \tag{4.35c}$$

$$E_a^{\text{cm}} = \frac{1}{2\sqrt{s}} (s + m_a^2 - m_b^2), \tag{4.35d}$$

and the Mandelstam variables are

$$s = m_c^2 + m_d^2 + 2E_c E_d - 2p_c p_d z_{cd}, \tag{4.36a}$$

$$t = m_c^2 + m_a^2 - 2E_c^{\text{cm}} E_a^{\text{cm}} + 2p_{\text{cm}} p'_{\text{cm}} z_{\text{cm}}, \tag{4.36b}$$

$$u = m_a^2 + m_b^2 + m_c^2 + m_d^2 - s - t. \tag{4.36c}$$

After the collision we know how to relate the (a, b) quantities with the (c, d) quantities in the CM frame, but we need E_a and E_b so we must boost back to a general frame

$$E_a = \gamma (E_a^{\text{cm}} + \mathbf{p}_{\text{cm}} \cdot \boldsymbol{\beta}_{\text{cm}}), \tag{4.37a}$$

$$E_b = \gamma (E_b^{\text{cm}} - \mathbf{p}_{\text{cm}} \cdot \boldsymbol{\beta}_{\text{cm}}), \tag{4.37b}$$

where the velocity of the CM in an arbitrary frame is given by

$$\begin{aligned}
\boldsymbol{\beta}_{\text{cm}} &= \frac{\mathbf{p}_c + \mathbf{p}_d}{E_c + E_d}, \\
\beta &\equiv |\boldsymbol{\beta}_{\text{cm}}| = \sqrt{1 - \frac{s}{(E_c + E_d)^2}}, \\
\gamma &\equiv \frac{1}{\sqrt{1 - \beta^2}} = \frac{E_c + E_d}{\sqrt{s}}. \tag{4.38}
\end{aligned}$$

To sum up, we need to find $\cos\theta_{\text{cm}}$ and relate it with our integration variables (E_c , E_d , $z_{cd} = \cos(\theta_c + \theta_d)$, $z_{\text{cm}} = \cos(\theta'_{\text{cm}} + \theta_{\text{cm}})$). We achieve this in two steps.

³

$$\delta(E_a^{\text{cm}} + E_b^{\text{cm}} - \sqrt{s}) = \frac{E_a^{\text{cm}} E_b^{\text{cm}}}{p_{\text{cm}} \sqrt{s}} \delta(p_{\text{cm}} - p_{\text{cm}}^0) \theta(\sqrt{s} - m_a - m_b)$$

I) First we will calculate θ'_{cm} in terms of \mathbf{E}_c , \mathbf{E}_d and z_{cd} .

II) Then, we will use z_{cm} to find $\cos\theta_{\text{cm}}$.

We can compute $\cos\theta'_{\text{cm}}$ from

$$\mathbf{E}_c = \gamma(\mathbf{E}_c^{\text{cm}} + \boldsymbol{\beta} \cdot \mathbf{p}'_{\text{cm}}) = \gamma(\mathbf{E}_c^{\text{cm}} + \beta p'_{\text{cm}} \cos\theta'_{\text{cm}}), \quad (4.39a)$$

$$\mathbf{E}_d = \gamma(\mathbf{E}_d^{\text{cm}} - \boldsymbol{\beta} \cdot \mathbf{p}'_{\text{cm}}) = \gamma(\mathbf{E}_d^{\text{cm}} - \beta p'_{\text{cm}} \cos\theta'_{\text{cm}}), \quad (4.39b)$$

so we have

$$\cos\theta'_{\text{cm}} = \frac{1}{\beta p'_{\text{cm}}} \left(\frac{\mathbf{E}_c}{\gamma} - \mathbf{E}_c^{\text{cm}} \right) = \frac{1}{\beta p'_{\text{cm}}} \left(-\frac{\mathbf{E}_d}{\gamma} + \mathbf{E}_d^{\text{cm}} \right). \quad (4.40)$$

Two cases of particular interest are:

- If $m_c = m_d$,

$$\cos\theta'_{\text{cm}} = \frac{\mathbf{E}_c - \mathbf{E}_d}{2\beta\gamma p'_{\text{cm}}}. \quad (4.41)$$

- If $m_c = 0$,

$$\cos\theta'_{\text{cm}} = \frac{1}{\beta} \left(\frac{\mathbf{E}_c}{\gamma E_c^{\text{cm}}} - 1 \right). \quad (4.42)$$

4.3.2 External field process

Let us consider a $2 \rightarrow 3$ process where one of the particles in the initial and final state is much heavier than the others. The heavy particle in this case ensures the conservation of momentum without contributing significantly to the energy balance. It can be effectively described as an external field ($1 + \text{EF} \rightarrow 2$). The rate equation in this case is

$$Q_a = n_h S \int \mathbf{E}_a \mathcal{D}p_a \int (1 \pm f_b) \mathcal{D}p_b \int f_c \mathcal{D}p_c (2\pi) \delta(\mathbf{E}_a + \mathbf{E}_b - \mathbf{E}_c) \sum_{\text{spins}} |\mathcal{M}|^2, \quad (4.43)$$

where n_h is the number density of heavy particles and $|\mathcal{M}|$ is the matrix element for the process $c + \text{EF} \rightarrow a + b$.

4.3.3 Two-particle annihilation

The general formula for a process $c + d \rightarrow a$ is

$$Q_a = S \int \mathbf{E}_a \mathcal{D}p_a \int f_c \mathcal{D}p_c \int f_d \mathcal{D}p_d (2\pi)^4 \delta(p_a - p_c - p_d) \sum_{\text{spins}} |\mathcal{M}|^2. \quad (4.44)$$

In this case, it is easier to integrate over p_a in the CM frame

$$\begin{aligned} Q_a &= S \int f_c \mathcal{D}p_c \int f_d \mathcal{D}p_d \frac{\mathbf{E}_a}{2m_a} (2\pi) \delta(m_a - \sqrt{s}) \sum_{\text{spins}} |\mathcal{M}|^2 \\ &= \frac{S}{4(2\pi)^3} \int_{m_c}^{\infty} f_c p_c dE_c \int_{m_d}^{\infty} f_d p_d dE_d \int_{-1}^1 dz_{cd} \frac{\mathbf{E}_c + \mathbf{E}_d}{m_a} \delta(m_a - \sqrt{s}) \sum_{\text{spins}} |\mathcal{M}|^2. \end{aligned} \quad (4.45)$$

4.4 Plasma processes

4.4.1 Photon-photon annihilation

There is only one Feynman diagram contributing to the process

$$h_{\mu\nu} = -2i\kappa\epsilon^\alpha(k_1)\epsilon^\beta(k_2)V_{(\mu\nu)\alpha\beta}(k_1, k_2)\epsilon^{*\mu\nu}(k_1 + k_2). \quad (4.46)$$

This scattering amplitude verifies the Ward identity⁴

$$k_1^\alpha V_{(\mu\nu)\alpha\beta} = k_2^\beta V_{(\mu\nu)\alpha\beta} = 0. \quad (4.47)$$

If both photons are on-shell it also verifies the equivalent identity for external gravitons

$$(k_1 + k_2)^\mu V_{(\mu\nu)\alpha\beta} = 0. \quad (4.48)$$

Summing over initial and final spins, we can easily obtain the matrix element

$$\sum_{\text{spins}} |\mathcal{M}|^2 = 4\kappa^2 S^{\mu\nu\mu'\nu'} V_{\mu\nu\alpha\beta} V_{\mu'\nu'\alpha\beta} = -8\kappa^2 (k_1 k_2)^2 = 2\kappa^2 s^2. \quad (4.49)$$

Now we can plug it in our Boltzmann equation, with the appropriate Bose-Einstein distributions and a symmetry factor $S = 1/2$ for identical particles in the initial state, to compute the energy loss

$$Q_\gamma = -\frac{\kappa^2 m^4 T^3}{2(2\pi)^3} \int_0^\infty \frac{\omega d\omega}{e^\omega - 1} \log\left(1 - e^{-\frac{m^2}{4T^2\omega}}\right), \quad (4.50)$$

where $s = 2\omega_c\omega_d(1 - z_{cd})$ is the center of mass energy and $z_{cd} \equiv \cos(\theta_{cd})$ is the cosine of the angle between the incident photons.

4.4.2 Gravi-Compton process

The Gravi-Compton process consists on four diagrams, see Figure 4.3. The matrix element for the process is

$$i\mathcal{M} \equiv -i\kappa e \mathcal{A}_{\mu\nu\alpha} \epsilon^{*\mu\nu}(q) \epsilon^\alpha(k), \quad (4.51)$$

⁴In this case it is really an identity, stemming from the structure of $V_{(\mu\nu)\alpha\beta}$ and irrespective of whether the particles are on-shell or not.

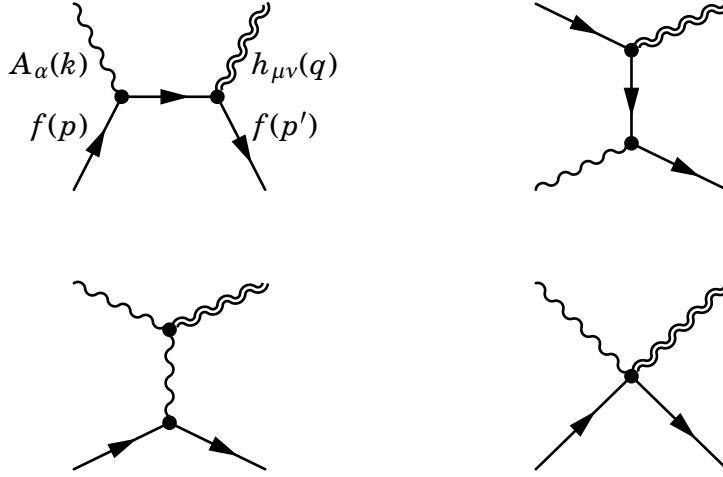


Figure 4.3: Gravi-Compton process.

where

$$\begin{aligned} \mathcal{A}_{\mu\nu\alpha}^{(\text{I})} &= \bar{u} \frac{p_\mu + k_\mu - q_\mu/2}{(p+k)^2 + m_e^2} \gamma_\nu (\not{p} + \not{k} - m_e) \gamma_\alpha u \\ &\quad + \bar{u} \frac{\eta_{\mu\nu}}{(k+p)^2 + m_e^2} (k+p - q/2 + 2m_e)(k+p - m_e) \gamma_\alpha u, \end{aligned} \quad (4.52a)$$

$$\begin{aligned} \mathcal{A}_{\mu\nu\alpha}^{(\text{II})} &= \bar{u} \frac{p_\mu - q_\mu/2}{(p-q)^2 + m_e^2} \gamma_\alpha (\not{p} - \not{q} - m_e) \gamma_\nu u \\ &\quad + \bar{u} \frac{\eta_{\mu\nu}}{(p-q)^2 + m_e^2} \gamma_\alpha (\not{p} - \not{q} - m_e) (\not{p} - \not{q}/2 + 2m_e) u, \end{aligned} \quad (4.52b)$$

$$\mathcal{A}_{\mu\nu\alpha}^{(\text{III})} = \frac{2}{(q-k)^2} \bar{u} \gamma^\beta V_{\mu\nu\beta\alpha}(q-k, k) u, \quad (4.52c)$$

$$\mathcal{A}_{\mu\nu\alpha}^{(\text{IV})} = \bar{u} (\gamma_\mu \eta_{\nu\alpha} - \eta_{\mu\nu} \gamma_\alpha) u, \quad (4.52d)$$

$$\mathcal{A}_{\mu\nu\alpha} \equiv \mathcal{A}_{(\mu\nu)\alpha}^{(\text{I})} + \mathcal{A}_{(\mu\nu)\alpha}^{(\text{II})} + \mathcal{A}_{(\mu\nu)\alpha}^{(\text{III})} + \mathcal{A}_{(\mu\nu)\alpha}^{(\text{IV})}. \quad (4.52e)$$

The scattering amplitude, for particles on-shell, verifies

$$k^\alpha \mathcal{A}_{\mu\nu\alpha} \epsilon^{*\mu\nu}(q) = 0, \quad (4.53)$$

$$q^\mu \mathcal{A}_{\mu\nu\alpha} \epsilon^\alpha(k) = 0, \quad (4.54)$$

where we have used the fact that the polarization tensor for photons satisfies $k^\alpha \epsilon_\alpha(k) = 0$. The squared matrix element, summing over spins, is

$$\begin{aligned} \sum_{\text{spins}} |\mathcal{M}|^2 &= (\kappa e)^2 S^{\mu\nu\mu'\nu'} \text{Tr} \left[\mathcal{A}_{\mu\nu\alpha} (\not{p} - m_e) \bar{\mathcal{A}}_{\mu'\nu'\alpha} (\not{p}' - m_e) \right] \\ &= (\kappa e)^2 F(s, t), \end{aligned} \quad (4.55)$$

where $F(s, t)$ is a lengthy function of the Mandelstam variables s, t and the masses of the particles, that we will integrate numerically later on. The final result for the

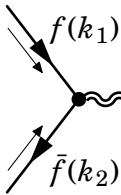
process $\gamma(c) + e(d) \rightarrow e(b) + G(a)$ is

$$\begin{aligned} Q_{\text{gcp}} = & \frac{\kappa^2 e^2}{8(2\pi)^5} \int_0^\infty \frac{E_c dE_c}{e^{E_c/T} - 1} \int_{m_e}^\infty \frac{p_d dE_d}{e^{(E_d - \mu)/T} + 1} \int_{-1}^1 dz_{cd} \int_{-1}^1 dz_{\text{cm}} (1 - f_{\text{F}}(E_b)) \\ & \times \frac{p_{\text{cm}} E_a}{\sqrt{s}} \theta(\sqrt{s} - m - m_e) F(s, t). \end{aligned} \quad (4.56)$$

The different variables can be related to the integration variables as explained in Section 4.3.1.

4.4.3 Electron-positron annihilation

The population of positrons is negligible in the Sun and in red giants. Processes involving positrons will only be important in supernovae, where the electrons are highly relativistic ($m_e \ll T_{\text{SN}}$) so we can safely set $m_e \simeq 0$. However, we will first check the consistency of the scattering amplitudes for a finite m_e and then set $m_e = 0$ at the cross-section level. Two electron-positron processes are relevant. The first process $e^+ e^- \rightarrow G$ is equivalent to the photon-photon annihilation



$$h_{\mu\nu} = -\frac{i\kappa}{2} \bar{v}(k_2) W_{(\mu\nu)}(k_1, -k_2) u(k_1) \epsilon^{*\mu\nu}(k_1 + k_2). \quad (4.57)$$

We can check that if the electrons are on-shell

$$(k_1 + k_2)^\mu \bar{v}(k_2) W_{(\mu\nu)}(k_1, -k_2) u(k_1) = 0. \quad (4.58)$$

The matrix element is easily computed

$$\begin{aligned} \sum_{\text{spins}} |\mathcal{M}|^2 &= \frac{\kappa^2}{4} (k_1 - k_2)_\mu (k_1 - k_2)_{\mu'} S^{\mu'\nu'\mu\nu} \text{Tr} \left[\gamma_\nu (k_1 - m_e) \gamma_{\nu'} (k_2 + m_e) \right] \\ &= \frac{\kappa^2}{2} \left(s^2 + \frac{4}{3} m_e^2 s - \frac{32}{3} m_e^4 \right) \simeq \frac{\kappa^2}{2} s^2, \end{aligned} \quad (4.59)$$

In the last line we have used the fact that this process will only be relevant in physical situations where $m_e/T \simeq 0$. The energy-loss rate is

$$Q_{ee1} = \frac{\kappa^2 m^4 T^3}{8(2\pi)^3} \int_0^\infty \frac{E dE}{e^{E+\mu/T} + 1} \log \left(1 + e^{-\frac{m^2}{4T^2 E} + \mu/T} \right) + (\mu \rightarrow -\mu), \quad (4.60)$$

where μ is the chemical potential for electrons. The second kind of electron-positron annihilation involves a photon and a hidden graviton in the final state, Figure 4.4, so it is also kinematically allowed in the massless limit. The amplitude and cross section for this case can be adapted from the Compton process (4.55) using the crossing symmetry

$$\sum_{\text{spins}} |\mathcal{M}|^2 = (\kappa e)^2 F(t, s). \quad (4.61)$$

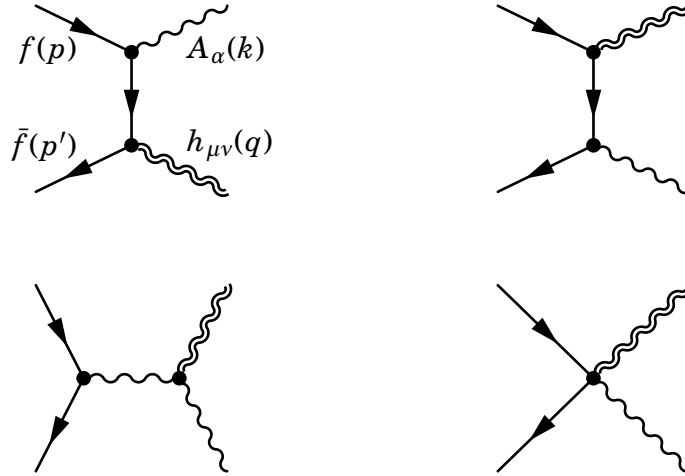


Figure 4.4: Electron-positron annihilation.

In the limit $m_e \rightarrow 0$, the function $F(t, s)$ takes a simple form

$$F(t, s) \simeq \frac{(m^4 - 2m^2t + s^2 + 2t(s+t))(4t(s+t) - m^2(s+4t))}{st(s+t-m^2)}. \quad (4.62)$$

The final result for the process $\bar{e}(c) + e(d) \rightarrow \gamma(b) + G(a)$ is

$$\begin{aligned} Q_{ee2} = & \frac{\kappa^2 e^2}{8(2\pi)^5} \int_0^\infty \frac{E_c dE_c}{e^{(E_c+\mu)/T} + 1} \int_0^\infty \frac{E_d dE_d}{e^{(E_d-\mu)/T} + 1} \int_{-1}^1 dz_{cd} \int_{-1}^1 dz_{cm} (1 + f_B(E_b)) \\ & \times \frac{p_{cm} E_a}{\sqrt{s}} \theta(\sqrt{s} - m) F(t, s). \end{aligned} \quad (4.63)$$

4.4.4 Gravi-bremsstrahlung

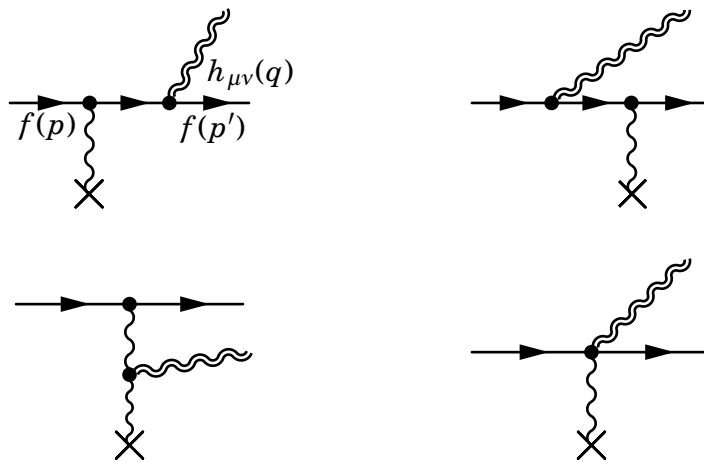


Figure 4.5: Gravi-bremsstrahlung process.

For this process we can adapt the result (4.55). Now the photon is off-shell, see Figure 4.5. It is a Coulomb field produced by a static heavy nucleus. In the external field approximation, we must substitute the polarization vector $\epsilon^\alpha(k)$ with the

external Coulomb field $A^\alpha = -\eta^{0\alpha} Z e / k^2$, $k^\mu = (0, \mathbf{q} + \mathbf{p}' - \mathbf{p})$. We are also neglecting the emission of hidden gravitons from the nucleus, since its contribution is strongly suppressed by its large mass. The matrix element is

$$\begin{aligned} \sum_{\text{spins}} |\mathcal{M}|^2 &= \frac{(\kappa Z e^2)^2}{k^4} S^{\mu\nu\mu'\nu'} \text{Tr} \left[\mathcal{A}_{\mu\nu 0}(\mathbf{p} + m_e) \bar{\mathcal{A}}_{\mu'\nu' 0}(\mathbf{p}' + m_e) \right] \\ &= (\kappa Z e^2)^2 M(s, t, u), \end{aligned} \quad (4.64)$$

where $M(s, t, u)$ is a lengthy, rational function of the Mandelstam variables and the masses of the particles. In the end, the energy-loss rate for the process $e(c) + \text{EF} \rightarrow e(b) + G(a)$ is

$$\begin{aligned} Q_{\text{gb}} &= \frac{\kappa^2 e^4}{4(2\pi)^5} \sum_j Z_j^2 n_j \int_{m_e}^{\infty} dE_b dE_c \theta(E_c - E_b - m) \int_{-1}^1 dz_a \int_{-1}^1 dz_c p_b p_c (E_c - E_b) \\ &\quad \times \sqrt{(E_c - E_b)^2 - m^2} f_{\text{F}}(E_c) (1 - f_{\text{F}}(E_b)) M(s, t, u), \end{aligned} \quad (4.65)$$

where we have summed over all the different nuclei present in the medium. If we assume that the star only contains fully ionized hydrogen and helium,

$$\sum_j Z_j^2 n_j = \sum_j Z_j^2 \frac{X_j \rho}{A_j m_u} = \frac{\rho}{m_u}, \quad (4.66)$$

where Z_j is the atomic number of the element j , X_j is the mass fraction, A_j is the atomic weight and m_u is the atomic mass unit. This should be a fair approximation, but it may underestimate the energy production in stars with appreciable metallicity. The heaviest nuclei, even in small amounts, can contribute significantly to this mechanism, for they also have higher charge Z .

4.4.5 Nucleon bremsstrahlung

As mentioned in the Section 4.1, most of the previous work on astrophysical constraints with massive gravitons was motivated by the ADD proposal [ADD98]. Shortly after, these authors studied the phenomenological implications of the model in [ADD99] and, using order-of-magnitude estimates, pointed out the relevance of two-nucleon processes $N + N \rightarrow N + N + G$ in supernovae.

Since then, considerable efforts have been devoted to detailed calculations of this energy-loss mechanism. In [CP99] and [Bar+99] the authors adopted a derivative and a Yukawa coupling for the nucleon-pion interaction, respectively, and computed the energy-loss rate relying on the one-pion-exchange approximation for the nucleon-nucleon scattering.

An alternative approach was adopted in [Han+01], where the authors dropped the one-pion-exchange approximation and used low-energy theorems to set bounds in a nearly model-independent way. The main assumptions in this case were that the emitted gravitons are soft and that the emission rate is dominated by two-body collisions. In this soft limit, the energy of the hidden graviton is much smaller than the other scales and it is possible to separate the details of the nucleon-nucleon scattering from the emission process. This result allows to use the measured nucleon-nucleon scattering cross-section and dramatically simplifies the calculations.

Finally, it is worth mentioning the results obtained in [HR03], where the authors derived some semiclassical formulas for the emission and absorption of hidden gravitons in a nuclear medium, such as a supernova or a neutron star.

For this work, we will just quote the results of [Han+01] for a single hidden graviton in a neutron gas (neutron-proton and proton-proton processes are subdominant). The energy emitted, in a nuclear bremsstrahlung process in the form of soft hidden gravitons, is

$$Q_{\text{nb}} = S \frac{2^{15/2} G_h M^{9/2} T^{13/2}}{5\pi^6} \int_{\delta}^{\infty} du_r \int_{-1}^1 d(\cos(\theta)) \int_0^{\infty} du_P \int_0^{u_r - \delta} du'_r \int_{-1}^1 d(\cos\theta') \\ u_r^{1/2} u_P^{1/2} u_r'^{1/2} \bar{u}^2 \xi[\delta/(u_r - u'_r)] f_1 f_2 (1 - f'_1)(1 - f'_2) \int_0^{2\pi} \frac{d\phi}{2\pi} \sin^2 \theta_{\text{cm}} |\mathcal{A}(\theta_{\text{cm}}, 2T\bar{u})|^2, \quad (4.67)$$

where $S = 1/4$ is the symmetry factor in this case, M is the neutron mass, T is the temperature of the neutron gas, $\mu = yT$ is the chemical potential and $m = 2T\delta$ is the hidden graviton mass. Other definitions are

$$f_i = \frac{1}{e^{(u_i - y_i)} + 1}, \quad u_{1,2} = u_P + u_r \pm 2\sqrt{u_P u_r} \cos \theta, \quad (4.68a)$$

$$f'_i = \frac{1}{e^{(u'_i - y_i)} + 1}, \quad u'_{1,2} = u_P + u'_r \pm 2\sqrt{u_P u'_r} \cos \theta', \quad (4.68b)$$

$$\bar{u} = (u_r + u'_r)/2, \quad (4.68c)$$

$$\xi[x] = \sqrt{1 - x^2} \left(\frac{19}{18} + \frac{11}{9} x^2 + \frac{2}{9} x^4 \right), \quad (4.68d)$$

$$\cos \theta_{\text{cm}} = \cos \theta \cos \theta' + \sin \theta \sin \theta' \cos \phi. \quad (4.68e)$$

Moreover, in the region of interest there is a weak dependence of the neutron-neutron scattering cross-section on the angle and the energy, so we can use the approximate result

$$\frac{M^2 |\mathcal{A}|^2}{32\pi} \simeq \sigma_0 = 25 \text{ mb}. \quad (4.69)$$

The formula (4.67) is strictly valid only when the emitted hidden gravitons are soft ($E \ll \frac{\bar{p}^2}{M} \rightarrow \frac{|u_r - u'_r|}{u_r + u'_r} \ll 1$). In particular, it is not valid in our whole range of masses. It works up to $m \sim 100$ MeV, but for these high masses the phase-space effects dominate the energy loss, so the results should not be significantly modified.

4.5 Astrophysical constraints

Stellar objects offer unique opportunities to study the behaviour of Nature under extreme conditions of temperature and density. They can be used as laboratories to constrain the properties of known particles, like neutrinos, or hypothetical new fields, like axions. The methods used to study new light particles with stars have been reviewed in Section 1.4.

In this section, we will apply the preceding results and the energy-loss argument of Section 1.4 to hidden gravitons. The relevant quantity for these constraints is the emissivity

$$\epsilon = \frac{Q}{\rho}, \quad (4.70)$$

i.e. the energy emitted per unit of mass. For each process (4.50, 4.56, 4.60, 4.63, 4.65, 4.67) under different medium conditions, relevant for the Sun (1.19), red giants (1.21) and supernovae (1.23) we can apply the relevant restrictions. The main results are collected in Figure 4.6.

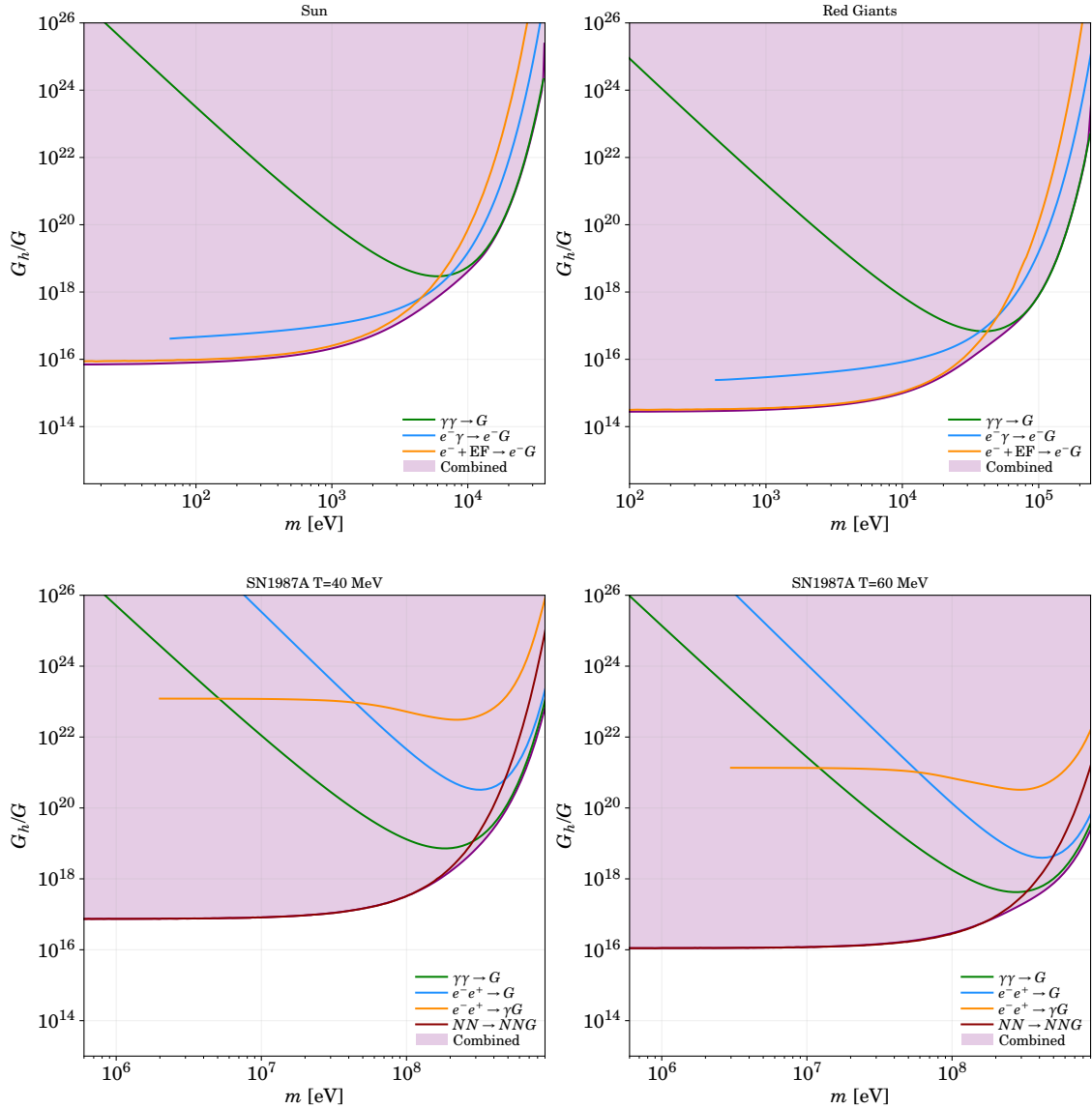


Figure 4.6: Constraints coming from the processes considered under different astrophysical conditions, along with the combined bounds for each object. The shadowed region is excluded. In the supernova case, as there is uncertainty about its temperature, we plot the results for two different temperatures. For the final limits we will use the more conservative estimate of $T = 40$ MeV.

Some authors have derived semiclassical formulas for the emission of soft particles from stars, and applied them to the case of standard massless gravitons. These formulas can be used to check the order of magnitude of our computations, by comparing them with our results for very low masses (where the energy loss reaches a plateau). The first one was derived in [Wei65] and applies to our gravi-

bremsstrahlung process

$$\epsilon \simeq \frac{32}{5} G (3T)^{3/2} m_e^{-1/2} n_e^2 \frac{4}{\rho} \simeq 4.525 \times 10^{-17} \text{ erg g}^{-1} \text{ s}^{-1}, \quad (\text{Sun}) \quad (4.71)$$

that compares to our result $\sim 9.60 \times 10^{-17} \text{ erg g}^{-1} \text{ s}^{-1}$. The other formula derived in [HR03] applies to the nuclear bremsstrahlung process

$$\epsilon \simeq \frac{512 \log 2}{5\pi^{3/2}} G \sigma_0 \rho T^{7/2} M^{-5/2} \simeq 4.96 \times 10^2 \text{ erg g}^{-1} \text{ s}^{-1}, \quad (\text{SN}, T = 40 \text{ MeV}) \quad (4.72)$$

while our result is $\sim 1.35 \times 10^2 \text{ erg g}^{-1} \text{ s}^{-1}$. Both results show a good agreement.

We can combine these bounds with the ones obtained from fifth-forces, as shown in Figure 4.7. These astrophysical bounds complement the fifth-force constraints and are orders of magnitude more competitive than other restrictions in the same range of masses, like tests on atomic systems [MT15].

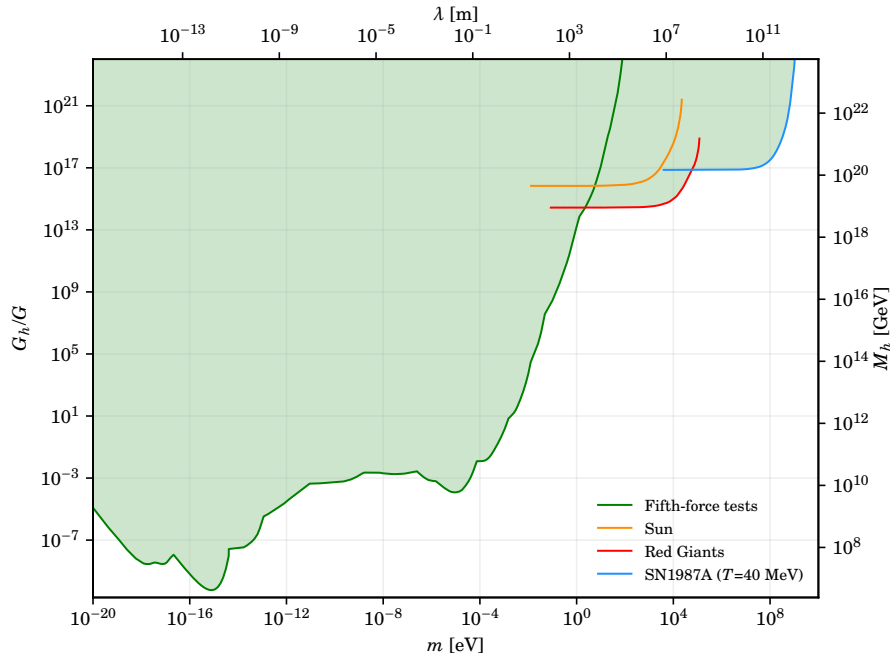


Figure 4.7: Constraints on the hidden-graviton mass and coupling G_h , relative to the standard-graviton coupling. The shadowed region is excluded by fifth-force tests and energy-loss restrictions, derived in this work. The two additional axes represent the distance scale $\lambda = 1/m$ and the energy scale $M_h = 1/\sqrt{8\pi G_h}$.

5

Repulsive Fuzzy Dark Matter

A second way to modify the standard dark sector is to go beyond the simplest dark energy or dark matter models. In this context, we consider a model where dark matter is ultralight and self-interacting: *repulsive fuzzy dark matter*. In Section 5.1, we start discussing the relevance of fuzzy dark matter (FDM) for astrophysics and cosmology. We introduce our model, and all the relevant equations to follow its evolution through different regimes, in Section 5.2. Finally, in Section 5.3 we determine its cosmological evolution and compare it with CMB and LSS data, constraining the mass and self-interaction strength of this new candidate.

5.1 FDM and coherent cosmological fields

5.1.1 Astrophysical behaviour

The challenges that Λ CDM faces at small scales have prompted the search for alternative models of dark matter. One of them, that has grown to be extremely popular in recent years, is fuzzy dark matter (FDM). It was initially proposed in [HBG00] that if the mass of the dark matter particles were ultralight ($m \sim 10^{-22}$ eV), their Compton wavelength (m^{-1}) would reach astrophysical scales. In this way the *core-cusp* problem, see Section 1.3, is neatly solved: the wave nature of particles on the smallest scales makes them impossible to localize, preventing the formation of cusps.

The usual approach to describe FDM is to start with a real scalar field¹

$$\square\phi = m^2\phi, \quad (5.1)$$

that will act as dark matter. In an astrophysical setting it is common to neglect the expansion of the Universe and work in the Newtonian limit. Expressing the real scalar field ϕ in terms of a complex scalar [Hui+17]

$$\phi \equiv \frac{1}{\sqrt{2m}} \left(\psi e^{-imt} + \psi^* e^{imt} \right), \quad (5.2)$$

and working in the non-relativistic limit, $|\dot{\psi}| \ll m|\psi|$, we arrive at

$$i\dot{\psi} = \left(-\frac{1}{2m}\nabla^2 + m\Phi \right) \psi, \quad (5.3a)$$

$$\nabla^2\Phi = 4\pi G\rho, \quad (5.3b)$$

¹ There was some debate in the early literature about whether ultralight scalar fields (produced through a misalignment mechanism) could be regarded as Bose-Einstein condensates and modelled as classical fields. This debate seems to be settled, see e.g. [SY09; Dav15; GHP15], and the classical-field picture is widely regarded as an appropriate description.

that is known as the Schrödinger-Poisson system. The eigenvalues of the time-independent version of (5.3) can be found for spherically symmetric configurations [Hui+17]. The ground state gives rise to the so-called solitonic core.

The first N -body simulation, taking (5.3) as the starting point, was performed in 2014 [SCB14]. The authors showed that the wave-like properties of this DM candidate lead to the formation of cores, obtaining the best fit to real galaxies for a mass of about $m \sim 10^{-22}$ eV.

It is common to perform a Madelung transformation

$$\psi \equiv \sqrt{\frac{\rho}{m}} e^{i\theta}, \quad (5.4a)$$

$$\mathbf{v} \equiv \frac{1}{m} \nabla \theta, \quad (5.4b)$$

obtaining two first-order differential equations for ρ and \mathbf{v} , equivalent to the continuity and Euler equations. Performing this change of variables, a new “quantum pressure” term appears in the Euler equation [Hui+17]. The advantage of this approach is that standard hydrodynamical N -body codes can be adapted to FDM just by adding the new source of pressure [Zha+18; NB18; LHB19].

The equivalence between the Schrödinger-Poisson (FDM) and Vlasov-Poisson (CDM) systems has been thoroughly studied in the literature for different dynamical configurations [KVS17; Moc+18]. Interestingly enough, prior to the FDM proposal, the Schrödinger-Poisson system (5.3) was explored as an alternative way to simulate CDM [WK93].

5.1.2 Cosmological behaviour

The present cosmological observations strongly favour a CDM-like behaviour for dark matter. As we will show now, FDM behaves as a rapidly oscillating coherent scalar field, thus recovering a CDM behaviour on cosmological scales.

In his groundbreaking work [Tur83], Turner analyzed a homogeneous oscillating scalar field in an expanding universe

$$\ddot{\phi} + 2\mathcal{H}\dot{\phi} + a^2 V'(\phi) = 0. \quad (5.5)$$

For a simple massive field we have

$$\ddot{\phi} + 2\mathcal{H}\dot{\phi} + m^2 a^2 \phi = 0. \quad (5.6)$$

This is just the equation for a damped harmonic oscillator with time-varying coefficients. In the regime where the time scale of variation of these coefficients, $\mathcal{O}(\mathcal{H}^{-1})$, is larger than the time scale of the system, $\mathcal{O}((ma)^{-2})$, i.e. $H/m \ll 1$, it is possible to find a WKB solution

$$\phi = \frac{\phi_0}{\alpha^{3/2}} \cos\left(\int m a d\tau\right) + \mathcal{O}\left(\frac{H}{m}\right). \quad (5.7)$$

The energy density and pressure, that can be obtained from (2.30), for this field are

$$\rho = \frac{1}{2}m^2\phi_0^2a^{-3} + \mathcal{O}\left(\frac{H}{m}\right), \quad (5.8a)$$

$$P = -\frac{1}{2}m^2\phi_0^2a^{-3} \cos\left(2 \int ma \, d\tau\right) + \mathcal{O}\left(\frac{H}{m}\right). \quad (5.8b)$$

Since the field oscillates with a frequency much larger than the expansion rate, the Einstein equations can be approximately solved using an averaged energy-momentum tensor

$$G_{\mu\nu} = 8\pi G \langle T_{\mu\nu} \rangle, \quad (5.9)$$

where

$$\langle T_{\mu\nu} \rangle(t) = \frac{1}{T} \int_{t-T/2}^{t+T/2} T_{\mu\nu}(t') \, dt', \quad (5.10)$$

and $\omega^{-1} \ll T \ll \mathcal{H}^{-1}$, where ω is the effective frequency of the field ($\omega = ma$ in the massive case). The averaging error introduced by this procedure is $\mathcal{O}(\mathcal{H}T)$ [CMN16]. The effective equation of state is

$$w = \frac{\langle P \rangle}{\langle \rho \rangle} = 0 + \mathcal{O}\left(\frac{H}{m}\right). \quad (5.11)$$

It behaves as CDM at the background level. In the original reference [Tur83], Turner further shows that, for a power-law potential $V(\phi) \propto \phi^n$,

$$w = \frac{n-2}{n+2} + \mathcal{O}\left(\frac{\mathcal{H}}{\omega}\right). \quad (5.12)$$

This result, and more general ones, can be obtained from a version of the virial theorem [JK08; CMN16].

After Turner's pioneering work, ultralight scalar fields have been thoroughly studied at the perturbation level [JK08; HN09; PHN12; Hlo+15; CMN16], proving that the same conclusion holds. Perturbations of coherent oscillating scalar fields admit an effective fluid description with an effective sound speed nearly zero, like CDM. The main cosmological signature of these models is the suppression of growth at small scales. Below some Jeans scale k_J^{-1} the modes do not grow appreciably, translating into a cut-off in the matter power spectrum [Hlo+15]. Additionally, there are important effects in the CMB temperature, lensing and polarization spectra. These effects were analyzed in [Hlo+17; HMG18] using the publicly available code AXIONCAMB. Although the work on ultralight fields has been mainly concerned with scalar fields, there are recent results on higher spin fields. It has been shown that abelian vectors at the background [Cem+12] and perturbation level [CMN17], non-abelian vectors [CMN13] and arbitrary-spin fields [CMN14] behave in a similar way. Interestingly, the results of [CMN14] show that it is possible to achieve an isotropic model of higher-spin dark matter as long as it is rapidly oscillating.

5.1.3 Axion-like particles

These ideas have been applied to the axion, a particularly well-motivated DM candidate. The standard QCD axion was initially proposed to solve the strong CP problem [PQ77; Wil78; Wei78] in particle physics. Likewise, the appearance of many

light scalar fields seems to be a generic feature of different string-theory scenarios. Some of these fields have a similar origin as the QCD axion, arising from the breaking of an approximate shift symmetry, and are usually known as axion-like particles (ALPs) or ultralight axions (ULAs) [Mar16; Hui+17]. ALPs present similar periodic potentials but with a mass much smaller than the QCD axion that could lie in the range of ultralight fields $m \sim 10^{-22}$ eV. While behaving like FDM, ALPs have a rich phenomenology based on their presumed interaction with matter. Aside from the standard searches for axions, there is a wealth of dedicated searches and projected experiments on the lookout for ultralight axions. These include studies of the neutral hydrogen distribution in the Universe [Sar+16; Kob+17], laboratory constraints based on nuclear interactions [Abe+17], variation of fundamental constants [SF15; SF16], astrophysical bounds [Ban+17; HSB18; Con+18], gravitational wave searches [Bri+17b; Bri+17a] and analysis of CMB spectral distortions [SSD17; DW17].

5.2 Repulsive FDM

The simplest model of fuzzy dark matter only involves a mass term in the potential. To extend the model one could add new couplings to matter or introduce a more complex potential. The axion model that we discussed in Section 5.1.3 explores both possibilities. Not only does the axion couple directly to photons, but it also has a non-trivial potential that introduces corrections over the mass term in FDM. These corrections arise, to first order, as quartic corrections in the potential with the opposite sign of the mass term, i.e. attractive self-interactions. The consequences of these self-interactions, as well as the effect of the full axion potential, have been studied and the impact on the linear power spectrum seems to be negligible [UG16; CGU17]. Beyond linear theory, it seems that self-interactions could play a role in the formation of non-linear structures [DKR18].

Another possibility involves introducing a positive quartic correction, i.e. repulsive self-interactions. It is more difficult to find particle-physics models in this case [Fan16], but the model is nonetheless well motivated as the simplest modification leading to a stable potential. This modification has been previously analyzed in some works [KMZ85; Goo00; LRS14; SC17; DLO17; LSR17]. The additional source of pressure from the repulsive self-interactions helps to solve the *core-cusp* problem with larger masses [Fan16]. Additionally, unlike the axion case, it could explain the formation of vortices in galaxies [RS12].

In this section we will study a FDM model with an additional quartic self-interaction. We first derive in Section 5.2.1 the equations describing a cosmological scalar field, both at the background and perturbation level. We will explore a region of the parameter space where the field will behave as a rapidly oscillating coherent field. The exact evolution equations can then be substituted by an approximate scheme where we follow only the behaviour of average quantities. This procedure is outlined in Section 5.2.2. This way we will gain physical insight while obtaining a set of equations suitable for a numerical implementation. We conclude in Section 5.2.3 with some analytical estimates that allow us to infer observational constraints

on our parameters without solving the evolution. These preliminary limits will be contrasted with the full numerical results in Section 5.3.

5.2.1 Exact description

Let us assume a scalar field with Lagrangian

$$\mathcal{L} = \frac{1}{2} g^{\mu\nu} \partial_\mu \phi \partial_\nu \phi - V(\phi) , \quad (5.13)$$

and potential

$$V(\phi) = \frac{1}{2} m^2 \phi^2 + \frac{1}{4} \lambda \phi^4 , \quad (5.14)$$

in a homogeneous and isotropic universe with a flat Robertson-Walker metric in conformal time (3.1). The equation of motion for a homogeneous scalar field in this background is

$$\ddot{\phi} + 2\mathcal{H}\dot{\phi} + a^2 V'(\phi) = 0 . \quad (5.15)$$

The components of the energy-momentum tensor are

$$T^0_0 = -\rho , \quad T^0_i = 0 , \quad T^i_j = \delta^i_j P , \quad (5.16)$$

where the density and pressure are

$$\rho = \frac{1}{2\alpha^2} \dot{\phi}^2 + V(\phi) , \quad (5.17)$$

$$P = \frac{1}{2\alpha^2} \dot{\phi}^2 - V(\phi) . \quad (5.18)$$

We choose initial conditions

$$\phi = \phi_0 , \quad (5.19)$$

$$\dot{\phi} = 0 . \quad (5.20)$$

The value ϕ_0 will be chosen to match the desired energy density ρ_ϕ today. Section 5.3.1 contains more details about how this matching is performed. These are the usual initial conditions when the axion-like particles are produced through a misalignment mechanism [DM17] and the field starts its evolution frozen. It is important to note that the choice of initial conditions has a deep impact in the subsequent evolution. In [LRS14], the authors considered a case similar to ours, but with an initial velocity $\dot{\phi} \neq 0$. In this case, there is an initial phase of stiff-matter ($w \simeq 1$) domination, absent in our case, constrained to be short enough not to spoil BBN.

Next, we study perturbations over this background solution. The metric perturbations are parameterized according to the general form (3.33) or to the scalar-vector-tensor version (3.126). The equation of motion for the scalar field perturbation is

$$\begin{aligned} \delta\ddot{\phi} + 2\mathcal{H}\delta\dot{\phi} + (k^2 + a^2 V''(\phi)) \delta\phi &= -\frac{1}{2} \left(\dot{A} - 2ik^i B_i + \dot{H}^i_i \right) \dot{\phi} + a^2 A V'(\phi) \\ &= (\dot{\Psi} + 3\dot{\Phi} - k^2(B - \dot{E})) \dot{\phi} - 2a^2 \Psi V'(\phi) . \end{aligned} \quad (5.21)$$

The components of the perturbed energy-momentum tensor are

$$\delta T^0_0 = -\frac{1}{a^2} (\dot{\phi} \delta \dot{\phi} - \Psi \dot{\phi}^2) - V' \delta \phi = -\delta \rho, \quad (5.22a)$$

$$\delta T^0_i = -\frac{ik_i}{a^2} \dot{\phi} \delta \phi = \delta Q_i, \quad (5.22b)$$

$$\delta T^i_j = \frac{1}{a^2} (\dot{\phi} \delta \dot{\phi} - \Psi \dot{\phi}^2) \delta^i_j - V' \delta \phi \delta^i_j = \delta P \delta^i_j. \quad (5.22c)$$

Notice that there is no anisotropic stress and that only scalar metric perturbations appear. It will be convenient to work in the synchronous gauge (3.162), in which case

$$\delta \ddot{\phi} + 2\mathcal{H} \delta \dot{\phi} + (k^2 + a^2 V'') \delta \phi = \frac{1}{2} \dot{h} \dot{\phi}, \quad (5.23)$$

and

$$\delta \rho = \frac{1}{a^2} \dot{\phi} \delta \dot{\phi} + V' \delta \phi, \quad (5.24)$$

$$\delta P = \frac{1}{a^2} \dot{\phi} \delta \dot{\phi} - V' \delta \phi, \quad (5.25)$$

$$(\rho + P)\theta = ik^i \delta Q_i = \frac{k^2}{a^2} \dot{\phi} \delta \phi. \quad (5.26)$$

Instead of solving the field equation (5.23), we will pursue the fluid analogy further and rewrite the system using the continuity and Euler equations. We introduce an alternative velocity variable

$$u \equiv \frac{1+w}{k} \theta = \frac{ik^i \delta Q_i}{\rho}, \quad (5.27)$$

that is numerically more stable when $w \simeq -1$. In absence of anisotropic stress ($\sigma = 0$), the conservation equations (D.64) and (D.68) for a generic fluid in the synchronous gauge are

$$\dot{\delta} + 3\mathcal{H}(c_s^2 - w)\delta + ku + \frac{1}{2}(1+w)\dot{h} = 0, \quad (5.28a)$$

$$\dot{u} + \mathcal{H}(1-3w)u - kc_s^2 \delta = 0. \quad (5.28b)$$

We need to find w and c_s^2 to close the system. The equation of state is just

$$w \equiv \frac{P}{\rho} = \frac{\dot{\phi}^2 - 2a^2 V(\phi)}{\dot{\phi}^2 + 2a^2 V(\phi)}. \quad (5.29)$$

It can be used to compute the adiabatic sound speed

$$c_{\text{ad}}^2 \equiv \frac{\dot{P}}{\dot{\rho}} = w - \frac{\dot{w}}{3\mathcal{H}(1+w)} = 1 + \frac{2}{3} \frac{a^2 V'}{\mathcal{H} \dot{\phi}}, \quad (5.30)$$

where we have used the background equation of motion (5.15). The sound speed *in the synchronous gauge* is²

$$c_s^2 = 1 + 3\mathcal{H}(1 - c_{\text{ad}}^2) \frac{u}{k\delta}. \quad (5.31)$$

²This result can be obtained directly using the expressions for δ and u in terms of $\delta\phi$ and $\delta\dot{\phi}$. It is also possible to compute the sound speed in the *comoving gauge*, where $\delta\phi = 0$ and $c_s^2 = 1$, and then transform it back to the synchronous gauge.

The final equations of motion are

$$\dot{\delta} = -3\mathcal{H}(1-w)\delta - ku - 9\mathcal{H}^2(1-c_{\text{ad}}^2)\frac{u}{k} - \frac{1}{2}(1+w)\dot{h}, \quad (5.32a)$$

$$\dot{u} = 2\mathcal{H}u + k\delta + 3(w - c_{\text{ad}}^2)\mathcal{H}u. \quad (5.32b)$$

Following the analysis of [Hlo+15] we provide initial conditions for the system

$$\delta = 0 + \mathcal{O}((k\tau)^4), \quad (5.33)$$

$$u = 0 + \mathcal{O}((k\tau)^4). \quad (5.34)$$

The overall evolution can be summarized as follows. The scalar field starts its evolution frozen in a value ϕ_0 with an equation of state $w \simeq -1$. As the Universe expands, the field starts rolling down the potential. When it reaches the minimum, a phase of fast oscillations sets in. This phase takes place when the effective frequency of the field, $\omega_{\text{eff}} \sim \sqrt{V''(\phi)}$, becomes larger than the expansion rate, \mathcal{H} .

On the numerical side, this wide separation of scales turns the problem intractable. It becomes prohibitively expensive to compute the exact evolution of the field, following every oscillation. This problem could be ameliorated choosing a different set of dynamical variables but, instead of trying to find a clever field redefinition, we will implement an entirely different strategy in the next section.

5.2.2 Averaged description

The averaged effective description that we described in Section 5.1.2 will be extended now to encompass our potential (5.14). The massive case ($\lambda = 0$) is particularly simple and the equation of motion (5.15) can be solved through a WKB expansion. Thanks to this adiabatic expansion in the parameter \mathcal{H}/ma , the averages can be performed explicitly, isolating the rapidly oscillating contributions and integrating by parts. This procedure for the massive case is discussed in [CMN16].

We are interested in anharmonic corrections to the mass term. Our first goal is to find the leading order correction in λ to the effective equation of state (5.11). We can start assuming that the WKB expansion (5.7) still holds to lowest order in λ

$$\phi(\tau) \simeq \frac{\phi_c}{a^{3/2}} \cos\left(\int ma(\tau')d\tau'\right) + \mathcal{O}\left(\frac{\mathcal{H}}{ma}\right). \quad (5.35)$$

With this WKB expression, to lowest order in λ , we have

$$\langle\phi^4\rangle \simeq \frac{3}{2}\langle\phi^2\rangle\langle\phi^2\rangle + \mathcal{O}\left(\frac{\mathcal{H}}{ma}\right), \quad (5.36)$$

$$\langle\rho\rangle \simeq m^2\langle\phi^2\rangle + \mathcal{O}\left(\frac{\mathcal{H}}{ma}\right), \quad (5.37)$$

so the first anharmonic correction to the equation of state is

$$w \simeq \frac{3\lambda}{8m^4}\langle\rho\rangle. \quad (5.38)$$

In this effective description, the background evolution of the field is described through its density and its effective equation of state, using the conservation equation

$$\partial_\tau\langle\rho\rangle = -3\mathcal{H}(1+w)\langle\rho\rangle. \quad (5.39)$$

For the equation of state w , when solving numerically the evolution, we will use the formula

$$w = \frac{\frac{3\lambda}{8m^4} \langle \rho \rangle}{1 + \frac{9\lambda}{8m^4} \langle \rho \rangle}, \quad (5.40)$$

that smoothly interpolates between the radiation-like $w \simeq 1/3$ and matter-like $w \simeq 0$ behaviour whenever the quartic or the quadratic part dominates³. The same technique can be applied to the perturbed fluid variables, obtaining the same results as in (5.28)

$$\dot{\delta} = 3\mathcal{H}(w - c_s^2)\delta - ku - \frac{1}{2}(1+w)\dot{h}, \quad (5.41a)$$

$$\dot{u} = -\mathcal{H}(1-w)u + kc_s^2\delta, \quad (5.41b)$$

but where now $\delta \equiv \langle \delta\rho \rangle / \langle \rho \rangle$ and $u \equiv ik^i \langle \delta Q_i \rangle / \langle \rho \rangle$ are defined with respect to the averaged energy-momentum tensor. To complete the system, there only remains to compute the effective sound speed

$$c_s^2 = \frac{\langle \delta P \rangle}{\langle \delta\rho \rangle}. \quad (5.42)$$

In contrast with the adiabatic sound speed, c_s^2 is gauge-dependent. However, as we will show now, the gauge ambiguities remain of order $\mathcal{O}(\mathcal{H}/\omega_{\text{eff}})$ so our effective sound speed turns out to be gauge-independent. In fact, identical expressions have previously been obtained working in the comoving gauge [LRS14] and in the Newtonian gauge [CMN16]. To leading order we have

$$\langle \partial_\tau(\dot{\phi}\delta\phi + \phi\dot{\delta}\phi) \rangle = 0 + \mathcal{O}\left(\frac{\mathcal{H}}{\omega_{\text{eff}}}\right). \quad (5.43)$$

Then, using (5.21) and (5.43) we can obtain the result

$$\langle \dot{\phi}\dot{\delta}\phi \rangle = \frac{1}{2} \langle a^2 V' \delta\phi + (k^2 + a^2 V'') \phi \delta\phi \rangle + \Psi \langle a^2 V' \phi \rangle + \mathcal{O}\left(\frac{\mathcal{H}}{\omega_{\text{eff}}}\right), \quad (5.44)$$

and finally compute the effective sound speed for a generic gauge

$$c_s^2 = \frac{\langle V' \delta\phi + ((k/a)^2 + V'') \phi \delta\phi - 2V' \delta\phi \rangle - 2\Psi \langle \dot{\phi}^2/a^2 - V' \phi \rangle}{\langle V' \delta\phi + ((k/a)^2 + V'') \phi \delta\phi + 2V' \delta\phi \rangle - 2\Psi \langle \dot{\phi}^2/a^2 - V' \phi \rangle} + \mathcal{O}\left(\frac{\mathcal{H}}{\omega_{\text{eff}}}\right) \quad (5.45)$$

$$= \frac{\langle ((k/a)^2 + V'') \phi \delta\phi - V' \delta\phi \rangle}{\langle ((k/a)^2 + V'') \phi \delta\phi + 3V' \delta\phi \rangle} + \mathcal{O}\left(\frac{\mathcal{H}}{\omega_{\text{eff}}}\right). \quad (5.46)$$

As we anticipated, the gauge ambiguities in the metric perturbations remain of order $\mathcal{O}(\mathcal{H}/\omega_{\text{eff}})$, so the final expression holds in any gauge. Moreover, it can be rewritten in a manifestly gauge-invariant form substituting $\delta\phi$ by its gauge-invariant

³Remember the result (5.12). The scalar field behaves (effectively) as radiation when the quartic field dominates.

perturbation⁴

$$\delta\phi_{\text{GI}} = \delta\phi + \dot{\phi}(B - \dot{E}), \quad (5.47)$$

and using the relations

$$\langle V' \dot{\phi} \rangle = \langle \partial_\tau(V) \rangle = 0 + \mathcal{O}\left(\frac{\mathcal{H}}{\omega_{\text{eff}}}\right), \quad (5.48)$$

$$\langle V'' \phi \dot{\phi} \rangle = \langle \phi \partial_\tau(V') \rangle = -\langle V' \dot{\phi} \rangle + \mathcal{O}\left(\frac{\mathcal{H}}{\omega_{\text{eff}}}\right) = 0 + \mathcal{O}\left(\frac{\mathcal{H}}{\omega_{\text{eff}}}\right), \quad (5.49)$$

we obtain

$$c_s^2 = \frac{\langle ((k/a)^2 + V'')\phi\delta\phi_{\text{GI}} - V'\delta\phi_{\text{GI}} \rangle}{\langle ((k/a)^2 + V'')\phi\delta\phi_{\text{GI}} + 3V'\delta\phi_{\text{GI}} \rangle} + \mathcal{O}\left(\frac{\mathcal{H}}{\omega_{\text{eff}}}\right). \quad (5.50)$$

This expression agrees with the result obtained in [CMN16] working in the Newtonian gauge, so the same conclusions apply. In particular, a generic feature of this kind of models is a suppression of growth $c_s^2 \simeq 1$ for small scales $k \gg \omega_{\text{eff}}$. In the case of a power-law potential $V(\phi) \propto \phi^n$, for large scales $k \ll \omega_{\text{eff}}$ we have

$$c_s^2 = \frac{n-2}{n+2} + \mathcal{O}\left(\frac{\mathcal{H}}{\omega_{\text{eff}}}\right). \quad (5.51)$$

For a harmonic potential $n = 2$, the zero-order term drops out and we must calculate the first-order corrections in k . Our potential of interest is a polynomial $V(\phi) = \frac{1}{2}m^2\phi^2 + \frac{\lambda}{4}\phi^4$, i.e. a mass term plus an anharmonic correction, in this case we have [CMN16]

$$c_s^2 = \frac{k^2}{4m^2a^2} + \frac{3}{4} \frac{\lambda}{m^4} \rho, \quad (5.52)$$

where ρ is the energy density of the scalar field and the anharmonic correction is assumed to be small. In our numerical solution we will use an effective sound speed

$$c_s^2 = \frac{\left(\frac{k}{2ma}\right)^2 + \frac{3}{4} \frac{\lambda}{m^4} \rho}{1 + \left(\frac{k}{2ma}\right)^2 + \frac{9}{4} \frac{\lambda}{m^4} \rho}, \quad (5.53)$$

suggested by the form of (5.46) and that smoothly interpolates between all the regimes of interest.

⁴Using the definition of δQ_i (5.22b) and its gauge transformation properties (3.155b) it is easy to deduce the gauge transformation properties for $\delta\phi$

$$\Delta\delta\phi = T\dot{\phi}.$$

One could obtain the same result making use of the fact that ϕ transforms as a scalar. From (3.159), we know that $\Delta(B - \dot{E}) = -T$ and then

$$\delta\phi_{\text{GI}} = \delta\phi + \dot{\phi}(B - \dot{E}),$$

is gauge invariant, i.e. $\Delta\delta\phi_{\text{GI}} = 0$.

5.2.3 Heuristic analysis

In this section we will discuss the simplest limits that constrain the model and the region of parameter space where we expect observable signatures. With this objective in mind, let us assume a simple cosmology composed of radiation, cosmological constant and our scalar field playing the role of dark matter

$$\mathcal{H}^2 = a^2 H_0^2 (\Omega_\phi(a) + \Omega_{\text{rad}} a^{-4} + \Omega_\Lambda) . \quad (5.54)$$

- *Limits on λ from background evolution.* The position of the peaks in the CMB temperature spectrum, especially the first one, is very sensitive to the amount of matter and the redshift of equality z_{eq} . We can assume that to have a viable model of dark matter this quantities remain essentially the same as in Λ CDM. In this case, to have a dark matter behaviour that resemble CDM, the anharmonic corrections at this time should be small

$$1 \gg w \simeq \frac{3}{8} \frac{\lambda}{m^4} \rho_\phi(a_{\text{eq}}) . \quad (5.55)$$

This imposes an upper limit on λ , namely

$$\lambda < \frac{8}{3} \frac{m^4}{\rho_\phi(a_{\text{eq}})} , \quad (5.56)$$

excluding the orange region in Figure 5.1.

- *Limits on m from perturbation evolution.* If λ is small enough, the background evolution of the effective fluid is identical to CDM. In this case, we can obtain limits from the behaviour of the perturbations. From (5.41a) and (5.41b) it can be seen that if we neglect the expansion rate, $c_s^2 k^2 \gg \mathcal{H}^2$, density perturbations evolve according to

$$\ddot{\delta} \simeq -c_s^2 k^2 \delta . \quad (5.57)$$

producing an oscillatory behaviour instead of the standard growth. To avoid a clear disagreement with observations, the effect of a non-negligible sound speed must be small

$$c_s^2 k^2 < \mathcal{H}^2 . \quad (5.58)$$

Translating into a lower bound for the allowed masses

$$m > \frac{k^2}{2a\mathcal{H}} . \quad (5.59)$$

As before, we assume that z_{eq} corresponds to the standard value and we apply the condition (5.59) at this redshift, that will give us the most conservative limit. For the wavenumber, we choose $k = 0.2 \text{ Mpc}^{-1}$, the highest mode observed in LSS at the linear level. The constraint is

$$m \gtrsim 10^{-26} \text{ eV} , \quad (5.60)$$

excluding the blue region in Figure 5.1.

- *Observable effects of anharmonic corrections.* Finally, there is a region in the parameter space that we cannot yet exclude and where the effects of anharmonic corrections to the sound speed may be important. At late times, repulsive FDM has a small but finite sound speed

$$c_s^2 \simeq \frac{k^2}{4m^2 a^2} + \frac{3}{4} \frac{\lambda}{m^4} \rho_\phi, \quad (5.61)$$

as compared with $c_s^2 = 0$ for standard CDM. This finite sound speed leads to a characteristic suppression in the matter power spectrum. If we want to observe the effects of λ , we must impose that the second term dominates over the harmonic contribution, yielding an upper bound

$$\lambda > \frac{k^2 m^2}{3 \rho_\phi a^2}. \quad (5.62)$$

This corresponds to a region where effects of the anharmonic correction to the sound speed are to be expected, but that we cannot exclude right away.

An additional result that can be obtained from (5.58) is the Jeans wavenumber

$$c_s^2 k_J^2 = \mathcal{H}^2. \quad (5.63)$$

Sub-Hubble modes below this Jeans wavenumber, $k < k_J$, grow while modes with $k > k_J$ are suppressed. In the massive case with $\lambda = 0$ we obtain

$$k_J^2 = 2a\mathcal{H}m. \quad (5.64)$$

Now, since we have seen that the quartic correction affects the sound speed, it will also affect the Jeans scale. It is natural to ask what combination of parameters (m , λ) can have a similar impact on structure formation as the case (\tilde{m} , $\tilde{\lambda} = 0$). To this end, we look for the combination that gives the same Jeans scale at the matter-radiation equality. Since its scaling in time is not significantly modified, this simple estimate should capture the essential features of structure formation in both models. Equating both sound speeds and inserting the result (5.64) we have an estimate for λ

$$\lambda = 4.96 \times 10^{-100} \left(\frac{\tilde{m}}{10^{-24} \text{ eV}} \right)^3 \left(\frac{1-r^2}{r^4} \right), \quad r \equiv \frac{\tilde{m}}{m}. \quad (5.65)$$

This simple result suggests for instance that, at the linear level, structure formation should be similar in the models ($\tilde{m} = 10^{-26}$ eV, $\tilde{\lambda} = 0$) and ($m = 10^{-24}$ eV, $\lambda \simeq 4.96 \times 10^{-98}$), a result that we will check with the full numerical solution. This estimate is represented in Figure 5.1 for two different masses \tilde{m} .

After discussing some approximate bounds on our model and its physical origin, we will devote the next section to the full numerical solution.

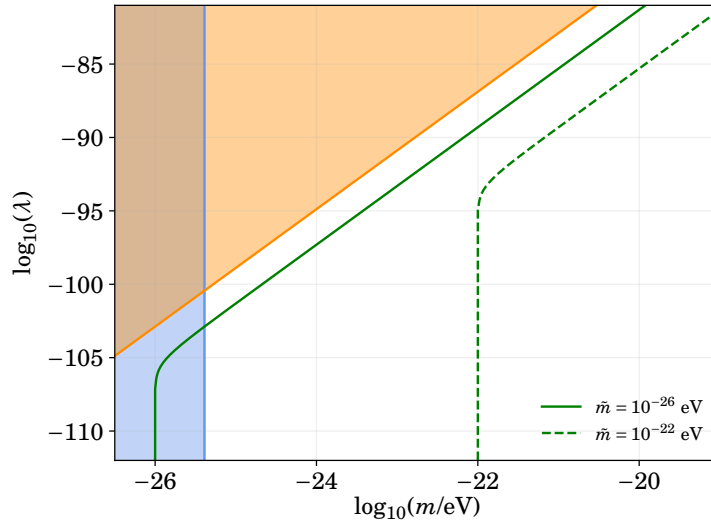


Figure 5.1: Different heuristic bounds. Orange region corresponds to the parameter-space excluded for the effects of λ on the background evolution. In the blue region, the effect of a non-negligible sound speed results in a strong disagreement with observations, hence it is excluded. The green curves represent (5.65) for two different masses. According to the argument in the main text, points along each curve should give similar structure-formation results.

5.3 Cosmological evolution and constraints

5.3.1 Numerical implementation

We modify the publicly available Boltzmann code CLASS [BLT11] and include this ultralight scalar field as a new species, that will assume the role of dark matter. Now, we summarize the key changes in the code and the evolution scheme chosen for the scalar field.

- At the background level, we start solving the equation (5.15) with initial conditions $\dot{\phi} = 0$ and $\phi = \phi_0$. The initial value ϕ_0 is chosen internally with a built-in shooting algorithm such as to match the required energy density $\Omega_\phi(\text{today})$. As a technical aside, it is critical to start with a sensible initial guess for ϕ_0 , so that the shooting algorithm converges quickly. In [Hlo+15] the authors provide analytical formulae for the initial guess in the harmonic case, that works as well if the anharmonic corrections are small. If the quadratic and quartic terms are comparable it is more difficult to find analytical expressions that fit our purposes. In our case, we precompute an interpolation table for different values of m , λ and ϕ_0 yielding some value $\Omega_\phi(m, \lambda, \phi_0)$. We only compute a coarse table, so that we still use the shooting algorithm to adjust ϕ_0 and achieve the desired precision in Ω_ϕ .

Another technical point involves the choice of the initial condition for $\dot{\phi}$. Since CLASS starts the integration at a finite $a_{\text{ini}} = 10^{-14}$, it is not strictly valid to set $\dot{\phi}(a_{\text{ini}}) = 0$. The proper way to account for this finite initial time is to use

the slow-roll approximation to obtain the analytic evolution at early times

$$\dot{\phi} \simeq -\frac{a_{\text{ini}}^3 V(\phi_0)}{3H_0}. \quad (5.66)$$

However, we have checked that, in practice, evolution starts early enough to be equivalent to use $\dot{\phi}(a_{\text{ini}}) = 0$. As long as the field starts in the slow-roll regime, the results are not significantly modified by the initial choice of $\dot{\phi}$.

With the initial conditions provided, the field starts its evolution frozen, slowly rolling down the potential until its natural frequency term in (5.15) dominates and it undergoes rapid oscillations. In this case it is computationally expensive to follow every oscillation so we turn to the averaged equations when $\sqrt{V''(\phi)} > 3H$.

In the averaged regime, we solve (5.39), matching continuously with the solution in the exact regime, and compute the pressure using the effective equation of state (5.40).

- At the perturbation level, we first solve (5.28) with adiabatic initial conditions $\delta = u = 0$. For each mode k we start the integration early enough to ensure that we start well within the exact regime, $\sqrt{V''(\phi)} \ll 3H$. In the averaged regime, $\sqrt{V''(\phi)} > 3H$, we solve (5.41) with the sound speed given by (5.53).

Some results for the temperature and matter power spectra are shown in Figures 5.2 and 5.3. They show the impact of different choices of m and λ , while the other cosmological parameters are fixed to their *Planck* [Ade+16a] best-fit values. As anticipated, the main cosmological signature is the appearance of a cut-off in the matter power spectrum. This cut-off has already been discussed in the harmonic case [Hlo+15]. In our case, we see that the anharmonic terms produce a similar effect.

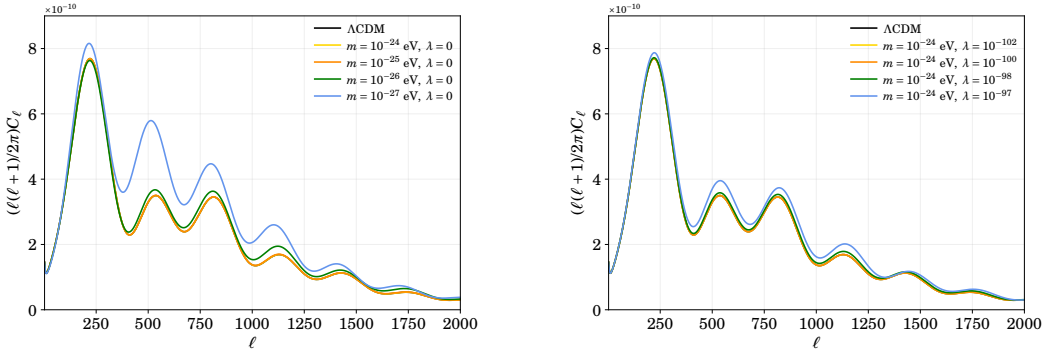


Figure 5.2: Temperature power spectrum. (Left) Results for a massive scalar field without self-interaction. (Right) Results for different self-interaction strengths for a mass that is indistinguishable from CDM with $\lambda = 0$.

5.3.2 Physical effects

The main physical effect responsible for the appearance of a cut-off in the matter power spectrum has already been discussed. In the averaged regime, the scalar field

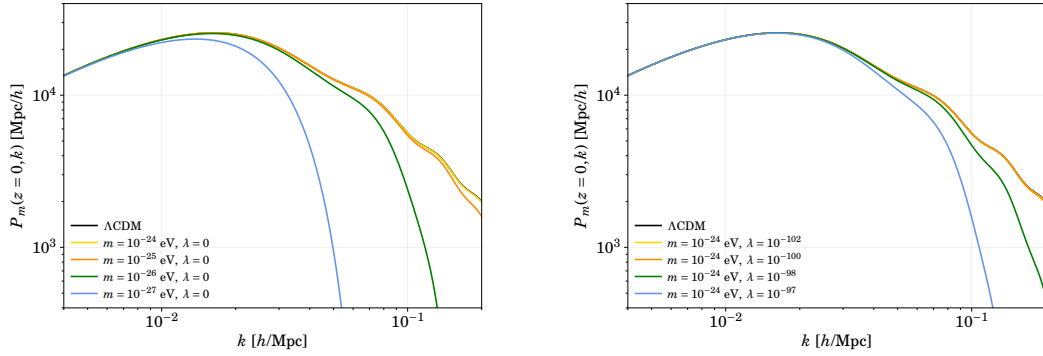


Figure 5.3: Matter power spectrum. (Left) Results for a massive scalar field without self-interaction. (Right) Results for different self-interaction strengths for a mass that is indistinguishable from CDM with $\lambda = 0$.

that supplies the dark matter component behaves like a fluid with a non-negligible sound speed. On small scales, above a certain Jeans scale k_J , the density perturbations oscillate and the growth is suppressed. This effect is illustrated in the Figure 5.4 for modes above and below k_J .

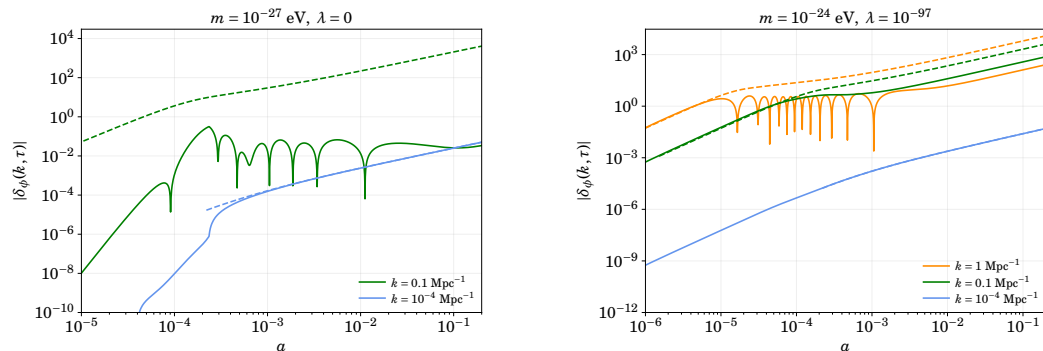


Figure 5.4: Evolution in time of the dark matter transfer functions compared to the standard ΛCDM evolution, represented by dotted lines, with Jeans scale at equality $k_J(z_{\text{eq}}) = 0.03 \text{ Mpc}^{-1}$ and $k_J(z_{\text{eq}}) = 0.11 \text{ Mpc}^{-1}$ respectively.

In the case of the CMB temperature power spectrum, it is far more difficult to disentangle the physical effect responsible for each feature. We split the effects in two categories, those coming from the modified background evolution and those coming from the perturbations. Furthermore, we will refer to two extreme cases ($m = 10^{-27}$, $\lambda = 0$) and ($m = 10^{-24}$, $\lambda = 10^{-97}$) as m -case and λ -case respectively. To gain some insight into the CMB spectrum structure, we will rely on simplified, analytical estimates [HS96b; Wei08; Les13], and work in the Newtonian gauge. In particular, we will analyze the evolution of the background and the perturbations. The thermodynamic part of the evolution, i.e. redshift of recombination and decoupling, is not appreciably modified since it takes place well after equality, when the scalar field closely resembles CDM.

Background evolution

The modified equation of state (5.40) changes the background evolution, modifying in particular the redshift of matter-radiation equality z_{eq} and in general the expansion history $a(\tau)$. In the m -case, the field transitions directly from the frozen phase with $w \simeq -1$ to a matter-like phase, while in the λ -case there is an intermediate radiation-like phase. There are two key effects.

- *First peak position.* The position ℓ_{peak} of the first peak in the CMB spectrum can be estimated as

$$\theta_{\text{peak}} = \frac{\pi}{\ell_{\text{peak}}} \simeq \frac{r_{\text{s}}|_{\text{dec}}}{d_{\text{A}}|_{\text{dec}}}, \quad (5.67)$$

where the angular diameter d_{A} distance is defined as

$$d_{\text{A}}|_{\text{dec}} = \int_{\tau_{\text{dec}}}^{\tau_0} d\tau, \quad (5.68)$$

$r_{\text{s}}|_{\text{dec}}$ is the sound horizon of the photon-baryon plasma evaluated at decoupling

$$r_{\text{s}}|_{\text{dec}} = \int_0^{\tau_{\text{dec}}} c_{\text{s}\gamma} d\tau, \quad (5.69)$$

and the sound speed for the baryon-photon plasma is

$$c_{\text{s}\gamma}^2 = \frac{1}{3(1+R)}, \quad R \equiv \frac{3\rho_{\text{b}}}{4\rho_{\gamma}}. \quad (5.70)$$

The angular diameter distance is almost unaffected but the sound horizon is slightly modified. Compared to Λ CDM we obtain relative deviations on ℓ_{peak} of about +2%, shift to the left, in the m -case and -0.7% , shift to the right, in the λ -case. Both are compatible with the tiny deviations observed in Figure 5.2.

- *Damping envelope.* Another physical scale that is modified is the diffusion length⁵

$$\lambda_{\text{D}}|_{\text{dec}} = \left(- \int_0^{\tau_{\text{dec}}} \frac{d\tau}{\dot{\kappa}} \right)^{1/2}, \quad (5.71)$$

The diffusion length governs the damping envelope, $e^{-(\ell/\ell_{\text{D}})^2}$, through the relation

$$\theta_{\text{D}} = \frac{\pi}{\ell_{\text{D}}} \simeq \frac{\lambda_{\text{D}}|_{\text{dec}}}{d_{\text{A}}|_{\text{dec}}}. \quad (5.72)$$

For a reference multipole $\ell = 820$, corresponding to the third acoustic peak, in the λ -case we obtain a modified damping envelope that produces an enhancement of 6% compared to Λ CDM, that can explain the overall increase of power in Figure 5.2. For the m -case, we obtain the puzzling result of a *suppression* of 0.7%, in clear disagreement with the observed effect. However, we will shortly see how a novel effect in the perturbation evolution can account for this overall amplification.

⁵This is an approximate expression that fit our purposes. For a more accurate estimation see [Ade+14a].

Perturbation evolution

In the tightly coupled regime, the photon density fluctuation (in the Newtonian gauge) evolves according to

$$\ddot{\delta}_\gamma + \frac{\dot{R}}{1+R}\dot{\delta}_\gamma + k^2 c_{s\gamma}^2 \delta_\gamma = -\frac{4k^2}{3}\Psi + \frac{4\dot{R}}{1+R}\dot{\Phi} + 4\ddot{\Phi}. \quad (5.73)$$

In the standard scenario, ignoring slow changes in R , Φ and Ψ from the expansion, we have

$$\ddot{\delta}_\gamma + k^2 c_{s\gamma}^2 \delta_\gamma \simeq -\frac{k^2}{3}\Psi. \quad (5.74)$$

This produces an oscillatory pattern with frequency $\omega = kc_{s\gamma}$ and zero-point displaced by an amount $-4(1+R)\Psi$. The main part of the temperature Sachs-Wolfe effect comes from the contribution $|\delta_\gamma/4 + \Psi|^2|_{\text{dec}}$, remember (3.236), so the displacement of the zero-point of the oscillations gives the characteristic asymmetry between odd and even peaks in the CMB temperature spectrum. Our modified dark matter model produces two interrelated effects: oscillation and suppression of growth at small scales.

- *Effects of suppression of growth at small scales.* The suppression of dark matter density perturbations at small scales also suppresses the gravitational wells Ψ , shifting the zero-point of the oscillation back to zero. This effect, alone, reduces the asymmetry among the peaks, decreasing the odd and increasing the even peaks. This explains the characteristic enhancement of the second peak with respect to the third one in Figure 5.2.
- *Effects of oscillatory behaviour.* There only remains to explain one effect: the striking gain in peak amplitude in the m -case. According to the modification in the damping envelope, the peaks should be slightly suppressed and their enhancement is actually related to a resonance effect. In the standard scenario, the term Ψ behaves like a constant external force, shifting the equilibrium position of the photon oscillations. In our case, it is not constant anymore, but oscillates with a frequency kc_s given by the sound speed of the dark matter perturbations (5.53). These two frequencies, kc_s and $kc_{s\gamma}$, are comparable for a range of k values, as shown in Figure 5.5, producing a resonant effect that increases the height of the peaks, as shown in Figure 5.6.

Moreover, since according to (5.53) the scale of the crossover in Figure 5.5 evolves $\propto a$, as we go from decoupling back in time it moves to smaller k . That is to say, although the crossover at decoupling is located around $k \simeq 0.1 \text{ Mpc}^{-1}$, smaller k have also fulfilled the resonance condition at earlier times, so they have also been amplified.

5.3.3 Observational constraints

To compare this model with CMB and LSS observations and refine the heuristic constraints obtained in Section 5.2.3, we use the public parameter-estimation code MontePython [Aud+13]. We will compare our results with two different data sets:

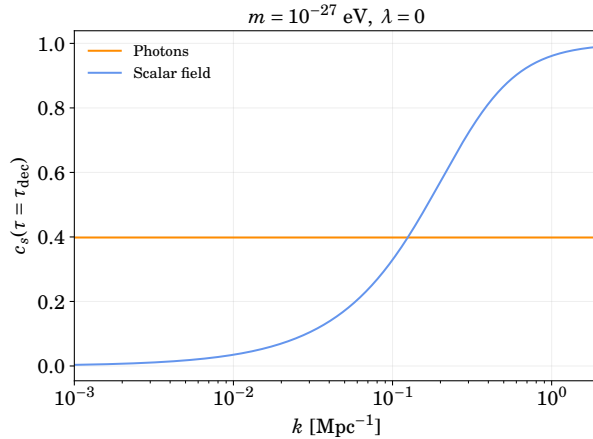


Figure 5.5: Sound speed at decoupling for photons and dark matter. Around $k \simeq 0.1 \text{ Mpc}^{-1}$ the sound speeds for both fluids, hence the oscillation frequencies too, are close and we have a resonant driving.

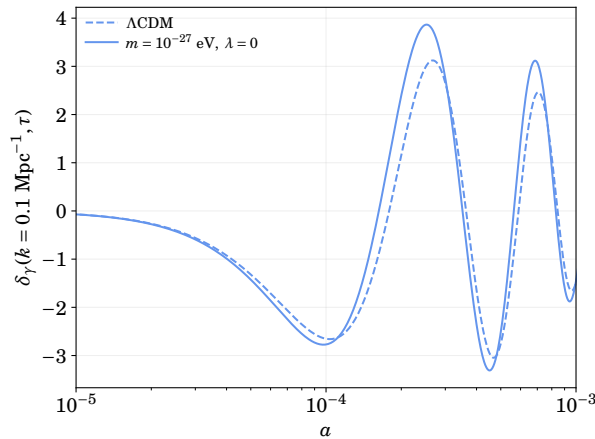


Figure 5.6: Evolution in time of the mode $k = 0.1 \text{ Mpc}^{-1}$, corresponding approximately to the third acoustic peak, until decoupling.

CMB measurements by *Planck* 2015 [Ade+16a] and LSS information by WiggleZ [Par+12]. We perform two analysis, *Planck* only and *Planck*+WiggleZ. In each case we vary the six Λ CDM base model parameters, the foreground parameters, plus m and λ , the mass and self-interaction strength. We choose logarithmic priors in our model parameters, as shown in Table 5.1.

It is important to note that to perform an accurate comparison with LSS data we must restrict our analysis to linear scales $k \lesssim 0.2 h/\text{Mpc}$. The non-linear module in CLASS includes HALOFIT [BVH12], but since it has not been calibrated for our model we restrict our analysis to linear scales without non-linear corrections. It is to be expected that, in the future, as more N -body simulations with ultralight fields become available, non-linear information will allow us to tighten the constraints.

We do not observe any significant degeneracy between m , λ and the rest of cosmological parameters. Best-fit results are shown in Table 5.2, while the marginalized contour for our model parameters is represented in Figure 5.7.

The presence of self-interactions in the ultralight field potential can lead to the

Parameter	minimum	maximum
$\Omega_b h^2$	–	–
$\Omega_\phi h^2$	–	–
h	–	–
$\log(10^{10} A_s)$	–	–
n_s	–	–
κ_{reio}	0.04	–
$\log_{10}(m/\text{eV})$	–26	–23.3
$\log_{10}(\lambda)$	–111	–98

Table 5.1: Prior ranges on the base Λ CDM parameters and the model parameters m and λ . A symbol – means that there is no prior. Additionally, the fixed parameters include the neutrino properties. In our case, two massless neutrinos plus a massive one with $m = 0.06$ eV, such that $N_{\text{eff}} = 3.046$ and $m_\nu/\Omega_\nu = 93.14$ eV.

Base parameters	<i>Planck</i>	<i>Planck+WiggleZ</i>
$\Omega_b h^2$	0.02223 ± 0.00047	$0.02212^{+0.00042}_{-0.00041}$
$\Omega_\phi h^2$	$0.1189^{+0.0044}_{-0.0041}$	$0.1204^{+0.0032}_{-0.0034}$
h	0.677 ± 0.019	$0.670^{+0.016}_{-0.014}$
$\log(10^{10} A_s)$	$3.070^{+0.056}_{-0.053}$	$3.057^{+0.046}_{-0.041}$
n_s	$0.965^{+0.016}_{-0.021}$	$0.963^{+0.011}_{-0.010}$
κ_{reio}	$0.070^{+0.028}_{-0.029}$	$0.061^{+0.024}_{-0.021}$
$\log_{10}(m/\text{eV})$	> -24.5	> -24.4
$\log_{10}(\lambda)$	–	< -99.0
Derived parameters		
z_{reio}	$9.2^{+2.6}_{-2.7}$	$8.4^{+2.2}_{-2.1}$
Ω_Λ	$0.690^{+0.024}_{-0.027}$	0.681 ± 0.021
Y_{He}	0.24778 ± 0.00020	0.24773 ± 0.00018
$100\theta_*$	$1.04193^{+0.00098}_{-0.00099}$	$1.04182^{+0.00084}_{-0.00083}$

Table 5.2: Best-fit results with 95% confidence level.

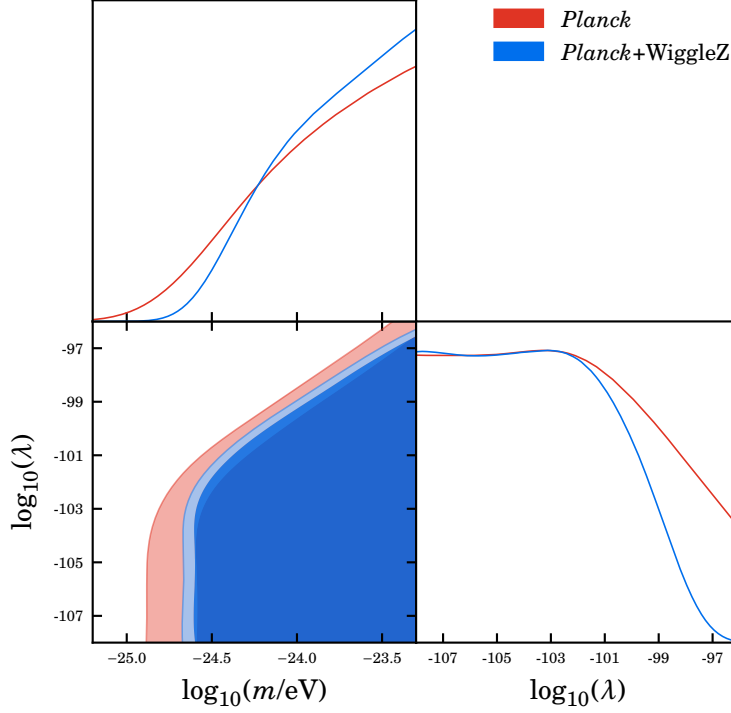


Figure 5.7: Contour plots with 95% and 99% confidence levels and 1d marginalized distributions.

appearance of new background-evolution phases, like the radiation-like phase due to our quartic potential. This modified background evolution, and especially its critical effect on the sound speed of dark matter perturbations, can lead to significant differences from observations. The observational signatures of the anharmonic contribution are similar to the mass term, the most prominent being the appearance of a cut-off in the matter power spectrum. This produces constraints for masses that would be otherwise indistinguishable from CDM, i.e. $m \gtrsim 10^{-24}$ eV. Our constraints on λ complement other bounds present in the literature, e.g. [DLO17]. These bounds on λ follow a scaling law with m^4 according to (5.56). We can extrapolate the results to higher masses using the 2σ region of Figure 5.7, obtaining an approximate constraint on λ

$$\log_{10}(\lambda) < -91.86 + 4\log_{10}\left(\frac{m}{10^{-22} \text{ eV}}\right), \quad (5.75)$$

for masses $m > 10^{-24}$ eV.

6

Non-comoving Cosmology

The last route to find an alternative to the Λ +CDM dark sector is to change a fundamental hypothesis. One of such hypotheses is the underlying Λ CDM assumption that large-scale motions, i.e. bulk flows, of the different components are negligible. In this chapter we will show that cosmological bulk flows can be introduced while still retaining an isotropic background and being compatible with current observations. This chapter is structured mimicking Chapter 3, highlighting the differences with the Λ CDM cosmology. In Section 6.1 we first motivate the existence of such large-scale flows in the Universe. Section 6.2 describes the background evolution of a set of fluids with bulk velocities, addressing the notions of isotropy and homogeneity in this context. The kinetic description is generalized in Section 6.3, as well as the Boltzmann equation in Section 6.4. In Section 6.5 we follow a different approach to the SVT decomposition and develop the Boltzmann hierarchy for scalar and vector modes. The Einstein equations remain unchanged and are collected in Section 6.6. Also in this section, we derive the modified gauge transformations. In order to obtain the first quantitative predictions of the model, we introduce the fluid approximation in Section 6.7 and study a reduced version of the system. The initial conditions for scalar and vector modes are collected in Section 6.8. In Section 6.9 we discuss our numerical implementation and obtain the first numerical results. Finally, Section 6.10 is devoted to the definition and computation of different observables.

6.1 Cosmology with large-scale motions

The isotropy and homogeneity of the Universe on large scales are two foundational assumptions of the standard cosmological model. These two assumptions are usually grouped under the name of Cosmological Principle. All the observational evidence, ranging from the extremely isotropic cosmic microwave background [Ade+16b; Saa+16; Akr+18a] to the galaxy number counts and the measured expansion from SNIa [KL01; AP10; BSL15], supports the conclusion that the Universe is very nearly isotropic on large scales. However, the notions of homogeneity and isotropy are inextricably linked with the election of a privileged frame. For any observer moving with respect to this frame, the Universe will appear anisotropic and inhomogeneous. This is precisely our situation on the Solar System.

Starting with the early CMB measurements [Kog+93; Lin+96], a significant dipole modulation, much larger than any other anisotropy, was found. This was readily interpreted as a kinematical effect: a Doppler-shifting effect arising from the relative motion of the Solar System with respect to the CMB rest frame, i.e. a frame in which the CMB looks isotropic. Recent analysis by the *Planck* Collaboration [Agh+14; Ade+16b] explored other kinematical effects, like the violation of

statistical isotropy induced by the observer motion, and reported an independent measurement of our relative velocity with respect to the CMB frame. This measured velocity can, given the uncertainties, fully account for the observed dipole, supporting its kinematical origin. Even if it is mostly kinematical, it may still contain an intrinsic contribution. Some authors have proposed searches for the intrinsic dipole, e.g. using spectral distortions [YP17].

A different kind of dipole should appear in the distribution of galaxies, induced by our motion with respect to the matter frame, i.e. a frame in which the matter distribution looks isotropic. The origin of the LSS dipole lies in a combination of Doppler shifting and aberration effects in the galaxy number counts [EB84; GH12]. Unfortunately, current observations can only loosely constrain its amplitude and direction, yielding a value compatible with the CMB dipole [Con+98; IYT10]. Future surveys like *Euclid* [Ame+18] and SKA [Maa+15] will measure it with unprecedented accuracy.

To complete the picture, we only need to know the relative velocity between the matter and CMB frames. Concerning this point, Λ CDM contains the underlying assumption, that usually goes by unnoticed, that both frames coincide. Λ CDM assumes matter and CMB to be *comoving*. As we will see in this chapter, it is possible to relax this condition. The homogeneous and isotropic Robertson-Walker metric can be sourced, at the background level, using non-comoving fluids. Thus, we will show that it is possible to construct a viable cosmological model for non-comoving fluids, with interesting phenomenological consequences and without any flagrant isotropy violation.

Early theoretical work concerning non-comoving fluids was mostly developed under the framework of tilted universes. The term was coined in the groundbreaking work by King and Ellis [KE73]. The authors considered a class of homogeneous models sourced by a single moving fluid, i.e. models in which the fluid 4-velocity is tilted with respect to the homogeneous hypersurfaces. These tilted models produce homogeneous but anisotropic universes. In a different context, Coley and Tupper [CT86] analyzed two-fluid cosmological models with general imperfect and non-comoving fluids. In order to source homogeneous and isotropic RW metrics, only very special configurations with radial velocities were considered. Later on, Turner [Tur91] proposed a theoretical mechanism to produce a mismatch between matter and CMB velocities. In Turner's tilted universes, the presence of a near-horizon-sized perturbation, remnant of inflation, could introduce a spatial gradient, driving the velocity of matter. More recently, the analysis of tilted models has been extended to Lemaître-Tolman-Bondi and Szekeres space-times [HDI11; Her+12; HDC18].

The analysis of non-comoving fluids has been extended to dark energy as well. Given our fundamental ignorance about the behaviour of the dark sector, it is conceivable that it has not ever been coupled to ordinary matter and that it does not share the same rest frame. Following this idea, a model of moving dark energy was proposed in [Mar06]. In this case, for a dynamical dark energy fluid, even if the matter and CMB frames coincide initially, they differ at late times. Different models of moving homogeneous dark energy were analyzed in [BM07; GMM16], as well as its possible impact in observables like the CMB quadrupole. The construction of a fully anisotropic model in which the full dark sector, i.e. dark energy and

dark matter, is non-comoving with the CMB and ordinary matter was carried out in [HL13]. The authors analyzed a Bianchi I universe in which dark matter and dark energy had different relative velocities with respect to the frame of ordinary matter and then derived some observables, like a modified luminosity-distance relation and CMB quadrupole.

From the observational point of view, a signal of the relative motion of the matter and CMB frames would be the detection of a large-scale bulk flow. In recent years, several works have claimed measurements of matter flows well in excess the Λ CDM predictions on different scales and at different statistical confidence levels [Kas+09; Ade+14b; Atr+15; Scr+16]. Although there seems to be a broad agreement on the direction of the flow, the amplitude is still subject to controversy [Ade+14b]. Such flows would be an indication of the existence of a cosmological preferred spatial direction. On the other hand, detected anomalies in the low multipoles of the CMB temperature power spectrum [Ade+16b], such as the low-multipole alignment and the dipolar or hemispherical anomalies, also suggest the presence of a preferred cosmological direction [Sch+16]. This fact has triggered the search for mechanisms which could break isotropy while keeping the predictions of standard cosmology.

The work in this chapter builds upon these previous studies, but we will present the first complete analysis for the evolution of a set of fluids with cosmological bulk flows, from the early to the late Universe, both at the background and perturbation level. As we will see later, it is reasonable to assume that any pair of tightly coupled fluids share the same velocity. Hence, we can expect that photons, baryons and neutrinos, being in thermal contact in the early Universe, shared a common rest frame, i.e. a frame in which the plasma looked isotropic. However, there is no *a priori* reason to assume the same about the dark sector. The dark sector, regardless of its composition, may very well possess its own rest frame, with a given global velocity with respect to the visible sector. The only reasonable assumption is that there is *one* frame that observes a homogeneous and isotropic universe, i.e. a RW background.

6.2 Perfect fluids with bulk velocity

6.2.1 Physical setting

Let us consider a perfect fluid, with an energy-momentum tensor given by (2.9), in a flat Robertson-Walker metric

$$ds^2 = \alpha^2(\tau) \left(-d\tau^2 + \delta_{ij} dx^i dx^j \right). \quad (6.1)$$

Now we will consider the situation where the fluid possesses a bulk velocity with respect to the frame in which the metric takes the form (6.1). Parameterizing the four-velocity as

$$u_\mu = \alpha \gamma (-1, v_i), \quad (6.2)$$

from the normalization condition, $u_\mu u^\mu = -1$, we have

$$\gamma = \frac{1}{\sqrt{1 - v^i v_i}}, \quad (6.3)$$

where the spatial indices in v_i are lowered and raised using δ_{ij} . With this parameterization the components of the energy-momentum tensor are

$$T^0_0 = -\rho - (\rho + P)\gamma^2 v^2, \quad (6.4a)$$

$$T^0_i = (\rho + P)\gamma^2 v_i, \quad (6.4b)$$

$$T^i_j = P\delta^i_j + (\rho + P)\gamma^2 v^i v_j. \quad (6.4c)$$

Since the non-diagonal components are not zero, this moving fluid cannot act as a source for the geometry (6.1). Let us show how to construct a valid source for the homogeneous and isotropic metric (6.1) using a collection of fluids.

Isotropy. For fluids moving with non-relativistic velocities ($v_i \ll 1$), the only non-diagonal component, to first order in v , is

$$T^0_i = (\rho + P)v_i. \quad (6.5)$$

If instead of a single fluid we have several fluids in relative motion, they can act as a source for (6.1) if they satisfy

$$T^0_i = \sum_s T_s^0_i = \sum_s (\rho_s + P_s)v_{si} = 0. \quad (6.6)$$

The physical content of this condition is that of a kind of *center of mass* frame condition. An isotropic source can be constructed, to first order in v , out of two non-relativistic fluids if the momentum density of one fluid is counterbalanced by that of the other fluid. We will see later that this constraint is conserved in time, so it can be implemented with an appropriate choice of the initial conditions. In [BM07] it is discussed how to transform to this frame, starting from an arbitrary configuration of the fluids.

Homogeneity. Homogeneity is easily implemented when the fluids are at rest, but we need to be cautious in our context. Consider two observers locally related by a boost:

- (τ, \mathbf{x}) , \mathcal{O} frame in which (6.6) is satisfied and the metric takes the form (6.1).
- $(\tilde{\tau}, \tilde{\mathbf{x}})$, $\tilde{\mathcal{O}}$ frame moving with respect to \mathcal{O} with velocity $\boldsymbol{\beta}$.

In the $\tilde{\mathcal{O}}$ frame, the transformed coordinates are obtained applying a local Lorentz transformation

$$d\tilde{x}^\mu = \Lambda^\mu_\nu(\boldsymbol{\beta})dx^\nu, \quad (6.7)$$

and the metric looks inhomogeneous

$$ds^2 = a^2(\tau(\tilde{\tau}, \tilde{\mathbf{x}})) \left(-d\tilde{\tau}^2 + \delta_{ij}d\tilde{x}^i d\tilde{x}^j \right). \quad (6.8)$$

The same applies to other time-dependent quantities like ρ and P . To provide a consistent source, we will require that the energy-momentum tensor of each fluid is homogeneous in the \mathcal{O} frame, i.e. the frame that observes an isotropic and homogeneous metric, *not* in the comoving frame with the fluid.

Finally, notice that on the tangent space at a given space-time point we can always define an orthonormal basis \mathbf{e}_a , see (2.102). For the flat RW metric, it is given by

$$\mathbf{e}_a = e^\mu{}_a \frac{\partial}{\partial x^\mu}, \quad e^\mu{}_a = a^{-1}(\tau) \delta^\mu{}_a, \quad (6.9)$$

and the corresponding orthonormal basis in the $\tilde{\mathcal{O}}$ frame reads

$$\tilde{\mathbf{e}}_a = \tilde{e}^\mu{}_a \frac{\partial}{\partial \tilde{x}^\mu}, \quad \tilde{e}^\mu{}_a = a^{-1}(\tau(\tilde{x})) \delta^\mu{}_a. \quad (6.10)$$

Thus, as expected, the two basis are just related by a Lorentz transformation on the tangent space

$$\tilde{\mathbf{e}}_a = (\Lambda^{-1}(\beta))^b{}_a \mathbf{e}_b. \quad (6.11)$$

To sum up, we can source a flat RW metric (6.1) with a collection of non-relativistic moving fluids as long as

I) We are in the center of mass frame, where

$$\sum_s (\rho_s + P_s) v_s^i = 0. \quad (6.12)$$

II) The energy-momentum tensor is homogeneous in that frame

$$\partial_i T^\mu{}_\nu = 0. \quad (6.13)$$

6.2.2 Evolution

Finally, in this subsection we will analyze the evolution of a perfect fluid with bulk velocity. Assuming homogeneity

$$\partial_i T^\mu{}_\nu = 0, \quad (6.14)$$

the conservation equation

$$\nabla_\mu T^\mu{}_\nu = 0, \quad (6.15)$$

for a flat RW metric in conformal time (6.1) yields the equations of motion

$$\partial_\tau (a^3 T^0{}_0) = \mathcal{H} a^3 T^i{}_i, \quad (6.16)$$

$$\partial_\tau (a^4 T^0{}_i) = 0. \quad (6.17)$$

As it was anticipated, (6.17) proves that the center of mass constraint (6.6) is conserved in time. Writing explicitly the components (6.4), the equations of motion can be rewritten in terms of v_i and ρ . The equation for the velocity can be expressed as

$$\partial_\tau v_i - \partial_\tau \log((1+w)a^4 \gamma^2 \rho) v_i = 0. \quad (6.18)$$

In the absence of interactions, the velocity does not change its direction, so we only need to follow the evolution of its magnitude. Combining (6.16) and (6.17), it is possible to obtain

$$\dot{\rho} = \frac{(v^2 - 3)(1+w)}{1-wv^2} \mathcal{H} \rho + \frac{\dot{w}}{1-wv^2} v^2 \rho, \quad (6.19)$$

$$\dot{v} = \frac{(1-v^2)(3w-1)}{1-wv^2} \mathcal{H} v + \frac{\dot{w}}{1+w} \frac{1-v^2}{1-wv^2} v, \quad (6.20)$$

assuming $w \neq -1$. It is worth particularizing these results to two kind of fluids.

- *Radiation*, $w = 1/3$.

$$\dot{\rho} = -4\mathcal{H}\rho , \quad (6.21)$$

$$\dot{v} = 0 . \quad (6.22)$$

The fluid moves with constant velocity and with the usual scaling $\rho \propto a^{-4}$.

- *Matter*, $w = 0$.

$$\dot{\rho} = (v^2 - 3)\mathcal{H}\rho , \quad (6.23)$$

$$\dot{v} = -(1 - v^2)\mathcal{H}v . \quad (6.24)$$

The equations can be solved analytically in this case

$$\rho = \frac{\rho_0}{a^2 \sqrt{v_0^2 + a^2(1 - v_0^2)}} , \quad (6.25)$$

$$v = \frac{v_0}{\sqrt{v_0^2 + a^2(1 - v_0^2)}} , \quad (6.26)$$

$$\gamma^2 \rho = \frac{\rho_0}{a^4(1 - v_0^2)} \sqrt{v_0^2 + a^2(1 - v_0^2)} , \quad (6.27)$$

where v_0 and ρ_0 are the velocity and density today. If the fluid starts with ultrarelativistic initial conditions, it behaves as radiation, $-T^0_0 = \gamma^2 \rho \propto a^{-4}$, until the velocity drops down and it enters the non-relativistic regime. In the non-relativistic regime, to first order in v , the velocity slows down with the expansion $v \propto a^{-1}$ and the density scales as usual $\gamma^2 \rho \simeq \rho \propto a^{-3}$.

Analytic expressions for a generic equation of state $w(a)$ can be obtained in the regime of small velocities

$$\rho = \rho_0 \exp\left(-3 \int \frac{da}{a} (1 + w)\right) + \mathcal{O}(v^2) , \quad (6.28)$$

$$v = \frac{v_0(1 + w_0)}{a^4(1 + w)} \exp\left(3 \int \frac{da}{a} (1 + w)\right) + \mathcal{O}(v^2) , \quad (6.29)$$

where w_0 is the value of the equation of state today. For the particular case $w = \text{const.}$, we have [Mar06; BM07]

$$\rho = \rho_0 a^{-3(1+w)} + \mathcal{O}(v^2) , \quad (6.30)$$

$$v = v_0 a^{-(1-3w)} + \mathcal{O}(v^2) . \quad (6.31)$$

6.3 Kinetic approach

As has been discussed in Section 3.2, in order to describe accurately the evolution of ultrarelativistic species and the photon-baryon decoupling, we must drop the perfect fluid framework. In this section we generalize the kinetic approach to include cosmological bulk flows. We will split the discussion into two parts. Since our main modification with respect to standard comoving cosmology concerns the definition of the unperturbed distribution function, we will focus on the background in the Section 6.3.1. Section 6.3.2 contains the complete treatment of perturbations.

6.3.1 Background

The definitions of the momentum variables follow those of Section 3.2. The formalism developed in that section to describe a Λ CDM cosmology must be adapted to accomodate the motion of the fluids. We introduce again two related frames.

- \mathcal{O} , frame in which the metric takes the RW form (6.1).
- $\tilde{\mathcal{O}}$, frame moving with respect to \mathcal{O} with velocity $\boldsymbol{\beta}$.

The local Lorentz transformation (6.7) that connects both frames yields

$$\tilde{\epsilon} \equiv \Lambda_\beta \epsilon = \gamma(\epsilon - \mathbf{q} \cdot \boldsymbol{\beta}) , \quad (6.32a)$$

$$\tilde{q}^i \equiv \Lambda_\beta q^i = \mathcal{P}_j^i q^j - \gamma \epsilon \beta^i , \quad (6.32b)$$

$$\boldsymbol{\beta} \cdot \tilde{\mathbf{q}} = \gamma(\mathbf{q} \cdot \boldsymbol{\beta} - \epsilon \beta) . \quad (6.32c)$$

We have defined

$$\mathcal{P}_j^i \equiv \delta_j^i + (\gamma - 1) \hat{\beta}^i \hat{\beta}_j , \quad (6.33a)$$

$$\gamma \equiv (1 - \beta^2)^{-1/2} , \quad (6.33b)$$

where $\hat{\beta}^i$ is a unit vector along $\boldsymbol{\beta}$ and every spatial index has been lowered or raised with δ_{ij} . Next, we consider a homogeneous distribution function in the \mathcal{O} frame

$$f(\tau, \mathbf{x}, \mathbf{q}) = f_0(\tau, \mathbf{q}) . \quad (6.34)$$

With this distribution function, we can define the usual fluid quantities (3.24)

$$\begin{aligned} \rho &\equiv a^{-4} g_* \int \frac{d^3 q}{(2\pi)^3} \epsilon f_0 , & P &\equiv a^{-4} g_* \int \frac{d^3 q}{(2\pi)^3} \frac{q^2}{3\epsilon} f_0 , \\ Q^i &\equiv a^{-4} g_* \int \frac{d^3 q}{(2\pi)^3} q^i f_0 , & n &\equiv a^{-3} g_* \int \frac{d^3 q}{(2\pi)^3} f_0 , \\ \Pi^{ij} &\equiv a^{-4} g_* \int \frac{d^3 q}{(2\pi)^3} \left(\frac{q^i q^j}{\epsilon} - \frac{q^2}{3\epsilon} \delta^{ij} \right) f_0 , & V^i &\equiv a^{-3} g_* \int \frac{d^3 q}{(2\pi)^3} \frac{q^i}{\epsilon} f_0 . \end{aligned} \quad (6.35)$$

To relate this set of quantities with those computed in the boosted $\tilde{\mathcal{O}}$ frame, we can either use their tensorial character under local Lorentz transformations or the fact that f transforms as a scalar

$$\tilde{f}_0(\tilde{\tau}, \tilde{\mathbf{x}}, \tilde{\mathbf{q}}) = f_0(\tau(\tilde{\tau}, \tilde{\mathbf{x}}), \mathbf{q}(\tilde{\mathbf{q}})) , \quad (6.36)$$

where, from now on, we will denote $\tilde{f}_0(\tilde{\tau}, \tilde{\mathbf{x}}, \tilde{\mathbf{q}})$ just as $\tilde{f}_0(\tau, \tilde{\mathbf{q}})$. With this property and the Lorentz-invariant volume element we can write, for instance,

$$\tilde{Q}^i = a^{-4} g_* \int \frac{d^3 \tilde{q}}{(2\pi)^3} \tilde{q}^i \tilde{f}_0(\tau, \tilde{\mathbf{q}}) = a^{-4} g_* \int \frac{d^3 q}{(2\pi)^3} \frac{(\Lambda_\beta \epsilon)(\Lambda_\beta q^i)}{\epsilon} f_0(\tau, \mathbf{q}) . \quad (6.37)$$

Using this procedure, one can obtain

$$\tilde{\rho} = \rho + \gamma^2 \left(\beta_k \beta_l \Pi^{kl} - 2\beta_k Q^k \right) + \gamma^2 \beta^2 (\rho + P), \quad (6.38a)$$

$$\tilde{Q}^i = \gamma \mathcal{P}_j^i \left(Q^j - \beta_k \Pi^{kj} \right) - \gamma^2 \beta^i \left(\rho + P - Q^j \beta_j \right), \quad (6.38b)$$

$$\begin{aligned} \tilde{\Pi}^{ij} = & \left(\mathcal{P}_k^i \mathcal{P}_l^j - \frac{1}{3} \gamma^2 \beta_k \beta_l \delta^{ij} \right) \Pi^{kl} - \gamma \left(\beta^i \mathcal{P}_k^j + \beta^j \mathcal{P}_k^i - \frac{2}{3} \gamma \delta^{ij} \beta_k \right) Q^k \\ & + \gamma^2 \left(\beta^i \beta^j - \frac{1}{3} \beta^2 \delta^{ij} \right) (\rho + P), \end{aligned} \quad (6.38c)$$

$$\tilde{P} = P + \frac{1}{3} \gamma^2 \left(\beta_k \beta_l \Pi^{kl} - 2\beta_k Q^k \right) + \frac{1}{3} \gamma^2 \beta^2 (\rho + P), \quad (6.38d)$$

$$\tilde{n} = \gamma (n - V^j \beta_j), \quad (6.38e)$$

$$\tilde{V}^i = \mathcal{P}_j^i V^j - \gamma \beta^i n. \quad (6.38f)$$

It is important to stress that the preceding relations hold as well if the quantities are defined with the full distribution function f , instead of using just the background part f_0 , and we will make use of them when we study perturbations.

There remains the question of how to describe the moving fluids of Section 6.2 in terms of a distribution function. We will describe the different constituents of the Universe with an unperturbed distribution function that satisfies

$$f_0(\tau, \mathbf{q}) = \tilde{f}_0(\tau, \tilde{\mathbf{q}}). \quad (6.39)$$

That is, the distribution function is homogeneous in the \mathcal{O} frame, i.e. the frame that observes a homogeneous and isotropic universe, and isotropic in the $\tilde{\mathcal{O}}$ frame, i.e. the frame comoving with the fluid. This parallels the discussion in Section 6.2 and allows us to describe a fluid moving with velocity $\boldsymbol{\beta}$. The condition (6.39) is the main physical assumption in our work. For instance, applying it to a blackbody spectrum for massless particles, using (6.32) we obtain the usual boosted distribution function

$$\tilde{f}_0(\tilde{\mathbf{q}}) = \frac{1}{e^{\tilde{q}/\tilde{T}} - 1} = \frac{1}{e^{q/T(\mathbf{q})} - 1} = f_0(\mathbf{q}), \quad T(\mathbf{q}) \equiv \gamma^{-1} \left(1 - \frac{\mathbf{q} \cdot \boldsymbol{\beta}}{q} \right)^{-1} \tilde{T}. \quad (6.40)$$

If the distribution function satisfies (6.39) we have

$$\tilde{\Pi}_{ij} = 0, \quad \tilde{V}_i = \tilde{Q}_i = 0, \quad (6.41)$$

so $\tilde{\mathcal{O}}$ is indeed the comoving frame with the (perfect) fluid. In this case, the relation between both sets of fluid variables is

$$\rho = \tilde{\rho} + \gamma^2 \beta^2 (\tilde{\rho} + \tilde{P}), \quad (6.42a)$$

$$Q^i = \gamma^2 \beta^i (\tilde{\rho} + \tilde{P}), \quad (6.42b)$$

$$\Pi^{ij} = \gamma^2 \left(\beta^i \beta^j - \frac{1}{3} \delta^{ij} \beta^2 \right) (\tilde{\rho} + \tilde{P}), \quad (6.42c)$$

$$P = \tilde{P} + \frac{1}{3} \gamma^2 \beta^2 (\tilde{\rho} + \tilde{P}), \quad (6.42d)$$

$$n = \gamma \tilde{n}, \quad (6.42e)$$

$$V^i = \gamma \beta^i \tilde{n}. \quad (6.42f)$$

Using the definition of the energy-momentum tensor (3.25), we can write its components as

$$T^0_0 = -\rho = -\tilde{\rho} - \gamma^2(\tilde{\rho} + \tilde{P})\beta^2, \quad (6.43a)$$

$$T^0_i = Q_i = \gamma^2(\tilde{\rho} + \tilde{P})\beta_i, \quad (6.43b)$$

$$T^i_j = P\delta^i_j + \Pi^i_j = \tilde{P}\delta^i_j + \gamma^2(\tilde{\rho} + \tilde{P})\beta^i\beta_j. \quad (6.43c)$$

These expressions agree with the ones obtained for a perfect fluid (6.4). Both approaches are equivalent at this level. To first order in β we have

$$T^0_0 = -\tilde{\rho}, \quad (6.44a)$$

$$T^0_i = (\tilde{\rho} + \tilde{P})\beta_i, \quad (6.44b)$$

$$T^i_j = \tilde{P}\delta^i_j. \quad (6.44c)$$

The total energy-momentum tensor for a collection of fluids is homogeneous, as it was imposed in (6.39), and it is also isotropic, to first order in β , if the velocities of the fluids satisfy the constraint

$$\sum_s (\tilde{\rho}_s + \tilde{P}_s)\beta_s^i = 0, \quad (6.45)$$

which is the same condition obtained in (6.6). It is clear from (6.43b) that a similar constraint can always be imposed, to all orders in β , to achieve $T^0_i = 0$ but this is not enough to source a RW geometry. Already to second order in β , (6.43c) contains a quadrupolar anisotropy that cannot be compensated by the other fluids. In this case, we should go one step further and consider a Bianchi universe. However, for the values of β that we will consider, this quadrupole lies well below the observed value [BM07]. Therefore, in this work we will restrict ourselves to first order and a RW background.

In Section 6.7.1 we will analyze in detail the evolution of the different fluids. It is important to stress here that, in our scenario, we will assume that all the components of the visible sector shared a common velocity in the early Universe, since they were in thermal contact. Then, the constraint (6.45) completely determines the evolution of the momentum of the dark sector. This leaves us with only one additional free parameter (β_0) over standard Λ CDM, i.e. the initial velocity of the visible sector in the cosmic center of mass frame.

6.3.2 Perturbations

Our starting point now is a perturbed flat RW metric (3.33). We express the distribution function again in terms of the momentum \mathbf{q} defined in (3.23) and introduce a perturbation

$$f(\tau, \mathbf{x}, \mathbf{q}) = f_0(\tau, \mathbf{q}) + \delta f(\tau, \mathbf{x}, \mathbf{q}), \quad (6.46)$$

If we compare this equation with the Λ CDM result (3.40), we can see that the only difference is that now f_0 depends also on the direction \hat{n} . The perturbed fluid variables are defined in the usual way (3.41) but now the components of the full energy-

momentum tensor are

$$\delta T^0_0 = -\delta\rho + B^i Q_i, \quad (6.47a)$$

$$\delta T^0_i = \delta Q_i + \frac{1}{2} A Q_i + \frac{1}{2} H_i^j Q_j, \quad (6.47b)$$

$$\delta T^i_j = \delta P \delta_j^i + \delta \Pi_j^i - B^i Q_j + \frac{1}{2} \left(H_j^k \Pi_k^i - H_k^i \Pi_j^k \right), \quad (6.47c)$$

that can be compared with the Λ CDM result (3.42). Expressing the background quantities in the $\tilde{\mathcal{O}}$ frame

$$\delta T^0_0 = -\delta\rho + \gamma^2 (\tilde{\rho} + \tilde{P}) B_i \beta^i, \quad (6.48a)$$

$$\delta T^0_i = \delta Q_i + \frac{1}{2} \gamma^2 (\tilde{\rho} + \tilde{P}) \left(A \delta_i^j + H_i^j \right) \beta_j, \quad (6.48b)$$

$$\delta T^i_j = \delta P \delta_j^i + \delta \Pi_j^i - \gamma^2 (\tilde{\rho} + \tilde{P}) B^i \beta_j + \frac{1}{2} \gamma^2 (\tilde{\rho} + \tilde{P}) \left(\beta^i H_j^k \beta_k - \beta_j H_k^i \beta^k \right). \quad (6.48c)$$

It is easy to show that, to first order in β , once we apply the center of mass condition (6.45), every metric variable cancels out and does not appear in the definition of the total energy-momentum tensor.

Non-relativistic limit

We conclude with a few remarks about the NR expansion that has been already analyzed in the context of a Λ CDM cosmology¹. Although this kind of approximation is standard, we must be careful when taking the NR limit in a moving frame. The proper way to account for this limit is to take it in the frame comoving with the fluid, i.e. $\tilde{\mathcal{O}}$. To first NR order we have

$$\delta \tilde{\Pi}^{ij} \simeq 0, \quad \delta \tilde{P} \simeq 0. \quad (6.49)$$

However, in the \mathcal{O} frame, using (6.38), it can be seen that we do have pressure and anisotropic stress

$$\delta P \simeq \frac{2}{3} \gamma^2 \beta_k \delta \tilde{Q}^k + \frac{1}{3} \gamma^2 \beta^2 \delta \tilde{\rho}, \quad (6.50a)$$

$$\delta \Pi^{ij} \simeq \gamma \left(\beta^i \mathcal{P}_k^j + \beta^j \mathcal{P}_k^i - \frac{2}{3} \gamma \delta^{ij} \beta_k \right) \delta \tilde{Q}^k + \gamma^2 \left(\beta^i \beta^j - \frac{1}{3} \beta^2 \delta^{ij} \right) \delta \tilde{\rho}. \quad (6.50b)$$

To first NR order and to first order in β , we have the following useful results

$$\begin{aligned} \delta P &\simeq \frac{2}{3} \beta_k \delta Q^k, & \delta V^i &\simeq \frac{\delta Q^i}{m}, \\ \delta \Pi^{ij} &\simeq \left(\beta^i \delta_k^j + \beta^j \delta_k^i - \frac{2}{3} \delta^{ij} \beta_k \right) \delta Q^k, & \delta \tilde{V}^i &\simeq \frac{1}{m} \left(\delta Q^i - \beta^i \delta \rho \right), \\ \delta \tilde{n} &\simeq \frac{\delta \tilde{\rho}}{m} \simeq \frac{1}{m} \left(\delta \rho - 2 \beta_k \delta Q^k \right), & \delta n &\simeq \frac{1}{m} \left(\delta \rho - \beta_k \delta Q^k \right). \end{aligned} \quad (6.51)$$

¹We will only keep the first NR order, neglecting the pressure and the sound speed of baryons.

Note that the preceding results hold as well for the corresponding unperturbed quantities, see (6.35). Finally, the full energy-momentum tensor for a non-relativistic species to first order in β is

$$T^0_0 + \delta T^0_0 \simeq -\tilde{\rho} - \delta\rho + \tilde{\rho}\beta^i B_i, \quad (6.52a)$$

$$T^0_i + \delta T^0_i \simeq m\delta V_i + \tilde{\rho}\left(\delta_i^j + \frac{1}{2}\delta_i^j A + \frac{1}{2}H_i^j\right)\beta_j, \quad (6.52b)$$

$$T^i_j + \delta T^i_j \simeq m\left(\beta^i\delta V_j - \beta_j\delta V^i\right) + \tilde{\rho}\beta_j B^i. \quad (6.52c)$$

6.4 Boltzmann equation

The evolution of the distribution function is described by the Boltzmann equation

$$\frac{Df}{d\tau} = a\left(1 - \frac{1}{2}A\right)\mathcal{C}[f]. \quad (6.53)$$

In the presence of bulk velocities, both sides are modified with respect to the results of Section 3.3. We address the relevant modifications to the free-streaming and collision terms in the next two sections.

6.4.1 Liouville operator

The left-hand side of the Boltzmann equation (6.53) is evaluated in the \mathcal{O} frame, where the geodesics are computed,

$$\frac{Df}{d\tau} \equiv \frac{\partial f}{\partial \tau} + \frac{dx^i}{d\tau} \frac{\partial f}{\partial x^i} + \frac{dq^i}{d\tau} \frac{\partial f}{\partial q^i}. \quad (6.54)$$

The expression for the geodesics is not modified, see (3.51) and (3.52), but the background distribution function is now anisotropic in this frame. We will assume that the distribution function takes the form

$$\begin{aligned} f(\tau, \mathbf{x}, \mathbf{q}) &= f_0(\tau, \mathbf{q}) + \delta f(\tau, \mathbf{x}, \mathbf{q}) \\ &= \tilde{f}_0(\tau, \Lambda\beta\epsilon) + \delta f(\tau, \mathbf{x}, \mathbf{q}), \end{aligned} \quad (6.55)$$

where $\tilde{f}_0(\tau, \tilde{\epsilon})$ is the standard isotropic distribution in the comoving $\tilde{\mathcal{O}}$ frame. Since (3.52) is already first order in perturbations, the left-hand side of the Boltzmann equation can be recast as

$$\frac{Df}{d\tau} = \frac{\partial f_0}{\partial \tau} + \frac{\partial \delta f}{\partial \tau} + \frac{dx^i}{d\tau} \frac{\partial \delta f}{\partial x^i} + \frac{dq^i}{d\tau} \frac{\partial f_0}{\partial q^i}. \quad (6.56)$$

Massless particles

For massless particles the Lorentz transformations (6.33) take a simpler form

$$\tilde{q} = \gamma(1 - \hat{n} \cdot \boldsymbol{\beta})q, \quad (6.57a)$$

$$\tilde{q}^i = \left(\mathcal{P}_j^i n^j - \gamma\beta^i\right)q, \quad (6.57b)$$

Using the Boltzmann equation, it can be directly checked that the unperturbed distribution function in the $\tilde{\mathcal{O}}$ frame only depends on \tilde{q} , if there is no zero-order collision term,

$$\tilde{f}_0(\tau, \tilde{q}) = \tilde{f}_0(\tilde{q}). \quad (6.58)$$

We work with the reduced phase-space density

$$\mathcal{F}(\tau, \mathbf{x}, \hat{n}) \equiv \frac{1}{\tilde{\mathcal{N}}} \int q^3 dq \delta f(\tau, \mathbf{x}, \mathbf{q}), \quad (6.59)$$

where the constant $\tilde{\mathcal{N}}$ is related to the comoving energy density computed in the $\tilde{\mathcal{O}}$ frame

$$\tilde{\mathcal{N}} \equiv \int \tilde{q}^3 d\tilde{q} \tilde{f}_0(\tilde{q}) = \frac{2\pi^2}{g_*} a^4 \tilde{\rho}. \quad (6.60)$$

Integrating over the momentum magnitude, we obtain, to all orders in β ,

$$\int q^3 dq \frac{Df}{d\tau} = \tilde{\mathcal{N}} \left[\frac{\partial}{\partial \tau} \frac{1}{\gamma^4 (1 - \hat{n} \cdot \boldsymbol{\beta})^4} + \dot{\mathcal{F}} + n^i \partial_i \mathcal{F} - \frac{4}{\gamma^4 (1 - \hat{n} \cdot \boldsymbol{\beta})^5} \left(\frac{1}{2} n^i \partial_i A \right. \right. \\ \left. \left. + n^i n^j C_{ij} - \frac{1}{2} \beta^i \partial_i A - \beta^i n^j C_{ij} - \beta^i n^j n^k D_{ijk} \right) \right]. \quad (6.61)$$

Expanding it to first order in β , we have

$$\int q^3 dq \frac{Df}{d\tau} = \tilde{\mathcal{N}} \left[4\hat{n} \cdot \dot{\boldsymbol{\beta}} + \dot{\mathcal{F}} + n^i \partial_i \mathcal{F} - 4 \left(\frac{1}{2} n^i \partial_i A + n^i n^j C_{ij} \right) (1 + 5\hat{n} \cdot \boldsymbol{\beta}) \right. \\ \left. + 4\beta^i \left(\frac{1}{2} \partial_i A + n^j C_{ij} + n^j n^k D_{ijk} \right) \right]. \quad (6.62)$$

The first two moments of the distribution can be found integrating over the solid angle

$$\int \frac{d\Omega}{4\pi} \int q^3 dq \frac{Df}{d\tau} = \tilde{\mathcal{N}} \left[\dot{\delta} + \frac{4}{3} \partial_i \delta v^i - \frac{4}{3} C_{ij} \delta^{ij} - \frac{4}{3} \beta^i \partial_i A - \frac{4}{3} D_{ijk} \delta^{ij} \beta^k \right], \quad (6.63)$$

$$\int \frac{d\Omega}{4\pi} n^i \int q^3 dq \frac{Df}{d\tau} = \frac{4}{3} \tilde{\mathcal{N}} \left[\dot{\beta}^i + \delta v^i + \frac{3}{4} \partial_j \pi^{ij} + \frac{1}{4} \partial^i \delta - \frac{1}{2} \partial^i A \right. \\ \left. - (\delta^{ij} \beta^k + \delta^{jk} \beta^i) C_{jk} \right], \quad (6.64)$$

where we have defined

$$\delta \equiv \int \frac{d\Omega}{4\pi} \mathcal{F} = \frac{\delta \rho}{\tilde{\rho}}, \quad (6.65a)$$

$$\delta \mathbf{v} \equiv \frac{3}{4} \int \frac{d\Omega}{4\pi} \hat{n} \mathcal{F} = \frac{\delta \mathbf{Q}}{\tilde{\rho} + \tilde{P}}, \quad (6.65b)$$

$$\pi^{ij} \equiv \int \frac{d\Omega}{4\pi} \left(n^i n^j - \frac{1}{3} \delta^{ij} \right) \mathcal{F} = \frac{\delta \Pi^{ij}}{\tilde{\rho}}. \quad (6.65c)$$

Massive particles

The energy density contrast, equation of state and sound speed are defined as

$$\delta \equiv \frac{\delta \rho}{\tilde{\rho}}, \quad w \equiv \frac{\tilde{P}}{\tilde{\rho}}, \quad c_s^2 \equiv \frac{\delta P}{\delta \rho}. \quad (6.66)$$

Note that in these definitions the background quantities are referred to the $\tilde{\mathcal{O}}$ frame while the perturbed quantities are defined in the \mathcal{O} frame. The election of intermediate variables is a matter of choice, provided that we write the energy-momentum tensor consistently in terms of these variables. We stick to this convention throughout this work. The final results for the first moments of the distribution are:

- *Number density.*

$$a^{-3} g_* \int \frac{d^3 q}{(2\pi)^3} \frac{Df}{d\tau} = a^{-3} \frac{\partial}{\partial \tau} (\gamma a^3 \tilde{n}) + a^{-3} \frac{\partial}{\partial \tau} (a^3 \delta n) + \partial_i \delta V^i - \gamma \tilde{n} \left[\frac{1}{2} \beta^i \partial_i A + \delta^{ij} C_{ij} + D_{ijk} \delta^{ij} \beta^k \right]. \quad (6.67)$$

- *Energy.*

$$a^{-4} g_* \int \frac{d^3 q}{(2\pi)^3} \epsilon \frac{Df}{d\tau} = \frac{\partial}{\partial \tau} [\gamma^2 (\tilde{\rho} + \beta^2 \tilde{P})] + 3\mathcal{H}(\tilde{\rho} + \tilde{P}) \left(1 + \frac{4}{3} \beta^2 \gamma^2 \right) + \tilde{\rho} (\dot{\delta} + 3\mathcal{H} \delta (c_s^2 - w)) + \delta (\dot{\tilde{\rho}} + 3\mathcal{H}(\tilde{\rho} + \tilde{P})) + \partial_i \delta Q^i - \gamma^2 (\tilde{\rho} + \tilde{P}) \left[\beta^i \partial_i A + \delta^{ij} C_{ij} + \beta^i \beta^j C_{ij} + D_{ijk} \delta^{ij} \beta^k \right]. \quad (6.68)$$

- *Momentum.*

$$a^{-4} g_* \int \frac{d^3 q}{(2\pi)^3} q^i \frac{Df}{d\tau} = a^{-4} \frac{\partial}{\partial \tau} \left[\gamma^2 \beta^i a^4 (\tilde{\rho} + \tilde{P}) \right] + a^{-4} \frac{\partial}{\partial \tau} (a^4 \delta Q^i) + \partial_j (\delta \Pi^{ij} + \delta^{ij} \delta P) - \gamma^2 (\tilde{\rho} + \tilde{P}) \left[\frac{1}{2} (\delta^{il} + \beta^i \beta^l) \partial_l A + (\delta^{jk} \beta^i + \delta^{ij} \beta^k) (C_{jk} + D_{jkl} \beta^l) \right]. \quad (6.69)$$

These results are exact to all orders in β , for relativistic and non-relativistic particles alike. They can be shown to reproduce (6.63) and (6.64) for massless particles. Next we define

$$\delta_n \equiv \frac{\delta n}{\tilde{n}}, \quad \delta v^i \equiv \frac{\delta V^i}{\tilde{n}}. \quad (6.70)$$

Assuming that the zero-order Boltzmann equation (without collisions) is satisfied, so we keep only cosmological perturbations and terms with β , and expanding to first NR order and to first order in β we have

- *Number density.*

$$a^{-3} g_* \int \frac{d^3 q}{(2\pi)^3} \frac{Df}{d\tau} \simeq \tilde{n} \left\{ \dot{\delta}_n + \partial_i \delta v^i - \frac{1}{2} \beta^i \partial_i A - \delta^{ij} C_{ij} - D_{ijk} \delta^{ij} \beta^k \right\}. \quad (6.71)$$

- *Energy.*

$$a^{-4} g_* \int \frac{d^3 q}{(2\pi)^3} \epsilon \frac{Df}{d\tau} \simeq \tilde{\rho} \left\{ \dot{\delta} + 2\mathcal{H} \beta_k \delta v^k + \partial_i \delta v^i - \beta^i \partial_i A - \delta^{ij} C_{ij} - D_{ijk} \delta^{ij} \beta^k \right\}. \quad (6.72)$$

- *Momentum.*

$$a^{-4} g_* \int \frac{d^3 q}{(2\pi)^3} q^i \frac{Df}{d\tau} \simeq \bar{\rho} \left\{ \beta^i + \mathcal{H} \beta^i + \delta v^i + \left(\beta^i \delta_k^j + \beta^j \delta_k^i \right) \partial_j \delta v^k + \mathcal{H} \delta v^i - \frac{1}{2} \partial^i A - \left(\delta^{jk} \beta^i + \delta^{ij} \beta^k \right) C_{jk} \right\}. \quad (6.73)$$

6.4.2 Collision term

In this section we will examine in detail the changes introduced in the collision term by the inclusion of relative bulk velocities. The starting point is the collision term of Section 3.3.2, see (3.73), under the same standard assumptions. For the process $e(p_e) + \gamma(p) \leftrightarrow e(p'_e) + \gamma(p')$ we have

$$\mathcal{C}[f(\mathbf{p})] = \frac{1}{4p} \int \mathcal{D}p_e \mathcal{D}p' \mathcal{D}p'_e (2\pi)^4 \delta(p^\mu + p_e^\mu - p'^\mu - p_e'^\mu) \times \left[f(\mathbf{p}') f_e(\mathbf{p}'_e) - f(\mathbf{p}) f_e(\mathbf{p}_e) \right] \sum_{\text{spins}} |\mathcal{M}|^2, \quad (6.74)$$

In our setting, we must implement the fact that the fluids are moving. The collision term is defined in the cosmic center of mass, \mathcal{O} frame, and in this frame both photons and electrons have their own bulk velocity. We will represent it schematically as

$$\mathcal{C}[f] = \frac{1}{4p} \int \mathcal{D}p_e \mathcal{D}p' \mathcal{D}p'_e (2\pi)^4 \delta(p^\mu + p_e^\mu - p'^\mu - p_e'^\mu) \times \left[\bar{f}(\Lambda_{\beta_\gamma} \mathbf{p}') \tilde{f}_e(\Lambda_{\beta_e} \mathbf{p}'_e) - \bar{f}(\Lambda_{\beta_\gamma} \mathbf{p}) \tilde{f}_e(\Lambda_{\beta_e} \mathbf{p}_e) \right] \sum_{\text{spins}} |\mathcal{M}|^2, \quad (6.75)$$

where \bar{f} and \tilde{f}_e are the distribution functions of photons and electrons in their comoving frame, moving with bulk velocities β_γ and β_e , respectively, with respect to the \mathcal{O} frame.

Previously, the $\tilde{\mathcal{O}}$ frame was defined as the frame comoving with the fluid. In this case, we are facing two moving fluids. We take $\tilde{\mathcal{O}}$ to be the frame moving with velocity β_e with respect to \mathcal{O} , i.e. the frame comoving with the *electrons*. Performing the integration in this frame, we have

$$\mathcal{C}[f] = \frac{1}{4p} \int \mathcal{D}\tilde{p}_e \mathcal{D}\tilde{p}' \mathcal{D}\tilde{p}'_e (2\pi)^4 \delta(\tilde{p}^\mu + \tilde{p}_e^\mu - \tilde{p}'^\mu - \tilde{p}'_e^\mu) \times \left[\bar{f}(\Lambda_{\beta_\gamma} \Lambda_{\beta_e}^{-1} \tilde{\mathbf{p}}') \tilde{f}_e(\tilde{\mathbf{p}}'_e) - \bar{f}(\Lambda_{\beta_\gamma} \Lambda_{\beta_e}^{-1} \tilde{\mathbf{p}}) \tilde{f}_e(\tilde{\mathbf{p}}_e) \right] \sum_{\text{spins}} |\mathcal{M}|^2. \quad (6.76)$$

The previous two equations may seem devoid of any additional content with respect to (6.74). As they stand, without defining f and f_e , they correspond just to a renaming of functions and reshuffling of variables. The physical content lies in (6.55), i.e. in the structure and relation of the background distribution function in \mathcal{O} and $\tilde{\mathcal{O}}$. The $\tilde{\mathcal{O}}$ frame is comoving with the electrons and observes a standard

isotropic equilibrium distribution. It is in this frame that we can perform the usual NR expansion to get the result analogous to (3.90)

$$C[f] = \frac{\sigma_T}{4\pi p} \int \tilde{p}' d\tilde{p}' d\tilde{\Omega}' \left[\tilde{n}_e^{\text{full}} \delta(\tilde{p} - \tilde{p}') + \tilde{n}_e \tilde{\mathbf{u}}_e^{\text{full}} \cdot (\tilde{\mathbf{p}} - \tilde{\mathbf{p}}') \frac{\partial \delta(\tilde{p} - \tilde{p}')}{\partial \tilde{p}'} \right] \times \left(\tilde{f}(\Lambda_{\beta_\gamma} \Lambda_{\beta_e}^{-1} \tilde{\mathbf{p}}') - \tilde{f}(\Lambda_{\beta_\gamma} \Lambda_{\beta_e}^{-1} \tilde{\mathbf{p}}) \right), \quad (6.77)$$

where σ_T is the Thomson cross section and we have defined

$$\tilde{n}_e^{\text{full}} \equiv 2 \int \frac{d^3 \tilde{p}_e}{(2\pi)^3} \tilde{f}_e(\tilde{\mathbf{p}}_e), \quad \tilde{n}_e \tilde{\mathbf{u}}_e^{\text{full}} \equiv 2 \int \frac{d^3 \tilde{p}_e}{(2\pi)^3} \frac{\tilde{\mathbf{p}}_e}{\tilde{E}_{p_e}} \tilde{f}_e(\tilde{\mathbf{p}}_e), \quad (6.78)$$

where \tilde{f} , \tilde{f}_e correspond to the full distribution functions. Just as we did for the Liouville operator in Section 6.4.1, we will split the distribution functions into a background and a perturbation part and integrate out the magnitude of the photon momentum. The whole process, to all orders in β , is detailed in the Appendix E. Here we present only the final results. To first order in β , we get

$$\frac{1}{\tilde{\mathcal{N}}} \int q^3 dq C[f] = \tilde{n}_e \sigma_T \left[-(1 - \hat{n} \cdot \boldsymbol{\beta}_e) \mathcal{F}_\gamma + (1 + 3\hat{n} \cdot \boldsymbol{\beta}_e) \delta_\gamma - \frac{8}{3} \boldsymbol{\beta}_e \cdot \delta \mathbf{v}_\gamma - 4\hat{n} \cdot \Delta \boldsymbol{\beta} - \frac{8}{3} \delta \mathbf{v}_e \cdot \Delta \boldsymbol{\beta} + 4(\hat{n} \cdot \delta \mathbf{v}_e)(\hat{n} \cdot \Delta \boldsymbol{\beta}) + 4\delta \mathbf{v}_e \cdot (\hat{n} - \boldsymbol{\beta}_e + 4\hat{n}(\hat{n} \cdot \boldsymbol{\beta}_e)) - 4\hat{n} \cdot \boldsymbol{\beta}_\gamma \delta_{n_e} \right], \quad (6.79)$$

where \tilde{n}_e is the number density of free electrons in the $\tilde{\mathcal{O}}$ frame, δ_{n_e} and $\delta \mathbf{v}_e$ are defined in (6.70) and the velocity difference is

$$\Delta \boldsymbol{\beta} \equiv \boldsymbol{\beta}_\gamma - \boldsymbol{\beta}_e. \quad (6.80)$$

Since, to first order in β , the background quantities like ρ or n coincide in the \mathcal{O} and $\tilde{\mathcal{O}}$ frames, we will drop the distinction. The first two moments of the photon collision term are

$$\frac{1}{\tilde{\mathcal{N}}} \int \frac{d\Omega}{4\pi} \int q^3 dq C[f(\mathbf{p})] = -\frac{4}{3} n_e \sigma_T \left[\boldsymbol{\beta}_e \cdot (\delta \mathbf{v}_\gamma - \delta \mathbf{v}_e) + \delta \mathbf{v}_e \cdot \Delta \boldsymbol{\beta} \right], \quad (6.81)$$

$$\frac{1}{\tilde{\mathcal{N}}} \int \frac{d\Omega}{4\pi} n^i \int q^3 dq C[f(\mathbf{p})] = -\frac{4}{3} n_e \sigma_T \left[\delta v_\gamma^i - \delta v_e^i + \Delta \beta^i + \beta_\gamma^i \delta_{n_e} - \beta_e^i \delta_\gamma - \frac{3}{4} \beta_{e,j} \pi_\gamma^{ij} \right]. \quad (6.82)$$

The conclusions about conserved quantities at the end of Section 3.3.2 still hold. We can obtain the first two moments of the electron collision term from the previous results using the conservation of energy (3.104) and momentum (3.105).

6.4.3 Boltzmann equation for different components

In this section we gather the Boltzmann equations for all the species. Notice that, as in Λ CDM, the baryons can be treated as a single tightly-coupled fluid and we can trade $(\boldsymbol{\beta}_e, \delta \mathbf{v}_e)$ with $(\boldsymbol{\beta}_b, \delta \mathbf{v}_b)$, i.e. the velocities of electrons, protons and the full baryonic fluid are equal.

Photons

The reduced Boltzmann equation for photons is obtained combining the Liouville operator (6.62) and the collision term (6.79). To zero order in cosmological perturbations, it describes the evolution of the bulk velocity β_γ

$$\dot{\beta}_\gamma^i = -an_e\sigma_T\Delta\beta^i. \quad (6.83)$$

To first order in cosmological perturbations and β , we get the evolution of the reduced phase-space density

$$\begin{aligned} \dot{\mathcal{F}}_\gamma + n^i\partial_i\mathcal{F}_\gamma - 4\left(\frac{1}{2}n^i\partial_i A + n^in^jC_{ij}\right)(1+5\hat{n}\cdot\boldsymbol{\beta}_\gamma) + 4\beta_\gamma^i\left(\frac{1}{2}\partial_i A + n^jC_{ij} + n^jn^kD_{ijk}\right) \\ = an_e\sigma_T\left[-(1-\hat{n}\cdot\boldsymbol{\beta}_b)\mathcal{F}_\gamma + (1+3\hat{n}\cdot\boldsymbol{\beta}_b)\delta_\gamma - \frac{8}{3}\boldsymbol{\beta}_b\cdot\delta\mathbf{v}_\gamma - \frac{8}{3}\delta\mathbf{v}_b\cdot\Delta\boldsymbol{\beta} \right. \\ \left. + 4(\hat{n}\cdot\delta\mathbf{v}_b)(\hat{n}\cdot\Delta\boldsymbol{\beta}) + 4\delta\mathbf{v}_b\cdot(\hat{n}-\boldsymbol{\beta}_b+4\hat{n}(\hat{n}\cdot\boldsymbol{\beta}_b)) - 4\hat{n}\cdot\boldsymbol{\beta}_\gamma\delta_{n_e} \right. \\ \left. + 2\hat{n}\cdot\Delta\boldsymbol{\beta}A\right]. \end{aligned} \quad (6.84)$$

The equations for the density, combining (6.63) and (6.81), and the velocity, combining (6.64) and (6.82), are

$$\begin{aligned} \dot{\delta}_\gamma + \frac{4}{3}\partial_i\delta v_\gamma^i - \frac{4}{3}C_{ij}\delta^{ij} - \frac{4}{3}\beta_\gamma^i\partial_i A - \frac{4}{3}D_{ijk}\delta^{ij}\beta_\gamma^k \\ = -\frac{4}{3}an_e\sigma_T\left[\boldsymbol{\beta}_b\cdot(\delta\mathbf{v}_\gamma - \delta\mathbf{v}_b) + \delta\mathbf{v}_b\cdot\Delta\boldsymbol{\beta}\right], \end{aligned} \quad (6.85)$$

$$\begin{aligned} \delta\dot{v}_\gamma^i + \frac{3}{4}\partial_j\pi_\gamma^{ij} + \frac{1}{4}\partial^i\delta_\gamma - \frac{1}{2}\partial^i A - (\delta^{ij}\beta_\gamma^k + \delta^{jk}\beta_\gamma^i)C_{jk} \\ = -an_e\sigma_T\left[\delta v_\gamma^i - \delta v_b^i + \beta_\gamma^i\delta_{n_e} - \beta_b^i\delta_\gamma - \frac{3}{4}\beta_{bj}\pi_\gamma^{ij} - \frac{1}{2}\Delta\beta^i A\right]. \end{aligned} \quad (6.86)$$

Baryons

The evolution of the baryon density can be found using the left-hand side (6.72) and energy conservation (3.104). For the velocity, we must use the left-hand side (6.73) and momentum conservation (3.105). To zero order in cosmological perturbations, we find the evolution of the bulk velocity β_b

$$\dot{\beta}_b^i + \mathcal{H}\beta_b^i = \frac{4\rho_\gamma}{3\rho_b}an_e\sigma_T\Delta\beta^i. \quad (6.87)$$

To first order in cosmological perturbations and β , the evolution of the first two moments of the distribution is

$$\begin{aligned} \dot{\delta}_b + 2\mathcal{H}\boldsymbol{\beta}_b\cdot\delta\mathbf{v}_b + \partial_i\delta v_b^i - \beta_b^i\partial_i A - \delta^{ij}C_{ij} - D_{ijk}\delta^{ij}\beta_b^k \\ = \frac{4\rho_\gamma}{3\rho_b}an_e\sigma_T\left[\boldsymbol{\beta}_b\cdot(\delta\mathbf{v}_\gamma - \delta\mathbf{v}_b) + \delta\mathbf{v}_b\cdot\Delta\boldsymbol{\beta}\right], \end{aligned} \quad (6.88)$$

$$\begin{aligned} \delta\dot{v}_b^i + \mathcal{H}\delta v_b^i + \left(\beta_b^i\delta_k^j + \beta_b^j\delta_k^i\right)\partial_j\delta v_b^k - \frac{1}{2}\partial^i A - \left(\delta^{jk}\beta_b^i + \delta^{ij}\beta_b^k\right)C_{jk} \\ = \frac{4\rho_\gamma}{3\rho_b}an_e\sigma_T\left[\delta v_\gamma^i - \delta v_b^i + \beta_\gamma^i\delta_{n_e} - \beta_b^i\delta_\gamma - \frac{3}{4}\beta_{bj}\pi_\gamma^{ij} - \frac{1}{2}\Delta\beta^i A\right]. \end{aligned} \quad (6.89)$$

Massless neutrinos

Since we will neglect both the mass and coupling of neutrinos, they only free-stream with the same left-hand side as photons. The equation for β_ν is

$$\dot{\beta}_\nu^i = 0. \quad (6.90)$$

The equation for the evolution of the reduced phase-space density is

$$\begin{aligned} \dot{\mathcal{F}}_\nu + n^i \partial_i \mathcal{F}_\nu - 4 \left(\frac{1}{2} n^i \partial_i A + n^i n^j C_{ij} \right) (1 + 5 \hat{n} \cdot \boldsymbol{\beta}_\nu) \\ + 4 \beta_\nu^i \left(\frac{1}{2} \partial_i A + n^j C_{ij} + n^j n^k D_{ijk} \right) = 0. \end{aligned} \quad (6.91)$$

Cold dark matter

The equation for β_c is

$$\dot{\beta}_c^i + \mathcal{H} \beta_c^i = 0. \quad (6.92)$$

The relevant equations for the perturbations are

$$\dot{\delta}_c + 2\mathcal{H} \boldsymbol{\beta}_c \cdot \delta \mathbf{v}_c + \partial_j \delta v_c^i - \beta_c^i \partial_i A - \delta^{ij} C_{ij} - D_{ijk} \delta^{ij} \beta_c^k = 0, \quad (6.93)$$

$$\delta \dot{v}_c^i + \mathcal{H} \delta v_c^i + \left(\beta_c^i \delta_k^j + \beta_c^j \delta_k^i \right) \partial_j \delta v_c^k - \frac{1}{2} \partial^i A - \left(\delta^{jk} \beta_c^i + \delta^{ij} \beta_c^k \right) C_{jk} = 0. \quad (6.94)$$

Total fluid

The total energy-momentum tensor, adding all the components, does not contain any explicit β contribution after enforcing the cosmic center of mass condition. The equations of motion take the same form as in Λ CDM, see (3.115) and (3.116).

6.5 Harmonic analysis

The cosmological perturbations can be classified according to their behaviour under the group of spatial rotations. This yields the usual splitting into scalar, vector and tensor perturbations, that has been discussed in Section 3.4. In the standard Λ CDM cosmology, the three types of perturbations are decoupled at the linear level. This result, known as decomposition theorem, ultimately stems from the isotropy of the background. Under these conditions, each perturbation type can be studied separately. In particular, the vector modes are decaying and are usually neglected. The tensor modes are ignored as well, except when polarization is taken into account, and the focus is set on the scalar perturbations.

In Λ CDM, the only explicit dependence on the line-of-sight vector \hat{n} in the Boltzmann equation comes from factors of the form $(\hat{n} \cdot \hat{k})$, see (3.106). It is reasonable then to write a multipole expansion in terms of Legendre polynomials (3.135). The Boltzmann equation unfolds into a whole hierarchy of coupled differential equations for the coefficients \mathcal{F}_ℓ of this expansion, as in (3.136).

The key difference in our scenario is the existence of a new direction $\hat{\beta}$, that introduces new angular dependencies in the Boltzmann equation (6.84). This means that we must resort to a full decomposition in terms of spherical harmonics

$$\mathcal{F}(\tau, \mathbf{k}, \hat{n}) = \sqrt{4\pi} \sum_{\ell=0}^{\infty} \sum_{m=-\ell}^{\ell} (-i)^{\ell+m} \sqrt{2\ell+1} \mathcal{F}_{\ell}^m(\tau, \mathbf{k}) Y_{\ell}^m(\hat{n}). \quad (6.95)$$

The coefficients have been defined to match the standard definition (3.135) for the scalar modes ($m = 0$). It can be checked, plugging the previous expansion into the modified Boltzmann equation (6.84), that the decomposition theorem no longer holds. The term $(\hat{n} \cdot \hat{\beta})$ introduces, in addition to the usual coupling to the $\ell - 1$ and $\ell + 1$ modes, new couplings to the $m - 1$ and $m + 1$ modes.

In the next section we will compute explicitly the equations for the lowest moments of (6.95) in order to see how these new couplings arise. Following this analysis, the modified Boltzmann hierarchy is presented in Section 6.5.2, along with some minor additions to the truncation scheme in Section 6.5.3.

6.5.1 Helicity basis

The usual scalar-vector-tensor decomposition takes \hat{k} as a reference axis to classify the perturbations. It is convenient to write the line-of-sight vector \hat{n} in a basis adapted to this decomposition. Its components can be explicitly written as

$$\hat{n} = \sin\theta \cos\phi \hat{x} + \sin\theta \sin\phi \hat{y} + \cos\theta \hat{z} \quad (6.96a)$$

$$= \frac{1}{\sqrt{2}} e^{i\phi} \sin\theta \hat{e}_+ + \frac{1}{\sqrt{2}} e^{-i\phi} \sin\theta \hat{e}_- + \cos\theta \hat{k} \quad (6.96b)$$

$$= \sqrt{\frac{4\pi}{3}} (-Y_1^{+1} \hat{e}_+ + Y_1^{-1} \hat{e}_- + Y_1^0 \hat{k}), \quad (6.96c)$$

where we have chosen the so-called *helicity basis*²

$$\hat{k} \equiv \hat{z}, \quad (6.97a)$$

$$\hat{e}_{\pm} \equiv \frac{1}{\sqrt{2}} (\hat{x} \mp i\hat{y}). \quad (6.97b)$$

Our convention for the spherical harmonics and related functions is discussed in Appendix C. This basis will allow us to deal systematically with more complex scalar-vector-tensor decompositions. As an example, let us derive a new result using this language.

The first moments of the Boltzmann equation have already been obtained in the previous sections, with $\ell = 0$ corresponding to the density (6.85) and $\ell = 1$ to the velocity (6.86). The next moment $\ell = 2$ can be obtained via direct integration of the Boltzmann equation (6.84) and corresponds to the shear tensor (6.65c). Performing

²Notice that some authors, e.g. [Dur08], choose the opposite sign convention for \hat{e}_{\pm} .

the appropriate integral, we find

$$\begin{aligned}
& \dot{\pi}_{ij} + \partial_k \int \frac{d\Omega}{4\pi} n^k n_i n_j \mathcal{F}_\gamma - \frac{4}{9} \delta_{ij} \partial_k \delta v_\gamma^k - \frac{4}{3} \left(\beta_{\gamma(i} \partial_{j)} - \frac{1}{3} \delta_{ij} \beta_\gamma^k \partial_k \right) A \\
& \quad - \frac{8}{15} \left(C_{(ij)} - \frac{1}{3} \delta_{ij} \delta^{kl} C_{kl} \right) + \frac{8}{15} \beta_\gamma^m \left(D_{m(ij)} - \frac{1}{3} \delta_{ij} D_{mkl} \delta^{kl} \right) \\
& = -an_e \sigma_T \left[\pi_{ij} - \beta_b^k \int \frac{d\Omega}{4\pi} n_k n_i n_j \mathcal{F}_\gamma + \frac{4}{9} \boldsymbol{\beta}_b \cdot \delta \mathbf{v}_\gamma \delta_{ij} \right. \\
& \quad \left. - \frac{32}{15} \left(\delta v_{b(i} \beta_{b j)} - \frac{1}{3} \delta_{ij} \delta \mathbf{v}_b \cdot \boldsymbol{\beta}_b \right) \right. \\
& \quad \left. - \frac{8}{15} \left(\delta v_{b(i} \Delta \beta_{j)} - \frac{1}{3} \delta_{ij} \delta \mathbf{v}_b \cdot \Delta \boldsymbol{\beta} \right) \right]. \tag{6.98}
\end{aligned}$$

The different components of this expression can be computed projecting in the helicity basis

$$\pi_{33} \equiv \hat{k}^i \hat{k}^j \pi_{ij}, \quad \pi_{3+} \equiv \hat{k}^i \hat{e}_+^j \pi_{ij}, \quad \pi_{++} \equiv \hat{e}_+^i \hat{e}_+^j \pi_{ij}. \tag{6.99}$$

The projection of a vector is computed in a similar way

$$V_3 \equiv \hat{k} \cdot \mathbf{V}, \quad V_\pm \equiv \hat{e}_\pm \cdot \mathbf{V}. \tag{6.100}$$

Projecting the equations of motion we get

$$\begin{aligned}
& \dot{\pi}_{33} + ik \int \frac{d\Omega}{4\pi} (\hat{n} \cdot \hat{k})^3 \mathcal{F}_\gamma - \frac{4}{9} \theta_\gamma - \frac{8i}{9} \boldsymbol{\beta}_\gamma \cdot \mathbf{k} A - \frac{8}{15} \left(C_{33} - \frac{1}{3} C^k_k \right) \\
& \quad + \frac{8}{15} \left(\beta_\gamma^m D_{m33} - \frac{1}{3} \beta_\gamma^m D_{mkl} \delta^{kl} \right) \\
& = -an_e \sigma_T \left[\pi_{33} - \int \frac{d\Omega}{4\pi} (\boldsymbol{\beta}_b \cdot \hat{n}) (\hat{k} \cdot \hat{n})^2 \mathcal{F}_\gamma + \frac{4}{9} \boldsymbol{\beta}_b \cdot \delta \mathbf{v}_\gamma \right. \\
& \quad \left. - \frac{32}{15} \left(\delta v_b^3 \beta_b^3 - \frac{1}{3} \delta \mathbf{v}_b \cdot \boldsymbol{\beta}_b \right) - \frac{8}{15} \left(\delta v_b^3 \Delta \beta_3 - \frac{1}{3} \delta \mathbf{v}_b \cdot \Delta \boldsymbol{\beta} \right) \right], \tag{6.101}
\end{aligned}$$

$$\begin{aligned}
& \dot{\pi}_{3+} + ik \int \frac{d\Omega}{4\pi} (\hat{n} \cdot \hat{k})^2 (\hat{n} \cdot \hat{e}_+) \mathcal{F}_\gamma - \frac{2}{3} i \beta_\gamma^+ k A - \frac{4}{15} (C_{3+} + C_{+3}) \\
& \quad + \frac{4}{15} \beta_\gamma^j (D_{j3+} + D_{j+3}) \\
& = -an_e \sigma_T \left[\pi_{3+} - \int \frac{d\Omega}{4\pi} (\boldsymbol{\beta}_b \cdot \hat{n}) (\hat{n} \cdot \hat{k}) (\hat{n} \cdot \hat{e}_+) \mathcal{F}_\gamma \right. \\
& \quad \left. - \frac{16}{15} (\delta v_b^3 \beta_b^+ + \delta v_b^+ \beta_b^3) - \frac{8}{15} (\delta v_b^3 \Delta \beta^+ + \delta v_b^+ \Delta \beta^3) \right], \tag{6.102}
\end{aligned}$$

$$\begin{aligned}
& \dot{\pi}_{++} + ik \int \frac{d\Omega}{4\pi} (\hat{n} \cdot \hat{k}) (\hat{n} \cdot \hat{e}_+)^2 \mathcal{F}_\gamma - \frac{8}{15} C_{++} + \frac{8}{15} \beta_\gamma^m D_{m++} \\
& = -an_e \sigma_T \left[\pi_{++} - \int \frac{d\Omega}{4\pi} (\boldsymbol{\beta}_b \cdot \hat{n}) (\hat{n} \cdot \hat{e}_+)^2 \mathcal{F}_\gamma - \frac{32}{15} \delta v_b^+ \beta_b^+ - \frac{8}{15} \delta v_b^+ \Delta \beta^+ \right]. \tag{6.103}
\end{aligned}$$

It is easy to prove that with the splitting (3.125), the projections correspond to the scalar part and one of the two vector and tensor helicities

$$\pi_{33} = -\frac{4}{3}\sigma, \quad \pi_{3+} = ik\pi_+^V, \quad \pi_{++} = \pi_{++}^T. \quad (6.104)$$

The same applies to the velocities, with the splitting (3.122),

$$\delta v^3 = -\frac{i}{k}\theta, \quad \delta v^+ = \chi^+. \quad (6.105)$$

There remains to perform a couple of angular integrals, writing down the appropriate coefficients of the expansion (6.95), and to substitute the metric variables, defined in (3.53, 3.54, 3.127). After these simplifications and rearranging terms, the first moments of the Boltzmann equation for photons are the following.

- *Scalar.* ($m = 0, \ell = 0, 1, 2$)

$$\begin{aligned} & \dot{\delta}_\gamma + \frac{4}{3}\theta_\gamma + \frac{4k^2}{3}(B - \dot{E}) - 4\dot{\Phi} + \frac{8i}{3}(\boldsymbol{\beta}_\gamma \cdot \mathbf{k})(\Psi - \Phi) + \frac{2k^2}{3}\boldsymbol{\beta}_\gamma \cdot \mathbf{F} \\ & = -\frac{4}{3}an_e\sigma_T \left[\boldsymbol{\beta}_b \cdot (\boldsymbol{\chi}_\gamma - \boldsymbol{\chi}_b) + \boldsymbol{\chi}_b \cdot \Delta\boldsymbol{\beta} - \frac{i}{k}\hat{k} \cdot (\boldsymbol{\beta}_b(\theta_\gamma - \theta_b) + \theta_b\Delta\boldsymbol{\beta}) \right], \end{aligned} \quad (6.106)$$

$$\begin{aligned} & \dot{\theta}_\gamma - \frac{k^2}{4}(\delta_\gamma - 4\sigma_\gamma) - k^2\Psi - 4i(\boldsymbol{\beta}_\gamma \cdot \mathbf{k})\dot{\Phi} \\ & \quad + 2ik^2(\boldsymbol{\beta}_\gamma \cdot \mathbf{k})(B - \dot{E}) - k^2\boldsymbol{\beta}_\gamma \cdot \left(\mathbf{S} + \frac{1}{2}\mathbf{F}\right) \\ & = -an_e\sigma_T \left[\theta_\gamma - \theta_b - i\mathbf{k} \cdot (\boldsymbol{\beta}_b(\delta_\gamma - \sigma_\gamma) - \boldsymbol{\beta}_\gamma\delta_{n_e}) \right. \\ & \quad \left. - \frac{3ik}{4}\boldsymbol{\beta}_\gamma \cdot \boldsymbol{\pi}_\gamma^V + i\Psi\Delta\boldsymbol{\beta} \cdot \mathbf{k} \right], \end{aligned} \quad (6.107)$$

$$\begin{aligned} & \dot{\sigma}_\gamma - \frac{4}{15}\theta_\gamma + \frac{3k}{10}\mathcal{F}_3^0 - \frac{4i}{15}(\boldsymbol{\beta}_\gamma \cdot \mathbf{k})(\Phi + 5\Psi) - \frac{4}{15}k^2(B - \dot{E}) - \frac{2}{15}k^2\boldsymbol{\beta}_\gamma \cdot \mathbf{F} \\ & = -an_e\sigma_T \left[\sigma_\gamma - \frac{4i}{15k}\hat{k} \cdot (\boldsymbol{\beta}_b\theta_\gamma + 4\boldsymbol{\beta}_b\theta_b + \Delta\boldsymbol{\beta}\theta_b) \right. \\ & \quad \left. + \frac{3i}{10} \left((\boldsymbol{\beta}_b \cdot \hat{k})\mathcal{F}_3^0 - i\sqrt{\frac{2}{3}} \left((\boldsymbol{\beta}_b \cdot \hat{e}_+)\mathcal{F}_3^{-1} + (\boldsymbol{\beta}_b \cdot \hat{e}_-)\mathcal{F}_3^{+1} \right) \right) \right. \\ & \quad \left. - \frac{2}{15}(\boldsymbol{\beta}_b \cdot \boldsymbol{\chi}_\gamma + 4\boldsymbol{\beta}_b \cdot \boldsymbol{\chi}_b + \Delta\boldsymbol{\beta} \cdot \boldsymbol{\chi}_b) \right]. \end{aligned} \quad (6.108)$$

- *Vector.* ($m = +1, \ell = 1, 2$)

$$\begin{aligned} & \dot{\chi}_\gamma^+ - \frac{3k^2}{4}\pi_+^V - 4\beta_\gamma^+\dot{\Phi} + \beta_\gamma^+k^2(B - \dot{E}) + \frac{i}{2}\boldsymbol{\beta}_\gamma \cdot \mathbf{k}\dot{F}_+ + \frac{1}{2}\beta_\gamma^-\dot{h}_{++} \\ & = -an_e\sigma_T \left[\chi_\gamma^+ - \chi_b^+ + \beta_\gamma^+\delta_{n_e} - \beta_b^+\delta_\gamma - \frac{1}{2}\beta_b^+\sigma_\gamma - \frac{3i}{4}(\boldsymbol{\beta}_b \cdot \hat{k})\pi_+^V \right. \\ & \quad \left. - \frac{3}{4}\beta_b^-\pi_{++} + \Psi\Delta\beta_+ \right], \end{aligned} \quad (6.109)$$

$$\begin{aligned}
& \dot{\pi}_+^V + \frac{4}{15} \left(\chi_\gamma^+ + \sqrt{\frac{3}{2}} \mathcal{F}_3^{+1} \right) + \frac{4}{15} \beta_\gamma^+ (\Phi + 5\Psi) + \frac{4}{15} (S_+ + \dot{F}_+) \\
& \quad - \frac{2}{15} \beta_\gamma^- h_{++} + \frac{2i}{15} \boldsymbol{\beta}_\gamma \cdot \mathbf{k} F_+ \\
& = -an_e \sigma_T \left[\pi_+^V + \frac{4}{15k^2} \beta_b^+ (\theta_\gamma + k \mathcal{F}_3^0) + \frac{1}{k} \sqrt{\frac{2}{15}} \beta_b^- \mathcal{F}_3^{+2} \right. \\
& \quad + \frac{4i}{15k} \hat{\mathbf{k}} \cdot \boldsymbol{\beta}_b \left(\chi_\gamma^+ + \sqrt{\frac{3}{2}} \mathcal{F}_3^{+1} \right) + \frac{4}{15k^2} (\Delta\beta_+ \theta_b + 4\beta_b^+ \theta_b) \\
& \quad \left. + \frac{4i}{15k} \hat{\mathbf{k}} \cdot (\Delta\boldsymbol{\beta} + 4\boldsymbol{\beta}_b) \chi_b^+ \right]. \tag{6.110}
\end{aligned}$$

- *Tensor.* ($m = +2$, $\ell = 2$)

$$\begin{aligned}
& \dot{\pi}_{++} + k \sqrt{\frac{2}{15}} \mathcal{F}_3^{+2} + \frac{4}{15} \dot{h}_{++} + \frac{4}{15} i (\boldsymbol{\beta}_\gamma \cdot \mathbf{k}) h_{++} \\
& = -an_e \sigma_T \left[\pi_{++} - \frac{8}{15} (\beta_b^+ \chi_\gamma^+ + 4\beta_b^+ \chi_b^+ + \Delta\beta_+ \chi_b^+) \right]. \tag{6.111}
\end{aligned}$$

The corresponding results for the opposite helicity can be obtained substituting $- \leftrightarrow +$ in every sub and superscript. Several comments are in order now.

- We will work to first order in β and to first order in cosmological perturbations, keeping cross-products. We have been implicitly working under this assumption, since the RW background is only correct to first order in β , but we will carry it through.
- The results to zero order in β reproduce Λ CDM. Thus, as we have justified in Section 3.4.1, we assume that there are no zero-order vector or tensor perturbations. Under this assumption, the hierarchy is greatly simplified. Since they are initially zero, and remain so in Λ CDM, their production can only occur through their new couplings, i.e. it is proportional to β . The vector modes are then $\mathcal{O}(\beta)$ and the tensor modes are $\mathcal{O}(\beta^2)$. In general, we can neglect the backreaction of higher m modes into lower m modes. As we will see in Section 6.6, the Einstein equations are not modified, so we can apply the same reasoning to the metric variables, i.e. \mathbf{S} and \mathbf{F} are $\mathcal{O}(\beta)$ and h_{ij} is $\mathcal{O}(\beta^2)$.
- The results of this section are everything we need in the fluid approximation, that is if we truncate at $\ell = 2$. The fluid approximation has been widely used in approximate computations of the CMB and for analytic estimates [HS96a]. It can introduce up to 10% errors in computations of the CMB spectrum [Hu+95]. The accuracy of the approximation also depends on the kind of truncation. The crudest truncation scheme, where we set to zero all higher moments, is known to introduce spurious growth at small scales in the ultrarelativistic species. Nonetheless, this simple approach may prove accurate enough to study large-scale structure, where the late time behaviour of ultrarelativistic species is irrelevant. We will come back to this point in Section 6.7.

Within the fluid approximation, better results can be obtained introducing the improved truncation scheme (3.139) or an effective viscosity in the equations for ultrarelativistic species [Hu98], although for truly accurate results one ought to solve the Boltzmann hierarchy.

6.5.2 Boltzmann hierarchy

The Boltzmann hierarchy for the modified Boltzmann equation (6.84) can be systematically written down. However, such general results are needlessly complicated for our purposes. Once the assumptions of the last section are taken into account, i.e. keep first order in β and neglect backreaction of higher m harmonics, we get a modified scalar hierarchy and a vector hierarchy coupled to the scalar one.

Scalar hierarchy. The full scalar hierarchy is

0, 0)

$$\begin{aligned} \dot{\delta}_\gamma + \frac{4}{3}\theta_\gamma + \frac{4}{3}k^2(B - \dot{E}) - 4\dot{\Phi} - \frac{8i}{3}(\boldsymbol{\beta}_\gamma \cdot \mathbf{k})(\Phi - \Psi) \\ = -an_e\sigma_T \frac{4i}{3k} \left\{ (\boldsymbol{\beta}_b \cdot \hat{\mathbf{k}})\Delta\theta + (\Delta\boldsymbol{\beta} \cdot \hat{\mathbf{k}})\theta_b \right\}, \end{aligned} \quad (6.112)$$

1, 0)

$$\begin{aligned} \dot{\theta}_\gamma - \frac{k^2}{4}(\delta_\gamma - 4\sigma_\gamma) - k^2\Psi + 2i(\boldsymbol{\beta}_\gamma \cdot \mathbf{k})k^2(B - \dot{E}) - 4i(\boldsymbol{\beta}_\gamma \cdot \mathbf{k})\dot{\Phi} \\ = -an_e\sigma_T \left\{ \Delta\theta + i\mathbf{k} \cdot \left(\boldsymbol{\beta}_\gamma \delta_{n_e} - \boldsymbol{\beta}_b(\delta_\gamma - \sigma_\gamma) + \Delta\boldsymbol{\beta}\Psi \right) \right\}, \end{aligned} \quad (6.113)$$

2, 0)

$$\begin{aligned} \dot{\sigma}_\gamma - \frac{4}{15}\theta_\gamma + \frac{3k}{10}\mathcal{F}_3^0 - \frac{4}{15}k^2(B - \dot{E}) - \frac{4i}{15}(\boldsymbol{\beta}_\gamma \cdot \mathbf{k})(\Phi + 5\Psi) \\ = -an_e\sigma_T \left\{ \sigma_\gamma - \frac{4i}{15k}\hat{\mathbf{k}} \cdot (\boldsymbol{\beta}_b\theta_\gamma + 4\boldsymbol{\beta}_b\theta_b + \Delta\boldsymbol{\beta}\theta_b) + \frac{3i}{10}(\boldsymbol{\beta}_b \cdot \hat{\mathbf{k}})\mathcal{F}_3^0 \right\}, \end{aligned} \quad (6.114)$$

3, 0)

$$\begin{aligned} \dot{\mathcal{F}}_3^0 - \frac{6k}{7}\sigma_\gamma + \frac{4k}{7}\mathcal{F}_4^0 - \frac{8i}{7}(\boldsymbol{\beta}_\gamma \cdot \mathbf{k})k(B - \dot{E}) \\ = -an_e\sigma_T \left\{ \mathcal{F}_3^0 - \frac{6i}{7}(\boldsymbol{\beta}_b \cdot \hat{\mathbf{k}})\sigma_\gamma + \frac{4i}{7}(\boldsymbol{\beta}_b \cdot \hat{\mathbf{k}})\mathcal{F}_4^0 \right\}, \end{aligned} \quad (6.115)$$

$\ell > 3, 0)$

$$\begin{aligned} \dot{\mathcal{F}}_\ell^0 - \frac{k}{2\ell+1}(\ell\mathcal{F}_{\ell-1}^0 - (\ell+1)\mathcal{F}_{\ell+1}^0) \\ = -an_e\sigma_T \left\{ \mathcal{F}_\ell^0 - \frac{i(\boldsymbol{\beta}_b \cdot \hat{\mathbf{k}})}{2\ell+1}(\ell\mathcal{F}_{\ell-1}^0 - (\ell+1)\mathcal{F}_{\ell+1}^0) \right\}. \end{aligned} \quad (6.116)$$

It can be supplemented with the classic truncation scheme (3.139)

$$\mathcal{F}_{(\ell_{\max}+1)}^0 \simeq \frac{2\ell_{\max}+1}{k\tau} \mathcal{F}_{\ell_{\max}}^0 - \mathcal{F}_{(\ell_{\max}-1)}^0, \quad (6.117)$$

so that the last moment that we integrate verifies the equation

$$\begin{aligned} & \dot{\mathcal{F}}_{\ell}^0 + \frac{\ell+1}{\tau} \mathcal{F}_{\ell}^0 - k \mathcal{F}_{\ell-1}^0 \\ &= -an_e \sigma_T \left\{ \mathcal{F}_{\ell}^0 + i(\boldsymbol{\beta}_b \cdot \hat{\mathbf{k}}) \left(\frac{\ell+1}{k\tau} \mathcal{F}_{\ell}^0 - \mathcal{F}_{\ell-1}^0 \right) \right\}, \quad \ell = \ell_{\max}. \end{aligned} \quad (6.118)$$

Vector hierarchy. The new vector hierarchy is coupled to the scalar perturbations

1, +1)

$$\begin{aligned} & \dot{\chi}_{\gamma}^+ - \frac{3k^2}{4} \pi_{+\gamma}^V + \beta_{\gamma}^+ k^2 (B - \dot{E}) - 4\beta_{\gamma}^+ \dot{\Phi} \\ &= -an_e \sigma_T \left\{ \chi_{\gamma}^+ - \chi_b^+ + \beta_{\gamma}^+ \delta_{n_e} - \beta_b^+ \left(\delta_{\gamma} + \frac{1}{2} \sigma_{\gamma} \right) + \Delta \beta^+ \Psi \right\}, \end{aligned} \quad (6.119)$$

2, +1)

$$\begin{aligned} & \dot{\pi}_{+\gamma}^V + \frac{4}{15} \chi_{\gamma} + \frac{2}{5} \sqrt{\frac{2}{3}} \mathcal{F}_3^{+1} + \frac{4}{15} (S_+ + \dot{F}_+) + \frac{4\beta_{\gamma}^+ k}{15} (\Phi + 5\Psi) \\ &= -an_e \sigma_T \left\{ \pi_{+\gamma}^V + \frac{4}{15k^2} (\beta_b^+ \theta_{\gamma} + 4\beta_b^+ \theta_b + \Delta \beta^+ \theta_b) + \frac{\beta_b^+}{5k} \mathcal{F}_3^0 \right\}, \end{aligned} \quad (6.120)$$

3, +1)

$$\begin{aligned} & \dot{\mathcal{F}}_3^{+1} + \frac{2k^2 \sqrt{6}}{7} \pi_{+\gamma}^V + \frac{k\sqrt{15}}{7} \mathcal{F}_4^{+1} - \frac{8}{7} \sqrt{\frac{2}{3}} \beta_{\gamma}^+ k^2 (B - \dot{E}) \\ &= -an_e \sigma_T \left\{ \mathcal{F}_3^{+1} - \beta_b^+ \frac{\sqrt{6}}{7} (2\sigma_{\gamma} + \mathcal{F}_4^0) \right\}, \end{aligned} \quad (6.121)$$

$\ell > 3$, +1)

$$\begin{aligned} & \dot{\mathcal{F}}_{\ell}^{+1} - \frac{k}{2\ell+1} \left(\sqrt{\ell^2-1} \mathcal{F}_{\ell-1}^{+1} - \sqrt{\ell(\ell+2)} \mathcal{F}_{\ell+1}^{+1} \right) \\ &= -an_e \sigma_T \left\{ \mathcal{F}_{\ell}^{+1} - \frac{\beta_b^+ \sqrt{\ell(\ell+1)}}{\sqrt{2} (2\ell+1)} (\mathcal{F}_{\ell-1}^0 + \mathcal{F}_{\ell+1}^0) \right\}. \end{aligned} \quad (6.122)$$

At first sight, it is not clear how to truncate this hierarchy. We analyze this issue in the coming section.

6.5.3 Truncation

Let us first define the functions

$$\bar{\mathcal{F}}_\ell \equiv \frac{\mathcal{F}_\ell^{+1}}{\sqrt{\ell(\ell+1)}}, \quad i_\ell(x) \equiv \frac{j_\ell(x)}{x}. \quad (6.123)$$

On the one hand, from (6.122) we see that $\bar{\mathcal{F}}_\ell$ satisfies the modified equation of motion

$$\begin{aligned} & \dot{\bar{\mathcal{F}}}_\ell - \frac{k}{2\ell+1} ((\ell-1)\bar{\mathcal{F}}_{\ell-1} - (\ell+2)\bar{\mathcal{F}}_{\ell+1}) \\ & = -an_e\sigma_T \left\{ \bar{\mathcal{F}}_\ell - \frac{\beta_b^+}{\sqrt{2(2\ell+1)}} (\mathcal{F}_{\ell-1}^0 + \mathcal{F}_{\ell+1}^0) \right\}. \end{aligned} \quad (6.124)$$

On the other hand, from the properties of the Bessel functions (C.4), we can prove

$$i'_\ell(x) = \frac{1}{2\ell+1} ((\ell-1)i_{\ell-1}(x) - (\ell+2)i_{\ell+1}(x)) \quad (6.125)$$

$$= \frac{\ell-1}{x} i_\ell(x) - i_{\ell+1}(x) \quad (6.126)$$

$$= i_{\ell-1}(x) - \frac{\ell+2}{x} i_\ell(x), \quad (6.127)$$

and

$$\frac{i_\ell(x)}{x} = \frac{1}{2\ell+1} (i_{\ell-1}(x) + i_{\ell+1}(x)). \quad (6.128)$$

Then, comparing (6.124) and (6.125), we can argue³ that the free-streaming solution satisfies

$$\bar{\mathcal{F}}_\ell \sim i_\ell(k\tau), \quad (6.129)$$

and propose a truncation scheme

$$\bar{\mathcal{F}}_{(\ell_{\max}+1)} \simeq \frac{2\ell_{\max}+1}{k\tau} \bar{\mathcal{F}}_{\ell_{\max}} - \bar{\mathcal{F}}_{(\ell_{\max}-1)}. \quad (6.130)$$

In terms of the original variables, the truncation scheme is

$$\mathcal{F}_{(\ell_{\max}+1)}^{+1} \simeq \frac{2\ell_{\max}+1}{k\tau} \sqrt{\frac{\ell_{\max}+2}{\ell_{\max}}} \mathcal{F}_{\ell_{\max}}^{+1} - \sqrt{\frac{(\ell_{\max}+1)(\ell_{\max}+2)}{(\ell_{\max}-1)\ell_{\max}}} \mathcal{F}_{(\ell_{\max}-1)}^{+1}. \quad (6.131)$$

Applying this truncation, the evolution equation for the last multipole is

$$\begin{aligned} & \dot{\mathcal{F}}_\ell^{+1} + \frac{\ell+2}{\tau} \mathcal{F}_\ell^{+1} - k \sqrt{\frac{\ell+1}{\ell-1}} \mathcal{F}_{\ell-1}^{+1} \\ & - an_e\sigma_T \left\{ \mathcal{F}_\ell^{+1} - \frac{\beta_b^+}{\sqrt{2}} \frac{\sqrt{\ell(\ell+1)}}{2\ell+1} (\mathcal{F}_{\ell-1}^0 + \mathcal{F}_{\ell+1}^0) \right\}, \quad \ell = \ell_{\max}. \end{aligned} \quad (6.132)$$

³This claim will be put in a firmer basis once we develop the line-of-sight approach in Chapter 7.

6.6 Einstein equations and gauge transformations

6.6.1 Einstein equations

The metric sector of the Einstein equations has not been modified. We can still use the Einstein equations (1), but we must carefully reevaluate the source (the total energy-momentum tensor). In this section we also include the Einstein equations for vector and tensor modes. The latter is only included for the sake of completeness.

It is worth remembering that, to first order in β , the background quantities we are interested in, e.g. ρ and P , are equal in the \mathcal{O} and $\tilde{\mathcal{O}}$ frames. Hence, as in previous sections, we will drop the distinction. The full energy-momentum tensor for each component is

$$T^0_0 + \delta T^0_0 = -\rho - \delta\rho - (\rho + P)B_i\beta^i, \quad (6.133a)$$

$$T^0_i + \delta T^0_i = \delta Q_i + (\rho + P)\left(\delta_i^j + \frac{1}{2}A\delta_i^j + \frac{1}{2}H_i^j\right)\beta_j, \quad (6.133b)$$

$$T^i_j + \delta T^i_j = P\delta_j^i + \delta P\delta_j^i + \delta\Pi_j^i + (\rho + P)\beta_j B^i, \quad (6.133c)$$

where β is different for each component. We must write now the Einstein equations with this source for the perturbed RW metric (3.126). The background evolution obeys the standard Friedmann equations plus the cosmic center of mass constraint

$$\mathcal{H}^2 = \frac{8\pi G a^2}{3} \sum_s \rho_s, \quad (6.134)$$

$$0 = \sum_s \beta_s(\rho_s + P_s), \quad (6.135)$$

$$\dot{\mathcal{H}} + \frac{1}{2}\mathcal{H}^2 = -4\pi G a^2 \sum_s P_s. \quad (6.136)$$

Applying the condition (6.135), the explicit β contributions to the total energy-momentum tensor vanish

$$\delta T^0_0 = \sum_s \delta T^0_{s0} = -\sum_s \delta\rho_s, \quad (6.137a)$$

$$\delta T^0_i = \sum_s \delta T^0_{si} = \sum_s \delta Q_{si}, \quad (6.137b)$$

$$\delta T^i_j = \sum_s \delta T^i_{sj} = \sum_s \left(\delta P_s \delta_j^i + \delta\Pi_s^{ij}\right). \quad (6.137c)$$

This time, the non-relativistic species have pressure and anisotropic stress of order β . Splitting the sources into relativistic and non-relativistic components we have

$$\delta\rho = \sum_{\text{NR}} \delta\rho + \sum_{\text{R}} \delta\rho, \quad (6.138)$$

$$\delta P = \frac{2}{3} \sum_{\text{NR}} \rho \beta_k \delta v^k + \frac{1}{3} \sum_{\text{R}} \delta\rho, \quad (6.139)$$

$$\delta Q^i = \sum_{\text{NR}} \rho \delta v^i + \frac{4}{3} \sum_{\text{R}} \rho \delta v^i, \quad (6.140)$$

$$\delta\Pi^{ij} = \sum_{\text{NR}} \rho \left(\beta^i \delta v^j + \beta^j \delta v^i - \frac{2}{3} \delta^{ij} \beta_k \delta v^k\right) + \sum_{\text{R}} \delta\Pi^{ij}. \quad (6.141)$$

Finally, the Einstein equations projected in the helicity basis read

(0,0)

$$2k^2\Phi + 6\mathcal{H}(\dot{\Phi} + \mathcal{H}\Psi) - 2k^2\mathcal{H}(B - \dot{E}) = -8\pi G\alpha^2\delta\rho. \quad (6.142)$$

(0,i)

$$ik(\dot{\Phi} + \mathcal{H}\Psi) = -4\pi G\alpha^2\delta Q_3, \quad (6.143)$$

$$k^2(S_+ + \dot{F}_+) = 16\pi G\alpha^2\delta Q_+. \quad (6.144)$$

(i,j)

$$k^2(\Phi - \Psi) - k^2(\partial_\tau + 2\mathcal{H})(B - \dot{E}) = -12\pi G\alpha^2\delta\Pi_{33}, \quad (6.145)$$

$$(\partial_\tau + 2\mathcal{H})(\dot{\Phi} + \mathcal{H}\Psi) + (\dot{\mathcal{H}} - \mathcal{H}^2)\Psi = 4\pi G\alpha^2(\delta P + \delta\Pi_{33}), \quad (6.146)$$

$$ik(\partial_\tau + \mathcal{H})(S_+ + \dot{F}_+) = 16\pi G\alpha^2\delta\Pi_{+3}, \quad (6.147)$$

$$\frac{1}{2}(\partial_\tau^2 + 2\mathcal{H}\partial_\tau + k^2)h_{++} = 8\pi G\alpha^2\delta\Pi_{++}. \quad (6.148)$$

Again, the results for the $-$ helicity can be obtained substituting $- \leftrightarrow +$ in every sub and superscript. The projections can be written in terms of the variables defined previously

$$\begin{aligned} \delta\Pi_{33} &= \frac{4}{3}\rho\sigma, & \delta\Pi_{3+} &= ik\rho\pi_+^V, & \delta\Pi_{++} &= \rho\pi_{++}^T, \\ \delta Q_3 &= ik(\rho + P)\theta, & \delta Q_+ &= (\rho + P)\chi_+. \end{aligned} \quad (6.149)$$

The equations for the scalar modes in the synchronous gauge are the standard ones, see (3.163). The vector metric perturbations can be grouped into a single variable

$$\mathbf{W} \equiv \mathbf{S} + \dot{\mathbf{F}}, \quad (6.150)$$

whose evolution is described by

$$W_+ = \frac{16\pi G\alpha^2}{k^2}(\rho + P)\chi_+, \quad (6.151)$$

$$\dot{W}_+ + \mathcal{H}W_+ = 16\pi G\alpha^2\rho\pi_+^V. \quad (6.152)$$

The vector metric perturbation is completely determined by (6.151). The condition (6.152) is identically satisfied once we impose the conservation of the energy-momentum tensor.

6.6.2 Gauge transformations

The gauge transformation properties of the metric variables and the energy-momentum tensor are not modified with respect to those elaborated in Section 3.5.2. However, the perturbed fluid variables are defined in a different way

$$\delta\rho = \alpha^2 T_{00} - \rho + A\rho + 2(\rho + P)\beta_i B^i, \quad (6.153a)$$

$$\delta Q_i = -\alpha^2 T_{0i} + (\rho + P)\beta_i - \frac{1}{2}(\rho + P)(H^j{}_i - A\delta^i{}_j)\beta_j + B_i P, \quad (6.153b)$$

$$\delta P = \frac{1}{3}\alpha^2 T^i{}_i - P - \frac{1}{3}H^i{}_i P, \quad (6.153c)$$

$$\delta\Pi_{ij} = \alpha^2 \left(T_{ij} - \frac{1}{3}\delta_{ij}T^k{}_k \right) - \left(H_{ij} - \frac{1}{3}\delta_{ij}H^k{}_k \right) P. \quad (6.153d)$$

The transformation rules are modified accordingly

$$\Delta\delta\rho = T\dot{\rho} - 2(\rho + P)\beta^i\partial_i T, \quad (6.154a)$$

$$\Delta\delta Q_i = -(\rho + P)\partial_i T + T\partial_\eta(\beta_i(\rho + P)) + \frac{1}{2}(\rho + P)\beta^j(\partial_i L_j - \partial_j L_i), \quad (6.154b)$$

$$\Delta\delta P = T\dot{P} - \frac{2}{3}\beta^i\partial_i T(\rho + P), \quad (6.154c)$$

$$\Delta\delta\Pi_{ij} = -(\rho + P)\left(\beta_i\partial_j T + \beta_j\partial_i T - \frac{2}{3}\delta_{ij}\beta^k\partial_k T\right). \quad (6.154d)$$

Using these results, the rules to trade between the Newtonian and the synchronous gauge are⁴

$$\delta(\text{Newt}) - \delta(\text{Syn}) = T\frac{\dot{\rho}}{\rho} - 2i(1+w)(\boldsymbol{\beta} \cdot \mathbf{k})T, \quad (6.155a)$$

$$\theta(\text{Newt}) - \theta(\text{Syn}) = k^2 T + i(\dot{\boldsymbol{\beta}} \cdot \mathbf{k})T + i(\boldsymbol{\beta} \cdot \mathbf{k})\frac{\dot{\rho} + \dot{P}}{\rho + P}T, \quad (6.155b)$$

$$\chi_+(\text{Newt}) - \chi_+(\text{Syn}) = T\dot{\beta}_+ + T\beta_+\frac{\dot{\rho} + \dot{P}}{\rho + P}, \quad (6.155c)$$

$$\delta P(\text{Newt}) - \delta P(\text{Syn}) = T\dot{P} - \frac{2i}{3}(\boldsymbol{\beta} \cdot \mathbf{k})T(\rho + P), \quad (6.155d)$$

$$\sigma(\text{Newt}) - \sigma(\text{Syn}) = i(\boldsymbol{\beta} \cdot \mathbf{k})(1+w)T, \quad (6.155e)$$

$$\pi_+^V(\text{Newt}) - \pi_+^V(\text{Syn}) = -\beta_+(1+w)T, \quad (6.155f)$$

$$\pi_{++}^T(\text{Newt}) - \pi_{++}^T(\text{Syn}) = 0. \quad (6.155g)$$

We are omitting the results for the $-$ helicity, that can be obtained substituting $- \leftrightarrow +$ in every sub and superscript.

6.7 Reduced system: fluid approximation

The main pieces of the non-comoving scenario have been set in place: we have described the behaviour of moving fluids, at the background and perturbation level, and closed the system with the Einstein equations. This section will be devoted to a deeper analysis of the system, after reducing it into a more manageable form. To this end, we defer the study of the full Boltzmann hierarchy to Chapter 7 and introduce here instead the fluid approximation.

The fluid approximation, that has been discussed in Section 6.5, consists on truncating the Boltzmann equation at $\ell = 2$. At this point we will not aim at describing the late time behaviour of photons or neutrinos in great detail. This will be the subject of Chapter 7, where we will solve the full Boltzmann hierarchy. We focus for now on the behaviour of non-relativistic components, which will allow us to predict new LSS signatures. The fluid approximation is well suited for this purpose, since it fails only when the ultrarelativistic species are almost negligible for

⁴We have neglected terms like βL_+ that, under our assumptions, are second order in β . This can be seen from (3.159) where it is clear that the transverse part of \mathbf{L} is proportional to the vector perturbations, i.e. $\mathcal{O}(\beta)$.

the overall evolution of LSS observables. In this context, it is also justified to use the simplest truncation scheme, setting to zero all moments with $\ell > 2$.

Section 6.7.1 analyzes the behaviour of the bulk velocities (β) of the fluids, an information that is essential for any further computation. The next two Sections 6.7.2 and 6.7.3 are devoted to the scalar and vector modes, respectively. The reason why the discussion can be splitted in two sections lies in the fact that the *modified* evolution of scalar and vector modes can actually be decoupled. This crucial fact, that has nothing to do with the fluid approximation, has already been treated in detail in Section 6.5.

6.7.1 Bulk velocities

The evolution of the different fluids is governed by

$$\dot{\beta}_\gamma = -\frac{1}{\tau_c} \Delta\beta, \quad (6.156a)$$

$$\dot{\beta}_\nu = 0, \quad (6.156b)$$

$$\dot{\beta}_b = -\mathcal{H}\beta_b + \frac{1}{R\tau_c} \Delta\beta, \quad (6.156c)$$

$$\dot{\beta}_c = -\mathcal{H}\beta_c \quad (6.156d)$$

where, again, $\Delta\beta \equiv \beta_\gamma - \beta_b$. The initial conditions are chosen according to the constraint

$$\sum_s (\rho_s + P_s) \beta_s = 0, \quad (6.157)$$

so the cosmic center of mass condition is maintained in the evolution. Moreover, we will assume that all the bulk velocities ($\beta_\gamma, \beta_\nu, \beta_b, \beta_c$) are aligned along the $\hat{\beta}$ axis in the \mathcal{O} frame. As we will shortly see, and can be inferred from (6.156a) and (6.156c), when two species are tightly coupled their velocities evolve to become equal. Once a particle species decouples, the magnitude of its velocity evolves independently but, in the absence of additional interactions or other sources of anisotropy, it does not change its direction. We assume that the whole visible sector was in thermal equilibrium in the very early Universe, even if some species, like neutrinos, decoupled later. In this case, all its components must have velocities pointing in the same direction $\hat{\beta}$. The only remaining contribution is the dark sector, with DM among its components. The dark sector in the \mathcal{O} frame counterbalance the momentum density of the visible sector to achieve an isotropic universe, so it must point in the $-\hat{\beta}$ direction.

CDM and neutrinos are decoupled, but the photon-baryon system must be treated with some care. In the tight-coupling limit, $\tau_c \ll 1$, it is easy to see that the velocities converge in direction and magnitude and we can look for an approximate solution of this system. Expanding perturbatively in the small parameter τ_c we have

$$\dot{\beta}_\gamma = -\mathcal{A}\mathcal{H}\beta_\gamma + \mathcal{O}(\tau_c), \quad (6.158)$$

$$\Delta\beta = \mathcal{A}\mathcal{H}\beta_\gamma\tau_c + \mathcal{O}(\tau_c^2). \quad (6.159)$$

The differential equation can be solved to yield

$$\beta_\gamma = \frac{\beta_0}{1+R}, \quad (6.160)$$

where β_0 is the initial velocity of the visible sector in the \mathcal{O} frame, the only additional free parameter in our model. In a similar way, the neutrino and CDM equations can be solved to give

$$\beta_\nu = \beta_0, \quad (6.161)$$

$$\beta_c = \beta_c^{\text{today}} a^{-1}. \quad (6.162)$$

Using the scaling (6.162) and enforcing the constraint (6.157) during the tightly coupled regime, the value of β_c^{today} is found to be

$$\beta_c^{\text{today}} = -\frac{4}{3}\beta_0 \frac{\Omega_\gamma + \Omega_\nu}{\Omega_c}. \quad (6.163)$$

It is important to notice that according to the evolution of β_c (6.162), early enough in time, the condition $\beta_c \ll 1$ could break down. However, this is only the case if the DM keeps the non-relativistic distribution at early times. If the DM were light enough it could behave as a radiation-like fluid well before its bulk velocity reaches $\beta_c = 1$. In this case, β_c would remain constant and small. On the other hand, if the DM is heavy, its bulk velocity can reach the relativistic regime. In this case, it is worth mentioning that even if the anisotropies that would arise at the background level are $\mathcal{O}(\beta_0)$ and not $\mathcal{O}(\beta_0^2)$, their effects can only be relevant well before the matter-dominated era, with no observational consequences.

In order to avoid choosing any particular framework for the dark sector, we will not follow the dark matter evolution using (6.162). Instead, we follow the evolution of photons (6.156a), neutrinos (6.156b) and baryons (6.156c), and then the momentum of the dark sector, regardless of its composition, can be obtained imposing the center of mass condition (6.157). Thus, our only assumptions regarding the dark sector are that it is subdominant at early times and that it behaves as cold matter plus cosmological constant at late times.

6.7.2 Scalar modes

Here we provide only the equations for the photon-baryon system. As usual, neutrinos and CDM satisfy the same equations without the coupling term. The evolution of the photon perturbations is described by the equations (6.112, 6.113, 6.114). Under the approximation scheme already discussed, i.e. neglecting backreaction of vector modes and neglecting moments higher than $\ell = 2$, these equations take the

form

$$\begin{aligned} \dot{\delta}_\gamma + \frac{4}{3}\theta_\gamma + \frac{4k^2}{3}(B - \dot{E}) - 4\dot{\Phi} + \frac{8}{3}\mathbf{i}(\boldsymbol{\beta}_\gamma \cdot \mathbf{k})(\Psi - \Phi) \\ = -\frac{4}{3\tau_c} \left[-\frac{\mathbf{i}}{k} \hat{\mathbf{k}} \cdot (\boldsymbol{\beta}_b \Delta\theta + \theta_b \Delta\boldsymbol{\beta}) \right], \end{aligned} \quad (6.164a)$$

$$\begin{aligned} \dot{\theta}_\gamma - \frac{k^2}{4}(\delta_\gamma - 4\sigma_\gamma) - k^2\Psi - 4\mathbf{i}(\boldsymbol{\beta}_\gamma \cdot \mathbf{k})\dot{\Phi} + 2\mathbf{i}k^2(\boldsymbol{\beta}_\gamma \cdot \mathbf{k})(B - \dot{E}) \\ = -\frac{1}{\tau_c} \left[\Delta\theta - \mathbf{i}\mathbf{k} \cdot (\boldsymbol{\beta}_b(\delta_\gamma - \sigma_\gamma) - \boldsymbol{\beta}_\gamma\delta_{n_e} - \Delta\boldsymbol{\beta}\Psi) \right], \end{aligned} \quad (6.164b)$$

$$\begin{aligned} \dot{\sigma}_\gamma - \frac{4}{15}\theta_\gamma - \frac{4}{15}k^2(B - \dot{E}) - \frac{4\mathbf{i}}{15}(\boldsymbol{\beta}_\gamma \cdot \mathbf{k})(\Phi + 5\Psi) \\ = -\frac{1}{\tau_c} \left[\sigma_\gamma - \frac{4\mathbf{i}}{15k} \hat{\mathbf{k}} \cdot (\boldsymbol{\beta}_b\theta_\gamma + 4\boldsymbol{\beta}_b\theta_b + \Delta\boldsymbol{\beta}\theta_b) \right]. \end{aligned} \quad (6.164c)$$

Neutrinos are described by the same system, without collision term. For baryons, we apply our approximation scheme to equations (6.88) and (6.89) obtaining

$$\begin{aligned} \dot{\delta}_b + \theta_b - 3\dot{\Phi} + k^2(B - \dot{E}) - 2\mathbf{i}\mathcal{H} \frac{(\boldsymbol{\beta}_b \cdot \hat{\mathbf{k}})}{k} \theta_b + 2\mathbf{i}(\boldsymbol{\beta}_b \cdot \mathbf{k})(\Psi - \Phi) \\ = \frac{1}{R\tau_c} \left[-\frac{\mathbf{i}}{k} \hat{\mathbf{k}} \cdot (\boldsymbol{\beta}_b \Delta\theta + \theta_b \Delta\boldsymbol{\beta}) \right], \end{aligned} \quad (6.165a)$$

$$\begin{aligned} \dot{\theta}_b + \mathcal{H}\theta_b - k^2\Psi + 2\mathbf{i}(\boldsymbol{\beta}_b \cdot \mathbf{k})\theta_b - 4\mathbf{i}(\boldsymbol{\beta}_b \cdot \mathbf{k})\dot{\Phi} + 2\mathbf{i}k^2(\boldsymbol{\beta}_b \cdot \mathbf{k})(B - \dot{E}) \\ = \frac{1}{R\tau_c} \left[\Delta\theta - \mathbf{i}\mathbf{k} \cdot (\boldsymbol{\beta}_b(\delta_\gamma - \sigma_\gamma) - \boldsymbol{\beta}_\gamma\delta_{n_e} - \Delta\boldsymbol{\beta}\Psi) \right]. \end{aligned} \quad (6.165b)$$

Again, CDM equations take the same form, but without collision term. The evolution of the total energy-momentum tensor is described by

$$\dot{\delta} + 3\mathcal{H}(c_s^2 - w)\delta + (1+w)\theta - (1+w)(3\dot{\Phi} - k^2(B - \dot{E})) = 0, \quad (6.166a)$$

$$\dot{\theta} + (1-3w)\mathcal{H}\theta + \frac{\dot{w}}{1+w}\theta - \frac{k^2}{1+w}c_s^2\delta + \frac{4k^2}{3(1+w)}\sigma - k^2\Psi = 0, \quad (6.166b)$$

where

$$c_s^2\delta = \frac{1}{\rho} \left(\frac{1}{3}\rho_\gamma\delta_\gamma + \frac{1}{3}\rho_\nu\delta_\nu - \frac{2\mathbf{i}\rho_c\beta_c\theta_c}{3k} - \frac{2\mathbf{i}\rho_b\beta_b\theta_b}{3k} \right), \quad (6.167)$$

$$\sigma = \frac{1}{\rho} \left(\rho_\gamma\sigma_\gamma + \rho_\nu\sigma_\nu + \frac{\mathbf{i}\rho_c\beta_c\theta_c}{k} + \frac{\mathbf{i}\rho_b\beta_b\theta_b}{k} \right). \quad (6.168)$$

In Section 3.7, we saw how the linearity of these equations allows us to regard them indistinctly as a system for the evolution of the transfer functions, factoring out the initial conditions. There is however a striking difference between these equations and the ones in Λ CDM: the appearance of imaginary terms, e.g. compare (6.164) and (3.136).

Usually, even though the Fourier coefficients are generally complex, the evolution equations are real. In this case, both real and imaginary parts of the transfer function satisfy the same equation. Owing to linearity, with a judicious choice of the initial global phase, the transfer function can be rendered purely real. With the

appearance of complex coefficients, real and imaginary parts constitute a coupled system with different equations of motion.

We will assume that the global phase has been chosen so that the imaginary parts are initially zero, or at most $\mathcal{O}(\beta)$. Even if they are initially zero, the terms proportional to β couple the imaginary to the real parts, driving them to a finite value proportional to β . Then we are in the same situation as with the vector modes: the imaginary parts of the scalar modes are determined by the real parts, but do not backreact on them. The real parts follow the standard cosmological evolution. Therefore, the transfer function of a generic perturbation g can be splitted as

$$g(\tau, \mathbf{k}) = g^R(\tau, k) + i(\hat{\beta} \cdot \hat{k})g^I(\tau, k), \quad (6.169)$$

where now g^R and g^I are purely real and do not depend on the direction of \hat{k} . The previous discussion can be summarized as follows.

- The real part of the perturbations, g^R , follows the standard Λ CDM evolution. In particular, it only contains adiabatic perturbations.
- The real parts act as external sources in the system for the imaginary parts, via contributions $\mathcal{O}(\beta)$. The imaginary part of the perturbations, g^I , is $\mathcal{O}(\beta)$.

Performing this splitting and working in the synchronous gauge (3.162), the final set of equations for the photon perturbations is

$$\begin{aligned} \dot{\delta}_\gamma^I + \frac{4}{3}\theta_\gamma^I + \frac{2}{3}\dot{h}^I - \frac{8\beta_\gamma k}{3}\eta^R \\ = \frac{4}{3k\tau_c} \left[\beta_b \Delta\theta^R + \theta_b^R \Delta\beta \right], \end{aligned} \quad (6.170a)$$

$$\begin{aligned} \dot{\theta}_\gamma^I - \frac{k^2}{4}(\delta_\gamma^I - 4\sigma_\gamma^I) + \beta_\gamma k (\dot{h}^R + 2\dot{\eta}^R) \\ = -\frac{1}{\tau_c} \left[\Delta\theta^I - k \left(\beta_b (\delta_\gamma^R - \sigma_\gamma^R) - \beta_\gamma \delta_{n_e}^R \right) \right], \end{aligned} \quad (6.170b)$$

$$\begin{aligned} \dot{\sigma}_\gamma^I - \frac{4}{15}\theta_\gamma^I - \frac{2}{15}(\dot{h}^I + 6\dot{\eta}^I) - \frac{4\beta_\gamma k}{15}\eta^R \\ = -\frac{1}{\tau_c} \left[\sigma_\gamma^I - \frac{4}{15k} \left(\beta_b \theta_\gamma^R + 4\beta_b \theta_b^R + \Delta\beta \theta_b^R \right) \right]. \end{aligned} \quad (6.170c)$$

The equations for neutrinos are the same, setting the collision part to zero. For the baryons we have

$$\begin{aligned} \dot{\delta}_b^I + \theta_b^I + \frac{1}{2}\dot{h}^I - \frac{2\mathcal{H}\beta_b}{k}\theta_b^R - 2\beta_b k\eta^R \\ = -\frac{1}{kR\tau_c} \left[\beta_b \Delta\theta^R + \theta_b^R \Delta\beta \right], \end{aligned} \quad (6.171a)$$

$$\begin{aligned} \dot{\theta}_b^I + \mathcal{H}\theta_b^I + 2\beta_b k\theta_b^R + \beta_b k (\dot{h}^R + 2\dot{\eta}^R) \\ = \frac{1}{R\tau_c} \left[\Delta\theta^I - k \left(\beta_b (\delta_\gamma^R - \sigma_\gamma^R) - \beta_\gamma \delta_{n_e}^R \right) \right]. \end{aligned} \quad (6.171b)$$

And finally for the total fluid

$$\dot{\delta}^I + 3\mathcal{H}(c_s^2 - w)\delta^I + (1+w)\theta^I + \frac{1}{2}(1+w)\dot{h}^I = 0, \quad (6.172a)$$

$$\dot{\theta}^I + (1-3w)\mathcal{H}\theta^I + \frac{\dot{w}}{1+w}\theta^I - \frac{k^2}{1+w}c_s^2\delta^I + \frac{4k^2}{3(1+w)}\sigma^I = 0, \quad (6.172b)$$

where, in the synchronous gauge,

$$c_s^2\delta^I = \frac{1}{\rho} \left(\frac{1}{3}\rho_\gamma\delta_\gamma^I + \frac{1}{3}\rho_\nu\delta_\nu^I - \frac{2\rho_b\beta_b\theta_b^R}{3k} \right), \quad (6.173)$$

$$\sigma^I = \frac{1}{\rho} \left(\rho_\gamma\sigma_\gamma^I + \rho_\nu\sigma_\nu^I + \frac{\rho_b\beta_b\theta_b^R}{k} \right). \quad (6.174)$$

To complete the system, we compute the variables η and $a\dot{h}$ using a combination of the Einstein equations

$$\dot{\eta}^I = \frac{3\mathcal{H}^2}{2k^2}(1+w)\theta^I, \quad (6.175)$$

$$\partial_\tau(a\dot{h}^I) = -3a(1+3c_s^2)\mathcal{H}^2\delta^I. \quad (6.176)$$

Usually, one would integrate the equations for photons, baryons, neutrinos and CDM. Then, after adding all the components, one would compute the sources for the metric perturbations, i.e. the total energy-momentum tensor. As we stressed before, in our setup we found it more convenient to follow a different route. Instead of tracking the behaviour of the dark sector, thus choosing a particular DM framework, we follow the evolution of the whole fluid (6.166). Using these equations, the only underlying assumptions are:

- The dark sector is subdominant with respect to neutrinos and photons at early times, i.e. before the matter-domination era.
- There is a transition to a Λ +CDM behaviour at late times.

Under these assumptions, the only CDM contribution to the total fluid goes into the equation of state w , since in the synchronous gauge it does not contribute to δP or σ at first order in β . The evolution of the dark sector can be obtained afterwards subtracting the contributions of photons, baryons and neutrinos from the total energy-momentum tensor.

These equations still need to be complemented with an appropriate description of the tight-coupling and radiation-streaming approximations, see Section 3.6 for details. Before that, we describe the impact of perturbed recombination. It is usually neglected in Λ CDM but it will be important in our case.

Perturbed recombination

The disturbances in the photon temperature field produce perturbations in the ionization fraction of the electrons. In standard Λ CDM, this inhomogeneous recombination only produces second order effects in the CMB, but it has proven important

at late times when computing other observables, like the 21 cm radiation, through its effects in the gas temperature [NB05; Lew07].

Boltzmann codes like CAMB [LB02] and CLASS [BLT11] have implemented perturbed recombination at late times. These implementations follow the formulae of RECFAST [SSS00], including perturbations into the recombination coefficient that effectively takes into account multilevel atom computations. These codes also track the evolution of the gas temperature and its perturbations, that modify significantly the baryon sound speed.

The study of the dark ages in detail is beyond the scope of this work, but, in our case, perturbed recombination plays a role in the photon-baryon system to first order in β , where a perturbation in the number of *free* electrons δn_e appears, e.g. see (6.84). The baryon sound speed has been neglected in our calculations (it is only important at very small scales) and we will neglect the perturbations in the gas temperature and the recombination coefficient as well. Defining the ionization fraction [KT94; SSS00] as

$$x_e \equiv \frac{n_e}{n_b}, \quad (6.177)$$

where n_e and n_b are the number densities of free electrons and baryons, respectively, we have

$$\delta n_e = \delta_b + \delta_{x_e}, \quad (6.178)$$

where $\delta_{x_e} \equiv \delta x_e / x_e$ is the relative perturbation in the ionization fraction. Since δn_e always appears multiplied by β , to study its evolution it suffices to take (6.67) with $\beta = 0$. After a few manipulations we obtain

$$\dot{\delta}_{n_e} - \frac{\partial}{\partial \tau} \left(\frac{1}{a^3 n_e} \right) a^3 \delta n_e + \theta_b + \frac{1}{2} \dot{h} = 0. \quad (6.179)$$

Substituting the definition (6.178) we get the final evolution equation

$$\dot{\delta}_{x_e} + \frac{\dot{x}_e}{x_e} (\delta_b + \delta_{x_e}) = 0. \quad (6.180)$$

Tight-coupling expansion

During the tightly coupled phase, $\tau_c \ll 1$, the system can be perturbatively expanded in the small parameter τ_c . The only difference with respect to Section 3.6.1 is that now we must plug in the TC results for β and the real parts as well. Solving simultaneously for $\Delta\theta^I$ and σ^I we get

$$\begin{aligned} \Delta\theta^I &= \beta_\gamma k \left(\delta_\gamma^R - \delta_b^R - \delta_{x_e}^R \right) + \tau_c \left\{ \frac{k^2}{4} \mathcal{A} \delta_\gamma^I + \mathcal{A} \mathcal{H} \theta_\gamma^I \right. \\ &\quad + \beta_\gamma k \left[\mathcal{A}(\mathcal{A} - 1) \mathcal{H} \left(\delta_\gamma^R - \delta_b^R - \delta_{x_e}^R \right) - \mathcal{A} \mathcal{H} \delta_\gamma^R + \mathcal{A} \theta_\gamma^R \right. \\ &\quad \left. \left. - \frac{4}{15} \theta_\gamma^R + \mathcal{A} \dot{\delta}_{x_e}^R + \frac{\mathcal{A}}{6} \dot{h}^R - \frac{2}{15} \left(\dot{h}^R + 6\dot{\eta}^R \right) \right] \right\} + \mathcal{O}(\tau_c^2), \quad (6.181) \end{aligned}$$

$$\begin{aligned} \sigma_\gamma^I &= \frac{4\beta_\gamma}{3k} \theta_\gamma^R + \frac{\tau_c}{15} \left\{ 4\theta_\gamma^I + \left(\dot{h}^I + 6\dot{\eta}^I \right) \right. \\ &\quad \left. + \beta_\gamma \left[k(\mathcal{A} - 5) \delta_\gamma^R + 4k\eta^R + \frac{8\mathcal{A}\mathcal{H}}{k} \theta_\gamma^R \right] \right\} + \mathcal{O}(\tau_c^2). \quad (6.182) \end{aligned}$$

The final equations of motion of the photon-baryon plasma during the tightly coupled phase are

$$\begin{aligned} \dot{\delta}_b^I + \theta_\gamma^I + \frac{1}{2}\dot{h}^I \\ = \beta_\gamma \left[\frac{k\mathcal{A}}{4}\delta_\gamma^R + k \left(\frac{3}{4}\delta_\gamma^R - \delta_b^R - \delta_{x_e}^R \right) + 2k\eta^R + \frac{2\mathcal{A}\mathcal{H}}{k}\theta_\gamma^R \right], \end{aligned} \quad (6.183)$$

$$\begin{aligned} \dot{\delta}_\gamma^I + \frac{4}{3}\theta_\gamma^I + \frac{2}{3}\dot{h}^I \\ = \beta_\gamma \left[\frac{k\mathcal{A}}{3}\delta_\gamma^R + \frac{8k}{3}\eta^R + \frac{8\mathcal{A}\mathcal{H}}{3k}\theta_\gamma^R \right], \end{aligned} \quad (6.184)$$

$$\begin{aligned} \dot{\theta}_\gamma^I + \mathcal{A}\mathcal{H}\theta_\gamma^I + \frac{k^2}{4}(\mathcal{A}-1)\delta_\gamma^I \\ = \beta_\gamma k \left[\mathcal{A}(1-\mathcal{A})\mathcal{H} \left(\delta_\gamma^R - \delta_b^R - \delta_{x_e}^R \right) \right. \\ \left. - \mathcal{A}\theta_\gamma^R - \frac{4}{3}\theta_\gamma^R - \mathcal{A}\delta_{x_e}^R - 2\dot{\eta}^R - \left(1 + \frac{\mathcal{A}}{6} \right) \dot{h}^R \right]. \end{aligned} \quad (6.185)$$

Radiation-streaming approximation

RSA can be handled like in Section 3.6.2, starting with a modified second-order equation for the neutrino density

$$\ddot{\delta}_\nu^I = -\frac{k^2}{3}(\delta_\nu^I - 4\sigma_\nu^I) + \frac{4\beta_\nu k}{3}(\dot{h}^R + 4\dot{\eta}^R) - \frac{2}{3}\ddot{h}^I, \quad (6.186)$$

The non-oscillatory particular solution in the sub-Hubble regime is

$$\delta_\nu^I = -\frac{2}{k^2}\ddot{h}^I + \frac{4\beta_\nu}{k}(\dot{h}^R + 4\dot{\eta}^R), \quad (6.187a)$$

$$\theta_\nu^I = -\frac{1}{2}\dot{h}^I + 2\beta_\nu k\eta^R, \quad (6.187b)$$

$$\sigma_\nu^I = 0. \quad (6.187c)$$

6.7.3 Vector modes

We will describe now the evolution of the vector modes, following the same steps as in the previous section. Since the evolution equations, and the initial conditions, are the same for both helicities, we can rewrite the vorticity for the species s as

$$\chi_s = \chi_s \left((\hat{\beta} \cdot \hat{e}_+) \hat{e}_- + (\hat{\beta} \cdot \hat{e}_-) \hat{e}_+ \right) \quad (6.188a)$$

$$= \chi_s \left((\hat{\beta} \cdot \hat{x}) \hat{x} + (\hat{\beta} \cdot \hat{y}) \hat{y} \right) \quad (6.188b)$$

$$= \chi_s \left(\hat{\beta} - (\hat{\beta} \cdot \hat{k}) \hat{k} \right). \quad (6.188c)$$

Then, we do not need to distinguish between helicities and we can just write one equation for χ_s . The same applies to the vector part of the shear tensor π_s^V . Starting from (6.119) and (6.120), under our approximation scheme, i.e. neglecting tensor

modes and moments higher than $\ell = 2$, the evolution of the photon vector modes is described by

$$\dot{\chi}_\gamma + \frac{1}{2}\beta_\gamma(\dot{h} - 2\dot{\eta}) - \frac{3k^2}{4}\pi_\gamma^V = -\frac{1}{\tau_c} \left[\Delta\chi + \left(\beta_\gamma\delta_{n_e} - \beta_b \left(\delta_\gamma + \frac{1}{2}\sigma_\gamma \right) \right) \right], \quad (6.189a)$$

$$\dot{\pi}_\gamma^V + \frac{4}{15}\chi_\gamma + \frac{4}{15}(S + \dot{F}) + \frac{4}{15}\beta_\gamma\eta = -\frac{1}{\tau_c} \left[\pi_\gamma^V + \frac{4}{15k^2}(\beta_b\theta_\gamma + 4\beta_b\theta_b + \Delta\beta\theta_b) \right], \quad (6.189b)$$

where we have defined

$$\Delta\chi \equiv \chi_\gamma - \chi_b. \quad (6.190)$$

Again, the behaviour of neutrinos can be obtained from these equations, setting to zero the collision term. From (6.89) and (6.94), baryons and dark matter evolve according to

$$\dot{\chi}_b + \mathcal{H}\chi_b + \beta_b\theta_b + \frac{1}{2}\beta_b(\dot{h} - 2\dot{\eta}) = \frac{1}{\tau_c R} \left[\Delta\chi + \left(\beta_\gamma\delta_{n_e} - \beta_b \left(\delta_\gamma + \frac{1}{2}\sigma_\gamma \right) \right) \right], \quad (6.191)$$

$$\dot{\chi}_c + \mathcal{H}\chi_c + \frac{1}{2}\beta_c(\dot{h} - 2\dot{\eta}) = 0. \quad (6.192)$$

The evolution of the total vorticity is

$$\dot{\chi} + \mathcal{H}(1 - 3w)\chi + \frac{\dot{w}}{1+w}\chi - \frac{k^2}{1+w}\pi^V = 0, \quad (6.193)$$

where

$$\pi^V = \frac{1}{\rho} \left(\rho_v\pi_v^V + \rho_\gamma\pi_\gamma^V - \frac{1}{k^2}\beta_b\theta_b \right). \quad (6.194)$$

Finally, the relevant Einstein equation is

$$S + \dot{F} = \frac{16\pi G a^2}{k^2}(\rho + P)\chi. \quad (6.195)$$

Tight coupling expansion

As in the previous section, we need to find the approximate equations to follow the tightly coupled phase. Performing the same manipulations, and inserting the TC solutions for β and the scalar modes, we get

$$\begin{aligned} \Delta\chi = & \beta_\gamma(\delta_\gamma - \delta_b - \delta_{x_e}) + \tau_c \left\{ \mathcal{A}\mathcal{H}\chi_\gamma + \beta_\gamma \left[\mathcal{A}(\mathcal{A} - 1)\mathcal{H}(\delta_\gamma - \delta_b - \delta_{x_e}) \right. \right. \\ & \left. \left. - \mathcal{A}\mathcal{H}\delta_\gamma + \frac{\mathcal{A}}{3}\theta_\gamma + \frac{2}{15}\theta_\gamma + \mathcal{A}\dot{\delta}_{x_e} + \frac{\mathcal{A}}{6}\dot{h} + \frac{1}{15}(\dot{h} + 6\dot{\eta}) \right] \right\} + \mathcal{O}(\tau_c^2), \end{aligned} \quad (6.196)$$

$$\pi_\gamma^V = -\frac{4\beta_\gamma}{3k^2}\theta_\gamma - \frac{4}{15}\tau_c \left\{ \chi_\gamma + (S + \dot{F}) - \beta_\gamma \left[\frac{5}{4}\delta_\gamma - \eta - \frac{\mathcal{A}}{4}\delta_\gamma - \frac{2\mathcal{A}\mathcal{H}}{k^2}\theta_\gamma \right] \right\}. \quad (6.197)$$

The equation governing the evolution of the photon vorticity during TC is

$$\begin{aligned} \dot{\chi}_\gamma = & -\mathcal{A}\mathcal{H}\chi_\gamma - \beta_\gamma\theta_\gamma - \frac{1}{2}\beta_\gamma(\dot{h} - 2\dot{\eta}) \\ & + \beta_\gamma\mathcal{A} \left[(1 - \mathcal{A})\mathcal{H}(\delta_\gamma - \delta_b - \delta_{x_e}) - \frac{1}{3}\theta_\gamma - \frac{1}{6}\dot{h} - \dot{\delta}_{x_e} \right]. \end{aligned} \quad (6.198)$$

Radiation streaming approximation

The equations (6.189a) and (6.189b) for neutrinos, or photons after decoupling, can be combined into a second order differential equation

$$\ddot{\chi}_\nu = -\frac{k^2}{5}\chi_\nu - \frac{k^2}{5}(S + \dot{F}) - \frac{k^2}{5}\beta_\nu\eta - \frac{1}{2}\beta_\nu(\ddot{h} - 2\ddot{\eta}) . \quad (6.199)$$

During the period of rapid oscillations, we are in the situation in which $|\ddot{\chi}_\nu| \ll |k^2\chi_\nu|$ and $|\dot{\chi}_\nu| \ll |k^2\pi_\nu^V|$. From the previous equation and (6.189a), the approximate non-oscillating particular solution is found to be

$$\chi_\nu = -(S + \dot{F}) - \beta_\nu\eta + \frac{5}{2k^2}\beta_\nu(\ddot{h} - 2\ddot{\eta}) , \quad (6.200)$$

$$\pi_\nu^V = \frac{2}{3k^2}\beta_\nu(\dot{h} - 2\dot{\eta}) . \quad (6.201)$$

Semi-analytic solutions

The equations obtained admit semi-analytic solutions in some regimes. During the TC regime, from (6.196) and (6.198), we find, to lowest order in τ_c ,

$$(1+R)\chi_\gamma = -\frac{1}{2}\beta_0(h-2\eta) + \beta_0\mathcal{A}(\delta_\gamma - \delta_b - \delta_{x_e}) - \frac{\beta_0}{3}\int\left(1 + \frac{\mathcal{A}}{4}\right)\theta_\gamma d\tau + C_\gamma , \quad (6.202)$$

$$(1+R)\chi_b = -\frac{1}{2}\beta_0(h-2\eta) - \frac{\beta_0}{1+R}(\delta_\gamma - \delta_b - \delta_{x_e}) - \frac{\beta_0}{3}\int\left(1 + \frac{\mathcal{A}}{4}\right)\theta_\gamma d\tau + C_\gamma , \quad (6.203)$$

where C_γ is a constant of integration, to be set with the initial condition, and β_0 is the initial velocity of the photon-baryon plasma. Another result that can be obtained, integrating (6.192), is the evolution of CDM

$$a\chi_c = -\frac{1}{2}\beta_c^{\text{today}}(h-2\eta) + C_c . \quad (6.204)$$

As discussed before, we do not specify the behaviour of the dark sector at early times. Hence, we do not use this equation. We solve the system instead using the total vorticity (6.193) and we then obtain the vorticity of the dark sector subtracting the other components.

6.8 Initial conditions

We need to find the appropriate initial conditions for the system of scalar and vector modes developed in Sections 6.7.2 and 6.7.3. We will consider the most general initial condition and then study the physical restrictions that we must impose. For $\beta = 0$ our system reproduces the standard cosmology. This case has been studied in detail in Section 3.7 and the relevant modes, i.e. one adiabatic and four isocurvature, have been identified. In this new setup, the presence of an external source gives rise to the existence of a new “mode” of the system, in the sense that we have a non-trivial evolution even if the usual adiabatic and isocurvature modes are absent. First, we will identify this particular solution, setting to zero the other modes of the

system. Note that the external sources only contain variables that evolve according to standard Λ CDM, so for these variables only adiabatic initial conditions are considered. After identifying the effect of the sources, the most general perturbation can be constructed adding to the sourced mode the adiabatic and isocurvature modes. Finally, we must analyze what physical requirements constrain our choice of initial conditions. In particular, we impose that neutrinos and photons, being tightly coupled in the very early Universe, share a common initial velocity. Every other initial condition that is not fixed by this condition is set to zero. This programme is carried out in detail in the next sections.

6.8.1 Scalar modes

Adopting the notation of Section 3.7, we will look for regular super-Hubble solutions and expand every cosmological variable as

$$\delta_\gamma^I = D_{\delta_\gamma}^{(0)} + D_{\delta_\gamma}^{(0)}\tau + D_{\delta_\gamma}^{(1)}\tau^2 + D_{\delta_\gamma}^{(3)}\tau^3 + \dots \quad (6.205)$$

We assume that the mode is in the tight-coupling regime and in the radiation-dominated era. The results for the sourced mode can be obtained setting to zero the initial conditions for η^I , \dot{h}^I , δ_γ^I , δ_b^I and θ_γ^I . In addition, we must use the series solution of Section 3.7 for the adiabatic mode of the real parts with

$$\eta^R(\tau = 0) = \frac{4\mathcal{R}_\nu + 15}{4\mathcal{R}_\nu + 10}, \quad (6.206)$$

where we have set $\mathcal{R}_k = 1$. Plugging all these expansions in the system and solving it order by order in τ , we get the coefficients $D^{(n)}$ for the new sourced mode.

$$D_{\delta_\gamma}^{(0)} = 0, \quad D_{\delta_\gamma}^{(1)} = \frac{4\beta_0 k (4\mathcal{R}_\nu + 15)}{3(2\mathcal{R}_\nu + 5)}, \quad (6.207a)$$

$$D_{\delta_\nu}^{(0)} = 0, \quad D_{\delta_\nu}^{(1)} = \frac{4\beta_0 k (\mathcal{R}_\nu - 1)(4\mathcal{R}_\nu + 15)}{3\mathcal{R}_\nu(2\mathcal{R}_\nu + 5)}, \quad (6.207b)$$

$$D_{\delta_b}^{(0)} = 0, \quad D_{\delta_b}^{(1)} = \frac{\beta_0 k (4\mathcal{R}_\nu + 15)}{2\mathcal{R}_\nu + 5}, \quad (6.207c)$$

$$D_{\delta}^{(0)} = 0, \quad D_{\delta}^{(1)} = 0. \quad (6.207d)$$

$$D_{\delta_\gamma}^{(2)} = -\frac{H_0 \sqrt{S_{\gamma\nu}} \mathcal{R}_b \beta_0 k (\mathcal{R}_\nu - 3)(4\mathcal{R}_\nu + 15)}{4(\mathcal{R}_\nu - 1)(2\mathcal{R}_\nu + 5)}, \quad (6.208a)$$

$$D_{\delta_\nu}^{(2)} = -\frac{H_0 \sqrt{S_{\gamma\nu}} \mathcal{R}_b \beta_0 k (4\mathcal{R}_\nu + 15)}{4(2\mathcal{R}_\nu + 5)}, \quad (6.208b)$$

$$D_{\delta_b}^{(2)} = -\frac{3H_0 \sqrt{S_{\gamma\nu}} \mathcal{R}_b \beta_0 k (\mathcal{R}_\nu - 3)(4\mathcal{R}_\nu + 15)}{16(\mathcal{R}_\nu - 1)(2\mathcal{R}_\nu + 5)}, \quad (6.208c)$$

$$D_{\delta}^{(2)} = \frac{H_0 \sqrt{S_{\gamma\nu}} \mathcal{R}_b \beta_0 k (4\mathcal{R}_\nu + 15)}{4(2\mathcal{R}_\nu + 5)}. \quad (6.208d)$$

$$D_{\delta_\gamma}^{(3)} = \frac{H_0^2 S_{\gamma\nu} \mathcal{R}_b \beta_0 k (4\mathcal{R}_\nu + 15) (5\mathcal{R}_\nu \mathcal{R}_{bc} (\mathcal{R}_\nu - 1) - 3\mathcal{R}_b (\mathcal{R}_\nu - 6))}{60 (\mathcal{R}_\nu - 1)^2 (2\mathcal{R}_\nu + 5)} + \frac{4\beta_0 k^3 (44\mathcal{R}_\nu + 65)}{45 (4\mathcal{R}_\nu + 5) (2\mathcal{R}_\nu + 5)}, \quad (6.209a)$$

$$D_{\delta_\nu}^{(3)} = -\frac{H_0^2 S_{\gamma\nu} \mathcal{R}_b \beta_0 k (4\mathcal{R}_\nu + 15) (3\mathcal{R}_b - 5\mathcal{R}_{bc} (\mathcal{R}_\nu - 1))}{60 (\mathcal{R}_\nu - 1) (2\mathcal{R}_\nu + 5)} + \frac{2\beta_0 k^3 (32\mathcal{R}_\nu + 45)}{45 \mathcal{R}_\nu (2\mathcal{R}_\nu + 5)}, \quad (6.209b)$$

$$D_{\delta}^{(3)} = \frac{3H_0^2 S_{\gamma\nu} \mathcal{R}_b \beta_0 k (4\mathcal{R}_\nu + 15) (2\mathcal{R}_b - 5\mathcal{R}_{bc} (\mathcal{R}_\nu - 1))}{80 (\mathcal{R}_\nu - 1) (2\mathcal{R}_\nu + 5)} + \frac{\beta_0 k^3 (80\mathcal{R}_\nu^2 + 392\mathcal{R}_\nu + 545)}{90 (4\mathcal{R}_\nu + 5) (2\mathcal{R}_\nu + 5)}. \quad (6.209c)$$

$$D_{\theta_\gamma}^{(0)} = 0, \quad D_{\theta_\gamma}^{(1)} = 0, \quad (6.210a)$$

$$D_{\theta_\nu}^{(0)} = \frac{\beta_0 k (4\mathcal{R}_\nu + 15)}{\mathcal{R}_\nu (2\mathcal{R}_\nu + 5)}, \quad D_{\theta_\nu}^{(1)} = 0, \quad (6.210b)$$

$$D_{\theta}^{(0)} = 0, \quad D_{\theta}^{(1)} = 0. \quad (6.210c)$$

$$D_{\theta_\gamma}^{(2)} = -\frac{5\beta_0 k^3}{6(2\mathcal{R}_\nu + 5)}, \quad (6.211a)$$

$$D_{\theta_\nu}^{(2)} = -\frac{\beta_0 k^3 (44\mathcal{R}_\nu^2 + 151\mathcal{R}_\nu + 135)}{6\mathcal{R}_\nu (4\mathcal{R}_\nu + 5) (2\mathcal{R}_\nu + 5)}, \quad (6.211b)$$

$$D_{\theta}^{(2)} = -\frac{\beta_0 k^3 (\mathcal{R}_\nu + 2) (4\mathcal{R}_\nu + 15)}{3(4\mathcal{R}_\nu + 5) (2\mathcal{R}_\nu + 5)}. \quad (6.211c)$$

$$D_{\sigma_\nu}^{(0)} = 0, \quad (6.212a)$$

$$D_{\sigma_\nu}^{(1)} = \frac{2\beta_0 k (\mathcal{R}_\nu + 2) (4\mathcal{R}_\nu + 15)}{3\mathcal{R}_\nu (4\mathcal{R}_\nu + 5) (2\mathcal{R}_\nu + 5)}, \quad (6.212b)$$

$$D_{\sigma_\nu}^{(2)} = \frac{2H_0 \sqrt{S_{\gamma\nu}} \mathcal{R}_{bc} \beta_0 k (\mathcal{R}_\nu + 2)}{(4\mathcal{R}_\nu + 5) (2\mathcal{R}_\nu + 5)}, \quad (6.212c)$$

$$D_{\sigma_\nu}^{(3)} = \frac{H_0^2 S_{\gamma\nu} \mathcal{R}_{bc}^2 \beta_0 k (\mathcal{R}_\nu + 2) (4\mathcal{R}_\nu - 45)}{6(2\mathcal{R}_\nu + 15) (4\mathcal{R}_\nu + 5) (2\mathcal{R}_\nu + 5)} - \frac{\beta_0 k^3 (32\mathcal{R}_\nu^4 + 224\mathcal{R}_\nu^3 + 914\mathcal{R}_\nu^2 + 2097\mathcal{R}_\nu + 1620)}{54\mathcal{R}_\nu (2\mathcal{R}_\nu + 15) (4\mathcal{R}_\nu + 5) (2\mathcal{R}_\nu + 5)}. \quad (6.212d)$$

$$D_{\eta}^{(0)} = 0, \quad D_{\eta}^{(1)} = -\frac{2\beta_0 k (\mathcal{R}_\nu + 2) (4\mathcal{R}_\nu + 15)}{3(4\mathcal{R}_\nu + 5) (2\mathcal{R}_\nu + 5)}, \quad (6.213a)$$

$$D_h^{(0)} = D_h^{(0)}, \quad D_h^{(1)} = 0. \quad (6.213b)$$

$$D_\eta^{(2)} = \frac{H_0 \sqrt{S_{\gamma\nu}} \beta_0 k (-\mathcal{R}_b (4\mathcal{R}_\nu + 5)(4\mathcal{R}_\nu + 15) + 40\mathcal{R}_{bc}(\mathcal{R}_\nu + 2))}{16(4\mathcal{R}_\nu + 5)(2\mathcal{R}_\nu + 5)}, \quad (6.214a)$$

$$D_h^{(2)} = \frac{3H_0 \sqrt{S_{\gamma\nu}} \mathcal{R}_b \beta_0 k (4\mathcal{R}_\nu + 15)}{8(2\mathcal{R}_\nu + 5)}. \quad (6.214b)$$

$$\begin{aligned} D_\eta^{(3)} = & -\frac{H_0^2 S_{\gamma\nu} \mathcal{R}_b^2 \beta_0 k (4\mathcal{R}_\nu + 15)}{80(\mathcal{R}_\nu - 1)(2\mathcal{R}_\nu + 5)} + \frac{H_0^2 S_{\gamma\nu} \mathcal{R}_b \mathcal{R}_{bc} \beta_0 k (4\mathcal{R}_\nu + 15)}{48(2\mathcal{R}_\nu + 5)} \\ & + \frac{5H_0^2 S_{\gamma\nu} \mathcal{R}_{bc}^2 \beta_0 k (\mathcal{R}_\nu + 2)(4\mathcal{R}_\nu - 45)}{24(2\mathcal{R}_\nu + 15)(4\mathcal{R}_\nu + 5)(2\mathcal{R}_\nu + 5)} \\ & + \frac{\beta_0 k^3 (-80\mathcal{R}_\nu^3 + 568\mathcal{R}_\nu^2 + 4525\mathcal{R}_\nu + 4950)}{270(2\mathcal{R}_\nu + 15)(4\mathcal{R}_\nu + 5)(2\mathcal{R}_\nu + 5)}, \end{aligned} \quad (6.215a)$$

$$\begin{aligned} D_h^{(3)} = & \frac{H_0^2 S_{\gamma\nu} \mathcal{R}_b \beta_0 k (4\mathcal{R}_\nu + 15)(3\mathcal{R}_b - 5\mathcal{R}_{bc}(\mathcal{R}_\nu - 1))}{40(\mathcal{R}_\nu - 1)(2\mathcal{R}_\nu + 5)} \\ & - \frac{\beta_0 k^3 (80\mathcal{R}_\nu^2 + 528\mathcal{R}_\nu + 655)}{90(4\mathcal{R}_\nu + 5)(2\mathcal{R}_\nu + 5)}. \end{aligned} \quad (6.215b)$$

Once we have the new behaviour of the system, we need to evaluate the assignment of initial conditions. It seems reasonable to give zero initial values to our modification but there is one further physical requirement that we must impose. As mentioned above, if neutrinos and photons were in thermal contact in the primeval Universe, it is physically sensible to impose that they shared the same velocity

$$\theta_\nu(\tau = 0) = \theta_\gamma(\tau = 0) = \theta_\gamma^{(0)}. \quad (6.216)$$

In the standard scenario this leads to $\theta_\gamma^{(0)} = 0$ and to the absence of neutrino velocity isocurvature modes. However, in our case, if we consider a neutrino isocurvature velocity mode on top of the sourced mode, upon imposing this restriction we get

$$\theta_\gamma^{(0)} = \frac{4\mathcal{R}_\nu + 15}{2\mathcal{R}_\nu + 5} \beta_0 k. \quad (6.217)$$

In order to obtain the correct initial conditions, we must consider the combination of the sourced mode with a neutrino isocurvature velocity mode with the previous

initial condition. The final results are

$$\delta_Y^I = \delta_v^I = \delta_b^I = \delta^I = 0 + \mathcal{O}(\tau^3), \quad (6.218a)$$

$$\theta_Y^I = \frac{\beta_0 k (4\mathcal{R}_v + 15)}{2\mathcal{R}_v + 5} + \frac{3H_0 \sqrt{S_{\gamma v}} \mathcal{R}_b \beta_0 k (4\mathcal{R}_v + 15)}{4(\mathcal{R}_v - 1)(2\mathcal{R}_v + 5)} \tau$$

$$+ \frac{3H_0^2 S_{\gamma v} \mathcal{R}_b \beta_0 k (4\mathcal{R}_v + 15) ((\mathcal{R}_v - 1)\mathcal{R}_{bc} + 3\mathcal{R}_b)}{16(\mathcal{R}_v - 1)^2 (2\mathcal{R}_v + 5)} \tau^2$$

$$- \frac{2\beta_0 k^3 (\mathcal{R}_v + 5)}{3(2\mathcal{R}_v + 5)} \tau^2 + \mathcal{O}(\tau^3), \quad (6.218b)$$

$$\theta_v^I = \frac{\beta_0 k (4\mathcal{R}_v + 15)}{2\mathcal{R}_v + 5} - \frac{\beta_0 k^3 (8\mathcal{R}_v^2 + 62\mathcal{R}_v + 95)}{3(4\mathcal{R}_v + 5)(2\mathcal{R}_v + 5)} \tau^2 + \mathcal{O}(\tau^3), \quad (6.218c)$$

$$\theta^I = -\frac{\mathcal{R}_v \beta_0 k^3 (4\mathcal{R}_v + 15)}{(4\mathcal{R}_v + 5)(2\mathcal{R}_v + 5)} \tau^2 + \mathcal{O}(\tau^3), \quad (6.218d)$$

$$\sigma_v^I = \frac{2\beta_0 k (4\mathcal{R}_v + 15)}{(4\mathcal{R}_v + 5)(2\mathcal{R}_v + 5)} \tau + \frac{6H_0 \sqrt{S_{\gamma v}} \mathcal{R}_v \mathcal{R}_{bc} \beta_0 k}{(4\mathcal{R}_v + 5)(2\mathcal{R}_v + 5)} \tau^2 + \mathcal{O}(\tau^3), \quad (6.218e)$$

$$h^I = 0 + \mathcal{O}(\tau^3), \quad (6.218f)$$

$$\eta^I = -\frac{2\mathcal{R}_v \beta_0 k (4\mathcal{R}_v + 15)}{(4\mathcal{R}_v + 5)(2\mathcal{R}_v + 5)} \tau + \frac{15H_0 \sqrt{S_{\gamma v}} \mathcal{R}_v \mathcal{R}_{bc} \beta_0 k}{2(4\mathcal{R}_v + 5)(2\mathcal{R}_v + 5)} \tau^2 + \mathcal{O}(\tau^3). \quad (6.218g)$$

6.8.2 Vector modes

Considering adiabatic perturbations in the scalar contributions, during TC and deep in the radiation era, the super-Hubble evolution is

$$D_{\chi_Y}^{(0)} = D_{\chi_Y}^{(0)}, \quad D_{\chi_Y}^{(1)} = \frac{3D_{\chi_Y}^{(0)} H_0 \sqrt{S_{\gamma v}} \mathcal{R}_b}{4(\mathcal{R}_v - 1)}, \quad (6.219a)$$

$$D_{\chi_v}^{(0)} = -\frac{\beta_0 (4\mathcal{R}_v + 15)}{2(2\mathcal{R}_v + 5)}, \quad D_{\chi_v}^{(1)} = 0, \quad (6.219b)$$

$$D_{\chi}^{(0)} = 0, \quad D_{\chi}^{(1)} = 0, \quad (6.219c)$$

$$D_{\chi_Y}^{(2)} = \frac{3D_{\chi_Y}^{(0)} H_0^2 S_{\gamma v} \mathcal{R}_b (3\mathcal{R}_b + \mathcal{R}_{bc} (\mathcal{R}_v - 1))}{16(\mathcal{R}_v - 1)^2} - \frac{\beta_0 k^2 (8\mathcal{R}_v + 25)}{12(2\mathcal{R}_v + 5)}, \quad (6.220a)$$

$$D_{\chi_v}^{(2)} = -\frac{\beta_0 k^2 (8\mathcal{R}_v + 25)}{12(2\mathcal{R}_v + 5)}, \quad (6.220b)$$

$$D_{\chi}^{(2)} = 0, \quad (6.220c)$$

$$D_{\chi}^{(3)} = 0, \quad (6.221a)$$

$$D_{\chi}^{(4)} = \frac{25\beta_0 k^4}{8(8\mathcal{R}_v + 45)(2\mathcal{R}_v + 5)}, \quad (6.221b)$$

$$D_{\pi_\nu}^{(0)} = 0, \quad (6.222a)$$

$$D_{\pi_\nu}^{(1)} = 0, \quad (6.222b)$$

$$D_{\pi_\nu}^{(2)} = 0, \quad (6.222c)$$

$$D_{\pi_\nu}^{(3)} = \frac{\beta_0 k^2 (32\mathcal{R}_v^2 + 268\mathcal{R}_v + 375)}{54(8\mathcal{R}_v + 45)(2\mathcal{R}_v + 5)}, \quad (6.222d)$$

$$D_{S+\dot{F}}^{(0)} = 0, \quad (6.223a)$$

$$D_{S+\dot{F}}^{(1)} = 0, \quad (6.223b)$$

$$D_{S+\dot{F}}^{(2)} = \frac{25\beta_0 k^2}{(8\mathcal{R}_v + 45)(2\mathcal{R}_v + 5)}. \quad (6.223c)$$

Again, imposing the physical requirement that photons and neutrinos had the same velocity in the very early Universe, we are led to

$$D_{\chi_\gamma}^{(0)} = -\frac{\beta_0(4\mathcal{R}_v + 15)}{2(2\mathcal{R}_v + 5)}. \quad (6.224)$$

The initial conditions provided for the numerical integration are

$$\begin{aligned} \chi_\gamma = & -\frac{\beta_0(4\mathcal{R}_v + 15)}{2(2\mathcal{R}_v + 5)} - \frac{3H_0\sqrt{S_{\gamma\nu}}\mathcal{R}_b\beta_0(4\mathcal{R}_v + 15)}{8(\mathcal{R}_v - 1)(2\mathcal{R}_v + 5)}\tau, \\ & - \frac{3H_0^2 S_{\gamma\nu}\mathcal{R}_b\beta_0(4\mathcal{R}_v + 15)(\mathcal{R}_{bc}(\mathcal{R}_v - 1) + 3\mathcal{R}_b)}{32(\mathcal{R}_v - 1)^2(2\mathcal{R}_v + 5)}\tau^2 \\ & - \frac{\beta_0 k^2(8\mathcal{R}_v + 25)}{12(2\mathcal{R}_v + 5)}\tau^2 + \mathcal{O}(\tau^3), \end{aligned} \quad (6.225a)$$

$$\chi_\nu = -\frac{\beta_0(4\mathcal{R}_v + 15)}{2(2\mathcal{R}_v + 5)} - \frac{\beta_0 k^2(8\mathcal{R}_v + 25)}{12(2\mathcal{R}_v + 5)}\tau^2 + \mathcal{O}(\tau^3), \quad (6.225b)$$

$$\chi = \frac{25\beta_0 k^4}{8(8\mathcal{R}_v + 45)(2\mathcal{R}_v + 5)}\tau^4 + \mathcal{O}(\tau^5), \quad (6.225c)$$

$$\pi_\nu^\vee = \frac{\beta_0 k^2(4\mathcal{R}_v(8\mathcal{R}_v + 67) + 375)}{54(8\mathcal{R}_v + 45)(2\mathcal{R}_v + 5)}\tau^3 + \mathcal{O}(\tau^4), \quad (6.225d)$$

$$S + \dot{F} = \frac{25\beta_0 k^2}{(8\mathcal{R}_v + 45)(2\mathcal{R}_v + 5)}\tau^2 + \mathcal{O}(\tau^3). \quad (6.225e)$$

6.9 Numerical implementation and first results

6.9.1 Implementation details

The first step is the integration of the background and the determination of the bulk velocities, that will be common to any subsequent computation. We proceed as follows.

- I) The background and the thermodynamic variables follow a Λ CDM behaviour. We compute them using CLASS [BLT11] with the base Λ CDM parameters [Agh+18], that are summarized in Table 1.1.
- II) This information is used to compute the bulk velocities. We integrate (6.156a), (6.156b), (6.156c), and apply the center of mass constraint (6.157) to infer the momentum of the dark sector. At very early times, the TC solution (6.160) is used and then joined smoothly with the exact evolution.

Once we have these results, we can solve our modified evolution for the perturbations. In particular, we evolve the simplified system of Section 6.7. The main ingredients for the integration of the scalar modes are summarized below.

- I) The real parts of the perturbations, labelled with R , follow the standard evolution and act as external sources in our system. We use CLASS to precompute these sources, with adiabatic initial conditions.
- II) Once the sources have been computed, we solve the system for the imaginary parts, labelled with I . The system consists of (6.170, 6.171, 6.172, 6.175, 6.176) and a neutrino contribution equal to (6.170) but without collisions.
- III) The appropriate initial conditions for the system are discussed in Section 6.8. We use the expressions (6.218), starting the integration at the same time as CLASS.
- IV) To take into account perturbed recombination, see Section 6.7.2, we also integrate (6.180). Each mode starts with initial conditions $\delta_{x_e}(\tau = \tau_{\text{ini}}) = 0$. We use the full ionization history $x_e(\tau)$ provided by the thermodynamics module in CLASS, computed using RECFAST [SSS00].
- V) We need two approximation schemes to follow the numerical evolution, the so-called tight-coupling approximation and radiation-streaming approximation. The relevant equations can be found in Section 6.7.2. Both are switched on and off using the same criteria as CLASS.

The recipe for the integration of the vector modes is similar.

- I) The scalar perturbations evolve according to standard Λ CDM and act as external sources for the vector modes. We use CLASS to precompute these sources.
- II) The system to be integrated consists of (6.189, 6.191, 6.193, 6.195) and a neutrino contribution equal to (6.189) but without collisions.
- III) The initial conditions are described in Section 6.8.2 and correspond to (6.225).
- IV) The relevant TCA and RSA equations are collected in Section 6.7.3.

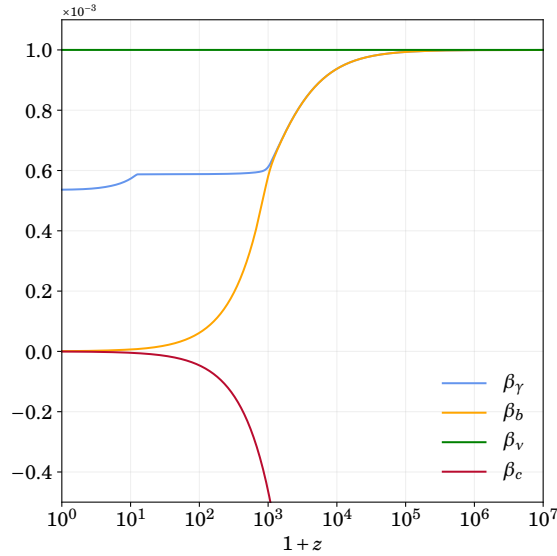


Figure 6.1: Time evolution of the bulk velocities for the different components. The dark matter velocity is obtained enforcing the cosmic center of mass condition (6.135). Massless neutrinos behave as an uncoupled ultrarelativistic species throughout the evolution and maintain a constant velocity. The photon-baryon plasma behaves as a single fluid, either matter- or radiation-like, until decoupling $z_{\text{dec}} \simeq 1090$. Around $z \simeq 11$ there is a small effect in the photon velocity due to reionization.

6.9.2 Time evolution and transfer functions

The time evolution of the bulk velocities for the different components is represented in Figure 6.1. All the components in the visible sector start their evolution with the same velocity in the center of mass frame, and its momentum is counterbalanced by the dark sector. The velocity of the neutrinos, since we are neglecting their masses, is always constant. The velocity of the photon-baryon plasma is constant deep in the radiation-dominated era. Once the baryonic contribution to the energy density becomes important, the plasma velocity drops down as a^{-1} , see (6.160), until decoupling. After decoupling, the velocity of the baryons keeps scaling as a^{-1} , like CDM, while the photons keep a constant velocity, with a slight late-time effect from reionization. Today, the cosmic center of mass, i.e. the \mathcal{O} frame, almost coincides with the matter frame but photons and neutrinos possess a sizeable velocity.

Before turning to the evolution of the perturbations, we must clarify a few points concerning our choice of fluid variables. In particular, it is important to relate the intermediate variables we have used with the physical velocities. The velocity that would appear in the energy-momentum tensor of a fluid (2.9) is the velocity of a frame in which the energy flux (or momentum density), i.e. the component T_{0i} , is zero [LL59]. Using the boost-transformation properties (6.38b) we can obtain an equation for the physical velocity U^i of the fluid

$$\bar{\gamma} \bar{\mathcal{P}}_j^i \left(Q^j - U_k \Pi^{kj} \right) - \bar{\gamma}^2 U^i \left(\rho + P - Q^j U_j \right) = 0, \quad (6.226)$$

where

$$\bar{\gamma} \equiv (1 - U^2)^{-1/2}, \quad \bar{\mathcal{P}}_j^i \equiv \delta_j^i + (\bar{\gamma} - 1) \frac{U^i U_j}{U^2}. \quad (6.227)$$

Working to first order in β and in cosmological perturbations we have

$$U^i = \beta^i + \frac{1}{\bar{\rho} + \bar{P}} \left(\delta Q^i - \beta^k \delta \Pi_k^i - \beta^i (\delta \rho + \delta P) \right). \quad (6.228)$$

The physical velocity has two parts, a bulk velocity β_i plus a peculiar contribution δu^i . For ultrarelativistic particles, the peculiar velocity can be expressed in terms of our previously defined variables (6.65) as

$$\delta u^i = \delta v^i - \frac{3}{4} \beta^k \pi_k^i - \beta^i \delta. \quad (6.229)$$

It can be splitted into a scalar and a vector part

$$\delta u^i = -\frac{i \hat{k}^i}{k} \vartheta + \zeta^i, \quad (6.230)$$

so that we have

$$\vartheta = \theta - i(\boldsymbol{\beta} \cdot \mathbf{k})(\delta - \sigma), \quad (6.231a)$$

$$\zeta^\pm = \chi^\pm - (\boldsymbol{\beta} \cdot \hat{\mathbf{e}}_\pm) \left(\delta + \frac{1}{2} \sigma \right). \quad (6.231b)$$

For non-relativistic species, the results are identical setting $\sigma = 0$. It is worth noting that this is not the only physically sensible definition of the velocity of a fluid. It can alternatively be defined as the velocity of the frame in which the flux of particles (6.38f) is zero [Wei72]. Both definitions agree for non-relativistic fluids if the number of particles is conserved.

Finally, we present the transfer functions evaluated today for a range of k and their time evolution for a fixed value $k = 10^{-2} \text{ Mpc}^{-1}$, as a sample from the full results for the evolution of the perturbations. All the results concerning cosmological perturbations are computed in the synchronous gauge and then transformed back to the Newtonian gauge, that can be more easily interpreted in the Newtonian limit [Maa98; EEM01]. Figures 6.2, 6.3, and 6.4 contain the density and velocity of CDM, baryons and the total fluid. Figure 6.5 contains the metric variables, i.e. Newtonian potentials and vector metric perturbations. The quantities with an R superscript follow the standard evolution and are computed using CLASS with the *Planck* 2018 [Agh+18] input values. The modified contributions, with an I superscript, remain smaller than the standard ones for most values of k , but not as small as could be expected. The difference at scales of 0.1 Mpc^{-1} is just one order of magnitude, instead of three as could be naively anticipated from $\beta_0 = 10^{-3}$, and the modifications could grow even larger above the non-linearity scale.

6.10 Observables

6.10.1 Power spectra

The distribution and redshift of galaxies give us information about density perturbations and peculiar velocities. This class of observables, related to the clustering

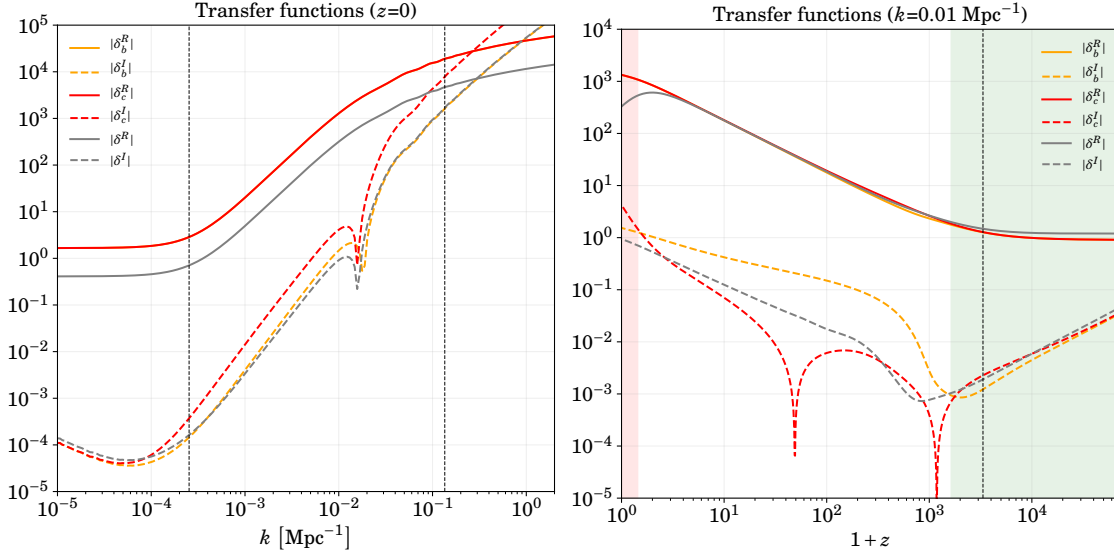


Figure 6.2: Transfer functions, with initial curvature perturbation normalized to one, in the Newtonian gauge. Both panels represent the evolution of the density contrast, both the standard and our modification. The imaginary parts are proportional to β_0 . We show the results for $\beta_0 = 10^{-3}$. (Left) The vertical line indicates the super-Hubble and non-linearity scales, respectively. (Right) The vertical line marks the horizon crossing. In the red and green shaded regions the RSA and TCA, respectively, are switched on.

of matter, contains information about the present distribution of CDM and baryons, as well as their evolution at very late times. The results of Section 6.9 allow us to predict new features in these observables arising from the non-comoving scenario.

The main LSS observable is the matter power spectrum, but our modification does not leave a first order imprint on it. On general grounds, if we consider a cosmological quantity g splitted as in (6.169), we have

$$|g(\tau, \mathbf{k})|^2 = |g^R(\tau, \mathbf{k})|^2 + \mathcal{O}(\beta^2), \quad (6.232)$$

i.e. the Λ CDM result. However, in the cross-correlation between two cosmological perturbations g_1 and g_2 we get a first order dipolar contribution

$$g_1 g_2^* = g_1^R g_2^{R*} + i(\hat{\beta} \cdot \hat{k}) \left(g_1^I g_2^{R*} - g_1^R g_2^{I*} \right) + \mathcal{O}(\beta^2). \quad (6.233)$$

Every cross-correlation between cosmological quantities contains a dipole modification with this structure. This effect could be observed in the future in the cross-correlations between matter density and velocity [Teg+04], as the precision of the surveys increases. It is conceivable that this effect could appear in cross-correlations between baryon and CDM densities as well, even though a thorough analysis using lensing information would be in order. Finally, the generation of vorticity, purely decaying in Λ CDM, is another distinctive feature of our model.

We stick to the following conventions for the definition of the spectra. In the

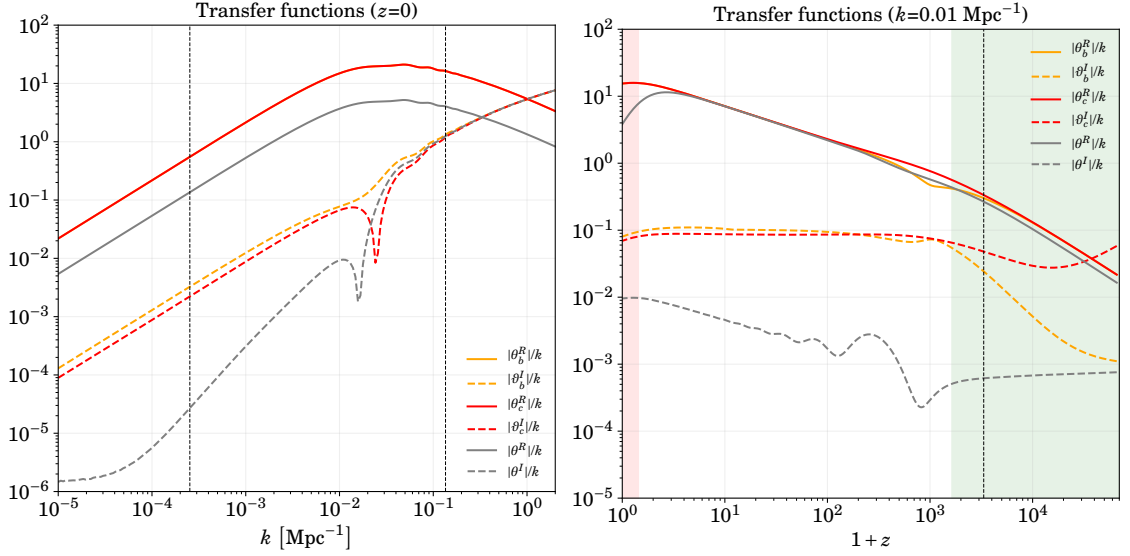


Figure 6.3: Transfer functions, with initial curvature perturbation normalized to one, in the Newtonian gauge. Both panels represent the evolution of the velocity divergence, where the imaginary parts have been redefined according to (6.231). The imaginary parts are proportional to β_0 . We show the results for $\beta_0 = 10^{-3}$. (Left) The vertical line indicates the super-Hubble and non-linearity scales, respectively. (Right) The vertical line marks the horizon crossing. In the red and green shaded regions the RSA and TCA, respectively, are switched on.

first place, we define the spectrum of a single variable as

$$\langle \delta(z, \mathbf{k}) \delta^*(z, \mathbf{k}') \rangle \equiv (2\pi)^3 \delta(\mathbf{k} - \mathbf{k}') P_{\delta\delta}(z, k) \quad (6.234)$$

$$= (2\pi)^3 \delta(\mathbf{k} - \mathbf{k}') |\delta^R(z, k)|^2 \frac{2\pi^2}{k^3} \mathcal{P}_{\mathcal{R}}(k) + \mathcal{O}(\beta^2), \quad (6.235)$$

where $\delta^R(z, k)$ is the real part of the transfer function and $\mathcal{P}_{\mathcal{R}}(k)$ is the usual nearly scale-invariant curvature spectrum. For the cross-correlations we define

$$\text{Re} \langle \delta(z, \mathbf{k}) \theta^*(z, \mathbf{k}') \rangle \equiv (2\pi)^3 \delta(\mathbf{k} - \mathbf{k}') P_{\delta\theta}^R(z, k) \quad (6.236)$$

$$= (2\pi)^3 \delta(\mathbf{k} - \mathbf{k}') \delta^R(z, k) \theta^R(z, k) \frac{2\pi^2}{k^3} \mathcal{P}_{\mathcal{R}}(k) + \mathcal{O}(\beta^2), \quad (6.237)$$

$$\text{Im} \langle \delta(z, \mathbf{k}) \theta^*(z, \mathbf{k}') \rangle \equiv (2\pi)^3 \delta(\mathbf{k} - \mathbf{k}') (\hat{\beta} \cdot \hat{k}) P_{\delta\theta}^I(z, k) \quad (6.238)$$

$$= (2\pi)^3 \delta(\mathbf{k} - \mathbf{k}') (\hat{\beta} \cdot \hat{k}) \times \left(\delta^I(z, k) \theta^R(z, k) - \delta^R(z, k) \theta^I(z, k) \right) \times \frac{2\pi^2}{k^3} \mathcal{P}_{\mathcal{R}}(k) + \mathcal{O}(\beta^2). \quad (6.239)$$

The vorticity spectrum is defined in a similar way, according to definition (6.231),

$$\langle \zeta(z, \mathbf{k}) \cdot \zeta^*(z, \mathbf{k}') \rangle \equiv (2\pi)^3 \delta(\mathbf{k} - \mathbf{k}') (1 - (\hat{\beta} \cdot \hat{k})^2) P_{\zeta\zeta}(z, k) \quad (6.240)$$

$$= (2\pi)^3 \delta(\mathbf{k} - \mathbf{k}') (1 - (\hat{\beta} \cdot \hat{k})^2) \times |\zeta(z, k)|^2 \frac{2\pi^2}{k^3} \mathcal{P}_{\mathcal{R}}(k) + \mathcal{O}(\beta^3), \quad (6.241)$$

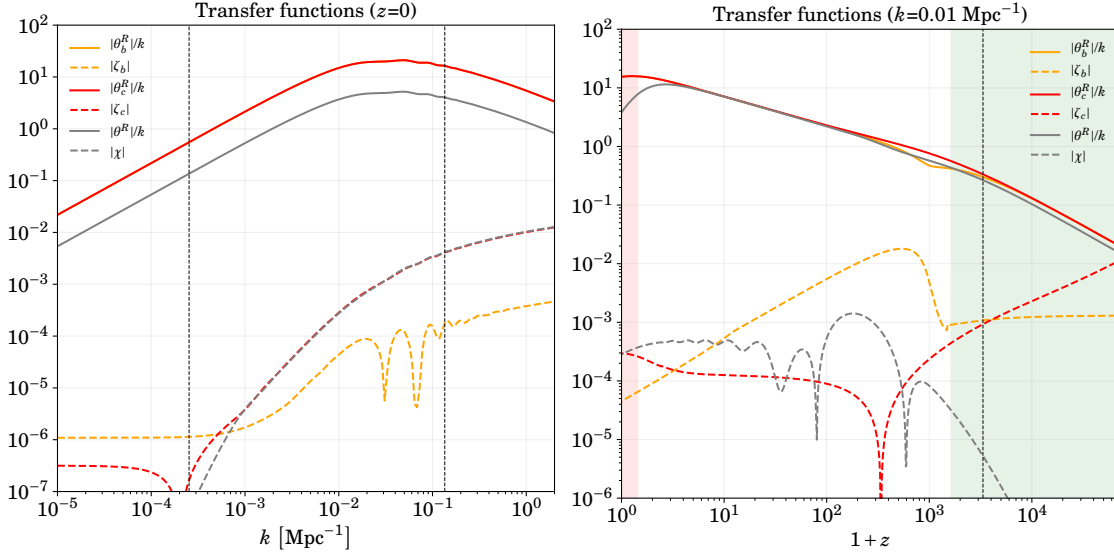


Figure 6.4: Transfer functions, with initial curvature perturbation normalized to one, in the Newtonian gauge. Both panels represent the evolution of the vorticity, compared with the velocity divergence. Again, the vorticity has been redefined according to (6.231). The vorticity is proportional to β_0 . We show the results for $\beta_0 = 10^{-3}$. (Left) The vertical line indicates the super-Hubble and non-linearity scales, respectively. (Right) The vertical line marks the horizon crossing. In the red and green shaded regions the RSA and TCA, respectively, are switched on.

The results for the velocity spectrum and the density cross-correlation for CDM are represented in Figure 6.6. In addition to this information, the velocity-density cross-correlation induced by our modification shows a distinctive dipolar pattern. In the same way, the vorticity autocorrelation, even though its amplitude is very small, deviates from statistical isotropy, with a quadrupole term in addition to the monopole. Figure 6.7 shows the cross-correlation between the matter density and the lensing potential, defined as $\Psi_W \equiv \Phi + \Psi$. This combination is observable using weak-lensing information [Dur08; SUR05]. Again, our additional contribution becomes important at small scales, being just one order of magnitude below the standard result at scales $k = 0.1 \text{ Mpc}^{-1}$ instead of three as might be inferred from $\beta_0 = 10^{-3}$. Both vorticity and deviations from statistical isotropy are absent in standard Λ CDM. Their presence, with the structure proposed, is a testable effect that could be used to confirm, or disprove, the non-comoving scenario.

As we have seen, in our modified setting, velocity spectra are the most easily accessible LSS observables that show significant deviations. Peculiar velocity surveys provide useful complementary information but currently are not competitive with other cosmological observables to constrain standard cosmology [Teg+04; Kod+14; Joh+14].

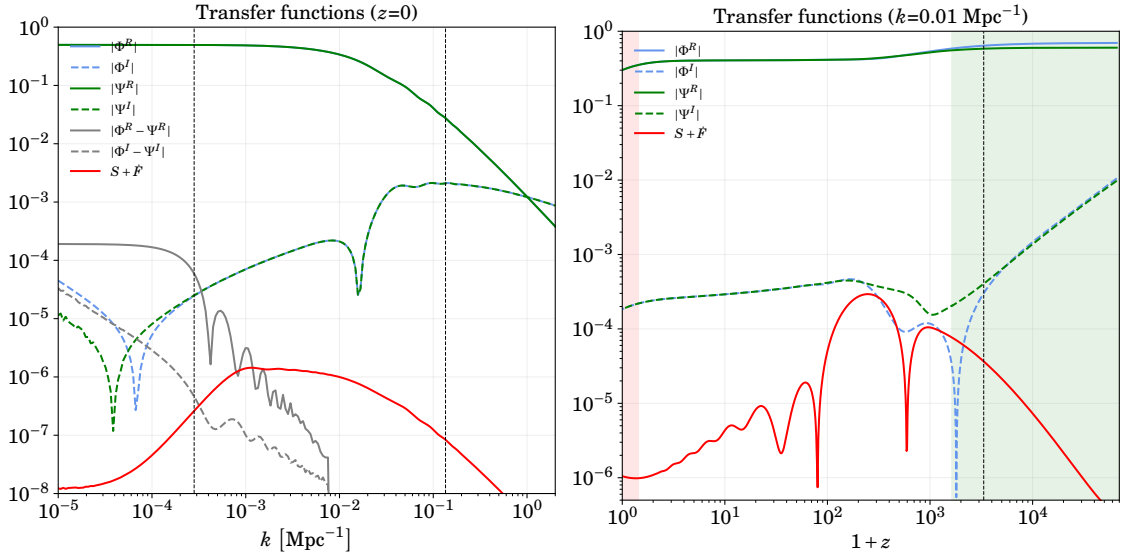


Figure 6.5: Transfer functions, with initial curvature perturbation normalized to one, in the Newtonian gauge. Both panels represent the evolution of the Newtonian potentials, their difference and the vector metric perturbation. The imaginary parts and the vector modes are proportional to β_0 . We show the results for $\beta_0 = 10^{-3}$. (Left) The vertical line indicates the super-Hubble and non-linearity scales, respectively. The sharp drop in the difference between the Newtonian potentials at small scales is a consequence of the RSA. On those scales we are setting the shear of ultrarelativistic species to zero, since it has a negligible impact in our observables. (Right) The vertical line marks the horizon crossing. In the red and green shaded regions the RSA and TCA, respectively, are switched on.

6.10.2 CMB temperature anisotropy

Temperature perturbation

Once we have constructed a consistent system of equations, we must discuss which of the intermediate variables correspond to physical observables. One of the main observables in cosmology is the distribution of temperature anisotropies in the CMB. The CMB is very nearly isotropic and described, at the background level, by an equilibrium Bose-Einstein distribution

$$f_0 = \frac{1}{e^{p/T} - 1}. \quad (6.242)$$

Deviations from this background distribution are usually parameterized as temperature perturbations

$$f(\tau, \mathbf{x}, p, \hat{n}) = \left[\exp\left(\frac{p}{T[1 + \Theta(\tau, \mathbf{x}, \hat{n})]}\right) - 1 \right]^{-1}. \quad (6.243)$$

The temperature perturbation can then be written in terms of the distribution function as

$$(1 + \Theta)^4 - 1 = \frac{\int p^3 dp (f - f_0)}{\int p^3 dp f_0} \equiv \Delta. \quad (6.244)$$

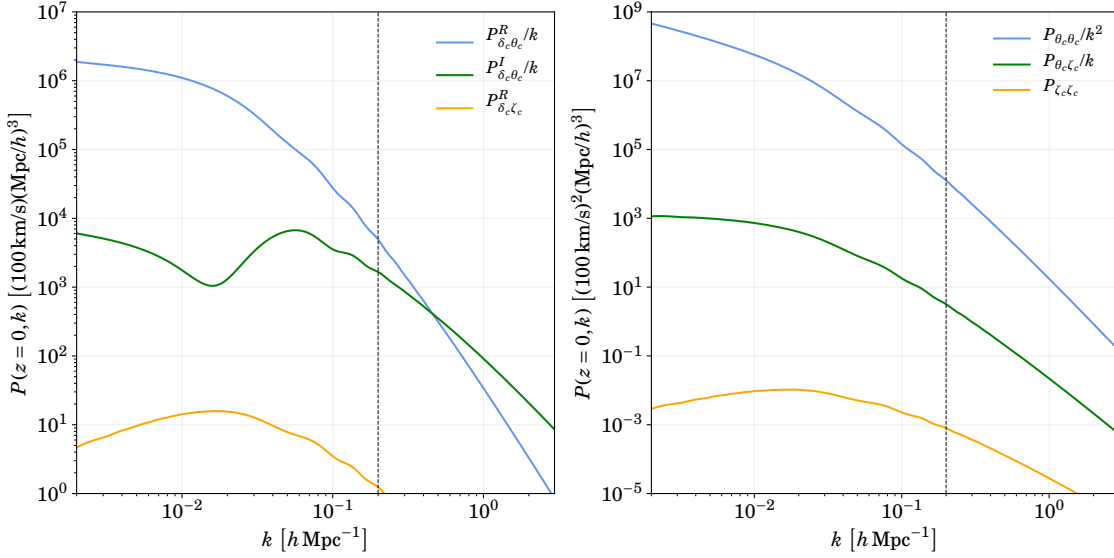


Figure 6.6: The vertical line indicates the scale of non-linearity. (Left) Cross-correlation spectra of dark matter densities and velocities, including the standard as well as the dipolar contribution, both for the divergence and for the vorticity. $P_{\delta_c \theta_c}^I$ and $P_{\delta_c \zeta_c}^R$ are given in units of $(\beta_0/10^{-3})(100 \text{ km/s})(\text{Mpc}/h)^3$, i.e. the curves are plotted for $\beta_0 = 10^{-3}$ but the spectra are proportional to this value. (Right) Autocorrelation spectra of dark matter velocity, as well as the cross-correlation spectrum between vorticity and the divergence of the velocity. $P_{\theta_c \zeta_c}$ and $P_{\zeta_c \zeta_c}$ are given in units $(\beta_0/10^{-3})(100 \text{ km/s})^2(\text{Mpc}/h)^3$ and $(\beta_0/10^{-3})^2(100 \text{ km/s})^2(\text{Mpc}/h)^3$, respectively.

With our definition for the distribution function (6.55), the deviations from (6.242) are

$$\Delta = \frac{1}{\gamma^4(1 - \hat{n} \cdot \boldsymbol{\beta}_\gamma)^4} - 1 + \mathcal{F}_\gamma. \quad (6.245)$$

To first order in cosmological perturbations we have

$$\begin{aligned} \Theta &= \frac{1}{\gamma(1 - \hat{n} \cdot \boldsymbol{\beta}_\gamma)} - 1 + \frac{1}{4}\gamma^3(1 - \hat{n} \cdot \boldsymbol{\beta}_\gamma)^3 \mathcal{F}_\gamma, \\ &= \hat{n} \cdot \boldsymbol{\beta}_\gamma + \frac{1}{4}\left(1 - 3(\hat{n} \cdot \boldsymbol{\beta}_\gamma) + \mathcal{O}(\beta^2)\right) \mathcal{F}_\gamma + \mathcal{O}(\beta^2). \end{aligned} \quad (6.246)$$

This would be the temperature perturbation observed in the \mathcal{O} frame. From the Sun's reference system, the observed temperature perturbation Θ_\odot is

$$1 + \Theta_\odot = \gamma_\odot(1 - \hat{n} \cdot \boldsymbol{\beta}_\odot)(1 + \Theta), \quad (6.247)$$

where $\boldsymbol{\beta}_\odot$ is the velocity of the Solar System in the \mathcal{O} frame. Expanding to leading order in β_γ and β_\odot we get

$$\Theta_\odot = (\boldsymbol{\beta}_\gamma - \boldsymbol{\beta}_\odot) \cdot \hat{n} + \frac{1}{4}\left(1 + \hat{n} \cdot (\boldsymbol{\beta}_\gamma - \boldsymbol{\beta}_\odot) - 4(\hat{n} \cdot \boldsymbol{\beta}_\gamma)\right) \mathcal{F}_\gamma + \mathcal{O}(\beta^2). \quad (6.248)$$

The reduced distribution function can be decomposed schematically as

$$\mathcal{F}_\gamma(\hat{n}, \boldsymbol{\beta}_\gamma) = \mathcal{F}_\gamma^{\text{CDM}}(\hat{n}) + (\hat{n} \cdot \boldsymbol{\beta}_\gamma) \mathcal{F}_\gamma^\beta(\hat{n}) + \mathcal{O}(\beta^2), \quad (6.249)$$

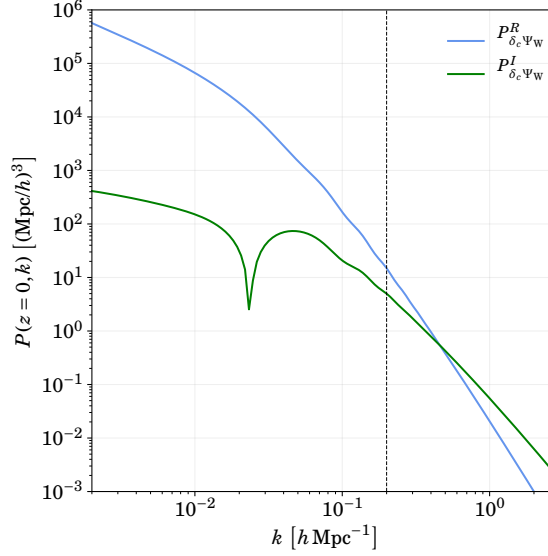


Figure 6.7: Cross-correlation spectra of dark matter density and lensing potential $\Psi_W \equiv \Phi + \Psi$, including both the standard and the dipolar contribution. $P_{\delta_c \Psi_W}^I$ is given in units $(\beta_0/10^{-3})(\text{Mpc}/h)^3$. The vertical line indicates the scale of non-linearity.

where $\mathcal{F}_\gamma^{\Lambda\text{CDM}}$ follows the standard evolution and \mathcal{F}_γ^β contains our modification, i.e. the imaginary part of the scalar modes and the vector modes. Finally, we need to take into account the aberration effects. The direction \hat{n}_\odot observed from the Solar System is related to the direction \hat{n} in the \mathcal{O} frame as

$$n_\odot^i = \frac{\mathcal{P}_{\odot j}^i n^j - \gamma_\odot \beta_\odot^i}{\gamma_\odot (1 - \hat{n} \cdot \boldsymbol{\beta}_\odot)}. \quad (6.250)$$

Then, to first order in β , we can express the direction as

$$n^i = n_\odot^i - \left(\delta_j^i - n_\odot^i n_{\odot j} \right) (\beta_{\text{CMB}}^{\odot j} - \beta_\gamma^j) + \mathcal{O}(\beta^2), \quad (6.251)$$

where we have defined the relative velocity between the Sun and the CMB rest frame

$$\boldsymbol{\beta}_{\text{CMB}}^\odot \equiv \boldsymbol{\beta}_\gamma - \boldsymbol{\beta}_\odot. \quad (6.252)$$

It is customary [Agh+14; Pan+19] to express the deflection instead as

$$\boldsymbol{\beta} - (\hat{n} \cdot \boldsymbol{\beta}) \hat{n} = \nabla(\hat{n} \cdot \boldsymbol{\beta}). \quad (6.253)$$

Taking everything into account, the temperature perturbation that would be measured from the Solar System in the direction \hat{n}_\odot is

$$\begin{aligned} \Theta_\odot(\hat{n}_\odot) &= \hat{n}_\odot \cdot \boldsymbol{\beta}_{\text{CMB}}^\odot \\ &+ \frac{1}{4} \left(1 + \hat{n}_\odot \cdot \boldsymbol{\beta}_{\text{CMB}}^\odot - 4(\hat{n}_\odot \cdot \boldsymbol{\beta}_\gamma) \right) \mathcal{F}_\gamma^{\Lambda\text{CDM}} \left(\hat{n}_\odot - \nabla(\hat{n}_\odot \cdot \boldsymbol{\beta}_{\text{CMB}}^\odot) + \nabla(\hat{n}_\odot \cdot \boldsymbol{\beta}_\gamma) \right) \\ &+ \frac{1}{4} (\hat{n}_\odot \cdot \boldsymbol{\beta}_\gamma) \mathcal{F}_\gamma^\beta(\hat{n}_\odot) + \mathcal{O}(\beta^2). \end{aligned} \quad (6.254)$$

The first term represents the usual kinematic dipole, i.e. the Doppler-shifting effect associated with the relative motion of the observer with respect to the CMB. The second term contains a dipolar modulation and aberration effects. Both effects produce a kinematic mixing of the multipole coefficients. The third term is a purely dynamical contribution, i.e. the effect of a relative motion between different species during the evolution. While recovering standard results [Agh+14] for $\beta = 0$, in our setting we observe two kinds of new effects. First, the directions of the dipole, the dipolar modulation and the aberration effects do not coincide. This effect comes from the fact that, in our scenario, the standard Λ CDM evolution is recovered in the \mathcal{O} frame and *not* in the CMB rest frame. In standard cosmology both frames coincide and this difference does not arise. The second effect is an additional source of statistical anisotropy, coming from the modified evolution, with a dipolar pattern.

The CMB dipole is very well measured, with the latest *Planck* value being $\beta_{\text{CMB}}^{\circ} = (1.23357 \pm 0.00036) \times 10^{-3}$ [Akr+18a]. It is widely accepted that its origin is mostly kinematical, so it gives us a very precise measurement of our relative motion with respect to the CMB. The *Planck* Collaboration also measured our relative motion using the kinematic correlations induced between different multipoles and the resultant anisotropic signal [Agh+14; Ade+16b]. Even though the uncertainties are large in this case, and there seems to be some tension [Ade+16b], the velocity inferred using this method is compatible with the dipole, supporting its kinematical origin. The relative velocity with respect to the CMB frame is usually interpreted as the result of peculiar motions of the Sun and the Local Group [Tul+08]. However, in our scenario, the relative velocity would arise as a combination of the local motion, with respect to the matter frame, and the relative motion between the matter and CMB frames.

It is very important to notice that our model produces a distinctive signature in the CMB. In the standard picture, as mentioned before, the motion of the Solar System produces a violation of statistical isotropy in the CMB. In our case, there would be an additional, purely dynamical, source of statistical anisotropy, caused by the relative motion between matter and radiation during the evolution. Both effects could in principle be disentangled.

The local motion of the Solar System also leaves an imprint in the observed galaxy distribution [EB84; GH12; Pan+19], even though the analysis is not straightforward in this case. Upcoming galaxy surveys like *Euclid* [Ame+18] or SKA [Maa+15] will measure the induced dipole with high precision. A significant difference between this dipole and the CMB result would be difficult to accommodate in standard Λ CDM, but could be easily interpreted as the result of a relative velocity between the CMB and matter frames. Even if no such difference is measured, the bulk motion can still be smaller than the local one, and yet lead to observational signatures.

Two-point function

The two-point function will be analyzed in Chapter 7, after developing a modified line-of-sight approach. In this section we will only prove that there is not an imprint in the temperature power spectrum, i.e. in the C_{ℓ} 's. Here we use a simple argument but it will be proven again in Chapter 7 by other means. Take a two-point function

that also depends on a (small) parameter $\boldsymbol{\beta}$. If we Taylor-expand it, the most general structure to first order is⁵

$$C(\hat{n}, \hat{n}'; \boldsymbol{\beta}) = C_{\Lambda\text{CDM}}(\hat{n} \cdot \hat{n}') + (\hat{n} \cdot \boldsymbol{\beta})C_{\beta}(\hat{n} \cdot \hat{n}') + (\hat{n}' \cdot \boldsymbol{\beta})\tilde{C}_{\beta}(\hat{n} \cdot \hat{n}') + \boldsymbol{\beta} \cdot (\hat{n} \wedge \hat{n}')\tilde{C}_{\beta}(\hat{n} \cdot \hat{n}') + \mathcal{O}(\beta^2) . \quad (6.255)$$

If we compute now the temperature power spectrum, see (3.254),

$$C_{\ell} \equiv \frac{1}{2\ell+1} \sum_{m=-\ell}^{\ell} \langle |a_{\ell m}|^2 \rangle = \frac{1}{4\pi} \int d\hat{n} d\hat{n}' P_{\ell}(\hat{n} \cdot \hat{n}') C(\hat{n}, \hat{n}'; \boldsymbol{\beta}) . \quad (6.256)$$

It is straightforward to check⁶

$$\int d\hat{n} d\hat{n}' (\boldsymbol{\beta} \cdot \hat{n}) P_{\ell}(\hat{n} \cdot \hat{n}') P_{\ell'}(\hat{n} \cdot \hat{n}') = 0 , \quad (6.257)$$

$$\int d\hat{n} d\hat{n}' \boldsymbol{\beta} \cdot (\hat{n} \wedge \hat{n}') P_{\ell}(\hat{n} \cdot \hat{n}') P_{\ell'}(\hat{n} \cdot \hat{n}') = 0 , \quad (6.258)$$

so that finally

$$C_{\ell} = \frac{1}{4\pi} \int d\hat{n} d\hat{n}' P_{\ell}(\hat{n} \cdot \hat{n}') C_{\Lambda\text{CDM}}(\hat{n} \cdot \hat{n}') + \mathcal{O}(\beta^2) . \quad (6.259)$$

The observed temperature power spectrum is not modified to first order in β .

Bulk flows

At the background level, the non-coincidence of the CMB and matter frames produces a global motion of large-scale structures with respect to the CMB. This effect could be potentially observed as a bulk flow on the largest scales. Measurements of bulk flows, at different scales, have been carried out in peculiar velocity surveys and using the kinetic Sunyaev-Zeldovich (kSZ) effect [Kas+09; Ade+14b; Atr+15]. See, e.g., Table 5 of [Scr+16] and references therein for a collection of recent measurements. Although there is a long history of conflicting measurements and anomalously large flows on cosmological scales, in this thesis we adopt the reported limit of *Planck* [Ade+14b] for two reasons. In the first place, it extends to the largest scales, up to 2 Gpc, where a cleaner determination of our global flow is expected. In the second place, it sets the more conservative bound in our parameter β_0 , in the sense of being the more restrictive to us. From the reported *Planck* value $v < 254$ km/s (95% CL), and according to the time evolution of β_{γ} in Figure 6.1, we obtain

$$\beta_0 < 1.6 \times 10^{-3} \text{ (95\% CL)} . \quad (6.260)$$

Note that, since we are performing a first-order computation, all our results scale trivially and we have written them explicitly in units of β_0 . The previous constraint is wholly compatible with the local measurements of peculiar motions mentioned

⁵Of course, the two-point function of the temperature perturbation is symmetric under the exchange $\hat{n} \leftrightarrow \hat{n}'$ by construction, but the argument does not rely on this.

⁶The first equality follows from the fact that every integration over an *odd* number of unitary vectors \hat{n} or \hat{n}' is zero. The second equality follows from symmetry.

above. The peculiar velocity of the Local Group (LG), and other higher order structures, with respect to the CMB is inferred from the movement of the Sun with respect to both of them. The constraint (6.260) yields a value $\beta_\gamma < 0.85 \times 10^{-3}$ today, of the same order as the measured velocity $\beta_{\text{LG}}^\odot = (1.00 \pm 0.05) \times 10^{-3}$ [Akr+18a], so it can be accommodated without fine-tuning the directions of these relative velocities. Potentially, it could even constitute a component of unaccounted peculiar motions of the largest structures [Tul+08]. This constraint also justifies our first order computation. In Section 6.2 it was discussed how to construct a RW background to $\mathcal{O}(\beta)$ and how the $\mathcal{O}(\beta^2)$ terms introduce anisotropies, i.e. a Bianchi background. Using (6.260) we can see that the terms $\mathcal{O}(\beta^2)$ are in fact smaller than a typical cosmological perturbation. Therefore, it is completely justified to take the RW metric (6.1) as the background geometry.

7

Non-comoving Cosmology: CMB

The previous chapter set up the stage for a cosmology with large-scale bulk motions. We proved that there is no leading order effect in the CMB temperature power spectrum, so we focused on LSS signatures. In this chapter we will find the leading order effects in the CMB, beyond the power spectrum. Notice that, while it was possible to reduce the complexity of the system to study LSS, if we want to compare with CMB observations we need to solve the full Boltzmann hierarchy. The main CMB observable is the two-point temperature correlation function, that we cover in Section 7.1. In this section we analyze the generic structure of a two-point function when we introduce a small vector parameter $\boldsymbol{\beta}$. We find that it is possible to define a set of multipoles (similar to the C_ℓ) encoding the modification. As an example, we apply this procedure to the modification that arises from the motion of the Solar System with respect to the CMB frame. In Section 7.2, we extend the line-of-sight approach of Section 3.8 to include cosmological bulk flows. Using this result, we give the expressions needed to compute the modified set of multipoles that we developed in the previous section.

7.1 Generic two-point function

7.1.1 Temperature perturbation and transfer function

The temperature perturbation (3.246) depends on time, the spatial position \mathbf{x} and the direction of observation \hat{n} . Evaluating it today at the origin, it can be written as

$$\Theta(\hat{n}) \equiv \Theta(\tau = \tau_0, \mathbf{x} = 0, \hat{n}) = \int \frac{d^3k}{(2\pi)^3} \Theta(\mathbf{k}, \hat{n}) = \int \frac{d^3k}{(2\pi)^3} \mathcal{T}(\mathbf{k}, \hat{n}) \mathcal{R}_{\mathbf{k}}, \quad (7.1)$$

where \mathcal{R} is the primordial curvature perturbation and \mathcal{T} is the transfer function. The two-point temperature correlation function is

$$\begin{aligned} C(\hat{n}, \hat{n}') &\equiv \langle \Theta(\hat{n}) \Theta(\hat{n}') \rangle = \int \frac{d^3\mathbf{k}}{(2\pi)^3} \frac{d^3\mathbf{k}'}{(2\pi)^3} \mathcal{T}(\mathbf{k}, \hat{n}) \mathcal{T}^*(\mathbf{k}', \hat{n}') \langle \mathcal{R}_{\mathbf{k}} \mathcal{R}_{\mathbf{k}'}^* \rangle \\ &= \int \frac{k^2 dk}{(2\pi)^3} P_{\mathcal{R}}(k) \int d^2\hat{k} \mathcal{T}(\mathbf{k}, \hat{n}) \mathcal{T}^*(\mathbf{k}, \hat{n}'). \end{aligned} \quad (7.2)$$

In Λ CDM, the transfer function only depends on the directions \hat{n} and \hat{k} through the combination $\mu \equiv \hat{n} \cdot \hat{k}$. If we include a new direction in the problem, through a small new parameter $\boldsymbol{\beta}$, to leading order the generic structure of the transfer function is

$$\mathcal{T}(\mathbf{k}, \hat{n}) = \mathcal{T}_A(k, \mu) + i(\boldsymbol{\beta} \cdot \hat{k}) \mathcal{T}_B(k, \mu) + (\hat{n} \cdot \boldsymbol{\beta}) \mathcal{T}_C(k, \mu) + i\hat{k} \cdot (\boldsymbol{\beta} \wedge \hat{n}) \mathcal{T}_D(k, \mu). \quad (7.3)$$

Here $\mathcal{T}_A(k, \mu)$ represents the Λ CDM part. We can write each of the terms as¹

$$\begin{aligned}\mathcal{T}_A &= \sum_{\ell} (-i)^{\ell} \bar{a}_{\ell} Y_{\ell}^0(\hat{n}), & \mathcal{T}_C &= \sum_{\ell} (-i)^{\ell} \bar{c}_{\ell} Y_{\ell}^0(\hat{n}), \\ \mathcal{T}_B &= \sum_{\ell} (-i)^{\ell} \bar{b}_{\ell} Y_{\ell}^0(\hat{n}), & \mathcal{T}_D &= \sum_{\ell} (-i)^{\ell} \bar{d}_{\ell} Y_{\ell}^0(\hat{n}),\end{aligned}\quad (7.4)$$

and we have, to leading order,

$$\begin{aligned}\mathcal{T}(\mathbf{k}, \hat{n}) \mathcal{T}^*(\mathbf{k}, \hat{n}') &= \mathcal{T}(\mathbf{k}, \hat{n}) \mathcal{T}(-\mathbf{k}, \hat{n}') \\ &= \sum_{\ell, \ell'} (-i)^{\ell + \ell'} Y_{\ell}^0(\hat{n}) Y_{\ell'}^0(-\hat{n}') \left\{ \bar{a}_{\ell} \bar{a}_{\ell'} + i(\hat{\beta} \cdot \hat{k})(\bar{a}_{\ell} \bar{b}_{\ell'} - \bar{a}_{\ell'} \bar{b}_{\ell}) \right. \\ &\quad + (\hat{n} \cdot \hat{\beta}) \bar{a}_{\ell'} \bar{c}_{\ell} + (\hat{n}' \cdot \hat{\beta}) \bar{a}_{\ell} \bar{c}_{\ell'} \\ &\quad \left. + i\hat{k} \cdot (\hat{\beta} \wedge \hat{n}) \bar{a}_{\ell'} \bar{d}_{\ell} - i\hat{k} \cdot (\hat{\beta} \wedge \hat{n}') \bar{a}_{\ell} \bar{d}_{\ell'} \right\}.\end{aligned}\quad (7.5)$$

The two-point function can be reduced to

$$\begin{aligned}C(\hat{n}, \hat{n}') &= \int \frac{k^2 dk}{(2\pi)^3} P_{\mathcal{R}}(k) \sum_{\ell, \ell'} (-i)^{\ell + \ell'} \left\{ \bar{a}_{\ell} \bar{a}_{\ell'} I_{\ell\ell'}^{(1)}(\hat{n}, -\hat{n}') \right. \\ &\quad + ((\hat{n} \cdot \hat{\beta}) \bar{a}_{\ell'} \bar{c}_{\ell} + (\hat{n}' \cdot \hat{\beta}) \bar{a}_{\ell} \bar{c}_{\ell'}) I_{\ell\ell'}^{(1)}(\hat{n}, -\hat{n}') \\ &\quad + i(\bar{a}_{\ell'} \bar{b}_{\ell} - \bar{a}_{\ell} \bar{b}_{\ell'}) \hat{\beta} \cdot \mathbf{I}_{\ell\ell'}^{(2)}(\hat{n}, -\hat{n}') \\ &\quad + i\bar{a}_{\ell'} \bar{d}_{\ell} (\hat{\beta} \wedge \hat{n}) \cdot \mathbf{I}_{\ell\ell'}^{(2)}(\hat{n}, -\hat{n}') \\ &\quad \left. - i\bar{a}_{\ell} \bar{d}_{\ell'} (\hat{\beta} \wedge \hat{n}') \cdot \mathbf{I}_{\ell\ell'}^{(2)}(\hat{n}, -\hat{n}') \right\},\end{aligned}\quad (7.6)$$

where the two angular integrals that appear are

$$I_{\ell\ell'}^{(1)}(\hat{n}, \hat{n}') = \int Y_{\ell}^0(\hat{n}) Y_{\ell'}^0(\hat{n}') d^2 \hat{k}, \quad (7.7)$$

$$\mathbf{I}_{\ell\ell'}^{(2)}(\hat{n}, \hat{n}') = \int \hat{k} Y_{\ell}^0(\hat{n}) Y_{\ell'}^0(\hat{n}') d^2 \hat{k}. \quad (7.8)$$

We can compute them explicitly²

$$I_{\ell\ell'}^{(1)}(\hat{n}, \hat{n}') = \delta_{\ell\ell'} P_{\ell}(\hat{n} \cdot \hat{n}'), \quad (7.9)$$

$$\mathbf{I}_{\ell\ell'}^{(2)}(\hat{n}, \hat{n}') = \mathbf{H}_{\ell}(\hat{n}', \hat{n}) \delta_{\ell+1, \ell'} + \mathbf{H}_{\ell'}(\hat{n}, \hat{n}') \delta_{\ell, \ell'+1}, \quad (7.10)$$

where we have defined the function

$$\begin{aligned}\mathbf{H}_{\ell}(\hat{n}, \hat{n}') &\equiv \frac{\ell + 1}{\sqrt{(2\ell + 1)(2\ell + 3)}} \frac{1}{1 - (\hat{n} \cdot \hat{n}')^2} \left\{ (\hat{n} - (\hat{n} \cdot \hat{n}') \hat{n}') P_{\ell} \right. \\ &\quad \left. + (\hat{n}' - (\hat{n} \cdot \hat{n}') \hat{n}) P_{\ell+1} \right\} \\ &= \frac{\ell + 1}{\sqrt{(2\ell + 1)(2\ell + 3)}} \left\{ \hat{n} P_{\ell} - \frac{P'_{\ell}}{\ell + 1} (\hat{n}' - (\hat{n} \cdot \hat{n}') \hat{n}) \right\},\end{aligned}\quad (7.11)$$

with the properties

$$\mathbf{H}_{\ell}(\hat{n}, -\hat{n}') = (-1)^{\ell} \mathbf{H}_{\ell}(\hat{n}, \hat{n}'), \quad (7.12a)$$

$$\mathbf{H}_{\ell}(-\hat{n}', \hat{n}) = -(-1)^{\ell} \mathbf{H}_{\ell}(\hat{n}', \hat{n}). \quad (7.12b)$$

¹The coefficients \bar{a}_{ℓ} , \bar{b}_{ℓ} , \bar{c}_{ℓ} and \bar{d}_{ℓ} are taken to be real. Notice that $Y_{\ell}^0(\hat{n}) = \sqrt{(2\ell + 1)/4\pi} P_{\ell}(\hat{n} \cdot \hat{k})$.

²More details can be found in Appendix C.

We will also need its symmetric combination

$$\mathbf{H}_\ell(\hat{n}, \hat{n}') + \mathbf{H}_\ell(\hat{n}', \hat{n}) = (\hat{n} + \hat{n}')S_\ell(\hat{n} \cdot \hat{n}'), \quad (7.13)$$

with

$$\begin{aligned} S_\ell(x) &\equiv \frac{\ell+1}{\sqrt{(2\ell+1)(2\ell+3)}} \frac{1}{1+x} (P_\ell(x) + P_{\ell+1}(x)) \\ &= \frac{\ell+1}{\sqrt{(2\ell+1)(2\ell+3)}} \left(P_\ell(x) - \frac{P'_\ell(x)}{\ell+1} (1-x) \right). \end{aligned} \quad (7.14)$$

Using these results, one can prove that

$$(\hat{\beta} \wedge \hat{n}) \cdot \mathbf{I}_{\ell\ell'}^{(2)}(\hat{n}, -\hat{n}') - (\hat{\beta} \wedge \hat{n}') \cdot \mathbf{I}_{\ell\ell'}^{(2)}(-\hat{n}', \hat{n}) = 0. \quad (7.15)$$

This implies that the coefficients \bar{d}_ℓ do not contribute to the two-point function

$$\begin{aligned} C(\hat{n}, \hat{n}') &= \int \frac{k^2 dk}{(2\pi)^3} \mathcal{P}_{\mathcal{R}}(k) \left\{ \sum_\ell \bar{a}_\ell^2 P_\ell(\hat{n} \cdot \hat{n}') \right. \\ &\quad \left. + (\hat{n} + \hat{n}') \cdot \hat{\beta} \sum_\ell \left(\bar{a}_\ell \bar{c}_\ell P_\ell(\hat{n} \cdot \hat{n}') + (\bar{a}_{\ell+1} \bar{b}_\ell - \bar{a}_\ell \bar{b}_{\ell+1}) S_\ell(\hat{n} \cdot \hat{n}') \right) \right\}. \end{aligned} \quad (7.16)$$

The last portion can be recast as³

$$\begin{aligned} \sum_\ell (\bar{a}_{\ell+1} \bar{b}_\ell - \bar{a}_\ell \bar{b}_{\ell+1}) S_\ell(\hat{n} \cdot \hat{n}') &= \sum_\ell \bar{a}_\ell (\bar{b}_{\ell-1} S_{\ell-1} - b_{\ell+1} S_\ell) \\ &= \sum_\ell \frac{\bar{a}_\ell}{\sqrt{2\ell+1}} \left(\frac{\ell}{\sqrt{2\ell-1}} \bar{b}_{\ell-1} - \frac{\ell+1}{\sqrt{2\ell+3}} \bar{b}_{\ell+1} \right) P_\ell(\hat{n} \cdot \hat{n}') \\ &\quad + \sum_\ell \frac{\bar{a}_\ell}{\sqrt{2\ell+1}} \left(\frac{\bar{b}_{\ell-1}}{\sqrt{2\ell-1}} + \frac{\bar{b}_{\ell+1}}{\sqrt{2\ell+3}} \right) (1 - (\hat{n} \cdot \hat{n}')) P'_\ell(\hat{n} \cdot \hat{n}'). \end{aligned} \quad (7.17)$$

After redefining the coefficients

$$\begin{aligned} a_\ell &\equiv \frac{\bar{a}_\ell}{\sqrt{4\pi(2\ell+1)}}, & b'_\ell &\equiv \ell b_{\ell-1} - (\ell+1)b_{\ell+1}, \\ b_\ell &\equiv \frac{\bar{b}_\ell}{\sqrt{4\pi(2\ell+1)}}, & \tilde{b}_\ell &\equiv b_{\ell-1} + b_{\ell+1}, \\ c_\ell &\equiv \frac{\bar{c}_\ell}{\sqrt{4\pi(2\ell+1)}}, \end{aligned} \quad (7.18)$$

the two-point function is

$$\begin{aligned} C(\hat{n}, \hat{n}') &= \int \frac{dk}{k} \mathcal{P}_{\mathcal{R}}(k) \left\{ \sum_\ell (2\ell+1) a_\ell^2 P_\ell \right. \\ &\quad \left. + (\hat{n} + \hat{n}') \cdot \hat{\beta} \sum_\ell (2\ell+1) a_\ell (b'_\ell + c_\ell) P_\ell \right. \\ &\quad \left. + (\hat{n} + \hat{n}') \cdot \hat{\beta} \sum_\ell (2\ell+1) a_\ell \tilde{b}_\ell (1 - (\hat{n} \cdot \hat{n}')) P'_\ell \right\}. \end{aligned} \quad (7.19)$$

³We are defining $\bar{b}_{-1} \equiv 0$.

7.1.2 Alternative power spectrum

The modified two-point function has the structure

$$C(\hat{n}, \hat{n}') = C_{\Lambda\text{CDM}}(\hat{n} \cdot \hat{n}') + \hat{\beta} \cdot (\hat{n} + \hat{n}') C_{\beta}(\hat{n} \cdot \hat{n}') . \quad (7.20)$$

For the ΛCDM part, it is usual to define the temperature power spectrum as

$$C_{\Lambda\text{CDM}}(\hat{n} \cdot \hat{n}') = \sum_{\ell=0}^{\infty} \frac{2\ell+1}{4\pi} C_{\ell} P_{\ell}(\hat{n} \cdot \hat{n}') . \quad (7.21)$$

With our previous definitions,

$$C_{\ell} = \int \frac{dk}{4\pi k} \mathcal{P}_{\mathcal{R}}(k) \alpha_{\ell}^2(k) . \quad (7.22)$$

These C_{ℓ} agree with the ones obtained using the definition (3.254), based on the harmonic decomposition of the temperature perturbation ($a_{\ell m}$). As argued in Section 6.10.2, our modification C_{β} does not contribute, to leading order, to the C_{ℓ} defined through (3.254). Focusing on the modified part, in general we get

$$\begin{aligned} C_{\beta}(\hat{n} \cdot \hat{n}') &= \int \frac{dk}{k} \mathcal{P}_{\mathcal{R}}(k) \left\{ \sum_{\ell} (2\ell+1) \alpha_{\ell} \alpha_{\ell} P_{\ell} + \sum_{\ell} (2\ell+1) \alpha_{\ell} \beta_{\ell} (1 - (\hat{n} \cdot \hat{n}')) P'_{\ell} \right\} \\ &= \int \frac{dk}{k} \mathcal{P}_{\mathcal{R}}(k) \left\{ \sum_{\ell} (2\ell+1) \alpha_{\ell} \alpha_{\ell} P_{\ell} + \sum_{\ell, \ell'} (2\ell+1) \alpha_{\ell} \beta_{\ell'} \mathcal{Q}_{\ell\ell'} P_{\ell'} \right\} \\ &= \int \frac{dk}{k} \mathcal{P}_{\mathcal{R}}(k) \left\{ \sum_{\ell} (2\ell+1) \left(\alpha_{\ell} \alpha_{\ell} + \sum_{\ell'} \frac{2\ell'+1}{2\ell+1} \alpha_{\ell'} \beta_{\ell'} \mathcal{Q}_{\ell\ell'} \right) P_{\ell} \right\} , \end{aligned} \quad (7.23)$$

where $\alpha_{\ell}, \beta_{\ell}$ are generic variables. Since C_{β} only depends on the product $(\hat{n} \cdot \hat{n}')$, we can define its Legendre expansion and an equivalent set of multipoles that encode the information about our modification

$$C_{\ell}^{\beta} = \int \frac{dk}{4\pi k} \mathcal{P}_{\mathcal{R}}(k) \left(\alpha_{\ell} \alpha_{\ell} + \sum_{\ell'} \frac{2\ell'+1}{2\ell+1} \alpha_{\ell'} \beta_{\ell'} \mathcal{Q}_{\ell\ell'} \right) . \quad (7.24)$$

The coefficients $\mathcal{Q}_{\ell\ell'}$ have been defined in a such a way that

$$(1 - (\hat{n} \cdot \hat{n}')) P'_{\ell}(\hat{n} \cdot \hat{n}') = \sum_{\ell'} \mathcal{Q}_{\ell\ell'} P_{\ell'}(\hat{n} \cdot \hat{n}') . \quad (7.25)$$

Equivalently⁴

$$\mathcal{Q}_{\ell\ell'} = \frac{2\ell+1}{2} \int_{-1}^1 d\mu (1-\mu) P'_{\ell'}(\mu) P_{\ell}(\mu) = \begin{cases} 0 , & \ell' < \ell , \\ -\ell , & \ell' = \ell , \\ -(-1)^{\ell'+\ell} (2\ell+1) , & \ell' > \ell . \end{cases} \quad (7.26)$$

The final result is

$$C_{\ell}^{\beta} = \int \frac{dk}{4\pi k} \mathcal{P}_{\mathcal{R}}(k) \left(\alpha_{\ell} (\alpha_{\ell} - \ell \beta_{\ell}) - (-1)^{\ell} \sum_{\ell'=\ell+1}^{\infty} (-1)^{\ell'} (2\ell'+1) \alpha_{\ell'} \beta_{\ell'} \right) . \quad (7.27)$$

⁴The integral is performed in the Appendix C.

7.1.3 Solar System motion

To conclude this section we will apply the previous results to a case particularly simple: the kinematic effects produced by the Solar System motion. As discussed in Section 6.10, the motion of the solar frame with respect to the CMB rest frame is a source of statistical anisotropy. Within Λ CDM, in the CMB rest frame (3.245)

$$\Theta_{\text{rest}}(\hat{n}) = \frac{1}{4} \mathcal{F}_\gamma(\hat{n}), \quad (7.28)$$

and the two-point function in this frame is

$$C_{\text{rest}}(\hat{n} \cdot \hat{n}') = \int \frac{dk}{k} \mathcal{P}_{\mathcal{R}}(k) \sum_{\ell} (2\ell + 1) \alpha_{\ell}^2 P_{\ell}(\hat{n} \cdot \hat{n}'). \quad (7.29)$$

In a moving frame, we get in general⁵

$$\Theta(\hat{n}) = \hat{n} \cdot \mathbf{d}_{\text{kin}} + \frac{1}{4} (1 + \hat{n} \cdot \mathbf{d}_{\text{m}}) \mathcal{F}(\hat{n} - \nabla(\hat{n} \cdot \mathbf{d}_{\text{a}})), \quad (7.30)$$

where

$$\nabla(\hat{n} \cdot \mathbf{d}_{\text{a}}) = \mathbf{d}_{\text{a}} - (\hat{n} \cdot \mathbf{d}_{\text{a}}) \hat{n}. \quad (7.31)$$

The two-point function in this case is

$$\begin{aligned} \langle \Theta(\hat{n}) \Theta(\hat{n}') \rangle &= \frac{1}{16} (1 + (\hat{n} + \hat{n}') \cdot \mathbf{d}_{\text{m}}) \langle \mathcal{F}(\hat{n} - \nabla(\hat{n} \cdot \mathbf{d}_{\text{a}})) \mathcal{F}(\hat{n}' - \nabla(\hat{n}' \cdot \mathbf{d}_{\text{a}})) \rangle \\ &= (1 + (\hat{n} + \hat{n}') \cdot \mathbf{d}_{\text{m}}) C_{\text{rest}} \left(\hat{n} \cdot \hat{n}' - (\hat{n} + \hat{n}') \cdot \mathbf{d}_{\text{a}} (1 - (\hat{n} \cdot \hat{n}')) \right) \\ &= \int \frac{dk}{k} \mathcal{P}_{\mathcal{R}}(k) \left\{ \sum_{\ell} (2\ell + 1) \alpha_{\ell}^2 P_{\ell} + (\hat{n} + \hat{n}') \cdot \mathbf{d}_{\text{m}} \sum_{\ell} (2\ell + 1) \alpha_{\ell}^2 P_{\ell} \right. \\ &\quad \left. - (\hat{n} + \hat{n}') \cdot \mathbf{d}_{\text{a}} \sum_{\ell} (2\ell + 1) \alpha_{\ell}^2 (1 - (\hat{n} \cdot \hat{n}')) P_{\ell}' \right\}. \quad (7.32) \end{aligned}$$

The modification has the structure (7.23) with

$$\alpha_{\ell} = d_{\text{m}} a_{\ell}, \quad \beta_{\ell} = -d_{\text{a}} a_{\ell}. \quad (7.33)$$

Writing $d_{\text{m}} = d_{\text{a}} = \beta_{\text{CMB}}^{\circ}$, the power spectrum of the modification, (7.27), is

$$C_{\ell}^{\beta} = \beta_{\text{CMB}}^{\circ} \left((\ell + 1) C_{\ell} + (-1)^{\ell} \sum_{\ell'=\ell+1}^{\infty} (-1)^{\ell'} (2\ell' + 1) C_{\ell'} \right), \quad (7.34)$$

where C_{ℓ} stands for the standard multipoles in the CMB rest frame.

7.2 Modified line-of-sight integral

7.2.1 Modified source

Our starting point is the Boltzmann equation for photons (6.84). It can be written as

$$\dot{\mathcal{F}} + (\mathbf{i}(\mathbf{k} \cdot \hat{n}) + \dot{\kappa}_{\beta}(\hat{\beta} \cdot \hat{n}) - \dot{\kappa}) \mathcal{F} + D + \hat{n} \cdot \mathbf{U} + (\hat{\beta} \cdot \hat{n}) n^i n^j S_{ij} + n^i n^j T_{ij} = 0, \quad (7.35)$$

⁵Of course, in this particular case $\mathbf{d}_{\text{kin}} = \mathbf{d}_{\text{m}} = \mathbf{d}_{\text{a}} \equiv \beta_{\text{CMB}}^{\circ}$. See (6.254) with $\beta = 0$.

where

$$\kappa_\beta \equiv \int_\tau^{\tau_0} \beta_b a n_e \sigma_T d\tau, \quad (7.36)$$

and the different coefficients are

$$D = 2i(\boldsymbol{\beta}_\gamma \cdot \mathbf{k})A + \dot{\kappa} \left[\delta_\gamma - \frac{8}{3} \boldsymbol{\beta}_b \cdot \delta \mathbf{v}_\gamma - \frac{8}{3} \Delta \boldsymbol{\beta} \cdot \delta \mathbf{v}_b - 4 \boldsymbol{\beta}_b \cdot \delta \mathbf{v}_b \right], \quad (7.37a)$$

$$U_j = -2ik_j A + 4\beta_\gamma^i C_{ij} + \dot{\kappa} [3\beta_{bj} \delta_\gamma + 4\delta v_{bj} - 4\beta_{\gamma j} \delta_{n_e} + 2\Delta \beta_j A], \quad (7.37b)$$

$$S_{ij} = -20\beta_\gamma C_{(ij)}, \quad (7.37c)$$

$$T_{ij} = -4C_{(ij)} + 4\beta_\gamma^k D_{k(ij)} - 10ik_{(i} \beta_{\gamma j)} A + 4\dot{\kappa} [\delta v_{b(i} \Delta \beta_{j)} + 4\delta v_{b(i} \beta_{b j)}]. \quad (7.37d)$$

Repeating the same steps that led us to (3.234), we find the integral solution

$$\begin{aligned} \mathcal{F}|_{\tau_0} = & - \int_0^{\tau_0} \left(D + \hat{n} \cdot \mathbf{U} + (\hat{\beta} \cdot \hat{n}) n^i n^j S_{ij} + n^i n^j T_{ij} \right) \\ & \times \exp(i(\mathbf{k} \cdot \hat{n})(\tau - \tau_0) - \kappa + \kappa_\beta (\hat{\beta} \cdot \hat{n})) d\tau. \end{aligned} \quad (7.38)$$

Using the fact that $\kappa_\beta \ll \kappa$ we can Taylor-expand the exponential and write⁶

$$\mathcal{F}|_{\tau_0} = \int_0^{\tau_0} \tilde{S} \exp(i(\mathbf{k} \cdot \hat{n})(\tau - \tau_0) - \kappa) d\tau, \quad (7.39)$$

with

$$\tilde{S} \equiv -D - \hat{n} \cdot \mathbf{U} - n^i n^j T_{ij} - (\hat{\beta} \cdot \hat{n}) \left\{ n^i n^j S_{ij} + \kappa_\beta \left(D + \hat{n} \cdot \mathbf{U} + n^i n^j T_{ij} \right) \right\}. \quad (7.40)$$

We will use the short-hand definitions

$$\boldsymbol{\xi} \equiv \mathbf{B} - \dot{\mathbf{E}}, \quad \mathbf{W} \equiv \mathbf{S} + \dot{\mathbf{F}}. \quad (7.41)$$

Since the vector modes are sourced only by β , we have (6.188)

$$\mathbf{W} \equiv W(\hat{\beta} - (\hat{\beta} \cdot \hat{k})\hat{k}), \quad \boldsymbol{\chi} \equiv \chi(\hat{\beta} - (\hat{\beta} \cdot \hat{k})\hat{k}). \quad (7.42)$$

Using all the previous definitions, the different contributions to the source are

$$D = -4i(\boldsymbol{\beta}_\gamma \cdot \mathbf{k})\Psi + \dot{\kappa} \left[\delta_\gamma + \frac{8i}{3k} (\hat{k} \cdot \boldsymbol{\beta}_b) \theta_\gamma + \frac{8i}{3k} (\hat{k} \cdot \Delta \boldsymbol{\beta}) \theta_b + \frac{4i}{k} (\hat{k} \cdot \boldsymbol{\beta}_b) \theta_b \right], \quad (7.43a)$$

$$\begin{aligned} \hat{n} \cdot \mathbf{U} = & 4i(\hat{n} \cdot \mathbf{k})\Psi + 4(\hat{n} \cdot \boldsymbol{\beta}_\gamma) \dot{\Phi} - 4(\hat{n} \cdot \mathbf{k})(\boldsymbol{\beta}_\gamma \cdot \mathbf{k})\xi \\ & + \dot{\kappa} \left[3(\hat{n} \cdot \boldsymbol{\beta}_b) \delta_\gamma - \frac{4i}{k} (\hat{n} \cdot \hat{k}) \theta_b + 4\chi_b ((\hat{n} \cdot \hat{\beta}) - (\hat{\beta} \cdot \hat{k})(\hat{n} \cdot \hat{k})) \right. \\ & \left. - 4(\hat{n} \cdot \boldsymbol{\beta}_\gamma) \delta_{n_e} - 4(\hat{n} \cdot \Delta \boldsymbol{\beta}) \Psi \right], \end{aligned} \quad (7.43b)$$

$$n^i n^j S_{ij} = -20\beta_\gamma \dot{\Phi} + 20\beta_\gamma (\hat{n} \cdot \mathbf{k})^2 \xi, \quad (7.43c)$$

$$\begin{aligned} n^i n^j T_{ij} = & -4\dot{\Phi} + 20i(\hat{n} \cdot \mathbf{k})(\hat{n} \cdot \boldsymbol{\beta}_\gamma) \Psi + 4(\hat{n} \cdot \mathbf{k})^2 \xi + 4i((\hat{n} \cdot \boldsymbol{\beta}_\gamma)(\hat{n} \cdot \mathbf{k}) - (\boldsymbol{\beta}_\gamma \cdot \mathbf{k})) \Phi \\ & + 4i(\hat{n} \cdot \mathbf{k}) W((\hat{n} \cdot \hat{\beta}) - (\hat{n} \cdot \hat{k})(\hat{\beta} \cdot \hat{k})) \\ & - \frac{4i}{k} \dot{\kappa} (\hat{n} \cdot \hat{k}) \left[(\hat{n} \cdot \Delta \boldsymbol{\beta}) \theta_b + 4(\hat{n} \cdot \boldsymbol{\beta}_b) \theta_b \right]. \end{aligned} \quad (7.43d)$$

⁶Notice that even if $\beta_b \ll 1$, $a n_e \sigma_T$ can still grow very large making $\kappa_\beta \gg 1$. However, in this case the contribution to the integral is strongly suppressed by $e^{-\kappa}$.

Stripping the explicit dependence on $\hat{\beta}$, the modified source can be written as

$$\tilde{S} = \tilde{S}_A + i(\hat{\beta} \cdot \hat{k})\tilde{S}_B + (\hat{n} \cdot \hat{\beta})\tilde{S}_C, \quad (7.44)$$

where

$$\tilde{S}_A = -\dot{\kappa}\delta_\gamma + 4\dot{\Phi} - 4i(\hat{n} \cdot \mathbf{k})\left(\Psi - \frac{\dot{\kappa}\theta_b}{k^2}\right) - 4(\hat{n} \cdot \mathbf{k})^2\xi, \quad (7.45a)$$

$$\begin{aligned} \tilde{S}_B = & -\frac{4\beta_\gamma\dot{\kappa}}{k}\left(\theta_b + \frac{2}{3}\theta_\gamma\right) + 4\beta_\gamma k(\Phi + \Psi) + \frac{4\dot{\beta}_\gamma}{3k}(\theta_b + 2\theta_\gamma) \\ & - 4i(\hat{n} \cdot \mathbf{k})\left(\beta_\gamma k\xi + \frac{\dot{\kappa}}{k}\chi_b\right) + \frac{4(\hat{n} \cdot \mathbf{k})^2}{k}W, \end{aligned} \quad (7.45b)$$

$$\begin{aligned} \tilde{S}_C = & \dot{\kappa}\left(\beta_\gamma(4\delta_{n_e} - 3\delta_\gamma) - 4\chi_b - \kappa_\beta\delta_\gamma\right) + \dot{\beta}_\gamma(4\Psi + 3\delta_\gamma) + 4(\kappa_\beta + 4\beta_\gamma)\dot{\Phi} \\ & - 4i(\hat{n} \cdot \mathbf{k})\left(\beta_\gamma(\Phi + 5\Psi) + \kappa_\beta\Psi + W - \frac{\dot{\kappa}}{k^2}(\kappa_\beta + 4\beta_\gamma)\theta_b + \frac{3\dot{\beta}_\gamma\theta_b}{k^2}\right) \\ & - 4(\hat{n} \cdot \mathbf{k})^2(\kappa_\beta + 5\beta_\gamma)\xi. \end{aligned} \quad (7.45c)$$

As we did in Section 3.8, after integration by parts and neglecting the boundary terms, we can substitute

$$(\hat{n} \cdot \mathbf{k}) \rightarrow i\frac{d}{d\tau}, \quad (\hat{n} \cdot \mathbf{k})^2 \rightarrow -\frac{d^2}{d\tau^2}. \quad (7.46)$$

Once we add the optical depth to the source term

$$S \equiv e^{-\kappa}\tilde{S} = S_A + i(\hat{\beta} \cdot \hat{k})S_B + (\hat{n} \cdot \hat{\beta})S_C, \quad (7.47)$$

the line-of-sight integral can be expressed as

$$\mathcal{F}|_{\tau_0} = \int_0^{\tau_0} d\tau \exp(i(\hat{n} \cdot \mathbf{k})(\tau - \tau_0)) (S_A + i(\hat{\beta} \cdot \hat{k})S_B + (\hat{n} \cdot \hat{\beta})S_C). \quad (7.48)$$

The different terms can be written alternatively as (equal upon integration by parts)

$$S_A = g(\delta_\gamma + 4\Psi + 4\dot{\xi}) + 4e^{-\kappa}(\dot{\Phi} + \dot{\Psi} + \dot{\xi}) + \frac{4}{k^2}\frac{d}{d\tau}\left(g(\theta_b + k^2\xi)\right) \quad (7.49a)$$

$$= g(\delta_\gamma - 4\Phi) + \frac{4}{k^2}\frac{d}{d\tau}\left\{g(\theta_b + k^2\xi) + k^2e^{-\kappa}(\Phi + \Psi + \dot{\xi})\right\}, \quad (7.49b)$$

$$\begin{aligned} S_B = & \frac{4g}{k}\left(\beta_\gamma\left(\theta_b + \frac{2}{3}\theta_\gamma + k^2\xi\right) - \dot{W}\right) - 4e^{-\kappa}\left(\beta_\gamma k(\Phi + \Psi + \dot{\xi}) - \frac{1}{k}\ddot{W}\right) \\ & + \frac{4\dot{\beta}_\gamma}{k}e^{-\kappa}\left(\frac{1}{3}(\theta_b + 2\theta_\gamma) + k^2\xi\right) - \frac{4}{k}\frac{d}{d\tau}\left(g(\chi_b + W)\right) \end{aligned} \quad (7.50a)$$

$$\begin{aligned} = & \frac{4}{k}g\beta_\gamma\left(\theta_b + \frac{2}{3}\theta_\gamma + k^2\xi\right) + 4\beta_\gamma ke^{-\kappa}(\Phi + \Psi + \dot{\xi}) \\ & + \frac{4\dot{\beta}_\gamma}{k}e^{-\kappa}\left(\frac{1}{3}(\theta_b + 2\theta_\gamma) + k^2\xi\right) - \frac{4}{k}\frac{d}{d\tau}\left\{g(\chi_b + W) + e^{-\kappa}\dot{W}\right\}, \end{aligned} \quad (7.50b)$$

$$\begin{aligned}
S_C = & g \{ \beta_\gamma (3\delta_\gamma - 4\delta_{n_e} + 4\Phi + 16\Psi + 16\dot{\xi}) + \kappa_\beta (\delta_b + 4\Psi + 4\dot{\xi}) + 4(\chi_b + W) \} \\
& + \dot{\beta}_\gamma e^{-\kappa} \{ 3\delta_\gamma + 4(\Phi + 5\Psi) + 16\dot{\xi} \} + 4e^{-\kappa} \{ (\kappa_\beta + 5\beta_\gamma) (\dot{\Phi} + \dot{\Psi} + \dot{\xi}) + \dot{W} \} \\
& + \frac{4}{k^2} \frac{d}{d\tau} \left\{ g(\kappa_\beta + 4\beta_\gamma - 3\Delta\beta)(\theta_b + k^2\xi) - k^2 g\Delta\beta\xi \right\} \tag{7.51a}
\end{aligned}$$

$$\begin{aligned}
= & g \left\{ 3\beta_\gamma \left(\delta_\gamma - \frac{4}{3}\delta_{n_e} - 4\Phi \right) + \kappa_\beta (\delta_b - 4\Phi) + 4(\chi_b + W) \right\} \\
& + 3\dot{\beta}_\gamma e^{-\kappa} \left\{ \delta_\gamma - 4\Phi + \frac{4}{3}\Psi \right\} + 4e^{-\kappa} \dot{W} \\
& + \frac{4}{k^2} \frac{d}{d\tau} \left\{ g(\kappa_\beta + 4\beta_\gamma - 3\Delta\beta)(\theta_b + k^2\xi) - k^2 g\Delta\beta\xi \right. \\
& \quad \left. + k^2 e^{-\kappa} (\kappa_\beta + 5\beta_\gamma) (\Phi + \Psi + \dot{\xi}) \right\}. \tag{7.51b}
\end{aligned}$$

The results have been rendered in the traditional form (3.236), where the terms associated to the SW, ISW and Doppler effects can be clearly identified. There is an additional ISW-like term proportional to $\dot{\beta}$, that is nearly zero after decoupling except for a small change at reionization time. We still need to split S_A into real and imaginary part ($S_A = S_A^R + i(\hat{\beta} \cdot \hat{k})S_A^I$). Once we do this, S_A^I can be reabsorbed into the definition of S_B in (7.48) and all the source terms become real, since any imaginary part would be $\mathcal{O}(\beta^2)$.

7.2.2 Modified two-point function

In order to relate the modification induced by the cosmological bulk flows with the previous results for a modified two-point function, it is convenient to define the following coefficients

$$a_\ell \equiv \frac{1}{4} \int_0^{\tau_0} d\tau j_\ell(k(\tau_0 - \tau)) S_A^R(\tau, k), \tag{7.52a}$$

$$b_\ell \equiv \frac{1}{4} \int_0^{\tau_0} d\tau j_\ell(k(\tau_0 - \tau)) (S_B(\tau, k) + S_A^I(\tau, k)), \tag{7.52b}$$

$$c_\ell \equiv \frac{1}{4} \int_0^{\tau_0} d\tau j_\ell(k(\tau_0 - \tau)) S_C(\tau, k), \tag{7.52c}$$

$$b'_\ell \equiv \frac{1}{4} \int_0^{\tau_0} d\tau j'_\ell(k(\tau_0 - \tau)) (S_B(\tau, k) + S_A^I(\tau, k)), \tag{7.52d}$$

$$\tilde{b}_\ell \equiv \frac{1}{4} \int_0^{\tau_0} d\tau \frac{j_\ell(k(\tau_0 - \tau))}{k(\tau_0 - \tau)} (S_B(\tau, k) + S_A^I(\tau, k)). \tag{7.52e}$$

For simplicity, we will omit the argument of the Bessel functions and the R superscripts from now on, unless there is risk of confusion. The first of these coefficients represents the usual Λ CDM contribution

$$\begin{aligned}
a_\ell = & \frac{1}{4} \int_0^{\tau_0} d\tau j_\ell \left\{ g(\delta_\gamma - 4\Phi) \right\} \\
& + \int_0^{\tau_0} d\tau j'_\ell \left\{ g \left(\frac{\theta_b}{k} + k\xi \right) + k e^{-\kappa} (\Phi + \Psi + \dot{\xi}) \right\}. \tag{7.53}
\end{aligned}$$

The next coefficient, that arises from our modification, is

$$\begin{aligned}
b'_\ell = & \frac{1}{4} \int_0^{\tau_0} d\tau j'_\ell \left\{ g(\delta_\gamma^I - 4\Phi^I) \right\} \\
& + \int_0^{\tau_0} d\tau j''_\ell \left\{ g \left(\frac{\theta_b^I}{k} + k\xi^I \right) + k e^{-\kappa} (\Phi^I + \Psi^I + \xi^I) \right\} \\
& + \int_0^{\tau_0} d\tau j'_\ell \left\{ g\beta_\gamma \left(\frac{\theta_b}{k} + \frac{2}{3} \frac{\theta_\gamma}{k} + k\xi \right) + \beta_\gamma k e^{-\kappa} (\Phi + \Psi + \xi) \right. \\
& \quad \left. + \dot{\beta}_\gamma e^{-\kappa} \left(\frac{1}{3k} (\theta_b + 2\theta_\gamma) + k\xi \right) \right\} \\
& - \int_0^{\tau_0} d\tau j''_\ell \left\{ g(\chi_b + W) + e^{-\kappa} \dot{W} \right\} .
\end{aligned} \tag{7.54}$$

The same expression holds for \tilde{b}_ℓ , after substituting

$$j'_\ell \rightarrow \frac{j_\ell}{k(\tau_0 - \tau)} = \frac{1}{\ell} (j'_\ell + j_{\ell+1}) , \tag{7.55a}$$

$$j''_\ell \rightarrow \frac{d}{d\tau} \left(\frac{j_\ell}{k(\tau_0 - \tau)} \right) . \tag{7.55b}$$

The last coefficient is

$$\begin{aligned}
c_\ell = & \int_0^{\tau_0} d\tau j_\ell \left\{ \frac{1}{4} g \left[3\beta_\gamma \left(\delta_\gamma - \frac{4}{3} \delta_{n_e} - 4\Phi \right) + \kappa\beta(\delta_b - 4\Phi) + 4(\chi_b + W) \right] \right. \\
& \quad \left. + e^{-\kappa} \dot{W} + \frac{3\dot{\beta}_\gamma}{4} e^{-\kappa} \left[\delta_\gamma - 4\Phi + \frac{4}{3} \Psi \right] \right\} \\
& + \int_0^{\tau_0} d\tau j'_\ell \left\{ g(\kappa\beta + 4\beta_\gamma - 3\Delta\beta) \left(\frac{\theta_b}{k} + k\xi \right) - g\Delta\beta k\xi \right. \\
& \quad \left. + k e^{-\kappa} (\kappa\beta + 5\beta_\gamma) (\Phi + \Psi + \xi) \right\} .
\end{aligned} \tag{7.56}$$

In our scenario, if we assume that we are working with a CMB map corrected for the Solar System motion (with the value measured from the kinematic dipole) there is still a remanent dipolar modulation and aberration

$$\mathbf{d}_m = -4\boldsymbol{\beta}_\gamma , \quad \mathbf{d}_a = -\boldsymbol{\beta}_\gamma . \tag{7.57}$$

Using the expression (7.32) to evaluate the effect of a dipolar modulation and aberration, the coefficients that appear in the modified two-point function (7.23) are

$$\alpha_\ell = b'_\ell + c_\ell - 4\beta_\gamma \alpha_\ell , \tag{7.58a}$$

$$\beta_\ell = \tilde{b}_\ell + \beta_\gamma \alpha_\ell . \tag{7.58b}$$

8

Non-comoving Cosmology: Magnetic fields

This chapter establishes a connection between the existence of large-scale bulk flows and the production of cosmological magnetic fields. Section 8.1 summarizes the current observations of magnetic fields at different scales and some proposed mechanisms to produce them. Until now, we have always treated the baryons as a single, tightly coupled fluid. In Section 8.2 we will dig deeper into the behaviour of this plasma. In particular, we will analyze an electron-proton-photon plasma sourcing (and coupled to) macroscopic electromagnetic fields. Section 8.3 outlines the physical mechanism responsible for the production of magnetic fields and presents the final results.

8.1 Magnetic fields in the Universe

The origin of the magnetic fields found in galaxies, with strengths in the range of the μG , and permeating the intergalactic medium in clusters is a long-standing question in astrophysics and cosmology [Wid02]. Even more puzzling is the presence of magnetic fields in voids with strengths 3×10^{-16} G as those detected in [NV10]. The evolution of primordially generated magnetic fields from the early Universe to the onset of structure formation seems to be well understood [BJ04; DN13; Sub16], and there are compelling astrophysical mechanisms, i.e. dynamos, that can amplify a preexisting magnetic field several orders of magnitude [DLT99; Wid02]. However, a definite mechanism that can *produce* the primordial seed fields is still lacking.

There are different proposed solutions, that can be classified as cosmological or astrophysical, addressing the origin of the primordial fields. In the cosmological mechanisms, magnetic fields are generated in the very early Universe, typically during inflation [TW88; Mar01] or in the electroweak [Vac91] or QCD [QLS89] phase transitions. On the other hand, in astrophysical mechanisms, magnetic fields are generated by motions in the plasma during galaxy formation. In general, the amplitude of the seeds generated by these mechanisms is too small to explain the observed fields even with dynamo amplification. Depending on the dynamo amplification rate, a seed field with a strength in the range $10^{-23} - 10^{-16}$ G at galaxy formation and coherent on comoving scales of 10 kpc is required to reach the amplitude of the detected galactic fields [DLT99].

Among the astrophysical proposals, a particularly appealing one is the so-called Harrison mechanism. In his pioneering work [Har70], Harrison realized that vorticity in the photon-baryon plasma would lead to the production of electromagnetic fields. The main obstacle [Ree87] for the Harrison mechanism to work is to achieve vortical motions in the fluid. Within ΛCDM , to first order in perturbation theory, vorticity and vector modes decay so, even if they are initially large, only small mag-

netic fields can be generated [ITS12]. Different routes have been explored to overcome this difficulty. It is possible to source vector modes, e.g. via topological defects, but it was shown in [Hol+08] that if vorticity is transferred only by gravitational interactions, it does not lead to production of magnetic fields. On the other hand, vorticity and magnetic fields are indeed generated to second order in perturbation theory in standard Λ CDM [Tak+05; FPM11; Sag+15], but are consequently very small.

In Chapter 6 we showed that vorticity in the photon-baryon plasma can also be produced if bulk flows of matter with respect to radiation are present. In such a case, first order scalar metric perturbations induce non-decaying vortical motions in the different plasma components. As has been previously discussed, the existence of large-scale bulk flows in excess of Λ CDM predictions has been a matter of debate in recent years. While some papers claim to find evidence of unusually large flows [Kas+09; Atr+15], most of the works find results consistent with Λ CDM [Ade+14b; Scr+16]. In particular, the largest-scale limits to date on the amplitude of the bulk flow has been set by the *Planck* collaboration [Ade+14b] from measurements of the kinetic Sunyaev-Zeldovich effect in clusters and is given by $\beta < 8.5 \times 10^{-4}$ at 95% CL on 2 Gpc scales¹. We will devote this chapter to show that a small background bulk velocity, compatible with the *Planck* limit, is able to generate vorticity to source magnetic fields above the dynamo threshold through the Harrison mechanism.

8.2 Electron-proton-photon plasma

8.2.1 Full system

The full electron-proton-photon plasma, including both Coulomb and Thomson scattering, is described by a set of coupled Boltzmann equations

$$\frac{Df_\gamma}{dt} = C_{\gamma e}[f_\gamma] + C_{\gamma p}[f_\gamma], \quad (8.1a)$$

$$\frac{Df_e}{dt} = C_{e\gamma}[f_e] + C_{ep}[f_e], \quad (8.1b)$$

$$\frac{Df_p}{dt} = C_{p\gamma}[f_p] + C_{pe}[f_p]. \quad (8.1c)$$

The evolution of the momentum for each fluid can be found performing the appropriate integral over the phase-space distributions. Defining

$$\frac{DQ_s^i}{d\tau} \equiv 2a^{-4} \int \frac{d^3q}{(2\pi)^3} q^i \frac{Df_s}{d\tau}, \quad s = \gamma, e, p, \quad (8.2)$$

¹The limit (6.260) applies to the *primordial* bulk flow β_0 . In this chapter we use the more conventional bulk flow measured *today* and denote it as β . Note that both parameterizations are perfectly equivalent.

we have

$$\frac{DQ_\gamma^i}{d\tau} = C_{\gamma e}^i + C_{\gamma p}^i, \quad (8.3a)$$

$$\frac{DQ_e^i}{d\tau} = C_{e\gamma}^i + C_{ep}^i, \quad (8.3b)$$

$$\frac{DQ_p^i}{d\tau} = C_{p\gamma}^i + C_{pe}^i, \quad (8.3c)$$

where, as usual, $dt = \alpha(1 - A/2)d\tau$. Additionally, from momentum conservation in Coulomb and Thomson scattering, we have $C_{s_1s_2}^i = -C_{s_2s_1}^i$. The collision term for Thomson scattering in our case is (6.86),

$$C_{\gamma e}^i = \frac{4}{3}\rho_\gamma a n_e \sigma_T \left(\Delta\beta_{\gamma e}^i + \Delta v_{\gamma e}^i + \beta_\gamma^i \delta n_e - \beta_e^i \delta\gamma - \frac{3}{4}\beta_{ej}\pi_\gamma^{ij} - \frac{1}{2}\Delta\beta_{\gamma e}^i A \right). \quad (8.4)$$

The collision term for Thomson scattering between photons and protons can be obtained changing the subscripts $e \rightarrow p$ and $\sigma_T \rightarrow (m_e/m_p)^2\sigma_T$. For the Coulomb coupling we have [FPM11]

$$C_{ep}^i = -e^2 a n_p n_e \eta_C \left(\Delta\beta_{ep}^i + \Delta v_{ep}^i + \Delta\beta_{ep}^i \delta n_e - \beta_e^i \Delta n_{ep} - \frac{1}{2}\Delta\beta_{ep}^i A \right). \quad (8.5)$$

where η_C is the electrical resistivity, that we will introduce later. We have defined, for two species a and b ,

$$\Delta n_{ab} \equiv \delta n_a - \delta n_b, \quad \Delta\beta_{ab}^i \equiv \beta_a^i - \beta_b^i, \quad \Delta v_{ab}^i \equiv \delta v_a^i - \delta v_b^i. \quad (8.6)$$

The left-hand side of the Boltzmann equation is also modified. It can be splitted into the usual geodesic evolution plus a term taking into account the Lorentz force, that can be written as

$$\left(\frac{dq_i}{d\tau} \right)_{\text{EM}} = Q \left(e_i + \varepsilon_{ijk} \frac{q^j}{\epsilon} b^k \right), \quad (8.7)$$

where e_i and b_i are the electric and magnetic components, respectively. These electromagnetic fields are sourced in its turn by the plasma, forming a set of coupled differential equations. Details on the definition of the electromagnetic fields and the Maxwell equations, as well as the Liouville operator with electromagnetic fields, can be consulted in Appendix F.

8.2.2 Electron-proton plasma

We focus now on the electron-proton plasma. We will assume that we have neutrality of charge at the background level, so that $n_p = n_e$.

- *Number density.* Since both Thomson and Coulomb scattering conserve the number of particles, there is no collision term and we have

$$\dot{\delta n}_e + \alpha \delta n_e + \partial_i \delta v_e^i - \delta^{ij} C_{ij} - \mathcal{M}_{\beta_e} = 0, \quad (8.8a)$$

$$\dot{\delta n}_p + \alpha \delta n_p + \partial_i \delta v_p^i - \delta^{ij} C_{ij} - \mathcal{M}_{\beta_p} = 0, \quad (8.8b)$$

where $\alpha \equiv \dot{x}_e/x_e$ and \mathcal{M}_β is defined in (F.38). Subtracting both equations and substituting the metric variables

$$\Delta \dot{n}_{ep} + \alpha \Delta n_{ep} + \Delta \theta_{ep} + i(\Psi + 2\Phi)k_i \Delta \beta_{ep}^i = 0. \quad (8.9)$$

As we have seen, the imaginary parts of the scalars are $\mathcal{O}(\beta)$. Then, to leading order, we get the standard result

$$\Delta \dot{n}_{ep} + \alpha \Delta n_{ep} + \Delta \theta_{ep} = 0. \quad (8.10)$$

- *Momentum.* The velocity evolution is governed by

$$\begin{aligned} m_e n_e \left\{ \dot{\beta}_e^i + (\mathcal{H} + \alpha) \beta_e^i + \delta \dot{v}_e^i + (\mathcal{H} + \alpha) \delta v_e^i + \left(\beta_e^i \delta_k^j + \beta_e^j \delta_k^i \right) \partial_j \delta v_e^k \right. \\ \left. - \frac{1}{2} \partial^i A - \mathcal{M}_{\beta_e}^i + \frac{e}{am_e} (1 + \delta_{n_e}) e^i + \frac{e}{am_e} \varepsilon^i{}_{jk} (\beta_e^j + \delta v_e^j) b^k \right\} \\ = C_{e\gamma}^i + C_{ep}^i, \end{aligned} \quad (8.11)$$

$$\begin{aligned} m_p n_e \left\{ \dot{\beta}_p^i + (\mathcal{H} + \alpha) \beta_p^i + \delta \dot{v}_p^i + (\mathcal{H} + \alpha) \delta v_p^i + \left(\beta_p^i \delta_k^j + \beta_p^j \delta_k^i \right) \partial_j \delta v_p^k \right. \\ \left. - \frac{1}{2} \partial^i A - \mathcal{M}_{\beta_p}^i - \frac{e}{am_p} (1 + \delta_{n_p}) e^i - \frac{e}{am_p} \varepsilon^i{}_{jk} (\beta_p^j + \delta v_p^j) b^k \right\} \\ = C_{p\gamma}^i + C_{pe}^i, \end{aligned} \quad (8.12)$$

where \mathcal{M}_β^i is defined in (F.40). Subtracting both equations, making use of the fact that $m_p \gg m_e$, and using the splitting (F.24) for the electromagnetic fields, we get

$$\begin{aligned} \Delta \dot{\beta}_{ep}^i + (\mathcal{H} + \alpha) \Delta \beta_{ep}^i + \Delta \dot{v}_{ep}^i + (\mathcal{H} + \alpha) \Delta v_{ep}^i - \mathcal{M}_{\Delta \beta_{ep}}^i \\ + \left[\left(\beta_e^i \delta_k^j + \beta_e^j \delta_k^i \right) \partial_j \delta v_e^k - \left(\beta_p^i \delta_k^j + \beta_p^j \delta_k^i \right) \partial_j \delta v_p^k \right] \\ + \frac{e}{am_e} \left(e_{(\beta)}^i + \delta e^i + \delta_{n_e} e_{(\beta)}^i \right) \\ \simeq \frac{1}{m_e n_e} \left(C_{e\gamma}^i + C_{ep}^i \right). \end{aligned} \quad (8.13)$$

This equation can be splitted into three different pieces: bulk velocity, divergence and vorticity. The $\mathcal{O}(\beta)$ contribution is

$$\Delta \dot{\beta}_{ep}^i + (\mathcal{H} + \alpha) \Delta \beta_{ep}^i + \frac{e}{am_e} e_{(\beta)}^i = \frac{4a\rho_\gamma\sigma_T}{3m_e} \Delta \beta_{\gamma e}^i - \frac{ae^2 n_e \eta C}{m_e} \Delta \beta_{ep}^i. \quad (8.14)$$

Taking the divergence and to zeroth order in β

$$\Delta \dot{\theta}_{ep} + (\mathcal{H} + \alpha) \Delta \theta_{ep} + \frac{e}{am_e} i k_i \delta e^i = \frac{4a\rho_\gamma\sigma_T}{3m_e} \Delta \theta_{\gamma e} - \frac{ae^2 n_e \eta C}{m_e} \Delta \theta_{ep}. \quad (8.15)$$

Keeping only the first order in β , the results for the vorticity are

$$\begin{aligned} \Delta \dot{\chi}_{ep}^+ + (\mathcal{H} + \alpha) \Delta \chi_{ep}^+ + \Delta \beta_{ep}^+ (k^2 (B - \dot{E}) - 4\dot{\Phi} + \theta_p) + \beta_e^+ \Delta \theta_{ep} \\ + \frac{e}{am_e} \left(\delta e^+ + \delta_{n_e} e_{(\beta)}^+ \right) \\ = \frac{4a\rho_\gamma\sigma_T}{3m_e} \left(\Delta \chi_{e\gamma}^+ + \beta_\gamma^+ \delta_{n_e} - \beta_e^+ \left(\delta_\gamma + \frac{1}{2} \sigma_\gamma \right) + \Psi \Delta \beta_{e\gamma}^+ \right) \\ - \frac{ae^2 n_e \eta C}{m_e} \left(\Delta \chi_{ep}^+ + \Delta \beta_{ep}^+ \delta_{n_e} - \beta_e^+ \Delta n_{ep} + \Psi \Delta \beta_{ep}^+ \right). \end{aligned} \quad (8.16)$$

An equivalent expression can be found for the opposite helicity.

8.2.3 Maxwell equations

We can particularize the Maxwell equations to our case, using the fact that the vorticity and the imaginary parts for scalars are $\mathcal{O}(\beta)$. At the background level, the only non-trivial Maxwell equation is (F.29)

$$\dot{\mathbf{e}}_{(\beta)} = ea^3 n_e \Delta \boldsymbol{\beta}_{ep} . \quad (8.17)$$

At the perturbation level, we must write the four Maxwell equations (F.30). The first one is

$$\hat{k} \cdot \delta \mathbf{e} = -\frac{ea^3 n_e}{ik} \Delta n_{ep} - S_{\partial e} , \quad (8.18)$$

$$S_{\partial e} \equiv (\Psi + 2\Phi) e_{(\beta)}^3 . \quad (8.19)$$

The second one, for both helicities, is²

$$\delta \dot{e}^\pm \mp kb^\pm = ea^3 n_e \Delta \chi_{ep}^\pm + S_e^\pm , \quad (8.20)$$

$$S_e^\pm \equiv (\dot{\Psi} + 2\dot{\Phi} - k^2(B - \dot{E})) e_{(\beta)}^\pm + 2ea^3 n_e \Psi \Delta \beta_{ep}^\pm . \quad (8.21)$$

The third Maxwell equation for both helicities is

$$\delta \dot{b}^\pm \pm k \delta e^\pm = S_b^\pm , \quad (8.22)$$

$$S_b^\pm \equiv \pm k \Phi e_{(\beta)}^\pm . \quad (8.23)$$

Finally, the last equation is

$$\hat{k} \cdot \delta \mathbf{b} = 0 . \quad (8.24)$$

8.2.4 Time scales

It is very important to notice that there are several, widely different, time scales in the problem. The most relevant for the scattering processes are listed below³.

- *Electrical resistivity.*

$$\eta \equiv \frac{\eta_C}{a} = \frac{\pi e^2 \sqrt{m_e} \log \Lambda}{\alpha T^{3/2}} \simeq 10^{-9} \text{ s} \left(\frac{1+z}{10^3} \right)^{-1/2} \left(\frac{\log \Lambda}{10} \right) . \quad (8.25)$$

In this work, the Coulomb logarithm [Jac98] is taken to be $\log \Lambda = 10$.

- *Coulomb time scale.*

$$\tau_C \equiv \frac{m_e}{ae^2 n_e \eta_C} \simeq \frac{2 \times 10^4 \text{ s}}{x_e} \left(\frac{1+z}{10^3} \right)^{-1/2} . \quad (8.26)$$

- *Thomson time scale.*

$$\tau_T \equiv \frac{m_e}{a \sigma_T \rho_\gamma} \simeq 5 \times 10^{11} \text{ s} \left(\frac{1+z}{10^3} \right)^{-3} . \quad (8.27)$$

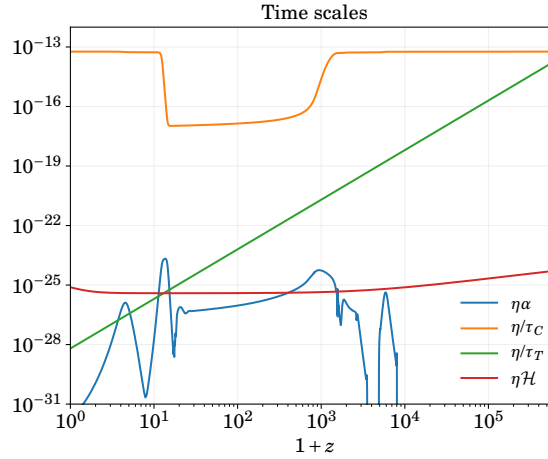


Figure 8.1: Relevant time scales for the problem.

There are other time scales in the problem, like the cosmological ones, \mathcal{H}^{-1} and $k^{-1} \simeq 10^{14} \text{ s}$ (Mpc^{-1}/k), or the time scale of recombination $\alpha = \dot{x}_e/x_e$. The different time scales, relative to η , are depicted in Figure 8.1. It is clear that there is a strong hierarchy of scales, with $\eta \ll \tau_C \ll \tau_T, \mathcal{H}^{-1}, \alpha^{-1}$. This circumstance will prove very convenient to find approximate solutions in the next section.

8.2.5 Evolution of subsystems

The evolution of the proton-electron-photon plasma can be splitted into three subsystems. They can be arranged in such a way that each subsystem does not back-react on the previous one. Moreover, the strong hierarchy of scales will allow us to find approximate solutions. The strategy can be summarized as follows.

- I) Find $\Delta \boldsymbol{\beta}_{ep}$ and $\mathbf{e}_{(\beta)}$.
- II) Find $\Delta \theta_{ep}$, Δn_{ep} and $\hat{k} \cdot \delta \mathbf{e}$.
- III) Find $\Delta \chi_{ep}^{\pm}$ and δe^{\pm} .
- IV) Use δe^{\pm} to compute the magnetic field produced.

At this point it is convenient to redefine the electromagnetic fields as

$$\mathcal{E}^i \equiv \frac{\delta e^i}{C}, \quad \mathcal{E}_{(\beta)}^i \equiv \frac{e_{(\beta)}^i}{C}, \quad \mathcal{B}^i \equiv \frac{\delta b^i}{C}, \quad C \equiv ea^{5/2}n_e\tau_C, \quad (8.28)$$

where $\dot{C} = 0$ in a matter-dominated universe⁴. We also have

$$\frac{e}{am_e} \delta e^i = \frac{1}{a^{1/2}\eta} \mathcal{E}^i. \quad (8.29)$$

²We have used $\varepsilon^{\pm jk} \partial_j b_k \rightarrow \pm k b^{\pm}$.

³Following [FPM11], for the numerical estimates we assume a matter-dominated universe.

⁴Even if we are in a radiation-dominated universe $\dot{C} = \mathcal{O}(\mathcal{H})$ and we will learn in this section that this kind of terms can be safely neglected.

Additionally, we can write

$$\mathcal{E}_{(\beta)} = \mathcal{E}_{(\beta)} \hat{\beta}, \quad (8.30a)$$

$$\begin{aligned} \mathcal{E} &= \mathcal{E}^\perp ((\hat{\beta} \cdot \hat{e}_+) \hat{e}_- + (\hat{\beta} \cdot \hat{e}_-) \hat{e}_+) + \mathcal{E}^\parallel \hat{k} \\ &= \mathcal{E}^\perp (\hat{\beta} - (\hat{\beta} \cdot \hat{k}) \hat{k}) + \mathcal{E}^\parallel \hat{k}, \end{aligned} \quad (8.30b)$$

$$\begin{aligned} \mathcal{B} &= \mathcal{B} ((\hat{\beta} \cdot \hat{e}_+) \hat{e}_- - (\hat{\beta} \cdot \hat{e}_-) \hat{e}_+) \\ &= i \mathcal{B} (\hat{\beta} \wedge \hat{k}). \end{aligned} \quad (8.30c)$$

as we did for the vorticity in (6.188). Finally, as we will see, the equations that we obtain are the standard ones for a charged plasma plus two kind of sources. The first type arises from the additional interaction of electrons with photons (Thomson dragging)

$$\mathcal{T}_\beta \equiv \frac{4}{3\tau_T} \Delta \beta_{\gamma e}, \quad (8.31a)$$

$$\mathcal{T}_\theta \equiv \frac{4}{3\tau_T} \Delta \theta_{\gamma e}, \quad (8.31b)$$

$$\mathcal{T}_\chi \equiv \frac{4}{3\tau_T} \left(\Delta \chi_{\gamma e} + \beta_\gamma \delta_{n_e} - \beta_e \left(\delta_\gamma + \frac{1}{2} \sigma_\gamma \right) + \Psi \Delta \beta_{\gamma e} \right). \quad (8.31c)$$

The second type of sources comes from the modifications $\mathcal{O}(\beta)$ in the evolution equations

$$\mathcal{S}_{\partial \mathcal{E}} \equiv (\Psi + 2\Phi) \mathcal{E}_{(\beta)}, \quad (8.32a)$$

$$\mathcal{S}_\mathcal{E} \equiv (\dot{\Psi} + 2\dot{\Phi} - k^2(\mathcal{B} - \dot{\mathcal{E}})) \mathcal{E}_{(\beta)} + \frac{2a^{1/2}}{\tau_C} \Psi \Delta \beta_{ep}, \quad (8.32b)$$

$$\mathcal{S}_\mathcal{B} \equiv k\Phi \mathcal{E}_{(\beta)}, \quad (8.32c)$$

$$\begin{aligned} \mathcal{S}_\chi &\equiv \beta_e \Delta \theta_{ep} + \Delta \beta_{ep} (\theta_p - 4\dot{\Phi} + k^2(\mathcal{B} - \dot{\mathcal{E}})) + \frac{1}{a^{1/2}\eta} \delta_{n_e} \mathcal{E}_{(\beta)} \\ &\quad + \frac{1}{\tau_C} (\Delta \beta_{ep} \delta_{n_e} - \beta_e \Delta n_{ep} + \Psi \Delta \beta_{ep}). \end{aligned} \quad (8.32d)$$

Now, we can proceed to solve the subsystems.

Bulk velocity

The evolution of the bulk velocity difference obeys

$$\Delta \dot{\beta}_{ep} + \left(\frac{1}{\tau_C} + \alpha + \mathcal{H} \right) \Delta \beta_{ep} + \frac{1}{a^{1/2}\eta} \mathcal{E}_{(\beta)} = \mathcal{T}_\beta, \quad (8.33a)$$

$$\dot{\mathcal{E}}_{(\beta)} - \frac{a^{1/2}}{\tau_C} \Delta \beta_{ep} = 0. \quad (8.33b)$$

It can be rewritten in matrix form

$$\frac{d}{d\tau} \begin{pmatrix} \Delta \beta_{ep} \\ \mathcal{E}_{(\beta)} \end{pmatrix} = - \overbrace{\begin{pmatrix} \gamma & \frac{1}{\eta} \\ -\frac{1}{\tau_C} & 0 \end{pmatrix}}^{\mathcal{M}} \begin{pmatrix} \Delta \beta_{ep} \\ \mathcal{E}_{(\beta)} \end{pmatrix} + \begin{pmatrix} \mathcal{T}_\beta \\ 0 \end{pmatrix}, \quad (8.34)$$

where

$$\gamma \equiv \frac{1}{\tau_C} + \alpha + \mathcal{H}, \quad \tilde{\eta} \equiv a^{1/2}\eta, \quad \tilde{\tau}_C \equiv a^{-1/2}\tau_C. \quad (8.35)$$

The eigenvalues of \mathcal{M} are

$$\lambda_{\pm} = \pm \frac{i}{\sqrt{\eta\tau_C}} + \frac{1}{2}\gamma \mp \frac{i\gamma^2\sqrt{\eta\tau_C}}{8} + \mathcal{O}(\eta). \quad (8.36)$$

The homogeneous solution oscillates with frequency $\omega = 1/\sqrt{\eta\tau_C}$ and is exponentially damped with characteristic time γ^{-1} . We can invert \mathcal{M}

$$\mathcal{M}^{-1} = \begin{pmatrix} 0 & -\tilde{\tau}_C \\ \tilde{\eta} & \gamma\tilde{\eta}\tilde{\tau}_C \end{pmatrix} \rightarrow \mathcal{M}^{-2} = \begin{pmatrix} -\tilde{\eta}\tilde{\tau}_C & -\gamma\tilde{\eta}\tilde{\tau}_C^2 \\ \gamma\tilde{\eta}^2\tilde{\tau}_C & \gamma^2\tilde{\eta}^2\tilde{\tau}_C^2 - \tilde{\eta}\tilde{\tau}_C \end{pmatrix}, \quad (8.37)$$

and then look for a particular solution

$$\begin{aligned} \begin{pmatrix} \Delta\beta_{ep} \\ \mathcal{E}_{(\beta)} \end{pmatrix} &= \mathcal{M}^{-1} \begin{pmatrix} \mathcal{T}_{\beta} \\ 0 \end{pmatrix} - \mathcal{M}^{-1} \frac{d}{d\tau} \begin{pmatrix} \Delta\beta_{ep} \\ \mathcal{E}_{(\beta)} \end{pmatrix} \\ &= \mathcal{M}^{-1} \begin{pmatrix} \mathcal{T}_{\beta} \\ 0 \end{pmatrix} - \mathcal{M}^{-1} \frac{d}{d\tau} (\mathcal{M}^{-1}) \begin{pmatrix} \mathcal{T}_{\beta} \\ 0 \end{pmatrix} - \mathcal{M}^{-2} \frac{d}{d\tau} \begin{pmatrix} \mathcal{T}_{\beta} \\ 0 \end{pmatrix} \\ &\quad + \mathcal{M}^{-2} \frac{d^2}{d\tau^2} \begin{pmatrix} \Delta\beta_{ep} \\ \mathcal{E}_{(\beta)} \end{pmatrix} + \mathcal{M}^{-1} \frac{d}{d\tau} (\mathcal{M}^{-1}) \frac{d}{d\tau} \begin{pmatrix} \Delta\beta_{ep} \\ \mathcal{E}_{(\beta)} \end{pmatrix}. \end{aligned} \quad (8.38)$$

Neglecting the time-scale of recombination and the expansion of the Universe we have $\gamma \simeq 1/\tau_C$ and $\frac{d}{d\tau}(\mathcal{M}^{-1}) \simeq 0$. Under these conditions

$$\begin{aligned} \begin{pmatrix} \Delta\beta_{ep} \\ \mathcal{E}_{(\beta)} \end{pmatrix} &\simeq \mathcal{M}^{-1} \begin{pmatrix} \mathcal{T}_{\beta} \\ 0 \end{pmatrix} - \mathcal{M}^{-2} \begin{pmatrix} \dot{\mathcal{T}}_{\beta} \\ 0 \end{pmatrix} + \mathcal{O}(\eta^2) \\ &\simeq \begin{pmatrix} 0 \\ \tilde{\eta}\mathcal{T}_{\beta} \end{pmatrix} + \begin{pmatrix} \tilde{\eta}\tilde{\tau}_C\dot{\mathcal{T}}_{\beta} \\ 0 \end{pmatrix} + \mathcal{O}(\eta^2). \end{aligned} \quad (8.39)$$

Finally, we have the following particular solution

$$\Delta\beta_{ep} \simeq \eta\tau_C\dot{\mathcal{T}}_{\beta} + \mathcal{O}(\eta^2), \quad (8.40a)$$

$$\mathcal{E}_{\beta} \simeq a^{1/2}\eta\mathcal{T}_{\beta} + \mathcal{O}(\eta^2), \quad (8.40b)$$

and, in particular,

$$e_{(\beta)} = \frac{4a^2\sigma_T\rho_{\gamma}}{3e}\Delta\beta_{\gamma e}. \quad (8.41)$$

Number density

The three equations governing the charge separation are

$$\Delta\dot{\theta}_{ep} + \left(\frac{1}{\tau_C} + \alpha + \mathcal{H}\right)\Delta\theta_{ep} + \frac{ik}{a^{1/2}\eta}\mathcal{E}^{\parallel} = \mathcal{T}_{\theta}, \quad (8.42a)$$

$$\Delta\dot{n}_{ep} + \alpha\Delta n_{ep} + \Delta\theta_{ep} = 0, \quad (8.42b)$$

$$\mathcal{E}^{\parallel} + \frac{a^{1/2}}{ik\tau_C}\Delta n_{ep} + \mathcal{S}_{\partial}\mathcal{E} = 0. \quad (8.42c)$$

We can reduce the system reintroducing \mathcal{E}^\parallel in the first equation. In this case we see that we can actually neglect $\mathcal{S}_{\partial\mathcal{E}}$ since only the imaginary parts of the scalars contribute, i.e. its contribution is $\mathcal{O}(\beta^2)$. The new system is

$$\Delta\dot{n}_{ep} + \alpha\Delta n_{ep} + \Delta\theta_{ep} = 0, \quad (8.43a)$$

$$\Delta\dot{\theta}_{ep} + \left(\frac{1}{\tau_C} + \alpha + \mathcal{H}\right)\Delta\theta_{ep} - \frac{1}{\tau_C\eta}\Delta n_{ep} = \mathcal{T}_\theta. \quad (8.43b)$$

Written in matrix form

$$\frac{d}{d\tau} \begin{pmatrix} \Delta n_{ep} \\ \Delta\theta_{ep} \end{pmatrix} = - \overbrace{\begin{pmatrix} \alpha & 1 \\ -\frac{1}{\eta\tau_C} & \gamma \end{pmatrix}}^{\mathcal{M}_\theta} \begin{pmatrix} \Delta n_{ep} \\ \Delta\theta_{ep} \end{pmatrix} + \begin{pmatrix} 0 \\ \mathcal{T}_\theta \end{pmatrix}. \quad (8.44)$$

The eigenvalues of \mathcal{M}_θ are

$$\lambda_\pm = \pm \frac{i}{\sqrt{\eta\tau_C}} + \frac{1}{2}\gamma + \mathcal{O}(\sqrt{\eta}). \quad (8.45)$$

The homogeneous solution has the same behaviour as the velocity difference. Following the same steps as in the previous section, we find the particular solution

$$\Delta n_{ep} \simeq -\eta\tau_C\mathcal{T}_\theta + \mathcal{O}(\eta^2), \quad (8.46a)$$

$$\Delta\theta_{ep} \simeq \eta\tau_C\dot{\mathcal{T}}_\theta + \mathcal{O}(\eta^2). \quad (8.46b)$$

Vorticity

The whole system is

$$\Delta\dot{\chi}_{ep} + \left(\frac{1}{\tau_C} + \alpha + \mathcal{H}\right)\Delta\chi_{ep} + \frac{1}{\alpha^{1/2}\eta}\mathcal{E}^\perp = \mathcal{T}_\chi - \mathcal{S}_\chi, \quad (8.47a)$$

$$\dot{\mathcal{E}}^\perp - k\mathcal{B} - \frac{\alpha^{1/2}}{\tau_C}\Delta\chi_{ep} = \mathcal{S}_\mathcal{E}, \quad (8.47b)$$

$$\dot{\mathcal{B}} + k\mathcal{E}^\perp = \mathcal{S}_\mathcal{B}. \quad (8.47c)$$

We can actually neglect the backreaction of the magnetic field⁵ so the system can be reduced to

$$\frac{d}{d\tau} \begin{pmatrix} \Delta\chi_{ep} \\ \mathcal{E}^\perp \end{pmatrix} = - \begin{pmatrix} \gamma & \frac{1}{\eta} \\ -\frac{1}{\tau_C} & 0 \end{pmatrix} \begin{pmatrix} \Delta\chi_{ep} \\ \mathcal{E}^\perp \end{pmatrix} + \begin{pmatrix} \mathcal{T}_\chi - \mathcal{S}_\chi \\ \mathcal{S}_\mathcal{E} \end{pmatrix}. \quad (8.48)$$

The homogeneous solution is the same as for the β system. The particular solution is

$$\Delta\chi_{ep} \simeq -\alpha^{-1/2}\tau_C\mathcal{S}_\mathcal{E} + \eta\tau_C(\dot{\mathcal{T}}_\chi - \dot{\mathcal{S}}_\chi) + \alpha^{-1/2}\eta\tau_C\dot{\mathcal{S}}_\mathcal{E} + \mathcal{O}(\eta^2), \quad (8.49a)$$

$$\mathcal{E}^\perp \simeq \alpha^{1/2}\eta(\mathcal{T}_\chi - \mathcal{S}_\chi) + \eta\mathcal{S}_\mathcal{E} + \eta\tau_C\dot{\mathcal{S}}_\mathcal{E} + \mathcal{O}(\eta^2). \quad (8.49b)$$

⁵This can be justified writing first the equation for $\dot{\mathcal{E}}^\perp$. Under our approximation scheme ($\eta \ll k^{-1}$) the effect of the magnetic field is equivalent to the change $\mathcal{T}_\chi - \mathcal{S}_\chi \rightarrow \mathcal{T}_\chi - \mathcal{S}_\chi + \alpha^{-1/2}k\tau_C\mathcal{S}_\mathcal{B}$. This new term would be second order in the final results, so we can neglect it altogether.

Plugging in the previous results, we have

$$\begin{aligned} \mathcal{S}_\chi &\simeq \delta_{n_e} \mathcal{T}_\beta + \eta \left(\dot{\mathcal{T}}_\beta \delta_{n_e} + \beta_e \mathcal{T}_\theta \right) + \eta \tau_C \beta_e \dot{\mathcal{T}}_\theta \\ &\quad + \eta \tau_C \dot{\mathcal{T}}_\beta (k^2(B - \dot{E}) - 4\dot{\Phi} + \theta_p) + \mathcal{O}(\eta^2) , \end{aligned} \quad (8.50a)$$

$$\mathcal{S}_\mathcal{E} \simeq a^{1/2} \eta (\dot{\Psi} + 2\dot{\Phi} - k^2(B - \dot{E})) \mathcal{T}_\beta + 2a^{1/2} \eta \Psi \dot{\mathcal{T}}_\beta + \mathcal{O}(\eta^2) , \quad (8.50b)$$

$$\mathcal{S}_\mathcal{B} \simeq a^{1/2} \eta k \Phi \mathcal{T}_\beta + \mathcal{O}(\eta^2) , \quad (8.50c)$$

and finally

$$\Delta \chi_{ep} \simeq \eta \tau_C \left\{ \dot{\mathcal{T}}_\chi - \dot{\mathcal{T}}_\beta \beta_\gamma (\delta_{n_e} + 2\Psi) - \mathcal{T}_\beta (\dot{\Psi} + 2\dot{\Phi} - k^2(B - \dot{E}) + \delta_{n_e}) \right\} + \mathcal{O}(\eta^2) , \quad (8.51a)$$

$$\mathcal{E}^\perp \simeq a^{1/2} \eta (\mathcal{T}_\chi - \delta_{n_e} \mathcal{T}_\beta) + \mathcal{O}(\eta^2) . \quad (8.51b)$$

Now we can use the third equation (8.47c) to compute the magnetic field produced

$$\begin{aligned} \dot{\mathcal{B}} &= -k \mathcal{E}^\perp + \mathcal{S}_\mathcal{B} \\ &= -a^{1/2} k \eta (\mathcal{T}_\chi - \mathcal{T}_\beta (\delta_{n_e} + \Phi)) , \end{aligned} \quad (8.52)$$

with

$$\mathcal{T}_\beta = \frac{4}{3\tau_T} \Delta \beta_{\gamma e} , \quad (8.53a)$$

$$\mathcal{T}_\chi = \frac{4}{3\tau_T} \left(\Delta \chi_{\gamma e} + \beta_\gamma \delta_{n_e} - \beta_e \left(\delta_\gamma + \frac{1}{2} \sigma_\gamma \right) + \Delta \beta_{\gamma e} \Psi \right) . \quad (8.53b)$$

8.3 Magnetic field production

Before moving on to the computation of the magnetic field produced, let us summarize what we have learnt in the previous sections. In the first place, we have seen that the evolution of electromagnetic fields and the velocity difference between electrons and protons are described by a coupled system of differential equations. This system contains different time scales, where the electrical resistivity η is by far the shortest, see (8.25). This allowed us to simplify the discussion, finding only the leading $\mathcal{O}(\eta)$ behaviour.

The three subsystems that we identified in Section 8.2.5, describing the electron-proton velocity difference, show a similar behaviour. The homogeneous part of these subsystems (without the sources \mathcal{T}) corresponds to the usual electron-proton plasma (without photons). There is an equilibrium configuration for the electron-proton plasma where the electric field is zero and there is no charge separation. If the system is placed out of this equilibrium configuration, an electric field is created in response, acting as a restoring force. These homogeneous solutions oscillate with characteristic frequency $\omega \simeq 1/\sqrt{\eta\tau_C}$ and are damped with a damping coefficient $\Gamma \simeq 1/2\tau_C$.

The presence of photons modifies this picture. Due to the large mass difference, $m_p \gg m_e$, the Thomson coupling of photons to electrons is much more effective than to protons, producing a differential dragging and introducing the sources \mathcal{T} in the electron-proton-photon plasma. The particular solutions of this system are

proportional to the sources, see (8.40, 8.46, 8.51), that in its turn are proportional to the velocity difference between photons and baryons. This is the essence of the Harrison mechanism: the Thomson dragging of the photons produces an electric field proportional to the photon-baryon velocity difference.

Cosmological bulk flows introduce two important differences with respect to Λ CDM. First of all, a homogeneous electric field is generated, pointing in the bulk flow direction and with an amplitude

$$\mathbf{E}_{(\beta)} \equiv a^{-2} \mathbf{e}_{(\beta)} = \frac{4\sigma_T \rho_\gamma}{3e} \Delta\beta_{\gamma e}. \quad (8.54)$$

Its evolution is represented in Figure 8.2. The detection of this weak field would

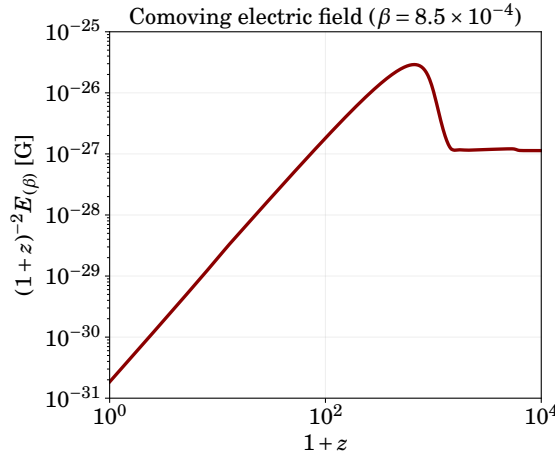


Figure 8.2: Comoving electric field at the background level.

be a smoking gun of the model, but its amplitude seems too small to have any observable effect. However, the most important difference with respect to Λ CDM is that now we have non-decaying vortical motions in the plasma, so can use the Harrison mechanism through (8.52) to produce magnetic fields. Rewritten in terms of the physical magnetic field $B \equiv a^{-2} \delta b$, and working in the Newtonian gauge, the final equation governing the magnetic field production is

$$\frac{d}{d\tau}(a^2 B) = -\frac{4a^2 k \sigma_T \rho_\gamma}{3e} \left(\Delta\chi_{\gamma e} + \beta_e \left(\delta_{n_e} - \delta_\gamma - \frac{1}{2} \sigma_\gamma \right) + \Delta\beta_{\gamma e} (\Psi - \Phi) \right). \quad (8.55)$$

This expression generalizes the Harrison mechanism to the case in which there are bulk flows in the plasma. It is also analogous to the one obtained in previous studies of production of magnetic fields in second order cosmological perturbation theory [FPM11; Sag+15]. As in previous chapters, the scalar perturbations follow the Λ CDM evolution while the behaviour of the bulk velocities is represented in Figure 6.1. The vorticity $\Delta\chi_{\gamma e}$ is computed by solving the Boltzmann hierarchy (6.119-6.122) truncated at $\ell_{\max} = 1000$.

The magnetic field power spectrum is defined by

$$\langle B_i(z, \mathbf{k}) B_j^*(z, \mathbf{k}') \rangle = (2\pi)^3 \delta(\mathbf{k} - \mathbf{k}') (\hat{\beta} \wedge \hat{k})_i (\hat{\beta} \wedge \hat{k})_j P_B(z, k), \quad (8.56)$$

as

$$P_B(z, k) = |T_B(z, k)|^2 \frac{2\pi^2}{k^3} \mathcal{P}_{\mathcal{R}}(k), \quad (8.57)$$

where $\mathcal{P}_{\mathcal{R}}(k)$ is the usual nearly scale-invariant primordial curvature power spectrum and $T_B(z, k)$ is the magnetic field transfer function computed using (8.55). In Figure 8.3 the comoving magnetic field $(1+z)^{-2}|T_B|\mathcal{P}_{\mathcal{R}}^{1/2}$ is plotted as a function of redshift and scale.

There are two points worth emphasizing. On the one hand, the magnetic power spectrum on small and large scales has a power-law behaviour

$$\sqrt{k^3 P_B(z < 100, k)} \propto \begin{cases} k^{1.2}, & k \gg 0.1 \text{ Mpc}^{-1}, \\ k^{2.8}, & k \ll 0.1 \text{ Mpc}^{-1}, \end{cases} \quad (8.58)$$

so that the magnetic field is steeply rising as $k^{1.2}$ on small scales, until the turbulence scale kicks in. On the other hand, the comoving magnetic field is continuously produced, with an important boost at recombination and remaining essentially constant for $z < 100$.

Following [FPM11], we also define the magnetic field smoothed over a comoving scale L as

$$B_L^2(z) = \frac{1}{2\pi^2} \int_0^\infty dk k^2 P_B(z, k) \exp\left(-\frac{k^2 L^2}{2}\right). \quad (8.59)$$

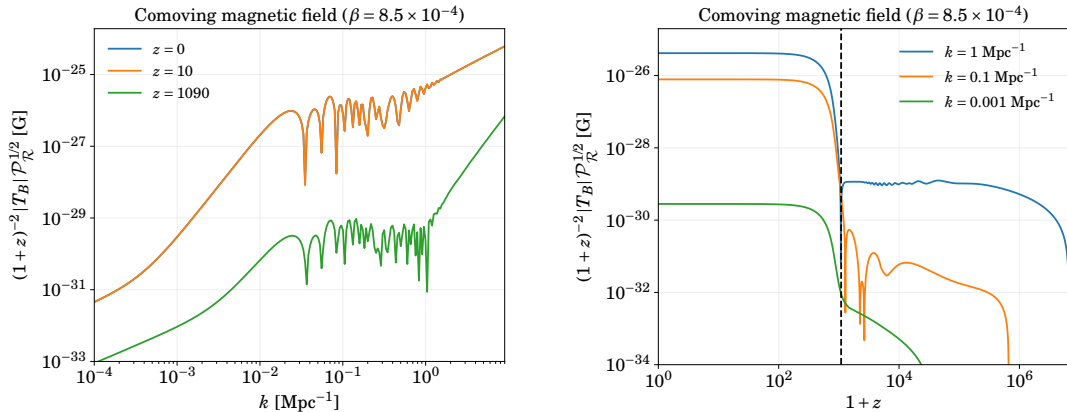


Figure 8.3: (Left) Comoving magnetic field as a function of the scale for different redshifts. Notice that the $z = 0$ and $z = 10$ curves overlap. Even though there is an important production immediately after decoupling, afterwards the comoving magnetic field is constant at all scales and it is not affected by reionization. (Right) Comoving magnetic field as a function of the redshift for different scales. The magnetic field presents some features inherited from the acoustic oscillations before decoupling. The main production takes place during and immediately after decoupling. Once the photon-baryon plasma is decoupled, the comoving magnetic field is constant.

The magnetic field B_L at the time of galaxy formation $z_{\text{gf}} = 10$ is depicted in Figure 8.4. The numerical computation of the transfer function becomes harder for smaller scales, and some of the usual approximations in CMB calculations cannot be trusted for scales $k > 10 \text{ Mpc}^{-1}$ [BLT11]. Therefore, we only compute the spectrum

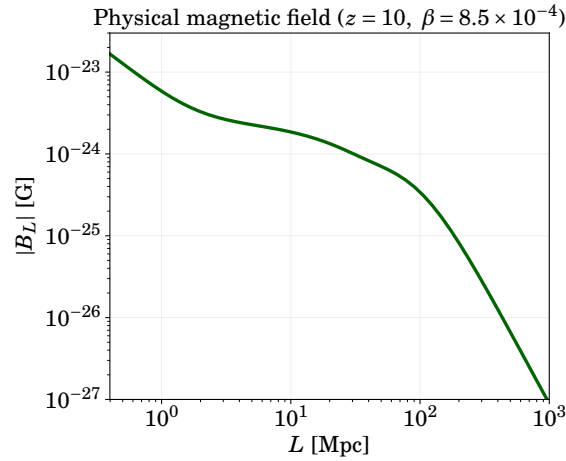


Figure 8.4: Physical magnetic field smoothed over a given scale L . It is evaluated at a redshift $z = 10$, where the dynamo mechanism should begin to operate [Wid02]. Since the comoving field is constant at late times, the results can be easily rescaled to any redshift.

up to scales $k = 9 \text{ Mpc}^{-1}$. The field B_L can be well approximated as a power law at small scales, yielding the approximate result

$$|B_L(z < 100)| \simeq 5.7 \times 10^{-24} \text{ G} \left(\frac{L}{\text{Mpc}} \right)^{-1.2} \left(\frac{1+z}{11} \right)^2 \left(\frac{\beta}{8.5 \times 10^{-4}} \right), \quad (8.60)$$

for $L < 1 \text{ Mpc}$ where β is the relative bulk velocity between photons and baryons (today). These results show that, although the field seems too weak to directly account for the intergalactic magnetic fields or magnetic fields in voids, the mechanism proposed provides a seed field large enough to potentially explain the galactic magnetic fields, after a suitable dynamo amplification.

III

CONCLUSIONS AND APPENDICES

Concluding remarks

This thesis has probed the viability of three different dark-sector models, that are representative examples of three different approaches to a cosmology beyond Λ CDM.

I) *Hidden gravitons*. In this work, we have derived constraints on the mass and coupling strength of an additional massive graviton. These new spin-2 particles are a generic feature of different extensions of the gravitational sector. In our analysis, we have introduced hidden gravitons in the simplest way: as an additional field described by a linear Fierz-Pauli Lagrangian. In addition to the standard fifth-force tests, we have worked out in detail the emission of these hidden gravitons from different astrophysical objects. The computed emission rates allow us to place limits on the parameters of the theory, to avoid anomalies in the observed energy-loss rates. The most important channels in the Sun and red giants are the Compton and the bremsstrahlung processes. However, in the supernova case, these processes are suppressed for two reasons: I) the electron gas is degenerated and the Pauli blocking becomes very efficient, II) the electric field created by the nucleus is screened, an effect that we have neglected for the other stars but that suppress decisively the bremsstrahlung emission in supernovae. Also in this case, there is an appreciable number of positrons in the medium, but their overall contribution to the energy loss turns out to be negligible. The dominant process, at these nuclear densities, turns out to be nucleon-nucleon bremsstrahlung, mediated by the strong interaction. In all the stars the photon-photon process, which is forbidden for massless gravitons, is found to be relevant.

The astrophysical bounds complement the fifth-force constraints and are orders of magnitude more competitive than other restrictions in the same range of masses, like tests on atomic systems [MT15]. Further work in this direction would involve a full numerical analysis and a modification of the stellar models. This kind of study has already been carried out in the case of axions and it would help to refine the constraints and clarify the impact on the stellar structure, as a novel form of energy transfer for large coupling strengths. Following the analogy with the axion case, another effect that might be relevant in our range of masses is the mixing of the hidden graviton with photons in electromagnetic fields [RS88]. This effect was originally studied for axions and massless gravitons, while in [BMR09] the analysis was extended to the massive-graviton case. The results of light-shining-through-walls experiments, that have been already used to place limits on the axion and hidden-photon properties, could be adapted to our case and may strengthen the constraints in a narrow range of masses.

II) *Repulsive fuzzy dark matter*. In this work we have studied the cosmological

effects of a repulsive self-coupling in a model of ultralight dark matter. As expected, if the coupling is small enough we recover the usual results for fuzzy dark matter: the scalar field starts its evolution frozen and then transitions to a phase where it is rapidly oscillating and behaves (on average) as CDM. On the other hand, if the quartic self-interaction is large, a new background phase appears. As the scalar field rolls down the potential and starts oscillating, it behaves first as radiation (on average) until finally settling down on the usual matter phase.

At the perturbation level, FDM models lead to a suppression of growth at small scales, as compared with CDM. We found that the self-interaction enhances this effect. This result could have been naively anticipated, since the quartic interaction introduces an additional source of pressure in the dark matter fluid. Interestingly enough, we also found that the large-scale structure results for a given FDM model (mass term only) can be mimicked by a repulsive FDM model (mass and quartic self-interaction) with a *higher* mass.

So far, we have only analyzed linear observables, but in fact larger effects on non-linear scales are expected. The available parameter space could be further constrained in the future using cosmological information with non-linear observables, as more simulations with ultralight fields become available. Even without non-linear information, using the aforementioned equivalence at the linear level, one could put forward the proposal that similar results on non-linear structure formation could be obtained for higher masses with a positive λ . For instance, results for $\tilde{m} = 10^{-22}$ eV might be reproduced with masses $m \simeq 10^{-5}$ eV adding a self-interaction of the order of $\lambda \simeq 10^{-24}$. Nevertheless, a definitive answer to this suggestive proposal requires a fully non-linear analysis.

III) *Cosmological bulk flows.* In this work we have developed the theoretical framework needed to analyze the cosmology of non-comoving fluids. We have shown that it is possible to relax one of the underlying assumptions of Λ CDM, comoving CMB and matter frames, while retaining a homogeneous and isotropic universe. The main ingredients of the model can be succinctly summarized as follows.

- If there exists a primordial bulk flow ($\beta \ll 1$) between the dark and the visible sectors, it is possible to define a *cosmic center of mass* frame that observes a RW background (up to corrections $\mathcal{O}(\beta^2)$). The model is characterized by a single additional free parameter. We take it to be the velocity of the visible sector with respect to the cosmic center of mass frame deep in the radiation era (β_0). Using *Planck* data, a conservative limit to be in agreement with all observations is $\beta_0 < 1.6 \times 10^{-3}$.
- The subsequent evolution gives rise to relative velocities between all the different components of the visible sector, e.g. between baryons and photons, even if they were initially comoving.

The background behaviour is the usual FLRW, but the couplings between the background bulk flows and the perturbations lead to a modified evolution. To

first order in the bulk flows, i.e. $\mathcal{O}(\beta)$, we reproduce the usual Λ CDM results for the main cosmological observables, like the matter power spectrum and the CMB temperature power spectrum. We find that, while the effects on the autocorrelation spectra are $\mathcal{O}(\beta^2)$, there are $\mathcal{O}(\beta)$ corrections on every cross-correlation between scalar perturbations. Additionally, these corrections present a dipolar pattern, producing deviations from statistical isotropy. We have observed that the additional contributions to the cross-correlation spectra become important for small scales.

A similar pattern of statistical anisotropy of order β arises in the CMB two-point function. Even though it is still under study, it may alleviate the tension that seems to arise when interpreting the anisotropic signal in the CMB as a pure kinematical effect [Ade+16b]. This tension corresponds to the dipolar modulation anomaly [Buc+16; Sch+16] that arises when analyzing low multipoles. The modulation points in a direction different from the kinematic dipole and seems to have a larger amplitude [Akr+19].

Another distinctive feature of this model is the production of vorticity, which is absent in Λ CDM. The relative motion of the fluids induces $\mathcal{O}(\beta)$ couplings between scalar and vector modes. This in its turn leads to the production of vorticity and vector metric perturbations, sourced by the scalar modes. This vector contribution also leaves a characteristic imprint in the velocity spectrum, with a statistically anisotropic quadrupolar modulation. The tensor modes that would be induced by scalar and vector perturbations are $\mathcal{O}(\beta^2)$.

More importantly, the production of vorticity in the photon-baryon plasma opens an avenue for the creation of magnetic fields. The origin of the galactic magnetic fields is a long-standing open question. The Harrison mechanism is a production mechanism that needs vorticity in the photon-baryon plasma to operate, but unfortunately it is absent in Λ CDM to first order in cosmological perturbation theory. Several studies have proven that in second-order cosmological perturbation theory vorticity and magnetic fields are created, but with an amplitude far too small to act as seed fields for the galactic dynamo amplification mechanism [Tak+05; FPM11; Sag+15]. Our setup is similar in some regards to a second order computation, but our relevant scale β_0 is larger than a typical cosmological perturbation and so it is our vorticity production. While being consistent with all observations, we produce magnetic fields that might be large enough to account for the origin of the observed galactic fields. The spectrum also has a distinctive tensor structure, related to the direction of the bulk flow, that could be further probed.

One direction for future work involves extending our analysis up to very early times. In this work we have treated the dark sector as a whole and we have only assumed that, while it behaves as CDM at late times, it is subdominant with respect to radiation at early times, at least during the period of interest. However, as pointed out before, at very early times some DM scenarios may induce $\mathcal{O}(\beta)$ anisotropic corrections on the background. These corrections are not sourced at later times, where the analysis of the present work holds, so their observation could be challenging. To extend the study in this direction or

to go one step further and find $\mathcal{O}(\beta^2)$ contributions would force us to include corrections over the background geometry. In particular, the lowest order corrections arising from the exact Bianchi geometry describing our configuration of moving fluids. Our present results can be interpreted as the zeroth order of a two-parameter expansion, where in addition to the standard cosmological perturbations the background contains corrections over RW. To tackle this kind of problems, a general N -parameter perturbation scheme has been developed [SBG04] and successfully applied to take into account the leading order effects of non-linear structures [GCM17]. It is important to keep in mind that once we go to higher orders in perturbation theory the definition of observables and its connection with gauge invariance becomes subtle [BS99] and must be carefully analyzed [YD17].

A

Conventions

A.1 Semantic conventions

When referring to the energy-momentum tensor

- full: background + perturbations
- total: adding all components

When referring to the cosmological history

- very late: up to $z \sim 2$
- late: after decoupling
- early: radiation dominated
- very early: before neutrino decoupling or nucleosynthesis

In general

- universe: a given cosmological model
- Universe: the observable one
- structure: loosely used to refer to ‘clumpy’ aggregates of matter in the Universe: galaxies, clusters, filaments...

A.2 Acronyms

ADD	Arkani-Hamed-Dimopoulos-Dvali
ALP	axion-like particles
BBN	Big Bang nucleosynthesis
BD	Boulware-Deser
CDM	cold dark matter
CMB	cosmic microwave background
CM	center of mass
DM	dark matter
dRGT	de Rham-Gabadadze-Tolley
FDM	fuzzy dark matter
FLRW	Friedmann-Lemaître-Robertson-Walker
GR	General Relativity

HB	horizontal branch
ISL	inverse-square law
ISW	integrated Sachs-Wolfe
KK	Kaluza-Klein
kSZ	kinetic Sunyaev-Zeldovich
LG	Local Group
LSS	large-scale structure
NFW	Navarro-Frenk-White
NR	non-relativistic
QCD	quantum chromodynamics
QED	quantum electrodynamics
QFT	quantum field theory
RG/RGB	red giant/red-giant branch
RSA	radiation-streaming approximation
RW	Robertson-Walker
SM	Standard Model
SN	supernova
SVT	scalar-vector-tensor
SW	Sachs-Wolfe
SZ	Sunyaev-Zeldovich
TC/TCA	tight coupling/tight-coupling approximation
ULA	ultralight axion
vDVZ	van Dam-Veltman-Zakharov
WIMP	weakly interacting massive particle
WKB	Wentzel-Kramers-Brillouin

A.3 Miscellanea

- We use natural units with $\hbar = c = k_B = 1$ and Lorentz-Heaviside electromagnetic units.
- Partial derivatives are denoted with ‘ ∂ ’ or ‘ $,$ ’. Covariant derivatives are denoted with ‘ ∇ ’ or ‘ $;$ ’.
- QFT-related conventions follow [Sre07].
- GR-related conventions follow [Wal10] and are summarized in Appendix D.
- $\varepsilon_{\mu\nu\rho\sigma}$ is the Levi-Civita symbol, with $\varepsilon_{0123} = 1$. The Levi-Civita pseudotensor is defined as $\epsilon_{\mu\nu\rho\sigma} \equiv \sqrt{-g} \varepsilon_{\mu\nu\rho\sigma}$.
- The Fourier transform is defined as

$$\mathcal{F}[f(\mathbf{x})] \equiv \tilde{f}(\mathbf{k}) \equiv \int d^3x e^{-i\mathbf{k}\cdot\mathbf{x}} f(\mathbf{x}). \quad (\text{A.1})$$

The inverse transformation is

$$\mathcal{F}^{-1}[\tilde{f}(\mathbf{k})] = f(\mathbf{x}) = \int \frac{d^3k}{(2\pi)^3} e^{i\mathbf{k}\cdot\mathbf{x}} \tilde{f}(\mathbf{k}). \quad (\text{A.2})$$

In general, we will use the same symbol for a variable and its Fourier transform, i.e. $\tilde{f} \equiv f$.

- Symmetrization and antisymmetrization of indices are defined as in [Wal10], e.g.

$$T_{[\mu\nu]} \equiv \frac{1}{2}(T_{\mu\nu} - T_{\nu\mu}) , \quad T_{(\mu\nu)} \equiv \frac{1}{2}(T_{\mu\nu} + T_{\nu\mu}) . \quad (\text{A.3})$$

B

Useful numbers

Most of the following conversion factors have been taken from the exceedingly useful tables of [KT94].

$$\begin{aligned} 1 \text{ eV} &= 1.7827 \times 10^{-33} \text{ g} & 1 \text{ g}^{-1} &= 5.6095 \times 10^{32} \text{ eV} \\ 1 \text{ eV} &= 5.0677 \times 10^4 \text{ cm}^{-1} & 1 \text{ cm}^{-1} &= 1.9733 \times 10^{-5} \text{ eV} \\ 1 \text{ eV} &= 1.5192 \times 10^{15} \text{ s}^{-1} & 1 \text{ s}^{-1} &= 6.5822 \times 10^{-16} \text{ eV} \\ 1 \text{ eV} &= 1.6022 \times 10^{-12} \text{ erg} & 1 \text{ erg} &= 6.2414 \times 10^{11} \text{ eV} \\ 1 \text{ eV} &= 1.1605 \times 10^4 \text{ K} & 1 \text{ K} &= 8.6170 \times 10^{-5} \text{ eV} \\ 1 \text{ eV} &= 1.5637 \times 10^{29} \text{ Mpc}^{-1} & 1 \text{ Mpc}^{-1} &= 6.3952 \times 10^{-30} \text{ eV} \end{aligned}$$

$$e = 0.30282$$

$$\begin{aligned} \sigma_T &= 6.6524 \times 10^{-25} \text{ cm}^2 = 1.7084 \times 10^{-15} \text{ eV}^{-2} \\ &= 6.9871 \times 10^{-74} \text{ Mpc}^2 \end{aligned}$$

$$\begin{aligned} G &= 6.6720 \times 10^{-8} \text{ cm}^3 \text{ g}^{-1} \text{ s}^{-2} = 6.7065 \times 10^{-57} \text{ eV}^{-2} \\ &= 2.7429 \times 10^{-115} \text{ Mpc}^2 \end{aligned}$$

$$\begin{aligned} H_0 &= 100h \text{ km s}^{-1} \text{ Mpc}^{-1} = \frac{h}{2997.9} \text{ Mpc}^{-1} \\ &= 2.33 \times 10^{-4} \left(\frac{h}{0.7} \right) \text{ Mpc}^{-1} = 1.5 \times 10^{-33} \left(\frac{h}{0.7} \right) \text{ eV} \end{aligned}$$

$$\begin{aligned} \rho_{\text{crit}} &= \frac{3H_0^2}{8\pi G} = 1.8791 \times 10^{-29} h^2 \text{ g cm}^{-3} = 1.0541 \times 10^4 h^2 \text{ eV cm}^{-3} \\ &= 8.0995 \times 10^{-11} h^2 \text{ eV}^4 \end{aligned}$$

$$\rho_\gamma = \frac{\pi}{15} T^4 = 2.0018 \times 10^{-15} \left(\frac{T}{2.7255 \text{ K}} \right)^4 \text{ eV}^4$$

$$\rho_\nu = N_{\text{eff}} \frac{7}{8} \left(\frac{4}{11} \right)^{4/3} \rho_\gamma = 1.3848 \times 10^{-15} \left(\frac{N_{\text{eff}}}{3.046} \right) \text{ eV}^4$$

$$1 \text{ s} = 2.9979 \times 10^{10} \text{ cm}$$

$$1 \text{ Mpc} = 3.2615 \times 10^6 \text{ year} = 3.0856 \times 10^{24} \text{ cm}$$

$$1 \text{ G} = 6.9256 \times 10^{-2} \text{ eV}^2 = 1.6934 \times 10^{57} \text{ Mpc}^{-2}$$

$$1 \text{ erg g}^{-1} \text{ s}^{-1} = 7.3237 \times 10^{-37} \text{ eV}$$

$$1 \text{ g cm}^{-3} = 4.3102 \times 10^{18} \text{ eV}^4$$

$$\begin{aligned}
10^{-23} \text{ eV} &= 1.5637 \times 10^6 \text{ Mpc}^{-1} \simeq 15.2 \text{ nHz} \simeq \frac{1}{2 \text{ year}} \\
10^{-5} \text{ eV} &= 1.5637 \times 10^{24} \text{ Mpc}^{-1} \simeq 15.2 \text{ GHz} \\
\frac{3\sigma_T}{8\pi G} &= 1.7957 \times 10^{-17} \frac{\text{G}}{\text{Mpc}^{-2}} \\
\frac{\pi G \rho}{m^2} &= 1.7064 \times 10^{-20} \left(\frac{10^{-23} \text{ eV}}{m} \right)^2 \left(\frac{\rho}{\rho_{\text{crit}}} \right) h^2
\end{aligned}$$

Table B.1 contains the values of the cosmological parameters obtained from the CMB and combining CMB and BAO measurements, as reported in [Agh+18]. Table B.2 contains some useful estimations, obtained with a cosmology given by the central values in Table B.1. We summarize here some definitions that have not been included in the introduction (even though some of them have been defined in Chapter 5). The coordinate time, related to the conformal time as $dt = a d\tau$, is

$$t = \int_0^a \frac{da}{\mathcal{H}}. \quad (\text{B.1})$$

The angular diameter distance is defined as

$$d_A = \int_a^1 \frac{da}{a\mathcal{H}}. \quad (\text{B.2})$$

The angular diameter distance allows us to compute the angle subtended by a physical length scale at a given redshift as

$$\theta = \frac{\lambda}{d_A} \quad (\text{B.3})$$

This angular scale in its turn can be (approximately) related with a multipole $\ell \simeq \pi/\theta$. The sound horizon for the photon-baryon plasma is

$$r_s = \int_0^a \frac{da}{a\mathcal{H}} \frac{1}{\sqrt{3(1+R)}}, \quad R \equiv \frac{3\rho_b}{4\rho_\gamma}. \quad (\text{B.4})$$

The characteristic wavenumber that sets the damping scale in the CMB is [Ade+14a]

$$k_D^{-2} = -\frac{1}{6} \int_0^\tau \frac{d\tau'}{\dot{\kappa}} \frac{R^2 + 16(1+R)/15}{(1+R)^2}. \quad (\text{B.5})$$

Another quantity that is commonly used in the literature to quantify the clustering is

$$\sigma_R^2 = \int \frac{k^2 dk}{2\pi^2} P_m(k) \left[\frac{3j_1(kR)}{kR} \right]^2, \quad (\text{B.6})$$

where it is usually evaluated at $R = 8h^{-1} \text{ Mpc}$.

Parameter	<i>Planck</i> only	<i>Planck</i> +BAO
$\Omega_b h^2$	0.02237 ± 0.00015	0.02242 ± 0.00014
$\Omega_c h^2$	0.1200 ± 0.0012	0.11933 ± 0.00091
$100\theta_{\text{MC}}$	1.04110 ± 0.00031	1.04101 ± 0.00029
τ	0.0544 ± 0.0073	0.0561 ± 0.0071
$\log(10^{10} A_s)$	3.044 ± 0.014	3.047 ± 0.014
n_s	0.9649 ± 0.0042	0.9665 ± 0.0038
h	0.6736 ± 0.0054	0.6766 ± 0.0042
Ω_m	0.3153 ± 0.0073	0.3111 ± 0.0056
$\Omega_m h^2$	0.1430 ± 0.0011	0.14240 ± 0.00087
Ω_Λ	0.6847 ± 0.0073	0.6889 ± 0.0056
σ_8	0.8111 ± 0.0060	0.8102 ± 0.0060
$10^9 A_s$	2.100 ± 0.030	2.105 ± 0.030
Age [Gyr]	13.797 ± 0.023	13.787 ± 0.020
z_{reio}	7.67 ± 0.73	7.82 ± 0.71
z_*	1089.92 ± 0.25	1089 ± 0.21
r_* [Mpc]	144.43 ± 0.26	144.57 ± 0.22
$100\theta_*$	1.04110 ± 0.00031	1.04119 ± 0.00029
z_{eq}	3402 ± 26	3387 ± 21
k_{eq} [Mpc $^{-1}$]	0.010384 ± 0.000081	0.010339 ± 0.000063
k_{D} [Mpc $^{-1}$]	0.14087 ± 0.00030	0.14078 ± 0.00028
Ω_K	$-0.011^{+0.013}_{-0.012}$	0.0007 ± 0.0037
$\sum m_\nu$ [eV]	< 0.241	< 0.120
N_{eff}	$2.89^{+0.36}_{-0.38}$	$2.99^{+0.34}_{-0.33}$
$r_{0.002}$	< 0.101	< 0.106
w_0	$-1.57^{+0.50}_{-0.40}$	$-1.04^{+0.10}_{-0.10}$

Table B.1: Constraints on the base- Λ CDM model (68% limits) using only CMB data and combining with BAO measurements, as reported in [Agh+18]. The middle part of the table presents some quantities that can be derived from the base parameters. These include: the fluctuation amplitude at $8h^{-1}$ Mpc (σ_8), the acoustic damping scale (k_{D}), the horizon scale and redshift at matter-radiation equality (k_{eq} , z_{eq}), the redshift, sound horizon and angular scale at decoupling (z_* , r_* , θ_*). On the lower part, some one-parameter extensions are included with 95% limits. The equation of state of dark energy (w_0) can be further constrained including measurements of the expansion history from supernovae. In this case, $w_0(+\text{SNe}) = -1.028 \pm 0.031$ (68% limit).

	z	a	τ [Mpc]	t [year]	d_A [Mpc]	h [Mpc $^{-1}$]	h [h /Mpc]	ℓ_{CMB}	
Today	0	1	1.4×10^4	1.4×10^{10}	0	2.2×10^{-4}	3.3×10^{-4}	$\mathcal{O}(1)$	
M- Λ eq.	0.29	0.78	1.3×10^4	1.0×10^{10}	1.2×10^3	2.0×10^{-4}	3.0×10^{-4}	$\mathcal{O}(1)$	
Reio.	7.82	0.11	5.1×10^3	6.6×10^8	9.1×10^3	3.8×10^{-4}	5.6×10^{-4}	$\mathcal{O}(1)$	
Dec.	1090	9.2×10^{-4}	280	3.7×10^5	1.4×10^4	4.8×10^{-3}	7.1×10^{-3}	33	
M-R eq.	3387	3.0×10^{-4}	113	5.1×10^4	–	0.010	0.015	72	
	1.3×10^4	7.6×10^{-5}	33	4051	–	0.032	0.048	221	CMB 1st peak
	3.4×10^4	2.9×10^{-5}	13	625	–	0.077	0.12	538	CMB 2nd peak
	5.2×10^4	1.9×10^{-5}	8.7	270	–	0.12	0.17	810	CMB 3rd peak
	6.4×10^4	1.6×10^{-5}	7.2	184	–	0.14	0.21	978	Damp. scale
	7.5×10^4	1.3×10^{-5}	6.1	133	–	0.17	0.25	1148	CMB 4th peak
	9.1×10^4	1.1×10^{-5}	5.0	90	–	0.2	0.3	1390	
R. era	10^7	10^{-7}	0.46	7.6×10^{-3}	–	22	32	1.5×10^5	Nonlin. scale

Table B.2: The first five rows correspond to important periods in the history of the Universe: the present time, matter-cosmological constant equality, reionization, decoupling and matter-radiation equality. For each of them we indicate the corresponding redshift, scale factor, time and angular diameter distance. We also include the horizon scale, $h = \mathcal{H}$, at that time and the CMB multipole that roughly corresponds to this scale. The following rows are the scales corresponding to the first CMB peaks, the acoustic damping scale and the non-linearity scale. The final row corresponds to a redshift deep in the radiation-dominated era. Before decoupling, d_A remains essentially constant with $d_A(z > z_{\text{dec}}) \simeq 1.4 \times 10^4$ and we omit it.

C

Special functions

Most of the results come from [AW01].

C.1 Spherical Bessel functions

The spherical Bessel functions are related to the ordinary Bessel functions through

$$j_\ell(x) = \sqrt{\frac{\pi}{2x}} J_{\ell+1/2}(x). \quad (\text{C.1})$$

Some particular values

$$j_0(x) = \frac{\sin x}{x}, \quad (\text{C.2a})$$

$$j_1(x) = \frac{\sin x}{x^2} - \frac{\cos x}{x}, \quad (\text{C.2b})$$

$$j_2(x) = \left(\frac{3}{x^3} - \frac{1}{x}\right) \sin x - \frac{3}{x^2} \cos x. \quad (\text{C.2c})$$

Limiting values

$$j_\ell(x) \simeq \frac{x^\ell}{(2\ell+1)!!}, \quad x \ll 2\sqrt{\frac{(2\ell+2)(2\ell+3)}{\ell+1}}, \quad (\text{C.3a})$$

$$j_\ell(x) \sim \frac{1}{x} \sin\left(x - \frac{\ell\pi}{2}\right), \quad x \gg 1. \quad (\text{C.3b})$$

Recurrence relations

$$\frac{j_\ell(x)}{x} = \frac{j_{\ell-1} + j_{\ell+1}}{2\ell+1}, \quad (\text{C.4a})$$

$$j'_\ell(x) = \frac{\ell j_{\ell-1} - (\ell+1)j_{\ell+1}}{2\ell+1}. \quad (\text{C.4b})$$

Integrals

$$\int_{-\infty}^{\infty} j_\ell(x) j_{\ell'}(x) dx = \frac{\pi}{2\ell+1} \delta_{\ell\ell'}, \quad (\text{C.5a})$$

$$\int_0^\infty j_\ell(ar) j_\ell(br) r^2 dr = \frac{\pi}{2a^2} \delta(a-b). \quad (\text{C.5b})$$

From equation (6.574.2) in [GR07] we have ($\lambda > 0$, $\nu + \mu + 1 > 0$)

$$\int_0^\infty J_\nu(t) J_\mu(t) t^{-\lambda} dt = \frac{\Gamma(\lambda) \Gamma\left(\frac{\nu+\mu-\lambda+1}{2}\right)}{2\lambda \Gamma\left(\frac{\mu-\nu+\lambda+1}{2}\right) \Gamma\left(\frac{\nu+\mu+\lambda+1}{2}\right) \Gamma\left(\frac{\nu-\mu+\lambda+1}{2}\right)}, \quad (\text{C.6})$$

and from this result we get ($n < 2$)

$$\int_0^\infty j_\ell(x) j_{\ell'}(x) \frac{dx}{x^{1-n}} = \frac{2^n \pi}{8} \frac{\Gamma(2-n) \Gamma\left(\frac{\ell+\ell'+n}{2}\right)}{\Gamma\left(\frac{\ell'-\ell-n}{2} + \frac{3}{2}\right) \Gamma\left(\frac{\ell'+\ell-n}{2} + 2\right) \Gamma\left(\frac{\ell-\ell'-n}{2} + \frac{3}{2}\right)}, \quad (\text{C.7})$$

$$\int_0^\infty (j_\ell(x))^2 \frac{dx}{x} = \frac{\pi}{8} \frac{\Gamma(2) \Gamma(\ell)}{(\Gamma(3/2))^2 \Gamma(\ell+2)} = \frac{1}{2\ell(\ell+1)}. \quad (\text{C.8})$$

Differential equation

$$x^2 \frac{d^2}{dx^2} j_\ell + 2x \frac{d}{dx} j_\ell + [x - \ell(\ell+1)] j_\ell = 0. \quad (\text{C.9})$$

From equation (9.3.1) in [AS72] we have

$$J_\nu(x) \sim \frac{1}{\sqrt{2\pi\nu}} \left(\frac{ex}{2\nu}\right)^\nu, \quad \nu \gg 1, \quad (\text{C.10})$$

$$j_\ell(x) \sim \frac{1}{2\ell} \left(\frac{e}{2}\right)^\ell \left(\frac{x}{\ell}\right)^{\ell+1/2}, \quad \ell \gg 1. \quad (\text{C.11})$$

C.2 Legendre polynomials

Some particular values are

$$\begin{aligned} P_0(x) &= 1, & P_2(x) &= \frac{1}{2}(3x^2 - 1), \\ P_1(x) &= x, & P_3(x) &= \frac{1}{2}(5x^3 - 3x). \end{aligned} \quad (\text{C.12})$$

Recurrence relation

$$(2\ell+1)xP_\ell(x) = (\ell+1)P_{\ell+1}(x) + \ell P_{\ell-1}(x), \quad (\text{C.13a})$$

$$P'_{\ell+1} - P'_{\ell-1} = (2\ell+1)P_\ell. \quad (\text{C.13b})$$

Some additional relations that can be derived include

$$\begin{aligned} P'_{\ell+1} &= (\ell+1)P_\ell + xP'_\ell, & (1-x^2)P'_\ell &= \ell P_{\ell-1} - \ell xP_\ell, \\ P'_{\ell-1} &= -\ell P_\ell + xP'_\ell, & (1-x^2)P'_\ell &= (\ell+1)xP_\ell - (\ell+1)P_{\ell+1}. \end{aligned} \quad (\text{C.14})$$

Special values

$$P_\ell(1) = 1, \quad (\text{C.15a})$$

$$P_{2\ell}(0) = \frac{(-1)^\ell (2\ell)!}{2^{2\ell} (\ell!)^2}, \quad (\text{C.15b})$$

$$P_{2\ell+1}(0) = 0. \quad (\text{C.15c})$$

Differential equation

$$(1-x^2) \frac{d^2}{dx^2} P_\ell - 2x \frac{d}{dx} P_\ell + \ell(\ell+1)P_\ell = 0. \quad (\text{C.16})$$

Parity

$$P_\ell(-x) = (-1)^\ell P_\ell(x). \quad (\text{C.17})$$

Orthogonality

$$\int_{-1}^1 dx P_\ell P_{\ell'} = \frac{2\delta_{\ell\ell'}}{2\ell+1}. \quad (\text{C.18})$$

Expansion of the exponential

$$e^{-i\mathbf{k}\cdot\mathbf{x}} = \sum_{\ell=0}^{\infty} (-i)^\ell (2\ell+1) j_\ell(kx) P_\ell(\hat{\mathbf{k}}\cdot\hat{\mathbf{x}}). \quad (\text{C.19})$$

C.3 Associated Legendre functions

Definition

$$P_n^m(x) = \frac{1}{2^n n!} (1-x^2)^{(m/2)} \frac{d^{m+n}}{dx^{m+n}} (x^2-1), \quad -n \leq m \leq n \quad (\text{C.20a})$$

$$P_n^m(x) = (1-x^2)^{(m/2)} \frac{d^m}{dx^m} P_n(x), \quad (\text{C.20b})$$

$$P_n^{-m}(x) = (-1)^m \frac{(n-m)!}{(n+m)!} P_n^m(x). \quad (\text{C.20c})$$

Parity

$$P_n^m(-x) = (-1)^{n+m} P_n^m(x). \quad (\text{C.21})$$

Orthogonality

$$\int_{-1}^1 P_p^m(x) P_q^m(x) dx = \frac{2}{2q+1} \frac{(q+m)!}{(q-m)!} \delta_{pq}, \quad (\text{C.22})$$

$$\int_{-1}^1 P_n^m(x) P_n^k(x) (1-x^2)^{-1} dx = \frac{(n+m)!}{m(n-m)!} \delta_{mk}. \quad (\text{C.23})$$

Miscellanea

$$P_n^0(x) = P_n(x), \quad (\text{C.24})$$

$$P_n^m(\pm 1) = 0, \quad \text{for } m \neq 0. \quad (\text{C.25})$$

Several recurrence relations can be found in [AW01, p.774].

C.4 Spherical harmonics

Definition

$$Y_n^m(\theta, \phi) = (-1)^m \sqrt{\frac{2n+1}{4\pi} \frac{(n-m)!}{(n+m)!}} P_n^m(\cos\theta) e^{im\phi}. \quad (\text{C.26})$$

Relation to Legendre polynomials

$$P_\ell(\cos\theta) = \sqrt{\frac{4\pi}{2\ell+1}} Y_\ell^0(\theta, \phi). \quad (\text{C.27})$$

Conjugation

$$Y_n^{m*} = (-1)^m Y_n^{-m}. \quad (\text{C.28})$$

Orthonormality

$$\int_0^{2\pi} d\phi \int_{-1}^1 d(\cos\theta) Y_{n_1}^{m_1*}(\theta, \phi) Y_{n_2}^{m_2}(\theta, \phi) = \delta_{n_1 n_2} \delta_{m_1 m_2}. \quad (\text{C.29})$$

Specific values with our convention

$$\begin{aligned} Y_0^0 &= \frac{1}{\sqrt{4\pi}}, & Y_2^0 &= \sqrt{\frac{5}{4\pi}} \left(\frac{3}{2} \cos^2\theta - \frac{1}{2} \right), \\ Y_1^0 &= \sqrt{\frac{3}{4\pi}} \cos\theta, & Y_2^{+1} &= -\sqrt{\frac{5}{24\pi}} 3 \sin\theta \cos\theta e^{i\phi}, \\ Y_1^{+1} &= -\sqrt{\frac{3}{8\pi}} \sin\theta e^{i\phi}, & Y_2^{+2} &= \sqrt{\frac{5}{96\pi}} 3 \sin^2\theta e^{2i\phi}. \end{aligned} \quad (\text{C.30})$$

Addition of angular momenta

$$\cos\theta Y_\ell^m = A_{\ell m}^c Y_{\ell+1}^m + B_{\ell m}^c Y_{\ell-1}^m, \quad (\text{C.31a})$$

$$e^{i\phi} \sin\theta Y_\ell^m = -A_{\ell m}^+ Y_{\ell+1}^{m+1} + B_{\ell m}^+ Y_{\ell-1}^{m+1}, \quad (\text{C.31b})$$

$$e^{-i\phi} \sin\theta Y_\ell^m = A_{\ell m}^- Y_{\ell+1}^{m-1} - B_{\ell m}^- Y_{\ell-1}^{m-1}, \quad (\text{C.31c})$$

where

$$\begin{aligned} A_{\ell m}^c &= \left(\frac{(\ell-m+1)(\ell+m+1)}{(2\ell+1)(2\ell+3)} \right)^{1/2}, & B_{\ell m}^c &= \left(\frac{(\ell-m)(\ell+m)}{(2\ell-1)(2\ell+1)} \right)^{1/2}, \\ A_{\ell m}^+ &= \left(\frac{(\ell+m+1)(\ell+m+2)}{(2\ell+1)(2\ell+3)} \right)^{1/2}, & B_{\ell m}^+ &= \left(\frac{(\ell-m)(\ell-m-1)}{(2\ell-1)(2\ell+1)} \right)^{1/2}, \\ A_{\ell m}^- &= \left(\frac{(\ell-m+1)(\ell-m+2)}{(2\ell+1)(2\ell+3)} \right)^{1/2}, & B_{\ell m}^- &= \left(\frac{(\ell+m)(\ell+m-1)}{(2\ell-1)(2\ell+1)} \right)^{1/2}. \end{aligned} \quad (\text{C.32})$$

Addition theorem

$$P_\ell(\hat{n} \cdot \hat{k}) = \frac{4\pi}{2\ell+1} \sum_{m=-\ell}^{\ell} Y_\ell^m(\hat{n}) Y_\ell^{m*}(\hat{k}). \quad (\text{C.33})$$

C.5 Proof of some results

Computation of $I_{\ell\ell'}^{(1)}(\hat{n}, \hat{n}')$. The integral to solve is

$$I_{\ell\ell'}^{(1)}(\hat{n}, \hat{n}') = \int Y_\ell^0(\hat{n} \cdot \hat{k}) Y_{\ell'}^0(\hat{n}' \cdot \hat{k}) d^2\hat{k}. \quad (\text{C.34})$$

Using the addition property (C.33) of the spherical harmonics we have

$$\begin{aligned}
I_{\ell\ell'}^{(1)}(\hat{n}, \hat{n}') &= \frac{\sqrt{(2\ell+1)(2\ell'+1)}}{4\pi} \int d^2\hat{k} P_\ell(\hat{n} \cdot \hat{k}) P_{\ell'}(\hat{n}' \cdot \hat{k}) \\
&= \frac{4\pi}{\sqrt{(2\ell+1)(2\ell'+1)}} \int d^2\hat{k} \sum_{m=-\ell}^{\ell} Y_\ell^m(\hat{n}) Y_\ell^{m*}(\hat{k}) \\
&\quad \times \sum_{m'=-\ell'}^{\ell'} Y_{\ell'}^{m'*}(\hat{n}') Y_{\ell'}^{m'}(\hat{k}) \\
&= \frac{4\pi}{\sqrt{(2\ell+1)(2\ell'+1)}} \sum_{m,m'} Y_\ell^m(\hat{n}) Y_{\ell'}^{m'*}(\hat{n}') \delta_{\ell'\ell} \delta_{m'm} \\
&= \frac{4\pi}{2\ell+1} \delta_{\ell'\ell} \sum_m Y_\ell^m(\hat{n}) Y_\ell^{m*}(\hat{n}') \\
&= \delta_{\ell'\ell} P_\ell(\hat{n} \cdot \hat{n}') .
\end{aligned} \tag{C.35}$$

Computation of $I_{\ell\ell'}^{(2)}(\hat{n}, \hat{n}')$. The integral to solve is¹

$$I_{\ell\ell'}^{(2)}(\hat{n}, \hat{n}') = \int (\hat{\beta} \cdot \hat{k}) Y_\ell^0(\hat{n} \cdot \hat{k}) Y_{\ell'}^0(\hat{n}' \cdot \hat{k}) d^2\hat{k} . \tag{C.36}$$

First we choose a frame

$$\hat{Z} = \hat{n} , \tag{C.37}$$

$$\begin{aligned}
\hat{Y} &= \frac{i}{\sqrt{2}} (\hat{E}_+ - \hat{E}_-) \\
&= \frac{1}{\sqrt{1 - (\hat{n} \cdot \hat{\beta})^2}} (\hat{n} \wedge \hat{\beta}) ,
\end{aligned} \tag{C.38}$$

$$\begin{aligned}
\hat{X} &= \frac{1}{\sqrt{2}} (\hat{E}_+ + \hat{E}_-) \\
&= \frac{1}{\sqrt{1 - (\hat{n} \cdot \hat{\beta})^2}} (\hat{\beta} - (\hat{n} \cdot \hat{\beta}) \hat{n}) .
\end{aligned} \tag{C.39}$$

Then we get the projection

$$\hat{\beta} \cdot \hat{k} = \frac{1}{\sqrt{2}} \sqrt{1 - (\hat{n} \cdot \hat{\beta})^2} \hat{k} \cdot (\hat{E}_+ + \hat{E}_-) + (\hat{n} \cdot \hat{\beta}) (\hat{n} \cdot \hat{k}) . \tag{C.40}$$

Our original integral can be splitted in two pieces

$$I_{\ell\ell'}^{(2)}(\hat{n}, \hat{n}') = (\hat{n} \cdot \hat{\beta}) \mathcal{I}_1 + \frac{1}{\sqrt{2}} \sqrt{1 - (\hat{n} \cdot \hat{\beta})^2} (\mathcal{I}_2 + \mathcal{I}_2^*) , \tag{C.41}$$

¹It is possible to derive the same results in a different way. One can argue that the integral must be of the form $I^{(2)} = (\hat{\beta} \cdot \hat{n})A + (\hat{\beta} \cdot \hat{n}')B$. Then we have

$$\begin{aligned}
3 \int \frac{d^2\hat{\beta}}{4\pi} (\hat{\beta} \cdot \hat{n}) I^{(2)} &= A + (\hat{n} \cdot \hat{n}') B = \int d^2\hat{k} (\hat{n} \cdot \hat{k}) Y_\ell^0(\hat{n} \cdot \hat{k}) Y_{\ell'}^0(\hat{n}' \cdot \hat{k}) \\
3 \int \frac{d^2\hat{\beta}}{4\pi} (\hat{\beta} \cdot \hat{n}') I^{(2)} &= (\hat{n} \cdot \hat{n}') A + B = \int d^2\hat{k} (\hat{n}' \cdot \hat{k}) Y_\ell^0(\hat{n} \cdot \hat{k}) Y_{\ell'}^0(\hat{n}' \cdot \hat{k})
\end{aligned}$$

Using the properties of the Legendre polynomials, we can straightforwardly compute the integrals on the right-hand side and then obtain A and B .

where

$$\begin{aligned}
\mathcal{I}_1 &= \int d^2\hat{k} (\hat{n} \cdot \hat{k}) Y_\ell^0(\hat{n} \cdot \hat{k}) Y_{\ell'}^0(\hat{n}' \cdot \hat{k}) \\
&= A_{\ell,0}^c \int d^2\hat{k} Y_{\ell+1}^0(\hat{n}) Y_{\ell'}^0(\hat{n}') + B_{\ell,0}^c \int d^2\hat{k} Y_{\ell-1}^0 Y_{\ell'}^0(\hat{n}') \\
&= A_{\ell,0}^c I_{\ell+1,\ell'}^{(1)}(\hat{n}, \hat{n}') + B_{\ell,0}^c I_{\ell-1,\ell'}^{(1)}(\hat{n}, \hat{n}') \\
&= \left(A_{\ell,0}^c \delta_{\ell+1,\ell'} + B_{\ell,0}^c \delta_{\ell-1,\ell'} \right) P_{\ell'}(\hat{n} \cdot \hat{n}'), \tag{C.42}
\end{aligned}$$

and

$$\begin{aligned}
\mathcal{I}_2 &= \int d^2\hat{k} (\hat{k} \cdot \hat{E}_+) Y_\ell^0(\hat{n} \cdot \hat{k}) Y_{\ell'}^0(\hat{n}' \cdot \hat{k}) \\
&= \sqrt{\frac{4\pi}{2\ell'+1}} \sum_{m'=-\ell'}^{\ell'} Y_{\ell'}^{m'}(\hat{n}') \int d^2\hat{k} Y_\ell^0(\hat{n} \cdot \hat{k}) (\hat{k} \cdot \hat{E}_+) Y_{\ell'}^{m'*}(\hat{k}) \\
&= \sqrt{\frac{4\pi}{2\ell'+1}} \sum_{m'=-\ell'}^{\ell'} Y_{\ell'}^{m'}(\hat{n}') \int_{-1}^1 d\mu Y_\ell^0(\mu) \\
&\quad \times \int \frac{d\varphi}{\sqrt{2}} \left(A_{\ell',m'}^- Y_{\ell'+1}^{m'-1*}(\mu, \varphi) - B_{\ell',m'}^- Y_{\ell'-1}^{m'-1*}(\mu, \varphi) \right) \tag{C.43}
\end{aligned}$$

$$\begin{aligned}
&= \frac{(2\pi)^{3/2}}{\sqrt{2\ell'+1}} Y_{\ell'}^{+1}(\hat{n}') \int_{-1}^1 d\mu Y_\ell^0(\mu) \left(A_{\ell',+1}^- Y_{\ell'+1}^0(\mu) - B_{\ell',+1}^- Y_{\ell'-1}^0(\mu) \right) \\
&= \sqrt{\frac{2\pi}{2\ell'+1}} Y_{\ell'}^{+1}(\hat{n}') \left(A_{\ell',+1}^- \delta_{\ell,\ell'+1} - B_{\ell',+1}^- \delta_{\ell,\ell'-1} \right). \tag{C.44}
\end{aligned}$$

In the basis we have chosen

$$\begin{aligned}
Y_{\ell'}^{+1} &= \frac{-1}{\sqrt{1-(\hat{n} \cdot \hat{\beta})^2}} \sqrt{\frac{2\ell'+1}{4\pi}} \frac{1}{\sqrt{\ell'(\ell'+1)}} \frac{P_{\ell'}^{+1}(\hat{n} \cdot \hat{n}')}{\sqrt{1-(\hat{n} \cdot \hat{n}')^2}} \\
&\quad \times \left\{ \hat{n}' \cdot \hat{\beta} - (\hat{n} \cdot \hat{\beta})(\hat{n} \cdot \hat{n}') - i \hat{n}' \cdot (\hat{n} \wedge \hat{\beta}) \right\}. \tag{C.45}
\end{aligned}$$

With these results, we have

$$\begin{aligned}
I_{\ell\ell'}^{(2)}(\hat{n}, \hat{n}') &= (\hat{n} \cdot \hat{\beta}) P_{\ell'}(\hat{n} \cdot \hat{n}') \left(A_{\ell,0}^c \delta_{\ell+1,\ell'} + B_{\ell'+1,0}^c \delta_{\ell,\ell'+1} \right) \\
&\quad - \frac{1}{\sqrt{\ell'(\ell'+1)}} \frac{P_{\ell'}^{+1}(\hat{n} \cdot \hat{n}')}{\sqrt{1-(\hat{n} \cdot \hat{n}')^2}} \left\{ \hat{n}' \cdot \hat{\beta} - (\hat{n} \cdot \hat{\beta})(\hat{n} \cdot \hat{n}') \right\} \\
&\quad \times \left(A_{\ell',+1}^- \delta_{\ell,\ell'+1} - B_{\ell'+1,+1}^- \delta_{\ell+1,\ell'} \right). \tag{C.46}
\end{aligned}$$

Using the properties of the Legendre polynomials

$$(2\ell+1)\sqrt{1-x^2}P_\ell^{+1} = \ell(\ell+1)(P_{\ell-1} - P_{\ell+1}), \tag{C.47}$$

$$P_\ell^{+1} = \sqrt{1-x^2}P'_\ell, \tag{C.48}$$

$$P'_{\ell+1} = (\ell+1)P_\ell + xP'_\ell, \tag{C.49}$$

$$P'_{\ell-1} = -\ell P_\ell + xP'_\ell, \tag{C.50}$$

we find

$$I_{\ell\ell'}^{(2)}(\hat{n}, \hat{n}') = H_\ell(\hat{n}', \hat{n})\delta_{\ell+1,\ell'} + H_{\ell'}(\hat{n}, \hat{n}')\delta_{\ell,\ell'+1}, \tag{C.51}$$

with

$$\begin{aligned}
H_\ell(\hat{n}, \hat{n}') &= \frac{\ell+1}{\sqrt{(2\ell+1)(2\ell+3)}} \left\{ (\hat{\beta} \cdot \hat{n}) P_\ell - \frac{P'_\ell}{\ell+1} ((\hat{\beta} \cdot \hat{n}') - (\hat{n} \cdot \hat{n}')(\hat{\beta} \cdot \hat{n})) \right\} \\
&= \frac{\ell+1}{\sqrt{(2\ell+1)(2\ell+3)}} \frac{1}{1 - (\hat{n} \cdot \hat{n}')^2} \left\{ ((\hat{\beta} \cdot \hat{n}) - (\hat{n} \cdot \hat{n}')(\hat{\beta} \cdot \hat{n}')) P_\ell \right. \\
&\quad \left. + ((\hat{\beta} \cdot \hat{n}') - (\hat{n} \cdot \hat{n}')(\hat{\beta} \cdot \hat{n})) P_{\ell+1} \right\}. \quad (\text{C.52})
\end{aligned}$$

Finally, note that $\hat{\beta}$ is an arbitrary vector so we can actually write these equations in vector form, as in the main text.

Computation of $Q_{\ell'\ell}$. We need to compute

$$Q_{\ell'\ell} = \frac{2\ell+1}{2} \int_{-1}^1 dx (1-x) P'_{\ell'}(x) P_\ell(x). \quad (\text{C.53})$$

Using the properties of the Legendre polynomials

$$(1-x)P'_\ell = P'_\ell + (\ell+1)P_\ell - P'_{\ell+1}, \quad (\text{C.54})$$

$$= P'_\ell - \ell P_\ell - P'_{\ell-1}, \quad (\text{C.55})$$

$$(1-x)P'_\ell = P'_{\ell+1} - (\ell+1)P_{\ell+1} - P'_\ell, \quad (\text{C.56})$$

we find the recurrence relation

$$(1-x)P'_{\ell+1} = (\ell+1)(P_\ell - P_{\ell+1}) - (1-x)P'_\ell. \quad (\text{C.57})$$

Then we can prove (by induction) that

$$(1-x)P'_\ell = -\ell P_\ell - (-1)^\ell \sum_{n=0}^{\ell-1} (-1)^n (2n+1) P_n. \quad (\text{C.58})$$

The coefficients are

$$\begin{aligned}
Q_{\ell'\ell} &= \frac{2\ell+1}{2} \left\{ -\ell' \int_{-1}^1 dx P_\ell P_{\ell'} - (-1)^{\ell'} \sum_{n=0}^{\ell'-1} (-1)^n (2n+1) \int_{-1}^1 dx P_\ell P_n \right\} \\
&= (2\ell+1) \left\{ -\ell \frac{\delta_{\ell'\ell}}{2\ell+1} - (-1)^{\ell'} \sum_{n=0}^{\ell'-1} (-1)^n \frac{2n+1}{2\ell+1} \delta_{n\ell} \right\}. \quad (\text{C.59})
\end{aligned}$$

We can distinguish three cases

$$Q_{\ell'\ell} = 0, \quad \ell' < \ell, \quad (\text{C.60a})$$

$$Q_{\ell'\ell} = -\ell, \quad \ell' = \ell, \quad (\text{C.60b})$$

$$Q_{\ell'\ell} = -(-1)^{\ell'+\ell} (2\ell+1), \quad \ell' > \ell. \quad (\text{C.60c})$$

D

Metric Formulae

D.1 Definitions

All the conventions follow [Wal10]. The signature of the metric is *mostly plus* $(-, +, +, +)$. The metric tensors are defined as

$$\Gamma^\rho{}_{\mu\nu} \equiv \frac{1}{2} g^{\rho\sigma} (\partial_\mu g_{\nu\sigma} + \partial_\nu g_{\mu\sigma} - \partial_\sigma g_{\mu\nu}) , \quad (\text{D.1a})$$

$$R^\sigma{}_{\rho\mu\nu} \equiv \partial_\mu \Gamma^\sigma{}_{\nu\rho} - \partial_\nu \Gamma^\sigma{}_{\mu\rho} + \Gamma^\sigma{}_{\mu\alpha} \Gamma^\alpha{}_{\nu\rho} - \Gamma^\sigma{}_{\nu\alpha} \Gamma^\alpha{}_{\mu\rho} , \quad (\text{D.1b})$$

$$R_{\mu\nu} \equiv R^\alpha{}_{\mu\alpha\nu} , \quad (\text{D.1c})$$

$$R \equiv g^{\mu\nu} R_{\mu\nu} , \quad (\text{D.1d})$$

$$G_{\mu\nu} \equiv R_{\mu\nu} - \frac{1}{2} g_{\mu\nu} R , \quad (\text{D.1e})$$

$$C_{\mu\nu\sigma\rho} \equiv R_{\mu\nu\sigma\rho} - g_{\mu[\sigma} R_{\rho]\nu} + g_{\nu[\sigma} R_{\rho]\mu} + \frac{1}{3} g_{\mu[\sigma} g_{\rho]\nu} R . \quad (\text{D.1f})$$

Two useful expressions relating Christoffel symbols and the metric are

$$\Gamma^\alpha{}_{\alpha\mu} = \partial_\mu \log \sqrt{-g} , \quad (\text{D.2})$$

$$\partial_\mu g_{\nu\sigma} = g_{\alpha\sigma} \Gamma^\alpha{}_{\nu\mu} + g_{\alpha\nu} \Gamma^\alpha{}_{\sigma\mu} . \quad (\text{D.3})$$

In terms of the Christoffel symbols, the covariant derivatives are

$$\nabla_\mu v^\nu = \partial_\mu v^\nu + \Gamma^\nu{}_{\mu\sigma} v^\sigma , \quad (\text{D.4a})$$

$$\nabla_\mu w_\nu = \partial_\mu w_\nu - \Gamma^\sigma{}_{\mu\nu} w_\sigma , \quad (\text{D.4b})$$

The divergence of a vector field can be expressed as

$$\nabla_\mu v^\mu = \frac{1}{\sqrt{-g}} \partial_\mu (\sqrt{-g} v^\mu) . \quad (\text{D.5})$$

For a perturbed metric

$$g_{\mu\nu} \equiv g_{\mu\nu}^{(0)} + \delta g_{\mu\nu} , \quad (\text{D.6})$$

$$g^{\mu\nu} \equiv g_{(0)}^{\mu\nu} + \delta g^{\mu\nu} , \quad (\text{D.7})$$

two useful expressions are

$$\delta g^{\mu\nu} \simeq -g_{(0)}^{\mu\alpha} g_{(0)}^{\nu\beta} \delta g_{\alpha\beta} , \quad (\text{D.8})$$

$$\det(g^{(0)} + \delta g) \simeq \left(1 + g_{(0)}^{\mu\nu} \delta g_{\mu\nu}\right) \det(g^{(0)}) . \quad (\text{D.9})$$

D.2 Perturbations on a FLRW space-time

D.2.1 Background

The line element for a flat FLRW space-time is

$$ds^2 = a^2(\tau) \left(-d\tau^2 + dx^i dx_i \right), \quad (\text{D.10})$$

For the background, we only display the non-zero components and we define $\mathcal{H} = \dot{a}/a$.

Christoffel symbols

$$\Gamma^0_{00} = \mathcal{H}, \quad (\text{D.11a})$$

$$\Gamma^0_{ij} = \delta_{ij} \mathcal{H}, \quad (\text{D.11b})$$

$$\Gamma^i_{0j} = \delta^i_j \mathcal{H}. \quad (\text{D.11c})$$

Ricci tensor

$$R_{00} = -3\dot{\mathcal{H}}, \quad (\text{D.12a})$$

$$R_{ij} = \delta_{ij} \left(\dot{\mathcal{H}} + 2\mathcal{H}^2 \right), \quad (\text{D.12b})$$

$$a^2 R^0_0 = 3\dot{\mathcal{H}}, \quad (\text{D.12c})$$

$$a^2 R^i_j = \delta^i_j \left(\dot{\mathcal{H}} + 2\mathcal{H}^2 \right), \quad (\text{D.12d})$$

$$R = 6a^{-2} \left(\dot{\mathcal{H}} + \mathcal{H}^2 \right). \quad (\text{D.12e})$$

Einstein tensor

$$G_{00} = 3\mathcal{H}^2, \quad (\text{D.13a})$$

$$G_{ij} = -\delta_{ij} \left(2\dot{\mathcal{H}} + \mathcal{H}^2 \right), \quad (\text{D.13b})$$

$$a^2 G^0_0 = -3\mathcal{H}^2, \quad (\text{D.13c})$$

$$a^2 G^i_j = -\delta^i_j \left(2\dot{\mathcal{H}} + \mathcal{H}^2 \right). \quad (\text{D.13d})$$

Riemann tensor

$$a^{-2} R_{0i0j} = \delta_{ij} \dot{\mathcal{H}}, \quad (\text{D.14a})$$

$$a^{-2} R_{0ijk} = 0, \quad (\text{D.14b})$$

$$a^{-2} R_{ijkl} = \mathcal{H}^2 \left(\delta_{ik} \delta_{lj} - \delta_{il} \delta_{jk} \right). \quad (\text{D.14c})$$

Weyl tensor

$$a^{-2}C_{0i0j} = 0, \quad (\text{D.15a})$$

$$a^{-2}C_{0ijk} = 0, \quad (\text{D.15b})$$

$$a^{-2}C_{ijkl} = 0. \quad (\text{D.15c})$$

D.2.2 General perturbations

We define a generic perturbation over the homogeneous RW metric as

$$ds^2 = a^2(\tau) \left(-(1-A)d\tau^2 + 2B_i d\tau dx^i + (\delta_{ij} + H_{ij}) dx^i dx^j \right), \quad (\text{D.16})$$

that is,

$$g_{\mu\nu} = a^2 \begin{pmatrix} -1+A & B_i \\ B_i & \delta_{ij} + H_{ij} \end{pmatrix}, \quad g^{\mu\nu} = \frac{1}{a^2} \begin{pmatrix} -1-A & B^i \\ B^i & \delta^{ij} - H^{ij} \end{pmatrix}. \quad (\text{D.17})$$

Christoffel symbols

$$\delta\Gamma^0_{00} = -\frac{1}{2}\dot{A}, \quad (\text{D.18a})$$

$$\delta\Gamma^0_{0i} = -\frac{1}{2}\partial_i A + \mathcal{H}B_i, \quad (\text{D.18b})$$

$$\delta\Gamma^i_{00} = B^i \mathcal{H} - \frac{1}{2}\partial^i A + \dot{B}^i, \quad (\text{D.18c})$$

$$\delta\Gamma^0_{ij} = -\frac{1}{2}(\partial_j B_i + \partial_i B_j) + \frac{1}{2}\dot{H}_{ij} + \mathcal{H}H_{ij} + \delta_{ij}A\mathcal{H}, \quad (\text{D.18d})$$

$$\delta\Gamma^i_{0j} = -\frac{1}{2}(\partial^i B_j - \partial_j B^i) + \frac{1}{2}\dot{H}^i_j, \quad (\text{D.18e})$$

$$\delta\Gamma^i_{jk} = \frac{1}{2}(\partial_k H_j^i + \partial_j H_k^i - \partial^i H_{jk}) - \mathcal{H}B^i \delta_{jk}. \quad (\text{D.18f})$$

Ricci tensor

$$\delta R_{00} = -\frac{1}{2}\partial^i \partial_i A + \partial_i \dot{B}^i - \frac{1}{2}\ddot{H}^i_i + \mathcal{H} \left(\partial_i B^i - \frac{3}{2}\dot{A} - \frac{1}{2}\dot{H}^i_i \right), \quad (\text{D.19a})$$

$$\delta R_{0i} = -\frac{1}{2}\partial^j \partial_j B_i + \frac{1}{2}\partial_i \partial_j B^j + \frac{1}{2}\partial_j \dot{H}^j_i - \frac{1}{2}\partial_i \dot{H}^j_j + B_i(\dot{\mathcal{H}} + 2\mathcal{H}^2) - \mathcal{H}\partial_i A, \quad (\text{D.19b})$$

$$\begin{aligned} \delta R_{ij} = & \frac{1}{2}\partial_i \partial_j A - \frac{1}{2}(\partial_j \dot{B}_i + \partial_i \dot{B}_j) + \frac{1}{2}\ddot{H}_{ij} + H_{ij}(\dot{\mathcal{H}} + 2\mathcal{H}^2) \\ & + \frac{1}{2}(\partial_i \partial_k H_j^k + \partial_j \partial_k H_i^k - \partial_i \partial_j H_k^k - \partial^k \partial_k H_{ij}) + \mathcal{H}(\dot{H}_{ij} - \partial_j B_i - \partial_i B_j) \\ & + \delta_{ij} \frac{1}{2}\mathcal{H} \left(\dot{A} - 2\partial_k B^k + \dot{H}^k_k \right) + \delta_{ij} A(\dot{\mathcal{H}} + 2\mathcal{H}^2), \end{aligned} \quad (\text{D.19c})$$

$$a^2 \delta R^0_0 = \frac{1}{2}\partial^i \partial_i A - \partial_i \dot{B}^i + \frac{1}{2}\ddot{H}^i_i + 3A\dot{\mathcal{H}} + \mathcal{H} \left(\frac{3}{2}\dot{A} - \partial_i B^i + \frac{1}{2}\dot{H}^i_i \right), \quad (\text{D.19d})$$

$$a^2 \delta R^0_i = \frac{1}{2}\partial^j \partial_j B_i - \frac{1}{2}\partial_i \partial_j B^j - \frac{1}{2}\partial_j \dot{H}^j_i + \frac{1}{2}\partial_i \dot{H}^j_j + \mathcal{H}\partial_i A, \quad (\text{D.19e})$$

$$a^2 \delta R^i{}_0 = -\frac{1}{2} \partial^j \partial_j B^i + \frac{1}{2} \partial^i \partial_j B^j + \frac{1}{2} \partial^j \dot{H}_j^i - \frac{1}{2} \partial^i \dot{H}_j^j - 2B^i (\dot{\mathcal{H}} - \mathcal{H}^2) - \mathcal{H} \partial^i A, \quad (\text{D.19f})$$

$$\begin{aligned} a^2 \delta R^i{}_j &= \frac{1}{2} \partial^i \partial_j A - \frac{1}{2} \partial^i \dot{B}_j - \frac{1}{2} \partial_j \dot{B}^i + \frac{1}{2} \dot{H}_j^i \\ &\quad + \frac{1}{2} \partial^i \partial^k H_{kj} + \frac{1}{2} \partial_j \partial_k H^{ik} - \frac{1}{2} \partial^k \partial_k H_j^i - \frac{1}{2} \partial^i \partial_j H_k^k \\ &\quad + \delta_j^i A (\dot{\mathcal{H}} + 2\mathcal{H}^2) + \mathcal{H} \left(\dot{H}_j^i - \partial^i B_j - \partial_j B^i + \frac{1}{2} \delta_j^i (\dot{A} - 2\partial_k B^k + \dot{H}_k^k) \right), \end{aligned} \quad (\text{D.19g})$$

$$\begin{aligned} a^2 \delta R &= \partial^i \partial_i A - 2\partial_i \dot{B}^i + \ddot{H}_i^i + \partial_i \partial_j H^{ij} - \partial^i \partial_i H_j^j \\ &\quad + 6A (\dot{\mathcal{H}} + \mathcal{H}^2) + 3\mathcal{H} (\dot{A} - 2\partial^i B_i + \dot{H}_i^i). \end{aligned} \quad (\text{D.19h})$$

Einstein tensor

$$\delta G_{00} = \frac{1}{2} \partial_i \partial_j H^{ij} - \frac{1}{2} \partial^i \partial_i H_j^j + \mathcal{H} (\dot{H}_i^i - 2\partial_i B^i), \quad (\text{D.20a})$$

$$\delta G_{0i} = -\frac{1}{2} \partial^j \partial_j B_i + \frac{1}{2} \partial_i \partial_j B^j + \frac{1}{2} \partial_j \dot{H}_i^j - \frac{1}{2} \partial_i \dot{H}_j^j - \mathcal{H} \partial_i A - 2 \left(\dot{\mathcal{H}} + \frac{1}{2} \mathcal{H}^2 \right) B_i, \quad (\text{D.20b})$$

$$\begin{aligned} \delta G_{ij} &= \frac{1}{2} \partial_i \partial_j A - \frac{1}{2} (\partial_i \dot{B}_j + \partial_j \dot{B}_i) + \frac{1}{2} \ddot{H}_{ij} - \frac{1}{2} \partial^k \partial_k H_{ij} \\ &\quad + \frac{1}{2} (\partial_i \partial_k H_j^k + \partial_j \partial_k H_i^k) - \frac{1}{2} \partial_i \partial_j H_k^k \\ &\quad - 2 \left(\dot{\mathcal{H}} + \frac{1}{2} \mathcal{H}^2 \right) H_{ij} + \mathcal{H} (\dot{H}_{ij} - \partial_i B_j - \partial_j B_i) \\ &\quad - \delta_{ij} \left\{ \frac{1}{2} \partial^k \partial_k A - \partial_k \dot{B}^k + \frac{1}{2} \ddot{H}_k^k + \frac{1}{2} \partial_k \partial_l H^{kl} - \frac{1}{2} \partial^k \partial_k H_l^l \right. \\ &\quad \left. + \mathcal{H} (\dot{A} - 2\partial_k B^k + \dot{H}_k^k) + 2 \left(\dot{\mathcal{H}} + \frac{1}{2} \mathcal{H}^2 \right) A \right\}, \end{aligned} \quad (\text{D.20c})$$

$$a^2 \delta G^0{}_0 = -\frac{1}{2} \partial_i \partial_j H^{ij} + \frac{1}{2} \partial^j \partial_j H_i^i + \mathcal{H} (2\partial_i B^i - \dot{H}_i^i) - 3\mathcal{H}^2 A, \quad (\text{D.20d})$$

$$a^2 \delta G^0{}_i = \frac{1}{2} \partial^j \partial_j B_i - \frac{1}{2} \partial_i \partial^j B_j - \frac{1}{2} \partial_j \dot{H}_i^j + \frac{1}{2} \partial_i \dot{H}_j^j + \mathcal{H} \partial_i A, \quad (\text{D.20e})$$

$$a^2 \delta G^i{}_0 = -\frac{1}{2} \partial^j \partial_j B^i + \frac{1}{2} \partial^i \partial^j B_j + \frac{1}{2} \partial_j \dot{H}^{ij} - \frac{1}{2} \partial^i \dot{H}_j^j - \mathcal{H} \partial^i A - 2B^i (\dot{\mathcal{H}} - \mathcal{H}^2), \quad (\text{D.20f})$$

$$\begin{aligned} a^2 \delta G^i{}_j &= \frac{1}{2} \partial^i \partial_j A - \frac{1}{2} (\partial_j \dot{B}^i + \partial^i \dot{B}_j) + \frac{1}{2} \ddot{H}_j^i - \frac{1}{2} \partial^k \partial_k H_j^i \\ &\quad + \frac{1}{2} \partial^k \partial_j H_k^i + \frac{1}{2} \partial^i \partial_k H_j^k - \frac{1}{2} \partial^i \partial_j H_k^k + \mathcal{H} (\dot{H}_j^i - \partial_j B^i - \partial^i B_j) \\ &\quad - \delta_j^i \left\{ \frac{1}{2} \partial^k \partial_k A - \partial_k \dot{B}^k + 2A \left(\dot{\mathcal{H}} + \frac{1}{2} \mathcal{H}^2 \right) + \mathcal{H} (\dot{A} - 2\partial_k B^k + \dot{H}_k^k) \right. \\ &\quad \left. + \frac{1}{2} \ddot{H}_k^k + \frac{1}{2} \partial_k \partial_l H^{kl} - \frac{1}{2} \partial^k \partial_k H_l^l \right\}. \end{aligned} \quad (\text{D.20g})$$

Riemann tensor

$$\begin{aligned} a^{-2} \delta R_{0i0j} &= -\frac{1}{2} \partial_i \partial_j A + \frac{1}{2} (\partial_i B_j + \partial_j B_i) - \frac{1}{2} \ddot{H}_{ij} - \dot{\mathcal{H}} H_{ij} \\ &\quad + \frac{1}{2} \mathcal{H} (\partial_i B_j + \partial_j B_i - \dot{H}_{ij} - \delta_{ij} \dot{A}), \end{aligned} \quad (\text{D.21a})$$

$$\alpha^{-2}\delta R_{0ijk} = \partial_i\partial_{[j}B_{k]} + \partial_{[k}\dot{H}_{j]i} + \mathcal{H}\delta_{i[j}\partial_{k]}A + 2\mathcal{H}^2\delta_{i[k}B_{j]} , \quad (\text{D.21b})$$

$$\begin{aligned} \alpha^{-2}\delta R_{ijkl} = & \partial_i\partial_{[l}H_{k]j} + \partial_j\partial_{[k}H_{l]i} - \frac{1}{2}\mathcal{H}\delta_{i[l}(\dot{H}_{k]j} + 2\mathcal{H}H_{k]j} - \partial_jB_{k]} - \partial_{k]}B_j) \\ & - \frac{1}{2}\mathcal{H}\delta_{j[k}(\dot{H}_{l]i} + 2\mathcal{H}H_{l]i} - \partial_iB_{l]} - \partial_{l]}B_i) + \mathcal{H}^2A(\delta_{ik}\delta_{jl} - \delta_{il}\delta_{jk}) . \end{aligned} \quad (\text{D.21c})$$

Weyl tensor

$$\begin{aligned} \alpha^{-2}\delta C_{0i0j} = & -\frac{1}{4}\partial_i\partial_jA + \frac{1}{4}(\partial_i\dot{B}_j + \partial_j\dot{B}_i) \\ & - \frac{1}{4}(\ddot{H}_{ij} + \partial_j\partial^k H_{ki} + \partial_i\partial^k H_{kj} - \partial^k\partial_k H_{ij} - \partial_i\partial_j H_k^k) \\ & + \frac{1}{12}\delta_{ij}(\partial^k\partial_k A - 2\partial^k\dot{B}_k + \ddot{H}_k^k - 2\partial^k\partial^l H_{kl} + 2\partial^l\partial_l H_k^k) , \end{aligned} \quad (\text{D.22a})$$

$$\alpha^{-2}\delta C_{0ijk} = \partial_i\partial_{[j}B_{k]} + \partial_{[k}\dot{H}_{j]i} + \frac{1}{2}\delta_{i[k}(\partial^l\partial_l B_{j]} - \partial_{j]}\partial^l B_l - \partial^l\dot{H}_{j]l} + \partial_{j]}\dot{H}_l^l) , \quad (\text{D.22b})$$

$$\begin{aligned} \alpha^{-2}\delta C_{ijkl} = & \partial_i\partial_{[l}H_{k]j} + \partial_j\partial_{[k}H_{l]i} \\ & + \frac{1}{2}\delta_{i[l}(\partial_{k]}\partial_j A - \partial_{k]}\dot{B}_j - \partial_j\dot{B}_{k]} + \ddot{H}_{k]j} + \partial_{k]}\partial^m H_{mj} + \partial_j\partial^m H_{k]m} \\ & \quad - \partial^m\partial_m H_{k]j} - \partial_{k]}\partial_j H_m^m) \\ & + \frac{1}{2}\delta_{j[k}(\partial_{l]}\partial_i A - \partial_{l]}\dot{B}_i - \partial_i\dot{B}_{l]} + \ddot{H}_{l]i} + \partial_{l]}\partial^m H_{mi} + \partial_i\partial^m H_{k]m} \\ & \quad - \partial^m\partial_m H_{l]i} - \partial_{l]}\partial_i H_m^m) \\ & + \frac{1}{3}\delta_{i[k}\delta_{l]j}(\partial^m\partial_m A - 2\partial^m\dot{B}_m + \ddot{H}_m^m + \partial^m\partial^n H_{mn} - \partial^n\partial_n H_m^m) . \end{aligned} \quad (\text{D.22c})$$

D.2.3 Scalar perturbations

For scalar perturbations we have

$$\begin{aligned} A &= -2\Psi , & B_i &= \partial_i B , \\ H_{ij} &= -2\Phi\delta_{ij} + 2\partial_i\partial_j E . \end{aligned} \quad (\text{D.23})$$

Christoffel symbols

$$\delta\Gamma_{(s)00}^0 = \dot{\Psi} , \quad (\text{D.24a})$$

$$\delta\Gamma_{(s)0i}^0 = \partial_i\Psi + \mathcal{H}\partial_i B , \quad (\text{D.24b})$$

$$\delta\Gamma_{(s)00}^i = \partial^i\Psi + \partial^i\dot{B} + \mathcal{H}\partial^i B , \quad (\text{D.24c})$$

$$\delta\Gamma_{(s)ij}^0 = -\partial_i\partial_j(B - \dot{E}) + 2\mathcal{H}(\partial_i\partial_j E - \delta_{ij}(\Phi + \Psi)) - \delta_{ij}\dot{\Phi} , \quad (\text{D.24d})$$

$$\delta\Gamma_{(s)0j}^i = \partial^i\partial_j\dot{E} - \delta_j^i\dot{\Phi} , \quad (\text{D.24e})$$

$$\delta\Gamma_{(s)jk}^i = \partial^i\partial_j\partial_k E - \delta_{jk}\mathcal{H}\partial^i B + \delta_{jk}\partial^i\Phi - \delta_k^i\partial_j\Phi - \delta_j^i\partial_k\Phi . \quad (\text{D.24f})$$

Ricci tensor

$$\delta R_{(s)00} = 3\ddot{\Phi} + \partial^i \partial_i \Psi + \partial^i \partial_i (\dot{B} - \dot{E}) + \mathcal{H} \left(3(\dot{\Phi} + \dot{\Psi}) + \partial^i \partial_i (B - \dot{E}) \right), \quad (\text{D.25a})$$

$$\delta R_{(s)0i} = 2\partial_i \dot{\Phi} + \left(\dot{\mathcal{H}} + 2\mathcal{H} \right) \partial_i B + 2\mathcal{H} \partial_i \Psi, \quad (\text{D.25b})$$

$$\begin{aligned} \delta R_{(s)ij} = & \partial_i \partial_j (\Phi - \Psi) - \partial_i \partial_j (\dot{B} - \dot{E}) + 2 \left(\dot{\mathcal{H}} + 2\mathcal{H}^2 \right) \partial_i \partial_j E - 2\mathcal{H} \partial_i \partial_j (B - \dot{E}) \\ & - \delta_{ij} \left\{ \ddot{\Phi} - \partial^k \partial_k \Phi + 2(\dot{\mathcal{H}} + 2\mathcal{H}^2)(\Phi + \Psi) \right. \\ & \left. + \mathcal{H} \left(\dot{\Psi} + 5\dot{\Phi} + \partial^k \partial_k (B - \dot{E}) \right) \right\}, \end{aligned} \quad (\text{D.25c})$$

$$\begin{aligned} \alpha^2 \delta R_{(s)0}^0 = & -3\ddot{\Phi} - \partial^i \partial_i \Psi - \partial^i \partial_i (\dot{B} - \dot{E}) - 6\dot{\mathcal{H}}\Psi \\ & - \mathcal{H} \left(3(\dot{\Phi} + \dot{\Psi}) + \partial^i \partial_i (B - \dot{E}) \right), \end{aligned} \quad (\text{D.25d})$$

$$\alpha^2 \delta R_{(s)i}^0 = -2\partial_i \dot{\Phi} - 2\mathcal{H} \partial_i \Psi, \quad (\text{D.25e})$$

$$\alpha^2 \delta R_{(s)0}^i = 2\partial^i \dot{\Phi} + 2\mathcal{H} \partial^i \Psi - 2(\dot{\mathcal{H}} - \mathcal{H}^2) \partial^i B, \quad (\text{D.25f})$$

$$\begin{aligned} \alpha^2 \delta R_{(s)i}^j = & \partial^i \partial_j (\Phi - \Psi) - \partial^i \partial_j (\dot{B} - \dot{E}) - 2\mathcal{H} \partial^i \partial_j (B - \dot{E}) \\ & - \delta_j^i \left\{ \ddot{\Phi} - \partial^k \partial_k \Phi + 2(\dot{\mathcal{H}} + 2\mathcal{H}^2)\Psi + \mathcal{H} \left(\dot{\Psi} + 5\dot{\Phi} + \partial^k \partial_k (B - \dot{E}) \right) \right\}, \end{aligned} \quad (\text{D.25g})$$

$$\begin{aligned} \alpha^2 \delta R_{(s)} = & -6\ddot{\Phi} + 4\partial_i \partial^i \Phi - 2\partial_i \partial^i \Psi - 2\partial_i \partial^i (\dot{B} - \dot{E}) - 12 \left(\dot{\mathcal{H}} + \mathcal{H}^2 \right) \Psi \\ & - 6\mathcal{H} \left(3\dot{\Phi} + \dot{\Psi} + \partial_i \partial^i (B - \dot{E}) \right). \end{aligned} \quad (\text{D.25h})$$

Einstein tensor

$$\delta G_{(s)00} = 2\partial_i \partial^i \Phi - 2\mathcal{H} \left(3\dot{\Phi} + \partial_i \partial^i (B - \dot{E}) \right), \quad (\text{D.26a})$$

$$\delta G_{(s)0i} = 2\partial_i \dot{\Phi} - 2 \left(\dot{\mathcal{H}} + \frac{1}{2} \mathcal{H}^2 \right) \partial_i B + 2\mathcal{H} \partial_i \Psi, \quad (\text{D.26b})$$

$$\begin{aligned} \delta G_{(s)ij} = & \partial_i \partial_j (\Phi - \Psi) - \partial_i \partial_j (\dot{B} - \dot{E}) - 4 \left(\dot{\mathcal{H}} + \frac{1}{2} \mathcal{H}^2 \right) \partial_i \partial_j E - 2\mathcal{H} \partial_i \partial_j (B - \dot{E}) \\ & + \delta_{ij} \left\{ 2\mathcal{H} \left(2\dot{\Phi} + \dot{\Psi} + \partial_k \partial^k (B - \dot{E}) \right) + 2\ddot{\Phi} - \partial_k \partial^k (\Phi - \Psi) \right. \\ & \left. + \partial_k \partial^k (\dot{B} - \dot{E}) + 4 \left(\dot{\mathcal{H}} + \frac{1}{2} \mathcal{H}^2 \right) (\Phi + \Psi) \right\}, \end{aligned} \quad (\text{D.26c})$$

$$\alpha^2 \delta G_{(s)0}^0 = -2\partial_i \partial^i \Phi + 6\mathcal{H}^2 \Psi + 2\mathcal{H} \left(3\dot{\Phi} + \partial_i \partial^i (B - \dot{E}) \right), \quad (\text{D.26d})$$

$$\alpha^2 \delta G_{(s)i}^0 = -2\partial_i (\dot{\Phi} + \mathcal{H}\Psi), \quad (\text{D.26e})$$

$$\alpha^2 \delta G_{(s)0}^i = 2\partial^i (\dot{\Phi} + \mathcal{H}\Psi) - 2 \left(\dot{\mathcal{H}} - \mathcal{H}^2 \right) \partial^i B, \quad (\text{D.26f})$$

$$\begin{aligned} \alpha^2 \delta G_{(s)i}^j = & \partial^i \partial_j (\Phi - \Psi) - \partial^i \partial_j (\dot{B} - \dot{E}) - 2\mathcal{H} \partial^i \partial_j (B - \dot{E}) \\ & + \delta_j^i \left\{ 2\mathcal{H} \left(2\dot{\Phi} + \dot{\Psi} + \partial_k \partial^k (B - \dot{E}) \right) + 2\ddot{\Phi} - \partial_k \partial^k (\Phi - \Psi) \right. \\ & \left. + \partial_k \partial^k (\dot{B} - \dot{E}) + 4 \left(\dot{\mathcal{H}} + \frac{1}{2} \mathcal{H}^2 \right) \Psi \right\}. \end{aligned} \quad (\text{D.26g})$$

Riemann tensor

$$\begin{aligned} \alpha^{-2} \delta R_{(s)0i0j} &= \partial_i \partial_j \Psi + \partial_i \partial_j (\dot{B} - \ddot{E}) + \delta_{ij} \left\{ \ddot{\Phi} + \mathcal{H}(\dot{\Phi} + \dot{\Psi}) + 2\dot{\mathcal{H}}\Phi \right\} \\ &\quad + \mathcal{H} \partial_i \partial_j (B - \dot{E}) - 2\dot{\mathcal{H}} \partial_i \partial_j E , \end{aligned} \quad (\text{D.27a})$$

$$\alpha^{-2} \delta R_{(s)0ijk} = 2\delta_{i[k} \partial_{j]} (\dot{\Phi} + \mathcal{H}\Psi + \mathcal{H}^2 B) , \quad (\text{D.27b})$$

$$\begin{aligned} \alpha^{-2} \delta R_{(s)ijkl} &= 2(\delta_{i[k} \partial_{l]} \partial_j + \delta_{j[l} \partial_{k]} \partial_i) \{ \Phi - \mathcal{H}(B - \dot{E}) + 2\mathcal{H}^2 E \} \\ &\quad + 4\delta_{i[l} \delta_{k]j} \mathcal{H} (\dot{\Phi} + \mathcal{H}(\Psi + 2\Phi)) . \end{aligned} \quad (\text{D.27c})$$

Weyl tensor

$$\alpha^{-2} \delta C_{(s)0i0j} = \frac{1}{2} \left(\partial_i \partial_j - \frac{1}{3} \delta_{ij} \partial^k \partial_k \right) \{ \Phi + \Psi + (\dot{B} - \ddot{E}) \} , \quad (\text{D.28a})$$

$$\alpha^{-2} \delta C_{(s)0ijk} = 0 , \quad (\text{D.28b})$$

$$\alpha^{-2} \delta C_{(s)ijkl} = \left(\delta_{i[k} \partial_{l]} \partial_j + \delta_{j[l} \partial_{k]} \partial_i + \frac{2}{3} \delta_{i[l} \delta_{k]j} \partial^m \partial_m \right) \{ \Phi + \Psi + (\dot{B} - \ddot{E}) \} . \quad (\text{D.28c})$$

D.2.4 Vector perturbations

For vector perturbations we have

$$\begin{aligned} A &= 0 , & B_i &= -S_i , \\ H_{ij} &= \partial_i F_j + \partial_j F_i , & \partial_i S^i &= \partial_i F^i = 0 . \end{aligned} \quad (\text{D.29})$$

Christoffel symbols

$$\delta \Gamma_{(v)00}^0 = 0 , \quad (\text{D.30a})$$

$$\delta \Gamma_{(v)0i}^0 = -\mathcal{H} S_i , \quad (\text{D.30b})$$

$$\delta \Gamma_{(v)00}^i = -\dot{S}^i - \mathcal{H} S^i , \quad (\text{D.30c})$$

$$\delta \Gamma_{(v)ij}^0 = \frac{1}{2} (\partial_i S_j + \partial_j S_i + \partial_i \dot{F}_j + \partial_j \dot{F}_i) + \mathcal{H} (\partial_i F_j + \partial_j F_i) , \quad (\text{D.30d})$$

$$\delta \Gamma_{(v)0j}^i = \frac{1}{2} (\partial^i S_j - \partial_j S^i) + \frac{1}{2} (\partial^i \dot{F}_j + \partial_j \dot{F}^i) , \quad (\text{D.30e})$$

$$\delta \Gamma_{(v)jk}^i = \partial_j \partial_k F^i + \delta_{jk} \mathcal{H} S^i . \quad (\text{D.30f})$$

Ricci tensor

$$\delta R_{(v)00} = 0 , \quad (\text{D.31a})$$

$$\delta R_{(v)0i} = \frac{1}{2} \partial^j \partial_j (S_i + \dot{F}_i) - S_i (\dot{\mathcal{H}} + 2\mathcal{H}^2) , \quad (\text{D.31b})$$

$$\begin{aligned} \delta R_{(v)ij} &= \frac{1}{2} (\partial_i \dot{S}_j + \partial_j \dot{S}_i) + \frac{1}{2} (\partial_i \ddot{F}_j + \partial_j \ddot{F}_i) + (\partial_i F_j + \partial_j F_i) (\dot{\mathcal{H}} + 2\mathcal{H}^2) \\ &\quad + \mathcal{H} (\partial_i S_j + \partial_j S_i + \partial_i \dot{F}_j + \partial_j \dot{F}_i) , \end{aligned} \quad (\text{D.31c})$$

$$\alpha^2 \delta R_{(v)0}^0 = 0 , \quad (\text{D.31d})$$

$$a^2 \delta R_{(v) i}^0 = -\frac{1}{2} \partial^j \partial_j (S_i + \dot{F}_i) , \quad (\text{D.31e})$$

$$a^2 \delta R_{(v) 0}^i = \frac{1}{2} \partial^j \partial_j (S^i + \dot{F}^i) + 2S^i (\dot{\mathcal{H}} - \mathcal{H}^2) , \quad (\text{D.31f})$$

$$a^2 \delta R_{(v) j}^i = \frac{1}{2} (\partial_j \dot{S}^i + \partial^i \dot{S}_j) + \frac{1}{2} (\partial_j \ddot{F}^i + \partial^i \ddot{F}_j) \\ + \mathcal{H} (\partial_j S^i + \partial^i S_j + \partial_j \dot{F}^i + \partial^i \dot{F}_j) , \quad (\text{D.31g})$$

$$\delta R_{(v)} = 0 . \quad (\text{D.31h})$$

Einstein tensor

$$\delta G_{(v) 00} = 0 , \quad (\text{D.32a})$$

$$\delta G_{(v) 0i} = \frac{1}{2} \partial^j \partial_j (S_i + \dot{F}_i) + 2S_i \left(\dot{\mathcal{H}} + \frac{1}{2} \mathcal{H}^2 \right) , \quad (\text{D.32b})$$

$$\delta G_{(v) ij} = \frac{1}{2} (\partial_i \dot{S}_j + \partial_j \dot{S}_i) + \frac{1}{2} (\partial_i \ddot{F}_j + \partial_j \ddot{F}_i) - 2 (\partial_i F_j + \partial_j F_i) \left(\dot{\mathcal{H}} + \frac{1}{2} \mathcal{H}^2 \right) \\ + \mathcal{H} (\partial_i S_j + \partial_j S_i + \partial_i \dot{F}_j + \partial_j \dot{F}_i) , \quad (\text{D.32c})$$

$$a^2 \delta G_{(v) 0}^0 = 0 , \quad (\text{D.32d})$$

$$a^2 \delta G_{(v) i}^0 = -\frac{1}{2} \partial^j \partial_j (S_i + \dot{F}_i) , \quad (\text{D.32e})$$

$$a^2 \delta G_{(v) 0}^i = \frac{1}{2} \partial^j \partial_j (S^i + \dot{F}^i) + 2S^i (\dot{\mathcal{H}} - \mathcal{H}^2) , \quad (\text{D.32f})$$

$$a^2 \delta G_{(v) j}^i = \frac{1}{2} (\partial_j \dot{S}^i + \partial^i \dot{S}_j) + \frac{1}{2} (\partial_j \ddot{F}^i + \partial^i \ddot{F}_j) \\ + \mathcal{H} (\partial_j S^i + \partial^i S_j + \partial_j \dot{F}^i + \partial^i \dot{F}_j) . \quad (\text{D.32g})$$

Riemann tensor

$$a^{-2} \delta R_{(v) 0i0j} = -\partial_{(i} \{ \dot{S}_{j)} + \ddot{F}_{j)} \} + \mathcal{H} (S_j + \dot{F}_j) + 2\dot{\mathcal{H}} F_j \} , \quad (\text{D.33a})$$

$$a^{-2} \delta R_{(v) 0ijk} = \partial_i \partial_{[k} (S_{j]} + \dot{F}_{j]}) + 2\mathcal{H}^2 \delta_{i[l} S_{k]} , \quad (\text{D.33b})$$

$$a^{-2} \delta R_{(v) ijkl} = \mathcal{H} \delta_{i[k} \{ \partial_{l]} (S_j + \dot{F}_j) + \partial_j (S_{l]} + \dot{F}_{l]}) + 2\mathcal{H} (\partial_{l]} F_j + \partial_j F_{l]}) \} \\ + \mathcal{H} \delta_{j[l} \{ \partial_{k]} (S_i + \dot{F}_i) + \partial_i (S_{k]} + \dot{F}_{k]}) + 2\mathcal{H} (\partial_{k]} F_i + \partial_i F_{k]}) \} . \quad (\text{D.33c})$$

Weyl tensor

$$a^{-2} \delta C_{(v) 0i0j} = -\frac{1}{2} \partial_{(i} (\dot{S}_{j)} + \ddot{F}_{j)}) , \quad (\text{D.34a})$$

$$a^{-2} \delta C_{(v) 0ijk} = \left(\partial_i \partial_{[k} - \frac{1}{2} \delta_{i[k} \partial^l \partial_{l]} \right) (S_{j]} + \dot{F}_{j]}) , \quad (\text{D.34b})$$

$$a^{-2} \delta C_{(v) ijkl} = -\frac{1}{2} \delta_{i[k} \{ \partial_{l]} (\dot{S}_j + \ddot{F}_j) + \partial_j (\dot{S}_{l]} + \ddot{F}_{l]}) \} \\ - \frac{1}{2} \delta_{j[l} \{ \partial_{k]} (\dot{S}_i + \ddot{F}_i) + \partial_i (\dot{S}_{k]} + \ddot{F}_{k]}) \} . \quad (\text{D.34c})$$

D.2.5 Tensor perturbations

For tensor perturbations we have

$$\begin{aligned} A = 0, \quad B_i = 0, \quad H_{ij} = h_{ij}, \\ \partial_i h_j^i = 0 \quad h^i_i = 0. \end{aligned} \quad (\text{D.35})$$

Christoffel symbols

$$\delta\Gamma_{(\text{T})00}^0 = 0, \quad (\text{D.36a})$$

$$\delta\Gamma_{(\text{T})0i}^0 = 0, \quad (\text{D.36b})$$

$$\delta\Gamma_{(\text{T})00}^i = 0, \quad (\text{D.36c})$$

$$\delta\Gamma_{(\text{T})ij}^0 = \frac{1}{2}\dot{h}_{ij} + \mathcal{H}h_{ij}, \quad (\text{D.36d})$$

$$\delta\Gamma_{(\text{T})0j}^i = \frac{1}{2}\dot{h}_j^i, \quad (\text{D.36e})$$

$$\delta\Gamma_{(\text{T})jk}^i = \frac{1}{2}\partial_k h_j^i - \frac{1}{2}\partial^i h_{jk} + \frac{1}{2}\partial_j h_k^i. \quad (\text{D.36f})$$

Ricci tensor

$$\delta R_{(\text{T})00} = 0, \quad (\text{D.37a})$$

$$\delta R_{(\text{T})0i} = 0, \quad (\text{D.37b})$$

$$\delta R_{(\text{T})ij} = \frac{1}{2}\ddot{h}_{ij} + \mathcal{H}\dot{h}_{ij} + \left(\dot{\mathcal{H}} + 2\mathcal{H}^2\right)h_{ij} - \frac{1}{2}\partial^k \partial_k h_{ij}, \quad (\text{D.37c})$$

$$a^2 \delta R_{(\text{T})0}^0 = 0, \quad (\text{D.37d})$$

$$a^2 \delta R_{(\text{T})i}^0 = 0, \quad (\text{D.37e})$$

$$a^2 \delta R_{(\text{T})0}^i = 0, \quad (\text{D.37f})$$

$$a^2 \delta R_{(\text{T})j}^i = \frac{1}{2}\ddot{h}_j^i + \mathcal{H}\dot{h}_j^i - \frac{1}{2}\partial^k \partial_k h_j^i, \quad (\text{D.37g})$$

$$\delta R_{(\text{T})} = 0. \quad (\text{D.37h})$$

Einstein tensor

$$\delta G_{(\text{T})00} = 0, \quad (\text{D.38a})$$

$$\delta G_{(\text{T})0i} = 0, \quad (\text{D.38b})$$

$$\delta G_{(\text{T})ij} = \frac{1}{2}\ddot{h}_{ij} + \mathcal{H}\dot{h}_{ij} - 2\left(\dot{\mathcal{H}} + \frac{1}{2}\mathcal{H}^2\right)h_{ij} - \frac{1}{2}\partial^k \partial_k h_{ij}, \quad (\text{D.38c})$$

$$a^2 \delta G_{(\text{T})0}^0 = 0, \quad (\text{D.38d})$$

$$a^2 \delta G_{(\text{T})i}^0 = 0, \quad (\text{D.38e})$$

$$a^2 \delta G_{(\text{T})0}^i = 0, \quad (\text{D.38f})$$

$$a^2 \delta G_{(\text{T})j}^i = \frac{1}{2}\ddot{h}_j^i + \mathcal{H}\dot{h}_j^i - \frac{1}{2}\partial^k \partial_k h_j^i. \quad (\text{D.38g})$$

Riemann tensor

$$a^{-2}\delta R_{(\tau)0i0j} = -\frac{1}{2}\left(\ddot{h}_{ij} + \mathcal{H}\dot{h}_{ij} + 2\dot{\mathcal{H}}h_{ij}\right), \quad (\text{D.39a})$$

$$a^{-2}\delta R_{(\tau)0ijk} = \frac{1}{2}\left(\partial_k \dot{h}_{ij} - \partial_j \dot{h}_{ik}\right), \quad (\text{D.39b})$$

$$a^{-2}\delta R_{(\tau)ijkl} = \partial_i \partial_{[l} h_{k]j} - \delta_{i[l} (\dot{h}_{k]j} + 2\mathcal{H}h_{k]j}) \\ + \partial_j \partial_{[k} h_{l]i} - \delta_{j[k} (\dot{h}_{l]i} + 2\mathcal{H}h_{l]i}). \quad (\text{D.39c})$$

Weyl tensor

$$a^{-2}\delta C_{(\tau)0i0j} = -\frac{1}{4}\left(\ddot{h}_{ij} + \partial^k \partial_k h_{ij}\right), \quad (\text{D.40a})$$

$$a^{-2}\delta C_{(\tau)0ijk} = \frac{1}{2}\left(\partial_k \dot{h}_{ij} - \partial_j \dot{h}_{ik}\right), \quad (\text{D.40b})$$

$$a^{-2}\delta C_{(\tau)ijkl} = \partial_i \partial_{[l} h_{k]j} + \frac{1}{2}\delta_{i[l} (\ddot{h}_{k]j} - \partial^m \partial_m h_{k]j}) \\ + \partial_j \partial_{[k} h_{l]i} + \frac{1}{2}\delta_{j[k} (\ddot{h}_{l]i} - \partial^m \partial_m h_{l]i}). \quad (\text{D.40c})$$

D.3 Geodesics

In this appendix we will compute in detail the geodesics for a general perturbed RW metric (D.16). Defining the proper-time parameter as $d\lambda \equiv \sqrt{-ds^2}$, the standard definitions for the four-velocity and four-momentum are

$$U^\mu \equiv \frac{dx^\mu}{d\lambda}, \quad (\text{D.41})$$

$$P_\mu \equiv mU_\mu, \quad (\text{D.42})$$

$$P_0 \equiv -\epsilon + \delta P_0. \quad (\text{D.43})$$

The geodesics are given by

$$\frac{dU^\mu}{d\lambda} + \Gamma^\mu_{\nu\rho} U^\nu U^\rho = 0, \quad (\text{D.44})$$

that can be conveniently rewritten as

$$\frac{dU_\mu}{d\lambda} = \frac{1}{2} \frac{\partial g_{\nu\rho}}{\partial x^\mu} U^\nu U^\rho. \quad (\text{D.45})$$

This last form is especially useful. Since the background metric is homogeneous, we can keep only the zero order in U_μ to compute the spatial part. Writing the evolution in terms of the conformal time we have

$$\frac{dP_i}{d\tau} = \frac{m}{U^0} \frac{dU_i}{d\lambda} = \frac{1}{2c} \left(\epsilon^2 \partial_i A + 2\epsilon P^j \partial_i B_j + P^j P^k \partial_i H_{jk} \right). \quad (\text{D.46})$$

The spatial momentum is redefined as

$$P_i \equiv \left(\delta^j_i + \frac{1}{2} H^j_i \right) q_j, \quad (\text{D.47})$$

$$a^2 P^i = -\epsilon B^i + \left(\delta^{ki} - \frac{1}{2} H^{ki} \right) q_k, \quad (\text{D.48})$$

where, from now on, every spatial index on a perturbed quantity is assumed to be raised or lowered using δ_{ij} . From the mass-shell condition, $P^\mu P_\mu = -m^2$, we obtain

$$\epsilon^2 = m^2 a^2 + q^2, \quad (\text{D.49})$$

$$P_0 = -\epsilon \left(1 - \frac{1}{2} A \right) + q_i B^i, \quad (\text{D.50})$$

$$P^0 = \frac{\epsilon}{a^2} \left(1 + \frac{1}{2} A \right). \quad (\text{D.51})$$

The geodesic equation can be written with this parameterization as

$$\frac{dq_i}{d\tau} = \frac{1}{2} \epsilon \partial_i A + q^j \partial_i B_j + \frac{1}{2\epsilon} q^j q^k (\partial_i H_{jk} - \partial_k H_{ij}) - \frac{1}{2} q^j \dot{H}_{ij}. \quad (\text{D.52})$$

Further decomposing q_i into direction \hat{n} and magnitude q

$$q_i \equiv q n_i \quad \rightarrow \quad n_i \delta^{ij} n_j = 1, \quad q^2 = \delta^{ij} q_i q_j, \quad (\text{D.53})$$

we have

$$\frac{dq}{d\tau} = n^i \frac{dq_i}{d\tau}, \quad (\text{D.54a})$$

$$\frac{dn_i}{d\tau} = \frac{1}{q} \left(\delta^j_i - n^j n_i \right) \frac{dq_j}{d\tau}. \quad (\text{D.54b})$$

Finally, using the following succinct redefinition of metric variables

$$C_{ij} \equiv \partial_i B_j - \frac{1}{2} \dot{H}_{ij}, \quad (\text{D.55})$$

$$D_{ijk} \equiv \frac{1}{2} (\partial_i H_{jk} - \partial_k H_{ij}), \quad (\text{D.56})$$

the final formulae needed to compute the geodesics, with the parameterization (D.47), are

$$\frac{dx^i}{d\tau} = \frac{q^i}{\epsilon} \left(1 - \frac{1}{2} A \right) - B^i - \frac{1}{2\epsilon} H^i_k q^k, \quad (\text{D.57a})$$

$$\frac{dq_i}{d\tau} = \frac{1}{2} \epsilon \partial_i A + q^j C_{ij} + \frac{q^j q^k}{\epsilon} D_{ijk}, \quad (\text{D.57b})$$

$$\frac{dq}{d\tau} = \frac{1}{2} \epsilon n^i \partial_i A + q n^i n^j C_{ij}, \quad (\text{D.57c})$$

$$\frac{dn_i}{d\tau} = \left(\delta^j_i - n^j n_i \right) \left(\frac{\epsilon}{2q} \partial_j A + n^k C_{jk} + \frac{q}{\epsilon} n^k n^l D_{jkl} \right). \quad (\text{D.57d})$$

Some relevant metric quantities, written in terms of the scalar-vector-tensor decomposition and in Fourier space, are

$$A = -2\Psi , \quad (\text{D.58a})$$

$$B_i = ik_i B - S_i , \quad (\text{D.58b})$$

$$H_{ij} = -2\Phi\delta_{ij} - 2k_i k_j E + i(k_i F_j + k_j F_i) + h_{ij} , \quad (\text{D.58c})$$

$$C_{ij} = \dot{\Phi}\delta_{ij} - k_i k_j (B - \dot{E}) - ik_i S_j - \frac{i}{2}(k_i \dot{F}_j + k_j \dot{F}_i) - \frac{1}{2}\dot{h}_{ij} , \quad (\text{D.58d})$$

$$D_{ijk} = -i(k_i \delta_{jk} - k_k \delta_{ij})\Phi - \frac{1}{2}(k_i k_j F_k - k_j k_k F_i) + \frac{i}{2}(k_i h_{jk} - k_k h_{ij}) . \quad (\text{D.58e})$$

D.4 Energy-momentum tensor conservation

The conservation of the energy-momentum tensor can be expressed as

$$\nabla_\mu T^\mu{}_\nu = \partial_\mu T^\mu{}_\nu + T^\mu{}_\nu \partial_\mu \log \sqrt{-g} - \Gamma^\sigma{}_{\mu\nu} T^\mu{}_\sigma = 0 , \quad (\text{D.59})$$

and its perturbed part is

$$\begin{aligned} \delta(\nabla_\mu T^\mu{}_\nu) &= \partial_\mu \delta T^\mu{}_\nu + \bar{T}^\mu{}_\nu \partial_\mu \left(\frac{\delta \sqrt{-g}}{\sqrt{-g}} \right) + \delta T^\mu{}_\nu \partial_\mu \log \sqrt{-g} \\ &\quad - \bar{\Gamma}^\sigma{}_{\mu\nu} \delta T^\mu{}_\sigma - \delta \Gamma^\sigma{}_{\mu\nu} \bar{T}^\mu{}_\sigma . \end{aligned} \quad (\text{D.60})$$

The components of the energy-momentum tensor are defined as

$$\bar{T}^0{}_0 = -\rho , \quad \delta T^0{}_0 = -\delta\rho , \quad (\text{D.61a})$$

$$\bar{T}^0{}_i = 0 , \quad \delta T^0{}_i = \delta Q_i , \quad (\text{D.61b})$$

$$\bar{T}^i{}_0 = 0 , \quad \delta T^i{}_0 = -\delta Q_i + (\rho + P)B_i , \quad (\text{D.61c})$$

$$\bar{T}^i{}_j = \delta^i{}_j P , \quad \delta T^i{}_j = \delta P \delta^i{}_j + \delta \Pi^i{}_j . \quad (\text{D.61d})$$

Then, the continuity equation is

$$\begin{aligned} \delta(\nabla_\mu T^\mu{}_0) &= - \left\{ (\partial_\tau + 3\mathcal{H})\delta\rho + \partial_i (\delta Q^i - (\rho + P)B^i) + 3\mathcal{H}\delta P + \frac{1}{2}(\rho + P)\dot{H}^i{}_i \right\} \\ &= -\rho \left\{ \dot{\delta} + 3\mathcal{H}(c_s^2 - w)\delta + (1+w)\partial_i (\delta v^i - B^i) + \frac{1}{2}(1+w)\dot{H}^i{}_i \right\} , \end{aligned} \quad (\text{D.62})$$

and the Euler equation is

$$\begin{aligned} \delta(\nabla_\mu T^\mu{}_i) &= (\partial_\tau + 4\mathcal{H})\delta Q_i + \partial_i \delta P + \partial_j \delta \Pi^j{}_i - \frac{1}{2}(\rho + P)\partial_i A \\ &= (\rho + P) \left\{ \delta \dot{v}_i + \mathcal{H}(1 - 3w)\delta v_i + \frac{\dot{w}}{1+w}\delta v_i + \frac{1}{1+w}\partial_i (c_s^2 \delta) \right. \\ &\quad \left. + \frac{1}{1+w}\partial_j \pi^j{}_i - \frac{1}{2}\partial_i A \right\} . \end{aligned} \quad (\text{D.63})$$

The usual set of equations is

$$\dot{\delta} + 3\mathcal{H}(c_s^2 - w)\delta + (1+w)\theta - (1+w)(3\dot{\Phi} - k^2(B - \dot{E})) = 0 , \quad (\text{D.64})$$

$$\dot{\theta} + \mathcal{H}(1 - 3w)\theta + \frac{\dot{w}}{1+w}\theta - \frac{k^2}{1+w}c_s^2\delta + \frac{4k^2}{3(1+w)}\sigma - k^2\Psi = 0 , \quad (\text{D.65})$$

$$\dot{\chi}_+ + \mathcal{H}(1 - 3w)\chi_+ + \frac{\dot{w}}{1+w}\chi_+ + \frac{ik}{1+w}\pi_{3+} = 0 . \quad (\text{D.66})$$

Sometimes, it is useful to redefine the velocity variable as

$$u \equiv \frac{1+w}{k} \theta . \quad (\text{D.67})$$

In terms of u , the Euler equation is

$$\dot{u} + \mathcal{H}(1-3w)u - kc_s^2\delta + \frac{4}{3}k\sigma - (1+w)k\Psi = 0 . \quad (\text{D.68})$$

E

Collision term with bulk flows

In this appendix we will compute the collision term in the presence of cosmological bulk flows (6.77). We will compute the results to all orders in β and then particularize to first order. Since the notation is baroque enough as it stands, throughout this appendix β will stand for β_γ , i.e. the bulk velocity of photons. \mathcal{P}_{ij} and γ are boost factors defined in (6.32) and computed with β_γ .

Starting from the collision term (6.77),

$$C[f] = \frac{\sigma_T}{4\pi p} \int \tilde{p}' d\tilde{p}' d\tilde{\Omega}' \left[\tilde{n}_e^{\text{full}} \delta(\tilde{p} - \tilde{p}') + \tilde{n}_e \tilde{\mathbf{u}}_e^{\text{full}} \cdot (\tilde{\mathbf{p}} - \tilde{\mathbf{p}}') \frac{\partial \delta(\tilde{p} - \tilde{p}')}{\partial \tilde{p}'} \right] \times \left(\bar{f}(\Lambda_\beta \Lambda_{\beta_e}^{-1} \tilde{\mathbf{p}}') - \bar{f}(\Lambda_\beta \Lambda_{\beta_e}^{-1} \tilde{\mathbf{p}}) \right), \quad (\text{E.1})$$

we need to solve two integrals

$$I_1 = \int \tilde{p}' d\tilde{p}' d\tilde{\Omega}' \delta(\tilde{p} - \tilde{p}') \left(\bar{f}(\Lambda_\beta \Lambda_{\beta_e}^{-1} \tilde{\mathbf{p}}') - \bar{f}(\Lambda_\beta \Lambda_{\beta_e}^{-1} \tilde{\mathbf{p}}) \right) = -4\pi \tilde{p} \bar{f}(\Lambda_\beta \Lambda_{\beta_e}^{-1} \tilde{\mathbf{p}}) + \tilde{p} \int d\tilde{\Omega}' \bar{f}(\Lambda_\beta \Lambda_{\beta_e}^{-1} \tilde{\mathbf{p}}') \Big|_{\tilde{p}'=\tilde{p}}, \quad (\text{E.2})$$

$$I_2 = \int \tilde{p}' d\tilde{p}' d\tilde{\Omega}' (\tilde{\mathbf{p}} - \tilde{\mathbf{p}}') \frac{\partial \delta(\tilde{p} - \tilde{p}')}{\partial \tilde{p}'} \left(\bar{f}(\Lambda_\beta \Lambda_{\beta_e}^{-1} \tilde{\mathbf{p}}') - \bar{f}(\Lambda_\beta \Lambda_{\beta_e}^{-1} \tilde{\mathbf{p}}) \right) = -\tilde{p} \int d\tilde{\Omega}' (\hat{n} - 2\hat{n}') \left(\bar{f}(\Lambda_\beta \Lambda_{\beta_e}^{-1} \tilde{\mathbf{p}}') \Big|_{\tilde{p}'=\tilde{p}} - \bar{f}(\Lambda_\beta \Lambda_{\beta_e}^{-1} \tilde{\mathbf{p}}) \right) + \tilde{p}^2 \int d\tilde{\Omega}' (\hat{n} - \hat{n}') \frac{\partial \bar{f}(\Lambda_\beta \Lambda_{\beta_e}^{-1} \tilde{\mathbf{p}})}{\partial \tilde{p}'} \Big|_{\tilde{p}'=\tilde{p}}. \quad (\text{E.3})$$

Now, we will integrate out the dependence on the momentum p in the \mathcal{O} frame, like we did with the left-hand side of the Boltzmann equation. First, for simplicity, we will assume that $\boldsymbol{\beta}$ and $\boldsymbol{\beta}_e$ point in the same direction, so we have

$$\Lambda_\beta \Lambda_{\beta_e}^{-1} = \Lambda_{\Delta\beta}, \quad \Delta\beta \equiv \frac{\beta - \beta_e}{1 - \beta\beta_e}. \quad (\text{E.4})$$

This assumption simplifies the derivation for arbitrary values of β , but it is not needed and in fact the first order results are independent of it. Since the expressions are already quite cumbersome, and this will be the only physical configuration of interest, we will adopt this assumption throughout this appendix. Some preliminary results and definitions are

$$\int q^3 dq \bar{f}_0(\Lambda_\beta q) = \frac{\tilde{\mathcal{N}}}{\gamma^4 (1 - \hat{n} \cdot \boldsymbol{\beta})^4}, \quad (\text{E.5a})$$

$$\int \frac{d^3 \tilde{q}}{4\pi} \tilde{q} \bar{f}_0(\Lambda_{\Delta\beta} \tilde{q}) = \tilde{\mathcal{N}} \gamma_{\Delta\beta}^2 \left(1 + \frac{\Delta\beta^2}{3} \right), \quad (\text{E.5b})$$

$$\int \frac{d^3 \tilde{q}}{4\pi} \tilde{q}^i \bar{f}_0(\Lambda_{\Delta\beta} \tilde{q}) = \frac{4}{3} \tilde{\mathcal{N}} \gamma_{\Delta\beta}^2 \Delta\beta^i, \quad (\text{E.5c})$$

where $\tilde{\mathcal{N}}$ is defined in (6.60) and \mathcal{P}_{ej}^i , γ_e correspond to (6.32), evaluated with β_e . We can proceed now to compute the integrals term by term. First for I_1

$$\int dq q^2 \tilde{q} \bar{f}(\Lambda_\beta \Lambda_{\beta_e}^{-1} \tilde{\mathbf{q}}) = \tilde{\mathcal{N}} \gamma_e (1 - \hat{n} \cdot \boldsymbol{\beta}_e) \left(\mathcal{F}_\gamma + \frac{1}{\gamma^4 (1 - \hat{n} \cdot \boldsymbol{\beta})^4} \right), \quad (\text{E.6a})$$

$$\begin{aligned} \int dq q^2 \tilde{q} \int d\tilde{\Omega} \bar{f}(\Lambda_\beta \Lambda_{\beta_e}^{-1} \tilde{\mathbf{q}}) &= \frac{4\pi \tilde{\mathcal{N}}}{\gamma_e^3 (1 - \hat{n} \cdot \boldsymbol{\beta}_e)^3} \left[\left(1 + \frac{\Delta\beta^2}{3} \right) \gamma_{\Delta\beta}^2 \right. \\ &\quad \left. + \gamma_e^2 \int \frac{d\Omega}{4\pi} (1 - 2\hat{n} \cdot \boldsymbol{\beta}_e + (\hat{n} \cdot \boldsymbol{\beta}_e)^2) \mathcal{F}_\gamma \right]. \end{aligned} \quad (\text{E.6b})$$

And for I_2

$$\int q^2 dq \tilde{q}^i \bar{f}_0(\Lambda_{\Delta\beta} \tilde{\mathbf{q}}) = \tilde{\mathcal{N}} \frac{\mathcal{P}_{ej}^i n^j - \gamma_e \beta_e^i}{\gamma^4 (1 - \hat{n} \cdot \boldsymbol{\beta})^4}, \quad (\text{E.7})$$

$$\int q^2 dq \tilde{q}^i \int d\tilde{\Omega} \bar{f}_0(\Lambda_{\Delta\beta} \tilde{\mathbf{q}}) = 4\pi \tilde{\mathcal{N}} \frac{\mathcal{P}_{ej}^i n^j - \gamma_e \beta_e^i}{\gamma_e^4 (1 - \hat{n} \cdot \boldsymbol{\beta}_e)^4} \gamma_{\Delta\beta}^2 \left(1 + \frac{\Delta\beta^2}{3} \right), \quad (\text{E.8})$$

$$\int q^2 dq \int d\tilde{\Omega} \tilde{q}^i \bar{f}_0(\Lambda_{\Delta\beta} \tilde{\mathbf{q}}) = \frac{16\pi}{3} \tilde{\mathcal{N}} \Delta\beta^i \frac{\gamma_{\Delta\beta}^2}{\gamma_e^3 (1 - \hat{n} \cdot \boldsymbol{\beta}_e)^3}, \quad (\text{E.9})$$

$$\int q^2 dq \tilde{q} \tilde{q}^i \int d\tilde{\Omega} \frac{\partial \bar{f}_0(\Lambda_{\Delta\beta} \tilde{\mathbf{q}})}{\partial \tilde{q}} = -16\pi \tilde{\mathcal{N}} \frac{\mathcal{P}_{ej}^i n^j - \gamma_e \beta_e^i}{\gamma_e^4 (1 - \hat{n} \cdot \boldsymbol{\beta}_e)^4} \gamma_{\Delta\beta}^2 \left(1 + \frac{\Delta\beta^2}{3} \right), \quad (\text{E.10})$$

$$\int q^2 dq \tilde{q} \int d\tilde{\Omega} \tilde{q}^i \frac{\partial \bar{f}_0(\Lambda_{\Delta\beta} \tilde{\mathbf{q}})}{\partial \tilde{q}} = -\frac{64\pi}{3} \tilde{\mathcal{N}} \Delta\beta^i \frac{\gamma_{\Delta\beta}^2}{\gamma_e^3 (1 - \hat{n} \cdot \boldsymbol{\beta}_e)^3}. \quad (\text{E.11})$$

Finally, for the electron quantities,

$$\tilde{n}_e^{\text{full}} \equiv 2 \int \frac{d^3 \tilde{\mathbf{p}}_e}{(2\pi)^3} \tilde{f}_e(\tilde{\mathbf{p}}_e) = \tilde{n}_e + \delta \tilde{n}_e, \quad (\text{E.12a})$$

$$\tilde{n}_e \tilde{\mathbf{u}}_e^{\text{full}} = 2 \int \frac{d^3 \tilde{\mathbf{p}}_e}{(2\pi)^3} \frac{\tilde{\mathbf{p}}_e}{\tilde{E}_{p_e}} \tilde{f}_e(\tilde{\mathbf{p}}_e) = 2 \int \frac{d^3 \tilde{\mathbf{p}}_e}{(2\pi)^3} \frac{\tilde{\mathbf{p}}_e}{\tilde{E}_{p_e}} \delta \tilde{f}_e(\tilde{\mathbf{p}}_e) = \tilde{n}_e \delta \tilde{\mathbf{v}}_e, \quad (\text{E.12b})$$

where \tilde{n}_e is the physical background electron number density, computed in its co-moving frame as every other background quantity. Using the Lorentz transformation properties

$$\delta \tilde{n}_e = \gamma_e \left(\delta n_e - \delta v_e^j \beta_{ej} \right), \quad (\text{E.13a})$$

$$\delta \tilde{v}_e^i = \mathcal{P}_{ej}^i \delta v_e^j - \gamma_e \beta_e^i \delta n_e. \quad (\text{E.13b})$$

The final results, to first order in β , are

$$\begin{aligned} \int q^2 dq I_1 &= -4\pi \tilde{\mathcal{N}} \left((1 - \hat{n} \cdot \boldsymbol{\beta}_e) \mathcal{F}_\gamma + 4\hat{n} \cdot \Delta\boldsymbol{\beta} - (1 + 3\hat{n} \cdot \boldsymbol{\beta}_e) \int \frac{d\Omega}{4\pi} \mathcal{F}_\gamma \right. \\ &\quad \left. + 2\boldsymbol{\beta}_e \cdot \int \frac{d\Omega}{4\pi} \hat{n} \mathcal{F}_\gamma \right), \end{aligned} \quad (\text{E.14a})$$

$$\int q^2 dq I_2 = 4\pi \tilde{\mathcal{N}} \left(-\frac{8}{3} \Delta\boldsymbol{\beta} + 4\hat{n} (\hat{n} \cdot \Delta\boldsymbol{\beta}) + 4(\hat{n} - \boldsymbol{\beta}_e + 4\hat{n} (\hat{n} \cdot \boldsymbol{\beta}_e)) \right), \quad (\text{E.14b})$$

$$\delta \tilde{n}_e = \delta n_e - \beta_{ej} \delta v_e^j, \quad (\text{E.14c})$$

$$\delta \tilde{v}_e^i = \delta v_e^i - \beta_e^i \delta n_e. \quad (\text{E.14d})$$

F Electrodynamics in a perturbed FLRW universe

F.1 Lorentz force in General Relativity

In this section we will study how the geodesics of charged particles are affected by the presence of an electromagnetic field. The conventions for the momentum variables are the same as in the main text and we will follow the same steps as in the Appendix D. The Lorentz force acting on a particle with charge Q is [Wal10]

$$\frac{dU^\mu}{d\lambda} + \Gamma^\mu_{\nu\rho} U^\nu U^\rho = \frac{Q}{m} g^{\mu\nu} F_{\nu\rho} U^\rho . \quad (\text{F.1})$$

We will focus on the electromagnetic part

$$\left(\frac{dU_\mu}{d\lambda} \right)_{\text{EM}} = \frac{Q}{m} F_{\nu\rho} U^\rho . \quad (\text{F.2})$$

Introducing the new definitions

$$\mathcal{P}_i^j \equiv \delta_i^j - \frac{1}{2} H_i^j , \quad \bar{\mathcal{P}}_i^j \equiv \delta_i^j + \frac{1}{2} H_i^j , \quad (\text{F.3})$$

and using the redefinition of momentum (3.35, 3.23), the new term that we must include in the Liouville operator (3.50) is

$$\left(\frac{dq_i}{d\tau} \right)_{\text{EM}} = Q \mathcal{P}_i^j \left\{ F_{j0} + F_{jk} \frac{dx^k}{d\tau} \right\} . \quad (\text{F.4})$$

We can split it into an ‘electric’ and ‘magnetic’ component¹

$$\left(\frac{dq_i}{d\tau} \right)_{\text{EM}} = Q \left\{ e_i + \varepsilon_{ijk} \frac{q^j}{\epsilon} b^k \right\} , \quad (\text{F.5})$$

where

$$e_i \equiv \mathcal{P}_i^j F_{j0} - \varepsilon_{ijk} B^j b^k , \quad (\text{F.6a})$$

$$b^i \equiv \frac{1}{2} \left(1 - \frac{1}{2} A \right) \varepsilon^{ijk} \mathcal{P}_j^l \mathcal{P}_k^m F_{lm} . \quad (\text{F.6b})$$

These relations can be recast into²

$$b^i = \frac{1}{2} \left(1 - \frac{1}{2} A - \frac{1}{2} H_j^j \right) \varepsilon^{lmk} \bar{\mathcal{P}}_k^i F_{lm} , \quad (\text{F.7a})$$

$$F_{i0} = \bar{\mathcal{P}}_i^j e_j + \varepsilon_{ijk} B^j b^k , \quad (\text{F.7b})$$

$$F_{jk} = \left(1 + \frac{1}{2} A + \frac{1}{2} H_i^i \right) \varepsilon_{jkl} \mathcal{P}_m^l b^m . \quad (\text{F.7c})$$

¹In Section F.4 we relate these variables with the physical electric and magnetic fields.

²Using $\varepsilon_{ijk} \mathcal{P}_n^j \mathcal{P}_l^k \varepsilon^{nlm} = 2(1 - \frac{1}{2} H_i^i) \bar{\mathcal{P}}_l^m$.

F.2 Electric current

The flux of particles (2.109) has been previously defined as

$$N^\mu \equiv \frac{g_*}{(2\pi)^3} \int \frac{d^3P}{\sqrt{-g}} \frac{P^\mu}{P^0} f = \frac{a^{-4} g_*}{(2\pi)^3} \int \left(1 + \frac{1}{2}A\right) d^3q \frac{P^\mu}{P^0} f, \quad (\text{F.8})$$

with components

$$N^0 = a^{-1} \left(1 + \frac{1}{2}A\right) (n + \delta n), \quad (\text{F.9a})$$

$$N^i = a^{-1} \mathcal{P}^{ij} (n\beta_j + \delta V_j) - a^{-1} n B^i. \quad (\text{F.9b})$$

As usual, the perturbations are defined in the cosmic center of mass frame. The electric current of a single species s is defined as

$$J_s^\mu \equiv Q_s N_s^\mu, \quad (\text{F.10})$$

and the total electric current is

$$J^\mu = \sum_s Q_s N_s^\mu. \quad (\text{F.11})$$

F.3 Maxwell equations

The free Maxwell equations in curved space-time have been already presented in (2.38) and (2.41). Here we will source them with an electric current. The Maxwell equations are³ [Wal10]

$$\nabla_\mu F^{\mu\nu} = -J^\nu, \quad (\text{F.12})$$

$$\nabla_{[\mu} F_{\nu\sigma]} = 0. \quad (\text{F.13})$$

In order to write them in terms of their components, the following alternative form is easier to handle

$$\partial_\mu (\sqrt{-g} F^{\mu\nu}) = -\sqrt{-g} J^\nu, \quad (\text{F.14})$$

$$\partial_\mu F_{\nu\sigma} + \partial_\sigma F_{\mu\nu} + \partial_\nu F_{\sigma\mu} = 0. \quad (\text{F.15})$$

We will expand them now with the perturbed RW metric (3.33), the field redefinition (F.6) and the electric current (F.11). Then we will particularize the results to the simplified version we will be interested in.

F.3.1 Full Maxwell equations

The first Maxwell equation is

$$\partial_\mu (\sqrt{-g} F^{\mu 0}) = -\sqrt{-g} J^0, \quad (\text{F.16})$$

³We use different charge conventions from [Wal10], hence the 4π factor difference.

where

$$\partial_\mu (\sqrt{-g} F^{\mu 0}) = -\partial_i \left\{ \left(1 + \frac{1}{2} A + \frac{1}{2} H_k^k \right) \mathcal{P}_j^i e^j \right\}, \quad (\text{F.17})$$

$$-\sqrt{-g} J^0 = -a^3 \left(1 + \frac{1}{2} H_k^k \right) \sum_s \mathcal{Q}_s (n_s + \delta n_s). \quad (\text{F.18})$$

The second Maxwell equation is

$$\partial_\mu (\sqrt{-g} F^{\mu i}) = -\sqrt{-g} J^i, \quad (\text{F.19})$$

where

$$\partial_\mu (\sqrt{-g} F^{\mu i}) = \partial_0 \left\{ \left(1 + \frac{1}{2} A + \frac{1}{2} H_k^k \right) \mathcal{P}_j^i e^j \right\} - \partial_j \left\{ e^i B^j - e^j B^i + \varepsilon^{ijkl} \bar{\mathcal{P}}_l^m b_m \right\}, \quad (\text{F.20})$$

$$\begin{aligned} -\sqrt{-g} J^i &= -a^3 \left(1 - \frac{1}{2} A + \frac{1}{2} H_k^k \right) \mathcal{P}_j^i \sum_s \mathcal{Q}_s \beta_s^j n_s - a^3 \sum_s \mathcal{Q}_s \delta V_s^i \\ &\quad + a^3 B^i \sum_s \mathcal{Q}_s n_s. \end{aligned} \quad (\text{F.21})$$

The third Maxwell equation is

$$\partial_0 \left\{ \left(1 + \frac{1}{2} A + \frac{1}{2} H_k^k \right) \mathcal{P}_j^i b^j \right\} + \partial_j \left\{ \varepsilon^{ijk} \bar{\mathcal{P}}_k^l e_l - b^i B^j + b^j B^i \right\} = 0. \quad (\text{F.22})$$

The fourth Maxwell equation is

$$\partial_i \left\{ \left(1 + \frac{1}{2} A + \frac{1}{2} H_k^k \right) \mathcal{P}_j^i b^j \right\} = 0. \quad (\text{F.23})$$

F.3.2 Simplified Maxwell equations

The Maxwell equations can be simplified if we assume that there are no background fields and that we can write

$$b^i = \delta b^i, \quad e^i = e_{(\beta)}^i + \delta e^i, \quad (\text{F.24})$$

where $e_{(\beta)}^i$ is a homogeneous contribution $\mathcal{O}(\beta)$, δe^i is first order in cosmological perturbations and δb^i is first order in cosmological perturbations and β (since we know that there is no magnetic field production in Λ CDM). Under these conditions, the first Maxwell equation for the evolution of the perturbations is

$$\partial_i \left\{ \delta e^i + \frac{1}{2} (A + H_j^j) e_{(\beta)}^i - \frac{1}{2} H_j^i e_{(\beta)}^j \right\} = a^3 \sum_s \mathcal{Q}_s \left\{ \delta n_s + \frac{1}{2} n_s H_j^j \right\}. \quad (\text{F.25})$$

The second Maxwell equation is

$$\begin{aligned} \partial_0 \left\{ \delta e^i + \frac{1}{2} (A + H_j^j) e_{(\beta)}^i - \frac{1}{2} H_j^i e_{(\beta)}^j \right\} - \partial_j \left\{ e_{(\beta)}^i B^j - e_{(\beta)}^j B^i + \varepsilon_{ijk} \delta b^k \right\} \\ = -a^3 \sum_s \mathcal{Q}_s n_s \left\{ \frac{\delta V_s^i}{n_s} - B^i - \frac{1}{2} (A - H_j^j) \beta_s^i + \frac{1}{2} H_j^i \beta_s^j \right\}. \end{aligned} \quad (\text{F.26})$$

The third Maxwell equation is

$$\delta \dot{b}^i + \varepsilon^{ijk} \partial_j \left\{ \delta e_k + \frac{1}{2} H_{kl} e_{(\beta)}^l \right\} = 0 . \quad (\text{F.27})$$

The fourth Maxwell equation is

$$\partial_i \delta b^i = 0 . \quad (\text{F.28})$$

Using the fact that we have neutrality of charge at the background level, $\sum_s Q_s n_s = 0$, the only relevant equation at this level is

$$\dot{e}_{(\beta)} = -a^3 \sum_s Q_s n_s \boldsymbol{\beta}_s . \quad (\text{F.29})$$

The whole set of Maxwell equations for the perturbations can be rewritten as⁴

$$\nabla \cdot \delta \mathbf{e} = a^3 \sum_s Q_s \delta n_s + S_{\partial e} , \quad (\text{F.30a})$$

$$\delta \dot{\mathbf{e}} - \nabla \wedge \delta \mathbf{b} = -a^3 \sum_s Q_s n_s \delta \mathbf{v}_s + \mathbf{S}_e , \quad (\text{F.30b})$$

$$\delta \dot{\mathbf{b}} + \nabla \wedge \delta \mathbf{e} = \mathbf{S}_b , \quad (\text{F.30c})$$

$$\nabla \cdot \delta \mathbf{b} = 0 . \quad (\text{F.30d})$$

We find the standard Maxwell equations for $\delta \mathbf{e}$ and $\delta \mathbf{b}$, plus external sources proportional to β

$$S_{\partial e} = -\frac{1}{2} e_{(\beta)}^j \partial_i \left\{ (A + H_k^k) \delta_j^i - H_j^i \right\} , \quad (\text{F.31a})$$

$$S_e^i = -\frac{1}{2} \left\{ (\dot{A} + \dot{H}_k^k) \delta_j^i - \dot{H}_j^i \right\} e_{(\beta)}^j + \partial_j \left(e_{(\beta)}^i B^j - e_{(\beta)}^j B^i \right) + a^3 A \sum_s Q_s n_s \beta_s^i , \quad (\text{F.31b})$$

$$S_b^i = -\frac{1}{2} e_{(\beta)}^l \varepsilon^{ijk} \partial_j H_{kl} . \quad (\text{F.31c})$$

F.4 Physical fields and gauge transformations

The physical strength tensor, that would be measured by a locally inertial observer, is

$$F_{ab}^{(\text{phys})} \equiv e^\mu_a e^\nu_b F_{\mu\nu} . \quad (\text{F.32})$$

The physical electric and magnetic fields that would be observed by a comoving observer are

$$E_i^{(\text{phys})} = F_{i0}^{(\text{phys})} = a^{-2} e_{(\beta)i} + a^{-2} \delta e_i + \frac{1}{2} a^{-2} A e_{(\beta)i} , \quad (\text{F.33a})$$

$$B^{(\text{phys})i} = \frac{1}{2} \varepsilon^{ijk} F_{jk}^{(\text{phys})} = a^{-2} \delta b^i . \quad (\text{F.33b})$$

Finally, we can compute the gauge-transformation properties of the fields. Following the analysis of Section 3.5.2, after an infinitesimal gauge transformation we have

$$\Delta F_{\mu\nu} = \varepsilon^\rho \partial_\rho F_{\mu\nu} + F_{\rho\mu} \partial_\mu \varepsilon^\rho + F_{\mu\rho} \partial_\nu \varepsilon^\rho . \quad (\text{F.34})$$

⁴Since we will apply them only to NR particles, we use the definition (6.70) of the velocity as $\delta V = n \delta v$.

This translates into

$$\Delta \delta e^i = T \dot{e}_{(\beta)}^i + \dot{T} e_{(\beta)}^i - \mathcal{H} T e_{(\beta)}^i, \quad (\text{F.35a})$$

$$\Delta E_i^{(\text{phys})} = T \partial_\tau (a^{-2} e_{(\beta)i}), \quad (\text{F.35b})$$

$$\Delta \delta b_i = a^2 \Delta B_i^{(\text{phys})} = -\varepsilon_{ijk} \partial^j T e_{(\beta)}^k. \quad (\text{F.35c})$$

F.5 Liouville operator with electromagnetic fields

The presence of electromagnetic fields modifies the trajectories of charged particles through (F.5). This new force must be included in the left-hand side of the Boltzmann equation. Since the only charged particles in our analysis (protons and electrons) are non-relativistic throughout the period of interest, in what follows we will take the NR limit. In particular, we have the results

$$g_* \int \frac{d^3 q}{(2\pi)^3} \left(\frac{dq^i}{d\tau} \right)_{\text{EM}} \frac{\partial f}{\partial q^i} = 0, \quad (\text{F.36a})$$

$$g_* \int \frac{d^3 q}{(2\pi)^3} \left(\frac{dq^i}{d\tau} \right)_{\text{EM}} \varepsilon \frac{\partial f}{\partial q^i} = -Q a^3 n e_i (\beta^i + \delta v^i), \quad (\text{F.36b})$$

$$g_* \int \frac{d^3 q}{(2\pi)^3} \left(\frac{dq^j}{d\tau} \right)_{\text{EM}} q^i \frac{\partial f}{\partial q^j} = -Q a^3 n (1 + \delta_n) e^i - Q a^3 n \varepsilon_{ijk} (\beta^j + \delta v^j) b^k. \quad (\text{F.36c})$$

Assuming that the zero-order Boltzmann equation is satisfied, expanding to first NR order and to first order in β we have:

- *Number density.*

$$g_* \int \frac{d^3 q}{(2\pi)^3} \frac{Df}{d\tau} \simeq a^3 n \left(\dot{\delta}_n + \alpha \delta_n + \partial_i \delta v^i - \delta^{ij} C_{ij} - \mathcal{M}_\beta \right), \quad (\text{F.37})$$

where $\alpha \equiv \partial_\tau (a^3 n) / (a^3 n)$ takes into account possible variations in the comoving number of particles, e.g. due to recombination. The metric-related variable is

$$\mathcal{M}_\beta \equiv \frac{1}{2} \beta^i \partial_i A + D_{ijk} \delta^{ij} \beta^k. \quad (\text{F.38})$$

- *Momentum.*

$$\begin{aligned} g_* \int \frac{d^3 q}{(2\pi)^3} q^i \frac{Df}{d\tau} &\simeq a^4 \rho \left\{ \dot{\beta}^i + (\mathcal{H} + \alpha) \beta^i + \delta \dot{v}^i + (\mathcal{H} + \alpha) \delta v^i \right. \\ &\quad \left. + (\beta^i \delta_k^j + \beta^j \delta_k^i) \partial_j \delta v^k - \frac{1}{2} \partial^i A - \mathcal{M}_\beta^i \right\} \\ &\quad - Q a^3 n (1 + \delta_n) e^i - Q a^3 n \varepsilon^{ijk} (\beta_j + \delta v_j) b_k, \end{aligned} \quad (\text{F.39})$$

where the metric-related variable is

$$\mathcal{M}_\beta^i \equiv (\delta^{jk} \beta^j + \delta^{ij} \beta^k) C_{jk}. \quad (\text{F.40})$$

It is worth keeping in mind that for non-relativistic particles we also have

$$n \simeq \frac{\rho}{m}, \quad \delta_n \simeq \delta - \beta_k \delta v^k. \quad (\text{F.41})$$

Abstract

The main task of cosmology is to understand both the current state of the Universe and its past history. It aims to answer fundamental questions like how has the Universe evolved or what are its constituents. Even though cosmology has developed over the last century, the last two decades have witnessed a revolution. During the XX century, there were many competing cosmological models with very definite observational predictions. However, the observations were not good enough to test these predictions. During the last twenty years the situation has been reversed. The amount and quality of empirical data have increased to the point where cosmology has become an observationally driven science.

These observations have also revealed unexpected (and puzzling) features of our Universe. In particular, they point towards the existence of a *dark sector*. The dark sector in cosmology gathers all the components that do not belong to the Standard Model of particle physics and whose only observed effects are gravitational. The standard model of cosmology, the Λ CDM model, assumes that the dark sector is composed of a cosmological constant (Λ) and cold dark matter (CDM). This simple choice allows to explain the current accelerated expansion (due to Λ) and the galaxy distribution (mainly due to CDM).

The Λ +CDM dark sector provides an excellent fit to many independent observations over a wide range of scales, but it lacks a solid theoretical motivation. Moreover, there are some observations that seem difficult to accommodate within the standard framework. Motivated by these facts, in this thesis we have explored models beyond the simplest Λ +CDM dark sector. In order to modify the dark sector, we have proceeded in three different ways:

- I) *Adding new species*. Since the standard Λ +CDM dark sector is already a two-component fluid, it seems natural to generalize it adding more fluids. In this thesis, we have analyzed the observational impact of an additional massive spin-2 field: a *hidden graviton*. In the first place, we used fifth-force tests to constrain its parameter space. Later on, we studied the production rate of these hypothetical new particles in stars. Using astrophysical observations, we were able to set bounds on the mass and coupling of hidden gravitons.
- II) *Changing the simplest paradigm*. Λ and CDM are the simplest examples of models of dark energy and dark matter, respectively. In this thesis, we have analyzed a dark-matter model beyond the CDM paradigm: *repulsive fuzzy dark matter*. Fuzzy dark matter is usually modelled as an ultralight scalar field, that can mimic CDM on cosmological scales while showing a distinctive behaviour on sub-galactic scales. We considered the implications of an additional (repulsive) self-interaction in the fuzzy dark matter model. After studying its phenomenology, we constrained the model parameters, mass and self-coupling, using cosmological information from the CMB and LSS.

III) *Modifying a fundamental assumption.* An important hypothesis underlying Λ CDM, that usually goes by unnoticed, is that the background velocities of the fluids (bulk flows) are negligible. In this thesis, we have studied in detail the consequences of such *cosmological bulk flows* on the evolution of the Universe. At the background level, we first showed that the existence of sizeable bulk flows is compatible with the usual notion of an isotropic Universe. We then moved on to study the behaviour of the perturbations, retracing all the steps of standard cosmological perturbation theory and readressing many of its underlying assumptions. Among the observable effects, we found violations of statistical isotropy that may be large enough to be measured in the foreseeable future. We also found that associated with the existence of large-scale bulk flows comes the creation of cosmological magnetic fields. The magnetic fields produced in this scenario are large enough to explain the origin of the galactic magnetic fields, a long-standing problem in cosmology and astrophysics.

Resumen

El principal objetivo de la cosmología es llegar a conocer la situación actual del Universo y su historia, tratando de desvelar cómo ha evolucionado y cuál es su composición. Aunque la cosmología moderna se ha venido desarrollando durante el último siglo, las últimas dos décadas han presenciado una auténtica revolución. Durante el siglo XX se propusieron diferentes modelos cosmológicos, con predicciones observacionales concretas, pero la precisión de las observaciones no era lo bastante alta para discriminar entre ellos. Sin embargo, la situación ha cambiado radicalmente en los últimos veinte años. La calidad y cantidad de datos empíricos ha aumentado drásticamente, hasta el punto en el que, hoy por hoy, las nuevas vías de investigación en cosmología se nutren de los últimos hallazgos observacionales.

Las recientes observaciones también han revelado sorprendentes (y hasta cierto punto desconcertantes) aspectos de nuestro Universo. En particular, todas apuntan a la existencia de un *sector oscuro*. El sector oscuro en cosmología aglutina todos los componentes que no pertenecen al Modelo Estándar de física de partículas y cuya presencia sólo es detectable por sus efectos gravitatorios. El modelo estándar de la cosmología, el modelo Λ CDM, asume que el sector oscuro se compone de una constante cosmológica (Λ) y materia oscura fría (CDM). Esta elección tan sencilla permite explicar la reciente expansión acelerada del Universo (debida a Λ) y las propiedades de la distribución de galaxias (principalmente debidas a la materia oscura).

Este sector oscuro $\Lambda + \text{CDM}$ ajusta exitosamente un gran número de observaciones a diferentes escalas. Adolece no obstante de una falta de motivación teórica y, además, aunque el acuerdo general es excelente, tiene dificultades para acomodar algunas observaciones. Estos motivos nos han llevado en esta tesis a estudiar diferentes alternativas al sector oscuro estándar $\Lambda + \text{CDM}$. Para modificar el sector oscuro, hemos explorado cada uno de los tres caminos posibles:

I) *Añadir nuevas especies*. Dado que el sector oscuro estándar $\Lambda + \text{CDM}$ ya es un fluido compuesto, parece natural extender el modelo añadiendo más fluidos. En esta tesis hemos analizado las consecuencias observacionales de la existencia de una nueva partícula de espín 2 con masa: un *gravitón oculto*. En primer lugar, hemos utilizado tests de quintas fuerzas para restringir una parte del espacio de parámetros. Una vez hecho esto, hemos estudiado el ritmo de producción de estas nuevas partículas en estrellas. Usando observaciones astrofísicas, ha sido posible restringir aún más la masa y constante de acoplo de los gravitones ocultos.

II) *Cambiar los paradigmas más simples*. Λ y la materia oscura fría son los ejemplos más sencillos de modelos más generales de energía y materia oscura, respectivamente. En esta tesis, hemos analizado un modelo de materia oscura alternativo: *materia oscura fuzzy repulsiva*. La materia oscura *fuzzy* se de-

scribe mediante un campo escalar ultraligero, que puede reproducir el comportamiento de la materia oscura fría a escalas cosmológicas pero que muestra características distintivas en escalas sub-galácticas. En particular, hemos considerado las implicaciones de una interacción adicional (repulsiva) en un modelo de materia oscura *fuzzy*. Tras estudiar su fenomenología, hemos encontrado cotas sobre los parámetros principales del modelo (la masa y la intensidad de la interacción repulsiva) comparando con datos observacionales del fondo de microondas y estructura a gran escala.

III) *Modificar suposiciones fundamentales.* Una importante hipótesis del modelo Λ CDM, que normalmente pasa desapercibida, es que las velocidades globales de los fluidos (flujos cosmológicos) son despreciables. En esta tesis, hemos estudiado en detalle los efectos de estos *flujos cosmológicos* sobre la evolución del Universo. Hemos estudiado primero la evolución de un universo sin perturbaciones, demostrando que la existencia de flujos cosmológicos con una amplitud considerable es compatible con las nociones usuales de homogeneidad e isotropía del Universo observable. Tras este análisis, hemos incluido las perturbaciones, reelaborando la teoría de perturbaciones cosmológicas y examinando críticamente muchas de sus suposiciones implícitas. Entre los efectos observables, hemos encontrado violaciones de la isotropía estadística que podrían llegar a ser detectadas en experimentos futuros. Uno de los resultados principales es que la existencia de movimientos a gran escala conduce a la producción de campos magnéticos cosmológicos. Los campos producidos en este escenario son lo bastante grandes para explicar la aparición de los campos magnéticos galácticos observados, cuyo origen ha supuesto un interrogante en cosmología y astrofísica durante años.

References

- [Aba+16] K. N. Abazajian et al. “CMB-S4 Science Book, First Edition” (2016). arXiv: [1610.02743](#).
- [Abb+18] T. M. C. Abbott et al. “Dark Energy Survey year 1 results: Cosmological constraints from galaxy clustering and weak lensing”. *Phys. Rev. D* 98.4 (2018). DOI: [10.1103/PhysRevD.98.043526](#). arXiv: [1708.01530](#).
- [Abe+08] S. A. Abel et al. “Kinetic Mixing of the Photon with Hidden U(1)s in String Phenomenology”. *JHEP* 07 (2008). DOI: [10.1088/1126-6708/2008/07/124](#). arXiv: [0803.1449](#).
- [Abe+09] P. A. Abell et al. “LSST Science Book, Version 2.0” (2009). arXiv: [0912.0201](#).
- [Abe+17] C. Abel et al. “Search for Axionlike Dark Matter through Nuclear Spin Precession in Electric and Magnetic Fields”. *Phys. Rev. X* 7.4 (2017). DOI: [10.1103/PhysRevX.7.041034](#). arXiv: [1708.06367](#).
- [ABK19] C. A. Argüelles, V. Brdar, and J. Kopp. “Production of keV Sterile Neutrinos in Supernovae: New Constraints and Gamma Ray Observables”. *Phys. Rev. D* 99.4 (2019). DOI: [10.1103/PhysRevD.99.043012](#). arXiv: [1605.00654](#).
- [ADD98] N. Arkani-Hamed, S. Dimopoulos, and G. R. Dvali. “The Hierarchy problem and new dimensions at a millimeter”. *Phys. Lett. B* 429 (1998). DOI: [10.1016/S0370-2693\(98\)00466-3](#). arXiv: [hep-ph/9803315](#).
- [ADD99] N. Arkani-Hamed, S. Dimopoulos, and G. R. Dvali. “Phenomenology, astrophysics and cosmology of theories with submillimeter dimensions and TeV scale quantum gravity”. *Phys. Rev. D* 59 (1999). DOI: [10.1103/PhysRevD.59.086004](#). arXiv: [hep-ph/9807344](#).
- [Ade+09] E. G. Adelberger et al. “Torsion balance experiments: A low-energy frontier of particle physics”. *Prog. Part. Nucl. Phys.* 62 (2009). DOI: [10.1016/j.pnpnp.2008.08.002](#).
- [Ade+14a] P. A. R. Ade et al. “Planck 2013 results. XVI. Cosmological parameters”. *Astron. Astrophys.* 571 (2014). DOI: [10.1051/0004-6361/201321591](#). arXiv: [1303.5076](#).
- [Ade+14b] P. A. R. Ade et al. “Planck intermediate results. XIII. Constraints on peculiar velocities”. *Astron. Astrophys.* 561 (2014). DOI: [10.1051/0004-6361/201321299](#). arXiv: [1303.5090](#).
- [Ade+16a] P. A. R. Ade et al. “Planck 2015 results. XIII. Cosmological parameters”. *Astron. Astrophys.* 594 (2016). DOI: [10.1051/0004-6361/201525830](#). arXiv: [1502.01589](#).

- [Ade+16b] P. A. R. Ade et al. “Planck 2015 results. XVI. Isotropy and statistics of the CMB”. *Astron. Astrophys.* 594 (2016). DOI: [10.1051/0004-6361/201526681](https://doi.org/10.1051/0004-6361/201526681). arXiv: [1506.07135](https://arxiv.org/abs/1506.07135).
- [Ade+19] P. Ade et al. “The Simons Observatory: Science goals and forecasts”. *JCAP* 1902 (2019). DOI: [10.1088/1475-7516/2019/02/056](https://doi.org/10.1088/1475-7516/2019/02/056). arXiv: [1808.07445](https://arxiv.org/abs/1808.07445).
- [Agh+14] N. Aghanim et al. “Planck 2013 results. XXVII. Doppler boosting of the CMB: Eppur si muove”. *Astron. Astrophys.* 571 (2014). DOI: [10.1051/0004-6361/201321556](https://doi.org/10.1051/0004-6361/201321556). arXiv: [1303.5087](https://arxiv.org/abs/1303.5087).
- [Agh+16] A. Aghamousa et al. “The DESI Experiment Part I: Science, Targeting, and Survey Design” (2016). arXiv: [1611.00036](https://arxiv.org/abs/1611.00036).
- [Agh+18] N. Aghanim et al. “Planck 2018 results. VI. Cosmological parameters” (2018). arXiv: [1807.06209](https://arxiv.org/abs/1807.06209).
- [AHN03] E. G. Adelberger, B. R. Heckel, and A. E. Nelson. “Tests of the gravitational inverse square law”. *Ann. Rev. Nucl. Part. Sci.* 53 (2003). DOI: [10.1146/annurev.nucl.53.041002.110503](https://doi.org/10.1146/annurev.nucl.53.041002.110503). arXiv: [hep-ph/0307284](https://arxiv.org/abs/hep-ph/0307284).
- [Akr+18a] Y. Akrami et al. “Planck 2018 results. I. Overview and the cosmological legacy of Planck” (2018). arXiv: [1807.06205](https://arxiv.org/abs/1807.06205).
- [Akr+18b] Y. Akrami et al. “Planck 2018 results. X. Constraints on inflation” (2018). arXiv: [1807.06211](https://arxiv.org/abs/1807.06211).
- [Akr+19] Y. Akrami et al. “Planck 2018 results. VII. Isotropy and Statistics of the CMB” (2019). arXiv: [1906.02552](https://arxiv.org/abs/1906.02552).
- [Ala+17] S. Alam et al. “The clustering of galaxies in the completed SDSS-III Baryon Oscillation Spectroscopic Survey: cosmological analysis of the DR12 galaxy sample”. *Mon. Not. Roy. Astron. Soc.* 470.3 (2017). DOI: [10.1093/mnras/stx721](https://doi.org/10.1093/mnras/stx721). arXiv: [1607.03155](https://arxiv.org/abs/1607.03155).
- [AM16] K. Aoki and S. Mukohyama. “Massive gravitons as dark matter and gravitational waves”. *Phys. Rev.* D94.2 (2016). DOI: [10.1103/PhysRevD.94.024001](https://doi.org/10.1103/PhysRevD.94.024001). arXiv: [1604.06704](https://arxiv.org/abs/1604.06704).
- [Ame+18] L. Amendola et al. “Cosmology and fundamental physics with the Euclid satellite”. *Living Rev. Rel.* 21.1 (2018). DOI: [10.1007/s41114-017-0010-3](https://doi.org/10.1007/s41114-017-0010-3). arXiv: [1606.00180](https://arxiv.org/abs/1606.00180).
- [Ant+98] I. Antoniadis et al. “New dimensions at a millimeter to a Fermi and superstrings at a TeV”. *Phys. Lett.* B436 (1998). DOI: [10.1016/S0370-2693\(98\)00860-0](https://doi.org/10.1016/S0370-2693(98)00860-0). arXiv: [hep-ph/9804398](https://arxiv.org/abs/hep-ph/9804398).
- [AP10] I. Antoniou and L. Perivolaropoulos. “Searching for a Cosmological Preferred Axis: Union2 Data Analysis and Comparison with Other Probes”. *JCAP* 1012 (2010). DOI: [10.1088/1475-7516/2010/12/012](https://doi.org/10.1088/1475-7516/2010/12/012). arXiv: [1007.4347](https://arxiv.org/abs/1007.4347).
- [APP13] H. An, M. Pospelov, and J. Pradler. “New stellar constraints on dark photons”. *Phys. Lett.* B725 (2013). DOI: [10.1016/j.physletb.2013.07.008](https://doi.org/10.1016/j.physletb.2013.07.008). arXiv: [1302.3884](https://arxiv.org/abs/1302.3884).

- [Ari+12] P. Arias et al. “WISPy Cold Dark Matter”. *JCAP* 1206 (2012). DOI: [10.1088/1475-7516/2012/06/013](https://doi.org/10.1088/1475-7516/2012/06/013). arXiv: [1201.5902](https://arxiv.org/abs/1201.5902).
- [AS72] M. Abramowitz and I. A. Stegun. *Handbook of Mathematical Functions: With Formulas, Graphs, and Mathematical Tables*. Applied Mathematics Series. U.S. Department of Commerce, National Bureau of Standards, 1972 [1964]. ISBN: 9780486612720.
- [Atr+15] F. Atrio-Barandela et al. “Probing the Dark Flow Signal in WMAP 9-year and Planck Cosmic Microwave Background Maps”. *Astrophys. J.* 810.2 (2015). DOI: [10.1088/0004-637X/810/2/143](https://doi.org/10.1088/0004-637X/810/2/143). arXiv: [1411.4180](https://arxiv.org/abs/1411.4180).
- [Aud+13] B. Audren et al. “Conservative Constraints on Early Cosmology: an illustration of the Monte Python cosmological parameter inference code”. *JCAP* 1302 (2013). DOI: [10.1088/1475-7516/2013/02/001](https://doi.org/10.1088/1475-7516/2013/02/001). arXiv: [1210.7183](https://arxiv.org/abs/1210.7183).
- [AW01] G. B. Arfken and H. J. Weber. *Mathematical methods for physicists*. Academic Press, 2001 [1966]. ISBN: 9780120598267.
- [Bab+16a] E. Babichev et al. “Bigravitational origin of dark matter”. *Phys. Rev. D* 94.8 (2016). DOI: [10.1103/PhysRevD.94.084055](https://doi.org/10.1103/PhysRevD.94.084055). arXiv: [1604.08564](https://arxiv.org/abs/1604.08564).
- [Bab+16b] E. Babichev et al. “Heavy spin-2 Dark Matter”. *JCAP* 1609.09 (2016). DOI: [10.1088/1475-7516/2016/09/016](https://doi.org/10.1088/1475-7516/2016/09/016). arXiv: [1607.03497](https://arxiv.org/abs/1607.03497).
- [Ban+17] N. Banik et al. “New astrophysical bounds on ultralight axionlike particles”. *Phys. Rev. D* 95.4 (2017). DOI: [10.1103/PhysRevD.95.043542](https://doi.org/10.1103/PhysRevD.95.043542). arXiv: [1701.04573](https://arxiv.org/abs/1701.04573).
- [Bar+99] V. D. Barger et al. “Astrophysical constraints on large extra dimensions”. *Phys. Lett. B* 461 (1999). DOI: [10.1016/S0370-2693\(99\)00795-9](https://doi.org/10.1016/S0370-2693(99)00795-9). arXiv: [hep-ph/9905474](https://arxiv.org/abs/hep-ph/9905474).
- [Bar80] J. M. Bardeen. “Gauge Invariant Cosmological Perturbations”. *Phys. Rev. D* 22 (1980). DOI: [10.1103/PhysRevD.22.1882](https://doi.org/10.1103/PhysRevD.22.1882).
- [BB17] J. S. Bullock and M. Boylan-Kolchin. “Small-Scale Challenges to the Λ CDM Paradigm”. *Ann. Rev. Astron. Astrophys.* 55 (2017). DOI: [10.1146/annurev-astro-091916-055313](https://doi.org/10.1146/annurev-astro-091916-055313). arXiv: [1707.04256](https://arxiv.org/abs/1707.04256).
- [BCW10] M. Bullimore, J. P. Conlon, and L. T. Witkowski. “Kinetic mixing of U(1)s for local string models”. *JHEP* 11 (2010). DOI: [10.1007/JHEP11\(2010\)142](https://doi.org/10.1007/JHEP11(2010)142). arXiv: [1009.2380](https://arxiv.org/abs/1009.2380).
- [BD11] C. Bonvin and R. Durrer. “What galaxy surveys really measure”. *Phys. Rev. D* 84 (2011). DOI: [10.1103/PhysRevD.84.063505](https://doi.org/10.1103/PhysRevD.84.063505). arXiv: [1105.5280](https://arxiv.org/abs/1105.5280).
- [BD72] D. G. Boulware and S. Deser. “Can gravitation have a finite range?” *Phys. Rev. D* 6 (1972). DOI: [10.1103/PhysRevD.6.3368](https://doi.org/10.1103/PhysRevD.6.3368).
- [BD84] N. D. Birrell and P. C. W. Davies. *Quantum Fields in Curved Space*. Cambridge Monographs on Mathematical Physics. Cambridge Univ. Press, 1984. ISBN: 0521278589, 9780521278584.

- [BDE92] M. Bruni, P. K. S. Dunsby, and G. F. R. Ellis. “Cosmological perturbations and the physical meaning of gauge invariant variables”. *Astrophys. J.* 395 (1992). DOI: [10.1086/171629](https://doi.org/10.1086/171629).
- [Ben+14] N. Benitez et al. “J-PAS: The Javalambre-Physics of the Accelerated Universe Astrophysical Survey” (2014). arXiv: [1403.5237](https://arxiv.org/abs/1403.5237).
- [Ben+96] C. L. Bennett et al. “Four year COBE DMR cosmic microwave background observations: Maps and basic results”. *Astrophys. J.* 464 (1996). DOI: [10.1086/310075](https://doi.org/10.1086/310075). arXiv: [astro-ph/9601067](https://arxiv.org/abs/astro-ph/9601067).
- [Ber88] J. Bernstein. *Kinetic Theory in the Expanding Universe*. Cambridge University Press, 1988. ISBN: 9780521360500.
- [Beu+11] F. Beutler et al. “The 6dF Galaxy Survey: Baryon Acoustic Oscillations and the Local Hubble Constant”. *Mon. Not. Roy. Astron. Soc.* 416 (2011). DOI: [10.1111/j.1365-2966.2011.19250.x](https://doi.org/10.1111/j.1365-2966.2011.19250.x). arXiv: [1106.3366](https://arxiv.org/abs/1106.3366).
- [BFP18] P. Brax, S. Fichet, and G. Pignol. “Bounding Quantum Dark Forces”. *Phys. Rev. D* 97.11 (2018). DOI: [10.1103/PhysRevD.97.115034](https://doi.org/10.1103/PhysRevD.97.115034). arXiv: [1710.00850](https://arxiv.org/abs/1710.00850).
- [BH18] G. Bertone and D. Hooper. “History of dark matter”. *Rev. Mod. Phys.* 90.4 (2018). DOI: [10.1103/RevModPhys.90.045002](https://doi.org/10.1103/RevModPhys.90.045002). arXiv: [1605.04909](https://arxiv.org/abs/1605.04909).
- [BJ04] R. Banerjee and K. Jedamzik. “The Evolution of cosmic magnetic fields: From the very early universe, to recombination, to the present”. *Phys. Rev. D* 70 (2004). DOI: [10.1103/PhysRevD.70.123003](https://doi.org/10.1103/PhysRevD.70.123003). arXiv: [astro-ph/0410032](https://arxiv.org/abs/astro-ph/0410032).
- [BLT11] D. Blas, J. Lesgourgues, and T. Tram. “The Cosmic Linear Anisotropy Solving System (CLASS) II: Approximation schemes”. *JCAP* 1107 (2011). DOI: [10.1088/1475-7516/2011/07/034](https://doi.org/10.1088/1475-7516/2011/07/034). arXiv: [1104.2933](https://arxiv.org/abs/1104.2933).
- [BM07] J. Beltrán Jiménez and A. L. Maroto. “Cosmology with moving dark energy and the CMB quadrupole”. *Phys. Rev. D* 76 (2007). DOI: [10.1103/PhysRevD.76.023003](https://doi.org/10.1103/PhysRevD.76.023003). arXiv: [astro-ph/0703483](https://arxiv.org/abs/astro-ph/0703483).
- [BMM01] M. Bordag, U. Mohideen, and V. M. Mostepanenko. “New developments in the Casimir effect”. *Phys. Rept.* 353 (2001). DOI: [10.1016/S0370-1573\(01\)00015-1](https://doi.org/10.1016/S0370-1573(01)00015-1). arXiv: [quant-ph/0106045](https://arxiv.org/abs/quant-ph/0106045).
- [BMR09] C. Biggio, E. Masso, and J. Redondo. “Mixing of photons with massive spin-two particles in a magnetic field”. *Phys. Rev. D* 79 (2009). DOI: [10.1103/PhysRevD.79.015012](https://doi.org/10.1103/PhysRevD.79.015012). arXiv: [hep-ph/0604062](https://arxiv.org/abs/hep-ph/0604062).
- [BMT00] M. Bucher, K. Moodley, and N. Turok. “The general primordial cosmic perturbation”. *Phys. Rev. D* 62 (2000). DOI: [10.1103/PhysRevD.62.083508](https://doi.org/10.1103/PhysRevD.62.083508). arXiv: [astro-ph/9904231](https://arxiv.org/abs/astro-ph/9904231).
- [BMT07] J. D. Barrow, R. Maartens, and C. G. Tsagas. “Cosmology with inhomogeneous magnetic fields”. *Phys. Rept.* 449 (2007). DOI: [10.1016/j.physrep.2007.04.006](https://doi.org/10.1016/j.physrep.2007.04.006). arXiv: [astro-ph/0611537](https://arxiv.org/abs/astro-ph/0611537).

- [BOT01] P. Bode, J. P. Ostriker, and N. Turok. “Halo formation in warm dark matter models”. *Astrophys. J.* 556 (2001). DOI: [10.1086/321541](https://doi.org/10.1086/321541). arXiv: [astro-ph/0010389](https://arxiv.org/abs/astro-ph/0010389).
- [Bri+17a] R. Brito et al. “Gravitational wave searches for ultralight bosons with LIGO and LISA”. *Phys. Rev. D* 96.6 (2017). DOI: [10.1103/PhysRevD.96.064050](https://doi.org/10.1103/PhysRevD.96.064050). arXiv: [1706.06311](https://arxiv.org/abs/1706.06311).
- [Bri+17b] R. Brito et al. “Stochastic and resolvable gravitational waves from ultralight bosons”. *Phys. Rev. Lett.* 119.13 (2017). DOI: [10.1103/PhysRevLett.119.131101](https://doi.org/10.1103/PhysRevLett.119.131101). arXiv: [1706.05097](https://arxiv.org/abs/1706.05097).
- [BS99] M. Bruni and S. Sonogo. “Observables and gauge invariance in the theory of nonlinear space-time perturbations: Letter to the editor”. *Class. Quant. Grav.* 16 (1999). DOI: [10.1088/0264-9381/16/7/101](https://doi.org/10.1088/0264-9381/16/7/101). arXiv: [gr-qc/9906017](https://arxiv.org/abs/gr-qc/9906017).
- [BSL15] J. Beltrán Jiménez, V. Salzano, and R. Lazkoz. “Anisotropic expansion and SNIa: an open issue”. *Phys. Lett. B* 741 (2015). DOI: [10.1016/j.physletb.2014.12.031](https://doi.org/10.1016/j.physletb.2014.12.031). arXiv: [1402.1760](https://arxiv.org/abs/1402.1760).
- [Buc+16] T. Buchert et al. “Observational Challenges for the Standard FLRW Model”. *Int. J. Mod. Phys. D* 25.03 (2016). DOI: [10.1142/S021827181630007X](https://doi.org/10.1142/S021827181630007X), [10.1142/9789813226609_0034](https://doi.org/10.1142/9789813226609_0034). arXiv: [1512.03313](https://arxiv.org/abs/1512.03313).
- [BVH12] S. Bird, M. Viel, and M. G. Haehnelt. “Massive Neutrinos and the Non-linear Matter Power Spectrum”. *Mon. Not. Roy. Astron. Soc.* 420 (2012). DOI: [10.1111/j.1365-2966.2011.20222.x](https://doi.org/10.1111/j.1365-2966.2011.20222.x). arXiv: [1109.4416](https://arxiv.org/abs/1109.4416).
- [Cem+12] J. A. R. Cembranos et al. “Isotropy theorem for cosmological vector fields”. *Phys. Rev. D* 86 (2012). DOI: [10.1103/PhysRevD.86.021301](https://doi.org/10.1103/PhysRevD.86.021301). arXiv: [1203.6221](https://arxiv.org/abs/1203.6221).
- [CG68] J. P. Cox and R. T. Giuli. *Principles of Stellar Structure: Applications to stars*. Principles of Stellar Structure. Gordon and Breach, 1968. ISBN: 0677019300, 9780677019307.
- [CGU17] F. X. L. Cedeño, A. X. González-Morales, and L. A. Ureña-López. “Cosmological signatures of ultralight dark matter with an axionlike potential”. *Phys. Rev. D* 96.6 (2017). DOI: [10.1103/PhysRevD.96.061301](https://doi.org/10.1103/PhysRevD.96.061301). arXiv: [1703.10180](https://arxiv.org/abs/1703.10180).
- [Cha+90] S. Chapman et al. *The Mathematical Theory of Non-uniform Gases: An Account of the Kinetic Theory of Viscosity, Thermal Conduction and Diffusion in Gases*. Cambridge Mathematical Library. Cambridge University Press, 1990. ISBN: 9780521408448.
- [Cha78] B. Chakraborty. *Principles of Plasma Mechanics*. Wiley, 1978. ISBN: 9780470217290, 0470217294.
- [Chi+03] J. Chiaverini et al. “New experimental constraints on non-Newtonian forces below 100 microns”. *Phys. Rev. Lett.* 90 (2003). DOI: [10.1103/PhysRevLett.90.151101](https://doi.org/10.1103/PhysRevLett.90.151101). arXiv: [hep-ph/0209325](https://arxiv.org/abs/hep-ph/0209325).

- [CMH92] E. D. Carlson, M. E. Machacek, and L. J. Hall. “Self-interacting dark matter”. *Astrophys. J.* 398 (1992). DOI: [10.1086/171833](https://doi.org/10.1086/171833).
- [CMN13] J. A. R. Cembranos, A. L. Maroto, and S. J. Núñez Jareño. “Isotropy theorem for cosmological Yang-Mills theories”. *Phys. Rev.* D87.4 (2013). DOI: [10.1103/PhysRevD.87.043523](https://doi.org/10.1103/PhysRevD.87.043523). arXiv: [1212.3201](https://arxiv.org/abs/1212.3201).
- [CMN14] J. A. R. Cembranos, A. L. Maroto, and S. J. Núñez Jareño. “Isotropy theorem for arbitrary-spin cosmological fields”. *JCAP* 1403 (2014). DOI: [10.1088/1475-7516/2014/03/042](https://doi.org/10.1088/1475-7516/2014/03/042). arXiv: [1311.1402](https://arxiv.org/abs/1311.1402).
- [CMN16] J. A. R. Cembranos, A. L. Maroto, and S. J. Núñez Jareño. “Cosmological perturbations in coherent oscillating scalar field models”. *JHEP* 03 (2016). DOI: [10.1007/JHEP03\(2016\)013](https://doi.org/10.1007/JHEP03(2016)013). arXiv: [1509.08819](https://arxiv.org/abs/1509.08819).
- [CMN17] J. A. R. Cembranos, A. L. Maroto, and S. J. Núñez Jareño. “Perturbations of ultralight vector field dark matter”. *JHEP* 02 (2017). DOI: [10.1007/JHEP02\(2017\)064](https://doi.org/10.1007/JHEP02(2017)064). arXiv: [1611.03793](https://arxiv.org/abs/1611.03793).
- [Con+18] J. P. Conlon et al. “Projected bounds on ALPs from Athena”. *Mon. Not. Roy. Astron. Soc.* 473 (2018). DOI: [10.1093/mnras/stx2652](https://doi.org/10.1093/mnras/stx2652). arXiv: [1707.00176](https://arxiv.org/abs/1707.00176).
- [Con+98] J. J. Condon et al. “The NRAO VLA Sky survey”. *Astron. J.* 115 (1998). DOI: [10.1086/300337](https://doi.org/10.1086/300337).
- [CP99] S. Cullen and M. Perelstein. “SN1987A constraints on large compact dimensions”. *Phys. Rev. Lett.* 83 (1999). DOI: [10.1103/PhysRevLett.83.268](https://doi.org/10.1103/PhysRevLett.83.268). arXiv: [hep-ph/9903422](https://arxiv.org/abs/hep-ph/9903422).
- [CS12] J. Chluba and R. A. Sunyaev. “The evolution of CMB spectral distortions in the early Universe”. *Mon. Not. Roy. Astron. Soc.* 419 (2012). DOI: [10.1111/j.1365-2966.2011.19786.x](https://doi.org/10.1111/j.1365-2966.2011.19786.x). arXiv: [1109.6552](https://arxiv.org/abs/1109.6552).
- [CT86] A. A. Coley and B. O. J. Tupper. “Two-fluid cosmological models”. *Journal of Mathematical Physics* 27.1 (1986).
- [Dav15] S. Davidson. “Axions: Bose Einstein Condensate or Classical Field?” *Astropart. Phys.* 65 (2015). DOI: [10.1016/j.astropartphys.2014.12.007](https://doi.org/10.1016/j.astropartphys.2014.12.007). arXiv: [1405.1139](https://arxiv.org/abs/1405.1139).
- [De 86] A. De Rujula. “On Weaker Forces than Gravity”. *Phys. Lett.* B180 (1986). DOI: [10.1016/0370-2693\(86\)90298-4](https://doi.org/10.1016/0370-2693(86)90298-4).
- [DFK12] J. B. Dent, F. Ferrer, and L. M. Krauss. “Constraints on Light Hidden Sector Gauge Bosons from Supernova Cooling” (2012). arXiv: [1201.2683](https://arxiv.org/abs/1201.2683).
- [DHR00] H. Davoudiasl, J. Hewett, and T. Rizzo. “Phenomenology of the Randall-Sundrum Gauge Hierarchy Model”. *Phys. Rev. Lett.* 84 (2000). DOI: [10.1103/PhysRevLett.84.2080](https://doi.org/10.1103/PhysRevLett.84.2080). arXiv: [hep-ph/9909255](https://arxiv.org/abs/hep-ph/9909255).
- [DKR18] V. Desjacques, A. Kehagias, and A. Riotto. “Impact of ultralight axion self-interactions on the large scale structure of the Universe”. *Phys. Rev.* D97.2 (2018). DOI: [10.1103/PhysRevD.97.023529](https://doi.org/10.1103/PhysRevD.97.023529). arXiv: [1709.07946](https://arxiv.org/abs/1709.07946).

- [DLO17] P. S. B. Dev, M. Lindner, and S. Ohmer. “Gravitational waves as a new probe of Bose–Einstein condensate Dark Matter”. *Phys. Lett.* B773 (2017). DOI: [10.1016/j.physletb.2017.08.043](https://doi.org/10.1016/j.physletb.2017.08.043). arXiv: [1609.03939](https://arxiv.org/abs/1609.03939).
- [DLT99] A.-C. Davis, M. Lilley, and O. Tornkvist. “Relaxing the bounds on primordial magnetic seed fields”. *Phys. Rev. D* 60 (1999). DOI: [10.1103/PhysRevD.60.021301](https://doi.org/10.1103/PhysRevD.60.021301). arXiv: [astro-ph/9904022](https://arxiv.org/abs/astro-ph/9904022).
- [DM17] A. Diez-Tejedor and D. J. E. Marsh. “Cosmological production of ultralight dark matter axions” (2017). arXiv: [1702.02116](https://arxiv.org/abs/1702.02116).
- [DN13] R. Durrer and A. Neronov. “Cosmological Magnetic Fields: Their Generation, Evolution and Observation”. *Astron. Astrophys. Rev.* 21 (2013). DOI: [10.1007/s00159-013-0062-7](https://doi.org/10.1007/s00159-013-0062-7). arXiv: [1303.7121](https://arxiv.org/abs/1303.7121).
- [Dod03] S. Dodelson. *Modern Cosmology*. Academic Press, 2003. ISBN: 0122191412, 9780122191411.
- [Dor05] M. Doran. “Speeding up cosmological Boltzmann codes”. *JCAP* 0506 (2005). DOI: [10.1088/1475-7516/2005/06/011](https://doi.org/10.1088/1475-7516/2005/06/011). arXiv: [astro-ph/0503277](https://arxiv.org/abs/astro-ph/0503277).
- [Dur08] R. Durrer. *The Cosmic Microwave Background*. Cambridge University Press, 2008. ISBN: 9780511817205.
- [DV70] H. van Dam and M. J. G. Veltman. “Massive and massless Yang-Mills and gravitational fields”. *Nucl. Phys.* B22 (1970). DOI: [10.1016/0550-3213\(70\)90416-5](https://doi.org/10.1016/0550-3213(70)90416-5).
- [DW17] J. A. D. Diacoumis and Y. Y. Y. Wong. “Using CMB spectral distortions to distinguish between dark matter solutions to the small-scale crisis”. *JCAP* 1709.09 (2017). DOI: [10.1088/1475-7516/2017/09/011](https://doi.org/10.1088/1475-7516/2017/09/011). arXiv: [1707.07050](https://arxiv.org/abs/1707.07050).
- [EB84] G. F. R. Ellis and J. E. Baldwin. “On the expected anisotropy of radio source counts”. *Monthly Notices of the Royal Astronomical Society* 206.2 (1984).
- [EE99] G. F. R. Ellis and H. van Elst. “Cosmological models: Cargese lectures 1998”. *NATO Sci. Ser. C* 541 (1999). DOI: [10.1007/978-94-011-4455-1_1](https://doi.org/10.1007/978-94-011-4455-1_1). arXiv: [gr-qc/9812046](https://arxiv.org/abs/gr-qc/9812046).
- [EEM01] G. F. R. Ellis, H. van Elst, and R. Maartens. “General relativistic analysis of peculiar velocities”. *Class. Quant. Grav.* 18 (2001). DOI: [10.1088/0264-9381/18/23/308](https://doi.org/10.1088/0264-9381/18/23/308). arXiv: [gr-qc/0105083](https://arxiv.org/abs/gr-qc/0105083).
- [Ehl73] J. Ehlers. “Survey of general relativity theory”. *Relativity, astrophysics and cosmology. Proceedings of the summer school held, 14-26 August, 1972 at the Banff Centre, Banff Alberta*. Ed. by W. Israel. D. Reidel Publishing Company, 1973. ISBN: 9027703698.
- [Fan16] J. Fan. “Ultralight Repulsive Dark Matter and BEC”. *Phys. Dark Univ.* 14 (2016). DOI: [10.1016/j.dark.2016.10.005](https://doi.org/10.1016/j.dark.2016.10.005). arXiv: [1603.06580](https://arxiv.org/abs/1603.06580).
- [FDT87] J. A. Frieman, S. Dimopoulos, and M. S. Turner. “Axions and Stars”. *Phys. Rev. D* 36 (1987). DOI: [10.1103/PhysRevD.36.2201](https://doi.org/10.1103/PhysRevD.36.2201).

- [Fix+96] D. J. Fixsen et al. “The Cosmic Microwave Background spectrum from the full COBE FIRAS data set”. *Astrophys. J.* 473 (1996). DOI: [10.1086/178173](https://doi.org/10.1086/178173). arXiv: [astro-ph/9605054](https://arxiv.org/abs/astro-ph/9605054).
- [Fix09] D. J. Fixsen. “The Temperature of the Cosmic Microwave Background”. *Astrophys. J.* 707 (2009). DOI: [10.1088/0004-637X/707/2/916](https://doi.org/10.1088/0004-637X/707/2/916). arXiv: [0911.1955](https://arxiv.org/abs/0911.1955).
- [FP39] M. Fierz and W. Pauli. “On relativistic wave equations for particles of arbitrary spin in an electromagnetic field”. *Proc. Roy. Soc. Lond.* A173 (1939). DOI: [10.1098/rspa.1939.0140](https://doi.org/10.1098/rspa.1939.0140).
- [FP94] R. A. Flores and J. R. Primack. “Observational and theoretical constraints on singular dark matter halos”. *Astrophys. J.* 427 (1994). DOI: [10.1086/187350](https://doi.org/10.1086/187350). arXiv: [astro-ph/9402004](https://arxiv.org/abs/astro-ph/9402004).
- [FPM11] E. Fenu, C. Pitrou, and R. Maartens. “The seed magnetic field generated during recombination”. *Mon. Not. Roy. Astron. Soc.* 414 (2011). DOI: [10.1111/j.1365-2966.2011.18554.x](https://doi.org/10.1111/j.1365-2966.2011.18554.x). arXiv: [1012.2958](https://arxiv.org/abs/1012.2958).
- [FT99] E. Fischbach and C. L. Talmadge. *The Search for Non-Newtonian Gravity*. Springer, 1999. ISBN: 9781461271444.
- [GCM17] S. R. Goldberg, T. Clifton, and K. A. Malik. “Cosmology on all scales: a two-parameter perturbation expansion”. *Phys. Rev.* D95.4 (2017). DOI: [10.1103/PhysRevD.95.043503](https://doi.org/10.1103/PhysRevD.95.043503). arXiv: [1610.08882](https://arxiv.org/abs/1610.08882).
- [GH12] C. Gibelyou and D. Huterer. “Dipoles in the Sky”. *Mon. Not. Roy. Astron. Soc.* 427 (2012). DOI: [10.1111/j.1365-2966.2012.22032.x](https://doi.org/10.1111/j.1365-2966.2012.22032.x). arXiv: [1205.6476](https://arxiv.org/abs/1205.6476).
- [GHP15] A. H. Guth, M. P. Hertzberg, and C. Prescod-Weinstein. “Do Dark Matter Axions Form a Condensate with Long-Range Correlation?” *Phys. Rev.* D92.10 (2015). DOI: [10.1103/PhysRevD.92.103513](https://doi.org/10.1103/PhysRevD.92.103513). arXiv: [1412.5930](https://arxiv.org/abs/1412.5930).
- [GMM16] C. García-García, A. L. Maroto, and P. Martín-Moruno. “Cosmology with moving bimetric fluids”. *JCAP* 1612.12 (2016). DOI: [10.1088/1475-7516/2016/12/022](https://doi.org/10.1088/1475-7516/2016/12/022). arXiv: [1608.06493](https://arxiv.org/abs/1608.06493).
- [GN10] A. S. Goldhaber and M. M. Nieto. “Photon and Graviton Mass Limits”. *Rev. Mod. Phys.* 82 (2010). DOI: [10.1103/RevModPhys.82.939](https://doi.org/10.1103/RevModPhys.82.939). arXiv: [0809.1003](https://arxiv.org/abs/0809.1003).
- [Goo+09] M. Goodsell et al. “Naturally Light Hidden Photons in LARGE Volume String Compactifications”. *JHEP* 11 (2009). DOI: [10.1088/1126-6708/2009/11/027](https://doi.org/10.1088/1126-6708/2009/11/027). arXiv: [0909.0515](https://arxiv.org/abs/0909.0515).
- [Goo00] J. Goodman. “Repulsive dark matter”. *New Astron.* 5 (2000). DOI: [10.1016/S1384-1076\(00\)00015-4](https://doi.org/10.1016/S1384-1076(00)00015-4). arXiv: [astro-ph/0003018](https://arxiv.org/abs/astro-ph/0003018).
- [GR07] I. S. Gradshteyn and I. M. Ryzhik. *Table of Integrals, Series, and Products*. Academic Press, 2007 [1967]. ISBN: 9780123736376.

- [GRW99] G. F. Giudice, R. Rattazzi, and J. D. Wells. “Quantum gravity and extra dimensions at high-energy colliders”. *Nucl. Phys.* B544 (1999). DOI: [10.1016/S0550-3213\(99\)00044-9](https://doi.org/10.1016/S0550-3213(99)00044-9). arXiv: [hep-ph/9811291](https://arxiv.org/abs/hep-ph/9811291).
- [GT00] J. Garriga and T. Tanaka. “Gravity in the brane world”. *Phys. Rev. Lett.* 84 (2000). DOI: [10.1103/PhysRevLett.84.2778](https://doi.org/10.1103/PhysRevLett.84.2778). arXiv: [hep-th/9911055](https://arxiv.org/abs/hep-th/9911055).
- [Had+18] C. C. Haddock et al. “Search for deviations from the inverse square law of gravity at nm range using a pulsed neutron beam”. *Phys. Rev.* D97.6 (2018). DOI: [10.1103/PhysRevD.97.062002](https://doi.org/10.1103/PhysRevD.97.062002). arXiv: [1712.02984](https://arxiv.org/abs/1712.02984).
- [Han+01] C. Hanhart et al. “Extra dimensions, SN1987a, and nucleon-nucleon scattering data”. *Nucl. Phys.* B595 (2001). DOI: [10.1016/S0550-3213\(00\)00667-2](https://doi.org/10.1016/S0550-3213(00)00667-2). arXiv: [nucl-th/0007016](https://arxiv.org/abs/nucl-th/0007016).
- [Har70] E. R. Harrison. “Generation of magnetic fields in the radiation era”. *Monthly Notices of the Royal Astronomical Society* 147.3 (1970).
- [Haz+19] M. Hazumi et al. “LiteBIRD: A Satellite for the Studies of B-Mode Polarization and Inflation from Cosmic Background Radiation Detection”. *J. Low. Temp. Phys.* 194.5-6 (2019). DOI: [10.1007/s10909-019-02150-5](https://doi.org/10.1007/s10909-019-02150-5).
- [HBG00] W. Hu, R. Barkana, and A. Gruzinov. “Cold and fuzzy dark matter”. *Phys. Rev. Lett.* 85 (2000). DOI: [10.1103/PhysRevLett.85.1158](https://doi.org/10.1103/PhysRevLett.85.1158). arXiv: [astro-ph/0003365](https://arxiv.org/abs/astro-ph/0003365).
- [HDC18] L. Herrera, A. Di Prisco, and J. Carot. “Tilted shear-free axially symmetric fluids”. *Phys. Rev.* D97.12 (2018). DOI: [10.1103/PhysRevD.97.124003](https://doi.org/10.1103/PhysRevD.97.124003). arXiv: [1806.01909](https://arxiv.org/abs/1806.01909).
- [HDI11] L. Herrera, A. Di Prisco, and J. Ibáñez. “Tilted Lemaitre-Tolman-Bondi Spacetimes: Hydrodynamic and Thermodynamic Properties”. *Phys. Rev.* D84 (2011). DOI: [10.1103/PhysRevD.84.064036](https://doi.org/10.1103/PhysRevD.84.064036). arXiv: [1105.4727](https://arxiv.org/abs/1105.4727).
- [Hee+17] A. Hees et al. “Testing General Relativity with stellar orbits around the supermassive black hole in our Galactic center”. *Phys. Rev. Lett.* 118.21 (2017). DOI: [10.1103/PhysRevLett.118.211101](https://doi.org/10.1103/PhysRevLett.118.211101). arXiv: [1705.07902](https://arxiv.org/abs/1705.07902).
- [Hei15] L. Heisenberg. “Quantum corrections in massive bigravity and new effective composite metrics”. *Class. Quant. Grav.* 32.10 (2015). DOI: [10.1088/0264-9381/32/10/105011](https://doi.org/10.1088/0264-9381/32/10/105011). arXiv: [1410.4239](https://arxiv.org/abs/1410.4239).
- [Hei19] L. Heisenberg. “A systematic approach to generalisations of General Relativity and their cosmological implications”. *Phys. Rept.* 796 (2019). DOI: [10.1016/j.physrep.2018.11.006](https://doi.org/10.1016/j.physrep.2018.11.006). arXiv: [1807.01725](https://arxiv.org/abs/1807.01725).
- [Her+12] L. Herrera et al. “Vorticity and entropy production in tilted Szekeres spacetimes”. *Phys. Rev.* D86 (2012). DOI: [10.1103/PhysRevD.86.044003](https://doi.org/10.1103/PhysRevD.86.044003). arXiv: [1207.2259](https://arxiv.org/abs/1207.2259).
- [Hin12] K. Hinterbichler. “Theoretical Aspects of Massive Gravity”. *Rev. Mod. Phys.* 84 (2012). DOI: [10.1103/RevModPhys.84.671](https://doi.org/10.1103/RevModPhys.84.671). arXiv: [1105.3735](https://arxiv.org/abs/1105.3735).

- [HL13] T. Harko and F. S. N. Lobo. “Cosmological anisotropy from non-comoving dark matter and dark energy”. *JCAP* 1307 (2013). DOI: [10.1088/1475-7516/2013/07/036](https://doi.org/10.1088/1475-7516/2013/07/036). arXiv: [1304.0757](https://arxiv.org/abs/1304.0757).
- [Hlo+15] R. Hlozek et al. “A search for ultralight axions using precision cosmological data”. *Phys. Rev. D* 91.10 (2015). DOI: [10.1103/PhysRevD.91.103512](https://doi.org/10.1103/PhysRevD.91.103512). arXiv: [1410.2896](https://arxiv.org/abs/1410.2896).
- [Hlo+17] R. Hložek et al. “Future CMB tests of dark matter: Ultralight axions and massive neutrinos”. *Phys. Rev. D* 95.12 (2017). DOI: [10.1103/PhysRevD.95.123511](https://doi.org/10.1103/PhysRevD.95.123511). arXiv: [1607.08208](https://arxiv.org/abs/1607.08208).
- [HLZ99] T. Han, J. D. Lykken, and R.-J. Zhang. “On Kaluza-Klein states from large extra dimensions”. *Phys. Rev. D* 59 (1999). DOI: [10.1103/PhysRevD.59.105006](https://doi.org/10.1103/PhysRevD.59.105006). arXiv: [hep-ph/9811350](https://arxiv.org/abs/hep-ph/9811350).
- [HMG18] R. Hložek, D. J. E. Marsh, and D. Grin. “Using the Full Power of the Cosmic Microwave Background to Probe Axion Dark Matter”. *Mon. Not. Roy. Astron. Soc.* 476.3 (2018). DOI: [10.1093/mnras/sty271](https://doi.org/10.1093/mnras/sty271). arXiv: [1708.05681](https://arxiv.org/abs/1708.05681).
- [HN09] J.-c. Hwang and H. Noh. “Axion as a Cold Dark Matter candidate”. *Phys. Lett. B* 680 (2009). DOI: [10.1016/j.physletb.2009.08.031](https://doi.org/10.1016/j.physletb.2009.08.031). arXiv: [0902.4738](https://arxiv.org/abs/0902.4738).
- [Hol+08] L. Hollenstein et al. “Challenges for creating magnetic fields by cosmic defects”. *Phys. Rev. D* 77 (2008). DOI: [10.1103/PhysRevD.77.063517](https://doi.org/10.1103/PhysRevD.77.063517). arXiv: [0712.1667](https://arxiv.org/abs/0712.1667).
- [Hop+18] P. F. Hopkins et al. “FIRE-2 Simulations: Physics versus Numerics in Galaxy Formation”. *Mon. Not. Roy. Astron. Soc.* 480.1 (2018). DOI: [10.1093/mnras/sty1690](https://doi.org/10.1093/mnras/sty1690). arXiv: [1702.06148](https://arxiv.org/abs/1702.06148).
- [Hos+85] J. K. Hoskins et al. “Experimental tests of the gravitational inverse square law for mass separations from 2-cm to 105-cm”. *Phys. Rev. D* 32 (1985). DOI: [10.1103/PhysRevD.32.3084](https://doi.org/10.1103/PhysRevD.32.3084).
- [HR01] S. Hannestad and G. G. Raffelt. “New supernova limit on large extra dimensions”. *Phys. Rev. Lett.* 87 (2001). DOI: [10.1103/PhysRevLett.87.051301](https://doi.org/10.1103/PhysRevLett.87.051301). arXiv: [hep-ph/0103201](https://arxiv.org/abs/hep-ph/0103201).
- [HR02] S. Hannestad and G. G. Raffelt. “Stringent neutron star limits on large extra dimensions”. *Phys. Rev. Lett.* 88 (2002). DOI: [10.1103/PhysRevLett.88.071301](https://doi.org/10.1103/PhysRevLett.88.071301). arXiv: [hep-ph/0110067](https://arxiv.org/abs/hep-ph/0110067).
- [HR03] S. Hannestad and G. G. Raffelt. “Supernova and neutron star limits on large extra dimensions reexamined”. *Phys. Rev. D* 67 (2003). [Erratum: *Phys. Rev. D* 69,029901(2004)]. DOI: [10.1103/PhysRevD.69.029901](https://doi.org/10.1103/PhysRevD.69.029901), [10.1103/PhysRevD.67.125008](https://doi.org/10.1103/PhysRevD.67.125008). arXiv: [hep-ph/0304029](https://arxiv.org/abs/hep-ph/0304029).
- [HR11] S. F. Hassan and R. A. Rosen. “On Non-Linear Actions for Massive Gravity”. *JHEP* 07 (2011). DOI: [10.1007/JHEP07\(2011\)009](https://doi.org/10.1007/JHEP07(2011)009). arXiv: [1103.6055](https://arxiv.org/abs/1103.6055).

- [HS93a] W. Hu and J. Silk. “Thermalization constraints and spectral distortions for massive unstable relic particles”. *Phys. Rev. Lett.* 70 (1993). DOI: [10.1103/PhysRevLett.70.2661](https://doi.org/10.1103/PhysRevLett.70.2661).
- [HS93b] W. Hu and J. Silk. “Thermalization and spectral distortions of the cosmic background radiation”. *Phys. Rev.* D48 (1993). DOI: [10.1103/PhysRevD.48.485](https://doi.org/10.1103/PhysRevD.48.485).
- [HS96a] W. Hu and N. Sugiyama. “Small scale cosmological perturbations: An Analytic approach”. *Astrophys. J.* 471 (1996). DOI: [10.1086/177989](https://doi.org/10.1086/177989). arXiv: [astro-ph/9510117](https://arxiv.org/abs/astro-ph/9510117).
- [HS96b] W. Hu and N. Sugiyama. “Small scale cosmological perturbations: an analytic approach”. *Astrophys. J.* 471 (1996). DOI: [10.1086/177989](https://doi.org/10.1086/177989). arXiv: [astro-ph/9510117](https://arxiv.org/abs/astro-ph/9510117).
- [HSB18] S. Hirano, J. M. Sullivan, and V. Bromm. “First star formation in ultralight particle dark matter cosmology”. *Mon. Not. Roy. Astron. Soc.* 473.1 (2018). DOI: [10.1093/mnrasl/slx146](https://doi.org/10.1093/mnrasl/slx146). arXiv: [1706.00435](https://arxiv.org/abs/1706.00435).
- [HT99] L. J. Hall and D. Tucker-Smith. “Cosmological constraints on theories with large extra dimensions”. *Phys. Rev.* D60 (1999). DOI: [10.1103/PhysRevD.60.085008](https://doi.org/10.1103/PhysRevD.60.085008). arXiv: [hep-ph/9904267](https://arxiv.org/abs/hep-ph/9904267).
- [Hu+95] W. Hu et al. “The effect of physical assumptions on the calculation of microwave background anisotropies”. *Phys. Rev.* D52 (1995). DOI: [10.1103/PhysRevD.52.5498](https://doi.org/10.1103/PhysRevD.52.5498). arXiv: [astro-ph/9505043](https://arxiv.org/abs/astro-ph/9505043).
- [Hu04] W. Hu. “Covariant linear perturbation formalism”. *Astroparticle physics and cosmology. Proceedings: Summer School, Trieste, Italy, Jun 17-Jul 5 2002*. 2004. arXiv: [astro-ph/0402060](https://arxiv.org/abs/astro-ph/0402060).
- [Hu98] W. Hu. “Structure formation with generalized dark matter”. *Astrophys. J.* 506 (1998). DOI: [10.1086/306274](https://doi.org/10.1086/306274). arXiv: [astro-ph/9801234](https://arxiv.org/abs/astro-ph/9801234).
- [Hui+17] L. Hui et al. “Ultralight scalars as cosmological dark matter”. *Phys. Rev.* D95.4 (2017). DOI: [10.1103/PhysRevD.95.043541](https://doi.org/10.1103/PhysRevD.95.043541). arXiv: [1610.08297](https://arxiv.org/abs/1610.08297).
- [Irs+17] V. Iršič et al. “New Constraints on the free-streaming of warm dark matter from intermediate and small scale Lyman- α forest data”. *Phys. Rev.* D96.2 (2017). DOI: [10.1103/PhysRevD.96.023522](https://doi.org/10.1103/PhysRevD.96.023522). arXiv: [1702.01764](https://arxiv.org/abs/1702.01764).
- [ITS12] K. Ichiki, K. Takahashi, and N. Sugiyama. “Constraint on the primordial vector mode and its magnetic field generation from seven-year Wilkinson Microwave Anisotropy Probe Observations”. *Phys. Rev.* D85 (2012). DOI: [10.1103/PhysRevD.85.043009](https://doi.org/10.1103/PhysRevD.85.043009). arXiv: [1112.4705](https://arxiv.org/abs/1112.4705).
- [Iwa70] Y. Iwasaki. “Consistency condition for propagators”. *Phys. Rev.* D2 (1970). DOI: [10.1103/PhysRevD.2.2255](https://doi.org/10.1103/PhysRevD.2.2255).

- [IYT10] Y. Itoh, K. Yahata, and M. Takada. “A dipole anisotropy of galaxy distribution: Does the CMB rest-frame exist in the local universe?” *Phys. Rev. D* 82 (2010). DOI: [10.1103/PhysRevD.82.043530](https://doi.org/10.1103/PhysRevD.82.043530). arXiv: [0912.1460](https://arxiv.org/abs/0912.1460).
- [Jac98] J. D. Jackson. *Classical Electrodynamics*. John Wiley & Sons, 1998 [1962]. ISBN: 9780471309321.
- [JK08] M. C. Johnson and M. Kamionkowski. “Dynamical and Gravitational Instability of Oscillating-Field Dark Energy and Dark Matter”. *Phys. Rev. D* 78 (2008). DOI: [10.1103/PhysRevD.78.063010](https://doi.org/10.1103/PhysRevD.78.063010). arXiv: [0805.1748](https://arxiv.org/abs/0805.1748).
- [JKG96] G. Jungman, M. Kamionkowski, and K. Griest. “Supersymmetric dark matter”. *Phys. Rept.* 267 (1996). DOI: [10.1016/0370-1573\(95\)00058-5](https://doi.org/10.1016/0370-1573(95)00058-5). arXiv: [hep-ph/9506380](https://arxiv.org/abs/hep-ph/9506380).
- [Joh+14] A. Johnson et al. “The 6dF Galaxy Survey: cosmological constraints from the velocity power spectrum”. *Mon. Not. Roy. Astron. Soc.* 444.4 (2014). DOI: [10.1093/mnras/stu1615](https://doi.org/10.1093/mnras/stu1615). arXiv: [1404.3799](https://arxiv.org/abs/1404.3799).
- [JS+98] J. V. José, E. J. Saletan, et al. *Classical Dynamics: A Contemporary Approach*. Cambridge University Press, 1998. ISBN: 9780521636360.
- [Kas+09] A. Kashlinsky et al. “A measurement of large-scale peculiar velocities of clusters of galaxies: results and cosmological implications”. *Astrophys. J.* 686 (2009). DOI: [10.1086/592947](https://doi.org/10.1086/592947). arXiv: [0809.3734](https://arxiv.org/abs/0809.3734).
- [KE73] A. R. King and G. F. R. Ellis. “Tilted homogeneous cosmological models”. *Commun. Math. Phys.* 31 (1973). DOI: [10.1007/BF01646266](https://doi.org/10.1007/BF01646266).
- [KL01] T. S. Kolatt and O. Lahav. “Constraints on cosmological anisotropy out to $z=1$ from supernovae Ia”. *Mon. Not. Roy. Astron. Soc.* 323 (2001). DOI: [10.1046/j.1365-8711.2001.04262.x](https://doi.org/10.1046/j.1365-8711.2001.04262.x). arXiv: [astro-ph/0008041](https://arxiv.org/abs/astro-ph/0008041).
- [KMW84] L. M. Krauss, J. E. Moody, and F. Wilczek. “A stellar energy loss mechanism involving axions”. *Phys. Lett.* B144 (1984). DOI: [10.1016/0370-2693\(84\)91285-1](https://doi.org/10.1016/0370-2693(84)91285-1).
- [KMZ85] M. Khlopov, B. A. Malomed, and I. B. Zeldovich. “Gravitational instability of scalar fields and formation of primordial black holes”. *Mon. Not. Roy. Astron. Soc.* 215 (1985).
- [Kob+17] T. Kobayashi et al. “Lyman- α constraints on ultralight scalar dark matter: Implications for the early and late universe”. *Phys. Rev. D* 96.12 (2017). DOI: [10.1103/PhysRevD.96.123514](https://doi.org/10.1103/PhysRevD.96.123514). arXiv: [1708.00015](https://arxiv.org/abs/1708.00015).
- [Kod+14] J. Koda et al. “Are peculiar velocity surveys competitive as a cosmological probe?” *Mon. Not. Roy. Astron. Soc.* 445.4 (2014). DOI: [10.1093/mnras/stu1610](https://doi.org/10.1093/mnras/stu1610). arXiv: [1312.1022](https://arxiv.org/abs/1312.1022).
- [Kog+93] A. Kogut et al. “Dipole anisotropy in the COBE DMR first year sky maps”. *Astrophys. J.* 419 (1993). DOI: [10.1086/173453](https://doi.org/10.1086/173453). arXiv: [astro-ph/9312056](https://arxiv.org/abs/astro-ph/9312056).

- [Kom+11] E. Komatsu et al. “Seven-Year Wilkinson Microwave Anisotropy Probe (WMAP) Observations: Cosmological Interpretation”. *Astrophys. J. Suppl.* 192 (2011). DOI: [10.1088/0067-0049/192/2/18](https://doi.org/10.1088/0067-0049/192/2/18). arXiv: [1001.4538](https://arxiv.org/abs/1001.4538).
- [KS84] H. Kodama and M. Sasaki. “Cosmological Perturbation Theory”. *Prog. Theor. Phys. Suppl.* 78 (1984). DOI: [10.1143/PTPS.78.1](https://doi.org/10.1143/PTPS.78.1).
- [KT94] E. W. Kolb and M. S. Turner. *The Early Universe*. Vol. 69. Frontiers in Physics. Addison-Wesley, 1994 [1990]. ISBN: 0813346452, 9780813346458.
- [KVS17] M. Kopp, K. Vattis, and C. Skordis. “Solving the Vlasov equation in two spatial dimensions with the Schrödinger method”. *Phys. Rev. D* 96.12 (2017). DOI: [10.1103/PhysRevD.96.123532](https://doi.org/10.1103/PhysRevD.96.123532). arXiv: [1711.00140](https://arxiv.org/abs/1711.00140).
- [LB02] A. Lewis and S. Bridle. “Cosmological parameters from CMB and other data: A Monte Carlo approach”. *Phys. Rev. D* 66 (2002). DOI: [10.1103/PhysRevD.66.103511](https://doi.org/10.1103/PhysRevD.66.103511). arXiv: [astro-ph/0205436](https://arxiv.org/abs/astro-ph/0205436).
- [LCL00] A. Lewis, A. Challinor, and A. Lasenby. “Efficient computation of CMB anisotropies in closed FRW models”. *Astrophys. J.* 538 (2000). DOI: [10.1086/309179](https://doi.org/10.1086/309179). arXiv: [astro-ph/9911177](https://arxiv.org/abs/astro-ph/9911177).
- [Les+13] J. Lesgourgues et al. *Neutrino cosmology*. Cambridge University Press, 2013.
- [Les13] J. Lesgourgues. “Cosmological Perturbations”. *Proceedings, Theoretical Advanced Study Institute in Elementary Particle Physics: Searching for New Physics at Small and Large Scales (TASI 2012): Boulder, Colorado, June 4-29, 2012*. 2013. DOI: [10.1142/9789814525220_0002](https://doi.org/10.1142/9789814525220_0002). arXiv: [1302.4640](https://arxiv.org/abs/1302.4640).
- [Lew07] A. Lewis. “Linear effects of perturbed recombination”. *Phys. Rev. D* 76 (2007). DOI: [10.1103/PhysRevD.76.063001](https://doi.org/10.1103/PhysRevD.76.063001). arXiv: [0707.2727](https://arxiv.org/abs/0707.2727).
- [LHB19] X. Li, L. Hui, and G. L. Bryan. “Numerical and Perturbative Computations of the Fuzzy Dark Matter Model”. *Phys. Rev. D* 99.6 (2019). DOI: [10.1103/PhysRevD.99.063509](https://doi.org/10.1103/PhysRevD.99.063509). arXiv: [1810.01915](https://arxiv.org/abs/1810.01915).
- [Lin+96] C. H. Lineweaver et al. “The dipole observed in the COBE DMR four-year data”. *Astrophys. J.* 470 (1996). DOI: [10.1086/177846](https://doi.org/10.1086/177846). arXiv: [astro-ph/9601151](https://arxiv.org/abs/astro-ph/9601151).
- [Lin66] R. W. Lindquist. “Relativistic transport theory”. *Annals of Physics* 37.3 (1966).
- [LL00] A. R. Liddle and D. H. Lyth. *Cosmological inflation and large scale structure*. Cambridge University Press, 2000. ISBN: 9780521828499.
- [LL59] L. D. Landau and E. M. Lifshitz. *Fluid mechanics*. Vol. 6. Course of Theoretical Physics. Pergamon Press, 1959. ISBN: 9780008091040.
- [Lon+03] J. C. Long et al. “Upper limits to submillimeter-range forces from extra space-time dimensions”. *Nature* 421 (2003). DOI: [10.1038/nature01432](https://doi.org/10.1038/nature01432).
- [LRS14] B. Li, T. Rindler-Daller, and P. R. Shapiro. “Cosmological Constraints on Bose-Einstein-Condensed Scalar Field Dark Matter”. *Phys. Rev. D* 89.8 (2014). DOI: [10.1103/PhysRevD.89.083536](https://doi.org/10.1103/PhysRevD.89.083536). arXiv: [1310.6061](https://arxiv.org/abs/1310.6061).

- [LSR17] B. Li, P. R. Shapiro, and T. Rindler-Daller. “Bose-Einstein-condensed scalar field dark matter and the gravitational wave background from inflation: new cosmological constraints and its detectability by LIGO”. *Phys. Rev. D* 96.6 (2017). DOI: [10.1103/PhysRevD.96.063505](https://doi.org/10.1103/PhysRevD.96.063505). arXiv: [1611.07961](https://arxiv.org/abs/1611.07961).
- [Maa+15] R. Maartens et al. “Overview of Cosmology with the SKA”. *PoS AASKA14* (2015). DOI: [10.22323/1.215.0016](https://doi.org/10.22323/1.215.0016). arXiv: [1501.04076](https://arxiv.org/abs/1501.04076).
- [Maa98] R. Maartens. “Covariant velocity and density perturbations in quasi-Newtonian cosmologies”. *Phys. Rev. D* 58 (1998). DOI: [10.1103/PhysRevD.58.124006](https://doi.org/10.1103/PhysRevD.58.124006). arXiv: [astro-ph/9808235](https://arxiv.org/abs/astro-ph/9808235).
- [Mar01] A. L. Maroto. “Primordial magnetic fields from metric perturbations”. *Phys. Rev. D* 64 (2001). DOI: [10.1103/PhysRevD.64.083006](https://doi.org/10.1103/PhysRevD.64.083006). arXiv: [hep-ph/0008288](https://arxiv.org/abs/hep-ph/0008288).
- [Mar06] A. L. Maroto. “Moving dark energy and the CMB dipole”. *JCAP* 0605 (2006). DOI: [10.1088/1475-7516/2006/05/015](https://doi.org/10.1088/1475-7516/2006/05/015). arXiv: [astro-ph/0512464](https://arxiv.org/abs/astro-ph/0512464).
- [Mar16] D. J. E. Marsh. “Axion Cosmology”. *Phys. Rept.* 643 (2016). DOI: [10.1016/j.physrep.2016.06.005](https://doi.org/10.1016/j.physrep.2016.06.005). arXiv: [1510.07633](https://arxiv.org/abs/1510.07633).
- [MB95] C.-P. Ma and E. Bertschinger. “Cosmological perturbation theory in the synchronous and conformal Newtonian gauges”. *Astrophys. J.* 455 (1995). DOI: [10.1086/176550](https://doi.org/10.1086/176550). arXiv: [astro-ph/9506072](https://arxiv.org/abs/astro-ph/9506072).
- [MFB92] V. F. Mukhanov, H. A. Feldman, and R. H. Brandenberger. “Theory of cosmological perturbations. Part 1. Classical perturbations. Part 2. Quantum theory of perturbations. Part 3. Extensions”. *Phys. Rept.* 215 (1992). DOI: [10.1016/0370-1573\(92\)90044-Z](https://doi.org/10.1016/0370-1573(92)90044-Z).
- [MN01] V. M. Mostepanenko and M. Novello. “Constraints on non-Newtonian gravity from the Casimir force measurements between two crossed cylinders”. *Phys. Rev. D* 63 (2001). DOI: [10.1103/PhysRevD.63.115003](https://doi.org/10.1103/PhysRevD.63.115003). arXiv: [hep-ph/0101306](https://arxiv.org/abs/hep-ph/0101306).
- [Moc+18] P. Mocz et al. “Schrödinger-Poisson–Vlasov-Poisson correspondence”. *Phys. Rev. D* 97.8 (2018). DOI: [10.1103/PhysRevD.97.083519](https://doi.org/10.1103/PhysRevD.97.083519). arXiv: [1801.03507](https://arxiv.org/abs/1801.03507).
- [Moo94] B. Moore. “Evidence against dissipationless dark matter from observations of galaxy haloes”. *Nature* 370 (1994). DOI: [10.1038/370629a0](https://doi.org/10.1038/370629a0).
- [MT15] J. Murata and S. Tanaka. “A review of short-range gravity experiments in the LHC era”. *Class. Quant. Grav.* 32.3 (2015). DOI: [10.1088/0264-9381/32/3/033001](https://doi.org/10.1088/0264-9381/32/3/033001). arXiv: [1408.3588](https://arxiv.org/abs/1408.3588).
- [MW84] J. E. Moody and F. Wilczek. “New Macroscopic Forces?” *Phys. Rev. D* 30 (1984). DOI: [10.1103/PhysRevD.30.130](https://doi.org/10.1103/PhysRevD.30.130).
- [NB05] S. Naoz and R. Barkana. “Growth of linear perturbations before the era of the first galaxies”. *Mon. Not. Roy. Astron. Soc.* 362 (2005). DOI: [10.1111/j.1365-2966.2005.09385.x](https://doi.org/10.1111/j.1365-2966.2005.09385.x). arXiv: [astro-ph/0503196](https://arxiv.org/abs/astro-ph/0503196).

- [NB18] M. Nori and M. Baldi. “AX-GADGET: a new code for cosmological simulations of Fuzzy Dark Matter and Axion models”. *Mon. Not. Roy. Astron. Soc.* 478.3 (2018). DOI: [10.1093/mnras/sty1224](https://doi.org/10.1093/mnras/sty1224). arXiv: [1801.08144](https://arxiv.org/abs/1801.08144).
- [NFW97] J. F. Navarro, C. S. Frenk, and S. D. M. White. “A universal density profile from hierarchical clustering”. *Astrophys. J.* 490 (1997). DOI: [10.1086/304888](https://doi.org/10.1086/304888). arXiv: [astro-ph/9611107](https://arxiv.org/abs/astro-ph/9611107).
- [NS11] A. E. Nelson and J. Scholtz. “Dark Light, Dark Matter and the Misalignment Mechanism”. *Phys. Rev.* D84 (2011). DOI: [10.1103/PhysRevD.84.103501](https://doi.org/10.1103/PhysRevD.84.103501). arXiv: [1105.2812](https://arxiv.org/abs/1105.2812).
- [NV10] A. Neronov and I. Vovk. “Evidence for strong extragalactic magnetic fields from Fermi observations of TeV blazars”. *Science* 328 (2010). DOI: [10.1126/science.1184192](https://doi.org/10.1126/science.1184192). arXiv: [1006.3504](https://arxiv.org/abs/1006.3504).
- [OS03] J. P. Ostriker and P. J. Steinhardt. “New light on dark matter”. *Science* 300 (2003). DOI: [10.1126/science.1085976](https://doi.org/10.1126/science.1085976). arXiv: [astro-ph/0306402](https://arxiv.org/abs/astro-ph/0306402).
- [Pad00] T. Padmanabhan. *Theoretical Astrophysics: Volume 3, Galaxies and Cosmology*. Cambridge University Press, 2000. ISBN: 9780521566308.
- [Pad93] T. Padmanabhan. *Structure Formation in the Universe*. Cambridge University Press, 1993. ISBN: 9780521424868.
- [Pan+19] N. Pant et al. “Measuring our velocity from fluctuations in number counts”. *JCAP* 1903 (2019). DOI: [10.1088/1475-7516/2019/03/023](https://doi.org/10.1088/1475-7516/2019/03/023). arXiv: [1808.09743](https://arxiv.org/abs/1808.09743).
- [Par+12] D. Parkinson et al. “The WiggleZ Dark Energy Survey: Final data release and cosmological results”. *Phys. Rev.* D86 (2012). DOI: [10.1103/PhysRevD.86.103518](https://doi.org/10.1103/PhysRevD.86.103518). arXiv: [1210.2130](https://arxiv.org/abs/1210.2130).
- [PHN12] C.-G. Park, J.-c. Hwang, and H. Noh. “Axion as a cold dark matter candidate: low-mass case”. *Phys. Rev.* D86 (2012). DOI: [10.1103/PhysRevD.86.083535](https://doi.org/10.1103/PhysRevD.86.083535). arXiv: [1207.3124](https://arxiv.org/abs/1207.3124).
- [PK86] A. Pantziris and K. Kang. “Axion Emission Rates in Stars and Constraints on Its Mass”. *Phys. Rev.* D33 (1986). DOI: [10.1103/PhysRevD.33.3509](https://doi.org/10.1103/PhysRevD.33.3509).
- [PQ77] R. D. Peccei and H. R. Quinn. “CP Conservation in the Presence of Instantons”. *Phys. Rev. Lett.* 38 (1977). DOI: [10.1103/PhysRevLett.38.1440](https://doi.org/10.1103/PhysRevLett.38.1440).
- [PS95] M. E. Peskin and D. V. Schroeder. *An Introduction to Quantum Field Theory*. Westview Press, 1995. ISBN: 9780201503975.
- [PS96] D. Polarski and A. A. Starobinsky. “Semiclassicality and decoherence of cosmological perturbations”. *Class. Quant. Grav.* 13 (1996). DOI: [10.1088/0264-9381/13/3/006](https://doi.org/10.1088/0264-9381/13/3/006). arXiv: [gr-qc/9504030](https://arxiv.org/abs/gr-qc/9504030).

- [QLS89] J. M. Quashnock, A. Loeb, and D. N. Spergel. “Magnetic Field Generation During the Cosmological QCD Phase Transition”. *Astrophys. J.* 344 (1989). DOI: [10.1086/185528](https://doi.org/10.1086/185528).
- [Raf86] G. G. Raffelt. “Astrophysical axion bounds diminished by screening effects”. *Phys. Rev. D* 33 (1986). DOI: [10.1103/PhysRevD.33.897](https://doi.org/10.1103/PhysRevD.33.897).
- [Raf90a] G. G. Raffelt. “Astrophysical methods to constrain axions and other novel particle phenomena”. *Phys. Rept.* 198 (1990). DOI: [10.1016/0370-1573\(90\)90054-6](https://doi.org/10.1016/0370-1573(90)90054-6).
- [Raf90b] G. G. Raffelt. “Axion bremsstrahlung in red giants”. *Phys. Rev. D* 41 (1990). DOI: [10.1103/PhysRevD.41.1324](https://doi.org/10.1103/PhysRevD.41.1324).
- [Raf96] G. G. Raffelt. *Stars as laboratories for fundamental physics: The astrophysics of neutrinos, axions, and other weakly interacting particles*. University of Chicago Press, 1996. ISBN: 0226702723, 9780226702728.
- [Raf99] G. G. Raffelt. “Particle physics from stars”. *Ann. Rev. Nucl. Part. Sci.* 49 (1999). DOI: [10.1146/annurev.nucl.49.1.163](https://doi.org/10.1146/annurev.nucl.49.1.163). arXiv: [hep-ph/9903472](https://arxiv.org/abs/hep-ph/9903472).
- [Red08] J. Redondo. “Helioscope Bounds on Hidden Sector Photons”. *JCAP* 0807 (2008). DOI: [10.1088/1475-7516/2008/07/008](https://doi.org/10.1088/1475-7516/2008/07/008). arXiv: [0801.1527](https://arxiv.org/abs/0801.1527).
- [Ree87] M. J. Rees. “The origin and cosmogonic implications of seed magnetic fields”. *Q. J. R. Astron. Soc.* 28 (Sept. 1987).
- [RGT11] C. de Rham, G. Gabadadze, and A. J. Tolley. “Resummation of Massive Gravity”. *Phys. Rev. Lett.* 106 (2011). DOI: [10.1103/PhysRevLett.106.231101](https://doi.org/10.1103/PhysRevLett.106.231101). arXiv: [1011.1232](https://arxiv.org/abs/1011.1232).
- [Rha14] C. de Rham. “Massive Gravity”. *Living Rev. Rel.* 17 (2014). DOI: [10.12942/lrr-2014-7](https://doi.org/10.12942/lrr-2014-7). arXiv: [1401.4173](https://arxiv.org/abs/1401.4173).
- [RHR14] C. de Rham, L. Heisenberg, and R. H. Ribeiro. “Ghosts and matter couplings in massive gravity, bigravity and multigravity”. *Phys. Rev. D* 90 (2014). DOI: [10.1103/PhysRevD.90.124042](https://doi.org/10.1103/PhysRevD.90.124042). arXiv: [1409.3834](https://arxiv.org/abs/1409.3834).
- [RHR15] C. de Rham, L. Heisenberg, and R. H. Ribeiro. “On couplings to matter in massive (bi-)gravity”. *Class. Quant. Grav.* 32 (2015). DOI: [10.1088/0264-9381/32/3/035022](https://doi.org/10.1088/0264-9381/32/3/035022). arXiv: [1408.1678](https://arxiv.org/abs/1408.1678).
- [RS12] T. Rindler-Daller and P. R. Shapiro. “Angular Momentum and Vortex Formation in Bose-Einstein-Condensed Cold Dark Matter Haloes”. *Mon. Not. Roy. Astron. Soc.* 422 (2012). DOI: [10.1111/j.1365-2966.2012.20588.x](https://doi.org/10.1111/j.1365-2966.2012.20588.x). arXiv: [1106.1256](https://arxiv.org/abs/1106.1256).
- [RS88] G. Raffelt and L. Stodolsky. “Mixing of the Photon with Low Mass Particles”. *Phys. Rev. D* 37 (1988). DOI: [10.1103/PhysRevD.37.1237](https://doi.org/10.1103/PhysRevD.37.1237).
- [RS99a] L. Randall and R. Sundrum. “A large mass hierarchy from a small extra dimension”. *Phys. Rev. Lett.* 83 (1999). DOI: [10.1103/PhysRevLett.83.3370](https://doi.org/10.1103/PhysRevLett.83.3370). arXiv: [hep-ph/9905221](https://arxiv.org/abs/hep-ph/9905221).

- [RS99b] L. Randall and R. Sundrum. “An alternative to compactification”. *Phys. Rev. Lett.* 83 (1999). DOI: [10.1103/PhysRevLett.83.4690](https://doi.org/10.1103/PhysRevLett.83.4690). arXiv: [hep-th/9906064](https://arxiv.org/abs/hep-th/9906064).
- [Saa+16] D. Saadeh et al. “How isotropic is the Universe?” *Phys. Rev. Lett.* 117.13 (2016). DOI: [10.1103/PhysRevLett.117.131302](https://doi.org/10.1103/PhysRevLett.117.131302). arXiv: [1605.07178](https://arxiv.org/abs/1605.07178).
- [Saf+18] M. S. Safronova et al. “Search for New Physics with Atoms and Molecules”. *Rev. Mod. Phys.* 90.2 (2018). DOI: [10.1103/RevModPhys.90.025008](https://doi.org/10.1103/RevModPhys.90.025008). arXiv: [1710.01833](https://arxiv.org/abs/1710.01833).
- [Sag+15] S. Saga et al. “Magnetic field spectrum at cosmological recombination revisited”. *Phys. Rev. D* 91.12 (2015). DOI: [10.1103/PhysRevD.91.123510](https://doi.org/10.1103/PhysRevD.91.123510). arXiv: [1504.03790](https://arxiv.org/abs/1504.03790).
- [Sar+16] A. Sarkar et al. “The effects of the small-scale DM power on the cosmological neutral hydrogen (HI) distribution at high redshifts”. *JCAP* 1604.04 (2016). DOI: [10.1088/1475-7516/2016/04/012](https://doi.org/10.1088/1475-7516/2016/04/012). arXiv: [1512.03325](https://arxiv.org/abs/1512.03325).
- [SBG04] C. F. Sopuerta, M. Bruni, and L. Gualtieri. “Nonlinear N parameter space-time perturbations: Gauge transformations”. *Phys. Rev. D* 70 (2004). DOI: [10.1103/PhysRevD.70.064002](https://doi.org/10.1103/PhysRevD.70.064002). arXiv: [gr-qc/0306027](https://arxiv.org/abs/gr-qc/0306027).
- [Sbi15] F. Sbisà. “Classical and quantum ghosts”. *Eur. J. Phys.* 36 (2015). DOI: [10.1088/0143-0807/36/1/015009](https://doi.org/10.1088/0143-0807/36/1/015009). arXiv: [1406.4550](https://arxiv.org/abs/1406.4550).
- [SC17] A. Suárez and P.-H. Chavanis. “Cosmological evolution of a complex scalar field with repulsive or attractive self-interaction”. *Phys. Rev. D* 95.6 (2017). DOI: [10.1103/PhysRevD.95.063515](https://doi.org/10.1103/PhysRevD.95.063515). arXiv: [1608.08624](https://arxiv.org/abs/1608.08624).
- [SCB14] H.-Y. Schive, T. Chiueh, and T. Broadhurst. “Cosmic Structure as the Quantum Interference of a Coherent Dark Wave”. *Nature Phys.* 10 (2014). DOI: [10.1038/nphys2996](https://doi.org/10.1038/nphys2996). arXiv: [1406.6586](https://arxiv.org/abs/1406.6586).
- [Sch+16] D. J. Schwarz et al. “CMB anomalies after Planck”. *Class. Quant. Grav.* 33.18 (2016). DOI: [10.1088/0264-9381/33/18/184001](https://doi.org/10.1088/0264-9381/33/18/184001). arXiv: [1510.07929](https://arxiv.org/abs/1510.07929).
- [Sch65] M. Schwarzschild. *Structure and evolution of the stars*. Dover Publications, 1965 [1958]. ISBN: 0486614794, 9780486614793.
- [Scr+16] M. I. Scrimgeour et al. “The 6dF Galaxy Survey: Bulk Flows on $50 - 70h^{-1}$ Mpc scales”. *Mon. Not. Roy. Astron. Soc.* 455.1 (2016). DOI: [10.1093/mnras/stv2146](https://doi.org/10.1093/mnras/stv2146). arXiv: [1511.06930](https://arxiv.org/abs/1511.06930).
- [SF15] Y. V. Stadnik and V. V. Flambaum. “Can dark matter induce cosmological evolution of the fundamental constants of Nature?” *Phys. Rev. Lett.* 115.20 (2015). DOI: [10.1103/PhysRevLett.115.201301](https://doi.org/10.1103/PhysRevLett.115.201301). arXiv: [1503.08540](https://arxiv.org/abs/1503.08540).
- [SF16] Y. V. Stadnik and V. V. Flambaum. “Improved limits on interactions of low-mass spin-0 dark matter from atomic clock spectroscopy”. *Phys. Rev. A* 94.2 (2016). DOI: [10.1103/PhysRevA.94.022111](https://doi.org/10.1103/PhysRevA.94.022111). arXiv: [1605.04028](https://arxiv.org/abs/1605.04028).

- [Smo+92] G. F. Smoot et al. “Structure in the COBE differential microwave radiometer first year maps”. *Astrophys. J.* 396 (1992). DOI: [10.1086/186504](https://doi.org/10.1086/186504).
- [Sre07] M. Srednicki. *Quantum Field Theory*. Cambridge University Press, 2007. ISBN: 9781139462761.
- [SS00] D. N. Spergel and P. J. Steinhardt. “Observational evidence for self-interacting cold dark matter”. *Phys. Rev. Lett.* 84 (2000). DOI: [10.1103/PhysRevLett.84.3760](https://doi.org/10.1103/PhysRevLett.84.3760). arXiv: [astro-ph/9909386](https://arxiv.org/abs/astro-ph/9909386).
- [SS16] A. Schmidt-May and M. von Strauss. “Recent developments in bimetric theory”. *J. Phys.* A49.18 (2016). DOI: [10.1088/1751-8113/49/18/183001](https://doi.org/10.1088/1751-8113/49/18/183001). arXiv: [1512.00021](https://arxiv.org/abs/1512.00021).
- [SSD17] A. Sarkar, S. K. Sethi, and S. Das. “The effects of the small-scale behaviour of dark matter power spectrum on CMB spectral distortion”. *JCAP* 1707.07 (2017). DOI: [10.1088/1475-7516/2017/07/012](https://doi.org/10.1088/1475-7516/2017/07/012). arXiv: [1701.07273](https://arxiv.org/abs/1701.07273).
- [SSS00] S. Seager, D. D. Sasselov, and D. Scott. “How exactly did the universe become neutral?” *Astrophys. J. Suppl.* 128 (2000). DOI: [10.1086/313388](https://doi.org/10.1086/313388). arXiv: [astro-ph/9912182](https://arxiv.org/abs/astro-ph/9912182).
- [Sta+87] F. D. Stacey et al. “Geophysics and the Law of Gravity”. *Rev. Mod. Phys.* 59 (1987). DOI: [10.1103/RevModPhys.59.157](https://doi.org/10.1103/RevModPhys.59.157).
- [Ste71] J. M. Stewart. *Non-equilibrium relativistic kinetic theory*. Springer, 1971. ISBN: 9783540056522.
- [Sub16] K. Subramanian. “The origin, evolution and signatures of primordial magnetic fields”. *Rept. Prog. Phys.* 79.7 (2016). DOI: [10.1088/0034-4885/79/7/076901](https://doi.org/10.1088/0034-4885/79/7/076901). arXiv: [1504.02311](https://arxiv.org/abs/1504.02311).
- [SUR05] C. Schimd, J.-P. Uzan, and A. Riazuelo. “Weak lensing in scalar-tensor theories of gravity”. *Phys. Rev.* D71 (2005). DOI: [10.1103/PhysRevD.71.083512](https://doi.org/10.1103/PhysRevD.71.083512). arXiv: [astro-ph/0412120](https://arxiv.org/abs/astro-ph/0412120).
- [SY09] P. Sikivie and Q. Yang. “Bose-Einstein Condensation of Dark Matter Axions”. *Phys. Rev. Lett.* 103 (2009). DOI: [10.1103/PhysRevLett.103.111301](https://doi.org/10.1103/PhysRevLett.103.111301). arXiv: [0901.1106](https://arxiv.org/abs/0901.1106).
- [SZ96] U. Seljak and M. Zaldarriaga. “A line-of-sight integration approach to cosmic microwave background anisotropies”. *Astrophys. J.* 469 (1996). DOI: [10.1086/177793](https://doi.org/10.1086/177793). arXiv: [astro-ph/9603033](https://arxiv.org/abs/astro-ph/9603033).
- [Tak+05] K. Takahashi et al. “Magnetic field generation from cosmological perturbations”. *Phys. Rev. Lett.* 95 (2005). DOI: [10.1103/PhysRevLett.95.121301](https://doi.org/10.1103/PhysRevLett.95.121301). arXiv: [astro-ph/0502283](https://arxiv.org/abs/astro-ph/0502283).
- [Tal+88] C. Talmadge et al. “Model Independent Constraints on Possible Modifications of Newtonian Gravity”. *Phys. Rev. Lett.* 61 (1988). DOI: [10.1103/PhysRevLett.61.1159](https://doi.org/10.1103/PhysRevLett.61.1159).
- [Tan+18] M. Tanabashi et al. “Review of Particle Physics”. *Phys. Rev. D* 98 (3 Aug. 2018). DOI: [10.1103/PhysRevD.98.030001](https://doi.org/10.1103/PhysRevD.98.030001).

- [TB17] K. S. Thorne and R. D. Blandford. *Modern Classical Physics: Optics, Fluids, Plasmas, Elasticity, Relativity, and Statistical Physics*. Princeton University Press, 2017. ISBN: 9781400848898.
- [Teg+04] M. Tegmark et al. “The 3-D power spectrum of galaxies from the SDSS”. *Astrophys. J.* 606 (2004). DOI: [10.1086/382125](https://doi.org/10.1086/382125). arXiv: [astro-ph/0310725](https://arxiv.org/abs/astro-ph/0310725).
- [Tol+16] E. Tollet et al. “NIHAO – IV: core creation and destruction in dark matter density profiles across cosmic time”. *Mon. Not. Roy. Astron. Soc.* 456.4 (2016). [Erratum: *Mon. Not. Roy. Astron. Soc.* 487, no. 2, 1764 (2019)]. DOI: [10.1093/mnras/stz1376](https://doi.org/10.1093/mnras/stz1376), [10.1093/mnras/stv2856](https://doi.org/10.1093/mnras/stv2856). arXiv: [1507.03590](https://arxiv.org/abs/1507.03590).
- [Tul+08] R. B. Tully et al. “Our Peculiar Motion Away from the Local Void”. *Astrophys. J.* 676 (2008). DOI: [10.1086/527428](https://doi.org/10.1086/527428). arXiv: [0705.4139](https://arxiv.org/abs/0705.4139).
- [Tur83] M. S. Turner. “Coherent Scalar Field Oscillations in an Expanding Universe”. *Phys. Rev. D* 28 (1983). DOI: [10.1103/PhysRevD.28.1243](https://doi.org/10.1103/PhysRevD.28.1243).
- [Tur91] M. S. Turner. “A Tilted Universe (and Other Remnants of the Preinflationary Universe)”. *Phys. Rev. D* 44 (1991). DOI: [10.1103/PhysRevD.44.3737](https://doi.org/10.1103/PhysRevD.44.3737).
- [TW88] M. S. Turner and L. M. Widrow. “Inflation Produced, Large Scale Magnetic Fields”. *Phys. Rev. D* 37 (1988). DOI: [10.1103/PhysRevD.37.2743](https://doi.org/10.1103/PhysRevD.37.2743).
- [TY18] S. Tulin and H.-B. Yu. “Dark Matter Self-interactions and Small Scale Structure”. *Phys. Rept.* 730 (2018). DOI: [10.1016/j.physrep.2017.11.004](https://doi.org/10.1016/j.physrep.2017.11.004). arXiv: [1705.02358](https://arxiv.org/abs/1705.02358).
- [UG16] L. A. Ureña-López and A. X. Gonzalez-Morales. “Towards accurate cosmological predictions for rapidly oscillating scalar fields as dark matter”. *JCAP* 1607.07 (2016). DOI: [10.1088/1475-7516/2016/07/048](https://doi.org/10.1088/1475-7516/2016/07/048). arXiv: [1511.08195](https://arxiv.org/abs/1511.08195).
- [Vac91] T. Vachaspati. “Magnetic fields from cosmological phase transitions”. *Phys. Lett.* B265 (1991). DOI: [10.1016/0370-2693\(91\)90051-Q](https://doi.org/10.1016/0370-2693(91)90051-Q).
- [Vai72] A. I. Vainshtein. “To the problem of nonvanishing gravitation mass”. *Phys. Lett.* B39 (1972). DOI: [10.1016/0370-2693\(72\)90147-5](https://doi.org/10.1016/0370-2693(72)90147-5).
- [Van73] P. Van Nieuwenhuizen. “On ghost-free tensor lagrangians and linearized gravitation”. *Nucl. Phys.* B60 (1973). DOI: [10.1016/0550-3213\(73\)90194-6](https://doi.org/10.1016/0550-3213(73)90194-6).
- [Wal10] R. M. Wald. *General relativity*. University of Chicago Press, 2010 [1984]. ISBN: 0226870332, 9780226870335.
- [Wan+15] L. Wang et al. “NIHAO project – I. Reproducing the inefficiency of galaxy formation across cosmic time with a large sample of cosmological hydrodynamical simulations”. *Mon. Not. Roy. Astron. Soc.* 454.1 (2015). DOI: [10.1093/mnras/stv1937](https://doi.org/10.1093/mnras/stv1937). arXiv: [1503.04818](https://arxiv.org/abs/1503.04818).
- [Wei08] S. Weinberg. *Cosmology*. Oxford University Press, 2008. ISBN: 9780198526827.

- [Wei65] S. Weinberg. “Infrared photons and gravitons”. *Phys. Rev.* 140 (1965). DOI: [10.1103/PhysRev.140.B516](https://doi.org/10.1103/PhysRev.140.B516).
- [Wei72] S. Weinberg. *Gravitation and Cosmology*. John Wiley & Sons, 1972. ISBN: 9780471925675.
- [Wei78] S. Weinberg. “A New Light Boson?” *Phys. Rev. Lett.* 40 (1978). DOI: [10.1103/PhysRevLett.40.223](https://doi.org/10.1103/PhysRevLett.40.223).
- [Wei95] S. Weinberg. *The Quantum Theory of Fields*. Vol. 1. Cambridge University Press, 1995. ISBN: 9780521670531.
- [Wid02] L. M. Widrow. “Origin of galactic and extragalactic magnetic fields”. *Rev. Mod. Phys.* 74 (2002). DOI: [10.1103/RevModPhys.74.775](https://doi.org/10.1103/RevModPhys.74.775). arXiv: [astro-ph/0207240](https://arxiv.org/abs/astro-ph/0207240).
- [Wil78] F. Wilczek. “Problem of Strong P and T Invariance in the Presence of Instantons”. *Phys. Rev. Lett.* 40 (1978). DOI: [10.1103/PhysRevLett.40.279](https://doi.org/10.1103/PhysRevLett.40.279).
- [WK93] L. M. Widrow and N. Kaiser. “Using the Schrödinger equation to simulate collisionless matter”. *Astrophys. J.* 416 (1993). DOI: [10.1086/187073](https://doi.org/10.1086/187073).
- [Woo15] R. P. Woodard. “Ostrogradsky’s theorem on Hamiltonian instability”. *Scholarpedia* 10.8 (2015). DOI: [10.4249/scholarpedia.32243](https://doi.org/10.4249/scholarpedia.32243). arXiv: [1506.02210](https://arxiv.org/abs/1506.02210).
- [YD17] J. Yoo and R. Durrer. “Gauge-Transformation Properties of Cosmological Observables and its Application to the Light-Cone Average”. *JCAP* 1709.09 (2017). DOI: [10.1088/1475-7516/2017/09/016](https://doi.org/10.1088/1475-7516/2017/09/016). arXiv: [1705.05839](https://arxiv.org/abs/1705.05839).
- [YP17] S. Yasini and E. Pierpaoli. “Beyond the Boost: Measuring the Intrinsic Dipole of the Cosmic Microwave Background Using the Spectral Distortions of the Monopole and Quadrupole”. *Phys. Rev. Lett.* 119.22 (2017). DOI: [10.1103/PhysRevLett.119.221102](https://doi.org/10.1103/PhysRevLett.119.221102). arXiv: [1610.00015](https://arxiv.org/abs/1610.00015).
- [Zak70] V. I. Zakharov. “Linearized gravitation theory and the graviton mass”. *JETP Lett.* 12 (1970). [Pisma Zh. Eksp. Teor. Fiz.12,447(1970)].
- [Zha+18] J. Zhang et al. “Ultralight Axion Dark Matter and its Impact on Dark Halo Structure in N -body Simulations”. *Astrophys. J.* 853.1 (2018). DOI: [10.3847/1538-4357/aaa485](https://doi.org/10.3847/1538-4357/aaa485). arXiv: [1611.00892](https://arxiv.org/abs/1611.00892).